C O M M U N I C A T I O N S

FACULTY OF SCIENCES
UNIVERSITY OF ANKARA

DE LA FACULTE DES SCIENCES
DE L'UNIVERSITE D'ANKARA

Series A1: Mathematics and Statistics

VOLUME: 72 **Number: 3** **YEAR: 2023**

Faculty of Sciences, Ankara University
06100 Beşevler, Ankara-Turkey

ISSN 1303-5991 e-ISSN 2618-6470

C O M M U N I C A T I O N S

FACULTY OF SCIENCES
UNIVERSITY OF ANKARA

DE LA FACULTE DES SCIENCES
DE L'UNIVERSITE D'ANKARA

Series A1: Mathematics and Statistics

Volume: 72 **Number: 3** **Year: 2023**

This Journal is published four issues in a year by the Faculty of Sciences, University of Ankara. Articles and any other material published in this journal represent the opinions of the author(s) and should not be construed to reflect the opinions of the Editor(s) and the Publisher(s).

Correspondence Address:
COMMUNICATIONS EDITORIAL OFFICE
Ankara University, Faculty of Sciences,
06100 Tandoğan, ANKARA – TURKEY
Tel: (90) 312-2126720 Fax: (90) 312-2235000
e-mail: commun@science.ankara.edu.tr
http://communications.science.ankara.edu.tr/index.php?series=A1

Print:
Ankara University Press
İncitaş Sokak No:10 06510 Beşevler
ANKARA – TURKEY
Tel: (90) 312-2136655

C O M M U N I C A T I O N S

FACULTY OF SCIENCES
UNIVERSITY OF ANKARA

DE LA FACULTE DES SCIENCES
DE L'UNIVERSITE D'ANKARA

Series A1: Mathematics and Statistics

VOLUME: 72 **Number: 3** **YEAR: 2023**

Faculty of Sciences, Ankara University
06100 Beşevler, Ankara-Turkey

ISSN 1303-5991 e-ISSN 2618-6470

C O M M U N I C A T I O N S

FACULTY OF SCIENCES
UNIVERSITY OF ANKARA

DE LA FACULTE DES SCIENCES DE
L'UNIVERSITE D'ANKARA

Series A1: Mathematics and Statistics

Volume: 72 **Number: 3** **Year: 2023**

Research Articles

http://communications.science.ankara.edu.tr

Commun.Fac.Sci.Univ.Ank.Ser. A1 Math. Stat.
Volume 72, Number 3, Pages 563–569 (2023)
DOI:10.31801/cfsuasmas.1229943
ISSN 1303-5991 E-ISSN 2618-6470

Research Article; Received: January 10, 2023; Accepted: February 28, 2023

ON SUBFLAT DOMAINS OF RD-FLAT MODULES

Mücahit BOZKURT[1] and Yılmaz DURĞUN[2]

[1]Department of Mathematics, Manisa Celal Bayar University, Manisa, TÜRKİYE
[2]Department of Mathematics, Çukurova University, Adana, TÜRKİYE

Abstract. The concept of subflat domain is used to measure how close (or far away) a module is to be flat. A right module is flat if its subflat domain is the entire class of left modules. In this note, we focus on of RD-flat modules that have subflat domain which is exactly the collection of all torsion-free modules, shortly tf-test modules. Properties of subflat domains and of tf-test modules are studied. New characterizations of left P-coherent rings and torsion-free rings by subflat domains of cyclically presented left R-modules are obtained.

1. Introduction

The rings R in this note are associative with identity, and every module is, if not specified otherwise, right R-module. We use $Mod-R$ ($R-Mod$) to denote the class of right (left) R-modules.

There are important subclasses of $Mod-R$ that shed light on the whole of $Mod-R$. The classes of all projectives, all injective modules and all flat modules are the prominent ones. Recently, many authors have studied on alternative ways to test projectivity, injectivity and flatness of modules. In general, they are trying to find test module whose test projectivity (injectivity or flatness) of modules ([1, 2, 4, 10, 11, 18]). In this paper, we test the flatness of the RD-flat modules by torsion-free modules.

Inspired by homological properties of torsion-free modules over an integral domain, Hattori in [9] defined and studied torsion-free modules over non-commutative rings. A right R-module X is called torsion-free if $\mathbf{T}or_1(X, R/Ra) = 0$ for all $a \in R$. Flat modules are torsion-free, but the converse is not true in general. Torsion-free modules are intimately related to relatively divisible (RD) exact sequences. A short exact sequence $0 \to K \to L \to M \to 0$ is called RD-exact if, for every $a \in R$, the

2020 *Mathematics Subject Classification.* 16D10, 18G15, 16D40.
Keywords. RD-flat module, subflat domain, torsion-free module.
[1] mucahit.bozkurt1@hotmail.com; 0000-0003-3265-1994
[2] ydurgun@cu.edu.tr-Corresponding author; 0000-0002-1230-8964.

induced homomorphism $Hom_R(R/Ra, L) \to Hom_R(R/Ra, M) \to 0$ is surjective, or equivalently, the induced map $(R/aR) \otimes K \to (R/aR) \otimes L$ is monic ([19, Proposition 2]). An R-module T (respectively, D) is torsion-free (respectively, divisible) if and only if every short exact sequence $0 \to D \to B \to T \to 0$ is RD-exact ([13]). Note that torsion-free (respectively, divisible) modules are called P-flat (rspectively, P-injective) by some authors. By the standard adjoint isomorphism, a module B is torsion-free if and only if its character module B^+ is a divisible left R-module. Obviously, every pure exact sequence is RD-exact. Moreover, every flat and fp-injective module is respectively torsion-free and divisible.

An R-module N is called RD-injective (respectively, RD-projective, RD-flat) if it has the injective (respectively, projective, flat) property with respect to every RD-exact sequence. The notions of RD-projective, RD-injective and RD-flat module were used by Stenström in [17]. Commutative rings for which each Artinian module is RD-injective (RD-flat) were completely characterized in [5]. In [13], the author studied main properties of RD-projective, RD-injective and RD-flat modules.

Inspired and motivated by Whitehead injective test modules (shortly, i-test modules) in [7,18], f-test modules is defined and studied in [2], through $\mathbf{T}or$ functor. A module F is called f-test provided that for every left R-module K, $\mathbf{T}or(F, K) = 0$ implies that K is flat. In the same vein as f-test module, the main objective of the present paper is to study test modules for torsion-freeness. A module K_R is said to be ${}_RL$-*subflat* if for every short exact sequence $0 \to U \to D \to L \to 0$ of left R-modules, the sequence $0 \to K \otimes U \to K \otimes D \to K \otimes L \to 0$ is exact. For any $K \in Mod - R$, we denote by $\mathfrak{F}^{-1}(K)$ the class $\{L \in R - Mod :$ K is L-subflat$\}$. Clearly, K_R is flat if and only if $\mathfrak{F}^{-1}(K) = R - Mod$. As can be seen from the definitions, all flat left R-modules are contained in $\mathfrak{F}^{-1}(K)$ for each module K. In particular, if M_R is RD-flat and ${}_RN$ is torsion-free, then M_R is ${}_RN$-subflat. So, the smallest possible subflat domain for an RD-flat module is the class of torsion-free modules. We call a left module K test module for torsion-free (shortly, tf-test) module if $\mathfrak{F}^{-1}(K)$ is exactly the class of torsion-free modules. We show that every ring has a tf-test module.

In Section 2, we first obtain elementary properties of subflat domains of modules. We present new characterizations for P-coherent rings and torsion-free rings by subflat domains. For example, a ring R is torsion-free if and only if the subflat domain of any cyclically presented left (or right) R-module is closed under submodules. In Section 3, we discuss tf-test modules.

In what follows, we write $\mathcal{TF}_R$(respectively, $\mathcal{F}_R, \mathcal{N}_R$) for the family of torsion-free (respectively, flat, nonsingular) modules. For a right R-module M, the character module $Hom_{\mathbb{Z}}(U, \mathbb{Q}/\mathbb{Z})$ is denoted by U^+. Given R-modules U and H, $Hom(U, H)$ (resp. $Ext^n(U, H)$) means $Hom_R(U, H)$ (resp. $Ext^n_R(U, H)$), and similarly $U \otimes H$ (resp. $\mathbf{T}or_n(U, H)$) denotes $U \otimes_R H$ (resp. $\mathbf{T}or^R_n(U, H)$) for an integer $n \geq 1$ unless otherwise specified.

2. Subflat Domains

This section is devoted to obtain some elementary properties of subflat domains of modules that will be needed later in the paper.

Given a left module X, a module T is X-subflat if and only if $\mathbf{T}or_1^R(T,X)=0$ by [2, Proposition 2.3]. Moreover, if $T \leq M$ and, T and M/T are N-subflat, then M is N-subflat.

Lemma 1. *Let $Y \in Mod-R$ and X be a pure submodule of Y. $\mathfrak{F}^{-1}(Y) \subseteq \mathfrak{F}^{-1}(X)$.*

Proof. Let $A \in \mathfrak{F}^{-1}(Y)$. Consider the following commutative diagram

$$\begin{array}{ccccccccc} 0 & \longrightarrow & X\otimes F_0 & \xrightarrow{\epsilon} & Y\otimes F_0 & \xrightarrow{\delta} & (Y/X)\otimes F_0 & \longrightarrow & 0 \\ & & \downarrow{\scriptstyle\alpha} & & \downarrow{\scriptstyle\gamma} & & \downarrow{\scriptstyle\theta} & & \\ 0 & \longrightarrow & X\otimes F_1 & \xrightarrow{\eta} & Y\otimes F_1 & \xrightarrow{\vartheta} & (Y/X)\otimes F_1 & \longrightarrow & 0, \end{array}$$

where $0 \to F_0 \to F_1 \to A \to 0$ is any short exact sequence. Since $A \in \mathfrak{F}^{-1}(Y)$, γ is monic. On the other hand, since X is pure submodule of Y, the rows are exact. Then, α is a monomorphism, because $\eta\alpha = \gamma\epsilon$ is monomorphism. □

For $Y \in Mod-R$, the flat dimension of Y (fd(Y)) ≤ 1 if and only if $\mathbf{T}or_2^R(Y,B)=0$, $\forall B \in R-Mod$ ([15, pp.239]).

Lemma 2. *Let $Y \in Mod-R$ and W be a submodule of Y. If $fd(Y/W) \leq 1$, then $\mathfrak{F}^{-1}(Y) \subseteq \mathfrak{F}^{-1}(W)$.*

Proof. Recall that $fd(Y/W) \leq 1$ if and only if then $\mathbf{T}or_2^R(Y/W,A)=0$ for every left R-module A. If $A \in \mathfrak{F}^{-1}(Y)$, then $\mathbf{T}or_1^R(Y,A)=0$ by [2, Proposition 2.3]. So the sequence $0 \to W \to Y \to \frac{Y}{W} \to 0$ implies that $0=\mathbf{T}or_2^R(\frac{Y}{W},A) \to \mathbf{T}or_1^R(W,A) \to \mathbf{T}or_1^R(Y,A)=0$ is exact. Therefore, W is A-subflat by [2, Proposition 2.3].

□

In general, for any R-module M, $\mathfrak{F}^{-1}(M)$ is closed under pure submodules.

Theorem 1. *Let $T \in Mod-R$. $fd(T) \leq 1$ if and only if $\mathfrak{F}^{-1}(T)$ is closed under submodules.*

Proof. Let $Z \in \mathfrak{F}^{-1}(T)$ and $H \subseteq Z$ be any submodule. From the sequence $0 \to H \to Z \to Z/H \to 0$, we have that $0=\mathbf{T}or_2^R(T,Z/H) \to \mathbf{T}or_1^R(T,H) \to \mathbf{T}or_1^R(T,Z)=0$. Then, T is H-subflat by [2, Proposition 2.3]. For the converse, let $Z \in R-Mod$ and consider the short exact sequence $0 \to H \to U \to Z \to 0$ with U projective. Since $U \in \mathfrak{F}^{-1}(T)$, $\mathbf{T}or_1^R(T,H)=0$ by our hypothesis. By the exactness of $0=\mathbf{T}or_2^R(T,U) \to \mathbf{T}or_2^R(T,Z) \to \mathbf{T}or_1^R(T,H)=0$, $\mathbf{T}or_2^R(T,Z)=0$. Therefore, $fd(T) \leq 1$. □

$wD(R) \leq 1$ if and only if $fd(X) \leq 1$ for all right (or left) modules X ([15, pp. 240]).

Corollary 1. *$wD(R) \leq 1$ if and only if $\mathfrak{F}^{-1}(X)$ is closed under submodules for every (finitely presented) left (or right) R-module X.*

We say R is torsion-free if all its (finitely generated) right (or left) ideals of R are torsion-free. The concept of a torsion-free ring is left and right symmetric ([6]). It is easy to see that a cyclic module is torsion-free if and only if it is flat. So, a ring is torsion-free if and only if it is a pf-ring, i.e. each principal ideal is flat. A cyclic module $M \cong R/I$ is called cyclically presented if $I = aR$ for some $a \in R$.

Corollary 2. *R is torsion-free ring if and only if the subflat domain of any cyclically presented (or RD-flat) right (or left) R-module is closed under submodules.*

Theorem 2. *Let U be a finitely presented module and $0 \to K \to H \to U \to 0$ be a short exact sequence with finitely generated projective module H. $\mathfrak{F}^{-1}(U)$ is closed under direct products if and only if K is finitely presented*

Proof. ($\Rightarrow$) $\mathbf{T}or_1^R(U, \prod R) = 0$ by our assumption. Consider the following commutative diagram

$$\begin{array}{ccccccc}
K \otimes (\prod R) & \xrightarrow{\beta} & H \otimes (\prod R) & \xrightarrow{\delta} & U \otimes (\prod R) & \longrightarrow & 0 \\
\downarrow{\scriptstyle\alpha} & & \downarrow{\scriptstyle\gamma} & & \downarrow{\scriptstyle\theta} & & \\
\prod K & \xrightarrow{\eta} & \prod H & \xrightarrow{\vartheta} & \prod U & \longrightarrow & 0
\end{array}$$

γ and θ are isomorphisms by [8, Theorem 3.2.22]. Then α is an isomorphism by the Five Lemma, therefore K is finitely presented by [8, Theorem 3.2.22].

($\Leftarrow$) Let $A \in \mathfrak{F}^{-1}(U)$, i.e. $\mathbf{T}or_1^R(U, A) = 0$. By the adjoint isomorphism, $Ext_R^1(U, A^+) = 0$. Note that $\mathbf{T}or_1^R(N, B^+) = Ext_R^1(N, B)^+$ for every $B \in R-Mod$ if a module N has a projective resolution $P_2 \to P_1 \to P_0 \to N \to 0$, where P_i is finitely generated for $i = 0, 1, 2$ (see [15, Remark, pp. 257]). Thus this implies that $\mathbf{T}or_1^R(U, A^{++}) = 0$, that is U is A^{++}-subflat.

Let $\{M_i\}_{i \in J}$ be a family of left R-modules in $\mathfrak{F}^{-1}(U)$. Then $\bigoplus_{i \in J} M_i \in \mathfrak{F}^{-1}(U)$ by main properties of $\mathbf{T}or$. So $(\bigoplus_{i \in J} M_i)^{++} \cong (\prod_{i \in J} M_i^+)^+$ is in $\mathfrak{F}^{-1}(U)$ by the preceding paragraph. But $\bigoplus_{i \in J} M_i^+$ is a pure submodule of $\prod_{i \in J} M_i^+$ by [12, Example 4.84(d)], hence $(\prod_{i \in J} M_i^+)^+ \to (\bigoplus_{i \in J} M_i^+)^+ \to 0$ is a splitting epimorphism. Therefore $(\bigoplus_{i \in J} M_i^+)^+ \cong \prod_{i \in J} M_i^{++}$ is in $\mathfrak{F}^{-1}(U)$. Since $\prod_{i \in J} M_i$ is a pure submodule of $\prod_{i \in J} M_i^{++}$ and $\mathfrak{F}^{-1}(U)$ is closed under pure submodules, $\prod_{i \in J} M_i$ is in $\mathfrak{F}^{-1}(U)$. □

R is called a right coherent (respectively, P-coherent) ring if every finitely generated (respectively, principal) right ideal is finitely presented ([14]).

Corollary 3. *R is right coherent(respectively, P-coherent) ring if and only if $\mathfrak{F}^{-1}(U)$ is closed under direct products for every finitely presented (respectively, cyclically presented) module U.*

3. RD-Flat Modules Having a Restricted Subflat Domain

In this section, we study existence of test modules for torsion-freeness. If U is RD-flat and N is torsion-free left R-module, then U is N-subflat. The next proposition shows that the subflat domain of any RD-flat module must contain at least the torsion-free modules. The following fact can be easily verified.

Proposition 1. *${}_R\mathcal{TF} = \bigcap_{M\in\Omega} \mathfrak{F}^{-1}(M)$, where Ω is the class of all RD-flat modules.*

Definition 1. *An RD-flat module K is called tf-test module if $\mathfrak{F}^{-1}(K) = \mathcal{TF}$, i.e. $\mathbf{T}or(K, X) \neq 0$ for every non-torsion-free left module X.*

Set $\mathfrak{CP} := \oplus_{C_i\in\Gamma} C_i$, where Γ is a set of representatives for cyclically presented right R-modules. Clearly, $\mathfrak{CP}$ is an RD-flat module.

Proposition 2. *$\mathfrak{CP}$ is a tf-test module.*

Proof. Let $U \in R - Mod$. Assume that $\mathbf{T}or_1^R(\mathfrak{CP}, U) = 0$. Since $\mathbf{T}or_1^R(\mathfrak{CP}, U) \cong \oplus_{C_i\in\Gamma}\mathbf{T}or_1^R(C_i, U)$, $\mathbf{T}or_1^R(C_i, U) = 0$ for each $C_i \in \Gamma$. This means that U is torsion-free. □

By Lemma 1 and Proposition 2, we get:

Corollary 4. *Any pure extension of the module $\mathfrak{CP}$ is a tf- test module.*

By Proposition 2 and Lemma 2, we get:

Corollary 5. *If $wD(R) \leq 1$, then $E(\mathfrak{CP})$ is a tf- test module.*

Remark 1. *Let K be a finitely presented module and $F_0 \to F_1 \to K \to 0$ be a minimal free resolution of K. The transpose of K, denoted by $Tr(K)$, is defined as the cokernel of dual map $Hom_R(F_1, R) \to Hom_R(F_0, R)$. The isomorphism classes of $Tr(K)$ do not depend on our choice of the minimal resolution. $Tr(K)$ is a finitely presented left R-module. ([3, 16]).*

A module K is said to be U-subprojective if the map $Hom_R(K, P) \to Hom_R(K, U)$ is an epimorphism for every epimorphism $P \to U$. The family of all modules U such that K is U-subprojective is called the subprojectivity domain of K, and is denoted by $\underline{\mathfrak{Pr}}^{-1}(K)$ ([11]). [16, Theorem 8.3] presents a double-sided path between subprojectivity domain and subflat domain.

Corollary 6. *For a finitely presented module K, $\underline{\mathfrak{Pr}}^{-1}(K) = \mathfrak{F}^{-1}(Tr(K))$ and $\underline{\mathfrak{Pr}}^{-1}(Tr(K)) = \mathfrak{F}^{-1}(K)$.*

Corollary 7. *For a finitely presented module K, the following are hold.*

(1) *K is RD-flat if and only if $Tr(K)$ is RD-projective module.*
(2) *$Tr(K)$ is RD-flat if and only if K is RD-projective module.*

By Corollary 6 and Corollary 7, we have the following.

Corollary 8. *A finitely presented RD-flat module U is tf-test if and only if* $\mathcal{TF} = \underline{\mathfrak{Pr}}^{-1}(Tr(U))$.

Lemma 3. *If an RD-flat module U is tf-test, then $Hom_R(C,U) \neq 0$ for each nonprojective finitely presented RD-flat module C.*

Proof. Assume contrarily that $Hom_R(C,U) = 0$ for some nonprojective finitely presented RD-flat module C. Given a short exact sequence $0 \to F_0 \to F_1 \to U \to 0$ where F_1 is projective, we have $0 \to Hom_R(C,F_0) \to Hom_R(C,F_1) \to Hom_R(C,U) = 0$. Then, by [16, Theorem 8.3], $0 \to F_0 \otimes Tr(C) \to F_1 \otimes Tr(C) \to U \otimes Tr(C) \to 0$ is exact, and hence $\mathbf{T}or(U,Tr(C)) = 0$. Since U is tf-test, $Tr(C)$ is torsion-free. But $Tr(C)$ is RD-flat, and so it is flat by [13, Corollary 2.5]. Again by [16, Theorem 8.3], C is projective. This contradicts with our hypothesis. Therefore, $Hom_R(C,U) \neq 0$. □

Author Contribution Statements The authors contributed equally to this article.

Declaration of Competing Interests The authors declare that they have no competing interest.

Acknowledgements This work was supported by the Scientific and Technological Research Council of Turkey (TUBITAK) (Project number: 119F176). The authors are deeply grateful to the referees for their careful reading of the paper and valuable suggestions.

References

[1] Alahmadi, A. N., Alkan, M., López-Permouth, S. R., Poor modules: The opposite of injectivity, *Glasgow Math. J.*, 52 (2010), 7-17. https://doi.org/10.1017/S001708951000025X

[2] Alizade, R., Durğun, Y., Test modules for flatness,*Rend. Semin. Mat. Univ. Padova*, 137 (2017), 75-91. https://doi.org/10.4171/RSMUP/137-4

[3] Auslander, M., Bridger, M., Stable Module Theory, American Mathematical Society, Providence, 1969.

[4] Büyükaşık, E., Enochs, E., Rozas, J. R. G., Kafkas-Demirci, G., Rugged modules: The opposite of flatness, *Comm. Algebra*, 137 (2018), 764-779. https://doi.org/10.1080/00927872.2017.1327066

[5] Couchot, F., RD-flatness and RD-injectivity, *Comm. Algebra*, 34(10) (2006), 3675–3689. https://doi.org/10.1080/00927870600860817,

[6] Dauns, J., Fuchs, L., Torsion-freeness for rings with zero divisor, *J. Algebra Appl.*, 3(3) (2004), 221–237. https://doi.org/10.1142/S0219498804000885

[7] Eklof, P. C., Trlifaj, J., How to make Ext vanish, *Bull. London Math. Soc.*, 33(1) (2001), 41-51. https://doi.org/10.1112/blms/33.1.41

[8] Enochs, E. E., Jenda, O. M. G., Relative Homological Algebra, Walter de Gruyter & Co., Berlin, 2000.

[9] Hattori, A., A foundation of torsion theory for modules over general rings, *Nagoya Math. J.*, 17 (1960), 147–158. http://projecteuclid.org/euclid.nmj/1118800457

[10] Holston, C., López-Permouth, S. R., Ertaş, N. O., Rings whose modules have maximal or minimal projectivity domain, *J. Pure Appl. Algebra*, 216(3) (2012), 673–678. https://doi.org/10.1016/j.jpaa.2011.08.002

[11] Holston, C., López-Permouth, S. R., Mastromatteo, J., Simental-Rodriguez, J. E., An alternative perspective on projectivity of modules, *Glasgow Math. J.*, 57(1) (2015), 83–99. https://doi.org/10.1017/S0017089514000135

[12] Lam, T. Y., Lectures on Modules and Rings, Springer-Verlag, New York, 1999.

[13] Mao, L., Properties of *RD*-projective and *RD*-injective modules, *Turkish J. Math.*, 35(2) (2011), 187–205. https://doi.org/10.3906/mat-0904-53

[14] Mao, L., Ding, N., On divisible and torsionfree modules, *Comm. Algebra*, 36(2) (2008), 708–731. https://doi.org/10.1080/00927870701724201

[15] Rotman, J., An Introduction to Homological Algebra, Academic Press, New York, 1979.

[16] Skljarenko, E. G., Relative homological algebra in the category of modules, *Uspehi Mat. Nauk*, 33(3) (1978), 85120.

[17] Stenström, B.T., Pure submodules, *Arkiv für Matematik*, 7(2) (1967), 159–171. https://doi.org/10.1007/BF02591032

[18] Trlifaj, J., Whitehead test modules, *Trans. Amer. Math. Soc.*, 348(4) (1996) 1521–1554. https://doi.org/10.1090/S0002-9947-96-01494-8

[19] Warfield, R. B., Purity and algebraic compactness for modules, *Pacific J. Math.*, 28 (1969) 699–719. http://projecteuclid.org/euclid.pjm/1102983324

http://communications.science.ankara.edu.tr

Commun.Fac.Sci.Univ.Ank.Ser. A1 Math. Stat.
Volume 72, Number 3, Pages 570–586 (2023)
DOI:10.31801/cfsuasmas.1211661
ISSN 1303-5991 E-ISSN 2618-6470

Research Article; Received: November 29, 2022; Accepted: March 25, 2023

RANDOM FIXED POINT RESULTS FOR GENERALIZED ASYMPTOTICALLY NONEXPANSIVE RANDOM OPERATORS

Isa YILDIRIM[1] and Muhammed Emin BATUHAN[2]

[1]Department of Mathematics, Faculty of Science, Atatürk University, 25240 Erzurum, TÜRKİYE
[2]Graduate School of Natural and Applied Sciences, Atatürk University, 25240 Erzurum, TÜRKİYE

Abstract. In this paper, we define an implicit random iterative process with errors for three finite families of generalized asymptotically nonexpansive random operators. We also prove some convergence theorems using this iteration method in separable Banach spaces.

1. Introduction and Preliminaries

Random analysis is one of the most important areas of mathematics. Particularly, random techniques have a very common use in pure and applied mathematics. Hans [9] and Spacek [17] proved random fixed point results for random contraction mappings on separable metric spaces. Later, many authors have worked on it using different operator classes and different spaces. Some of them are given in these references [1], [3], [4], [10], [11], [12] and [13].

Let $(\mho, \Sigma)$ be a measurable space and $\mathfrak{X}$ be a real Banach space. Assume that E is an operator from $\mho \times \mathfrak{X}$ to $\mathfrak{X}$. Here, the m-th iterate $E(\ell, E(\ell, \ldots, E(\ell, u_0)))$ of E is denoted by as $E^m(\ell, u_0)$.

Definition 1. *Let f be a mapping on $\mho$. If for any Borel subset $\mathfrak{X} \subset \mathbb{R}$ the set $f^{-1}(\mathfrak{X})$ is measurable, the mapping f is called measurable.*

Definition 2. *Let E be an operator from $\mho \times \mathfrak{X}$ to $\mathfrak{X}$. If $E(\cdot, u_0) : \mho \to \mathfrak{X}$ is measurable for every $u_0 \in \mathfrak{X}$, then it is called a random operator.*

2020 *Mathematics Subject Classification.* 47H09, 47H10.

Keywords. Generalized asymptotically nonexpansive random operators, measurable spaces, Banach spaces, condition(B^*), implicit random iteration.

[1] isayıldırım@atauni.edu.tr-Corresponding author; 0000-0001-6165-716X;
[2] emin.batuhan@gmail.com; 0000-0001-9318-4627.

Definition 3. *Let E be an operator from $\mho \times \mathfrak{X}$ to $\mathfrak{X}$. If $E(\ell, \cdot) : \mathfrak{X} \to \mathfrak{X}$ is continuous for each $\ell \in \mho$, it is continuous.*

Definition 4. *Let E be an operator from $\mho \times \mathfrak{X}$ to $\mathfrak{X}$. If $E(\ell, p(\ell)) = p(\ell), \forall \ell \in \mho$, p is called a random fixed point of the random operator E. Here, $p : \mho \to \mathfrak{X}$ is a measurable function. We denote by $RF(E)$ the set of random fixed points of E.*

Definition 5. ([2]) Let $\mathfrak{X}$ be a separable Banach space and Θ be a nonempty subset of $\mathfrak{X}$. Assume that $E : \mho \times \Theta \to \Theta$ is a random operator. Then E is called

(i) nonexpansive random operator if

$$\|E(\ell, u_0) - E(\ell, v_0)\| \leq \|u_0 - v_0\| \text{ for all } u_0, v_0 \in \Theta \text{ and for each } \ell \in \mho,$$

(ii) asymptotically nonexpansive random operator if there exists a sequence of measurable functions $r_m : \mho \to [1, \infty)$ with $\lim_{m\to\infty} r_m(\ell) = 1$ for each $\ell \in \mho$ such that

$$\|E^m(\ell, u_0) - E^m(\ell, v_0)\| \leq r_m(\ell)\|u_0 - v_0\|, \forall u_0, v_0 \in \Theta, m \in \mathbb{N},$$

(iii) asymptotically quasi-nonexpansive random operator if there exists a sequence of measurable functions $r_m : \mho \to [0, \infty)$ with $\lim_{m\to\infty} r_m(\ell) = 0, \forall \ell \in \mho$ such that

$$\|E^m(\ell, \eta(\ell)) - p(\ell)\| \leq (1 + r_m(\ell)) \|\eta(\ell) - p(\ell)\|,$$

where $p : \mho \to \Theta$ is a random fixed point of E and $\eta : \mho \to \Theta$ is a measurable mapping.

(iv) uniformly L-Lipschitzian random operator if for all $u_0, v_0 \in \Theta$ and for all $\ell \in \mho$

$$\|E^m(\ell, u_0) - E^m(\ell, v_0)\| \leq L\|u_0 - v_0\|,$$

where, $m \geq 1$ and $L > 0$.

(v) semi-compact random operator if for a sequence of measurable mappings $\{\varrho_m\}$ from $\mho$ to Θ, with $\lim_{m\to\infty} \|\varrho_m(\ell) - E(\ell, \varrho_m(\ell))\| = 0$ for all $\ell \in \mho$, we have a subsequence $\{\varrho_{m_k}\}$ of $\{\varrho_m\}$ such that $\varrho_{m_k}(\ell) \to \varrho(\ell)$ for each $\ell \in \mho$, where ϱ is a measurable mapping from $\mho$ to Θ.

In 1995, Choudhury gave the random Ishikawa iteration method and he proved some random fixed point theorems using this method in Hilbert spaces. Thus he contributed to the development of random iteration schemes. Later, some authors introduced different iteration methods for random fixed points of different operator classes ([2], [5], [6], [7], [8], [14], [15]). In 2005, Beg and Abbas [2] introduced the following implicit iteration process for weakly contractive and asymptotically nonexpansive random operators in Banach spaces. They also showed that this iteration method converges to the common random fixed point of a finite family of asymptotically quasi-nonexpansive random operators in Banach spaces.

Throughout the rest of this paper, I denote the set of the first $\aleph$ natural numbers, that is, $I = \{1, 2, \ldots, \aleph\}$. Also, $F = \bigcap_{i=1}^{\aleph} [RF(\mathcal{S}_i) \cap RF(E_i) \cap RF(\mathcal{K}_i)]$ shows the set of common fixed points of three finite families of mappings $\{\mathcal{S}_i : i \in I\}$, $\{E_i : i \in I\}$ and $\{\mathcal{K}_i : i \in I\}$.

Let $E_i : \mho \times \Theta \to \Theta$ be a finite family of random operators and $\varrho_0 : \mho \to \Theta$ be any measurable function. Let us define the sequence of functions $\{\varrho_m\}$ as follows:

$$\varrho_m(\ell) = \alpha_m \varrho_{m-1}(\ell) + (1-\alpha_m) E_{i(m)}^{k(m)}(\ell, \varrho_m(\ell)) \tag{1}$$

where $m = (k-1)\aleph + i$.

In 2007, Plubtieng et al. [14] introduced the following implicit iteration method and they obtained some convergence results for a common random fixed point of a finite family of asymptotically quasi-nonexpansive random operators under some conditions in uniformly convex separable Banach spaces.

Let $E_i : \mho \times \Theta \to \Theta$ be a finite family of random operators and $\varrho_0 : \mho \to \Theta$ be any measurable function. Also, let's assume that the sequence $\{f_m\}$ consists of measurable mappings from $\mho$ to Θ. For all $m \geq 1$ and $\forall \ell \in \mho$,

$$\varrho_m(\ell) = \alpha_m \varrho_{m-1}(\ell) + (1-\alpha_m) E_{i(m)}^{k(m)}(\ell, \varrho_m(\ell)) + f_m(\ell)$$

where $m = (k-1)\aleph + i$ and each $\{f_m(\ell)\}$ is summable sequence in Θ, that is, the series $\sum_{m=1}^{\infty} \|f_m(\ell)\|$ is convergent.

Afterwards, Banerjee and Choudhury [1] constructed an implicit random iterative process with errors for a finite family of asymptotically nonexpansive random operators in real Banach space. They also proved that this process converges to the common random fixed point of such operators in the setting of uniformly convex Banach spaces. Their iteration process is as follows:

Let $E_i : \mho \times \Theta \to \Theta$ be a finite family of random operators and $\varrho_0 : \mho \to \Theta$ be a measurable function. For all $m \geq 1$ and $\forall \ell \in \mho$,

$$\begin{aligned} \varrho_m(\ell) &= \alpha_m \varrho_{m-1}(\ell) + \beta_m E_{i(m)}^{k(m)}(\ell, \eta_m(\ell)) + \gamma_m f_m(\ell) \\ \eta_m(\ell) &= a_m \varrho_m(\ell) + b_m E_{i(m)}^{k(m)}(\ell, \varrho_m(\ell)) + c_m g_m(\ell), \end{aligned} \tag{2}$$

where $\{\alpha_m\}, \{\beta_m\}, \{\gamma_m\}, \{a_m\}, \{b_m\}, \{c_m\}$ are sequences in $[0,1]$ with $\alpha_m + \beta_m + \gamma_m = a_m + b_m + c_m = 1$ and $\{f_m\}, \{g_m\}$ are bounded sequences of measurable functions from $\mho$ to Θ.

Based on the above studies, we first present the idea of the generalized asymptotically nonexpansive random operators. We also give an implicit iteration method using three finite families of these operator classes. Then, we obtain some convergence results using this iteration process.

Definition 6. *Let $\mathfrak{X}$ be a separable Banach space and Θ be a nonempty subset of $\mathfrak{X}$. Also, let's assume that $E : \mho \times \Theta \to \Theta$ is a random operator. Then E is said to be a generalized asymptotically nonexpansive random operator if there exist two sequences of measurable functions $\mu_m(\ell) : \mho \to [0,\infty)$, $\nu_m(\ell) : \mho \to [0,\infty)$ with $\lim_{m\to\infty} \mu_m(\ell) = 0$ and $\lim_{m\to\infty} \nu_m(\ell) = 0$ for each $\ell \in \mho$ such that*

$$\|E^m(\ell, u_0) - E^m(\ell, \upsilon_0)\| \leq \|u_0 - \upsilon_0\| + \mu_m(\ell)\|u_0 - \upsilon_0\| + \nu_m(\ell)$$

for all $u_0, \upsilon_0 \in \Theta$ and for each $\ell \in \mho$.

Remark 1. *From above definitions, we can see that every asymptotically nonexpansive random operator is generalized asymptotically nonexpansive random operator. But, its converse is not true in general. We know also that every asymptotically nonexpansive random operator with $RF(T) \neq \emptyset$ is asymptotically quasi-nonexpansive random operator and every asymptotically nonexpansive and asymptotically quasi-nonexpansive random operator is uniformly L-Lipschitzian random operator.*

Definition 7. *Let $\mathfrak{X}$ be a separable Banach space and Θ be a nonempty subset of $\mathfrak{X}$ and $\mathcal{S}_i, E_i, \mathcal{K}_i : \mho \times \Theta \to \Theta$ be three finite families of random operators. Also, suppose that $\varrho_0 : \mho \to \Theta$ is a measurable function.*

Then our iteration method with errors is defined as follows:

$$\begin{cases} \varrho_1(\ell) = \alpha_1 \mathcal{S}_1(\ell, \varrho_0(\ell)) + \beta_1 E_1\left(\ell, a_1\varrho_1(\ell) + b_1\mathcal{K}_1\left(\ell, \varrho_1(\ell)\right) + c_1 g_1(\ell)\right) \\ \qquad +\gamma_1 f_1(\ell) \\ \varrho_2(\ell) = \alpha_2 \mathcal{S}_2(\ell, \varrho_1(\ell)) + \beta_2 E_2\left(\ell, a_2\varrho_2(\ell) + b_2\mathcal{K}_2\left(\ell, \varrho_2(\ell)\right) + c_2 g_2(\ell)\right) \\ \qquad +\gamma_2 f_2(\ell) \\ \ldots \\ \varrho_{\aleph}(\ell) = \alpha_{\aleph} \mathcal{S}_{\aleph}(\ell, \varrho_{\aleph-1}(\ell)) + \beta_{\aleph} E_{\aleph}(\ell, a_{\aleph}\varrho_{\aleph}(\ell) + b_{\aleph}\mathcal{K}_{\aleph}\left(\ell, \varrho_{\aleph}(\ell)\right) \\ \qquad +c_{\aleph} g_{\aleph}(\ell)) + \gamma_{\aleph} f_{\aleph}(\ell) \\ \varrho_{\aleph+1}(\ell) = \alpha_{\aleph+1} \mathcal{S}_{\aleph+1}(\ell, \varrho_{\aleph}(\ell)) + \beta_{\aleph+1} E_1^2(\ell, a_{\aleph+1}\varrho_{\aleph+1}(\ell) \\ \qquad\quad +b_{\aleph+1}\mathcal{K}_1^2\left(\ell, \varrho_{\aleph+1}(\ell)\right) + c_{\aleph+1} g_{\aleph+1}(\ell)) + \gamma_{\aleph+1} f_{\aleph+1}(\ell) \\ \ldots \\ \varrho_{\aleph}(\ell) = \alpha_{2\aleph} \mathcal{S}_{2\aleph}(\ell, \varrho_{2\aleph-1}(\ell)) + \beta_{2\aleph} E_{\aleph}^2(\ell, a_{2\aleph}\varrho_{2\aleph}(\ell) \\ \qquad +b_{2\aleph}\mathcal{K}_{\aleph}^2\left(\ell, \varrho_{\aleph}(\ell)\right) + c_{2\aleph} g_{2\aleph}(\ell)) + \gamma_{2\aleph} f_{\aleph}(\ell) \\ \varrho_{2\aleph+1}(\ell) = \alpha_{2\aleph+1} \mathcal{S}_{2\aleph+1}(\ell, \varrho_{2\aleph}(\ell)) + \beta_{2\aleph+1} E_1^3(\ell, a_{2\aleph+1}\varrho_{2\aleph+1}(\ell) \\ \qquad\quad +b_{2\aleph+1}\mathcal{K}_1^3\left(\ell, \varrho_{2\aleph+1}(\ell)\right) + c_{2\aleph+1} g_{2\aleph+1}(\ell)) + \gamma_{2\aleph+1} f_{2\aleph+1}(\ell) \\ \ldots \end{cases}$$

We can write compact form of above iteration as follows:

$$\begin{cases} \varrho_m(\ell) = \alpha_m \mathcal{S}_{i(m)}^{k(m)}(\ell, \varrho_{m-1}(\ell)) + \beta_m E_{i(m)}^{k(m)}\left(\ell, \eta_m(\ell)\right) + \gamma_m f_m(\ell) \\ \eta_m(\ell) = a_m \varrho_m(\ell) + b_m \mathcal{K}_{i(m)}^{k(m)}\left(\ell, \varrho_m(\ell)\right) + c_m g_m(\ell), \quad m \geq 1, \quad \forall \ell \in \mho \end{cases} \tag{3}$$

where $\{\alpha_m\}, \{\beta_m\}, \{\gamma_m\}, \{a_m\}, \{b_m\}, \{c_m\}$ are sequences in $[0,1]$ with $\alpha_m + \beta_m + \gamma_m = a_m + b_m + c_m = 1$ and $\{f_m\}, \{g_m\}$ are bounded sequences of measurable functions from $\mho$ to Θ.

Lemma 1. ([18]) Let $\{\mu_m\}, \{v_m\}$ and $\{\delta_m\}$ be sequences of nonnegative real numbers such that

$$\mu_{m+1} \leq (1 + \delta_m)\,\mu_m + v_m.$$

If $\sum \delta_m < \infty$ and $\sum v_m < \infty$, then

(i) $\lim_{m\to\infty} \mu_m$ exists,
(ii) $\lim_{m\to\infty} \mu_m = 0$ whenever $\liminf_{m\to\infty} \mu_m = 0$.

Lemma 2. ([16]) Let $\mathfrak{X}$ be a uniformly convex Banach space and $\{u_{0m}\}$ and $\{\upsilon_{0m}\}$ be two sequences in $\mathfrak{X}$ such that $\limsup_{m\to\infty}\|u_{0m}\|\leq r$, $\limsup_{m\to\infty}\|\upsilon_{0m}\|\leq r$ and $\lim_{m\to\infty}\|\ell_m u_{0m}+(1-\ell_m)\,\upsilon_{0m}\|=r$ satisfying for any $r\geq 0$. Also, let's assume that $0<p\leq \ell_m\leq q<1$. Then $\lim_{m\to\infty}\|u_{0m}-\upsilon_{0m}\|=0$.

2. Main results

Now, we will give some convergence theorems for generalized asymptotically nonexpansive random operators using our implicit random iteration scheme with errors.

Theorem 1. *Let $\mathfrak{X}$ be a separable Banach space and Θ be a nonempty closed convex subset of $\mathfrak{X}$. Let $\mathcal{S}_i, E_i, \mathcal{K}_i : \mho\times\Theta\to\Theta$ be generalized asymptotically nonexpansive random operators with the sequence of measurable mappings $\{r_{i_m}\}$: $\mho\to[1,\infty)$ satisfying $\sum_{m=1}^{\infty}(r_{i_m}(\ell)-1)<\infty$ for all $\ell\in\mho$ and for all $i\in I$. Suppose that $F\neq\emptyset$. Let the iteration $\{\varrho_m\}$ be defined by (3) with the additional assumption $0<\alpha\leq\alpha_m,\beta_m\leq\beta<1$ and $\sum_{m=1}^{\infty}\gamma_m<\infty,\sum_{m=1}^{\infty}c_m<\infty$. Then $\{\varrho_m\}$ converges strongly to a common random fixed point of the random operators $\mathcal{S}_i$,E_i and $\mathcal{K}_i$ if and only if for all $\ell\in\mho,\liminf_{m\to\infty}d(\varrho_m(\ell),F)=0$, where $d(\varrho_m(\ell),F)=\inf\{\|\varrho_m(\ell)-\varrho(\ell)\|:\varrho\in F\}$.*

Proof. Let ϱ be a fixed point, that is $\varrho\in F$. Since $\{f_m\}$ and $\{g_m\}$ are bounded sequences, we can write for each $\ell\in\mho$,

$$M(\ell)=\sup_{m\geq 1}\|f_m(\ell)-\varrho(\ell)\|\vee\sup_{m\geq 1}\|g_m(\ell)-\varrho(\ell)\|.$$

It is clear that $M(\ell)<\infty$ for each $\ell\in\mho$. Also assume that $r_m(\ell)=\{\max r_{i_m}(\ell): i=1,2,\ldots,\aleph\}$ for each $m\geq 1$. From the condition $\sum_{m=1}^{\infty}(r_{i_m}(\ell)-1)<\infty$ for each $\ell\in\mho$, we have that $\sum_{m=1}^{\infty}(r_m(\ell)-1)<\infty$. Using (3), we obtain that

$$\begin{aligned}
\|\eta_m(\ell)-\varrho(\ell)\| &= \left\|a_m\varrho_m(\ell)+b_m\mathcal{K}_{i(m)}^{k(m)}(\ell,\varrho_m(\ell))+c_m g_m(\ell)-\varrho(\ell)\right\| \qquad (4)\\
&\leq a_m\|\varrho_m(\ell)-\varrho(\ell)\|+b_m\left\|\mathcal{K}_{i(m)}^{k(m)}(\ell,\varrho_m(\ell))-\varrho(\ell)\right\|\\
&\quad +c_m\|g_m(\ell)-\varrho(\ell)\|\\
&\leq a_m\|\varrho_m(\ell)-\varrho(\ell)\|+b_m r_{k(m)}(\ell)\|\varrho_m(\ell)-\varrho(\ell)\|\\
&\quad +b_m v_m(\ell)+c_m M(\ell)\\
&= a_m\|\varrho_m(\ell)-\varrho(\ell)\|+b_m(1+\mu_m(\ell))\|\varrho_m(\ell)-\varrho(\ell)\|\\
&\quad +b_m v_m(\ell)+c_m M(\ell),\\
&\leq (1+\mu_m(\ell))\|\varrho_m(\ell)-\varrho(\ell)\|+b_m v_m(\ell)+c_m M(\ell).
\end{aligned}$$

where $\mu_m(\ell)=r_{k(m)}(\ell)-1$.Also,

$$\begin{aligned}
\|\varrho_m(\ell)-\varrho(\ell)\| &= \left\|\alpha_m\mathcal{S}_{i(m)}^{k(m)}(\ell,\varrho_{m-1}(\ell)+\beta_m E_{i(m)}^{k(m)}(\ell,\eta_m(\ell))+\gamma_m f_m(\ell)-\varrho(\ell)\right\|\\
&\leq \alpha_m\left\|\mathcal{S}_{i(m)}^{k(m)}(\ell,\varrho_{m-1}(\ell)-\varrho(\ell)\right\|+\beta_m\left\|E_{i(m)}^{k(m)}(\ell,\eta_m(\ell))-\varrho(\ell)\right\|
\end{aligned}$$

$$
\begin{aligned}
& +\gamma_m \|f_m(\ell) - \varrho(\ell)\| \\
\leq\ & \alpha_m r_{k(m)}(\ell) \left\|\varrho_{m-1}(\ell) - \varrho(\ell)\right\| + \alpha_m v_m(\ell) \\
& +\beta_m r_{k(m)}(\ell) \|\eta_m(\ell) - \varrho(\ell)\| + \gamma_m M(\ell) + \beta_m v_m(\ell) \\
\leq\ & \alpha_m (1 + \mu_m(\ell)) \left\|\varrho_{m-1}(\ell) - \varrho(\ell)\right\| \\
& +\beta_m (1 + \mu_m(\ell)) [(1 + \mu_m(\ell)) \|\varrho_m(\ell) - \varrho(\ell)\| + c_m M(\ell)] \\
& +\alpha_m v_m(\ell) + \beta_m v_m(\ell) + \gamma_m M(\ell) \\
=\ & \alpha_m (1 + \mu_m(\ell)) \left\|\varrho_{m-1}(\ell) - \varrho(\ell)\right\| \\
& +\beta_m (1 + \mu_m(\ell))^2 \|\varrho_m(\ell) - \varrho(\ell)\| \\
& +\beta_m c_m (1 + \mu_m(\ell)) M(\ell) + \beta_m v_m(\ell) + \beta_m (1 + \mu_m(\ell)) b_m v_m(\ell) \\
& +\alpha_m v_m(\ell) + \gamma_m M(\ell) \\
\leq\ & \alpha_m (1 + \mu_m(\ell)) \left\|\varrho_{m-1}(\ell) - \varrho(\ell)\right\| \\
& + (1 - \alpha_m) (1 + p_m(\ell)) \|\varrho_m(\ell) - \varrho(\ell)\| \\
& + [\beta_m c_m (1 + \mu_m(\ell)) + \gamma_m] M(\ell) + \beta_m v_m(\ell) \\
& +\beta_m (1 + \mu_m(\ell)) b_m v_m(\ell) + \alpha_m v_m(\ell), \\
\leq\ & \alpha_m \left\|\varrho_{m-1}(\ell) - \varrho(\ell)\right\| + (1 - \alpha_m + p_m(\ell)) \|\varrho_m(\ell) - \varrho(\ell)\| \\
& + [\beta_m c_m (1 + \mu_m(\ell)) + \gamma_m] M(\ell) + \beta_m v_m(\ell) \\
& +\beta_m (1 + \mu_m(\ell)) b_m v_m(\ell) + \alpha_m v_m(\ell).
\end{aligned}
$$

where $p_m(\ell) = 2\mu_m(\ell) + \mu_m(\ell)^2$. This implies that

$$
\begin{aligned}
\|\varrho_m(\ell) - \varrho(\ell)\| \leq\ & \left\|\varrho_{m-1}(\ell) - \varrho(\ell)\right\| + \frac{p_m(\ell)}{\alpha_m} \|\varrho_m(\ell) - \varrho(\ell)\| \\
& + \frac{\beta_m c_m (1 + \mu_m(\ell)) + \gamma_m}{\alpha_m} M(\ell) + v_m(\ell) \\
& + \frac{\beta_m v_m(\ell) + \beta_m (1 + \mu_m(\ell)) b_m v_m(\ell)}{\alpha_m} \\
\leq\ & \left\|\varrho_{m-1}(\ell) - \varrho(\ell)\right\| + \frac{p_m(\ell)}{\alpha} \|\varrho_m(\ell) - \varrho(\ell)\| \\
& + \frac{\beta_m c_m (1 + \mu_m(\ell)) + \gamma_m}{\alpha} M(\ell) + v_m(\ell) \\
& + \frac{\beta_m v_m(\ell) + \beta_m (1 + \mu_m(\ell)) b_m v_m(\ell)}{\alpha}
\end{aligned}
$$

and

$$
\|\varrho_m(\ell) - \varrho(\ell)\| \leq \frac{\alpha}{\alpha - p_m(\ell)} v_m(\ell) \left\|\varrho_{m-1}(\ell) - \varrho(\ell)\right\| \tag{5}
$$

$$+\left(\frac{\begin{array}{c}\beta_m c_m\left(1+\mu_m(\ell)\right)+\gamma_m+\beta_m v_m(\ell)\\+\beta_m\left(1+\mu_m(\ell)\right)b_m v_m(\ell)+v_m(\ell)\end{array}}{\alpha-p_m(\ell)}\right)M(\ell)$$

$$=\left(1+\frac{p_m(\ell)}{(\alpha-p_m(\ell))v_m(\ell)}\right)\left\|\varrho_{m-1}(\ell)-\varrho(\ell)\right\|$$

$$+\left(\frac{\begin{array}{c}\beta_m c_m\left(1+\mu_m(\ell)\right)+\gamma_m+\beta_m v_m(\ell)\\+\beta_m\left(1+\mu_m(\ell)\right)b_m v_m(\ell)+v_m(\ell)\end{array}}{\alpha-p_m(\ell)}\right)M(\ell).$$

From the condition $\sum_{m=1}^{\infty}\left(r_{k(m)}(\ell)-1\right)<\infty$ for each $\ell\in\mho$, we know that $\sum_{m=1}^{\infty}\mu_m(\ell)<\infty$ and hence $\sum_{m=1}^{\infty}p_m(\ell)<\infty$. So $\lim_{m\to\infty}p_m(\ell)=0$ for each $\ell\in\mho$. From the definition of generalized asymptotically nonexpansive random operator, we also have $\lim_{m\to\infty}v_m(\ell)=0$ for each $\ell\in\mho$. Then for $\ell\in\mho$, there exists $m_1\in\aleph$ such that $p_m(\ell)<\frac{\alpha}{2}$ for all $m\geq m_1$. Thus from (5) we have that, for all $m\geq m_1$

$$\begin{aligned}\left\|\varrho_m(\ell)-\varrho(\ell)\right\| &\leq \left(1+2\frac{p_m(\ell)}{\alpha v_m(\ell)}\right)\left(1+\mu_m(\ell)\right)\left\|\varrho_{m-1}(\ell)-\varrho(\ell)\right\| \\ &\quad+\left(\frac{\begin{array}{c}\beta_m c_m\left(1+\mu_m(\ell)\right)+\gamma_m+\beta_m v_m(\ell)\\+\beta_m\left(1+\mu_m(\ell)\right)b_m v_m(\ell)+v_m(\ell)\end{array}}{\alpha}\right)2M(\ell) \\ &= \left(1+\lambda_m(\ell)\right)\left\|\varrho_{m-1}(\ell)-\varrho(\ell)\right\|+\sigma_m(\ell),\end{aligned} \tag{6}$$

where

$$\lambda_m(\ell)=2\frac{p_m(\ell)}{\alpha v_m(\ell)}\left(1+\mu_m(\ell)\right)+\mu_m(\ell)$$

and

$$\sigma_m(\ell)=\frac{\beta_m c_m\left(1+\mu_m(\ell)\right)+\gamma_m+\beta_m v_m(\ell)+\beta_m\left(1+\mu_m(\ell)\right)b_m v_m(\ell)+v_m(\ell)}{\alpha}2M(\ell).$$

Therefore $\sum_{m=1}^{\infty}\lambda_m(\ell)<\infty$ and $\sum_{m=1}^{\infty}\sigma_m(\ell)<\infty$. This implies that

$$d\left(\varrho_m(\ell),F\right)\leq 1+\lambda_m(\ell)d\left(\varrho_{m-1}(\ell),F\right)+\sigma_m(\ell).$$

Using Lemma 2, we obtain that $\lim_{m\to\infty}d\left(\varrho_m(\ell),F\right)$ exists for each $\ell\in\mho$. Moreover, from the condition of the theorem we have for all $\ell\in\mho$,

$$\lim_{m\to\infty}d\left(\varrho_m(\ell),F\right)=0.$$

We can see that the sequence $\{\varrho_m(\ell)\}$ is a Cauchy sequence for each $\ell\in\mho$ using a similar method as in [2]. Therefore $\varrho_m(\ell)\to p(\ell)$ as $m\to\infty$ for each $\ell\in\mho$, where $p:\mho\to F$. Next, we will prove that $p\in F$. Since for each $\ell\in\mho$, $\varrho_m(\ell)\to p(\ell)$ as $m\to\infty$ there exists $m_3\in\aleph$ such that $\left\|\varrho_m(\ell)-p(\ell)\right\|<\frac{\epsilon}{3(1+r_1(\ell))}$ for all

$m \geq m_3$. Since $\lim_{m\to\infty} d(\varrho_m(\ell), F) = 0$ for each $\ell \in \mho$, there exists $m_4 \in \aleph$ such that $d(\varrho_m(\ell), F) < \frac{\epsilon}{3(1+r_1(\ell))}$ for all $m \geq m_4$. So there exists $\varrho^* \in F$ such that $\|\varrho_m(\ell) - \varrho^*(\ell)\| \leq \frac{\epsilon(\ell))}{3(1+r_1(\ell))}$ for all $m \geq m_4$. Since $\lim_{m\to\infty} \nu_m(\ell) = 0$ for each $\ell \in \mho$, there exists $m_5 \in \aleph$ such that $v_m(\ell) < \frac{\epsilon}{3(1+r_1(\ell))}$ for all $m \geq m_5$. Let $m_6 = \max\{m_3, m_4, m_5\}$. Now for all $l \in I$ and for all $m \geq m_6$

$$\begin{aligned}
\|\mathcal{S}_l(\ell, p(\ell)) - p(\ell)\| &\leq \|\mathcal{S}_l(\ell, p(\ell)) - \varrho^*(\ell)\| + \|\varrho^*(\ell) - p(\ell)\| \\
&\leq \|\mathcal{S}_l(\ell, p(\ell)) - \mathcal{S}_l(\ell, \varrho^*(\ell))\| + \|\varrho^*(\ell) - p(\ell)\| \\
&\leq r_1(\ell)\|\varrho^*(\ell) - p(\ell)\| + v_1(\ell) + \|\varrho^*(\ell) - p(\ell)\| \\
&= (1 + r_1(\ell))\|\varrho^*(\ell) - p(\ell)\| + v_1(\ell) \\
&\leq (1 + r_1(\ell))\|\varrho^*(\ell) - \varrho_m(\ell)\| + (1 + r_1(\ell))\|\varrho_m(\ell) - p(\ell)\| \\
&\quad + (1 + r_1(\ell))\, v_1(\ell) \\
&< (1 + r_1(\ell))\frac{\epsilon}{3(1 + r_1(\ell))} + (1 + r_1(\ell))\frac{\epsilon}{3(1 + r_1(\ell))} \\
&\quad + (1 + r_1(\ell))\frac{\epsilon}{3(1 + r_1(\ell))} \\
&= \epsilon
\end{aligned}$$

which implies that $\mathcal{S}_l(\ell, p(\ell)) = p(\ell)$ for all $l \in I$ and for each $\ell \in \mho$. Similarly, we can show that $E_l(\ell, p(\ell)) = p(\ell)$ and $\mathcal{K}_l(\ell, p(\ell)) = p(\ell)$ for all $l \in I$ and for each $\ell \in \mho$. Therefore, we can say that $p \in F$. That is, $\{\varrho_m\}$ converges strongly to a common random fixed point of $\mathcal{S}_i$, E_i and $\mathcal{K}_i$. □

Lemma 3. *Let $\mathfrak{X}$ be a uniformly convex separable Banach space and Θ be a nonempty closed convex subset of $\mathfrak{X}$. Let $\mathcal{S}_i, E_i, \mathcal{K}_i : \mho \times \Theta \to \Theta$ be uniformly L-Lipschitzian generalized asymptotically nonexpansive random operators with the sequence of measurable mappings $\{r_{i_m}\} : \mho \to [1, \infty)$ satisfying $\sum_{m=1}^{\infty}(r_{i_m}(\ell) - 1) < \infty$ for each $\ell \in \mho$ and for all $i \in I$. Suppose that $F \neq \emptyset$. Let the iteration $\{\varrho_m\}$ be defined by (3) with the additional assumption $0 < \alpha \leq \alpha_m, \beta_m \leq \beta < 1$ and $\sum_{m=1}^{\infty}\gamma_m < \infty, \sum_{m=1}^{\infty} c_m < \infty$. Then*

$$\lim_{m\to\infty}\|\varrho_m(\ell) - \mathcal{S}_l(\ell, \varrho_m(\ell))\| = 0\ ,\ \lim_{m\to\infty}\|\varrho_m(\ell) - E_l(\ell, \varrho_m(\ell))\| = 0$$

and

$$\lim_{m\to\infty}\|\varrho_m(\ell) - \mathcal{K}_l(\ell, \varrho_m(\ell))\| = 0$$

for each $\ell \in \mho$ and for all $l = 1, 2, \ldots, \aleph$.

Proof. Let $\varrho \in F$ be arbitrary. Since $\{f_m\}, \{g_m\}$ are bounded sequences of measurable functions from $\mho$ to Θ, so we can write as follows,

$$M(\ell) = \sup_{m\geq 1}\|f_m(\ell) - \varrho(\ell)\| \vee \sup_{m\geq 1}\|g_m(\ell) - \varrho(\ell)\|.$$

From above the equality, we have $M(\ell) < \infty$ for each $\ell \in \mho$. Assume that $r_m(\ell) = \{\max r_{i_m}(\ell) : i = 1, 2, \ldots, \aleph\}$ for each $m \geq 1$. This implies that $\sum_{m=1}^{\infty}(r_m(\ell) - 1) <$

∞ for each $\ell \in \mho$. Using (6) we know that

$$\|\varrho_m(\ell) - \varrho(\ell)\| \leq (1 + \lambda_m(\ell)) \left\|\varrho_{m-1}(\ell) - \varrho(\ell)\right\| + \sigma_m(\ell),$$

where $\sum_{m=1}^{\infty} \lambda_m(\ell) < \infty$ and $\sum_{m=1}^{\infty} \sigma_m(\ell) < \infty$. From Lemma 1, we obtain that $\lim_{m\to\infty} \|\varrho_m(\ell) - \varrho(\ell)\|$ exists for all $\varrho \in F$ and for each $\ell \in \mho$. We suppose that $\lim_{m\to\infty} \|\varrho_m(\ell) - \varrho(\ell)\| = a_\ell$. From (4), we have that

$$\|\eta_m(\ell) - \varrho(\ell)\| \leq (1 + \mu_m(\ell)) \|\varrho_m(\ell) - \varrho(\ell)\| + b_m v_m(\ell) + c_m M(\ell).$$

From the above inequality, we obtain that

$$\limsup_{m\to\infty} \|\eta_m(\ell) - \varrho(\ell)\| \leq a_\ell \text{ for each } \ell \in \mho. \tag{7}$$

Also

$$\begin{aligned} a_\ell &= \lim_{m\to\infty} \|\varrho_m(\ell) - \varrho(\ell)\| \qquad (8) \\ &= \lim_{m\to\infty} \left\|\alpha_m \mathcal{S}_{i(m)}^{k(m)}(\ell, \varrho_{m-1}(\ell) + \beta_m E_{i(m)}^{k(m)}(\ell, \eta_m(\ell)) + \gamma_m f_m(\ell) - \varrho(\ell)\right\| \\ &= \lim_{m\to\infty} \left\| \begin{array}{c} (1-\beta_m)\left(\mathcal{S}_{i(m)}^{k(m)}(\ell, \varrho_{m-1}(\ell) - \varrho(\ell) + \gamma_m(f_m(\ell) - \mathcal{S}_{i(m)}^{k(m)}(\ell, \varrho_{m-1}(\ell)))\right) \\ +\beta_m \left(E_{i(m)}^{k(m)}(\ell, \eta_m(\ell)) - \varrho(\ell) + \gamma_m\left(f_m(\ell) - \mathcal{S}_{i(m)}^{k(m)}(\ell, \varrho_{m-1}(\ell))\right)\right) \end{array} \right\|. \end{aligned}$$

For all $\ell \in \mho$, we have

$$\begin{aligned} &\left\|\mathcal{S}_{i(m)}^{k(m)}(\ell, \varrho_{m-1}(\ell) - \varrho(\ell) + \gamma_m\left(f_m(\ell) - \mathcal{S}_{i(m)}^{k(m)}(\ell, \varrho_{m-1}(\ell))\right)\right\| \\ \leq\; &\left\|\mathcal{S}_{i(m)}^{k(m)}(\ell, \varrho_{m-1}(\ell)) - \varrho(\ell)\right\| + \gamma_m \left\|f_m(\ell) - \mathcal{S}_{i(m)}^{k(m)}(\ell, \varrho_{m-1}(\ell))\right\|. \end{aligned}$$

Taking limsup on the both sides of above inequality, we obtain that

$$\begin{aligned} &\limsup_{m\to\infty} \left\| \begin{array}{c} \mathcal{S}_{i(m)}^{k(m)}(\ell, \varrho_{m-1}(\ell)) - \varrho(\ell) \\ +\gamma_m\left(f_m(\ell) - \mathcal{S}_{i(m)}^{k(m)}(\ell, \varrho_{m-1}(\ell))\right) \end{array} \right\| \qquad (9) \\ \leq\; &\limsup_{m\to\infty} \left(\left\|\mathcal{S}_{i(m)}^{k(m)}(\ell, \varrho_{m-1}(\ell)) - \varrho(\ell)\right\| + \gamma_m \left\|f_m(\ell) - \mathcal{S}_{i(m)}^{k(m)}(\ell, \varrho_{m-1}(\ell))\right\|\right) \\ \leq\; &\limsup_{m\to\infty} \left(\begin{array}{c} (1+\mu_m(\ell)) \left\|\varrho_{m-1}(\ell) - \varrho(\ell)\right\| + v_m(\ell) \\ +\gamma_m \left\|f_m(\ell) - \mathcal{S}_{i(m)}^{k(m)}(\ell, \varrho_{m-1}(\ell))\right\| \end{array} \right) = a_\ell. \end{aligned}$$

Also, we can write the following inequality

$$\begin{aligned} &\left\|E_{i(m)}^{k(m)}(\ell, \eta_m(\ell)) - \varrho(\ell) + \gamma_m\left(f_m(\ell) - \mathcal{S}_{i(m)}^{k(m)}(\ell, \varrho_{m-1}(\ell))\right)\right\| \\ \leq\; &\left\|E_{i(m)}^{k(m)}(\ell, \eta_m(\ell)) - \varrho(\ell)\right\| + \gamma_m \left\|f_m(\ell) - \mathcal{S}_{i(m)}^{k(m)}(\ell, \varrho_{m-1}(\ell))\right\| \\ \leq\; &r_{k(m)}(\ell) \|\eta_m(\ell) - \varrho(\ell)\| + v_m(\ell) + \gamma_m r_{k(m)}(\ell) \left\|f_m(\ell) - \varrho_{m-1}(\ell)\right\| + v_m(\ell). \end{aligned}$$

Taking again limsup at the above inequality, we get

$$\limsup_{m\to\infty}\left\|\begin{array}{c} E_{i(m)}^{k(m)}(\ell,\eta_m(\ell))-\varrho(\ell) \\ +\gamma_m\left(f_m(\ell)-\mathcal{S}_{i(m)}^{k(m)}(\ell,\varrho_{m-1}(\ell))\right) \end{array}\right\| \tag{10}$$

$$\leq \limsup_{m\to\infty}\left(\begin{array}{c} (1+\mu_m(\ell))\left\|\eta_m(\ell)-\varrho(\ell)\right\| \\ +v_m(\ell)+\gamma_m\left\|\left(f_m(\ell)-\mathcal{S}_{i(m)}^{k(m)}(\ell,\varrho_{m-1}(\ell))\right)\right\| \end{array}\right)\leq a_\ell.$$

From (8),(9),(10) and Lemma 2, we obtain that

$$\lim_{m\to\infty}\left\|E_{i(m)}^{k(m)}(\ell,\eta_m(\ell))-\mathcal{S}_{i(m)}^{k(m)}(\ell,\varrho_{m-1}(\ell))\right\|=0 \tag{11}$$

for each $\ell\in\mho$. For each $\ell\in\mho$, we have

$$\begin{aligned} & \left\|\varrho_m(\ell)-\mathcal{S}_{i(m)}^{k(m)}(\ell,\varrho_{m-1}(\ell))\right\| \qquad (12)\\ = & \left\|\begin{array}{c} \alpha_m\mathcal{S}_{i(m)}^{k(m)}(\ell,\varrho_{m-1}(\ell))+\beta_m E_{i(m)}^{k(m)}(\ell,\eta_m(\ell)) \\ +\gamma_m f_m(\ell)-\mathcal{S}_{i(m)}^{k(m)}(\ell,\varrho_{m-1}(\ell)) \end{array}\right\| \\ \leq & \beta_m\left\|E_{i(m)}^{k(m)}(\ell,\eta_m(\ell))-\mathcal{S}_{i(m)}^{k(m)}(\ell,\varrho_{m-1}(\ell))\right\| \\ & +\gamma_m\left\|f_m(\ell)-\mathcal{S}_{i(m)}^{k(m)}(\ell,\varrho_{m-1}(\ell))\right\| \\ \to & \ 0 \text{ as } m\to\infty. \end{aligned}$$

Hence for each $\ell\in\mho$ and for all $l\in I$,

$$\lim_{m\to\infty}\left\|\varrho_m(\ell)-\mathcal{S}_{i(m)}^{k(m)}(\ell,\varrho_{m+l}(\ell))\right\|=0.$$

Since

$$\begin{aligned} \left\|\varrho_m(\ell)-E_{i(m)}^{k(m)}(\ell,\eta_m(\ell))\right\| \leq & \left\|\varrho_m(\ell)-\mathcal{S}_{i(m)}^{k(m)}(\ell,\varrho_{m-1}(\ell))\right\| \\ & +\left\|\mathcal{S}_{i(m)}^{k(m)}(\ell,\varrho_{m-1}(\ell))-E_{i(m)}^{k(m)}(\ell,\eta_m(\ell))\right\|, \end{aligned}$$

by using (11),(12), we obtain that

$$\lim_{m\to\infty}\left\|\varrho_m(\ell)-E_{i(m)}^{k(m)}(\ell,\eta_m(\ell))\right\|=0 \tag{13}$$

for each $\ell\in\mho$. We also have

$$\begin{aligned} & \left\|\eta_m(\ell)-\varrho(\ell)\right\| \\ = & \left\|a_m\varrho_m(\ell)+b_m\mathcal{K}_{i(m)}^{k(m)}(\ell,\varrho_m(\ell))+c_m g_m(\ell)-\varrho_m(\ell)\right\| \\ \leq & b_m\left\|\mathcal{K}_{i(m)}^{k(m)}(\ell,\varrho_m(\ell))-\varrho_m(\ell)\right\|+c_m\left\|g_m(\ell)-\varrho_m(\ell)\right\|. \end{aligned}$$

Using (7), we have that $\limsup_{m\to\infty}\left\|\eta_m(\ell)-\varrho(\ell)\right\|\leq a_\ell$ for each $\ell\in\mho$. Also, we have

$$\liminf_{m\to\infty}\left\|\eta_m(\ell)-\varrho(\ell)\right\| \leq \liminf_{m\to\infty}\alpha_m r_m(\ell)\left\|\varrho_{m-1}(\ell)-\varrho(\ell)\right\|$$

$$+\beta_m r_m(\ell)\|\eta_m(\ell)-\varrho(\ell)\|+\gamma_m\|f_m(\ell)-\varrho(\ell)\|$$

which implies that

$$a_\ell \le \alpha_m a_\ell + \beta_m \liminf_{m\to\infty}\|\eta_m(\ell)-\varrho_m(\ell)\|.$$

From above inequality,

$$\begin{aligned}\frac{(1-\alpha_m)a_\ell}{\beta_m} &\le \liminf_{m\to\infty}\|\eta_m(\ell)-\varrho_m(\ell)\| \\ a_\ell &\le \liminf_{m\to\infty}\|\eta_m(\ell)-\varrho_m(\ell)\|.\end{aligned}$$

Now

$$\begin{aligned} a_\ell &= \lim_{m\to\infty}\|\eta_m(\ell)-\varrho(\ell)\| \\ &= \lim_{m\to\infty}\left\|a_m\varrho_m(\ell)+b_m\mathcal{K}_{i(m)}^{k(m)}(\ell,\varrho_m(\ell))+c_m g_m(\ell)-\varrho(\ell)\right\| \\ &= \lim_{m\to\infty}\left\|\begin{array}{c}(1-b_m)\left[\varrho_m(\ell)-\varrho(\ell)+c_m g_m(\ell)-\varrho_m(\ell)\right] \\ +b_m\left[\mathcal{K}_{i(m)}^{k(m)}(\ell,\varrho_m(\ell))-\varrho(\ell)+c_m g_m(\ell)-\varrho_m(\ell)\right]\end{array}\right\|.\end{aligned}$$

So

$$\begin{aligned} &\limsup_{m\to\infty}\|\varrho_m(\ell)+\varrho(\ell)+c_m(g_m(\ell)-\varrho_m(\ell))\| \\ \le\; &\limsup_{m\to\infty}\|\varrho_m(\ell)+\varrho(\ell)\|+c_m\|(g_m(\ell)-\varrho_m(\ell))\| \\ \le\; &a_\ell\end{aligned}$$

and

$$\begin{aligned} &\limsup_{m\to\infty}\left\|\mathcal{K}_{i(m)}^{k(m)}(\ell,\varrho_m(\ell))-\varrho(\ell)+c_m g_m(\ell)-\varrho_m(\ell)\right\| \\ \le\; &\limsup_{m\to\infty}\left\|\mathcal{K}_{i(m)}^{k(m)}(\ell,\varrho_m(\ell))-\varrho(\ell)\right\|+c_m\|g_m(\ell)-\varrho_m(\ell)\| \\ \le\; &\limsup_{m\to\infty} r_m(\ell)\|\varrho_m(\ell)-\varrho(\ell)\|+\upsilon_m(\ell)+c_m\|g_m(\ell)-\varrho_m(\ell)\| \\ \le\; &a_\ell.\end{aligned}$$

Taking Lemma 2

$$\left\|\mathcal{K}_{i(m)}^{k(m)}(\ell,\varrho_m(\ell))-\varrho_m(\ell)\right\|\to 0 \text{ as } m\to\infty$$

Using (13), we obtain that

$$\|\varrho_m(\ell)-\eta_m(\ell)\|\to 0 \text{ as } m\to\infty.$$

We have

$$\begin{aligned} &\left\|\mathcal{S}_{i(m)}^{k(m)}(\ell,\varrho_{m-1}(\ell))-E_m(\ell,\varrho_m(\ell))\right\| \qquad (14) \\ \le\; &\left\|\mathcal{S}_{i(m)}^{k(m)}(\ell,\varrho_{m-1}(\ell))-E_{i(m)}^{k(m)}(\ell,\eta_m(\ell))\right\|+\left\|E_{i(m)}^{k(m)}(\ell,\eta_m(\ell))-E_m(\ell,\varrho_m(\ell))\right\|\end{aligned}$$

$$
\begin{aligned}
&\leq \left\|\mathcal{S}_{i(m)}^{k(m)}(\ell,\varrho_{m-1}(\ell)) - E_{i(m)}^{k(m)}(\ell,\eta_m(\ell))\right\| + L\left\|E_{i(m)}^{k(m)-1}(\ell,\eta_m(\ell)) - \varrho_m(\ell)\right\| \\
&= \sigma_m(\ell) + L\left\|E_{i(m)}^{k(m)-1}(\ell,\eta_m(\ell)) - \varrho_m(\ell)\right\|
\end{aligned}
$$

where $\sigma_m(\ell) = \left\|\mathcal{S}_{i(m)}^{k(m)}(\ell,\varrho_{m-1}(\ell)) - E_{i(m)}^{k(m)}(\ell,\eta_m(\ell))\right\|$ for each $\ell \in \mho$. From (11), we get that $\sigma_m(\ell) \to 0$ for each $\ell \in \mho$ as $m \to \infty$. We also have

$$
\begin{aligned}
&\left\|E_{i(m)}^{k(m)-1}(\ell,\eta_m(\ell)) - \varrho_m(\ell)\right\| \qquad (15)\\
\leq\ & \left\|E_{i(m)}^{k(m)-1}(\ell,\eta_m(\ell)) - E_{i(m-\aleph)}^{k(m)-1}\left(\ell,\varrho_{m-\aleph}(\ell)\right)\right\| \\
&+\left\|E_{i(m-\aleph)}^{k(m)-1}\left(\ell,\varrho_{m-\aleph}(\ell)\right) - E_{i(m-\aleph)}^{k(m)-1}\left(\ell,\eta_{m-\aleph}(\ell)\right)\right\| \\
&+\left\|E_{i(m-\aleph)}^{k(m)-1}\left(\ell,\eta_{m-\aleph}(\ell)\right) - \mathcal{S}_{i(m-\aleph)}^{k(m-\aleph)}(\ell,\varrho_{(m-\aleph)-1}(\ell))\right\| \\
&+\left\|\mathcal{S}_{i(m-\aleph)}^{k(m-\aleph)}(\ell,\varrho_{(m-\aleph)-1}(\ell)) - \varrho_m(\ell)\right\|.
\end{aligned}
$$

for each $m > \aleph, m = (m-\aleph)(modN)$. Again since $m = (k(m)-1)\aleph + i(m)$, we have $k(m-\aleph) = k(m)-1$ and $i(m-\aleph) = i(m)$. Using (15), we can write

$$
\begin{aligned}
&\left\|E_{i(m)}^{k(m)-1}(\ell,\eta_m(\ell)) - \varrho_m(\ell)\right\| \qquad (16)\\
\leq\ & \left\|E_{i(m-\aleph)}^{k(m-\aleph)}(\ell,\eta_m(\ell)) - E_{i(m-\aleph)}^{k(m-\aleph)}\left(\ell,\varrho_{m-\aleph}(\ell)\right)\right\| \\
&+\left\|E_{i(m-\aleph)}^{k(m-\aleph)}\left(\ell,\varrho_{m-\aleph}(\ell)\right) - E_{i(m-\aleph)}^{k(m-\aleph)}\left(\ell,\eta_{m-\aleph}(\ell)\right)\right\| \\
&+\left\|E_{i(m-\aleph)}^{k(m-\aleph)}\left(\ell,\eta_{m-\aleph}(\ell)\right) - \mathcal{S}_{i(m-\aleph)}^{k(m-\aleph)}(\ell,\varrho_{(m-\aleph)-1}(\ell))\right\| \\
&+\left\|\mathcal{S}_{i(m-\aleph)}^{k(m-\aleph)}(\ell,\varrho_{(m-\aleph)-1}(\ell)) - \varrho_m(\ell)\right\| \\
\leq\ & L\left\|\eta_m(\ell) - \varrho_{m-\aleph}(\ell)\right\| + L\left\|\varrho_{m-\aleph}(\ell) - \eta_{m-\aleph}(\ell)\right\| + \sigma_{m-\aleph}(\ell) \\
&+\left\|\mathcal{S}_{i(m-\aleph)}^{k(m-\aleph)}(\ell,\varrho_{(m-\aleph)-1}(\ell)) - \varrho_m(\ell)\right\|.
\end{aligned}
$$

Also, we have

$$
\begin{aligned}
\left\|\varrho_m(\ell) - \varrho_{m-1}(\ell)\right\| &= \left\| \begin{array}{c} \alpha_m\mathcal{S}_{i(m)}^{k(m)}(\ell,\varrho_{m-1}(\ell)) + \beta_m E_{i(m)}^{k(m)}(\ell,\eta_m(\ell)) \\ +\gamma_m f_m(\ell) - \varrho_{m-1}(\ell) \end{array} \right\| \\
&\leq \alpha_m\left\|\mathcal{S}_{i(m)}^{k(m)}(\ell,\varrho_{m-1}(\ell)) - \varrho_{m-1}(\ell)\right\| \\
&\quad +\beta_m\left\|E_{i(m)}^{k(m)}(\ell,\eta_m(\ell)) - \varrho_{m-1}(\ell)\right\| \\
&\leq \alpha_m(\left\|\mathcal{S}_{i(m)}^{k(m)}(\ell,\varrho_{m-1}(\ell)) - \varrho_m(\ell)\right\| + \left\|\varrho_m(\ell) - \varrho_{m-1}(\ell)\right\|) \\
&\quad +\beta_m(\left\|E_{i(m)}^{k(m)}\ell,(\eta_m(\ell)) - \varrho_m(\ell)\right\| + \left\|\varrho_m(\ell) - \varrho_{m-1}(\ell)\right\|)
\end{aligned}
$$

and

$$\begin{aligned}
&= \alpha_m \left\|\mathcal{S}_{i(m)}^{k(m)}(\ell, \varrho_{m-1}(\ell)) - \varrho_m(\ell)\right\| + \beta_m \left\|E_{i(m)}^{k(m)}(\ell, \eta_m(\ell)) - \varrho_m(\ell)\right\| \\
&\quad +(\alpha_m + \beta_m) \left\|\varrho_m(\ell) - \varrho_{m-1}(\ell)\right\| \\
&\Longrightarrow (1-\alpha_m-\beta_m) \left\|\varrho_m(\ell) - \varrho_{m-1}(\ell)\right\| \leq \alpha_m \left\|\mathcal{S}_{i(m)}^{k(m)}(\ell, \varrho_{m-1}(\ell)) - \varrho_m(\ell)\right\| \\
&\quad +\beta_m \left\|E_{i(m)}^{k(m)}(\ell, \eta_m(\ell)) - \varrho_m(\ell)\right\| \\
&\Longrightarrow \left\|\varrho_m(\ell) - \varrho_{m-1}(\ell)\right\| \leq \frac{\begin{array}{c}\alpha_m \left\|\mathcal{S}_{i(m)}^{k(m)}(\ell, \varrho_{m-1}(\ell)) - \varrho_m(\ell)\right\| \\ +\beta_m \left\|E_{i(m)}^{k(m)}(\ell, \eta_m(\ell)) - \varrho_m(\ell)\right\|\end{array}}{(1-\alpha_m-\beta_m)} \\
&\leq \frac{\begin{array}{c}\alpha_m \left\|\mathcal{S}_{i(m)}^{k(m)}(\ell, \varrho_{m-1}(\ell)) - \varrho_m(\ell)\right\| \\ +\beta_m \left\|E_{i(m)}^{k(m)}(\ell, \eta_m(\ell)) - \varrho_m(\ell)\right\|\end{array}}{1-2\beta_m} \\
&\Longrightarrow \left\|\varrho_m(\ell) - \varrho_{m-1}(\ell)\right\| \to 0 \text{ as } m \to \infty \text{ for each } \ell \in \mho.
\end{aligned}$$

So from (14) and (16) we have for each $\ell \in \mho$,

$$\begin{aligned}
&\left\|\mathcal{S}_{i(m)}^{k(m)}(\ell, \varrho_{m-1}(\ell)) - E_m(\ell, \varrho_m(\ell))\right\| \\
\leq\ & \sigma_m(\ell) + L^2 \left\|\eta_m(\ell) - \varrho_{m-\aleph}(\ell)\right\| + L^2 \left\|\varrho_{m-\aleph}(\ell) - \eta_{m-\aleph}(\ell)\right\| + L\sigma_{m-\aleph}(\ell) \\
& +L \left\|\mathcal{S}_{i(m)}^{k(m)}(\ell, \varrho_{(m-\aleph)-1}(\ell)) - \varrho_m(\ell)\right\| \\
\leq\ & \sigma_m(\ell) + L^2 \left(\left\|\eta_m(\ell) - \varrho_m(\ell)\right\| + \left\|\varrho_m(\ell) - \varrho_{m-\aleph}(\ell)\right\|\right) + L^2 \left\|\varrho_{m-\aleph}(\ell) - \eta_{m-\aleph}(\ell)\right\| \\
& +L\sigma_{m-\aleph}(\ell) + L \left\|\mathcal{S}_{i(m)}^{k(m)}(\ell, \varrho_{(m-\aleph)-1}(\ell)) - \varrho_m(\ell)\right\|.
\end{aligned}$$

It follows that

$$\left\|\mathcal{S}_{i(m)}^{k(m)}(\ell, \varrho_{m-1}(\ell)) - E_m(\ell, \varrho_m(\ell))\right\| \to 0 \text{ as } m \to \infty \tag{17}$$

By (17) and (12) we obtain that

$$\begin{aligned}
& \left\|\varrho_m(\ell) - E_m(\ell, \varrho_m(\ell))\right\| \qquad (18) \\
\leq\ & \left\|\varrho_m(\ell) - \mathcal{S}_{i(m)}^{k(m)}(\ell, \varrho_{m-1}(\ell))\right\| + \left\|\mathcal{S}_{i(m)}^{k(m)}(\ell, \varrho_{m-1}(\ell)) - E_m(\ell, \varrho_m(\ell))\right\| \\
\to\ & 0 \text{ as } m \to \infty
\end{aligned}$$

Now for each $l \in \{1, 2, \ldots, \aleph\}$, by using (18) we get that

$$\begin{aligned}
\left\|\varrho_m(\ell) - \mathcal{S}_{m+l}(\ell, \varrho_m(\ell))\right\| &\leq \left\|\varrho_m(\ell) - \varrho_{m+l}(\ell)\right\| + \left\|\varrho_{m+l}(\ell) - \mathcal{S}_{m+l}\left(\ell, \varrho_{m+l}(\ell)\right)\right\| \\
&\quad + \left\|\mathcal{S}_{m+l}\left(\ell, \varrho_{m+l}(\ell)\right) - \mathcal{S}_{m+l}(\ell, \varrho_m(\ell))\right\| \\
&\leq \left\|\varrho_m(\ell) - \varrho_{m+l}(\ell)\right\| + \left\|\varrho_{m+l}(\ell) - \mathcal{S}_{m+l}\left(\ell, \varrho_{m+l}(\ell)\right)\right\| \\
&\quad +L \left\|\varrho_{m+l}(\ell) - \varrho_m(\ell)\right\|
\end{aligned}$$

$$\begin{aligned}
&\leq \left\|\varrho_m(\ell)-\varrho_{m+l}(\ell)\right\|+\left\|\varrho_{m+l}(\ell)-\varrho_{m+l-1}(\ell)\right\| \\
&\quad +\left\|\varrho_{m+l-1}(\ell)-\mathcal{S}_{m+l}\left(\ell,\varrho_{m+l}(\ell)\right)\right\| \\
&\quad +L\left\|\varrho_{m+l}(\ell)-\varrho_m(\ell)\right\| \\
&\leq \left\|\varrho_m(\ell)-\varrho_{m+l}(\ell)\right\|+\left\|\varrho_{m+l}(\ell)-\varrho_{m+l-1}(\ell)\right\| \\
&\quad +\left\|\varrho_{m+l-1}(\ell)-\varrho_{m+l}(\ell)\right\| \\
&\quad +\left\|\varrho_{m+l-1}(\ell)-\mathcal{S}_{m+l}\left(\ell,\varrho_{m+l}(\ell)\right)\right\| \\
&\quad +L\left\|\varrho_{m+l}(\ell)-\varrho_m(\ell)\right\| \\
&\to 0 \text{ as } m\to\infty \text{ for each } \ell\in\mho.
\end{aligned}$$

Therefore we have

$$\lim_{m\to\infty}\left\|\varrho_m(\ell)-\mathcal{S}_l\left(\ell,\varrho_m(\ell)\right)\right\|=0$$

for each $\ell\in\mho$ and for each $l\in I$. Similarly we have

$$\lim_{m\to\infty}\left\|\varrho_m(\ell)-E_l\left(\ell,\varrho_m(\ell)\right)\right\|=0 \text{ and } \lim_{m\to\infty}\left\|\varrho_m(\ell)-\mathcal{K}_l\left(\ell,\varrho_m(\ell)\right)\right\|=0$$

for each $\ell\in\mho$ and for each $l\in I$. □

Definition 8. *Let $\mathcal{S}_i, E_i, \mathcal{K}_i : \mho\times\Theta\to\Theta$ be continuous random operators with $F\neq\emptyset$. They is said to satisfy Condition (B^*) if there is a nondecreasing function f on $[0,\infty)$ with $f(0)=0$ and $f(t)>0$ for each $t\in(0,\infty)$ such that for each $\ell\in\mho$*

$$\begin{aligned}
f(d(u_0(\ell),F)) &\leq \max_{1\leq i\leq\aleph}\{\|u_0(\ell)-\mathcal{S}_i(\ell,u_0(\ell))\|\} \\
\text{or } f(d(u_0(\ell),F)) &\leq \max_{1\leq i\leq\aleph}\{\|u_0(\ell)-E_i(\ell,u_0(\ell))\|\} \\
\text{or } f(d(u_0(\ell),F)) &\leq \max_{1\leq i\leq\aleph}\{\|u_0(\ell)-\mathcal{K}_i(\ell,u_0(\ell))\|\}
\end{aligned}$$

where $u_0 : \mho\to\Theta$ is a measurable function.

Theorem 2. *Let $\mathfrak{X}$ be a uniformly convex separable Banach space and Θ be a nonempty closed convex subset of $\mathfrak{X}$. Let $\mathcal{S}_i, E_i, \mathcal{K}_i : \mho\times\Theta\to\Theta$ be uniformly L-Lipschitzian generalized asymptotically nonexpansive random operators with the sequence of measurable mappings $\{r_{i_m}\} : \mho\to[1,\infty)$ satisfying $\sum_{m=1}^{\infty}(r_{i_m}(\ell)-1)<\infty$ for each $\ell\in\mho$ and for all $i\in I$. Suppose that $F\neq\emptyset$. Let the iteration $\{\varrho_m\}$ be defined by (3) with the additional assumption $0<\alpha\leq\alpha_m,\beta_m\leq\beta<1$ and $\sum_{m=1}^{\infty}\gamma_m<\infty, \sum_{m=1}^{\infty}c_m<\infty$. If the families $\mathcal{S}_i, E_i$ and $\mathcal{K}_i$ satisfies Condition (B^*) for each $\ell\in\mho$, then $\{\varrho_m\}$ converges strongly to a common random fixed point of $\mathcal{S}_i, E_i$ and $\mathcal{K}_i$.*

Proof. From Theorem 1, we know that $\lim_{m\to\infty} d\left(\varrho_m(\ell),F\right)$ exists for each $\ell\in\mho$. Using Lemma 3 and Condition (B^*), we have that

$$\lim_{m\to\infty} f\left(d\left(\varrho_m(\ell),F\right)\right)=0.$$

From definition of f, we have $\lim_{m\to\infty} d\left(\varrho_m(\ell),F\right)=0$. Hence the result follows by Theorem 1. □

Theorem 3. *Let $\mathfrak{X}$ be a uniformly convex separable Banach space and Θ be a nonempty closed convex subset of $\mathfrak{X}$. Let $\mathcal{S}_i, E_i, \mathcal{K}_i : \mho \times \Theta \to \Theta$ be uniformly L-Lipschitzian generalized asymptotically nonexpansive random operators with the sequence of measurable mappings $\{r_{i_m}\} : \mho \to [1, \infty)$ satisfying $\sum_{m=1}^{\infty} (r_{i_m}(\ell) - 1) < \infty$ for each $\ell \in \mho$ and for all $i \in I$. Suppose that $F \neq \emptyset$ and at least one of member of the families $\mathcal{S}_i, E_i$ and $\mathcal{K}_i$ is semi-compact random operator. Let the iteration $\{\varrho_m\}$ be defined by (3) with the additional assumption $0 < \alpha \leq \alpha_m, \beta_m \leq \beta < 1$ and $\sum_{m=1}^{\infty} \gamma_m < \infty, \sum_{m=1}^{\infty} c_m < \infty$, then $\{\varrho_m\}$ converges strongly to a common random fixed point of $\mathcal{S}_i, E_i$ and $\mathcal{K}_i$.*

Proof. From Lemma 3, we know that $\lim_{m\to\infty} \|\varrho_m(\ell) - \mathcal{S}_l(\ell, \varrho_m(\ell))\| = 0$ for each $\ell \in \mho$ and for each $l \in I$. Assume that $\mathcal{S}_1$ is semi-compact random operator. Then there exists a subsequence $\{\varrho_{m_k}(\ell)\}$ of $\{\varrho_m(\ell)\}$ such that $\varrho_{m_k}(\ell) \to \varrho(\ell)$ for each $\ell \in \mho$, where ϱ is a measurable mapping from $\mho$ to Θ. Thus

$$\begin{aligned} \|\varrho(\ell) - \mathcal{S}_l(\ell, \varrho(\ell))\| &= \lim_{k\to\infty} \left\|\varrho_{m_k}(\ell) - \mathcal{S}_l\left(\ell, \varrho_{m_k}(\ell)\right)\right\| \\ &= 0 \quad \text{for each } \ell \in \mho \text{ and for each } l \in I. \end{aligned}$$

It follows that $\varrho \in F$. Since $\{\varrho_m(\ell)\}$ has a subsequence $\{\varrho_{m_k}(\ell)\}$ such that $\varrho_{m_k}(\ell) \to \varrho(\ell)$ for each $\ell \in \mho$, we have that $\liminf_{m\to\infty} d(\varrho_m(\ell), F) = 0$. Hence the result follows by Theorem 1 . □

Remark 2. *i) Theorem 1, Lemma 3 and Theorems 2-3 are also valid for asymptotically nonexpansive random operators and uniformly L-Lipschitzian asymptotically nonexpansive random operators. If we take $\nu_m(\ell) = 0$ for each $\ell \in \mho$ and for all $m \geq 1$, the conclusions of our theorems are immediate.*
ii) Taking $\mathcal{S}_{i(m)}^{k(m)}(\ell, \varrho_{m-1}(\ell)) = \varrho_{m-1}(\ell)$ for each $\ell \in \mho$ and $\mathcal{K} = E$ at the implicit iteration process (3), this reduces to the iteration process (2). So, Theorem 1, Lemma 3 and Theorems 2-3 extend and improve Theorem 3.1*, Lemma* 3.1 *and Theorems* 3.2-3.3 *of [1] for three finite families of generalized asymptotically nonexpansive random operators.*
iii) Taking $\mathcal{S}_{i(m)}^{k(m)}(\ell, \varrho_{m-1}(\ell)) = \varrho_{m-1}(\ell)$, $f_m(\ell) = 0$ for each $\ell \in \mho$, $a_m = b_m = c_m = 0$ for all $m \in \mathbb{N}$ at the implicit iteration process (3), we get that the iteration process (1). Thus, our results extend Theorem 4.1 *and Theorem* 4.2 *of [2] respectively. Moreover, our results extend and improve the corresponding results of [14].*

Author Contribution Statements All authors contributed equally to the writing of this paper and they read and approved the final of it.

Declaration of Competing Interests The authors declare that they have no competing interests.

Acknowledgements The second author would like to thank TUBITAK (Scientific and Technological Research Council of Turkey) for financial support with the

TUBITAK 2211 Domestic Graduate Scholarship Program during his graduate studies.

References

[1] Banerjee, S., Choudhury, B. S., Composite implicit random iterations for approximating common random fixed point for a finite family of asymptotically nonexpansive random operators, *Communications of the Korean Mathematical Society*, 26(1) (2011), 23-35. https://doi.org/10.4134/CKMS.2011.26.1.023

[2] Beg, I., Abbas, M., Iterative procedures for solutions of random operator equations in Banach spaces, *J. Math. Anal. Appl.*, 315(1) (2006), 181-201. https://doi.org/10.1016/j.jmaa.2005.05.073

[3] Beg, I., Shahzad, N., Random fixed point theorems for nonexpansive and contractive type random operators on Banach spaces, *J. Appl. Math. Stochastic Anal.*, 7(4) (1994), 569-580. https://doi.org/10.1155/S1048953394000444

[4] Choudhury, B. S., A common unique fixed point theorem for two random operators in Hilbert spaces, *International Journal of Mathematics and Mathematical Sciences*, 32(3) (2002), 177-182. https://doi.org/10.1155/S0161171202005616

[5] Choudhury, B. S., A random fixed point iteration For three random operators on uniformly convex Banach spaces, *Analysis in Theory and Application* 19(2) (2003), 99-107. https://doi.org/10.1007/BF02835233

[6] Choudhury, B. S., An iteration for finding a common random fixed point, *Journal of Applied Mathematics and Stochastic Analysis*, 2004(4) (2004), 385-394. https://doi.org/10.1155/S1048953304208012

[7] Choudhury, B. S., Random Mann iteration scheme, *Appl. Math. Lett.* 16(1) (2003), 93-96. https://doi.org/10.1016/S0893-9659(02)00149-0

[8] Choudhury, B. S., Upadhyay A., An iteration leading to random solutions and fixed points of operators, *Soochow J. Math.* 25(4) (1999), 395-400.

[9] Hans, O., Random fixed point theorems, Transactions of the 1st Prague Conf. on Information Theory, Statistics, Decision Functions and Random Processes, Czeschosl. Acad. Sci., Prague (1957), 105-125.

[10] Itoh, S., Random fixed point theorems with an application to random differential equations in Banach spaces, *J. Math. Anal. Appl.*, 67(2) (1979), 261-273. https://doi.org/10.1016/0022-247X(79)90023-4

[11] Khan, A. R., Thaheem, A. B., Hussain, N., Random fixed points and random approximations in nonconvex domains, *J. Appl. Math. Stochastic Anal.*, 15(3) (2002), 247-253. https://doi.org/10.1155/S1048953302000217

[12] Lin, T. C., Random approximations and random fixed point theorems for continuous 1-set-contractive random maps, *Proc. Amer. Math. Soc.*, 123(4) (1995), 1167-1176. https://doi.org/10.2307/2160715

[13] O'Regan, D., Random fixed point theory for multivalued maps, *Stochastic Analysis and Applications*, 17(4) (1999), 597-607. https://doi.org/10.1080/07362999908809623

[14] Plubtieng, S., Kumam, P.,Wangkeeree, R., Approximation of a common random fixed point for a finite family of random operators, *Int. J. Math. Math. Sci.*, (2007). https://doi.org/10.1155/2007/69626

[15] Rhoades, B. E., Iteration to obtain random solutions and fixed points of operators in uniformly convex Banach spaces, *Soochow J. Math.*, 27(4) (2001), 401-404.

[16] Schu, J., Weak and strong convergence of fixed points of asymptotically nonexpansive mappings, *Bull. Austral. Math. Soc.* 43(1) (1991), 153-159. https://doi.org/10.1017/S0004972700028884

[17] Spacek, A., Zuffalige gleichungen, *Czech. Math. Jour.*, 80(5) (1955), 462-466. https://doi.org/10.21136/CMJ.1955.100162

[18] Tan, K. K., Xu, H. K., Approximating fixed points of nonexpansive mapping by the Ishikawa iteration process, *J. Math. Anal. Appl.*, 178(2) (1993), 301-308. https://doi.org/10.1006/jmaa.1993.1309

http://communications.science.ankara.edu.tr

Commun.Fac.Sci.Univ.Ank.Ser. A1 Math. Stat.
Volume 72, Number 3, Pages 587–605 (2023)
DOI:10.31801/cfsuasmas.1252070
ISSN 1303-5991 E-ISSN 2618-6470

Research Article; Received: February 16, 2023; Accepted: March 28, 2023

TESTING EQUALITY OF MEANS IN ONE-WAY ANOVA USING THREE AND FOUR MOMENT APPROXIMATIONS

Gamze GUVEN
Department of Statistics, Eskisehir Osmangazi University, 26040 Eskisehir, TÜRKIYE

Abstract. In this study, we focus on two test statistics for testing the equality of treatment means in one-way analysis of variance (ANOVA). The first one is the well known Cochran (C_{LS}) test statistic based on least squares (LS) estimators and the second one is robust version of it (RC_{MML}) based on modified maximum likelihood (MML) estimators. These two test statistics are asymptotically distributed as chi-square. However, distributions of them are unknown for small samples. Therefore, three-moment chi-square and four moment F approximations to the null distributions of C_{LS} and RC_{MML} are derived inspired by Tiku and Wong [19]. To investigate the small and moderate sample properties of these tests based on the mentioned approximations, an extensive Monte-Carlo simulation study is performed when the underlying distribution is long-tailed symmetric (LTS). Simulation results show that four-moment F approximation provides better approximation than the three-moment chi-square approximation for both C_{LS} and RC_{MML} tests. Therefore, the simulated Type I error rates and powers of the C_{LS} and RC_{MML} test statistics are calculated using four-moment F approximation. According to simulation results, RC_{MML} test is more powerful than the corresponding C_{LS} test.

1. Introduction

Testing the equality of treatment means in one-way analysis of variance (ANOVA) is one of the oldest problems in theoretical and applied statistics. The problem of interest can be stated in the following hypothesis

$$\begin{aligned} &H_0 : \mu_1 = \mu_2 = \cdots = \mu_a = \mu \quad vs. \\ &H_1 : \mu_i \neq \mu_j \quad \text{for some} \quad i \neq j. \end{aligned} \tag{1}$$

2020 *Mathematics Subject Classification.* 62F03, 62F05, 62F35.
Keywords. Cochran test statistic, three moment chi-square approximation, four-moment F approximation, Monte Carlo simulation.

gamzeguven@ogu.edu.tr; 0000-0002-8821-3179.

Classical F test based on least squares (LS) estimators is appropriate for testing the null hypothesis in (1) when the usual ANOVA assumptions such as independent and identically distributed normal error terms with constant variance are satisfied. Although the F test is relatively robust in terms of the size performance, it may lose power under assumption violations, see Gamage and Weerahandi [4], Hampel [6], Schrader and Hettmansperger [14] and Şenoğlu and Tiku [15] etc. There is an extensive literature focusing on one-way ANOVA under normality and heterogeneiy of variances assumptions. Therefore, a variety of tests have been developed and compared, see for example Brown and Forsythe [2], Cochran [3], James [8], Krishnamoorthy et al. [9], Li et al. [10], Mehrotra [11], Weerahandi [22], Welch [23], etc. for detailed information.

In this study, we are interested in Cochran [3] test statistic based on least squares (LS) estimators, denoted as C_{LS}. The reason of why we focus on this statistic is that many tests available in the literature are based on the C_{LS}. For example, Welch test is a modification of Cochran's test. In addition, C_{LS} is often used as the standard test for testing homogeneity in meta-analysis, see Hartung et al. [7]. As it is well known that this test statistic is proposed under normality and heterogeneity of variances assumptions. However, nonnormal distributions are encountered more frequently in practice. Therefore, Guven et al. [5] considered robust version of the Cochran test statistic based on modified maximum likelihood (MML) estimators, denoted as RC_{MML}, and fiducial based test using RC_{MML} for testing the equality of means when the underlying distribution is long-tailed symmetric (LTS). MML estimators proposed by Tiku [16,17] are asymptotically equivalent to the maximum likelihood (ML) estimators and more efficient than the LS estimators under nonnormality. Also, MML estimators are robust to the outliers, see Aydogdu et al. [1], Tiku et al. [20] and references therein.

It should be noted that C_{LS} and RC_{MML} test statistics have asymptotic chi-square distribution with $a-1$ degrees of freedom under H_0. Here, a denotes the number of treatments. However, their null distributions are difficult to obtain for small samples, even at moderate sample sizes. If one uses asymptotic distribution in small samples this results in highly liberal tests. To deal with this problem, in this study, two useful moment approximations for the small sample distributions of the C_{LS} and RC_{MML} test statistics are derived by inspiring the Tiku and Wong [19]. The former is based on the first three moments of the chi-square distribution and the latter is based on the first four moments of the F distribution. To the best of our knowledge, this is the first study using three-moment chi-square and four moment F approximations to test the equality of treatment means in one-way ANOVA under heteroscedasticity and nonnormality. These approximations are applied to the various problems in the literature. For example, Tiku and Wong [19] used three-moment chi-square and four moment F approximations for testing a unit root in an AR(1) model. Sürücü and Sazak [13] studied the three-parameter Weibull distribution to monitor reliability. Also, they provided reasonably accurate results to the percentage points of the distribution of cumulative time between failures by using two and three moment approximations. Purutcuoğlu [12] extended Tiku and Wong's [19] work to skewed distributions, namely, gamma and generalized logistic.

The outline of this study is organized as follows. In Section 2, C_{LS} and RC_{MML} test statistics are reviewed. In Section 3, a brief description of the three moment chi-square and the four moment F approximations are given. In section 4, results of the simulation study are presented. Concluding remarks are given in Section 5.

2. Test Statistics

In this section, we briefly review the well known C_{LS} test based on LS estimators and RC_{MML} test based on MML estimators.

2.1. **Cochran Test.** Let $Y_{i1}, Y_{i2}, ..., Y_{in_i}$ be a random sample from $N(\mu_i, \sigma_i^2)$, $i = 1, 2, ..., a$ distribution.

C_{LS} test proposed by Cochran in 1937, which is also referred to as natural test statistic in the literature is defined as follows

$$C_{LS} = \sum_{i=1}^{a} \frac{n_i}{S_i^2} \left(\bar{Y}_i - \frac{\sum_{i=1}^{a} n_i \bar{Y}_i / S_i^2}{\sum_{i=1}^{a} n_i / S_i^2} \right)^2 . \tag{2}$$

Here, $\bar{Y}_i$ and S_i^2 are LS estimators of μ_i and σ_i^2, respectively and formulated as follows

$$\bar{Y}_i = \frac{1}{n_i} \sum_{j=1}^{n_i} Y_{ij} \quad \text{and} \quad S_i^2 = \sum_{j=1}^{n_i} (Y_{ij} - \bar{Y}_i)^2 / (n_i - 1). \tag{3}$$

2.2. **Robust Cochran Test.** Let $Y_{i1}, Y_{i2}, ..., Y_{in_i}$ be a random sample from LTS(p, μ_i, σ_i), $(i = 1, ..., a)$ distribution.

The probability density function (pdf) of LTS distribution is

$$f(y) = \frac{1}{\sqrt{k}\beta(1/2, p - 1/2)\sigma} \left(1 + \frac{(y-\mu)^2}{k\sigma^2} \right)^{-p}, -\infty < y < \infty; -\infty < \mu < \infty; \sigma > 0; p \geq 2 \tag{4}$$

where μ is location, σ is scale, p is shape parameter and $k = 2p - 3$, see [18]. It should be noted LTS distribution is used for modeling outlier(s) in data. It has a long tail when the shape parameter p is small and reduces to the normal distribution when p goes to infinity. If a random variable Y is distributed as LTS(p, μ, σ), then $t = \sqrt{(\nu/k)}((Y - \mu)/\sigma)$ is distributed as Student's t with $\nu = 2p - 1$ degrees of freedom.

RC_{MML} test proposed by Güven et al. in 2019 is given as follows

$$RC_{MML} = \sum_{i=1}^{a} \frac{M_i}{\hat{\sigma}_i^2} \left[\hat{\mu}_i - \frac{\sum_{i=1}^{a} M_i \hat{\mu}_i / \hat{\sigma}_i^2}{\sum_{i=1}^{a} M_i / \hat{\sigma}_i^2} \right]^2. \tag{5}$$

Here, $\hat{\mu}_i$ and $\hat{\sigma}_i^2$ are MML estimators of μ_i and σ_i^2, respectively and formulated as follows

$$\hat{\mu}_i = \frac{\sum_{j=1}^{n_i} \beta_{ij} y_{i(j)}}{m_i} \quad \text{and} \quad \hat{\sigma}_i = \frac{B_i + \sqrt{B_i^2 + 4A_i C_i}}{2\sqrt{A_i(A_i - 1)}}. \tag{6}$$

In Eq. (6), $A_i = n_i$, $B_i = \frac{2p}{k} \sum_{j=1}^{n_i} \alpha_{ij}(y_{i(j)} - \hat{\mu}_i)$, $C_i = \frac{2p}{k} \sum_{j=1}^{n_i} \beta_{ij}(y_{i(j)} - \hat{\mu}_i)^2$, $m_i = \sum_{j=1}^{n_i} \beta_{ij}$. $M_i = 2pm_i/k$ and

$$\alpha_{ij} = \frac{(2/k)t_{i(j)}^3}{\left(1 + (1/k)t_{i(j)}^2\right)^2} \quad \text{and} \quad \beta_{ij} = \frac{1 - (1/k)t_{i(j)}^2}{\left(1 + (1/k)t_{i(j)}^2\right)^2}.$$

It should be noted that $y_{i(j)}$, $i = 1, 2, ..., a$ and $j = 1, 2, ..., n_i$ are the ordered observations of a sample. The approximate values of the expected values of the ordered statistics, i.e, $t_{i(j)}$=$E(y_{i(j)})$ values are computed from the following equality

$$\int_{-\infty}^{t_{i(j)}} f(z)dz = \frac{j}{n_i + 1}.$$

Remark 1. *C_{LS} test statistic given in (2) and RC_{MML} test statistic given in (5) are asymptotically distributed as chi-square with $a - 1$ degrees of freedom, see [5, 9] for details. However, as mentioned earlier, the null distribution of these test statistics are unknown for small and moderate samples. To deal with this problem two approximations that can be used to calculate critical values are given.*

3. Moment Approximations

In this section, we briefly mentioned three moment chi-square and four-moment F approximations derived by Tiku and Wong [19].

3.1. **Three-moment chi-square approximation.** Let X^* be a random variable and

$$W_1 = \frac{X^* + a}{b}. \tag{7}$$

Here, W_1 has the central chi-square distribution with ν degrees of freedom. The values of a, b and ν are obtained by equating the first three moments on both sides of (7):

$$\nu = \frac{8}{\beta_1^*} \quad b = \sqrt{\frac{\mu_2}{2\nu}} \quad \text{and} \quad a = b\nu - \mu_1^{'} \tag{8}$$

where $\beta_1^* = \mu_3^2/\mu_2^3$ ($\mu_3 > 0$), $\mu_1^{'}$ is the mean of a random variable X^*, μ_2 is the variance of a random variable X^* and μ_3 is the third central moment of a random variable X^*.

It should be noted that for (7) to be valid β_1^* and β_2^* values of X^* should satisfy the following condition:

$$E = |\beta_2^* - (3 + 1.5\beta_1^*)| \le 0.5 \tag{9}$$

where $\beta_2^* = \mu_4/\mu_2^2$ and μ_4 is the fourth central moment of a random variable X^*.

Realize that $\beta_2^* = 3{+}1.5\beta_1^*$ is called the Type III line for a chi-square distribution, see Tiku and Yip [21] and references therein.

3.2. **Four-moment F approximation.** Let X^* be a random variable and

$$W_2 = \frac{X^* + g}{h}. \tag{10}$$

Here, W_2 has the central F distribution with (ν_1, ν_2) degrees of freedom. The values of ν_1, ν_2, g and h are obtained by equating the four moments on both sides of (10):

$$\begin{aligned}
\nu_2 &= 2\left[3 + \frac{\beta_2^* + 3}{\beta_2^* - (3 + 1.5\beta_1^*)}\right] \\
\nu_1 &= \frac{1}{2}(\nu_2 - 2)\left[-1 + \sqrt{1 + \frac{32(\nu_2 - 4)/(\nu_2 - 6)^2}{\beta_1^* - 32(\nu_2 - 4)/(\nu_2 - 6)^2}}\right] \\
h &= \sqrt{\left\{\frac{\nu_1(\nu_2 - 2)^2(\nu_2 - 4)}{2\nu_2^2(\nu_1 + \nu_2 - 2)}\right\}\mu_2} \\
g &= \frac{\nu_2}{\nu_2 - 2}h - \mu_1^{'}.
\end{aligned} \tag{11}$$

Here, $\beta_1^* = \mu_3^2/\mu_2^3$ ($\mu_3 > 0$), $\beta_2^* = \mu_4/\mu_2^2$, $\mu_1^{'}$ is the mean of a random variable X^*, μ_2 is the variance of a random variable X^*, μ_3 is the third central moment of a random variable X^* and μ_4 is the fourth central moment of a random variable X^*.

It should be noted that for (10) to be valid (β_1^*, β_2^*) values of X^* should satisfy the following conditions:

$$\beta_1^* > C_1 \quad \text{and} \quad \beta_2^* > C_2. \tag{12}$$

where $C_1 = \frac{32(\nu_2-4)}{(\nu_2-6)^2}$ and $C_2 = 3 + 1.5\beta_1^*$.

Realize that the inequalities in (12) determine the F region in the (β_1^*, β_2^*)-plane bounded by the χ^2-line and the reciprocal χ^2-line, see [12].

4. Monte Carlo Simulation Study

In this section, the performances of the RC_{MML} and C_{LS} test statistics based on approximations are compared when the underlying population distributions are LTS. Throughout the simulation study, the following parameter settings are used:

- Number of treatments: $a = 3$,
- Shape parameter: $p = 2$, 2.5, 3.5 and 5,
- Sample sizes: $(n_1, n_2, n_3) = (6, 6, 6)$, $(6, 9, 12)$, $(12, 12, 12)$, $(12, 15, 18)$ and $(20, 20, 20)$,
- Variances: $(\sigma_1^2, \sigma_2^2, \sigma_3^2) = (1, 1, 1)$, $(1, 1.5, 2.5)$ and $(1, 3, 5)$.

Based on the parameter settings, random samples with sample size (n_1, n_2, n_3) were generated from the $LTS(p, \mu_i, \sigma_i)$ distributions. Since it is very difficult to obtain the distribution of RC_{MML} and C_{LS} test statistics or their moments, we simulated (from 10,000 runs) their first four moments. The simulated mean, variance, β_1^* and β_2^* values of the test statistics RC_{MML} and C_{LS} are given in Table 1. In addition, the values for inequalities in (9) and (12) are also included in Table 1, to see whether the three-moment chi square and four-moment F approximations are applicable or not. If the condition in (9) is satisfied, then three-moment chi-square approximation provides accurate values for the percentage points of X^*. Thus, distributions belonging to the Type III region are approximated by this method. In other words, the $100(1-\alpha)\%$ point of X^* is approximately $b\chi^2_{(1-\alpha)}(\nu) - a$ where $\chi^2_{(1-\alpha)}(\nu)$ is the $100(1-\alpha)\%$ point of central chi-square distribution with ν degrees of freedom. Similarly, if the conditions in (12) are satisfied, then four-moment F approximation provides accurate values for the percentage points of X^*. Thus, distributions belonging to the F-region are approximated by this method. In other words, the $100(1-\alpha)\%$ point of X^* is approximately $hF_{(1-\alpha)}(\nu_1, \nu_2) - g$ where $F_{(1-\alpha)}(\nu_1, \nu_2)$ is the $100(1-\alpha)\%$ point of central central F distribution with (ν_1, ν_2) degrees of freedom.

According to the results given in Table 1, condition (9) is satisfied when the sample sizes are $(n_1, n_2, n_3) = (12, 12, 12), (12, 15, 18)$ and $(20, 20, 20)$ for all values of p except $p = 2$. However, when $p = 2$, if sample sizes are $(n_1, n_2, n_3) = (12, 15, 18)$ and $(20, 20, 20)$, then this condition is satisfied. It should be noted that

(β_1^*, β_2^*) values of RC_{MML} and C_{LS} test statistics satisfy the conditions in (12) for all sample sizes and p values. In other words, four moment F approximation is applicable for all parameter settings. Therefore, 95% points of the Eq. (10) and simulated type I error rates and powers of both tests are computed using four-moment F approximation. To illustrate the accuracy of four moment F approximation, the simulated values of the probabilities (based on 10,000 Monte Carlo runs) formulated as

$$P_1 = P(RC_{MML} \geq c_{MML} \,|H_0\,) \quad \text{and} \quad P_2 = P(C_{LS} \geq c_{LS} \,|H_0\,) \tag{13}$$

are given in Table 2. Here, c_{MML} and c_{LS} are the 95% points as determined by (10). The simulated values of the probabilities (based on 10,000 Monte Carlo runs)

$$P_3 = P(RC_{MML} \geq c\,|H_0\,) \quad \text{and} \quad P_4 = P(C_{LS} \geq c\,|H_0\,) \tag{14}$$

are also calculated and included in Table 2. Here, c is the 95% point of the chi-square distribution with $a-1$ degrees of freedom. The purpose here is to show that both test statistics are not distributed as chi-quare with $a-1$ degrees of freedom when the sample sizes are small and moderate.

As it is known that simulated values of the probabilities given in (13) and (14) are Type I error rates of the test statistics. According to Table 2, Type I error rates of both tests are very close to the nominal level $\alpha = 0.05$ based on the probabilities in (13). Therefore, four-moment F approximation performs quite well.

It should be noted that μ_i's $i = 1, 2, 3$ are taken to be 0 for calculating the Type I error rates. The simulated power values are presented in Table 3. They are obtained by substracting and adding a constant s to the observations in the first and third group, respectively.

From Table 3, it can be seen that RC_{MML} test is more powerful than the C_{LS} test. RC_{MML} test outperforms the C_{LS} test especially when $p = 2$ and 2.5. According to the results, it is clear that powers of two tests become very close to each other as expected as the shape parameter p increases, i.e. when the distribution converges to normal.

Table 1 Simulated values of the mean, variance, β_1^* and β_2^* of RC_{MML} and C_{LS} test statistics.

$(\sigma_1^2, \sigma_2^2, \sigma_3^2)$		Mean	Variance	β_1^*	β_2^*	C_1	C_2	E
$p = 2$								
(n_1, n_2, n_3)=(6,6,6)								
$(1, 1, 1)$	RC_{MML}	2.3096	8.0560	13.0149	27.7682	3.1930	22.5223	5.2459
	C_{LS}	2.5299	8.0138	11.7138	26.8661	4.0835	20.5707	6.2954
$(1, 1.5, 2.5)$	RC_{MML}	2.3589	8.3187	11.6877	24.9991	2.9603	20.5315	4.4676
	C_{LS}	2.5722	8.1623	9.1842	20.0265	2.5773	16.7763	3.2503
$(1, 3, 5)$	RC_{MML}	2.3634	8.1424	9.6312	19.8070	1.8271	17.4468	2.3602
	C_{LS}	2.5762	8.1160	8.1244	16.9847	1.5691	15.1866	1.7981
(n_1, n_2, n_3)=(6,9,12)								
$(1, 1, 1)$	RC_{MML}	2.1631	6.0217	8.4289	18.8903	2.7253	15.6434	3.2469
	C_{LS}	2.3272	6.0408	8.0179	19.9702	4.1843	15.0269	4.9433
$(1, 1.5, 2.5)$	RC_{MML}	2.1308	5.7908	7.6515	15.9360	1.3274	14.4773	1.4587
	C_{LS}	2.3022	5.5273	5.8677	12.9254	1.2088	11.8016	1.1238
$(1, 3, 5)$	RC_{MML}	2.0855	5.3528	6.3573	13.0810	0.5607	12.5359	0.5451
	C_{LS}	2.2886	5.3462	5.0975	11.5050	1.0033	10.6463	0.8587
(n_1, n_2, n_3)=(12,12,12)								
$(1, 1, 1)$	RC_{MML}	2.0800	5.4741	7.9669	17.6418	2.3582	14.9504	2.6914
	C_{LS}	2.2032	5.1416	5.9498	14.0425	2.2354	11.9247	2.1179
$(1, 1.5, 2.5)$	RC_{MML}	2.0619	5.0819	6.7256	14.0429	0.9464	13.0884	0.9546
	C_{LS}	2.2280	4.9446	5.2560	12.1676	1.4686	10.8840	1.2836
$(1, 3, 5)$	RC_{MML}	2.1180	5.6276	7.0758	13.9387	0.3129	13.6137	0.3250
	C_{LS}	2.2368	5.2004	5.4540	11.6230	0.4983	11.1810	0.4420
(n_1, n_2, n_3)=(12,15,18)								
$(1, 1, 1)$	RC_{MML}	2.0499	5.0062	6.2150	12.5231	0.2095	12.3224	0.2006
	C_{LS}	2.1970	4.8792	5.0956	10.9974	0.4149	10.6434	0.3541
$(1, 1.5, 2.5)$	RC_{MML}	2.0358	4.7405	5.2598	11.0816	0.2209	10.8897	0.1918
	C_{LS}	2.1673	4.5687	4.3740	9.9229	0.4607	9.5610	0.3620
$(1, 3, 5)$	RC_{MML}	2.0321	4.8645	5.9746	12.2518	0.3099	11.9619	0.2899
	C_{LS}	2.1854	4.7859	4.7202	10.5556	0.5806	10.0804	0.4753
(n_1, n_2, n_3)=(20,20,20)								
$(1, 1, 1)$	RC_{MML}	2.0226	4.4795	5.3256	11.3624	0.4275	10.9883	0.3740
	C_{LS}	2.1341	4.2243	3.9059	9.0935	0.3165	8.8588	0.2347
$(1, 1.5, 2.5)$	RC_{MML}	2.0160	4.5365	5.2599	11.3575	0.5381	10.8899	0.4676
	C_{LS}	2.1090	4.2262	3.7145	8.7742	0.2798	8.5717	0.2024
$(1, 3, 5)$	RC_{MML}	2.0648	4.9787	6.0703	12.5036	0.4215	12.1054	0.3982
	C_{LS}	2.1520	4.4884	4.0370	9.0617	0.0082	9.0556	0.0061

Table 1 Continued

$p = 2.5$								
$(\sigma_1^2, \sigma_2^2, \sigma_3^2)$		Mean	Variance	β_1^*	β_2^*	C_1	C_2	E
(n_1, n_2, n_3)=(6,6,6)								
$(1, 1, 1)$	RC_{MML}	2.4218	8.4302	10.6901	22.3395	2.3585	19.0352	3.3043
	C_{LS}	2.5581	8.5239	9.2394	18.9141	1.6411	16.8591	2.0550
$(1, 1.5, 2.5)$	RC_{MML}	2.4228	8.6027	12.0572	24.8101	2.4296	21.0858	3.7242
	C_{LS}	2.5597	8.7233	10.5542	21.6902	2.0672	18.8312	2.8590
$(1, 3, 5)$	RC_{MML}	2.4826	9.2056	12.0715	24.4862	2.2087	21.1072	3.3789
	C_{LS}	2.6070	9.1769	10.8083	22.3328	2.2136	19.2124	3.1204
(n_1, n_2, n_3)=(6,9,12)								
(1,1,1)	RC_{MML}	2.2667	7.0193	10.1246	22.4666	3.1407	18.1869	4.2798
	C_{LS}	2.3759	6.9486	8.7447	19.1618	2.5003	16.1170	3.0448
(1,1.5,2.5)	RC_{MML}	2.2354	6.5174	8.4731	17.5403	1.5531	15.7097	1.8306
	C_{LS}	2.3585	6.4990	7.2715	15.9467	1.9077	13.9072	2.0395
(1,3,5)	RC_{MML}	2.2131	5.9959	7.5144	16.2003	1.7687	14.2716	1.9287
	C_{LS}	2.3379	6.0546	6.2077	13.6899	1.4305	12.3115	1.3783
(n_1, n_2, n_3)=(12,12,12)								
(1,1,1)	RC_{MML}	2.1299	5.4463	6.2480	12.6131	0.2510	12.3720	0.2412
	C_{LS}	2.2468	5.4260	5.1322	10.9339	0.2751	10.6982	0.2356
(1,1.5,2.5)	RC_{MML}	2.1374	5.5258	6.1414	12.3430	0.1377	12.2121	0.1309
	C_{LS}	2.2439	5.5119	5.5494	11.5547	0.2575	11.3241	0.2306
(1,3,5)	RC_{MML}	2.1556	5.5529	6.0006	12.4211	0.4479	12.0009	0.4202
	C_{LS}	2.2780	5.4755	4.7076	10.1637	0.1253	10.0614	0.1023
(n_1, n_2, n_3)=(12,15,18)								
(1,1,1)	RC_{MML}	2.0891	4.8593	5.4115	11.5966	0.5427	11.1172	0.4794
	C_{LS}	2.2011	4.8299	4.6185	10.3151	0.4790	9.9278	0.3873
(1,1.5,2.5)	RC_{MML}	2.0681	4.9123	5.7607	11.7959	0.1693	11.6410	0.1549
	C_{LS}	2.1738	4.9129	5.0528	10.9016	0.3797	10.5792	0.3224
(1,3,5)	RC_{MML}	2.0624	4.7238	5.0612	11.0668	0.5584	10.5919	0.4749
	C_{LS}	2.1714	4.7558	4.2012	9.4379	0.1768	9.3019	0.1360
(n_1, n_2, n_3)=(20,20,20)								
(1,1,1)	RC_{MML}	2.0612	4.7198	4.9356	10.6220	0.2610	10.4033	0.2187
	C_{LS}	2.1347	4.6836	4.5503	10.3010	0.5924	9.8255	0.4755
(1,1.5,2.5)	RC_{MML}	2.0534	4.6072	4.7783	10.1984	0.0377	10.1674	0.0310
	C_{LS}	2.1400	4.6175	4.3784	9.9652	0.5058	9.5676	0.3977
(1,3,5)	RC_{MML}	2.0755	4.8576	5.3440	11.1513	0.1544	11.0161	0.1352
	C_{LS}	2.1376	4.8247	5.0309	10.9896	0.5230	10.5464	0.4433

Table 1 Continued

				$p = 3.5$				
$(\sigma_1^2, \sigma_2^2, \sigma_3^2)$		Mean	Variance	β_1^*	β_2^*	C_1	C_2	E
				(n_1, n_2, n_3)=(6,6,6)				
(1, 1, 1)	RC_{MML}	2.4878	9.2504	12.7133	25.9098	2.4074	22.0700	3.8398
	C_{LS}	2.5587	9.4876	12.5679	25.3752	2.2334	21.8518	3.5234
(1,1.5,2.5)	RC_{MML}	2.5112	9.8580	14.3304	28.8503	2.4866	24.4957	4.3546
	C_{LS}	2.5792	10.0060	14.0845	28.6982	2.6402	24.1268	4.5714
(1,3,5)	RC_{MML}	2.6010	10.9686	13.7113	27.6405	2.4100	23.5669	4.0736
	C_{LS}	2.6614	11.0235	12.7401	25.2558	1.9796	22.1101	3.1457
				(n_1, n_2, n_3)=(6,9,12)				
(1,1,1)	RC_{MML}	2.3729	7.3840	9.1295	18.6714	1.5930	16.6942	1.9772
	C_{LS}	2.4405	7.4683	8.2328	16.7771	1.2386	15.3492	1.4279
(1,1.5,2.5)	RC_{MML}	2.3098	6.7497	7.8150	16.4073	1.5096	14.7225	1.6848
	C_{LS}	2.3768	6.8880	7.6406	16.3291	1.6958	14.4609	1.8681
(1,3,5)	RC_{MML}	2.3133	6.5897	6.8536	14.1312	0.8341	13.2804	0.8508
	C_{LS}	2.3764	6.6548	6.7169	14.1695	1.0846	13.0753	1.0941
				(n_1, n_2, n_3)=(12,12,12)				
(1,1,1)	RC_{MML}	2.1419	5.5832	6.3234	12.7305	0.2535	12.4850	0.2454
	C_{LS}	2.2150	5.7049	6.0440	12.4456	0.4029	12.0660	0.3797
(1,1.5,2.5)	RC_{MML}	2.2279	5.8083	5.4341	11.2752	0.1403	11.1511	0.1241
	C_{LS}	2.2801	5.8356	5.1763	10.9279	0.1901	10.7644	0.1635
(1,3,5)	RC_{MML}	2.2066	5.7402	5.9609	12.4132	0.5049	11.9413	0.4719
	C_{LS}	2.2648	5.8047	5.5062	11.7500	0.5500	11.2593	0.4907
				(n_1, n_2, n_3)=(12,15,18)				
(1,1,1)	RC_{MML}	2.1052	4.9854	5.6536	11.8726	0.4331	11.4803	0.3923
	C_{LS}	2.1725	4.9796	4.9204	10.8199	0.5248	10.3805	0.4393
(1,1.5,2.5)	RC_{MML}	2.1222	5.3348	5.9678	11.9782	0.0284	11.9517	0.0265
	C_{LS}	2.1881	5.3890	5.6574	11.7592	0.3015	11.4861	0.2730
(1,3,5)	RC_{MML}	2.1788	5.2685	5.2153	11.2398	0.4822	10.8229	0.4169
	C_{LS}	2.2412	5.3480	4.8351	10.2684	0.0190	10.2527	0.0157
				(n_1, n_2, n_3)=(20,20,20)				
(1,1,1)	RC_{MML}	2.0968	4.8573	5.0836	10.6636	0.0449	10.6254	0.0382
	C_{LS}	2.1408	4.8398	4.8967	10.5150	0.2038	10.3450	0.1700
(1,1.5,2.5)	RC_{MML}	2.0911	4.8850	5.2287	10.9304	0.1009	10.8431	0.0873
	C_{LS}	2.1524	4.9565	4.8703	10.3574	0.0625	10.3055	0.0520
(1,3,5)	RC_{MML}	2.0905	4.9111	5.2425	11.2253	0.4169	10.8637	0.3615
	C_{LS}	2.1339	4.9440	4.7707	10.2893	0.1621	10.1560	0.1333

Table 1 Continued

				$p = 5$				
$(\sigma_1^2, \sigma_2^2, \sigma_3^2)$		Mean	Variance	β_1^*	β_2^*	C_1	C_2	E
				(n_1, n_2, n_3)=(6,6,6)				
(1, 1, 1)	RC_{MML}	2.5931	10.1696	10.4780	19.8989	0.8685	18.7169	1.1819
	C_{LS}	2.6224	10.2105	10.1684	19.3852	0.8505	18.2526	1.1326
(1,1.5,2.5)	RC_{MML}	2.5824	9.2375	8.2641	16.3544	0.8314	15.3961	0.9583
	C_{LS}	2.6117	9.3139	8.2007	16.2315	0.8116	15.3010	0.9305
(1,3,5)	RC_{MML}	2.6785	11.3840	12.1254	22.8392	1.0877	21.1881	1.6510
	C_{LS}	2.7104	11.4115	11.6371	22.0232	1.0651	20.4556	1.5675
				(n_1, n_2, n_3)=(6,9,12)				
(1,1,1)	RC_{MML}	2.4202	7.8965	8.2753	16.1644	0.6520	15.4129	0.7515
	C_{LS}	2.4478	7.8960	8.0382	15.8409	0.6931	15.0573	0.7835
(1,1.5,2.5)	RC_{MML}	2.3891	7.3910	7.6100	15.2101	0.7291	14.4150	0.7951
	C_{LS}	2.4176	7.4448	7.5063	15.1283	0.8036	14.2594	0.8689
(1,3,5)	RC_{MML}	2.3322	6.7876	6.8458	14.3607	1.0698	13.2686	1.0920
	C_{LS}	2.3615	6.8576	6.6484	13.8872	0.9135	12.9726	0.9146
				(n_1, n_2, n_3)=(12,12,12)				
(1,1,1)	RC_{MML}	2.2527	6.0280	6.1148	12.5301	0.3773	12.1722	0.3579
	C_{LS}	2.2829	6.0599	5.8781	12.1358	0.3440	11.8171	0.3187
(1,1.5,2.5)	RC_{MML}	2.2251	5.7954	5.7693	12.0057	0.3840	11.6539	0.3518
	C_{LS}	2.2525	5.8256	5.5710	11.8138	0.5092	11.3565	0.4573
(1,3,5)	RC_{MML}	2.2721	6.3965	6.7848	13.6628	0.4799	13.1771	0.4857
	C_{LS}	2.2959	6.3694	6.6065	13.4051	0.4977	12.9098	0.4953
				(n_1, n_2, n_3)=(12,15,18)				
(1,1,1)	RC_{MML}	2.1660	5.1636	5.0322	10.8800	0.3916	10.5482	0.3318
	LS	2.1890	5.2156	4.9121	10.5098	0.1695	10.3682	0.1416
(1,1.5,2.5)	RC_{MML}	2.1914	5.2469	4.9893	10.7124	0.2711	10.4839	0.2285
	C_{LS}	2.2216	5.3025	4.7285	10.2224	0.1584	10.0927	0.1297
(1,3,5)	RC_{MML}	2.1852	5.3835	5.4095	11.5094	0.4477	11.1142	0.3952
	C_{LS}	2.2144	5.3921	5.1696	11.0698	0.3667	10.7544	0.3154
				(n_1, n_2, n_3)=(20,20,20)				
(1,1,1)	RC_{MML}	2.1482	4.9962	4.9164	10.3884	0.0164	10.3747	0.0137
	C_{LS}	2.1717	5.0489	5.0828	10.9542	0.3872	10.6243	0.3299
(1,1.5,2.5)	RC_{MML}	2.0912	4.7621	5.1844	11.1729	0.4599	10.7766	0.3963
	C_{LS}	2.1220	4.8095	4.9371	10.6404	0.2800	10.4057	0.2347
(1,3,5)	RC_{MML}	2.1392	5.2311	5.4792	11.3733	0.1739	11.2188	0.1545
	C_{LS}	2.1688	5.3126	5.2535	10.9122	0.0368	10.8803	0.0320

Table 2 Simulated critical values and the probabilities
$P_1 = P(RC_{MML} \geq c_{MML} \,|H_0\,)$, $P_2 = P(C_{LS} \geq c_{LS} \,|H_0\,)$,
$P_3 = P(RC_{MML} \geq c \,|H_0\,)$, $P_4 = P(C_{LS} \geq c \,|H_0\,)$ and $c = 5.9915$.

(n_1, n_2, n_3)	$(\sigma_1^2, \sigma_2^2, \sigma_3^2)$		$p = 2$ critical value	$p = 2$ P_1 / P_2	$p = 2$ P_3 / P_4	$p = 2.5$ critical value	$p = 2.5$ P_1 / P_2	$p = 2.5$ P_3 / P_4
(6,6,6)	(1,1,1)	c_{MML}	7.6647	0.0488	0.0823	7.9867	0.0484	0.0907
		c_{LS}	7.8448	0.0478	0.0899	8.2283	0.0474	0.0956
	(1,1.5,2.5)	c_{MML}	7.8346	0.0489	0.0864	8.0174	0.0471	0.0894
		c_{LS}	8.0483	0.0493	0.0948	8.2436	0.0467	0.0963
	(1,3,5)	c_{MML}	7.8853	0.0495	0.0896	8.2841	0.0442	0.0930
		c_{LS}	8.1243	0.0469	0.0994	8.4219	0.0452	0.0993
(6,9,12)	(1,1,1)	c_{MML}	6.8603	0.0518	0.0708	7.3034	0.0487	0.0780
		c_{LS}	6.9498	0.0494	0.0728	7.4359	0.0467	0.0818
	(1,1.5,2.5)	c_{MML}	6.8381	0.0506	0.0674	7.2065	0.0485	0.0745
		c_{LS}	6.9046	0.0476	0.0707	7.2969	0.0495	0.0814
	(1,3,5)	c_{MML}	6.6798	0.0504	0.0650	6.9674	0.0492	0.0711
		c_{LS}	6.8224	0.0497	0.0721	7.1381	0.0484	0.0765
(12,12,12)	(1,1,1)	c_{MML}	6.5818	0.0522	0.0643	6.7971	0.0473	0.0648
		c_{LS}	6.5636	0.0513	0.0648	6.8911	0.0490	0.0715
	(1,1.5,2.5)	c_{MML}	6.5034	0.0481	0.0595	6.8512	0.0463	0.0667
		c_{LS}	6.5510	0.0483	0.0635	6.9328	0.0487	0.0701
	(1,3,5)	c_{MML}	6.8559	0.0453	0.0625	6.8449	0.0486	0.0701
		c_{LS}	6.7639	0.0468	0.0643	6.9529	0.0495	0.0758
(12,15,18)	(1,1,1)	c_{MML}	6.5290	0.0460	0.0562	6.4603	0.0495	0.0619
		c_{LS}	6.5855	0.0479	0.0620	6.5512	0.0493	0.0631
	(1,1.5,2.5)	c_{MML}	6.3847	0.0508	0.0603	6.5065	0.0461	0.0578
		c_{LS}	6.3940	0.0487	0.0594	6.5804	0.0488	0.0619
	(1,3,5)	c_{MML}	6.4353	0.0483	0.0588	6.3653	0.0525	0.0614
		c_{LS}	6.5075	0.0516	0.0655	6.5095	0.0484	0.0634
(20,20,20)	(1,1,1)	c_{MML}	6.2296	0.0483	0.0532	6.3909	0.0492	0.0599
		c_{LS}	6.1992	0.0516	0.0576	6.4054	0.0520	0.0620
	(1,1.5,2.5)	c_{MML}	6.2378	0.0485	0.0551	6.3530	0.0500	0.0597
		c_{LS}	6.1721	0.0523	0.0568	6.3847	0.0497	0.0599
	(1,3,5)	c_{MML}	6.5082	0.0477	0.0581	6.4863	0.0496	0.0617
		c_{LS}	6.3803	0.0482	0.0573	6.4893	0.0481	0.0607

Table 2 Continued

			$p = 3.5$			$p = 5$		
(n_1, n_2, n_3)	$(\sigma_1^2, \sigma_2^2, \sigma_3^2)$		critical value	P_1 P_2	P_3 P_4	critical value	P_1 P_2	P_3 P_4
(6,6,6)	(1,1,1)	c_{MML}	8.2775	0.0462	0.0920	8.8412	0.0479	0.0999
		c_{LS}	8.4364	0.0459	0.0950	8.8920	0.0475	0.1011
	(1,1.5,2.5)	c_{MML}	8.4453	0.0460	0.0924	8.5783	0.0472	0.1070
		c_{LS}	8.5552	0.0438	0.0963	8.6353	0.0465	0.1080
	(1,3,5)	c_{MML}	8.8812	0.0467	0.1031	9.2216	0.0461	0.1086
		c_{LS}	9.0109	0.0453	0.1068	9.2778	0.0453	0.1109
(6,9,12)	(1,1,1)	c_{MML}	7.6554	0.0452	0.0830	7.9833	0.0464	0.0899
		c_{LS}	7.7920	0.0454	0.0874	8.0084	0.0462	0.0907
	(1,1.5,2.5)	c_{MML}	7.3755	0.0485	0.0781	7.7680	0.0476	0.0851
		c_{LS}	7.4786	0.0497	0.0797	7.8084	0.0471	0.0892
	(1,3,5)	c_{MML}	7.3827	0.0487	0.0802	7.4531	0.0491	0.0837
		c_{LS}	7.4452	0.0495	0.0819	7.5242	0.0485	0.0848
(12,12,12)	(1,1,1)	c_{MML}	6.8673	0.0465	0.0661	7.1474	0.0486	0.0765
		c_{LS}	6.9734	0.0483	0.0688	7.1926	0.0493	0.0776
	(1,1.5,2.5)	c_{MML}	7.0540	0.0521	0.0742	7.0208	0.0493	0.0732
		c_{LS}	7.1076	0.0507	0.0773	7.0444	0.0491	0.0744
	(1,3,5)	c_{MML}	6.9678	0.0488	0.0703	7.3045	0.0465	0.0766
		c_{LS}	7.0428	0.0485	0.0744	7.3154	0.0469	0.0769
(12,15,18)	(1,1,1)	c_{MML}	6.5469	0.0466	0.0583	6.6820	0.0500	0.0645
		c_{LS}	6.5912	0.0474	0.0645	6.7506	0.0493	0.0678
	(1,1.5,2.5)	c_{MML}	6.7658	0.0482	0.0669	6.7563	0.0496	0.0682
		c_{LS}	6.8207	0.0487	0.0674	6.8186	0.0497	0.0704
	(1,3,5)	c_{MML}	6.7338	0.0496	0.0674	6.7962	0.0504	0.0694
		c_{LS}	6.8771	0.0492	0.0702	6.8344	0.0492	0.0715
(20,20,20)	(1,1,1)	c_{MML}	6.5162	0.0484	0.0599	6.6309	0.0479	0.0632
		c_{LS}	6.5309	0.0481	0.0602	6.6387	0.0488	0.0637
	(1,1.5,2.5)	c_{MML}	6.5188	0.0487	0.0607	6.4234	0.0473	0.0583
		c_{LS}	6.6109	0.0472	0.0626	6.4906	0.0485	0.0600
	(1,3,5)	c_{MML}	6.4954	0.0503	0.0620	6.7159	0.0476	0.0642
		c_{LS}	6.5732	0.0519	0.0655	6.7944	0.0478	0.0653

Table 3 Simulated powers of the RC_{MML} and C_{LS} tests based on four-moment F approximation.

$p = 2$									
(n_1, n_2, n_3)	$(\sigma_1^2, \sigma_2^2, \sigma_3^2) = (1, 1, 1)$			$(\sigma_1^2, \sigma_2^2, \sigma_3^2) = (1, 1.5, 2.5)$			$(\sigma_1^2, \sigma_2^2, \sigma_3^2) = (1, 3, 5)$		
	s	RC_{MML}	C_{LS}	s	RC_{MML}	C_{LS}	s	RC_{MML}	C_{LS}
(6,6,6)	0.00	0.0488	0.0478	0.00	0.0489	0.0493	0.00	0.0495	0.0469
	0.15	0.08	0.08	0.18	0.08	0.08	0.22	0.08	0.07
	0.30	0.19	0.19	0.36	0.18	0.18	0.44	0.16	0.16
	0.45	0.37	0.36	0.54	0.35	0.34	0.66	0.32	0.32
	0.60	0.58	0.57	0.72	0.55	0.53	0.88	0.52	0.50
	0.75	0.75	0.73	0.90	0.71	0.68	1.10	0.69	0.66
	0.90	0.87	0.84	1.08	0.84	0.82	1.32	0.82	0.79
	1.05	0.93	0.91	1.26	0.92	0.90	1.54	0.90	0.88
	1.20	0.97	0.95	1.44	0.96	0.94	1.76	0.95	0.93
	1.35	0.98	0.97	1.62	0.98	0.96	1.98	0.97	0.96
	s	RC_{MML}	C_{LS}	s	RC_{MML}	C_{LS}	s	RC_{MML}	C_{LS}
(6,9,12)	0.00	0.0518	0.0494	0.00	0.0506	0.0476	0.00	0.0504	0.0497
	0.11	0.08	0.07	0.14	0.08	0.08	0.17	0.08	0.08
	0.22	0.17	0.17	0.28	0.17	0.16	0.34	0.18	0.17
	0.33	0.32	0.30	0.42	0.33	0.31	0.51	0.34	0.32
	0.44	0.50	0.47	0.56	0.53	0.49	0.68	0.53	0.48
	0.55	0.68	0.64	0.70	0.71	0.66	0.85	0.72	0.66
	0.66	0.81	0.77	0.84	0.84	0.80	1.02	0.84	0.79
	0.77	0.91	0.87	0.98	0.92	0.87	1.19	0.93	0.88
	0.88	0.95	0.92	1.12	0.96	0.93	1.36	0.96	0.93
	0.99	0.98	0.96	1.26	0.98	0.96	1.53	0.98	0.96
	s	RC_{MML}	C_{LS}	s	RC_{MML}	C_{LS}	s	RC_{MML}	C_{LS}
(12,12,12)	0.00	0.0522	0.0513	0.00	0.0481	0.0483	0.00	0.0453	0.0468
	0.09	0.08	0.08	0.11	0.08	0.07	0.14	0.07	0.07
	0.18	0.16	0.15	0.22	0.15	0.14	0.28	0.15	0.14
	0.27	0.31	0.27	0.33	0.29	0.26	0.42	0.29	0.27
	0.36	0.52	0.46	0.44	0.49	0.43	0.56	0.48	0.42
	0.45	0.70	0.62	0.55	0.66	0.59	0.70	0.66	0.59
	0.54	0.85	0.77	0.66	0.82	0.73	0.84	0.82	0.73
	0.63	0.92	0.86	0.77	0.91	0.84	0.98	0.91	0.84
	0.72	0.96	0.92	0.88	0.96	0.90	1.12	0.96	0.91
	0.81	0.99	0.96	0.99	0.98	0.94	1.26	0.98	0.95
	s	RC_{MML}	C_{LS}	s	RC_{MML}	C_{LS}	s	RC_{MML}	C_{LS}
(12,15,18)	0.00	0.0460	0.0479	0.00	0.0508	0.0487	0.00	0.0483	0.0516
	0.08	0.07	0.07	0.10	0.07	0.07	0.13	0.07	0.07
	0.16	0.15	0.13	0.20	0.16	0.14	0.26	0.17	0.15
	0.24	0.30	0.26	0.30	0.31	0.27	0.39	0.34	0.29
	0.32	0.51	0.43	0.40	0.50	0.43	0.52	0.54	0.46
	0.40	0.69	0.59	0.50	0.70	0.59	0.65	0.74	0.64
	0.48	0.83	0.73	0.60	0.83	0.73	0.78	0.87	0.77
	0.56	0.92	0.84	0.70	0.92	0.84	0.91	0.94	0.86
	0.64	0.97	0.91	0.80	0.97	0.91	1.04	0.98	0.92
	0.72	0.99	0.95	0.90	0.98	0.95	1.17	0.99	0.96
	s	RC_{MML}	C_{LS}	s	RC_{MML}	C_{LS}	s	RC_{MML}	C_{LS}
(20,20,20)	0.00	0.0483	0.0516	0.00	0.0485	0.0523	0.00	0.0477	0.0482
	0.06	0.07	0.07	0.08	0.07	0.07	0.11	0.07	0.06
	0.12	0.14	0.12	0.16	0.14	0.12	0.22	0.16	0.14
	0.18	0.26	0.22	0.24	0.28	0.22	0.33	0.31	0.25
	0.24	0.43	0.35	0.32	0.45	0.36	0.44	0.51	0.41
	0.30	0.60	0.50	0.40	0.64	0.51	0.55	0.70	0.58
	0.36	0.75	0.64	0.48	0.79	0.65	0.66	0.86	0.74
	0.42	0.87	0.76	0.56	0.89	0.78	0.77	0.94	0.85
	0.48	0.94	0.85	0.64	0.95	0.86	0.88	0.98	0.92
	0.54	0.98	0.92	0.72	0.98	0.92	0.99	0.99	0.96

Table 3 Continued

$p = 2.5$									
(n_1, n_2, n_3)	$(\sigma_1^2, \sigma_2^2, \sigma_3^2) = (1,1,1)$			$(\sigma_1^2, \sigma_2^2, \sigma_3^2) = (1,1.5,2.5)$			$(\sigma_1^2, \sigma_2^2, \sigma_3^2) = (1,3,5)$		
	s	RC_{MML}	C_{LS}	s	RC_{MML}	C_{LS}	s	RC_{MML}	C_{LS}
(6,6,6)	0.00	0.0484	0.0474	0.00	0.0471	0.0467	0.00	0.0442	0.0452
	0.16	0.08	0.08	0.20	0.08	0.07	0.25	0.07	0.07
	0.32	0.17	0.17	0.40	0.17	0.16	0.50	0.15	0.15
	0.48	0.32	0.32	0.60	0.31	0.30	0.75	0.30	0.30
	0.64	0.52	0.50	0.80	0.50	0.49	1.00	0.50	0.49
	0.80	0.69	0.68	1.00	0.67	0.66	1.25	0.68	0.67
	0.96	0.83	0.81	1.20	0.82	0.81	1.50	0.81	0.80
	1.12	0.92	0.90	1.40	0.91	0.90	1.75	0.91	0.90
	1.28	0.96	0.95	1.60	0.96	0.95	2.00	0.95	0.94
	1.44	0.98	0.98	1.80	0.98	0.98	2.25	0.98	0.97
	s	RC_{MML}	C_{LS}	s	RC_{MML}	C_{LS}	s	RC_{MML}	C_{LS}
(6,9,12)	0.00	0.0487	0.0467	0.00	0.0485	0.0495	0.00	0.0492	0.0484
	0.13	0.0799	0.0809	0.16	0.07	0.08	0.19	0.07	0.07
	0.26	0.1685	0.1638	0.32	0.16	0.16	0.38	0.16	0.15
	0.39	0.3213	0.3076	0.48	0.31	0.30	0.57	0.32	0.30
	0.52	0.5239	0.4966	0.64	0.50	0.48	0.76	0.50	0.48
	0.65	0.7009	0.6701	0.80	0.69	0.66	0.95	0.69	0.65
	0.78	0.8425	0.8117	0.96	0.83	0.80	1.14	0.83	0.80
	0.91	0.9268	0.9009	0.12	0.92	0.89	1.33	0.92	0.88
	1.04	0.9714	0.9525	1.28	0.96	0.94	1.52	0.96	0.94
	1.17	0.9875	0.9760	1.44	0.99	0.97	1.71	0.99	0.97
	s	RC_{MML}	C_{LS}	s	RC_{MML}	C_{LS}	s	RC_{MML}	C_{LS}
(12,12,12)	0.00	0.0473	0.0490	0.00	0.0463	0.0487	0.00	0.0486	0.0495
	0.11	0.07	0.07	0.13	0.07	0.07	0.16	0.08	0.07
	0.22	0.17	0.16	0.26	0.16	0.15	0.32	0.15	0.14
	0.33	0.34	0.31	0.39	0.28	0.26	0.48	0.29	0.27
	0.44	0.54	0.50	0.52	0.49	0.45	0.64	0.48	0.44
	0.55	0.74	0.68	0.65	0.67	0.62	0.80	0.66	0.61
	0.66	0.88	0.83	0.78	0.82	0.77	0.96	0.81	0.76
	0.77	0.95	0.91	0.91	0.92	0.87	1.12	0.91	0.86
	0.88	0.98	0.96	1.04	0.96	0.93	1.28	0.96	0.93
	0.99	0.99	0.98	1.17	0.99	0.97	1.44	0.99	0.97
	s	RC_{MML}	C_{LS}	s	RC_{MML}	C_{LS}	s	RC_{MML}	C_{LS}
(12,15,18)	0.00	0.0495	0.0493	0.00	0.0461	0.0488	0.00	0.0525	0.0484
	0.09	0.08	0.08	0.11	0.07	0.07	0.13	0.07	0.07
	0.18	0.16	0.15	0.22	0.15	0.14	0.26	0.14	0.13
	0.27	0.29	0.27	0.33	0.28	0.25	0.39	0.28	0.25
	0.36	0.49	0.44	0.44	0.47	0.42	0.52	0.44	0.39
	0.45	0.68	0.62	0.55	0.65	0.58	0.65	0.63	0.55
	0.54	0.83	0.76	0.66	0.81	0.74	0.78	0.78	0.71
	0.63	0.92	0.87	0.77	0.90	0.85	0.91	0.89	0.83
	0.72	0.97	0.93	0.88	0.96	0.92	1.04	0.96	0.91
	0.81	0.99	0.97	0.99	0.99	0.96	1.17	0.98	0.95
	s	RC_{MML}	C_{LS}	s	RC_{MML}	C_{LS}	s	RC_{MML}	C_{LS}
(20,20,20)	0.00	0.0492	0.0520	0.00	0.0500	0.0497	0.00	0.0496	0.0481
	0.07	0.07	0.07	0.09	0.07	0.07	0.11	0.07	0.07
	0.14	0.14	0.13	0.18	0.14	0.13	0.22	0.13	0.12
	0.21	0.25	0.22	0.27	0.26	0.23	0.33	0.24	0.22
	0.28	0.42	0.37	0.36	0.43	0.37	0.44	0.40	0.35
	0.35	0.60	0.53	0.45	0.61	0.54	0.55	0.58	0.52
	0.42	0.76	0.69	0.54	0.78	0.69	0.66	0.75	0.67
	0.49	0.88	0.81	0.63	0.89	0.81	0.77	0.88	0.80
	0.56	0.95	0.89	0.72	0.95	0.90	0.88	0.94	0.88
	0.63	0.98	0.95	0.81	0.98	0.95	0.99	0.98	0.94

Table 3 Continued

$p = 3.5$									
(n_1, n_2, n_3)	$(\sigma_1^2, \sigma_2^2, \sigma_3^2) = (1, 1, 1)$			$(\sigma_1^2, \sigma_2^2, \sigma_3^2) = (1, 1.5, 2.5)$			$(\sigma_1^2, \sigma_2^2, \sigma_3^2) = (1, 3, 5)$		
	s	RC_{MML}	C_{LS}	s	RC_{MML}	C_{LS}	s	RC_{MML}	C_{LS}
(6,6,6)	0.00	0.0462	0.0459	0.00	0.0460	0.0438	0.00	0.0467	0.0453
	0.17	0.07	0.07	0.21	0.07	0.07	0.27	0.07	0.07
	0.34	0.16	0.16	0.42	0.15	0.15	0.54	0.15	0.14
	0.51	0.31	0.31	0.63	0.28	0.28	0.81	0.28	0.28
	0.68	0.50	0.49	0.84	0.47	0.46	1.08	0.47	0.47
	0.85	0.68	0.67	1.05	0.66	0.65	1.35	0.66	0.65
	1.02	0.82	0.81	1.26	0.81	0.80	1.62	0.81	0.80
	1.19	0.91	0.91	1.47	0.90	0.89	1.89	0.90	0.89
	1.36	0.96	0.95	1.68	0.96	0.95	2.16	0.96	0.95
	1.53	0.99	0.98	1.89	0.98	0.98	2.43	0.98	0.97
	s	RC_{MML}	C_{LS}	s	RC_{MML}	C_{LS}	s	RC_{MML}	C_{LS}
(6,9,12)	0.00	0.0452	0.0454	0.00	0.0485	0.0497	0.00	0.0487	0.0495
	0.13	0.07	0.07	0.16	0.07	0.07	0.20	0.07	0.07
	0.26	0.14	0.13	0.32	0.14	0.13	0.40	0.15	0.13
	0.39	0.27	0.26	0.48	0.27	0.27	0.60	0.28	0.27
	0.52	0.44	0.43	0.64	0.44	0.44	0.80	0.45	0.44
	0.65	0.63	0.61	0.80	0.63	0.62	1.00	0.65	0.63
	0.78	0.78	0.77	0.96	0.78	0.77	1.20	0.80	0.79
	0.91	0.89	0.87	0.12	0.88	0.87	1.40	0.90	0.89
	1.04	0.95	0.94	1.28	0.94	0.93	1.60	0.96	0.95
	1.17	0.98	0.98	1.44	0.98	0.97	1.80	0.98	0.97
	s	RC_{MML}	C_{LS}	s	RC_{MML}	C_{LS}	s	RC_{MML}	C_{LS}
(12,12,12)	0.00	0.0465	0.0483	0.00	0.0521	0.0507	0.00	0.0488	0.0485
	0.11	0.07	0.07	0.13	0.06	0.06	0.16	0.07	0.07
	0.22	0.15	0.14	0.26	0.13	0.12	0.32	0.13	0.13
	0.33	0.29	0.28	0.39	0.24	0.23	0.48	0.24	0.23
	0.44	0.48	0.47	0.52	0.41	0.40	0.64	0.40	0.39
	0.55	0.66	0.64	0.65	0.59	0.57	0.80	0.58	0.56
	0.66	0.83	0.80	0.78	0.76	0.73	0.96	0.75	0.73
	0.77	0.92	0.90	0.91	0.87	0.85	1.12	0.87	0.85
	0.88	0.97	0.96	1.04	0.94	0.93	1.28	0.94	0.92
	0.99	0.99	0.98	1.17	0.98	0.97	1.44	0.98	0.97
	s	RC_{MML}	C_{LS}	s	RC_{MML}	C_{LS}	s	RC_{MML}	C_{LS}
(12,15,18)	0.00	0.0466	0.0474	0.00	0.0482	0.0487	0.00	0.0496	0.0492
	0.09	0.07	0.07	0.12	0.07	0.07	0.15	0.07	0.07
	0.18	0.14	0.13	0.24	0.14	0.13	0.30	0.14	0.13
	0.27	0.26	0.24	0.36	0.27	0.26	0.45	0.27	0.26
	0.36	0.42	0.41	0.48	0.45	0.43	0.60	0.47	0.44
	0.45	0.60	0.58	0.60	0.64	0.62	0.75	0.66	0.62
	0.54	0.76	0.73	0.72	0.78	0.76	0.90	0.81	0.78
	0.63	0.88	0.85	0.84	0.91	0.88	1.05	0.91	0.88
	0.72	0.95	0.93	0.96	0.96	0.94	1.20	0.97	0.95
	0.81	0.98	0.97	1.08	0.99	0.97	1.35	0.99	0.97
	s	RC_{MML}	C_{LS}	s	RC_{MML}	C_{LS}	s	RC_{MML}	C_{LS}
(20,20,20)	0.00	0.0484	0.0481	0.00	0.0487	0.0472	0.00	0.0503	0.0519
	0.08	0.07	0.07	0.10	0.07	0.07	0.13	0.07	0.07
	0.16	0.13	0.13	0.20	0.14	0.13	0.26	0.15	0.14
	0.24	0.27	0.26	0.30	0.26	0.24	0.39	0.28	0.27
	0.32	0.45	0.43	0.40	0.44	0.41	0.52	0.47	0.43
	0.40	0.63	0.60	0.50	0.63	0.59	0.65	0.65	0.62
	0.48	0.80	0.77	0.60	0.78	0.75	0.78	0.81	0.78
	0.56	0.91	0.88	0.70	0.90	0.87	0.91	0.92	0.89
	0.64	0.96	0.94	0.80	0.96	0.94	1.04	0.97	0.95
	0.72	0.99	0.98	0.90	0.98	0.97	1.17	0.99	0.98

Table 3 Continued

$p = 5$									
(n_1, n_2, n_3)	$(\sigma_1^2, \sigma_2^2, \sigma_3^2) = (1, 1, 1)$			$(\sigma_1^2, \sigma_2^2, \sigma_3^2) = (1, 1.5, 2.5)$			$(\sigma_1^2, \sigma_2^2, \sigma_3^2) = (1, 3, 5)$		
	s	RC_{MML}	C_{LS}	s	RC_{MML}	C_{LS}	s	RC_{MML}	C_{LS}
(6,6,6)	0.00	0.0479	0.0475	0.00	0.0472	0.0465	0.00	0.0461	0.0453
	0.17	0.07	0.07	0.22	0.07	0.07	0.27	0.07	0.07
	0.34	0.14	0.14	0.44	0.15	0.14	0.54	0.14	0.14
	0.51	0.28	0.28	0.66	0.29	0.29	0.81	0.26	0.26
	0.68	0.44	0.44	0.88	0.47	0.47	1.08	0.43	0.42
	0.85	0.64	0.64	1.10	0.66	0.65	1.35	0.62	0.61
	1.02	0.78	0.78	1.32	0.82	0.81	1.62	0.78	0.77
	1.19	0.89	0.89	1.54	0.91	0.90	1.89	0.89	0.88
	1.36	0.96	0.95	1.76	0.96	0.96	2.16	0.96	0.95
	1.53	0.98	0.98	1.98	0.99	0.98	2.43	0.98	0.98
	s	RC_{MML}	C_{LS}	s	RC_{MML}	C_{LS}	s	RC_{MML}	C_{LS}
(6,9,12)	0.00	0.0464	0.0462	0.00	0.0476	0.0471	0.00	0.0491	0.0485
	0.13	0.06	0.06	0.17	0.07	0.07	0.21	0.07	0.07
	0.26	0.13	0.13	0.34	0.14	0.14	0.42	0.15	0.14
	0.39	0.25	0.24	0.51	0.26	0.26	0.63	0.29	0.28
	0.52	0.40	0.39	0.68	0.45	0.44	0.84	0.47	0.46
	0.65	0.58	0.57	0.85	0.63	0.62	1.05	0.66	0.65
	0.78	0.74	0.74	1.02	0.79	0.78	1.26	0.82	0.81
	0.91	0.86	0.85	1.19	0.90	0.89	1.47	0.92	0.91
	1.04	0.93	0.93	1.36	0.96	0.95	1.68	0.96	0.96
	1.17	0.98	0.97	1.53	0.99	0.98	1.89	0.99	0.98
	s	RC_{MML}	C_{LS}	s	RC_{MML}	C_{LS}	s	RC_{MML}	C_{LS}
(12,12,12)	0.00	0.0486	0.0493	0.00	0.0493	0.0491	0.00	0.0465	0.0469
	0.11	0.07	0.07	0.14	0.07	0.07	0.17	0.07	0.07
	0.22	0.14	0.14	0.28	0.14	0.14	0.34	0.13	0.13
	0.33	0.27	0.26	0.42	0.26	0.26	0.51	0.25	0.25
	0.44	0.44	0.43	0.56	0.45	0.44	0.68	0.41	0.40
	0.55	0.62	0.61	0.70	0.63	0.63	0.85	0.59	0.58
	0.66	0.79	0.78	0.84	0.79	0.78	1.02	0.76	0.75
	0.77	0.90	0.89	0.98	0.90	0.89	1.19	0.87	0.86
	0.88	0.96	0.95	1.12	0.96	0.95	1.36	0.95	0.94
	0.99	0.99	0.98	1.26	0.99	0.98	1.53	0.98	0.98
	s	RC_{MML}	C_{LS}	s	RC_{MML}	C_{LS}	s	RC_{MML}	C_{LS}
(12,15,18)	0.00	0.0500	0.0493	0.00	0.0496	0.0497	0.00	0.0504	0.0492
	0.10	0.07	0.07	0.13	0.07	0.07	0.15	0.07	0.07
	0.20	0.14	0.14	0.26	0.15	0.14	0.30	0.13	0.13
	0.30	0.29	0.28	0.39	0.29	0.28	0.45	0.27	0.26
	0.40	0.47	0.46	0.52	0.49	0.48	0.60	0.44	0.43
	0.50	0.66	0.64	0.65	0.68	0.66	0.75	0.63	0.62
	0.60	0.82	0.80	0.78	0.84	0.82	0.90	0.79	0.77
	0.70	0.92	0.91	0.91	0.93	0.92	1.05	0.90	0.89
	0.80	0.97	0.96	1.04	0.98	0.97	1.20	0.96	0.95
	0.90	0.99	0.98	1.17	0.99	0.98	1.35	0.99	0.98
	s	RC_{MML}	C_{LS}	s	RC_{MML}	C_{LS}	s	RC_{MML}	C_{LS}
(20,20,20)	0.00	0.0479	0.0488	0.00	0.0473	0.0485	0.00	0.0476	0.0478
	0.08	0.07	0.07	0.11	0.08	0.08	0.13	0.07	0.06
	0.16	0.13	0.13	0.22	0.16	0.15	0.26	0.14	0.13
	0.24	0.25	0.24	0.33	0.30	0.29	0.39	0.26	0.25
	0.32	0.41	0.39	0.44	0.48	0.47	0.52	0.42	0.41
	0.40	0.60	0.58	0.55	0.68	0.67	0.65	0.62	0.60
	0.48	0.77	0.75	0.66	0.84	0.82	0.78	0.78	0.76
	0.56	0.88	0.87	0.77	0.93	0.92	0.91	0.89	0.88
	0.64	0.95	0.94	0.88	0.98	0.97	1.04	0.96	0.95
	0.72	0.98	0.99	0.99	0.99	0.99	1.17	0.99	0.98

5. Conclusion

This study examined small and moderate sample properties of the C_{LS} and RC_{MML} tests proposed in the literature for testing the equality of treatment means in one-way ANOVA when the underlying distribution is long tailed symmetric using three moment chi-square and four moment F approximations. Although the asymptotic distributions of the C_{LS} and RC_{MML} test statistics are known in large samples, the null distributions of both test statistics are not known for small and moderate sample sizes. This is the reason why three moment chi-square and four moment F approximations are needed. An extensive Monte Carlo simulation study is conducted to see whether two approximations are applicable to the test statistics or not and to compare the performances of the test statistics in terms of the Type I error rates and power. According to simulation results four moment F approximation is applicable to the C_{LS} and RC_{MML} test statistics regardless of the sample sizes and p values. Three moment chi-square approximation applicable when sample sizes are moderate. Also, using asymptotic distribution results in inflated type I error rates when sample sizes are small and moderate while Type I errror rates of the tests using F approximation are very close to the nominal level. Therefore, this approximation performs very well for C_{LS} and RC_{MML} test statistics. RC_{MML} test is more powerful than the C_{LS} especially when the shape parameter $p = 2$ and 2.5. Note also that, when the values of the shape parameter greater and equal 3.5 and 5 the RC_{MML} test is slightly more powerful than C_{LS} test.

Declaration of Competing Interests The author declares that there is no competing interest regarding the publication of this paper.

References

[1] Aydoğdu, H., Şenoğlu, B., Kara, M., Parameter estimation in geometric process with Weibull distribution. *Appl. Math. Comput.*, 217(6) (2010), 2657-2665. https://doi.org/10.1016/j.amc.2010.08.003

[2] Brown, M. B., Forsythe, A. B., The small sample behavior of some statistics which test the equality of several means. *Technometrics*, 16(1) (1974), 129-132. https://www.tandfonline.com/doi/abs/10.1080/00401706.1974.10489158.

[3] Cochran, W. G., Problems arising in the analysis of a series of similar experiments. *Suppl. J. R. Stat. Soc*, 4(1) (1937), 102-118. https://www.jstor.org/stable/2984123

[4] Gamage, J., Weerahandi, S., Size performance of some tests in one-way ANOVA, *Comm. Statist. Simulation Comput.*, 27(3) (1998), 625-640. https://www.tandfonline.com/doi/abs/10.1080/03610919808813500

[5] Güven, G., Gürer, Ö., Şamkar, H., Şenoglu, B., A fiducial-based approach to the one-way ANOVA in the presence of nonnormality and heterogeneous error variances. *J. Stat. Comput. Simul.*, 89(9) (2019), 1715-1729. https://doi.org/10.1080/00949655.2019.1593985

[6] Hampel, F. R., Robust estimation: A condensed partial survey, *Zeitschrift für Wahrscheinlichkeitstheorie und verwandte Gebiete*, 27(2) (1973), 87-104. https://link.springer.com/article/10.1007/BF00536619

[7] Hartung, J., Knapp, G., Sinha, B. K., Statistical meta-analysis with applications. John Wiley and Sons (2011)

[8] James, G. S., The comparison of several groups of observations when the ratios of the population variances are unknown. *Biometrika*, 38(3/4) (1951), 324-329. https://doi.org/10.2307/2332578.

[9] Krishnamoorthy, K., Lu, F., Mathew, T., A parametric bootstrap approach for ANOVA with unequal variances: Fixed and random models. *Comput. Stat. Data Anal.*, 51(12) (2007), 5731-5742. https://doi.org/10.1016/j.csda.2006.09.039

[10] Li, X., Wang, J., Liang, H., Comparison of several means: A fiducial based approach. *Comput. Stat. Data Anal.*, 55(5) (2011), 1993-2002. https://doi.org/10.1016/j.csda.2010.12.009

[11] Mehrotra, D. V., Improving the Brown-Forsythe solution to the generalized Behrens-Fisher problem. *Commun. Stat. Simul. Comput.*, 26(3) (1997), 1139-1145. https://doi.org/10.1080/03610919708813431

[12] Purutcuoğlu, V., Unit root problems in time series analysis, Master Thesis, Middle East Technical University, 2004.

[13] Sürücü, B., Sazak, H. S., Monitoring reliability for a three-parameter Weibull distribution. *Reliab. Eng. Syst. Saf.*, 94(2) (2009), 503-508. https://doi.org/10.1016/j.ress.2008.06.001

[14] Schrader, R. M., Hettmansperger, T. P., Robust analysis of variance based upon a likelihood ratio criterion, *Biometrika*, 67(1) (1980), 93-101. https://doi.org/10.1093/biomet/67.1.93

[15] Şenoğlu, B., Tiku, M. L., Analysis of variance in experimental design with non-normal error distributions. *Commun. Stat. Theory Methods*, 30(7) (2001), 1335-1352. https://www.tandfonline.com/doi/full/10.1081/STA-100104748

[16] Tiku, M. L., Estimating the mean and standard deviation from a censored normal sample. *Biometrika*, 54(1-2) (1967), 155-165. https://doi.org/10.1093/biomet/54.1-2.155

[17] Tiku, M. L., Estimating the parameters of log-normal distribution from censored samples. *J. Am. Stat. Assoc*, 63(321) (1968), 134-140. https://doi.org/10.1080/01621459.1968.11009228

[18] Tiku, M. L., Kumra, S., Expected values and variances and covariances of order statistics for a family of symmetric distributions (Student'st). *Selected tables in mathematical statistics*, 8 (1981), 141-270.

[19] Tiku, M. L., Wong, W. K., Testing for a unit root in an AR (1) model using three and four moment approximations: symmetric distributions, *Commun. Stat. Simul. Comput.*, 27(1) (1998), 185-198. https://www.tandfonline.com/doi/abs/10.1080/03610919808813474

[20] Tiku, M. L., Wong, W. K., Bian, G., Estimating parameters in autoregressive models in non-normal situations: Symmetric innovations. *Commun. Stat. Theory Methods*, 28(2) (1999), 315-341. https://doi.org/10.1080/03610929908832300

[21] Tiku, M. L., Yip, D. Y. N., A four-moment approximation based on the F distribution. *Austrian J. Stat.*, 20(3) (1978), 257-261. https://doi.org/10.1111/j.1467-842X.1978.tb01108.x

[22] Weerahandi, S., ANOVA under unequal error variances.*Biometrics*, 51(2) (1995), 589-599. https://doi.org/10.2307/2532947

[23] Welch, B. L., On the comparison of several mean values: an alternative approach. *Biometrika*, 38(3/4) (1951) , 330-336. https://doi.org/10.2307/2332579

http://communications.science.ankara.edu.tr

Commun.Fac.Sci.Univ.Ank.Ser. A1 Math. Stat.
Volume 72, Number 3, Pages 606–617 (2023)
DOI:10.31801/cfsuasmas.1147745
ISSN 1303-5991 E-ISSN 2618-6470

Research Article; Received: July 23, 2022; Accepted: March 27, 2023

ON THE EXTENDED WRIGHT HYPERGEOMETRIC MATRIX FUNCTION AND ITS PROPERTIES

Halil GEZER[1] and Cem KAANOĞLU[2]

[1,2] Cyprus International University, Faculty of Arts and Sciences, Department of Basic Sciences and Humanities, Nicosia, Mersin 10, TÜRKİYE

Abstract. Recently, Bakhet *et al.* [9] presented the Wright hypergeometric matrix function ${}_2\mathbf{R}_1^{(\tau)}(A,B;C;z)$ and derived several properties. Abdalla [6] has since applied fractional operators to this function. In this paper, with the help of the generalized Pochhammer matrix symbol $(A;B)_n$ and the generalized beta matrix function $\mathcal{B}(P,Q;\mathbb{X})$, we introduce and study an extended form of the Wright hypergeometric matrix function, ${}_2\mathbf{R}_1^{(\tau)}((A;\mathbb{A}),B;C;z;\mathbb{X})$. We establish several potentially useful results for this extended form, such as integral representations and fractional derivatives. We also derive some properties of the corresponding incomplete extended Wright hypergeometric matrix function.

1. Introduction

Let $\mathbb{C}^{r\times r}$ be the vector space of r-square matrices with complex entries. A square matrix $P\in\mathbb{C}^{r\times r}$ is said to be positive stable if $\Re(\lambda)>0$ for all $\lambda\in\sigma(P)$, where $\Re(\lambda)$ denotes the real part of a complex number λ and $\sigma(P)$ is the set of all eigenvalues of P.

Let P and Q be positive stable matrices in $\mathbb{C}^{r\times r}$. The gamma matrix function $\Gamma(P)$ and the beta matrix function $\mathfrak{B}(P,Q)$ were defined by Jódar and Cortés [12] as follows:

$$\Gamma(P)=\int_0^\infty e^{-t}t^{P-I}dt,\qquad t^{P-I}=\exp((P-I)\ln t)$$

and

$$\mathfrak{B}(P,Q)=\int_0^1 t^{P-I}(1-t)^{Q-I}dt, \tag{1}$$

2020 *Mathematics Subject Classification.* Primary 33C05, 33C20; Secondary 33C45, 33C90.
Keywords. Wright hypergeometric matrix function, generalized hypergeometric functions, Riemann–Liouville fractional derivative.
[1] hgezer@ciu.edu.tr-Corresponding author; 0000-0002-1248-989X;
[2] kaanoglu@ciu.edu.tr; 0000-0001-7733-041X.

respectively. The shifted factorial matrix function $(P)_n$ for $P \in \mathbb{C}^{r\times r}$, given by [13], is

$$(P)_n = \begin{cases} I, & n = 0, \\ P(P+I)\dots(P+(n-1)I), & n \geq 1. \end{cases}$$

Let $P \in \mathbb{C}^{r\times r}$, and suppose that

$$P + nI \text{ is invertible for all integers } n, \tag{2}$$

then the reciprocal gamma matrix function [12] is given by

$$\Gamma^{-1}(P) = (P)_n \Gamma^{-1}(P + nI).$$

Over the past two decades, several generalizations of the well-known special matrix functions have been studied by various authors (for example, [5], [7] and [10]). In particular, in 2015, Abul-Dahab *et al.* [7] introduced a generalized Pochhammer matrix symbol $(A; B)_n$. Let A and B be positive stable matrices in $\mathbb{C}^{r\times r}$ that satisfy the condition (2). Then

$$(A;B)_n = \begin{cases} \Gamma^{-1}(A)\Gamma(A+nI,B) & \big(B \neq \mathbf{0}\big) \\ \\ (A)_n & (B \doteq \mathbf{0}), \end{cases} \tag{3}$$

where $\mathbf{0} \in \mathbb{C}^{r\times r}$ is the zero matrix and $\Gamma(A, B)$ is the generalized gamma matrix function given by (see [7])

$$\Gamma(A,B) = \int_0^\infty t^{A-I}\, e^{-\left(It + \frac{B}{t}\right)} \mathrm{d}t,$$

so that the integral representation for the generalized Pochhammer matrix symbol is

$$(A;B)_n = \Gamma^{-1}(A) \int_0^\infty t^{A+(n-1)I}\, e^{-\left(It + \frac{B}{t}\right)} \mathrm{d}t, \tag{4}$$

where B and $A + nI$ are positive stable for all $n \geq 0$. Let A and B be positive stable matrices in $\mathbb{C}^{r\times r}$ that satisfy the condition (2). Then $\Gamma(A, B)$ is invertible; let its inverse be denoted by $\Gamma^{-1}(A, B)$.

Subsequently, in 2016, Abdalla and Bakhet [5] introduced the following extension of the beta matrix function:

$$\mathcal{B}(P,Q;\mathbb{X}) = \int_0^1 t^{P-1}(1-t)^{Q-1}\, \exp\left(-\frac{\mathbb{X}}{t(1-t)}\right)\, \mathrm{d}t, \tag{5}$$

where the matrices P, Q and $\mathbb{X}$ are positive stable and commutative matrices in $\mathbb{C}^{r\times r}$ satisfying the spectral condition (2).

The special case of (5) when $\mathbb{X} = \mathbf{0}$ gives the beta matrix function $\mathfrak{B}(P, Q)$ defined in (1) (see also [13]), that is,

$$\mathcal{B}(P,Q;\mathbf{0}) = \mathfrak{B}(P,Q).$$

Furthermore, under the given conditions we have the following identity (see [5]):

$$\mathcal{B}(P,Q;\mathbb{X}) = \Gamma(P,\mathbb{X})\Gamma(Q,\mathbb{X})\Gamma^{-1}(P+Q,\mathbb{X}).$$

In recent years, the generalized Pochhammer matrix symbol $(A;B)_n$ and the generalized beta matrix function $\mathcal{B}(P,Q;\mathbb{X})$ were used to introduce and investigate several extensions of hypergeometric matrix functions (see, for example, [4], [14]; see also the recent paper [20]).

On the other hand, Bakhet *et al.* [9] presented the Wright Kummer hypergeometric matrix function ${}_1\mathbf{R}_1^{(\tau)}$ and the Wright hypergeometric matrix function ${}_2\mathbf{R}_1^{(\tau)}$ as follows: let A, B and C be positive stable matrices in $\mathbb{C}^{r\times r}$ satisfying the condition (2). Then the Wright Kummer and Wright hypergeometric matrix functions are defined as

$${}_1\mathbf{R}_1^{(\tau)}(A;C;z) = \Gamma^{-1}(A)\Gamma(C)\sum_{n=0}^{\infty}\Gamma^{-1}(C+\tau nI)\Gamma(A+\tau nI)\,\frac{z^n}{n!},$$

and

$${}_2\mathbf{R}_1^{(\tau)}(A,B;C;z) = \Gamma^{-1}(B)\Gamma(C)\sum_{n=0}^{\infty}(A)_n\Gamma^{-1}(C+\tau nI)\Gamma(B+\tau nI)\,\frac{z^n}{n!},$$

where $\tau\in(0,\infty)$. In [9], the integral representations, differential formulas and fractional calculus of the Wright hypergeometric matrix function were studied. Furthermore, the incomplete Wright hypergeometric matrix function was defined and some of its properties were established. We remark in passing that the *incomplete* extension of the Pochhammer matrix symbol, which was also considered by Bakhet *et al.* [9], has also been used rather widely in the current literature on hypergeometric functions (see, for example, [2], [8], [18] and [19], and references therein). On the other hand, very recently, the authors (see [1,3,11]) introduced the extensions of the $(k;\tau)$-Gauss hypergeometric matrix function and obtained their various properties. Also, they used these functions to find the solutions of the generalization of fractional kinetic equation.

The goal of this paper is to introduce an extended form of ${}_2\mathbf{R}_1^{(\tau)}(A,B;C;z)$, which involves the Pochhammer matrix symbol $(A;B)_n$ defined by (3) and the extended beta matrix function $\mathcal{B}(P,Q;\mathbb{X})$ given by (5). The remainder of the paper is organized as follows. In Section 2, we define an extended form of the Wright hypergeometric matrix function,

$${}_2\mathbf{R}_1^{(\tau)}((A;\mathbb{A}),B;C;z;\mathbb{X}),$$

and obtain some useful results such as integral representations. In Section 3, we introduce the incomplete extended Wright hypergeometric matrix function with the help of the incomplete extended beta matrix function $\mathcal{B}_y(P,Q;\mathbb{X})$, and investigate some of its properties. In Section 4, we evaluate the Riemann–Liouville fractional derivative of this extended hypergeometric function. In Section 5, we make concluding remarks.

2. Extended Wright Hypergeometric Matrix Function

In this section, we introduce the extended Wright hypergeometric matrix function (EWHMF) ${}_2\mathbf{R}_1^{(\tau)}((A;\mathbb{A}),B;C;z;\mathbb{X})$ in terms of the generalized beta matrix function $\mathcal{B}(P,Q;\mathbb{X})$ defined by (5) and the generalized Pochhammer matrix symbol $(A;B)_n$ defined by (3).

Suppose that A, $\mathbb{A}$, B, C, $C-B$ and $\mathbb{X}$ are positive stable matrices in $\mathbb{C}^{r\times r}$ satisfying the condition (2), and suppose that B, C and $\mathbb{X}$ commute with each other. Then we introduce the EWHMF and the extended Wright Kummer hypergeometric matrix function (EWKHMF) as follows:

$$
{}_2\mathbf{R}_1^{(\tau)}((A;\mathbb{A}),B;C;z;\mathbb{X}) = \Gamma\binom{C}{B,C-B}\sum_{n=0}^{\infty}(A;\mathbb{A})_n\mathcal{B}(B+\tau nI,C-B;\mathbb{X})\,\frac{z^n}{n!}, \quad (6)
$$

$$
{}_1\mathbf{R}_1^{(\tau)}(B;C;z;\mathbb{X}) = \Gamma\binom{C}{B,C-B}\sum_{n=0}^{\infty}\mathcal{B}(B+\tau nI,C-B;\mathbb{X})\,\frac{z^n}{n!}, \quad (7)
$$

$$
|z|<1, \quad \tau\in(0,\infty),
$$

where $\Gamma\binom{C}{B,C-B} = \Gamma(C)\Gamma^{-1}(B)\Gamma^{-1}(C-B)$.

Remark 1. *In the particular case when $\mathbb{A}=\mathbb{X}=\mathbf{0}$, the definition (6) gives the Wright hypergeometric matrix function ${}_2\mathbf{R}_1^{(\tau)}(A,B;C;z)$ studied in [9], and the case with $\mathbb{A}=\mathbf{0}$ and $\tau=1$ gives the extended Gauss hypergeometric matrix function $F^{(\mathbb{X})}(A,B;C;z)$ given in [4]. Moreover, if we set $\mathbb{A}=\mathbb{X}=\mathbf{0}$ and $\tau=1$, the unification given in (6) reduces to the familiar Gauss hypergeometric matrix function ${}_2F_1(A,B;C;z)$ defined in [13]. On the other hand, if we consider $\mathbb{X}=\mathbf{0}$ in the definition (7), we get the Wright Kummer hypergeometric matrix function given in [9].*

We start with the following theorem.

Theorem 1. *Let A, $\mathbb{A}$, B, C, $C-B$ and $\mathbb{X}$ be positive stable matrices in $\mathbb{C}^{r\times r}$ satisfying the condition (2), and suppose that B, C and $\mathbb{X}$ commute with each other. Then the EWHMF ${}_2\mathbf{R}_1^{(\tau)}((A;\mathbb{A}),B;C;z;\mathbb{X})$ can be given in integral form as follows:*

$$
\begin{aligned}
{}_2\mathbf{R}_1^{(\tau)}((A;\mathbb{A}),B;C;z;\mathbb{X}) \;=\; & \Gamma\binom{C}{B,C-B,A}\int_0^{\infty}\int_0^1 u^{A-I}e^{-(Iu+\frac{\mathbb{A}}{u})}t^{B-I} \\
& \times(1-t)^{C-B-I}\exp\left(-\frac{\mathbb{X}}{t(1-t)}\right)e^{zut^{\tau}}\,dtdu.
\end{aligned}
$$

Proof. Using the integral representations (4) and (5), we get

$$
{}_2\mathbf{R}_1^{(\tau)}((A;\mathbb{A}),B;C;z;\mathbb{X}) \;=\; \Gamma\binom{C}{B,C-B,A}\int_0^{\infty}\int_0^1 u^{A-I}e^{-(Iu+\frac{\mathbb{A}}{u})}t^{B-I}
$$

$$\times(1-t)^{C-B-I}\exp\left(-\frac{\mathbb{X}}{t(1-t)}\right)\sum_{n=0}^{\infty}\frac{(zut^{\tau})^n}{n!}dtdu$$

$$= \Gamma\binom{C}{B, C-B, A}\int_0^{\infty}\int_0^1 u^{A-I}e^{-(Iu+\frac{\mathbb{A}}{u})}t^{B-I}$$

$$\times(1-t)^{C-B-I}\exp\left(-\frac{\mathbb{X}}{t(1-t)}\right)e^{zut^{\tau}}dtdu.$$

This completes the proof. □

Theorem 2. *Under the same conditions as Theorem 1, we have the following relation:*

$$_2\mathbf{R}_1^{(\tau)}((A;\mathbb{A}), B; C; z; \mathbb{X}) = \Gamma^{-1}(A)\int_0^{\infty} t^{A-I}e^{-(It+\frac{\mathbb{A}}{t})}{}_1\mathbf{R}_1^{(\tau)}(B; C; zt; \mathbb{X})dt.$$

Proof. Substituting the integral representation (4) into the definition (6), we have

$$_2\mathbf{R}_1^{(\tau)}((A;\mathbb{A}), B; C; z; \mathbb{X}) = \Gamma\binom{C}{B, C-B, A}\int_0^{\infty} t^{A-I}e^{-(It+\frac{\mathbb{A}}{t})}$$

$$\times\sum_{n=0}^{\infty}\mathcal{B}(B+\tau nI, C-B; \mathbb{X})\frac{(zt)^n}{n!}dt.$$

Now, using the definition (7) gives the result. □

Theorem 3. *Under the same conditions as Theorem 1, we have the following integral representation for the EWHMF:*

$$_2\mathbf{R}_1^{(\tau)}((A;\mathbb{A}), B; C; z; \mathbb{X}) = \Gamma\binom{C}{B, C-B}\int_0^1 t^{B-I}(1-t)^{C-B-I}\exp\left(-\frac{\mathbb{X}}{t(1-t)}\right)$$

$$\times{}_1F_0[(A;\mathbb{A}), -, zt^{\tau}]dt.$$

Proof. Substituting the integral representation (5) into the definition (6), we get

$$_2\mathbf{R}_1^{(\tau)}((A;\mathbb{A}), B; C; z; \mathbb{X})$$

$$= \Gamma\binom{C}{B, C-B}\int_0^1 t^{B-I}(1-t)^{C-B-I}\exp\left(-\frac{\mathbb{X}}{t(1-t)}\right)\sum_{n=0}^{\infty}(A;\mathbb{A})_n\frac{(zt^{\tau})^n}{n!}dt.$$

Since

$$_1F_0[(A;\mathbb{A}), -, zt^{\tau}] = \sum_{n=0}^{\infty}(A;\mathbb{A})_n\frac{(zt^{\tau})^n}{n!},$$

the result follows. □

3. Incomplete Extended Wright Hypergeometric Matrix Function

In this section, motivated by [21], we introduce the incomplete extended Wright hypergeometric matrix function (IEWHMF) with the help of the incomplete extended beta matrix function defined in (8). Let B, C and $\mathbb{X}$ be positive stable matrices in $\mathbb{C}^{r\times r}$ satisfying the condition (2), and suppose B, C and $\mathbb{X}$ commute with each other. The incomplete extended beta matrix function $\mathcal{B}_y(B,C;\mathbb{X})$ is defined as follows:

$$\mathcal{B}_y(B,C;\mathbb{X}) := \int_0^y t^{B-I}(1-t)^{C-I}\exp\left(-\frac{\mathbb{X}}{t(1-t)}\right)dt,\ 0\le y<1. \tag{8}$$

Let B, $C-B$ and $\mathbb{X}$ be positive stable matrices in $\mathbb{C}^{r\times r}$ satisfying the condition (2), and suppose B, C and $\mathbb{X}$ commute with each other. Then we introduce the incomplete extended beta matrix functions $[B,C;\mathbb{X};y]_n^{(\tau)}$ and $\{B,C;\mathbb{X};y\}_n^{(\tau)}$ as

$$[B,C;\mathbb{X};y]_n^{(\tau)} = \mathcal{B}_y(B+n\tau I, C-B;\mathbb{X}),$$

and

$$\{B,C;\mathbb{X};y\}_n^{(\tau)} = \mathcal{B}_{1-y}(C-B, B+n\tau I;\mathbb{X}),$$

where $0\le y<1$, respectively. It can be shown that

$$[B,C;\mathbb{X};y]_n^{(\tau)} + \{B,C;\mathbb{X};y\}_n^{(\tau)} = \mathcal{B}(B+n\tau I, C-B;\mathbb{X}).$$

Suppose that A, $\mathbb{A}$, B, C, $C-B$ and $\mathbb{X}$ are positive stable matrices in $\mathbb{C}^{r\times r}$ satisfying the condition (2), and that B, C and $\mathbb{X}$ commute with each other. Then we define the IEWHMFs as follows:

$$\begin{aligned} {}_2\mathbf{R}_1((A;\mathbb{A});[B,C;\mathbb{X};y]_n^{(\tau)};z;\mathbb{X}) &= \Gamma\begin{pmatrix} C \\ B, C-B\end{pmatrix} \\ &\quad\times\sum_{n=0}^{\infty}(A;\mathbb{A})_n\mathcal{B}_y(B+n\tau I, C-B;\mathbb{X})\frac{z^n}{n!}, \end{aligned} \tag{9}$$

and

$$\begin{aligned} {}_2\mathbf{R}_1((A;\mathbb{A});\{B,C;\mathbb{X};y\}_n^{(\tau)};z;\mathbb{X}) &= \Gamma\begin{pmatrix} C \\ B, C-B\end{pmatrix} \\ &\quad\times\sum_{n=0}^{\infty}(A;\mathbb{A})_n\mathcal{B}_{1-y}(C-B, B+n\tau I;\mathbb{X})\frac{z^n}{n!}. \end{aligned}$$

It can be seen that the IEWHMFs satisfy the following relation:

$$\begin{aligned} {}_2\mathbf{R}_1^{(\tau)}((A;\mathbb{A}),B;C;z;\mathbb{X}) &= {}_2\mathbf{R}_1((A;\mathbb{A});[B,C;\mathbb{X};y]_n^{(\tau)};z;\mathbb{X}) \\ &\quad+{}_2\mathbf{R}_1((A;\mathbb{A});\{B,C;\mathbb{X};y\}_n^{(\tau)};z;\mathbb{X}). \end{aligned}$$

Theorem 4. *Let A, $\mathbb{A}$, B, C, $C-B$ and $\mathbb{X}$ be positive stable matrices in $\mathbb{C}^{r\times r}$ satisfying the condition (2), and suppose that B, C and $\mathbb{X}$ commute with each other.*

Then we have the following integral representation for ${}_2\mathbf{R}_1((A;\mathbb{A});[B,C;\mathbb{X};y]_n^{(\tau)};z;\mathbb{X})$*:*

$$\begin{aligned}{}_2\mathbf{R}_1((A;\mathbb{A});[B,C;\mathbb{X};y]_n^{(\tau)};z;\mathbb{X}) &= \Gamma\binom{C}{B,C-B,A}y^B \\ &\times\int_0^\infty\int_0^1 u^{A-I}e^{-(Iu+\frac{\mathbb{A}}{u})}v^{B-I}(1-yv)^{C-B-I} \\ &\times\exp\left(-\frac{\mathbb{X}}{yv(1-yv)}\right)e^{uz(yv)^\tau}dvdu.\end{aligned}$$

Proof. From the definitions (3) and (8), straightforward calculations show that

$$\begin{aligned}{}_2\mathbf{R}_1((A;\mathbb{A});[B,C;\mathbb{X};y]_n^{(\tau)};z;\mathbb{X}) &= \Gamma\binom{C}{B,C-B,A}y^B \\ &\times\int_0^\infty\int_0^1 u^{A-I}e^{-(Iu+\frac{\mathbb{A}}{u})}v^{B-I}(1-yv)^{C-B-I} \\ &\times\exp\left(-\frac{\mathbb{X}}{yv(1-yv)}\right)\sum_{n=0}^\infty\frac{(uz(yv)^\tau)^n}{n!}dvdu,\end{aligned}$$

which proves the theorem. □

Theorem 5. *Under the conditions given in Theorem 4, let* $|z(uy)^\tau|<1$*. Then we have the following integral representation:*

$$\begin{aligned}{}_2\mathbf{R}_1((A;\mathbb{A});[B,C;\mathbb{X};y]_n^{(\tau)};z;\mathbb{X}) &= \Gamma\binom{C}{B,C-B}y^B \\ &\times\int_0^1 u^{B-I}(1-uy)^{C-B-I}\exp\left(-\frac{\mathbb{X}}{uy(1-uy)}\right) \\ &\times{}_1F_0((A;\mathbb{A}),-,z(uy)^\tau)du.\end{aligned}$$

Proof. Using the integral representation (8) and applying similar calculations as in Theorem 3 proves the theorem. □

Next, we give a derivative formula for the IEWHMF.

Theorem 6. *Let* ${}_2\mathbf{R}_1((A;\mathbb{A});[B,C;\mathbb{X};y]_n^{(\tau)};z;\mathbb{X})$ *be defined in* (9)*. Then we have the following derivative formula:*

$$\begin{aligned}&\frac{d^n}{dz^n}({}_2\mathbf{R}_1((A;\mathbb{A});[B,C;\mathbb{X};y]_n^{(\tau)};z;\mathbb{X})) \\ &=\Gamma\binom{C}{B,C-B}\Gamma\binom{C-B,B+\tau I}{C+\tau I}\Gamma\binom{C-B,B+2\tau I}{C+2\tau I}\ldots\Gamma\binom{C-B,B+\tau nI}{C+\tau nI} \\ &\times(A)_n\quad{}_2\mathbf{R}_1((A+nI;\mathbb{A});[B+\tau nI,C+\tau nI;\mathbb{X};y]_n^{(\tau)};z;\mathbb{X}).\end{aligned}$$

Proof. It is straightforward to obtain that

$$\frac{d}{dz}({}_2\mathbf{R}_1((A;\mathbb{A});[B,C;\mathbb{X};y]_n^{(\tau)};z;\mathbb{X}))$$

$$= \Gamma\binom{C}{B, C-B}\Gamma\binom{C-B, B+\tau I}{C+\tau I}A \times {}_2\mathbf{R}_1((A+I;\mathbb{A});[B+\tau I, C+\tau I;\mathbb{X};y]_n^{(\tau)};z;\mathbb{X}).$$

Repeating this n times proves the result. □

4. Fractional Derivative

In this section, we study the extended Riemann–Liouville fractional derivative of the EWHMF defined by (6). Let $\mathbb{X}$ be a positive stable matrix in $\mathbb{C}^{r\times r}$ and $\mu \in \mathbb{C}$. The extended Riemann–Liouville fractional derivative of order μ is given by [20]

$$D_z^{\mu,\mathbb{X}} f(z) = \frac{1}{\Gamma(-\mu)}\int_0^z f(t)(z-t)^{-\mu-1}\ \exp\left(-\frac{\mathbb{X}z^2}{t(z-t)}\right)\ \mathrm{d}t, \qquad (10)$$

$$\big(\Re(\mu)<0\big).$$

The particular case $\mathbb{X}=p$, $p\in\mathbb{C}^{1\times 1}$, such that $\Re(p)\geq 0$, gives the extended Riemann–Liouville fractional derivative given in [16] (see also [17]). Moreover, $\mathbb{X}=0$ yields the classical Riemann–Liouville fractional derivative operator D_z^{μ} (for details, see [15]).

In [20], the authors presented the extended Riemann-Liouville fractional derivative of the function $f(z)=z^A$.

Theorem 7. *([20]) Let A be a positive stable matrix in $\mathbb{C}^{r\times r}$ and $\Re(\mu)<0$. Then*

$$D_z^{\mu,\mathbb{X}}\{z^A\} = \frac{\mathcal{B}(A+I,-\mu I;\mathbb{X})}{\Gamma(-\mu)}\ z^{A-\mu I}.$$

Proof. According the definition (10), it is clear that

$$D_z^{\mu,\mathbb{X}}\{z^A\} = \frac{1}{\Gamma(-\mu)}\int_0^z t^A(z-t)^{-\mu-1}\ \exp\left(-\frac{\mathbb{X}z^2}{t(z-t)}\right)\ \mathrm{d}t. \qquad (11)$$

Upon setting $t=zu$ and $\mathrm{d}t = z\mathrm{d}u$ in (11) gives

$$\begin{aligned} D_z^{\mu,\mathbb{X}}\{z^A\} &= \frac{1}{\Gamma(-\mu)}\int_0^1 (uz)^A(z-uz)^{-\mu-1}\ \exp\left(-\frac{\mathbb{X}z^2}{uz(z-uz)}\right)\ z\mathrm{d}u \\ &= \frac{1}{\Gamma(-\mu)}z^{A-\mu I}\int_0^1 u^A(1-u)^{(-\mu-1)I}\ \exp\left(-\frac{\mathbb{X}}{u(1-u)}\right)\ \mathrm{d}u \\ &= \frac{\mathcal{B}(A+I,-\mu I;\mathbb{X})}{\Gamma(-\mu)}z^{A-\mu I}, \end{aligned}$$

which completes the proof. □

We now prove the following theorem.

Theorem 8. *Let A, $\mathbb{A}$ and $\mathbb{X}$ be positive stable matrices in $\mathbb{C}^{r\times r}$ satisfying the condition (2) and let $\Re(\mu) > \Re(\lambda) > 0$. Then for $|z^\tau| < 1$, the following relation holds true for the EWHMF:*

$$D_z^{\lambda-\mu,\mathbb{X}}\left\{z^{(\lambda-1)I}\,{}_1F_0[(A;\mathbb{A});\ —\ ;z^\tau]\right\} = \frac{\Gamma(\lambda)}{\Gamma(\mu)} z^{(\mu-1)I}\ {}_2\boldsymbol{R}_1^{(\tau)}((A;\mathbb{A}),\lambda I;\mu I;z^\tau;\mathbb{X}).$$

Proof. According to the extended fractional derivative formula (10), we have

$$\begin{aligned} &D_z^{\lambda-\mu,\mathbb{X}}\left\{z^{(\lambda-1)I}\ {}_1F_0[(A;\mathbb{A});\ —\ ;z^\tau]\right\} \\ &= \frac{1}{\Gamma(\mu-\lambda)}\int_0^z t^{(\lambda-1)I}\ {}_1F_0[(A;\mathbb{A});\ —\ ;t^\tau] \\ &\quad\times (z-t)^{\mu-\lambda-1}\ \exp\left(-\frac{\mathbb{X}z^2}{t(z-t)}\right)\ \mathrm{d}t. \end{aligned} \tag{12}$$

Let $t = zu$ in (12), then if we consider Theorem 3 we obtain the result asserted by Theorem 8. □

Theorem 9. *Suppose that A, $\mathbb{A}$, B, C, $C-B$ and $\mathbb{X}$ are positive stable matrices in $\mathbb{C}^{r\times r}$ satisfying the condition (2) and that B, C and $\mathbb{X}$ commute with each other. Let $\Re(\mu) < 0$, then for $|xz^\tau| < 1$, we have*

$$\begin{aligned} &D_z^{\mu,\mathbb{X}}\left\{z^{C-I}\ {}_2\boldsymbol{R}_1^{(\tau)}((A;\mathbb{A}),B;C;xz^\tau;\mathbb{X})\right\} \\ &= \Gamma\begin{pmatrix} C, C-B-\mu I \\ C-\mu I, C-B, -\mu I\end{pmatrix}\Gamma\begin{pmatrix} C-B, -\mu I;\mathbb{X} \\ C-B-\mu I\end{pmatrix} \\ &\quad\times {}_2\mathbf{R}_1^{(\tau)}((A;\mathbb{A}),B;C-\mu I;xz^\tau;\mathbb{X})z^{C-\mu I-I}, \end{aligned} \tag{13}$$

where $\Gamma\binom{C-B,-\mu I;\mathbb{X}}{C-B-\mu I} = \Gamma(C-B;\mathbb{X})\Gamma(-\mu I;\mathbb{X})\Gamma^{-1}(C-B-\mu I;\mathbb{X})$.

Proof. Consider the definitions (6) and (10) and let the left-hand side of (13) be denoted by $\mathfrak{D}$. Direct calculations yield that

$$\begin{aligned} \mathfrak{D} &= \frac{1}{\Gamma(-\mu)}\int_0^z t^{C-I}\ {}_2\boldsymbol{R}_1^{(\tau)}((A;\mathbb{A}),B;C;xt^\tau;\mathbb{X})(z-t)^{-\mu-1}\ \exp\left(-\frac{\mathbb{X}z^2}{t(z-t)}\right)\ \mathrm{d}t \\ &= \Gamma\begin{pmatrix} C \\ B, C-B\end{pmatrix}\frac{1}{\Gamma(-\mu)}\ \sum_{n=0}^{\infty}(A;\mathbb{A})_n\mathcal{B}(B+\tau nI, C-B;\mathbb{X})\ \frac{x^n}{n!} \\ &\quad\times\int_0^z t^{\tau nI+C-I}(z-t)^{-\mu-1}\ \exp\left(-\frac{\mathbb{X}z^2}{t(z-t)}\right)\ \mathrm{d}t. \end{aligned}$$

Then we have

$$\begin{aligned} \mathfrak{D} &= \Gamma\begin{pmatrix} C \\ B, C-B\end{pmatrix}\frac{1}{\Gamma(-\mu)}\ \sum_{n=0}^{\infty}(A;\mathbb{A})_n\mathcal{B}(B+\tau nI, C-B;\mathbb{X}) \\ &\quad\times\mathcal{B}(\tau nI+C,-\mu I;\mathbb{X})\frac{(z^\tau x)^n}{n!}z^{C-\mu I-I} \end{aligned}$$

$$
\begin{aligned}
&= \Gamma\binom{C}{B, C-B} \frac{1}{\Gamma(-\mu)} \Gamma(C-B;\mathbb{X})\Gamma(-\mu I;\mathbb{X}) \\
&\quad \times \sum_{n=0}^{\infty} (A;\mathbb{A})_n \Gamma(B+\tau n I;\mathbb{X})\Gamma^{-1}(C+\tau n I-\mu I;\mathbb{X})\ \frac{(z^\tau x)^n}{n!} z^{C-\mu I-I} \\
&= \Gamma\binom{C}{B, C-B} \Gamma\binom{C-B, -\mu I;\mathbb{X}}{C-B-\mu I} \frac{1}{\Gamma(-\mu)} \\
&\quad \times \sum_{n=0}^{\infty} (A;\mathbb{A})_n \mathcal{B}(B+\tau n I, C-B-\mu I;\mathbb{X})\ \frac{(z^\tau x)^n}{n!} z^{C-\mu I-I} \\
&= \Gamma\binom{C, C-B-\mu I}{C-\mu I, C-B, -\mu I} \Gamma\binom{C-B, -\mu I;\mathbb{X}}{C-B-\mu I} \\
&\quad \times \Gamma(C-\mu I)\Gamma^{-1}(C-B-\mu I)\Gamma^{-1}(B) \\
&\quad \times \sum_{n=0}^{\infty} (A;\mathbb{A})_n \mathcal{B}(B+\tau n I, C-B-\mu I;\mathbb{X})\ \frac{(z^\tau x)^n}{n!} z^{C-\mu I-I}.
\end{aligned}
$$

Thus the result follows by the definition (6) of the EWHMF. □

Theorem 10. *Suppose that A, $\mathbb{A}$, B, C, $C-B$, $\mathbb{X}_1$ and $\mathbb{X}_2$ are positive stable matrices in $\mathbb{C}^{r\times r}$ satisfying the condition (2) and that B, C and $\mathbb{X}_1$ commute with each other. Let $\Re(\mu) > \Re(\lambda) > 0$ and $\left|\frac{x}{1-z^{\tau_2}}\right| < 1$, then we have*

$$
\begin{aligned}
&D_z^{\lambda-\mu,\mathbb{X}_2}\left\{ z^{(\lambda-1)I}(1-z^{\tau_2})^{-A}\ {}_2\boldsymbol{R}_1^{(\tau_1)}\left((A;\mathbb{A}), B; C; \frac{x}{1-z^{\tau_2}};\mathbb{X}_1\right)\right\} \\
&= \Gamma^{-1}(\mu I)\Gamma(\lambda I) z^{(\mu-1)I} F_2^{(\tau_1,\tau_2)}(A, B, \lambda I; C, \mu I; x, z^{\tau_2};\mathbb{X}_1,\mathbb{X}_2;\mathbb{A}),
\end{aligned}
$$

where $\tau_1, \tau_2 \in (0,\infty)$ and $F_2^{(\tau_1,\tau_2)}(A, B, C; D, E; x, y;\mathbb{X}_1,\mathbb{X}_2;\mathbb{A})$ is a two-variable function defined by

$$
\begin{aligned}
&F_2^{(\tau_1,\tau_2)}(A, B, C; D, E; x, y;\mathbb{X}_1,\mathbb{X}_2;\mathbb{A}) \qquad (14)\\
&\quad = \Gamma\binom{D, E}{B, D-B, C, E-C} \sum_{m,n=0}^{\infty} (A;\mathbb{A})_m (A+mI)_n \\
&\qquad \times \mathcal{B}(B+\tau_1 m I, D-B;\mathbb{X}_1)\mathcal{B}(C+\tau_2 n I, E-C;\mathbb{X}_2)\ \frac{x^m}{m!}\ \frac{y^n}{n!}.
\end{aligned}
$$

Proof. Considering the definition (6) and Theorem 7, we get

$$
\begin{aligned}
&D_z^{\lambda-\mu,\mathbb{X}_2}\left\{ z^{(\lambda-1)I}(1-z^{\tau_2})^{-A}\ {}_2\boldsymbol{R}_1^{(\tau_1)}\left((A;\mathbb{A}), B; C; \frac{x}{1-z^{\tau_2}};\mathbb{X}_1\right)\right\} \\
&\quad = D_z^{\lambda-\mu,\mathbb{X}_2}\{\Gamma\binom{C}{B, C-B} z^{(\lambda-1)I}(1-z^{\tau_2})^{-A}
\end{aligned}
$$

$$\times \sum_{m=0}^{\infty}(A;\mathbb{A})_m\mathcal{B}(B+\tau_1 mI, C-B;\mathbb{X}_1)\ \frac{\left(\frac{x}{1-z^{\tau_2}}\right)^m}{m!}\}$$
$$=\Gamma\binom{C}{B, C-B}\sum_{m,n=0}^{\infty}(A;\mathbb{A})_m(A+mI)_n\mathcal{B}(B+\tau_1 mI, C-B;\mathbb{X}_1)$$
$$\times D_z^{\lambda-\mu,\mathbb{X}_2}\{z^{\tau_2 nI+(\lambda-1)I}\}\ \frac{x^m}{n!m!}$$
$$=\Gamma\binom{C}{B, C-B}\frac{z^{(\mu-1)I}}{\Gamma(\mu-\lambda)}\sum_{m,n=0}^{\infty}(A;\mathbb{A})_m(A+mI)_n\mathcal{B}(B+\tau_1 mI, C-B;\mathbb{X}_1)$$
$$\times \mathcal{B}(\tau_2 nI+\lambda I, (\mu-\lambda)I;\mathbb{X}_2)\ \frac{(z^{\tau_2})^n x^m}{n!m!}$$
$$=\Gamma^{-1}(\mu I)\Gamma(\lambda I)z^{(\mu-1)I}F_2^{(\tau_1,\tau_2)}(A,B,\lambda I;C,\mu I;x,z^{\tau_2};\mathbb{X}_1,\mathbb{X}_2;\mathbb{A}).$$

□

Remark 2. *Note that, when $\tau_1,\tau_2=1$, $\mathbb{A}=\mathbf{0}$ and $\mathbb{X}_1=\mathbb{X}_2$, the definition* (14) *gives the extended Appell hypergeometric matrix function $F_2(A,B,C;D,E;x,y;\mathbb{X})$ introduced in [20].*

5. Concluding Remarks

In our investigation here, we have introduced and studied the EWHMF

$${}_2\mathbf{R}_1^{(\tau)}((A;\mathbb{A}),B;C;z;\mathbb{X}).$$

We have presented various potentially useful properties of this family of extended hypergeometric matrix functions. Many of the results derived in this paper can be shown to reduce to known or new results about functions previously defined in the literature. For instance, in some particular cases, Theorems 8-10 yield new fractional-derivative formulas for various known families of hypergeometric functions.

Author Contribution Statement All authors jointly worked on the results and they read and approved the final manuscript.

Declaration of Competing Interests The authors declare that they have no competing interest.

References

[1] Abd-Elmageed, H., Hidan, M., Abdalla, M., Investigation for the k-analogue of τ-Gauss hypergeometric matrix functions and associated fractional calculus, Linear and Multilinear Algebra, (2022), 1-14. https://doi.org/10.1080/03081087.2022.2161459

[2] Abdalla, M., On the incomplete hypergeometric matrix functions, Ramanujan J., 43 (2017), 663-678. https://doi.org/10.1007/s11139-016-9795-z

[3] Abdalla, A., Akel, M., Contribution of using Hadamard fractional integral operator via Mellin integral transform for solving certain fractional kinetic matrix equations, Fractal and Fractional, 6(6) (2022), 305. https://doi.org/10.3390/ fractalfract6060305

[4] Abdalla, M., Bakhet, A., Extended Gauss hypergeometric matrix functions, Iran J Sci Technol Trans Sci., 42 (2018), 1465-1470. https://doi.org/10.1007/s40995-017-0183-3

[5] Abdalla, M., Bakhet, A., Extension of beta matrix function, Asian J Math Comput Res., 9 (2016), 253-264.

[6] Abdalla, M., Fractional operators for the Wright hypergeometric matrix functions, Advances in Difference Equations, (2020), 246. https://doi.org/10.1186/s13662-020-02704-y

[7] Abul-Dahab, M. A., Bakhet, A. K., A certain generalized gamma matrix functions and their properties, J. Ana. Num. Theor., 3(1) (2015), 63-68. https://dx.doi.org/10.12785/jant/030110

[8] Bakhet, A., Hyder, A. A., Almoneef, A. A., Niyaz, M., Soliman, A. H., On new matrix version extension of the incomplete Wright hypergeometric functions and their fractional calculus, Mathematics, 10(22) (2022), 4371. https://doi.org/10.3390/math10224371

[9] Bakhet, A., Jiao, Y., He, F., On the Wright hypergeomertric matrix functions and their fractional calculus, Integral Transforms Spec. Funct., 30 (2019), 138-156. https://doi.org/10.1080/10652469.2018.1543669

[10] Dwivedi, R., Sanjhira, R., On the matrix function ${}_pR_q(A;B;z)$ and its fractional calculus properties, Communications in Mathematics, 31(1) (2023), 43-56. https://doi.org/10.46298/cm.10205

[11] Hidan, M., Akel, M., Abd-Elmageed, H., Abdalla, M., Solution of fractional kinetic equations involving extended $(k;\tau)$-Gauss hypergeometric matrix functions, AIMS Math., 7(8) (2022), 14474-14491. https://doi.org/10.3934/math.2022798

[12] Jódar, L., Cortés, J. C., Some properties of gamma and beta matrix functions, Appl. Math. Lett., 11 (1998), 89-93. https://doi.org/10.1016/S0893-9659(97)00139-0

[13] Jódar, L., Cortés, J. C., On the hypergeometric matrix functions, J. Compute. Appl. Math., 99 (1998), 205-217. https://doi.org/10.1016/S0377-0427(98)00158-7

[14] Khammash, G. S., Agarwal, P., Choi, J., Extended k-gamma and k-beta functions of matrix arguments, Mathematics, 8 (2020), 1715. https://doi.org/10.3390/math8101715

[15] Kilbas, A. A., Srivastava, H. M. and Trujillo, J. J., Theory and Applications of Fractional Differential Equations, North-Holland Mathematical Studies, Elsevier (North-Holland) Science Publishers, Amsterdam, (2006), 204.

[16] Özarslan, M. A., Ustaoğlu, C., Incomplete Caputo fractional derivative operators, *Adv. Differ. Equ.*, (2018), 209. https://doi.org/10.1186/s13662-018-1656-1

[17] Özarslan, M. A., Ustaoğlu, C., Some incomplete hypergeometric functions and incomplete Riemann-Liouville fractional integral operators, *Mathematics*, 7 (2018), 483. https://doi.org/10.3390/math7050483

[18] Verma, A., On the incomplete Srivastava's triple hypergeometric matrix functions, *Quaest Math.*, (2020), 1-24. https://doi.org/10.2989/16073606.2020.1753123

[19] Verma, A., Yadav, S., On the incomplete second Appell hypergeometric matrix functions, *Linear Multilinear Algebra*, (2019). https://doi.org/10.1080/03081087.2019.1640178

[20] Verma, A., Dwivedi, R., Sahai, V., Some extended hypergeometric matrix functions and their fractional calculus, (2020), arXiv:2011.00772v1. https://doi.org/10.48550/arXiv.2011.00772

[21] Zou, C., Yu, M., Bakhet, A., He, F., On the matrix versions of incomplete extended gamma and beta functions and their applications for the incomplete Bessel, *Complexity*, (2020). https://doi.org/10.1155/2021/5586021

http://communications.science.ankara.edu.tr

Commun.Fac.Sci.Univ.Ank.Ser. A1 Math. Stat.
Volume 72, Number 3, Pages 618–632 (2023)
DOI:10.31801/cfsuasmas.1184273
ISSN 1303-5991 E-ISSN 2618-6470

COMMUNICATIONS SERIES A1

Research Article; Received:October 4, 2022; Accepted: April 3, 2023

ON THE TOPOLOGICAL CATEGORY OF NEUTROSOPHIC CRISP SETS

Samed ÖZKAN
Department of Mathematics, Nevşehir Hacı Bektaş Veli University, Nevşehir, TÜRKİYE

ABSTRACT. In this work, we explicitly characterize local separation axioms as well as generic separation axioms in the topological category of neutrosophic crisp sets, and examine their mutual relationship. Moreover, we characterize several distinct notions of closedness, compactness and connectedness in **NCSet**, and study their relationship with each other.

1. INTRODUCTION

As a generalization of crisp sets, Zadeh [30] introduced fuzzy set theory in 1965. Without a doubt, the fuzzy set theory is effective in dealing with imprecise estimates, yet it was unable to explain the level of dissatisfaction (non-membership). The intuitionistic fuzzy set (IFS) model was established by Atanassov [1] to address these weaknesses of fuzzy sets. This model is more accurate and useful than fuzzy sets since it can manage both membership and nonmembership degrees. The IFSs offer more space in terms of applications for decision-making because they can handle data both in favor (membership value) and against (non-membership value) of the possibilities given.

The concept of a neutrosophic set taking into account the degrees of membership, non-membership, and indeterminacy was first suggested by Smarandache [29] in 1998. Additionally, Salama and Smarandache [28] introduced the idea of a neutrosophic crisp set in a set in 2015. They also provided definitions of neutrosophic crisp empty (resp. whole) set as more than two types, inclusion between two neutrosophic crisp sets, complement of a neutrosophic crisp set and intersection (union) of two neutrosophic crisp sets. In 2017, Hur et al [18] defined several categorical

2020 *Mathematics Subject Classification.* 54B30, 18D15, 54D10, 06F07, 03E72.
Keywords. Topological category, neutrosophic crisp set, separation, closedness, compactness, connectedness.
ozkans@nevsehir.edu.tr; 0000-0003-3063-6168.

properties of neutrosophic crisp set and showed that **NCSet** (the category of neutrosophic crisp spaces and neutrosophic crisp maps) is a cartesian closed topological category.

Categorical topology is that field of mathematics where general topology and category theory overlap, was introduced by Herrlich [17] in 1971, and the purpose was to apply categorical concepts and results to topological settings and to explain not only the original topological phenomena but similar phenomena throughout topology as well as in other fields.

Due to huge importance of neutrosophic crisp sets in decision-making, it motivates us to characterize several fundamental concepts of topology including Hausdorffness, closedness, compactness and connectedness in the topological category of **NCSet**.

The following are the paper's main goals:

(i) to characterize local T_0, T_1, $PreT_2$ objects in the category of neutrosophic crisp sets and to examine how they are related,

(ii) to provide the characterization of generic separation axioms and several distinct version of Hausdorff objects in **NCSet**,

(iii) to give the explicit characterization of several notions of closedness, compactness and connectness in topological category of **NCSet**,

(iv) to compare our results with the ones in some other categories.

2. Preliminaries

All preliminary information and more about neutrosophic crisp spaces can be found in [28].

Definition 1. *[18, 28] Let A be a non-empty set.*

(1) *If $\mathcal{N}$ has the form $\mathcal{N} = (N_1, N_2, N_3)$, where N_1, N_2, and N_3 are subsets of A, then $\mathcal{N}$ is referred to as a neutrosophic crisp set (NCS) on A. The pair $(A, \mathcal{N})$ is called a neutrosophic crisp space (NCSp). The set of all NCSs on A will be represented by $NCS(A)$.*

(2) *The neutrosophic crisp empty set, $\emptyset_{nc}$ is an NCS on A defined by $\emptyset_{nc} = (\emptyset, \emptyset, A)$.*

(3) *The neutrosophic whole set, A_{nc} is an NCS on A defined by $A_{nc} = (A, A, \emptyset)$.*

(4) *Let $\{\mathcal{N}_i\}_{i\in I}$ be a family of NCSs on A, where $\mathcal{N}_i = (N_{i1}, N_{i2}, N_{i3})$. Then*

   (i) *$\bigcap_{i\in I} \mathcal{N}_i$, the intersection of $\{\mathcal{N}_i\}_{i\in I}$, is an NCS on A defined by*

$$\bigcap \mathcal{N}_i = (\bigcap N_{i1}, \bigcap N_{i2}, \bigcup N_{i3}),$$

   (ii) *$\bigcup_{i\in I} \mathcal{N}_i$, the union of $\{\mathcal{N}_i\}_{i\in I}$, is an NCS on A defined by*

$$\bigcup \mathcal{N}_i = (\bigcup N_{i1}, \bigcup N_{i2}, \bigcap N_{i3}).$$

Definition 2. *[18] Let $(A, \mathcal{N})$, $(B, \mathcal{M})$ be NCSps and $f\colon A \to B$ be a map. Then $f\colon (A, \mathcal{N}) \to (B, \mathcal{M})$ is called a morphism, if $\mathcal{N} \subset f^{-1}(\mathcal{M})$, equivalently, $N_1 \subset$*

$f^{-1}(M_1)$, $N_2 \subset f^{-1}(M_2)$ and $N_3 \supset f^{-1}(M_3)$, where $\mathcal{N} = (N_1, N_2, N_3)$ and $\mathcal{M} = (M_1, M_2, M_3)$.

Definition 3. *The category of neutrosophic crisp spaces,* **NCSet** *has the pairs $(A, \mathcal{N})$ as objects, where A is any non-empty set and $\mathcal{N}$ is a neutrosophic crisp set on A, and has morphisms. In this case, every morphism in* **NCSet** *is called a* **NCSet***-map.*

Lemma 1. *(cf. [18])*

(1) *Let A be a set, $\{(A_j, \mathcal{N}_j)\}_{j\in J}$ be any families of NCSps and $\{f_j : (A, \mathcal{N}_A) \to (A_j, \mathcal{N}_j)\}_{j\in J}$ be a source. Then,*

$$\mathcal{N}_A = \bigcap_{j\in J} f_j^{-1}(\mathcal{N}_j)$$

is an initial structure on A, where $\mathcal{N}_A = (N_{A1}, N_{A2}, N_{A3})$ and $\mathcal{N}_j = (N_{j1}, N_{j2}, N_{j3})$.

(2) *Let B be a set, $\{(A_j, \mathcal{N}_j)\}_{j\in J}$ be any families of NCSps and $\{g_j : (A_j, \mathcal{N}_j) \to (B, \mathcal{N}_B)\}_{j\in J}$ be a sink. Then,*

$$\mathcal{N}_B = \bigcup_{j\in J} g_j(\mathcal{N}_j)$$

is a final structure on B, where $\mathcal{N}_B = (N_{B1}, N_{B2}, N_{B3})$ and $\mathcal{N}_j = (N_{j1}, N_{j2}, N_{j3})$.

(3) *Let $(A, \mathcal{N})$ be a neutrosophic crisp space (NCSp).*
   (i) *A neutrosophic crisp structure on A is discrete whenever $\mathcal{N} = \emptyset_{nc}$.*
   (ii) *A neutrosophic crisp structure on A is indiscrete whenever $\mathcal{N} = A_{nc}$.*

Remark 1. *The forgetful functor $\mathcal{U}$:* **NCSet** $\to$ **Set** *is topological, i.e., the category* **NCSet** *is topological over* **Set** *[18], but the functor $\mathcal{U}$ is not normalized (i.e., subterminals, have a unique structure) since a singleton set $\{a\}$ has multiple neutrosophic crisp structures on it.*

3. Local Separation Axioms in Neutrosophic Crisp Sets

Let p be a point in a set B and $B \vee_p B$ be the *wedge product* of B at p ([2], p. 334), i.e., two disjoint copies of B identified at p. If a point b in $B \vee_p B$ is in the first component, it is denoted as b_1, and if it is in the second component, it is denoted as b_2.

Definition 4. *[2] Let B^2 denote the cartesian product of B.*

(1) *The map $\mathcal{A}_p : B \vee_p B \to B^2$ is called principal p-axis map iff*

$$\mathcal{A}_p(b_i) = \begin{cases} (b,p), & i = 1 \\ (p,b), & i = 2 \end{cases}$$

(2) *The map* $\mathcal{S}_p : B \vee_p B \to B^2$ *is called skewed* p*-axis map iff*

$$\mathcal{S}_p(b_i) = \begin{cases} (b,b), & i=1 \\ (p,b), & i=2 \end{cases}$$

(3) *The map* $\nabla_p : B \vee_p B \to B$ *is called fold map at* p *provided that* $\nabla_p(b_i) = b$ *for* $i = 1, 2$.

Definition 5. *[2] Let* $U : \mathcal{E} \to \mathbf{Set}$ *be topological,* $A \in Ob(\mathcal{E})$ *with* $U(A) = B$ *and* $p \in B$.

(i) *A is* $\overline{T_0}$ *at* p *iff the initial lift of the* U*-source* $\{\mathcal{A}_p : B \vee_p B \to U(A^2) = B^2$ *and* $\nabla_p : B \vee_p B \to UD(B) = B\}$ *is discrete, where* D *is the discrete functor.*

(ii) *A is* T_0' *at* p *iff the initial lift of the* $\mathcal{U}$*-source* $\{id : B \vee_p B \to \mathcal{U}(A \vee_p A) = B \vee_p B$ *and* $\nabla_p : B \vee_p B \to \mathcal{UD}(B) = B\}$ *is discrete, where* $A \vee_p A$ *is the wedge in* $\mathcal{E}$*, i.e., the final lift of the* $\mathcal{U}$*-sink* $\{i_1, i_2 : \mathcal{U}(A) = B \to B \vee_p B\}$ *where* i_1, i_2 *denote the canonical injections.*

(iii) *A is* T_1 *at* p *iff the initial lift of the* U*-source* $\{\mathcal{S}_p : B \vee_p B \to U(A^2) = B^2$ *and* $\nabla_p : B \vee_p B \to UD(B) = B\}$ *is discrete.*

(iv) *A is* $Pre\overline{T}_2$ *at* p *iff the initial lift of the* $\mathcal{U}$*-source* $\{\mathcal{A}_p : B \vee_p B \to \mathcal{U}(A^2) = B^2\}$ *and the initial lift of the* $\mathcal{U}$*-source* $\{\mathcal{S}_p : B \vee_p B \to \mathcal{U}(A^2) = B^2\}$ *agree.*

(v) *A is* $PreT_2'$ *at* p *iff the initial lift of the* $\mathcal{U}$*-source* $\{\mathcal{S}_p : B \vee_p B \to \mathcal{U}(A^2) = B^2\}$ *and the final lift of the* $\mathcal{U}$*-sink* $\{i_1, i_2 : \mathcal{U}(A) = B \to B \vee_p B\}$ *agree.*

(vi) *A is* $\overline{T}_2$ *at* p *iff A is* $\overline{T}_0$ *at* p *and* $Pre\overline{T}_2$ *at* p.

(vii) *A is* T_2' *at* p *iff A is* T_0' *at* p *and* $PreT_2'$ *at* p.

Remark 2. (1) *Particularly, we have the following for the category of topological spaces,* ***Top****:*

(a) $\overline{T}_0$ *at* p *and* T_0' *at* p *(resp.* T_1 *at* p*) reduce to for each* $x \in X$ *with* $x \neq p$*, there exists a neighborhood of* x *that doesn't contain* p *or (resp. and) there exists a neighborhood of* p *that doesn't contain* x *[5].*

(b) $Pre\overline{T}_2$ *at* p *and* $PreT_2'$ *at* p *are equivalent, and they both reduce to for each point* x *distinct from* p*, there exist disjoint neighborhoods of* x *and* p *if the set* $\{x, p\}$ *is not indiscrete [5].*

(c) $\overline{T}_2$ *at* p *and* T_2' *at* p *are equivalent, and they both reduce to for each* $x \in X$ *with* $x \neq p$*, there exist disjoint neighborhoods of* x *and* p *[5].*

(2) *Local separation axioms are used to introduce the notions of (strong) closedness in set-based topological categories which are defined in [3]. These notions are used in [2,9,10] to generalize each of the notions of Hausdorffness, compactness, perfectness and connectedness to arbitrary set-based topological categories. Additionally, it is shown in [9] that they constitute suitable closure operators in the sense of Dikranjan and Giuli [16] in various well-known topological categories.*

Theorem 1. *Let $(A,\mathcal{N})$, $(B,\mathcal{M})$ be NCSps and $f:(A,\mathcal{N})\to(B,\mathcal{M})$ be a* **NCSet***-map. If $(B,\mathcal{M})$ is discrete, then so is $(A,\mathcal{N})$, i.e., f reflects discreteness.*

Proof. Let $(B,\mathcal{M})$ be discrete, i.e., $\mathcal{M}=\emptyset_{nc}$, but $(A,\mathcal{N})$ be not discrete, i.e., $\mathcal{N}\neq\emptyset_{nc}$. Since $f:(A,\mathcal{N})\to(B,\mathcal{M})$ is in **NCSet**, it follows that $\mathcal{N}\subset f^{-1}(\mathcal{M}=\emptyset_{nc})=\emptyset_{nc}$ and consequently $\mathcal{N}=\emptyset_{nc}$, a contradiction. □

Theorem 2. *All objects in* **NCSet** *are $\overline{T_0}$ at p, T_0' at p, and T_1 at p.*

Proof. It is deduced from Definition 5 and Theorem 1. □

Theorem 3. *Let $(A,\mathcal{N})$ be a neutrosophic crisp space and $p\in A$. The following are equivalent.*

(1) *$(A,\mathcal{N})$ is $PreT_2'$ at p.*
(2) *$(A,\mathcal{N})$ is $Pre\overline{T}_2$ at p.*
(3) *$(A,\mathcal{N})$ is $\overline{T_2}$ at p.*
(4) *$(A,\mathcal{N})$ is T_2' at p.*
(5) *$\mathcal{N}=\emptyset_{nc}$ or $p\in\mathcal{N}$.*

Proof. (1) $\Longrightarrow$ (2) : By Theorem 3.1 of [8] we get the result.

(2) $\Longrightarrow$ (3) : It follows from Definition 5 and Theorem 2.

(3) $\Longrightarrow$ (4) : Suppose $(A,\mathcal{N})$ is $\overline{T_2}$ at p. Then by Definition 5, Lemma 1 and Theorem 2, $(\pi_1\mathcal{A}_p)^{-1}\mathcal{N}\cap(\pi_2\mathcal{A}_p)^{-1}\mathcal{N}=(\pi_1\mathcal{S}_p)^{-1}\mathcal{N}\cap(\pi_2\mathcal{S}_p)^{-1}\mathcal{N}$. It follows that $\mathcal{N}=\emptyset_{nc}$ or $p\in\mathcal{N}$. Otherwise the equality does not hold. Because, if $\mathcal{N}\neq\emptyset_{nc}$ and $p\notin\mathcal{N}$, then $(\pi_1\mathcal{A}_p)^{-1}\mathcal{N}\cap(\pi_2\mathcal{A}_p)^{-1}\mathcal{N}=\emptyset_{nc}$ and $(\pi_1\mathcal{S}_p)^{-1}\mathcal{N}\cap(\pi_2\mathcal{S}_p)^{-1}\mathcal{N}=\mathcal{N}\times p\subset A\vee_p A$ by definitions of principal and skewed $p-$axis maps. This is a contradiction.

If $\mathcal{N}=\emptyset_{nc}$, then clearly $(\pi_1\mathcal{S}_p)^{-1}\mathcal{N}\cap(\pi_2\mathcal{S}_p)^{-1}\mathcal{N}=i_1\mathcal{N}\cup i_2\mathcal{N}=\emptyset_{nc}$.

If $p\in\mathcal{N}$, then $(\pi_1\mathcal{S}_p)^{-1}\mathcal{N}\cap(\pi_2\mathcal{S}_p)^{-1}\mathcal{N}=i_1\mathcal{N}\cup i_2\mathcal{N}=\mathcal{N}\vee_p\mathcal{N}$. Hence $(A,\mathcal{N})$ is T_2' at p by Definition 5, Lemma 1 and Theorem 2.

(4) $\Longrightarrow$ (5) : Suppose $(A,\mathcal{N})$ is T_2' at p. Then by Definition 5, Lemma 1 and Theorem 2, $(\pi_1\mathcal{S}_p)^{-1}\mathcal{N}\cap(\pi_2\mathcal{S}_p)^{-1}\mathcal{N}=i_1\mathcal{N}\cup i_2\mathcal{N}$. We must show that $p\in\mathcal{N}$ if $\mathcal{N}\neq\emptyset_{nc}$. Let $\mathcal{N}\neq\emptyset_{nc}$ and $p\notin\mathcal{N}$, then $(\pi_1\mathcal{S}_p)^{-1}\mathcal{N}\cap(\pi_2\mathcal{S}_p)^{-1}\mathcal{N}=(\mathcal{N}\times p)\cap(\mathcal{N}\vee_p\mathcal{N})=\mathcal{N}\times p$ and $i_1\mathcal{N}\cup i_2\mathcal{N}=\mathcal{N}\vee_p\mathcal{N}$ by definitions of skewed $p-$axis map and canonical injections. It follows that $(\pi_1\mathcal{S}_p)^{-1}\mathcal{N}\cap(\pi_2\mathcal{S}_p)^{-1}\mathcal{N}\neq i_1\mathcal{N}\cup i_2\mathcal{N}$ since if $x\in\mathcal{N}$, then $i_2x=(p,x)\in\mathcal{N}\vee_p\mathcal{N}$ but $(p,x)\notin\mathcal{N}\times p$. Consequently, this is a contradiction. Thus $p\in\mathcal{N}$ if $\mathcal{N}\neq\emptyset_{nc}$.

(5) $\Longrightarrow$ (1) : Assume that $\mathcal{N}=\emptyset_{nc}$ or $p\in\mathcal{N}$. If $\mathcal{N}=\emptyset_{nc}$, then clearly $(\pi_1\mathcal{S}_p)^{-1}\mathcal{N}\cap(\pi_2\mathcal{S}_p)^{-1}\mathcal{N}=i_1\mathcal{N}\cup i_2\mathcal{N}=\emptyset_{nc}$. If $\mathcal{N}\neq\emptyset_{nc}$, then $p\in\mathcal{N}$ by assumption. It follows that $(\pi_1\mathcal{S}_p)^{-1}\mathcal{N}\cap(\pi_2\mathcal{S}_p)^{-1}\mathcal{N}=(\mathcal{N}\vee_p\mathcal{N})\cap(\mathcal{N}\vee_p\mathcal{N})=\mathcal{N}\vee_p\mathcal{N}$, $i_1\mathcal{N}\cup i_2\mathcal{N}=\mathcal{N}\vee_p\mathcal{N}$, and consequently, $(\pi_1\mathcal{S}_p)^{-1}\mathcal{N}\cap(\pi_2\mathcal{S}_p)^{-1}\mathcal{N}=i_1\mathcal{N}\cup i_2\mathcal{N}$. Hence, $(A,\mathcal{N})$ is $PreT_2'$ at p by Definition 5. □

4. Generic Separation Axioms in Neutrosophic Crisp Space

Let B be a non-empty set, B^2 be cartesian product of B with itself and $B^2 \vee_\Delta B^2$ be two distinct copies of B^2 identified along the diagonal. If a point (a,b) in $B^2 \vee_\Delta B^2$ is in the first (resp. second) component, it is denoted as $(a,b)_1$ $(resp.(a,b)_2)$ Clearly, $(a,b)_1 = (a,b)_2$ iff $a = b$ [2].

Definition 6. *[2]*

(1) *The map $\mathcal{A} : B^2 \vee_\Delta B^2 \to B^3$ is called principal axis map iff*

$$\mathcal{A}(a,b)_i = \begin{cases} (a,b,a), & i=1 \\ (a,a,b), & i=2 \end{cases}$$

(2) *The map $\mathcal{S} : B^2 \vee_\Delta B^2 \to B^3$ is called skewed axis map iff*

$$\mathcal{S}(a,b)_i = \begin{cases} (a,b,b), & i=1 \\ (a,a,b), & i=2 \end{cases}$$

(3) *The map $\nabla : B^2 \vee_\Delta B^2 \to B^2$ is called fold map iff $\nabla(a,b)_i = (a,b)$ for $i = 1,2$.*

Definition 7. *(cf. [2, 6]) Let $\mathcal{U} : \mathcal{E} \to$ **Set** be a topological functor, A an object in $\mathcal{E}$ with $\mathcal{U}(A) = B$.*

(1) *A is $\overline{T}_0$ iff the initial lift of the $\mathcal{U}-$source $\{\mathcal{A} : B^2 \vee_\Delta B^2 \to \mathcal{U}(A^3) = B^3$ and $\nabla : B^2 \vee_\Delta B^2 \to \mathcal{U}\mathcal{D}(B^2) = B^2\}$ is discrete, where $\mathcal{D}$ is the discrete functor that is a left adjoint to $\mathcal{U}$ [2].*
(2) *A is T_0' iff the initial lift of the $\mathcal{U}-$source $\{id : B^2 \vee_\Delta B^2 \to \mathcal{U}(B^2 \vee_\Delta B^2)' = B^2 \vee_\Delta B^2$ and $\nabla : B^2 \vee_\Delta B^2 \to \mathcal{U}\mathcal{D}(B^2) = B^2\}$ is discrete, where $(B^2 \vee_\Delta B^2)'$ is the final lift of the $\mathcal{U}-$sink $\{i_1, i_2 : \mathcal{U}(A^2) = B^2 \to B^2 \vee_\Delta B^2\}$, i_1 and i_2 are the canonical injections, and $\mathcal{D}(B^2)$ is the discrete structure on B^2 [2].*
(3) *A is T_0 iff A doesn't contain an indiscrete subspace with at least two points [23].*
(4) *A is T_1 iff the initial lift of the $\mathcal{U}-$source $\{\mathcal{S} : B^2 \vee_\Delta B^2 \to \mathcal{U}(A^3) = B^3$ and $\nabla : B^2 \vee_\Delta B^2 \to \mathcal{U}\mathcal{D}(B^2) = B^2\}$ is discrete [2].*
(5) *A is $Pre\overline{T}_2$ iff the initial lift of the $\mathcal{U}$-sources $\{\mathcal{A} : B^2 \vee_\Delta B^2 \to \mathcal{U}(A^3) = B^3\}$ and $\{\mathcal{S} : B^2 \vee_\Delta B^2 \to \mathcal{U}(A^3) = B^3\}$ agree.*
(6) *A is $PreT_2'$ iff the initial lift of the $\mathcal{U}$-source $\{\mathcal{S} : B^2 \vee_\Delta B^2 \to \mathcal{U}(A^3) = B^3\}$ and the final lift of the $\mathcal{U}$-sink $\{i_1, i_2 : \mathcal{U}(A^2) = B^2 \to B^2 \vee_\Delta B^2\}$ agree.*
(7) *A is $\overline{T}_2$ iff A is $Pre\overline{T}_2$ and $\overline{T}_0$.*
(8) *A is T_2' iff A is $PreT_2'$ and T_0'.*
(9) *A is KT_2 iff A is $Pre\overline{T}_2$ and T_0'.*
(10) *A is LT_2 iff A is $PreT_2'$ and $\overline{T}_0$.*
(11) *A is MT_2 iff A is $PreT_2'$ and T_0.*
(12) *A is NT_2 iff A is $Pre\overline{T}_2$ and T_0.*

Remark 3. *Note that for **Top**, all of T_0's or T_1 or $Pre\overline{T}_2$, $PreT_2'$ or all of T_2's reduce to usual T_0 or T_1 or $PreT_2$ (for each distinct pair x, y, there exist disjoint neighborhoods of x and y if the set $\{x, y\}$ is not indiscrete) or Hausdorff separation axioms, respectively [2, 23].*

Theorem 4. *Let $(A, \mathcal{N})$ be an object in* **NCSet**.

(1) $(A, \mathcal{N})$ *is* $\overline{T_0}$.
(2) $(A, \mathcal{N})$ *is* T_0'.
(3) $(A, \mathcal{N})$ *is* T_1.
(4) $(A, \mathcal{N})$ *is* $Pre\overline{T}_2$.
(5) $(A, \mathcal{N})$ *is* $PreT_2'$.
(6) $(A, \mathcal{N})$ *is* $\overline{T_2}$.
(7) $(A, \mathcal{N})$ *is* T_2'.
(8) $(A, \mathcal{N})$ *is* KT_2.
(9) $(A, \mathcal{N})$ *is* LT_2.

Proof. For $(1)-(3)$, the proofs are deduced from Definition 7 and Theorem 1.

Let $(A, \mathcal{N})$ be a neutrosophic crisp space and $(A^2, \mathcal{N}^2)$ be the product neutrosophic crisp space. Note that the product neutrosophic crisp structure $\mathcal{N}^2$ is given by $\mathcal{N}^2 = \pi_1^{-1}\mathcal{N} \cap \pi_2^{-1}\mathcal{N}$.

Let $\mathcal{M} = (\pi_1\mathcal{A})^{-1}\mathcal{N} \cap (\pi_2\mathcal{A})^{-1}\mathcal{N} \cap (\pi_3\mathcal{A})^{-1}\mathcal{N}$, $\mathcal{M}' = (\pi_1\mathcal{S})^{-1}\mathcal{N} \cap (\pi_2\mathcal{S})^{-1}\mathcal{N} \cap (\pi_3\mathcal{S})^{-1}\mathcal{N}$, $\mathcal{M}'' = i_1\mathcal{N}^2 \cup i_2\mathcal{N}^2$ and it follows that $\mathcal{M} = \mathcal{M}' = \mathcal{M}'' = \mathcal{N}^2 \vee_\Delta \mathcal{N}^2$. Then by Definition 7 and Lemma 1, $(A, \mathcal{N})$ is $Pre\overline{T}_2$ since $\mathcal{M} = \mathcal{M}'$, and by Definition 7 and Lemma 1, $(A, \mathcal{N})$ is $PreT_2'$ since $\mathcal{M}' = \mathcal{M}''$, and consequently, $(A, \mathcal{N})$ is $\overline{T_2}$, T_2', KT_2 and LT_2 by Definition 7. □

Theorem 5. $(A, \mathcal{N})$ *in* **NCSet** *is T_0 if and only if $cardA \leq 1$.*

Proof. Assume that $(A, \mathcal{N})$ is a T_0 neutrosophic crisp space and $cardA > 1$, i.e., A is not a one-point set. Then there exist distinct points a and b of A. It follows that $(\{a, b\}, \{a, b\}_{nc})$ is the indiscrete subspace of $(A, \mathcal{N})$ contradicting to $(A, \mathcal{N})$ is being T_0. Hence, $cardA \leq 1$.

If $cardA \leq 1$, i.e., $A = \emptyset$ or A is a one-point set, then clearly by Definition 7, $(A, \mathcal{N})$ is a T_0. □

Theorem 6. $(A, \mathcal{N})$ *in* **NCSet** *is MT_2 (resp. NT_2) if and only if $cardA \leq 1$.*

Proof. It is deduced from Definition 7 and Theorems 4, 5. □

5. Closedness, Compactness and Connectedness in NCSet

Let p be a point in a set B and $\vee_p^\infty B$ be the *infinite wedge product* of B at p, that is formed by taking countably separate copies of B and identifying them at p. If a point b in $\vee_p^\infty B$ is in the i-th component, it is denoted as b_i.

Definition 8. [3] *Let $\vee_p^\infty B$ be the infinite wedge product at p and $B^\infty = B \times B \times ...$ be the countable cartesian product of B with itself.*

(i) *The map* $\mathcal{A}_p^\infty : \vee_p^\infty B \to B^\infty$ *is called infinite principle axis map at* p *provided that* $\mathcal{A}_p^\infty(b_i) = (p, p, ..., p, b, p, ...)$.

(ii) *The map* $\nabla_p^\infty : \vee_p^\infty B \to B^\infty$ *is called infinite fold map at* p *provided that* $\nabla_p^\infty(b_i) = b$ *for all* $i \in I$.

Definition 9. *[3] Let* $\mathcal{U} : \mathcal{E} \to$ **Set** *be a topological functor,* $A \in Ob(\mathcal{E})$ *with* $\mathcal{U}(A) = B$ *and* $p \in B$. *Let* C *be a subset of* B. *We denote* A/C *as the final lift of the epi* $\mathcal{U}$*-sink* $q : \mathcal{U}(A) = B \to B/C = (B\backslash C) \cup \{*\}$, *where* q *is the epi map that is the identity on* $B\backslash C$ *and identifying* C *with a point* $\{*\}$.

(i) $\{p\}$ *is closed provided that the initial lift of the* $\mathcal{U}$*-source* $\{A_p^\infty : \vee_p^\infty B \to \mathcal{U}(A^\infty) = B^\infty$ *and* $\nabla_p^\infty : \vee_p^\infty B \to \mathcal{U}\mathcal{D}(B^\infty) = B^\infty\}$ *is discrete, where* $\mathcal{D}$ *is the discrete functor.*

(ii) $C \subset A$ *is closed provided that* $\{*\}$, *the image of* C, *is closed in* A/C *or* $C = \emptyset$.

(iii) $C \subset A$ *is strongly closed provided that* A/C *is* T_1 *at* $\{*\}$ *or* $C = \emptyset$.

(iv) $C \subset A$ *is (strongly) open provided that* C^c, *the complement of* C, *is (strongly) closed in* A.

Remark 4. *In* ***Top***, C *is strongly closed provided that* C *is closed and there exists a neighbourhood of* C *missing* x *for each* $x \notin C$, *and the notion of closedness coincides with the usual one. Moreover, the notions of strong closedness and closedness coincide for* T_1 *topological spaces [3].*

Theorem 7. *Every point is closed in* A *for* $(A, \mathcal{N})$ *in* **NCSet**.

Proof. It is deduced from Definition 9 and Theorem 1. □

Theorem 8. *Let* $(A, \mathcal{N})$ *be in* **NCSet**. *Each* $C \subset A$ *is both strongly closed and closed, so it is strongly open and open.*

Proof. It is deduced from Definition 9 and Theorem 1. □

Definition 10. *[7] Let* $\mathcal{E}$ *be a topological category over* **Set**, $A, B \in Ob(\mathcal{E})$, *and* $f : A \to B$ *a morphism.*

(1) f *is (strongly) closed provided that the image of each (strongly) closed subobject of* A *is a (strongly) closed subobject of* B.

(2) A *is (strongly) compact provided that for each* $B \in Ob(\mathcal{E})$, *the projection* $\pi_2 : A \times B \to B$ *is (strongly) closed.*

Remark 5. (1) *In* ***Top***, *the notions of compactness and closed morphism reduce to the usual ones ([15] p. 97 and 103).*

(2) *The notions of compactness and strong compactness are different for an arbitrary topological category, in general, since the notions of strong closedness and closedness are different, in general ([3] p. 393).*

Theorem 9. *Every neutrosophic crisp space is (strongly) compact.*

Proof. Let $(A, \mathcal{N})$ be a neutrosophic crisp space. By Definition 10, we need to show that $\pi_2 : (A, \mathcal{N}) \times (B, \mathcal{M}) \to (B, \mathcal{M})$ is (strongly) closed for all $(B, \mathcal{M})$ in **NCSet**. Suppose $C \subset A \times B$ is (strongly) closed. By Theorem 8, it follows that $\pi_2(C)$ is (strongly) closed and consequently, $(A, \mathcal{N})$ is (strongly) compact. □

Corollary 1. *Let $(A, \mathcal{N})$ and $(B, \mathcal{M})$ be in* **NCSet** *and $f : (A, \mathcal{N}) \to (B, \mathcal{M})$ be an* **NCSet***-map.*

(1) *Each* **NCSet***-map f is (strongly) closed.*
(2) *If $(A, \mathcal{N})$ is (strongly) compact, then $(f(A), \mathcal{M})$ is (strongly) compact.*

Now, we give the characterizations of the various notions of connected objects in **NCSet**.

Definition 11. *Let $\mathcal{E}$ be a topological category over* **Set** *and $A \in Ob(\mathcal{E})$.*

(i) *A is strongly connected (connected) provided that the only subsets of A both open (strongly open) and closed (strongly closed) are A and $\emptyset$ [10].*
(ii) *A is D-connected provided that any morphism from A to any discrete object is constant [10, 26].*
(iii) *A is (strongly) hereditarily disconnected provided that the only (strongly) connected subspaces of A are singletons and $\emptyset$ [11].*
(iv) *A is said to be (strongly) irreducible if X, Y are (strongly) closed subobjects of A and $A = X \cup Y$, then $X = A$ or $Y = A$ [13].*

Remark 6. *In* **Top***,*

(1) *The notions of D-connectedness and strong connectedness coincide with the usual notion of connectedness. Moreover, if a topological space X is T_1, then the notions of D-connectedness, connectedness and strong connectedness coincide [10].*
(2) *The notion of irreducibility coincides with the usual irreducibility [13]. Note that if a topological space (X, τ) is irreducible, then (X, τ) is connected, and if (X, τ) is T_1, then the notions of of irreducible spaces and strongly irreducible spaces coincide. [13].*

Theorem 10. *Let $(A, \mathcal{N})$ be a neutrosophic crisp space. Then the following are equivalent.*

(1) *$(A, \mathcal{N})$ is (strongly) connected.*
(2) *$(A, \mathcal{N})$ is (strongly) irreducible.*
(3) *$card A \leq 1$.*

Proof. (1) $\implies$ (2) : Let $(A, \mathcal{N})$ is strongly connected (resp. connected). Then the only subsets of A both open (strongly open) and closed (strongly closed) are A and $\emptyset$. Suppose $(A, \mathcal{N})$ is not (strongly) irreducible. Let B be a subset of A. By Theorem 8, B and B^c are closed (strongly closed). Since $A = B \cup B^c$ and $(A, \mathcal{N})$ is not (strongly) irreducible, then $B \neq A$ and $B^c \neq A$. It follows that $\emptyset \neq B \subset A$ is a both open (strongly open) and closed (strongly closed). Given that $(A, \mathcal{N})$

is strongly connected (resp. connected), this is a contradiction. Hence, $(A, \mathcal{N})$ is (strongly) irreducible.

(2) $\implies$ (3) : Suppose $(A, \mathcal{N})$ is (strongly) irreducible and $cardA > 1$. Then there exist distinct points a and b of A. By Theorem 8, both $\{a\}$ and $\{a\}^c$ are (strongly) closed subsets of A and $A = \{a\} \cup \{a\}^c$ contradicting to $(A, \mathcal{N})$ is being (strongly) irreducible. Hence, $cardA \leq 1$.

(3) $\implies$ (1) : Suppose $cardA \leq 1$. We show that $(A, \mathcal{N})$ is strongly connected (resp. connected). Since $cardA \leq 1$, $A = \emptyset$ or $A = \{a\}$ (one-point set). If $A = \{a\}$, then A and $A^c = \emptyset$ is closed (strongly closed). It follows that $A = \{a\}$ is both closed (strongly closed) and open (strongly open). Similarly, we have $A = \emptyset$ is both closed (strongly closed) and open (strongly open). Hence, $(A, \mathcal{N})$ is strongly connected (resp. connected). □

Theorem 11. *All objects in* **NCSet** *is (strongly) hereditarily disconnected.*

Proof. It is deduced from Definition 11 and Theorem 10. □

Theorem 12. $(A, \mathcal{N})$ *in* **NCSet** *is D-connected provided that $cardA \leq 1$ and $\mathcal{N} = \emptyset_{nc}$.*

Proof. Suppose $(A, \mathcal{N})$ is D-connected. Let $(B, \emptyset_{nc})$ be a discrete neutrosophic crisp space. By the definition of D-connectedness, every **NCSet**-map $f\colon (A, \mathcal{N}) \to (B, \emptyset_{nc})$ is constant. Since f is an **NCSet**-map, $\mathcal{N} \subset f^{-1}(\emptyset_{nc}) = \emptyset_{nc}$ and we have $\mathcal{N} = \emptyset_{nc}$. We show that $cardA \leq 1$. Suppose $cardA > 1$. Let $B = \{0, 1\}$, E be a non-empty proper subset of A and $f\colon A \to B$ be map given by

$$f(x) = \begin{cases} 0, & x \in E \\ 1, & x \in E^c \end{cases}$$

The map $f\colon (A, \emptyset_{nc}) \to (B, \emptyset_{nc})$ is an **NCSet**-map, but it is not constant. Given that $(A, \mathcal{N})$ is D-connected, this is a contradiction. Hence, $cardA \leq 1$.

Conversely, suppose that $cardA \leq 1$ and $\mathcal{N} = \emptyset_{nc}$. Let $(B, \emptyset_{nc})$ be a discrete neutrosophic crisp space. $A = \emptyset$ or $A = \{a\}$. If $A = \emptyset$, then $f\colon (\emptyset, \emptyset_{nc}) \to (B, \emptyset_{nc})$ is an **NCSet**-map. If $A = \{a\}$, then $f\colon (\{a\}, \emptyset_{nc}) \to (B, \emptyset_{nc})$ is an **NCSet**-map and it is constant. It follows that every morphism from A to $(B, \emptyset_{nc})$ is constant. By Definition 11, we have that $(A, \mathcal{N})$ is D-connected. □

6. Comparative Evaluation

In this section, we compare our results with the ones in some other categories.

(1) In **Top**,
   (a) All T_2's are equivalent, i.e., $\overline{T_2} = T_2' = KT_2 = LT_2 = MT_2 = NT_2$. Moreover, $\overline{T_2} \implies T_1 \implies \overline{T_0} = T_0' = T_0$ and $\overline{T_2} \implies Pre\overline{T}_2 = PreT_2'$ [6].
   (b) $\overline{T_2}$ at $p = T_2'$ at $p \implies T_1$ at $p \implies \overline{T_0}$ at $p = T_0'$ at p and $\overline{T_2}$ at $p \implies Pre\overline{T}_2$ at $p = PreT_2'$ at p [5].

(c) If a topological space (X, τ) is $\overline{T_0}$ (resp. T_0', T_1, $Pre\overline{T}_2$, $PreT_2'$, $\overline{T}_2$, or T_2'), then (X, τ) is $\overline{T}_0$ at p (resp. T_0' at p, T_1 at p, $Pre\overline{T}_2$ at p, $PreT_2'$ at p, $\overline{T}_2$ at p, or T_2' at p), since **Top** is a normalized category [5].

(d) Strong closedness implies closedness. In addition, in the realm of T_1 topological spaces, the notions of strong closedness and closedness coincide [3]. Based on this, the notions of strong compactness and compactness are different, in general, and in the realm of T_1 property, these notions coincide [7].

(e) D-connectedness and strong connectedness coincides with the usual connectedness [10], and in the realm of T_1 property, then all the notions of connectedness coincide [10]. Moreover, the notion of strong hereditary disconnectedness coincides with the usual hereditary disconnectedness [10], and if a topological space is T_1, then hereditary disconnectedness and strong hereditary disconnectedness coincide [11].

(f) The notion of irreducibility coincides with the usual irreducibility [13]. In addition, in the realm of T_1 topological spaces, the notions of irreducibility and strong irreducibility coincide. [13].

(2) In **NCSet**, we can infer the following results.

(a) By Theorems 2 and 3, if a neutrosophic crisp space $(A, \mathcal{N})$ is $Pre\overline{T}_2$ at p, $PreT_2'$ at p, $\overline{T_2}$ at p or T_2', then $(A, \mathcal{N})$ is $\overline{T_0}$ at p, T_0' at p or T_1 at p, but the reverse implication is not true, in general.

(b) By Theorems 4, 5, and 6, if a neutrosophic crisp space $(A, \mathcal{N})$ is T_0, NT_2 or MT_2, then $(A, \mathcal{N})$ is $\overline{T_0}$, T_0', T_1, $Pre\overline{T}_2$, $PreT_2'$, $\overline{T_2}$, T_2', KT_2 or LT_2, but the reverse implication is not true, in general.

(c) By Theorems 2 and 4, a neutrosophic crisp space $(A, \mathcal{N})$ is $\overline{T_0}$ (resp. T_0', or T_1) iff $(A, \mathcal{N})$ is $\overline{T_0}$ at p (resp. T_0' at p, or T_1 at p). But, by Theorems 3 and 4, if $(A, \mathcal{N})$ is $Pre\overline{T}_2$ (resp. $PreT_2'$, $\overline{T_2}$, or T_2'), then $(A, \mathcal{N})$ is not necessary to be $Pre\overline{T}_2$ at p (resp. $PreT_2'$ at p, $\overline{T_2}$ at p, or T_2' at p).

(d) By Theorems 8, closedness and strong closedness are equivalent, and all subsets of a neutrosophic crisp space are (strongly) closed.

(e) Let $(A, \mathcal{N})$ be a neutrosophic crisp space. By Theorems 9 and 11,
   (i) $(A, \mathcal{N})$ is (strongly) compact.
   (ii) $(A, \mathcal{N})$ is (strongly) hereditary disconnected.

(f) Let $(A, \mathcal{N})$ be a neutrosophic crisp space. By Theorems 5 and 10, the following are equivalent:
   (i) $A = \emptyset$ or A is a one-point set.
   (ii) $(A, \mathcal{N})$ is T_0.
   (iii) $(A, \mathcal{N})$ is (strongly) connected.
   (iv) $(A, \mathcal{N})$ is (strongly) irreducible.

   (g) By Theorems 10 and 12, D-connectedness implies (strong) connectedness or (strong) irreducibility, but in general, the converse of implication does not hold. For instance, if $A = \{a\}$ and $\mathcal{N} = A_{nc}$, then $(A, \mathcal{N})$ is (strongly) connected and (strongly) irreducible, but not D-connected.
   (h) By Theorems 10 and 11, (strong) connectedness or (strong) irreducibility implies hereditary disconnectedness, the reverse implication is not true, in general. For instance, the indiscrete neutrosophic crisp space $(A, \mathcal{N})$ with $cardA = 2$ is hereditary disconnected, but neither (strongly) connected nor (strongly) irreducible.

(3) In **Prox**, the category of proximity spaces and proximity maps,
   (a) $\overline{T_0} = T_1 = PreT_2' = \overline{T_2} = T_2' \implies T_0' = Pre\overline{T}_2$ [20].
   (b) $\overline{T_0}$ at $p = T_1$ at $p = PreT_2'$ at $p = \overline{T_2}$ at $p = T_2'$ at $p \implies T_0'$ at $p = Pre\overline{T}_2$ at p [19,22].
   (c) Since **Prox** is a normalized category, if a topological space (X, δ) is $\overline{T_0}$ (resp. T_0', T_1, $Pre\overline{T}_2$, $PreT_2'$, $\overline{T}_2$, or T_2'), then (X, δ) is $\overline{T}_0$ at p (resp. T_0' at p, T_1 at p, $Pre\overline{T}_2$ at p, $PreT_2'$ at p, $\overline{T}_2$ at p, or T_2' at p).
   (d) By Remark 4.11 of [19], the notions of closedness and strong closedness coincide. Moreover, by Lemma 4.3 of [21], (strong) closedness implies (strong) compactness since all objects are (strongly) compact.
   (e) By Theorem 4.5 of [25], a proximity space (X, δ) is (strongly) connected if and only if (X, δ) is (strongly) irreducible.

(4) In **L-GS**, the category of quantale-valued gauge spaces and $\mathcal{L}$-gauge morphisms,
   (a) $\overline{T_2} = T_1 \implies \overline{T_0} \implies T_0$. Moreover, an $\mathcal{L}$-gauge space $(X, \mathcal{G})$ is $\overline{T_2}$, then $(X, \mathcal{G})$ is both NT_2 and $Pre\overline{T_2}$, and in the realm of Pre-Hausdorff quantale-valued gauge spaces, $\overline{T_0}$, T_1 and $\overline{T_2}$ are equivalent [24].
   (b) By Theorems 3.6 and 3.9 of [27], T_1 at $p \implies \overline{T_0}$ at p, and if an $\mathcal{L}$-gauge space $(X, \mathcal{G})$ is $\overline{T_0}$ (or T_1), then $(X, \mathcal{G})$ is $\overline{T_0}$ at p (or T_1 at p) [24,27].
   (c) There is no relation between D-connectedness and the notion of closedness or T_1 at p [27].

(5) In **pqsMet**, the category of extended pseudo-quasi-semi metric spaces and contraction maps,
   (a) $T_1 = PreT_2' = T_2' = \overline{T_2} \implies \overline{T_0} \implies T_0 \implies T_0'$ and $\overline{T_2} \implies NT_2 \implies Pre\overline{T}_2 = KT_2$ [14].
   (b) T_1 at $p = PreT_2'$ at $p = T_2'$ at $p = \overline{T_2}$ at $p \implies \overline{T_0}$ at $p \implies T_0'$ at p and $\overline{T_2}$ at $p \implies Pre\overline{T}_2$ at p [12].
   (c) Since **pqsMet** is a normalized category, if an extended pseudo-quasi-semi metric space (X, d) is $\overline{T_0}$ (resp. T_0', T_1, $Pre\overline{T}_2$, $PreT_2'$, $\overline{T}_2$, or T_2'), then (X, d) is $\overline{T}_0$ at p (resp. T_0' at p, T_1 at p, $Pre\overline{T}_2$ at p, $PreT_2'$ at p, $\overline{T}_2$ at p, or T_2' at p).

   (d) By Theorem 3.4 of [13], strong closedness implies closedness. By Theorem 3.20 of [14], an extended pseudo-quasi-semi metric space (X, d) is KT_2 or NT_2, then the notions of strong closedness and closedness coincide. Moreover, in the realm of $\overline{T_2}$, T_2' or T_1 property, each subset of X is (strongly) closed.
   (e) By Theorem 4.9 of [13], an extended pseudo-quasi-semi metric space (X, d) is strongly connected, then (X, d) is connected. In addition, the notions of connectedness and D-connectedness coincide.
   (f) By Theorem 5.4 of [13], irreducibility implies strong irreducibility or strong connectedness. Also, strong irreducibility implies connectedness or D-connectedness.

(6) For any arbitrary topological category,
   (a) $\overline{T_0} \implies T_0'$ and there is no relationship between $\overline{T_0}$ or T_0' and T_0 [3]. In addition, it is shown in [6], that $\overline{T_2} \implies NT_2$ and $LT_2 \implies T_2'$, also the notions of $\overline{T_2}$ and NT_2, or T_2' and MT_2 are independent of each other, in general. Moreover, $PreT_2' \implies Pre\overline{T}_2$ [8].
   (b) Let $\mathcal{U} : \mathcal{E} \to \boldsymbol{Set}$ be a topological functor, A an object in $\mathcal{E}$ and $p \in \mathcal{U}(A)$ be a retract of A, i.e., the initial lift $h : \overline{1} \to A$ of the $\mathcal{U}$-source $p : 1 \to \mathcal{U}(A)$ is a retract, where 1 is the terminal object in $\boldsymbol{Set}$, or more precisely let $\mathcal{U}$ be normalized. Then if A is $\overline{T}_0$ (resp. T_1, $Pre\overline{T}_2$, or $\overline{T}_2$), then A is $\overline{T}_0$ at p (resp. T_1 at p, $Pre\overline{T}_2$ at p, or $\overline{T}_2$ at p), but the reverse implication is not true, in general ([4], Theorem 2.6 and Corollary 2.7).
   (c) The notions of closedness and strong closedness are independent of each other, in general [3]. Even if $A \in \mathcal{E}$ is T_1, where $\mathcal{E}$ is a topological category, then these notions are still independent of each other [3]. Based on this, the notions of compactness and strong compactness are different, in general.
   (d) There are no implications between the notions of strong connectedness and connectedness, or hereditary disconnectedness and strong hereditary disconnectedness [11].

Acknowledgments I would like to thank the referees for their valuable and kind suggestions that improved the paper.

Declaration of Competing Interests The author declares that he has no competing interest.

References

[1] Atanassov, K. T., Intuitionistic fuzzy sets, *Fuzzy Sets Syst.*, 20(1) (1986), 383-395. https://doi.org/10.1016/S0165-0114(86)80034-3
[2] Baran, M., Separation properties, *Indian J. Pure Appl. Math.*, 23 (1992), 333-341.

[3] Baran, M., The notion of closedness in topological categories, *Comment. Math. Univ. Carolin.*, 34(2) (1993), 383-395.
[4] Baran, M., Generalized local separation properties, *Indian J. Pure Appl. Math.*, 25(6) (1994), 615-620.
[5] Baran, M., Separation properties in topological categories, *Math. Balkanica*, 10(1) (1996), 39-48.
[6] Baran, M., Altındiş, H., T_2 objects in topological categories, *Acta Math. Hungar.*, 71(1-2) (1996), 41-48. https://doi.org/10.1007/BF00052193
[7] Baran, M., A notion of compactness in topological categories, *Publ. Math. Debrecen*, 50(3-4) (1997), 221-234.
[8] Baran, M., Completely regular objects and normal objects in topological categories, *Acta Math. Hungar.*, 80(3) (1998), 211-224. https://doi.org/10.1023/A:1006550726143
[9] Baran, M., Compactness, perfectness, separation, minimality and closedness with respect to closure operators, *Appl. Categ. Struct.*, 10(4) (2002), 403-415. https://doi.org/10.1023/A:1016388102703
[10] Baran, M., Kula, M., A note on connectedness, *Publ. Math. Debr.*, 68 (2006), 489-501.
[11] Baran, M., Separation, connectedness, and disconnectedness, *Turk. J. Math.*, 47(1) (2023), 279-295. https://doi.org/10.55730/1300-0098.3360
[12] Baran, T. M., Local T_2 extended pseudo-quasi-semi metric spaces, *Commun. Fac. Sci. Univ. Ank. Ser. A1 Math. Stat.*, 68(2) (2019), 2117-2127. https://doi.org/10.31801/cfsuasmas.497701
[13] Baran, T. M., Closedness, separation and connectedness in pseudo-quasi-semi metric spaces, *Filomat*, 34(14) (2020), 4757-4766. https://doi.org/10.2298/FIL2014757B
[14] Baran, T. M., Kula, M., Separation axioms, Urysohn's lemma and Tietze extention theorem for extended pseudo-quasi-semi metric spaces, *Filomat*, 36(2) (2022), 703-713. https://doi.org/10.2298/FIL2202703B
[15] Bourbaki, N., General Topology, Addison-Wesley Publ. Co., Massachusets, 1966.
[16] Dikranjan, D., Giuli, E., Closure operators I, *Topol. Appl.*, 27(2) (1987), 129-143. https://doi.org/10.1016/0166-8641(87)90100-3
[17] Herrlich, H., Categorical topology, *Gen. Topol. Appl.*, 1 (1971), 1-15.
[18] Hur, K., Lim, P. K., Lee, J. G., Kim, J., The category of neutrosophic crisp sets, *Ann. Fuzzy Math. Inform.*, 14(1) (2017), 43-54.
[19] Kula, M., Maraşlı, T., Özkan S., A note on closedness and connectedness in the category of proximity spaces, *Filomat*, 28(7) (2014), 1483-1492. https://doi.org/10.2298/FIL1407483K
[20] Kula, M., Özkan, S., Maraşlı, T., Pre-Hausdorff and Hausdorff proximity spaces, *Filomat*, 31(12) (2017), 3837-3846. https://doi.org/10.2298/FIL1712837K
[21] Kula, M., ST2, ΔT2, ST3, ΔT3, Tychonoff, compact and ∂-connected objects in the category of proximity spaces, *Hacet. J. Math. Stat.*, 48(2) (2019), 490-500.
[22] Kula, M., Özkan, S., T_2 and T_3 objects at p in the category of proximity spaces, *Math. Bohem.*, 145(2) (2020), 177-190. https://doi.org/10.21136/MB.2019.0144-17
[23] Marny, T., Rechts-Bikategoriestrukturen in Topologischen Kategorien, Dissertation, Freie Univ., Berlin, 1973.
[24] Özkan, S., Alsulami, S., Baran, T. M., Qasim, M., Pre-Hausdorffness and Hausdorffness in quantale-valued gauge spaces, *Mathematics*, 10(24) (2022), 4819. https://doi.org/10.3390/math10244819
[25] Özkan, S., Kula, M., Kula, S., Baran, T. M., Closure operators, irreducibility, Urysohn's lemma, and Tietze extension theorem for proximity spaces, *Turk. J. Math.*, 47(2) (2023), 870-882. https://doi.org/10.55730/1300-0098.3398
[26] Preuss, G., Theory of Topological Structures, An Approach to topological Categories, D. Reidel Publ. Co., Dordrecht, 1988.

[27] Qasim, M., Özkan, S., The notion of closedness and D-connectedness in quantale-valued approach spaces. *Categ. Gen. Algebr. Struct. Appl.*, 12(1) (2020), 149-173. https://doi.org/10.29252/CGASA.12.1.149

[28] Salama, A. A., Smarandache, F., Neutrosophic Crisp Set Theory, The Educational Publisher, Columbus, Ohio, 2015.

[29] Smarandache, F., Neutrosophy: Neutrisophic Property, Sets, and Logic, American Research Press, Rehoboth, USA, 1998.

[30] Zadeh, L. A., Fuzzy sets, *Inf. Control.*, 8 (1965), 338-356. https://doi.org/10.1016/S0019-9958(65)90241-X

http://communications.science.ankara.edu.tr

Commun.Fac.Sci.Univ.Ank.Ser. A1 Math. Stat.
Volume 72, Number 3, Pages 633–649 (2023)
DOI:10.31801/cfsuasmas.1224326
ISSN 1303-5991 E-ISSN 2618-6470

COMMUNICATIONS SERIES A1

Research Article; Received: December 26, 2022; Accepted: March 28, 2023

THE FELL APPROACH STRUCTURE

Meryem ATEŞ[1] and Sevda SAĞIROĞLU[2]

[1,2]Department of Mathematics, Faculty of Science, Ankara University, 06100, Ankara, TÜRKİYE

ABSTRACT. In the present paper we construct a new approach structure called Fell approach structure. We define the new structure by means of lower regular function frames and prove that the Top-coreflection of this new structure is the ordinary Fell topology. We also give analogue result for the extended Fell topology and investigate some properties of Fell approach structure.

1. Introduction

Hyperspaces of topological spaces were initiated by Felix Hausdorff (1868) and Leopold Vietoris (1891). The theory occupy an important place in the applications of convex analysis, optimization theory and the theory of Banach spaces. Hyperspaces of topological spaces are an important way of obtaining information on the structure of a topological space X. Although the most important and well-studied hyperspace topologies on $CL(X)$ are the Wijsman topology, the Hausdorff metric topology and the hit and miss topologies. These topologies are investigated in [6]. Lowen and Wuyts [16] investigated the corresponding approach structures of the Vietoris topology and the other are investigated by Lowen and Sioen in [11, 14]. In most of cases they obtained the well known hyperspace topologies as the Top-coreflections of their new constructed approach structures.

The Fell topology is also known as a useful construct in terms of applications, especially in convex analysis, probability theory and its applications to optimization [1, 2]. In this paper we construct a new approach structure in the setting of hyperspaces and we prove that its Top-coreflection is the well known Fell topology. We also investigate some properties of this new structure in the setting of approach theory.

2020 *Mathematics Subject Classification.* 54B20, 54B30.

Keywords. Distance, lower regular function frame, approach structure, approach space, contraction, Vietoris topology, Fell topology, index of compactness.

[1] mbiten@ankara.edu.tr-Corresponding author; 0000-0003-2393-0828;

[2] ssagir@science.ankara.edu.tr; 0000-0003-3084-0839.

We refer to R.Lowen [12,17] for extensive literature to study on approach spaces and we refer to G.Beer [4] for more information on hyperspace topologies.

2. Preliminaries

Throughout this work, given a nonempty set X, 2^X denotes the set of all subsets of X, $2^{(X)}$ denotes the set of all finite subsets of X. Given a topological space (X,τ) by $CL(X)$ we denote the set of all closed subsets of X and $K(X)$ represents the set of all compact subsets of X, in addition $\mathcal{W} = CL(X) \cup \{\emptyset\}$. The hit and miss sets of a subset A in X are defined as

$$A^- := \{B \in CL(X) \mid B \cap A \neq \emptyset\} \text{ and } A^+ := \{B \in CL(X) \mid B \subset A\},$$

respectively. We also consider $\mathbb{P}$:=[0,∞] with its usual order and complete lattice structure as an additive semigroup. For any $A \subset X$, the indicator of A is defined as

$$\begin{aligned} \theta_A : X &\longrightarrow \mathbb{P} \\ x &\longmapsto \theta_A(x) = \begin{cases} 0 & , \text{x} \in A \\ \infty & , \text{x} \notin A. \end{cases} \end{aligned}$$

For a Hausdorff space (X,τ), the lower-Vietoris topology τ_V^- and the upper-Vietoris topology τ_V^+ on $CL(X)$ are generated by the subbasis $\{V^- \mid V \in \tau\}$ and the basis $\{W^+ \mid W \in \tau\}$, respectively. The Vietoris topology is simply the supremum of its upper part and lower part, i.e. $\tau_V = \tau_V^- \bigvee \tau_V^+$ [6].
The upper-Fell topology τ_{Fell}^+ on $CL(X)$ is generated by the basis

$$\{W^+ \mid W \in \tau, W^c \in K(X)\}$$

and the **Fell topology** τ_{Fell} on $CL(X)$ is generated by the subbasis

$$\{V^- \mid V \in \tau\} \cup \{W^+ \mid W \in \tau, W^c \in K(X)\} \text{ [6]}.$$

Approach spaces can be described in terms of several equivalent mathematical structures; such as distance, limit operator, gauge, approach system, upper hull operator and lower regular function frame. Now we recall the definition of lower regular function frame.

A **lower regular function frame** [17] is a collection of functions $\mathcal{L} \subseteq \mathbb{P}^X$ with the following properties:
(LR1) $\forall \mathfrak{K} \subseteq \mathcal{L} : \bigvee \mathfrak{K} \in \mathcal{L}$,
(LR2) $\forall \mathfrak{K} \subseteq \mathcal{L}$ such that $\mathfrak{K}$ is finite : $\bigwedge \mathfrak{K} \in \mathcal{L}$ (that is stable for finite infima),
(LR3) $\forall \mu \in \mathcal{L}$, $\forall \alpha \in \mathbb{P} : \mu + \alpha \in \mathcal{L}$ (that is translation invariant),
(LR4) $\forall \mu \in \mathcal{L}$, $\forall \alpha \in [0, \inf \mu] : \mu - \alpha \in \mathcal{L}$.
A basis for a lower regular function frame $\mathcal{L}$ is a collection $\mathcal{B} \subset \mathcal{L}$ such that any function in $\mathcal{L}$ can be obtained as a supremum of functions in $\mathcal{B}$. In addition while Lowen and Wuyts [16] introducing the Vietoris approach structure, they gave a notion of a basis and a subbasis for a lower regular function frame. If the collection $\mathfrak{B} \subset \mathbb{P}^X$ is stable for finite infima then $\mathfrak{B}$ is a subbasis for a lower regular function frame defined on X and if the subbasis $\mathfrak{B}$ is translation invariant then $\mathfrak{B}$ is a basis

for a lower regular function frame on X. If $\mathfrak{B} \subset \mathbb{P}^X$, the smallest lower regular function frame containing $\mathfrak{B}$ (or the lower regular function frame generated by $\mathfrak{B}$) is defined as

$$[\mathfrak{B}] = \{\sup_{j\in J} \inf_{k\in K_j} \mu_{j,k} \mid \forall j \in J, \forall k \in K_j : K_j \text{ finite }, \mu_{j,k} \in \mathfrak{B}\}, \tag{1}$$

and in this case we call $\mathfrak{B}$ a subbasis of $[\mathfrak{B}]$, if moreover $\mathfrak{B}$ is closed for finite infima we call $\mathfrak{B}$ a basis for $[\mathfrak{B}]$.

In [12] it is proved that a lower regular function frame, a distance and an approach system are equivalent mathematical structures. In addition for a given lower regular function frame $\mathcal{L}$ the corresponding distance is defined as

$$\delta(x, A) = \sup\{\rho(x) \mid \rho \in \mathcal{L}, \rho_{|A=0}\} \tag{2}$$

and for a given distance δ the corresponding approach system $\mathcal{A}$ is defined as

$$\mathcal{A}(x) = \{\psi \in \mathbb{P}^X \mid \forall A \subset X : \inf_{y\in A} \psi(y) \leq \delta(x, A)\} \tag{3}$$

If (X, τ) is topological space, then

$$\mathcal{L}_\tau = \{\mu \in \mathbb{P}^X \mid \mu \text{ lower semicontinuous}\}$$

is a lower regular function frame on X. On the other hand; if there exists a topology τ on X such that $\mathcal{L} = \mathcal{L}_\tau$, then $(X, \mathcal{L})$ is called a **topological approach space** [12]. A function $f : (X, \mathcal{L}) \to (X', \mathcal{L}')$ between approach spaces is called a contraction if for all $\nu \in \mathcal{L}'$, $\nu \circ f \in \mathcal{L}$. The category whose objects are approach spaces and morphisms are contractions is denoted by **App**. App is a topological category and **Top** is embedded as a concretely coreflective subcategory of **App**. For any approach space $(X, \mathcal{L})$, Top-coreflection $\tau_{\mathcal{L}}^{tc}$ determined by $\mathcal{L}$ is the topology associated with the following topological closure operator:

$$cl_{\mathcal{L}}(A) = \Big\{x \in X \mid \sup_{\substack{\rho\in\mathcal{L} \\ \rho_{|A=0}}} \rho(x) = 0\Big\} \ ; \ A \subset X. \tag{4}$$

Note that the equality (4) can be written as

$$cl_{\mathcal{L}}(A) = \bigcap_{\substack{\rho\in\mathcal{L} \\ \rho_{|A}=0}} \{\rho = 0\} \tag{5}$$

Before describing the construction process of the Fell approach structure, let us give the definition of Vietoris approach structure investigated in [16] by means of regular function frames. If $\mu \in \mathbb{P}^X$, then the functions $\mu^\wedge$ and $\mu^\vee$ are defined as

$$\mu^\wedge : CL(X) \longrightarrow \mathbb{P} \qquad A \longmapsto \mu^\wedge(A) = \inf_{x\in A} \mu(x)$$

$$\mu^\vee : CL(X) \longrightarrow \mathbb{P} \qquad A \longmapsto \mu^\vee(A) = \sup_{x\in A} \mu(x).$$

Lowen and Wuyts obtained in [16] that for the function θ_A of $A \in CL(X)$, $\theta_A^{\wedge} = \theta_{A^-}$ and $\theta_A^{\vee} = \theta_{A^+}$ and for a subcollection $\mathcal{A}$ in $CL(X)$,

$$\theta_{\cap\mathcal{A}} = \sup_{A\in\mathcal{A}} \theta_A \text{ and } \theta_{\cup\mathcal{A}} = \inf_{A\in\mathcal{A}} \theta_A. \tag{6}$$

Given an approach space $(X,\mathcal{L})$, $\mathcal{L}^{\bigwedge} = \{\mu^{\wedge} \mid \mu \in \mathcal{L}\}$ is a basis for a lower regular function frame. The corresponding lower regular function frame is

$$\mathcal{L}_V^{\bigwedge} = \{\sup_{j\in J} \mu_j^{\wedge} \mid \forall j \in J : \mu_j \in \mathcal{L}\}.$$

This approach structure is called **Vietoris $\bigwedge$-structure**. Moreover, $\mathcal{L}^{\bigvee} = \{\mu^{\vee} | \mu \in \mathcal{L}\}$ is a subbasis for a lower regular function frame. The corresponding lower regular function frame is

$$\mathcal{L}_V^{\bigvee} = \{\sup_{j\in J} \inf_{k\in I_j} \mu_{j,k}^{\vee} \mid J \neq \emptyset, \forall j,k: \ I_j \subset J \ finite, \ \mu_{j,k} \in \mathcal{L}\}.$$

This approach structure is called **Vietoris $\bigvee$-structure**. Finally, the **Vietoris approach structure** is a lower regular function frame with the subbasis $\mathcal{L}^{\bigwedge} \cup \mathcal{L}^{\bigvee}$.

We denote the expression " such that " by " s.t. " briefly.

3. The Fell Approach Structure

In this section we construct a new approach structure corresponding to the Fell topology and investigate its properties. Here, $CL(X)$ and $K(X)$ denote the families of the closed and the compact subsets, respectively, of the Top-coreflection $\tau_{\mathcal{L}}^{tc}$ of the approach structure $\mathcal{L}$. To construct Fell approach structure, we modify the function $\mu^{\wedge}$ defined by Lowen and Wuyts [16] using compact sets. Let $\mu \in \mathbb{P}^X$ and B$\in$ K(X), we define the function

$$\mu_B^{\wedge} : CL(X) \longrightarrow \mathbb{P}$$
$$A \longmapsto \mu_B^{\wedge}(A) = \inf_{x\in A\cap B} \mu(x).$$

In the sequel the considered approach spaces are assumed to be Hausdorff approach spaces [15] $(X,\mathcal{L})$, that are the approach spaces such that their Top-coreflections are Hausdorff. In the following result we proved that being a Hausdorff approach space can be characterized by means of lower regular function frames.

Proposition 1. *For an approach space $(X,\mathcal{L})$, the following properties are equivalent.*

(i) $(X,\tau_{\mathcal{L}}^{tc})$ *is Hausdorff.*

(ii) $x \neq y \Longrightarrow (\exists \rho, \mu \in \mathcal{L} \ni \rho(x) > 0, \rho(y) = 0$ *and* $\mu(x) = 0, \mu(y) > 0)$.

Proof. Let $(X,\tau_{\mathcal{L}}^{tc})$ be a Hausdorff space. Then

$$\exists W, G \in \tau_{\mathcal{L}}^{tc} \text{ s.t. } x \in W, y \in G \text{ and } W \cap G = \emptyset$$

Since $W \in \tau_{\mathcal{L}}^{tc}$, we know that $y \in X - W = cl_{\mathcal{L}}(X - W)$ and $x \notin X - W$. Thus by (4) it is clear that

$$\forall \rho \in \mathcal{L} \text{ s.t. } \rho_{|X-W=0} : \rho(y) = 0$$

and

$$\exists \rho^{'} \in \mathcal{L} \text{ s.t. } \rho^{'}_{|X-W=0} : \rho^{'}(x) > 0.$$

Similarly, since $G \in \tau_{\mathcal{L}}^{tc}$, $x \in X - G$ and $y \notin X - G$, one can obtain that

$$\forall \mu \in \mathcal{L} \text{ s.t. } \mu_{|X-G=0} : \mu(x) = 0$$

and

$$\exists \mu^{'} \in \mathcal{L} \text{ s.t. } \mu^{'}_{|X-G=0} : \mu^{'}(y) > 0.$$

On the other hand, when (ii) holds we have three posibilities: If $\rho(x) < \mu(y)$, then by Proposition 2.2.8 in [17], $y \in \mu^{-1}(]\rho(x), +\infty[) \in \tau_{\mathcal{L}}^{tc}$ and $x \in \mu^{-1}([0, \rho(x)[) \in \tau_{\mathcal{L}}^{tc}$. Moreover,

$$\mu^{-1}(]\rho(x), +\infty[) \cap \mu^{-1}([0, \rho(x)[) = \emptyset$$

Hence $(X, \tau_{\mathcal{L}}^{tc})$ is Hausdorff. Similarly, if $\mu(y) < \rho(x)$ one can easily obtain the same fact. And if $\mu(y) = \rho(x)$, by the assumption since we have that both $\mu(y)$, $\rho(x)$ are positive, there exist a real number r such that $0 < r < \mu(y)$. Then $x \in \mu^{-1}([0, r[) \in \tau_{\mathcal{L}}^{tc}$ and $y \in \mu^{-1}(]r, +\infty[) \in \tau_{\mathcal{L}}^{tc}$. Moreover,

$$\mu^{-1}([0, r[) \cap \mu^{-1}(]r, +\infty[) = \emptyset$$

which completes the proof. □

Remark 1. *In [7] and [8] Baran and Qasim gave different definitions of T_0 and T_1 approach spaces. We hope that the characterization given in Proposition 1 will lead a way to give an analogue definition of T_2 spaces (Hausdorff spaces).*

The following result gives some basic properties of the modified function given in the beginning of this chapter.

Proposition 2. *If $(X, \mathcal{L})$ is an approach space, then the following statements are valid.*

(i) $\forall A, C \in CL(X)$, $\forall \mathcal{B} \subset K(X)$ *s.t.* $|\mathcal{B}| < \infty$:

$$\min_{B \in \mathcal{B}} \inf_{x \in B \cap C} \theta_A(x) = \inf_{x \in (\cup \mathcal{B}) \cap C} \theta_A(x),$$

(ii) $\forall A \in CL(X), \forall B \in K(X) : (\theta_A)^{\wedge}_{B} = \theta_{(A \cap B)^-}$,

(iii) $\forall \mathcal{A} \subset CL(X)$, $\forall B \in K(X) : (\theta_{\cup \mathcal{A}})^{\wedge}_{B} = \inf_{A \in \mathcal{A}} (\theta_A)^{\wedge}_{B}$,

(iv) $\forall A \in CL(X)$, $\mathcal{B} \subset K(X)$ *and* $|\mathcal{B}| < \infty : (\theta_A)^{\wedge}_{\cup \mathcal{B}} = \min_{B \in \mathcal{B}} (\theta_A)^{\wedge}_{B}$.

Proof. **(i)** It is straightforward. **(ii)** Let $C \in CL(X)$. Since $(\theta_A)^{\wedge}_{B}$ can only take on two values, ∞ or 0, we must consider two possible cases. Whenever $(\theta_A)^{\wedge}_{B}(C) = \infty$ then it means that $B \cap C = \emptyset$ or $A \cap B \cap C = \emptyset$. In both cases, clearly $C \notin (A \cap B)^-$ and thus $\theta_{(A\cap B)^-}(C) = \infty$. Also, whenever $\theta_{(A\cap B)^-}(C) = \infty$, one can easily show that $(\theta_A)^{\wedge}_{B}(C) = \infty$. For the second possibility, $(\theta_A)^{\wedge}_{B}(C) = 0$ iff $A \cap B \cap C \neq \emptyset$ which means that $C \in (A \cap B)^-$. Hence $\theta_{(A\cap B)^-}(C) = 0$.
(iii) Let $C \in CL(X)$. By (6) we obtain

$$(\theta_{\cup\mathcal{A}})^{\wedge}_{B}(C) = \inf_{x\in B\cap C} \theta_{\cup\mathcal{A}}(x) = \inf_{x\in B\cap C} \inf_{A\in\mathcal{A}} \theta_A(x)$$

and so if $B \cap C = \emptyset$, then

$$\inf_{A\in\mathcal{A}} (\theta_A)^{\wedge}_{B}(C) = \inf_{A\in\mathcal{A}} \inf_{x\in B\cap C} \theta_A(x) = \infty.$$

If $B \cap C \neq \emptyset$, then by (6) we obtain

$$\begin{aligned} (\theta_{\cup\mathcal{A}})^{\wedge}_{B}(C) &= \inf_{x\in B\cap C} \theta_{\cup\mathcal{A}}(x) \\ &= \inf_{x\in B\cap C} \inf_{A\in\mathcal{A}} \theta_A(x) \\ &= \inf_{A\in\mathcal{A}} \inf_{x\in B\cap C} \theta_A(x) \\ &= \inf_{A\in\mathcal{A}} (\theta_{\mathcal{A}})^{\wedge}_{B}(C). \end{aligned}$$

(iv) Let $C \in CL(X)$. For the finite subcollection $\mathcal{B} \subset K(X)$, if $(\cup\mathcal{B}) \cap C = \emptyset$, then

$$(\theta_A)^{\wedge}_{\cup\mathcal{B}}(C) = \inf_{x\in(\cup\mathcal{B})\cap C} \theta_A(x) = \infty$$

and

$$\min_{B\in\mathcal{B}} (\theta_A)^{\wedge}_{B}(C) = \min_{B\in\mathcal{B}} \inf_{x\in B\cap C} \theta_A(x) = \infty.$$

If $(\cup\mathcal{B}) \cap C \neq \emptyset$, then by (i) we obtain

$$\begin{aligned} \min_{B\in\mathcal{B}} (\theta_A)^{\wedge}_{B}(C) &= \min_{B\in\mathcal{B}} \inf_{x\in B\cap C} \theta_A(x) \\ &= \inf_{x\in(\cup B)\cap C} \theta_A(x) \\ &= (\theta_A)^{\wedge}_{\cup\mathcal{B}}(C). \end{aligned}$$

□

Proposition 3. *In an approach space* $(X, \mathcal{L})$*, the collection*

$$\mathcal{L}^{\bigwedge_{Fell}} = \{\mu^{\wedge}_{B} \mid \mu \in \mathcal{L}, B \in K(X)\}$$

is a subbasis for a lower regular function frame on $CL(X)$ *and the corresponding lower regular function frame is*

$$\mathcal{L}^{\bigwedge}_{Fell} = \left\{ \sup_{j\in J} \inf_{\substack{\mu\in\mathcal{L}_j \\ B\in K_j}} \mu^{\wedge}_{B} \mid J \neq \emptyset, \mathcal{L}_j \subset \mathcal{L}, K_j \subset K(X), \mathcal{L}_j \textit{ and } K_j \textit{ are finite} \right\}.$$

Proof. For all $\mu \in \mathcal{L}, B \in K(X)$, $\alpha > 0$ and $A \in CL(X)$, clearly

$$(\mu_B^{\wedge} + \alpha)(A) = \mu_B^{\wedge}(A) + \alpha = \inf_{x \in A \cap B} \mu(x) + \alpha = \inf_{x \in A \cap B} (\mu + \alpha)(x) = (\mu + \alpha)_B^{\wedge}(A).$$

Since $\mathcal{L}$ is translation invariant, we have $(\mu+\alpha)_B^{\wedge} \in \mathcal{L}^{\bigwedge_{Fell}}$ thus $\mathcal{L}^{\bigwedge_{Fell}}$ is translation invariant. Therefore, $\mathcal{L}^{\bigwedge_{Fell}}$ is a subbasis for a lower regular function frame. Thus we obtaine the following family;

$$\left\{ \inf_{\substack{\mu \in \mathcal{L}_j \\ B \in K_j}} \mu_B^{\wedge} \mid \mathcal{L}_j \subset \mathcal{L}, K_j \subset K(X), \mathcal{L}_j \textit{ and } K_j \textit{ are finite} \right\},$$

which is a basis for a lower regular function frame, and the lower regular function frame generated by this basis is

$$\mathcal{L}_{Fell}^{\bigwedge} = \left\{ \sup_{j \in J} \inf_{\substack{\mu \in \mathcal{L}_j \\ B \in K_j}} \mu_B^{\wedge} \mid J \neq \emptyset, \mathcal{L}_j \subset \mathcal{L}, K_j \subset K(X), \mathcal{L}_j \textit{ and } K_j \textit{ are finite} \right\}.$$

□

We call the approach structure $\mathcal{L}_{Fell}^{\bigwedge}$ as **Fell $\bigwedge$- approach structure**.

Theorem 1. *The collection $\mathcal{L}^{\bigvee} \cup \mathcal{L}^{\bigwedge_{Fell}}$ is a subbasis for the lower regular function frame;*

$$\mathcal{L}_{Fell} = \left\{ \sup_{j \in J} \Big(\inf_{\substack{\mu \in \mathcal{L}_j \\ B \in K_j}} \mu_B^{\wedge} \bigwedge \inf_{\mu \in \mathcal{L}_{t_j}} \mu^{\vee} \Big) \mid \mathcal{L}_j, \mathcal{L}_{t_j} \subset \mathcal{L}, K_j \subset K(X), \right.$$
$$\left. \mathcal{L}_j, \mathcal{L}_{t_j} \textit{ and } K_j \textit{ are finite} \right\}.$$

Proof. Since $\mathcal{L}^{\bigvee}$ and $\mathcal{L}^{\bigwedge_{Fell}}$ are both translation invariant, so $\mathcal{L}^{\bigvee} \cup \mathcal{L}^{\bigwedge_{Fell}}$ is. Thus this union is a subbasis for a lower regular function frame. Hence $\mathcal{L}^{\bigvee} \cup \mathcal{L}^{\bigwedge_{Fell}}$ generates a lower regular function frame (see (1)) which coincides with $\mathcal{L}_{Fell}$. □

We call the approach structure $\mathcal{L}_{Fell}$ as **Fell approach structure**. Now we should point out that this generalization is meaningful by introducing its relation with the ordinary Fell topology.

If $\mathcal{L}$ is a lower regular function frame, then it was shown in [16] that

$$\forall \mu \in \mathcal{L} : \{\mu = 0\}^{+} = \{\mu^{\vee} = 0\}. \tag{7}$$

The following lemma gives analogue equalities for our modified functions $\mu_B^{\wedge}$ whenever $\mu \in \mathcal{L}$, $B \in K(X)$.

Lemma 1. *In an approach space $(X, \mathcal{L})$, the following holds*
(i) $\forall \mu \in \mathcal{L}, \forall B \in K(X) : \{\mu_B^{\wedge} = 0\} = \big(\{\mu = 0\} \bigcap B\big)^{-}$,

(ii) *For all* $K \in K(X)$,

$$\Big(\bigcap_{\rho\in\mathcal{J}}\{\rho=0\}\Big)^{-} = \bigcap_{\rho\in\mathcal{J}}\{\rho=0\}^{-} = \bigcap_{\rho\in\mathcal{J}}\{\rho_K^{\wedge}=0\}$$

where $\mathcal{J}=\{\rho\in\mathcal{L}\mid \rho_{|_K}=0\}$.

Proof. **(i)** To prove the equality we shall show that $\mu : (X,\tau_{\mathcal{L}}^{tc}) \to \mathbb{P}$ is lower semicontinuous. For an arbitrary $\alpha>0$ if $x\notin\{\mu\leq\alpha\}$ since we can consider the mapping $\rho:=(\mu-\alpha)\bigvee 0$ that lies in $\mathcal{L}$, $x\notin\{\rho=0\}$. Thus by (5)

$$x\notin \bigcap_{\substack{\rho\in\mathcal{L}\\ \rho_{|_{\{\mu\leq\alpha\}}}=0}}\{\rho=0\} = cl_{\tau}\{\mu\leq\alpha\}.$$

Therefore $\{\mu\leq\alpha\}$ is a closed subset in the Top-coreflection $\tau_{\mathcal{L}}^{tc}$ of $\mathcal{L}$. Hence μ is lower semicontinuous. Now let us consider the claimed equality:

$$A\in\{\mu_B^{\wedge}=0\} \iff \inf_{x\in A\cap B}\mu(x)=0.$$

By the fact that a lower semicontinuous mapping takes on its infimum value on a compact set [9], we obtain

$$\begin{aligned}\inf_{x\in A\cap B}\mu(x)=0 &\iff \exists x\in A\cap B:\mu(x)=0\\ &\iff A\cap B\cap\{\mu=0\}\neq\emptyset\\ &\iff A\in(\{\mu=0\}\cap B)^{-}.\end{aligned}$$

(ii) Let $K\in K(X)$, then

$$\begin{aligned}A\in\Big(\bigcap_{\rho\in\mathcal{J}}\{\rho=0\}\Big)^{-} &\iff A\bigcap\Big(\bigcap_{\rho\in\mathcal{J}}\{\rho=0\}\Big)\neq\emptyset\\ &\iff \exists a\in A \text{ and } a\in\{\rho=0\} \text{ for all } \rho\in\mathcal{J}\\ &\iff A\cap\{\rho=0\}\neq\emptyset \text{ for all } \rho\in\mathcal{J}\\ &\iff A\in\bigcap_{\rho\in\mathcal{J}}\{\rho=0\}^{-}.\end{aligned}$$

For the second equality

$$\begin{aligned}A\in\bigcap_{\rho\in\mathcal{J}}\{\rho=0\}^{-} &\implies \forall\rho\in\mathcal{J}: A\in\{\rho=0\}^{-}\\ &\implies \forall\rho\in\mathcal{J}:\exists a\in A \text{ s.t. } \rho(a)=0\\ &\implies \forall\rho\in\mathcal{J}:\inf_{a\in A}\rho(a)=0.\end{aligned}$$

Moreover, since $K \in CL(X)$, by (5) we know that

$$K = cl_{\mathcal{L}}(K) = \bigcap_{\rho \in \mathcal{J}} \{\rho = 0\}.$$

Thus, if $A \in K^-$, then the first equality provides that

$$\forall \rho \in \mathcal{J} : \inf_{a \in A \cap K} \rho(a) = 0$$

thus

$$\forall \rho \in \mathcal{J} : A \in \{\rho_K^\wedge = 0\}.$$

Consequently, we obtain that $A \in \bigcap_{\rho \in \mathcal{J}} \{\rho_K^\wedge = 0\}$. Conversely, if $A \in \bigcap_{\rho \in \mathcal{J}} \{\rho_K^\wedge = 0\}$, then

$$\forall \rho \in \mathcal{J} : \inf_{a \in A \cap K} \rho(a) = 0.$$

By the lower semicontinuity of ρ and compactness of $A \cap K$,

$$\exists a \in A \cap K \text{ s.t. } \rho(a) = 0 \text{ for all } \rho \in \mathcal{J}.$$

Therefore

$$\forall \rho \in J : A \cap \{\rho = 0\} \neq \emptyset.$$

Hence, $A \in \bigcap_{\rho \in \mathcal{J}} \{\rho = 0\}^-$ which completes the proof.

□

Remark 2. *Lowen and Wuyts [16] proved that if $(X, \mathcal{L})$ is a topological approach space, then $(CL(X), \mathcal{L}_V^{\bigwedge}), (CL(X), \mathcal{L}_V^{\bigvee})$ and $(CL(X), \mathcal{L}_V)$ are topological approach spaces.*

With the following theorem we investigate the analogue fact for our new structures.

Theorem 2. *Whenever $\mathcal{L}$ is a topological approach structure on X, $\mathcal{L}_{Fell}^\wedge$ and $\mathcal{L}_{Fell}$ are topological approach structures on $CL(X)$.*

Proof. By Proposition 2.1.2 (5) in [17] (page 93-94), it suffices to prove that $\theta_{\{\mu_B^\wedge = 0\}} \in \mathcal{L}_{Fell}^\wedge$ for all $\mu \in \mathcal{L}$ and $B \in K(X)$. With respect to the same theorem (i) we know that $\theta_{\{\mu \leq \varepsilon\}} \in \mathcal{L}$ for all $\varepsilon > 0$. Thus $(\theta_{\{\mu \leq \varepsilon\}})_B^\wedge \in \mathcal{L}_{Fell}^\wedge$ for all $\varepsilon > 0$ and $B \in K(X)$. By Proposition 2 (ii) we have $(\theta_{\{\mu \leq \varepsilon\}})_B^\wedge = \theta_{(\{\mu \leq \varepsilon\} \cap B)^-}$. Therefore by (LR1); in order to complete the proof it is sufficient to show that $\theta_{\{\mu_B^\wedge = 0\}} = \sup_{\varepsilon > 0} \theta_{(\{\mu \leq \varepsilon\} \cap B)^-}$. Since the indicator function takes on only two values, we shall consider both of the possibilities. Let $A \in CL(X)$

$$\begin{aligned} \theta_{\{\mu_B^\wedge = 0\}}(A) = 0 \quad &\Longleftrightarrow \quad A \in \{\mu_B^\wedge = 0\} \\ &\Longleftrightarrow \quad \forall \varepsilon > 0 : \exists x_\varepsilon \in A \cap B \text{ s.t. } \mu(x_\varepsilon) \leq \varepsilon \\ &\Longleftrightarrow \quad \forall \varepsilon > 0 : A \cap B \cap \{\mu \leq \varepsilon\} \neq \emptyset \\ &\Longleftrightarrow \quad \forall \varepsilon > 0 : A \in (B \cap \{\mu \leq \varepsilon\})^- \end{aligned}$$

$$\begin{aligned}&\Longleftrightarrow \quad \forall \varepsilon > 0 : \theta_{(B\cap\{\mu\leq\varepsilon\})^-}(A) = 0\\ &\Longleftrightarrow \quad \sup_{\varepsilon>0}\theta_{(B\cap\{\mu\leq\varepsilon\})^-}(A) = 0.\end{aligned}$$

In addition

$$\begin{aligned}\sup_{\varepsilon>0}\theta_{(\{\mu\leq\varepsilon\}\cap B)^-}(A) = \infty \quad &\Longleftrightarrow \quad \exists\varepsilon > 0 \text{ s.t. } \theta_{(\{\mu\leq\varepsilon\}\cap B)^-}(A) = \infty\\ &\Longleftrightarrow \quad \exists\varepsilon > 0 \text{ s.t. } A \notin (\{\mu\leq\varepsilon\}\cap B)^-\\ &\Longleftrightarrow \quad \exists\varepsilon > 0 \text{ s.t. } A\cap(\{\mu\leq\varepsilon\}\cap B) = \emptyset\\ &\Longleftrightarrow \quad \exists\varepsilon > 0 \text{ s.t. } A\cap B\subset\{\mu>\varepsilon\}\\ &\Longrightarrow \quad \exists\varepsilon > 0 \text{ s.t. } \inf_{x\in A\cap B}\mu(x)\geq\varepsilon\\ &\Longrightarrow \quad \theta_{\{\mu_B^\wedge=0\}}(A) = \infty.\end{aligned}$$

On the other hand if $\theta_{\{\mu_B^\wedge=0\}}(A) = \infty$, then

$$\begin{aligned}A\notin\{\mu_B^\wedge=0\} \quad &\Longrightarrow \quad \inf_{x\in A\cap B}\mu(x) > 0\\ &\Longrightarrow \quad \exists\varepsilon > 0 \text{ s.t. } \inf_{x\in A\cap B}\mu(x) > \varepsilon\\ &\Longleftrightarrow \quad \exists\varepsilon > 0 \text{ s.t. } A\cap B\cap(\{\mu\leq\varepsilon\}) = \emptyset\\ &\Longleftrightarrow \quad \exists\varepsilon > 0 \text{ s.t. } A\notin(\{\mu\leq\varepsilon\}\cap B)^-\\ &\Longrightarrow \quad \exists\varepsilon > 0 \text{ s.t. } \theta_{(\{\mu\leq\varepsilon\}\cap B)^-}(A) = \infty\\ &\Longrightarrow \quad \sup_{\varepsilon>0}\theta_{(\{\mu\leq\varepsilon\}\cap B)^-}(A) = \infty\end{aligned}$$

Hence $\mathcal{L}^\wedge_{Fell}$ is a topological approach structure. Since $\mathcal{L}^\wedge_{Fell}$ and $\mathcal{L}^\vee_V$ are topological approach structures [16], one can obtain easily that $\mathcal{L}_{Fell}$ is a topological approach structure . □

The facts given in the following lemma are expressed by Lowen and Wuyts in [16] (see page 288 line 23). There $\mathcal{L}$ is expressed as a regular function frame and in [17] that structure is renamed as lower regular function frame.

Lemma 2. *Let $\mathcal{L}$ be a lower regular function frame on X then*
(i) *If $\mathcal{B}$ is a basis for $\mathcal{L}$, then $\mathcal{C} := \{\{\rho = 0\} \mid \rho\in\mathcal{B}\}$ is a basis for the collection of closed subsets of $\tau^{tc}_{\mathcal{L}}$.*
(ii) *If $\mathcal{S}$ is a subbasis for $\mathcal{L}$, then $\mathcal{T} := \{\{\mu = 0\} \mid \mu\in\mathcal{S}\}$ is a subbasis for the collection of closed subsets of $\tau^{tc}_{\mathcal{L}}$ [16].*

Remark 3. *It was proved by Lowen and Wuyts in [16] that Top-coreflections of $\mathcal{L}^{\bigwedge}_V, \mathcal{L}^{\bigvee}_V$ and $\mathcal{L}_V$ are τ^+_V, τ^-_V and τ_V, respectively. Lowen and Wuyts also showed that if $(X,\mathcal{L})$ is any approach space, Top-coreflection of $\mathcal{L}^{\bigvee}_V$ coincides with $(\tau^{tc}_{\mathcal{L}})^-_V$, whereas there is no relation between Top-coreflections of $\mathcal{L}^{\bigwedge}_V, \mathcal{L}_V$ and $(\tau^{tc}_{\mathcal{L}})^+_V, (\tau^{tc}_{\mathcal{L}})_V$, respectively on the whole of CL(X). Nevertheless, the following equalities hold only on $K(X)$, that is*

$$\tau^{tc}_{\mathcal{L}^{\wedge}_{V}} = (\tau^{tc}_{\mathcal{L}})^{+}_{V} \text{ and } \tau^{tc}_{\mathcal{L}_{V}} = (\tau^{tc}_{\mathcal{L}})_{V}.$$

Now we show that the Top-coreflection $\tau^{tc}_{\mathcal{L}^{\wedge}_{Fell}}$ of the approach structure $\mathcal{L}^{\wedge}_{Fell}$ is the upper Fell topology on CL(X) and Top-coreflection $\tau^{tc}_{\mathcal{L}_{Fell}}$ of the Fell approach structure $\mathcal{L}_{Fell}$ is the Fell topology on CL(X).

The following theorem is the main result of this paper.

Theorem 3. *For a lower regular function frame $\mathcal{L}$ on X, the following properties hold.*

(i) $\tau^{tc}_{\mathcal{L}^{\wedge}_{Fell}} = (\tau^{tc}_{\mathcal{L}})^{+}_{Fell}$,

(ii) $\tau^{tc}_{\mathcal{L}_{Fell}} = (\tau^{tc}_{\mathcal{L}})_{Fell}$.

Proof. **(i)** Since $\mathcal{L}^{\wedge_{Fell}} = \{\mu^{\wedge}_{B} | \mu \in \mathcal{L}, B \in K(X)\}$ is a subbasis for $\mathcal{L}^{\wedge}_{Fell}$, by Lemma 2 (ii) we obtain that the family

$$\mathcal{S} = \left\{ \{\mu^{\wedge}_{B} = 0\} \mid \mu \in \mathcal{L}, B \in K(X) \right\}$$

is a subbasis for the collection $\mathcal{F}_{\mathcal{L}^{\wedge}_{Fell}}$ of closed subsets of $(CL(X), \tau^{tc}_{\mathcal{L}^{\wedge}_{Fell}})$. Moreover,

$$\mathcal{B} = \{K^{-} \mid K \in K(X)\}$$

is a basis for the collection $\mathcal{F}^{+}_{\mathcal{L}_{Fell}}$ of closed subsets of $(CL(X), (\tau^{tc}_{\mathcal{L}})^{+}_{Fell})$. It is sufficient to prove that $\mathcal{S} \subset \mathcal{B}$ in order to obtain $\mathcal{F}_{\mathcal{L}^{\wedge}_{Fell}} \subset \mathcal{F}^{+}_{\mathcal{L}_{Fell}}$. Thus let $\mathcal{A} \in \mathcal{S}$, then

$$\exists \mu \in \mathcal{L}, \exists B \in K(X) \text{ s.t. } \mathcal{A} = \{\mu^{\wedge}_{B} = 0\}.$$

Therefore by Lemma 1 (i), $\mathcal{A} = \{\{\mu = 0\} \cap B\}^{-}$ and by the lower semicontinuity of μ, we obtain $\{\mu = 0\} \cap B \in K(X)$ and then $\mathcal{F}_{\mathcal{L}^{\wedge}_{Fell}} \subset \mathcal{F}^{+}_{\mathcal{L}_{Fell}}$. On the other hand, by the fact that $K(X) \subset CL(X)$ and by (5)

$$\begin{aligned} \mathcal{A} \in \mathcal{B} &\implies \exists K \in K(X) : \mathcal{A} = K^{-} \\ &\implies \mathcal{A} = \left(\bigcap_{\rho \in \mathcal{J}} \{\rho = 0\} \right)^{-}, \text{ where } \mathcal{J} = \{\rho \in \mathcal{L} \mid \rho_{|K=0}\}. \end{aligned}$$

Moreover, by Lemma 1 (ii) and since $\{\rho^{\wedge}_{K} = 0\} \in \mathcal{S}$ for all $\rho \in \mathcal{J}$ we obtain that $\mathcal{F}^{+}_{\mathcal{L}_{Fell}} \subset \mathcal{F}_{\mathcal{L}^{\wedge}_{Fell}}$.

(ii) We know that $\mathcal{L}^{\wedge_{Fell}} \bigcup \mathcal{L}^{\vee} = \{\mu^{\wedge}_{B} \mid \mu \in \mathcal{L}, B \in K(X)\} \bigcup \{\nu^{\vee} \mid \nu \in \mathcal{L}\}$ is a subbasis for $\mathcal{L}_{Fell}$. By Lemma 2 (ii),

$$\mathcal{S}_1 = \left\{ \{\eta = 0\} \mid \eta \in \mathcal{L}^{\wedge_{Fell}} \bigcup \mathcal{L}^{\vee} \right\}$$

is a subbasis for the collection $\mathcal{F}_{\mathcal{L}_{Fell}}$ of the closed sets of $(CL(X),\tau^{tc}_{\mathcal{L}_{Fell}})$. In addition

$$\mathcal{S}_2=\Big\{F^+ \mid F\in CL(X)\Big\}\bigcup\Big\{K^- \mid K\in K(X)\Big\},$$

is a subbasis for the collection $(\mathcal{F}_{\mathcal{L}})_{Fell}$ of closed subsets of $(CL(X),(\tau^{tc}_{\mathcal{L}})_{Fell})$. Now we shall prove that $\mathcal{S}_1\subset\mathcal{S}_2$ in order to obtain that $\mathcal{F}_{\mathcal{L}_{Fell}}\subset(\mathcal{F}_{\mathcal{L}})_{Fell}$. Let $\mathcal{A}\in\mathcal{S}_1$, then

$$\exists\eta\in\mathcal{L}^{\wedge_{Fell}}\bigcup\mathcal{L}^{\vee}:\mathcal{A}=\{\eta=0\}.$$

Thus we have two possibilities. If $\eta\in\mathcal{L}^{\wedge_{Fell}}$, then

$$\exists\mu\in\mathcal{L},\exists B\in K(X):\mathcal{A}=\{\mu^{\wedge}_{B}=0\}$$

Lemma 1 (i) provides that $\mathcal{A}\in\mathcal{S}_2$. If $\eta\in\mathcal{L}^{\vee}$, then

$$\exists\mu\in\mathcal{L}\ni\mathcal{A}=\{\mu^{\vee}=0\}$$

and by (7) $\mathcal{A}\in(\mathcal{F}_{\mathcal{L}})_{Fell}$. On the other hand when $\mathcal{A}\in\mathcal{S}_2$ we have two posibilities. If there exists $F\in CL(X)$ s.t. $\mathcal{A}=F^+$, by (5) and (7) we obtain

$$\mathcal{A}=\Bigg(\bigcap_{\substack{\rho\in\mathcal{L}\\ \rho_{|F}=0}}\{\rho=0\}\Bigg)^+=\bigcap_{\substack{\rho\in\mathcal{L}\\ \rho_{|F}=0}}\{\rho=0\}^+=\bigcap_{\substack{\rho\in\mathcal{L}\\ \rho_{|F}=0}}\{\rho^{\vee}=0\}\in(\tau_{\mathcal{L}_{Fell}})^c.$$

If there exists $K\in K(X)\subset CL(X)$ for which $\mathcal{A}=K^-$, then respectively (5) and Lemma 1 (ii) provides that

$$\mathcal{A}=K^-=\Bigg(\bigcap_{\substack{\rho\in\mathcal{L}\\ \rho_{|K}=0}}\{\rho=0\}\Bigg)^-=\bigcap_{\substack{\rho\in\mathcal{L}\\ \rho_{|K}=0}}\{\rho^{\wedge}_{K}=0\}\in\mathcal{F}_{\mathcal{L}_{Fell}}.$$

Hence it follows that $(\mathcal{F}_{\mathcal{L}})_{Fell}\subset\mathcal{F}_{\mathcal{L}_{Fell}}$. □

The following example gives rise to observe how one shall construct the members of the subbasis of the Fell approach structure step by step. To make it more clear we considered the topological case.

Example 1. *Let $\mathcal{L}_{\mathcal{U}}$ be the induced frame on $\mathbb{R}$, where $\mathcal{U}$ is the usual topology on $\mathbb{R}$. In this case, of course, $\tau^{tc}_{\mathcal{L}_{\mathcal{U}}}=\mathcal{U}$. Now we shall consider $CL(\mathbb{R})$ with its Fell approach structure. Here $\mathcal{L}^{\vee}=\{\mu^{\vee}|\mu:(\mathbb{R},\mathcal{U})\to\mathbb{P}$ lower semi continuous$\}$ and $\mathcal{L}^{\wedge_{Fell}}=\{\mu^{\wedge}_{B}|\mu:(\mathbb{R},\mathcal{U})\to\mathbb{P}$ lower semi continuous and $B\in K(\mathbb{R})\}$. If we let the lower semi continuous mapping $\mu:\mathbb{R}\longrightarrow\mathbb{P}$ defined as*

$$\mu(x)=\begin{cases}x^2, & x>1\\ 1-x^2, & x\leq 1\end{cases},$$

then $\mu^{\vee} \in \mathcal{L}^{\vee}$ *and* $\mu_B^{\wedge} \in \mathcal{L}^{\wedge_{Fell}}$. *For* $A \in CL(\mathbb{R})$, $\mu_B^{\wedge}(A) = \infty$ *whenever* $A \cap B = \emptyset$ *and if* $A \cap B \neq \emptyset$ *there exist* $x_0 \in A \cap B$ *such that* $\mu_B^{\wedge}(A) = \mu(x_0)$. *Particularly,* $\theta_A \in \mathcal{L}_{\mathcal{U}_{Fell}}$ *for each* $A \in CL(\mathbb{R})$. *Because if we let* $B = [0,1]$, *then by Proposition 2.1.2 (3) in [17],* $(\theta_{\{\mu=0\}})_B^{\wedge} \in \mathcal{L}_{\mathcal{U}_{Fell}}$. *And one can easily see that* $(\theta_{\{\mu=0\}})_B^{\wedge} = \theta_A$.

Now we construct an approach structure corresponding to the extended Fell topology. Extended Fell topology τ_{eFell} is a topology on $\mathcal{W} = CL(X) \cup \{\emptyset\}$ with subbasis

$$\{V^-|V \in \tau\} \bigcup \{W^+|W \in \tau, W^c \in K(X)\}$$

where W^+ is considered as the set of subsets of W which belongs to $\mathcal{W}$. While constructing the extended Fell approach space, the domains of $\mu_B^{\wedge}$ and $\mu^{\vee}$ are assumed to be $\mathcal{W}$ instead of $CL(X)$.

Proposition 4. *If* $(X, \mathcal{L})$ *is an approach space, then*

$$\mathcal{L}^{\bigwedge_{eFell}} = \{\mu_B^{\wedge} \mid \mu \in \mathcal{L}, B \in K(X)\}$$

is a subbasis for a lower regular function frame and the corresponding frame is

$$\mathcal{L}_{eFell}^{\bigwedge} = \left\{ \sup_{j\in J} \inf_{\substack{\mu\in\mathcal{L}_j \\ B\in K_j}} \mu_B^{\wedge} \mid J \neq \emptyset, \mathcal{L}_j \subset \mathcal{L}, K_j \subset K(X), \mathcal{L}_j \text{ and } K_j \text{ are finite} \right\}.$$

Proof. The proof goes along the same lines in Proposition 3. □

Theorem 4. *The collection* $\mathcal{L}^{\bigvee} \cup \mathcal{L}^{\bigwedge_{eFell}}$ *is a subbasis for a lower regular function frame. The corresponding lower regular function frame is*

$$\mathcal{L}_{eFell} = \left\{ \sup_{j\in J} \Big(\inf_{\substack{\mu\in\mathcal{L}_j \\ B\in K_j}} \mu_B^{\wedge} \bigwedge \inf_{\mu\in\mathcal{L}_{t_j}} \mu^{\vee} \Big) \mid \mathcal{L}_j, \mathcal{L}_{t_j} \subset \mathcal{L}, K_j \subset K(X), \right.$$

$$\left. \mathcal{L}_j, \mathcal{L}_{t_j} \text{ and } K_j \text{ are finite} \right\}$$

Proof. The proof goes along the same lines in Theorem 1. □

The approach structures $\mathcal{L}_{eFell}^{\bigwedge}$ and $\mathcal{L}_{eFell}$ are called **extended Fell $\bigwedge$-approach structure** and **extended Fell approach structure**, respectively. In the following result we give the fact that the Top-coreflection of extended Fell approach structure is the extended Fell topology on $\mathcal{W}$.

Theorem 5. *For a lower regular function frame* $\mathcal{L}$ *on* X*, the following properties hold*

(i) $\tau^{tc}_{\mathcal{L}^{\wedge}_{eFell}} = (\tau^{tc}_{\mathcal{L}})^{+}_{eFell}$,

(ii) $\tau^{tc}_{\mathcal{L}_{eFell}} = (\tau^{tc}_{\mathcal{L}})_{eFell}$.

Proof. The proof goes along the same lines in Theorem 3. □

In [16] the measure of compactness of an approach space $(X, \mathcal{L})$ is given as

$$\chi_c(X) = \sup_{\mathcal{F}\in F(X)} \inf_{x\in X} \sup_{F\in\mathcal{F}} \sup_{\substack{\rho\in\mathcal{L} \\ \rho_{|F}=0}} \rho(A)$$

where $F(X)$ is the set of all filters on X. If an approach space has an index of compactness equal to zero, then in [10] it is said to be 0-compact. Lowen and Wuyts [16] proved that the index of compactness of X can be reformulated in terms of FS-sets; that is a subset $\mathcal{B}$ of $\mathcal{L}$ such that $\inf_{\mu\in\mathcal{C}} \mu = 0$ for each finite subcollection $\mathcal{C}$ of $\mathcal{B}$. For a subbasis $\mathcal{B}$ of $\mathcal{L}$, if an FS-set is contained in $\mathcal{B}$ we say it is an FS-set in $\mathcal{B}$. The set of all FS-sets in $\mathcal{B}$ is denoted by $B_s(\mathcal{B})$ and the following equality holds.

$$\chi_c(X) = \sup_{\mathcal{I}\in B_s(\mathcal{B})} \inf_{x\in X} \bigvee \mathcal{I}(x)$$

Here, for clarity we shall write $\chi_c(X_{\mathcal{L}})$ instead of $\chi_c(X)$. In the following theorem we show that extended Fell $\wedge$-approach space is 0-compact and then it gives a result which mentions that the compactness index of $(\mathcal{W}, \mathcal{L}_{eFell})$ is zero.

Theorem 6. $\chi_c(CL(X_{\mathcal{L}^{\wedge}_{Fell}})) = 0$ *for any approach space* $(X, \mathcal{L})$.

Proof. Consider the subbasis $\mathcal{L}^{\bigwedge_{Fell}}$ for $\mathcal{L}^{\bigwedge}_{Fell}$. We shall prove that

$$\forall \mathcal{I} \in B_s(\mathcal{L}^{\bigwedge_{Fell}}) : \inf_{A\in CL(X)} \bigvee \mathcal{I}(A) = 0$$

Let $\mathcal{I} \in B_s(\mathcal{L}^{\bigwedge_{Fell}})$, i.e $\mathcal{I}$ is an FS-set in $\mathcal{L}^{\wedge}_{Fell}$, then for $\{\mu^{\wedge}_K\} \in 2^{(I)}$ where $\mu \in \mathcal{L}$ and $K \in K(X)$ we obtain that

$$\inf_{A\in CL(X)} \mu^{\wedge}_K(A) = 0$$

Clearly for all $A \in CL(X)$, $A \cap K \subset X$ and so $\mu^{\wedge}_K(X) \leq \mu^{\wedge}_K(A)$. Then

$$\mu^{\wedge}_K(X) \leq \inf_{A\in CL(X)} \mu^{\wedge}_K(A)$$

Therefore $\mu^{\wedge}_K(X) = 0$. Since $K \in K(X)$ is arbitrary it follows that

$$\bigvee \mathcal{I}(X) = \sup_{\mu^{\wedge}_B\in\mathcal{I}} \mu^{\wedge}_B(X) = 0.$$

Consequently $\inf_{A\in CL(X)} \bigvee \mathcal{I}(A) = 0$. □

Corollary 1. $\chi_c(\mathcal{W}_{\mathcal{L}_{eFell}}) = 0$ *for any approach space* $(X, \mathcal{L})$.

Proof. The compactness of $(\mathcal{W}, \tau_{eFell})$ is given in [4] and we know that an approach space with a compact topological coreflection is 0-compact [17]. By these two facts, Theorem 5 provides that the compactness index of the extended Fell approach space is zero. □

Proposition 5. *For a lower regular function frame $\mathcal{L}$ on X, the following properties hold.*

(i) If $\rho \in \mathcal{L}_{eFell}$ s.t. $\rho_{|_\mathcal{D}} = 0$ whenever $\mathcal{D} \subset CL(X)$, then $\rho_{|_{CL(X)}} \in \mathcal{L}_{Fell}$ and $(\rho_{|_{CL(X)}})_{|_\mathcal{D}} = 0$,

(ii) If $\nu \in \mathcal{A}_{eFell}(B)$, then $\nu_{|_{CL(X)}} \in \mathcal{A}_{Fell}(B)$ for an arbitrary $B \in CL(X)$.

Proof. **(i)** If $\rho \in \mathcal{L}_{eFell}$ s.t. $\rho_{|_\mathcal{D}} = 0$, then by the definition of $\mathcal{L}_{Fell}$ and the facts about restriction of a function, clearly $\rho_{|_{CL(X)}} \in \mathcal{L}_{Fell}$ and $(\rho_{|_{CL(X)}})_{|_\mathcal{D}} = 0$.
(ii) By (2) and (3) it is clear that

$$\mathcal{A}_{eFell}(B) = \left\{ \phi \in \mathbb{P}^{\mathcal{W}} \mid \forall \mathcal{D} \subset \mathcal{W} : \inf_{D \in \mathcal{D}} \phi(D) \leq \sup_{\substack{\rho \in \mathcal{L}_{eFell} \\ \rho_{|_\mathcal{D}} = 0}} \rho(B) \right\}.$$

If $\nu \in \mathcal{A}_{eFell}(B)$, then

$$\forall \mathcal{D} \subset \mathcal{W} : \inf_{D \in \mathcal{D}} \nu(D) \leq \sup_{\substack{\rho \in \mathcal{L}_{eFell} \\ \rho_{|_\mathcal{D}} = 0}} \rho(B). \tag{8}$$

Thus (8) is also true for an arbitrary subfamily $\mathcal{D}$ of $CL(X)$. In addition, for all $D \in \mathcal{D} \subset CL(X)$, it is obvious that $\nu_{|_{CL(X)}}(D) = \nu(D)$. Therefore

$$\inf_{D \in \mathcal{D}} \nu_{|_{CL(X)}}(D) = \inf_{D \in \mathcal{D}} \nu(D) \leq \sup_{\substack{\rho \in \mathcal{L}_{eFell} \\ \rho_{|_\mathcal{D}} = 0}} \rho(B).$$

To complete the proof we shall prove that

$$\sup_{\substack{\rho \in \mathcal{L}_{eFell} \\ \rho_{|_\mathcal{D}} = 0}} \rho(B) \leq \sup_{\substack{\mu \in \mathcal{L}_{Fell} \\ \mu_{|_\mathcal{D}} = 0}} \mu(B).$$

For an arbitrary $\alpha > 0$ suppose that

$$\forall \mu \in \mathcal{L}_{Fell} \text{ s.t. } \mu_{|_\mathcal{D}} = 0 : \mu(B) < \alpha \tag{9}$$

If $\rho \in \mathcal{L}_{eFell}$ s.t. $\rho_{|_\mathcal{D}} = 0$, then by **(i)** it is clear that $\rho_{|_{CL(X)}} \in \mathcal{L}_{Fell}$ and $(\rho_{|_{CL(X)}})_{|_\mathcal{D}} = 0$. Thus by (9) $\sup_{\substack{\rho \in \mathcal{L}_{eFell} \\ \rho_{|_\mathcal{D}} = 0}} \rho(B) \leq \alpha$ which completes the proof. □

An approach space $(X, \mathcal{L})$ is said to be LC1 iff its Top-coreflection is locally compact [13]. By using Corollary 5.1.4 in [4], we obtain the following result as an analogue of the same Corollary by means of approach theory.

Theorem 7. *If $(X, \mathcal{L})$ is a LC1-Hausdorff approach space, then $(\mathcal{W}, \mathcal{L}_{eFell})$ is a 0-compact Hausdorff approach space and $(CL(X), \mathcal{L}_{Fell})$ is a LC1 Hausdorff approach space.*

Proof. It was first observed in [5] that $(\mathcal{W}, \tau_{eFell})$ is a Hausdorff topological space. In Theorem 5 we proved that the Top-coreflection of $(\mathcal{W}, \mathcal{L}_{eFell})$ is $(\mathcal{W}, \tau_{eFell})$. Then by these two facts and Corollary 1 it is clear that $(\mathcal{W}, \mathcal{L}_{eFell})$ is a 0-compact Hausdorff space. Since $(X, \mathcal{L})$ is LC1, we know that $(X, \tau^{tc}_{\mathcal{L}})$ is locally compact. Then $(CL(X), (\tau^{tc}_{\mathcal{L}})_{Fell})$ is locally compact by Corollary 5.1.4 in [4]. Consequently $(CL(X), \mathcal{L}_{Fell})$ is LC1 by Theorem 3 (ii) and definition of the property LC1, respectively. Then the proof is completed since $(X, \tau^{tc}_{\mathcal{L}})$ is locally compact. Because, in [3], it is said that being locally compact provides that $(\mathcal{W}, \tau_{eFell})$ is Hausdorff and so the subhyperspace $(CL(X), \tau_{Fell})$ is. Thus by Theorem 3 clearly $(CL(X), \mathcal{L}_{Fell})$ is a Hausdorff approach space. In addition it can be easily seen by Proposition 1, whenever $(\mathcal{W}, \mathcal{L}_{eFell})$ is assumed to be a Hausdorff approach space. Let $A, B \in CL(X)$ and $A \neq B$, then

$$\exists \rho, \mu \in \mathcal{L}_{eFell} \ni \rho(A) > 0, \rho(B) = 0 \text{ and } \mu(A) = 0, \mu(B) > 0.$$

By Proposition 5 (i), we know that $\rho_{|_{CL(X)}}, \mu_{|_{CL(X)}} \in \mathcal{L}_{Fell}$. Therefore by the fact that, $\rho_{|_{CL(X)}}(A) = \rho(A)$ and $\mu_{|_{CL(X)}}(A) = \mu(A)$ for each $A \in CL(X)$, we obtain

$$\rho_{|_{CL(X)}}(A) > 0, \rho_{|_{CL(X)}}(B) = 0 \text{ and } \mu_{|_{CL(X)}}(A) = 0, \mu_{|_{CL(X)}}(B) > 0.$$

Hence $(CL(X), \mathcal{L}_{Fell})$ is a Hausdorff approach space. □

Author Contribution Statements All authors contributed equally and significantly in writing this article. All authors read and approved the final manuscript.

Declaration of Competing Interests On behalf of all authors, the corresponding author states that there is no conflict of interest.

Acknowledgements The authors would like to thank the referee for valuable suggestions and comments which improved the paper considerably.

References

[1] Beer, G., Kenderov, P. On the arg min multifunction for lower semicontinuous functions, *Proc. Amer. Math. Soc.*, 102 (1988), 107-113. https://doi.org/10.1090/S0002-9939-1988-0915725-3

[2] Beer, G., Luchetti, R., Convex optimization and epi-distance topology, *Trans. Amer. Math. Soc.*, 327 (1991), 795-813. https://doi.org/10.2307/2001823

[3] Beer, G., On the Fell topology, *Set Valued Analysis*, 1 (1993), 69-80. https://doi.org/10.1007/BF01039292

[4] Beer, G., Topologies on Closed Convex Sets, Kluwer Academic Publishers, 1993. http://dx.doi.org/10.1007/978-94-015-8149-3

[5] Fell, J., A Hausdorff topology for the closed subsets of locally compact non-Hausdorff space, *Proc. Amer. Math. Soc.*, 13 (1962), 472-476. https://doi.org/10.1090/S0002-9939-1962-0139135-6

[6] Hola, L., Levi, S., Decomposition properties of hyperspace topologies, *Set Valued Analysis, Kluwer Academic Publishers* (1997). https://doi.org/10.1023/A:1008608209952

[7] Baran, M., Qasim, M., Local T_0 approach spaces, *Mathematical Sciences and Applications E-Notes*, 5(1) (2017), 45-56.

[8] Baran, M., Qasim, M., T_1 approach spaces, *Communications Faculty of Sciences University of Ankara Series A1 Mathematics and Statistics*, 68(1) (2019), 784-800. https://doi.org/10.31801/cfsuasmas.478632

[9] Bourbaki, N., Theory of sets, Elements of Mathematics, Springer, Heidelberg, 2004.

[10] Lowen, R. Kuratowski's measure of noncompactness revisited, *Q.J. Math. Oxford*, 39 (1988), 235-254. https://doi.org/10.1093/qmath/39.2.235

[11] Lowen, R., Sioen, M., The Wijsman and Attouch-Wets topologies on hyperspaces revisited, *Topology Appl.*, 70 (1996), 179-197. https://doi.org/10.1016/0166-8641(95)00096-8

[12] Lowen, R., Approach Spaces: the Missing Link in the Topology Uniformity Metric Triad, Oxford Mathematical Monographs. Oxford University Press, New York, United States Springer, 1997.

[13] Lowen, R., Verbeeck, C., Local compactness in approach spaces I, *Internat. J. Math. Scie.*, 21 (1998), 429-438. https://doi.org/10.1155/S0161171203007646

[14] Lowen, R., Sioen, M., Proximal hypertopologies revisited, *Set Valued Analysis*, 6 (1998), 1-19. http://dx.doi.org/10.1023/A:1008646106442

[15] Lowen, R., Sioen, M., A note on seperation in Ap, *Applied General Topology*, 4 (2003), 475-486. http://dx.doi.org/10.4995/agt.2003.2046

[16] Lowen, R., Wuyts, P., The Vietoris hyperspace structure for approach spaces, *Acta Math. Hungar.*, 139, (2013), 286–302. http://dx.doi.org/10.1007/s10474-012-0292-6

[17] Lowen, R. Index Analysis, Approach Theory at Work, Springer, 2015. http://dx.doi.org/10.1007/978-1-4471-6485-2

http://communications.science.ankara.edu.tr

Commun.Fac.Sci.Univ.Ank.Ser. A1 Math. Stat.
Volume 72, Number 3, Pages 650–662 (2023)
DOI:10.31801/cfsuasmas.1127781
ISSN 1303-5991 E-ISSN 2618-6470

Research Article; Received: June 8, 2022; Accepted: December 10, 2022

DEVELOPABLE NORMAL SURFACE PENCIL

Mustafa DEDE

Department of Mathematics, Kilis 7 Aralık University, 79000 Kilis, TÜRKİYE

Abstract. In this paper, we introduce a new class of surfaces, called as normal surface pencil. We parameterize a normal surface pencil by using the principal normal vector $\mathbf{n}$ and the binormal vector $\mathbf{b}$ of the Frenet frame of a space curve $\alpha(s)$ as follows $\varphi(s,t) = \alpha(s) + y(s,t)\mathbf{n} + z(s,t)\mathbf{b}$. A well known example of normal surface pencil is a canal surface. Finally, we propose the sufficient conditions of a normal surface pencil being a developable surface. Then several new examples of developable normal surface pencil are constructed from these conditions.

1. Introduction

Let $\varphi = \varphi(u,v)$ be a local parametrization of a surface parameterized by

$$\varphi(u,v) = (x(u,v), y(u,v), z(u,v)).$$

A well known Gauss curvature K of a surface is given by

$$K = \frac{LN - M^2}{EG - F^2}, \tag{1}$$

where E, F, G and L, M, N are the coefficients of the first and the second fundamental forms of a surface, respectively [11].

An important topic in differential geometry is the study of curvature conditions of a surface [12, 13]. For instance, the surfaces with constant Gauss curvature are investigated in many papers [8]. Recently, Lopez and Moruz investigated the constant Gauss curvature of translation and homothetical surfaces [14]. A special case of constant Gauss curvature surface is flat ones. A surface with vanishing Gaussian curvature is called a flat surface ($K = 0$) [9, 18]. The geometric meaning of a flat surface is that if we flattened a developable surface (flat ruled surface) into

2020 *Mathematics Subject Classification.* 53A04, 65D17.
Keywords. Flat surfaces, Gauss curvature, surface pencil, developable.
mustafadede@kilis.edu.tr; 0000-0003-2652-637X.

a planar figure (with no distortion), any geodesic on it will be mapped to a straight line in the planar figure [4].

Let $\alpha(t)$ be a regular space curve [10], then the Frenet frame is defined as follows

$$\mathbf{t} = \frac{\alpha'}{\|\alpha'\|}, \mathbf{b} = \frac{\alpha' \wedge \alpha''}{\|\alpha' \wedge \alpha''\|}, \mathbf{n} = \mathbf{b} \wedge \mathbf{t}.$$

The well-known Frenet formulas are given by

$$\begin{bmatrix} \mathbf{t}' \\ \mathbf{n}' \\ \mathbf{b}' \end{bmatrix} = \|\alpha'(t)\| \begin{bmatrix} 0 & \kappa & 0 \\ -\kappa & 0 & \tau \\ 0 & -\tau & 0 \end{bmatrix} \begin{bmatrix} \mathbf{t} \\ \mathbf{n} \\ \mathbf{b} \end{bmatrix},$$

where the curvature κ and the torsion τ of the curve are given by

$$\kappa = \frac{\|\alpha' \wedge \alpha''\|}{\|\alpha'\|^3}, \tau = \frac{\det(\alpha', \alpha'', \alpha''')}{\|\alpha' \wedge \alpha''\|^2}.$$

Let us consider the Frenet frame $\{\mathbf{t}, \mathbf{n}, \mathbf{b}\}$ along a unit speed space curve $\alpha(s)$. By using the Frenet frame, we can define lots of special class of surfaces. For instance, we define the ruled surfaces $F(s,u) = \alpha(s) + u\mathbf{n}(s)$ or $F(s,u) = \alpha(s) + u\mathbf{b}(s)$ which are called the principal normal surface or principal binormal surface of the curve $\alpha(s)$, respectively [15]. The other example is that a canal surface is defined by $F(s,u) = \alpha(s) + r(s)\cos(u)\mathbf{n} + r(s)\sin(u)\mathbf{b}$ where $r(s)$ is radii function [3]. Moreover a pipe surface (tube) is a canal surface with a constant radii [2].

Theorem 1. *The principal normal or principal binormal surfaces are flat (developable) if and only if the corresponding curve is a planar [1].*

Theorem 2. *The regular canal surface is developable if and only if the canal surface is a cylinder or cone. That is, the curvature $\kappa(s) = 0$; the spine curve is a line and radii function $r(s)$ is a constant or linear function of s [3].*

A surface pencil can be parameterized by using the Frenet frame as follows

$$\varphi(s,t) = \alpha(s) + u(s,t)\mathbf{t}(s) + v(s,t)\mathbf{n}(s) + w(s,t)\mathbf{b}(s),$$

where $u(s,t)$,$v(s,t)$ and $w(s,t)$ are functions of s and t [4, 6]. Wang et al. used the surface pencil to answer the problem "assume we are given a space curve, how to characterize those surfaces that possess this curve as a common geodesic". The generalized solution of this problem is studied in [5]. The study of surface pencil has been extended Minkowski and Galilean spaces [7, 17]. Recently, Zhao and Wang derived the necessary and sufficient conditions to construct a developable surface through a given curve [16]. However they studied this problem with some constraints such as the curve is isoparametric on surface. In this paper we have studied this problem without any constraints. Moreover we derived possible parameterizations of flat normal surface pencil. Surprisingly we obtained new class of space curve which we call it the helical extension of a space curve. In [20] we give the characterization of this class of curve.

Rotation Minimizing Frame(RMF) or sometimes called as Bishop frame which is well defined even when the curve has vanishing second derivative in 3-dimensional Euclidean space [21]. Because Bishop frame is formed with the tangent vector and any convenient arbitrary basis for the remainder of the frame [22,23].

2. Flat Normal Surface Pencils

In this section, we introduce the normal surface pencil to generalize two special classes of surfaces, namely, the principal normal surfaces and the canal surfaces. Then we derive the necessary and sufficient conditions for a normal surface pencil to be flat.

Definition 1. *Let $\alpha(s)$ be a unit speed space curve with the Frenet frame $\{\mathbf{t}, \mathbf{n}, \mathbf{b}\}$, then a normal surface pencil is parameterized by*

$$\varphi(s,t) = \alpha(s) + y(s,t)\mathbf{n}(s) + z(s,t)\mathbf{b}(s), \tag{2}$$

where $y(s,t)$ and $z(s,t)$ are functions of s and t. For simplicity, we take the functions $y(s,t)$ and $z(s,t)$ that can be decomposed into two factors that allows us instead of solving partial differential equations we deal with ordinary differential equations

$$y(s,t) = y(s)w(t), z(s,t) = z(s)l(t).$$

Here $y(s), w(t), z(s)$ and $l(t)$ are all functions of s and t. Then a normal surface pencil is parameterized by

$$\varphi(s,t) = \alpha(s) + y(s)w(t)\mathbf{n} + z(s)l(t)\mathbf{b}. \tag{3}$$

Now, we can give the following theorems for classification of flat normal surface pencil.

Theorem 3. *Let $\alpha(s)$ be a unit speed space curve ($\tau \neq 0, \kappa \neq 0$). A normal surface pencil is flat, if and only if it is either*

(1) *a surface parameterized by $\varphi(s,t) = \alpha(s) + \dfrac{1}{\kappa(s)}\mathbf{n} + z(s)l(t)\mathbf{b}$,*

(2) *a surface parameterized by $\varphi(s,t) = \alpha(s) + y(s)w(t)\mathbf{n} - \int \dfrac{\tau}{\kappa} ds\mathbf{b}$,*

(3) *a surface parameterized by $\varphi(s,t) = \alpha(s) + z(s)(\tan \int \tau + c_{11})l(t)\mathbf{n} + z(s)l(t)\mathbf{b}$.*

If the curve $\alpha(s)$ is a unit speed plane curve ($\tau = 0$). Then a normal surface pencil is flat, if and only if it is either

(1) *a surface parameterized by $\varphi(s,t) = \alpha(s) + y(s)c_2\mathbf{n} + z(s)l(t)\mathbf{b}$*

(2) *a surface parameterized by $\varphi(s,t) = \alpha(s) + y(s)w(t)\mathbf{n} + c_7c_8\mathbf{b}$*

If the curve $\alpha(s)$ is a unit speed line ($\kappa = \tau = 0$). We use Rotation Minimizing Frame basis ($\mathbf{e}_1$ and $\mathbf{e}_2$), then a normal surface pencil is flat, if and only if it is either

(1) *a surface parameterized by* $\varphi(s,t) = \alpha(s) + c_3(c_4 s + c_5)w(t)\mathbf{e}_1 + (c_4 s + c_5)l(t)\mathbf{e}_2$.

(2) *a surface parameterized by* $\varphi(s,t) = \alpha(s) + y(s)w(t)\mathbf{e}_1 + z(s)c_6\mathbf{e}_2$.

where $c_i (i = 1..11) \in \mathbb{R}$.

The rest of the section is devoted to the proof of the above theorem.

Proof. From (1) and (3), it is easy to see that a surface is flat if and only if it satisfies the following equation:

$$\langle \varphi_s \wedge \varphi_t, \varphi_{ss} \rangle \langle \varphi_s \wedge \varphi_t, \varphi_{tt} \rangle - \langle \varphi_s \wedge \varphi_t, \varphi_{st} \rangle^2 = 0. \tag{4}$$

By using the well known Frenet formulas, we obtain the partial derivatives of the normal surface pencil as follows

$$\varphi_s = (1-\kappa(s)y(s)w(t))\mathbf{t} + (y_s(s)w(t) - \tau(s)z(s)l(t))\mathbf{n} + (\tau(s)y(s)w(t) + z_s(s)l(t))\mathbf{b}. \tag{5}$$

and

$$\varphi_t = y(s)w_t(t)\mathbf{n} + z(t)l_t(t)\mathbf{b}. \tag{6}$$

where φ_s and φ_t denote the partial derivatives of the surface with respect to s and t.

It follows that the cross product of φ_s and φ_t is obtained as

$$\varphi_s \wedge \varphi_t = ((y_s w - \tau z l)z l_t - (\tau y w + z_s l)y w_t)\mathbf{t} - (1-\kappa y w)z l_t \mathbf{n} + (1-\kappa y w)y w_t \mathbf{b}. \tag{7}$$

Combining the equations (4), (5), (6) and (7) and higher order partial derivatives of normal surface pencil, we have a non-linear partial differential equation (PDE) in the following form

$$\begin{aligned} \tau^2 z^4(-y^2w^2\kappa^2 + 2w\kappa y - 1)l_t^4 + (...)l_t^3 w_t + ... + (...)l_t - \\ y^4(z_s^2c^2\kappa^2 + \tau^2 + 2z_s c\kappa\tau)w_t^4 + (...)w_t^3 l_t + ... + (...)w_t = 0. \end{aligned} \tag{8}$$

We can rearrange the equation (8) as follows

$$\sum_{i=1}^{4} A_i(s,t)l_t^i(t) + B_i(s,t)w_t^i(t) + \sum_{i=1}^{3} C_i(s,t)l_t^i(t)w_t^{4-i}(t) = 0, \tag{9}$$

where upper "i" indicates the degree of function and the coefficients $A_i(s,t)$ $B_i(s,t)$ $(i = 1..4)$ and $C_i(s,t)$ $(i = 1..3)$ are smooth functions on s and t.

We will solve the equation (9) whether the set of functions $\{l, w\}$ is linearly independent or linearly dependent.

- If l and w functions are not linearly dependent. Then a normal surface pencil is flat if the coefficients $A_i(s,t), B_i(s,t)$ and $C_i(s,t)$ vanishes.

From (8) and (9) the coefficient $A_4(s,t)$ of $l_t^4(t)$ can be computed as follows

$$A_4 = -\tau^2 z^4 (yw\kappa - 1)^2. \tag{10}$$

It follows that the coefficient $A_4(s,t)$ vanishes if and only if $yw\kappa - 1 = 0, \tau(s) = 0, z(s) = 0$ or $l_t = 0$, respectively.

Now, we discuss these four cases:
Case 1) If $yw\kappa - 1 = 0$ then we have

$$y(s)w(t) = \frac{1}{\kappa(s)}. \tag{11}$$

Thus, observe that $w(t)$ is a constant function.
Combining (11) with (9) we obtain that all the coefficients A_i, B_i and C_i in (9) vanishes. Therefore, substituting (11) into (3) allow us to parameterize a flat normal surface pencil as follows

$$\varphi(s,t) = \alpha(s) + \frac{1}{\kappa(s)}\mathbf{n} + z(s)l(t)\mathbf{b}. \tag{12}$$

Conversely, a simply calculation implies that the Gauss curvature of the surface is zero.
Now, let us construct an example belonging to case 1.

Example 1. *Let us consider a space curve parameterized by*

$$\alpha(s) = (\cos(s), \sin(s), s).$$

It is easy to see that the curvature $\kappa = 1/2$. Hence, from (11) we have $y(s)w(t) = 2$. Then a flat normal surface pencil is illustrated in Figure 1, in which $z(s)l(t) = t\cosh(t)$, if we set $z(s)l(t) = t\cos(s)$, we obtain another member of flat normal surface pencil shown in Figure 1.

Case 2) If $l_t(t) = 0 (l(t) = c_1, c_1 \in \mathbb{R})$ in equation (10), then we have the coefficient $B_4(s,t)$ of $w_t^4(t)$ as follows

$$B_4 = -y^4(z_s^2 c_1^2 \kappa^2 + \tau^2 + 2z_s c_1 \kappa\tau).$$

It follows that for $y(s) \neq 0, w_t(t) \neq 0$ (in these cases it is not a surface) the coefficient $B_4(s,t)$ vanishes if and only if the following equation is satisfied:

$$z_s^2 c_1^2 \kappa^2 + 2z_s c_1 \kappa\tau + \tau^2 = 0.$$

The solution of the above differential equation can be obtained as

$$z(s) = -\int \frac{\tau(s)}{c_1\kappa(s)} ds. \tag{13}$$

It follows that substituting $l(t) = c_1$ and (13) into (9) gives a flat normal surface pencil parameterized by

$$\varphi(s,t) = \alpha(s) + y(s)w(t)\mathbf{n} - \int \frac{\tau}{\kappa} ds\mathbf{b}.$$

Note that if the curve $\alpha(s)$ is an arbitrary speed curve, then one calculates the function $z(s)$ as follows

$$z(s) = -\int \frac{\tau}{c_1\kappa} \|\alpha'\| \, ds. \tag{14}$$

Now, let us construct an example about case 2.

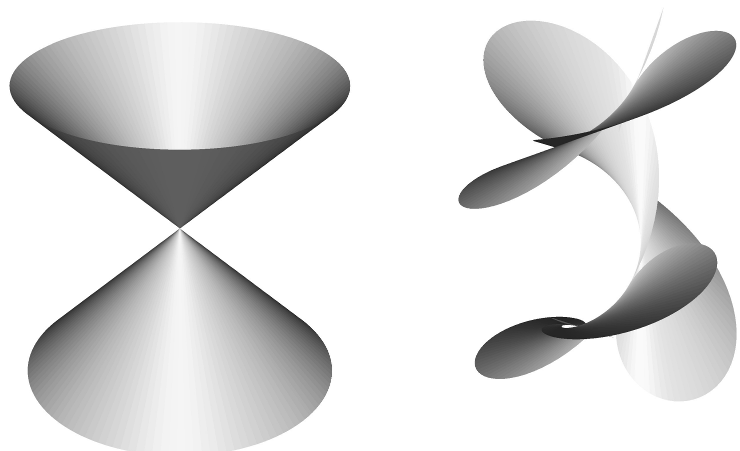

(a) A member of flat normal surface pencil, with $zl = tcosh(t)$.

(b) A member of flat normal surface pencil, with $zl = tcos(s)$.

FIGURE 1. Flat normal surface pencil.

Example 2. *Assume that a space curve is given by*

$$\alpha(s) = (\frac{3s^2-1}{3s^2+3}, \frac{s(s^2-3)}{3s^2+3}, \frac{2\sqrt{2}\sqrt{s^2+1}}{3}).$$

When $c_1 = 1$, from (14) we have

$$z(s) = -\frac{1}{2}s^2.$$

In addition, if we set $y(s)w(t) = 5\cos(t)\sin(t)$ or $y(s)w(t) = st$ then the flat normal surface pencils are illustrated in Figure 2.

Case 3) If the curve $\alpha(s)$ is a plane curve ($\tau = 0$) in equation (10) then the coefficient $B_4(s,t)$ of $w_t^4(t)$ is calculated as

$$B_4 = -y^4 z_s^2 l^2 \kappa^2. \tag{15}$$

Now, we distinguish the following five cases:

Subcase 3.1) If $w_t(t) = 0 (w(t) = c_2, c_2 \in \mathbb{R})$ in equation (15) then the Gauss curvature vanishes ($K = 0$), which implies that the normal surface pencil is a flat surface parameterized by

$$\varphi(s,t) = \alpha(s) + y(s)c_2\mathbf{n} + z(s)l(t)\mathbf{b}.$$

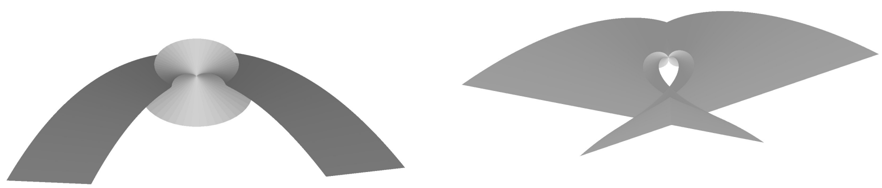

(a) A member of flat normal surface pencil, with $yw = 5cos(t)sin(t)$.

(b) A member of flat normal surface pencil, with $yw = st$.

FIGURE 2. Flat normal surface pencil.

Now, lets construct an example about subcase 3.1.

Example 3. *Assume that a plane curve is given by*

$$\alpha(s) = (\cos(s), \sin(s), 0).$$

A straightforward computation shows that $\tau = 0$*, therefore for* $w(t) = 3$*, we can set* $l(t) = \cos(t), y(s) = 2s/3$ *and* $z(s) = \cosh(s/5)$ *or* $l(t) = \cos(t), y(s) = \cos(s)$ *and* $z(s) = \cos(5s)$ *to construct members of flat normal surface pencil, shown in Figure 3.*

Subcase 3.2) If $y(s) = 0$ in equation (15) then the Gauss curvature vanishes, thus a flat normal surface pencil is parameterized by

$$\varphi(s,t) = \alpha(s) + z(s)l(t)\mathbf{b}.$$

It is easy to see that if we set $z(s) = 1$ and $l(t) = t$ in the above equation, then we have a principal binormal surface, therefore the above result coincides with Theorem 1.

Subcase 3.3) If $l(t) = 0$ in equation (15), then we have $K = 0$, thus a flat normal surface pencil is parameterized by

$$\varphi(s,t) = \alpha(s) + y(s)w(t)\mathbf{n}.$$

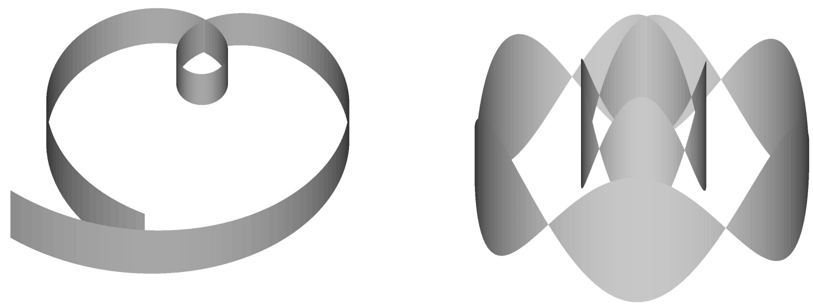

(a) A member of flat normal surface pencil, with $l = cos(t)$, $y = 2s/3$ and $z = cosh(s/5)$.

(b) A member of normal flat surface pencil, with $l = cos(t)$, $y = cos(s)$ and $z = cos(5s)$.

FIGURE 3. Flat normal surface pencil.

Note that when we set $y(s) = 1$ and $w(t) = t$ in the above equation, then we have a principal normal surface, therefore the above result coincides with Theorem 1.

Subcase 3.4) If the curve is a line ($\kappa(s) = 0$) then the coefficient $C_2(s,t)$ of $l_t^2(t)w_t^2(t)$ is calculated as

$$C_2 = 2y_s zyz_s - z^2y_s^2 - y^2z_s^2.$$

The condition $w_t = 0$ is investigated in subcase 3.1. Therefore, two subcases must be considered.

Subsubcase 3.4.1) If $2y_s zyz_s - z^2y_s^2 - y^2z_s^2 = 0$ then we have

$$y(s) = c_3z(s).$$

where $c_3 \in \mathbb{R}$.

With these conditions (9) becomes

$$c_3^2z^3z_{ss}(l_tw - w_tl)(l_{tt}w_t - l_tw_{tt}) = 0.$$

It is easy to see that $z(s) = 0$ and $l = kw,k \in \mathbb{R}$ contradiction. therefore, there is just one subcase:

If $z_{ss}(s) = 0(z(s) = c_4s + c_5)$ $c_4, c_5 \in \mathbb{R}$, then the normal surface pencil is a flat surface parameterized by

$$\varphi(s,t) = \alpha(s) + c_3(c_4s + c_5)w(t)\mathbf{e}_1 + (c_4s + c_5)l(t)\mathbf{e}_2. \tag{16}$$

Observe that if we set $c_3 = 1, w(t) = \cos(t)$ and $l(t) = \sin(t)$ in the equation (16), then the surface is a flat canal surface, therefore this result coincides with the Theorem 2. Now, let us construct an example about this case.

Example 4. *Assume that a line is given by*

$$\alpha(s) = (s, 3, 0).$$

In this case the Frenet frame is undefined, thus we can choose an arbitrary basis such as $\mathbf{n} = (0, 1, 0)$ *and* $\mathbf{b} = (0, 0, 1)$. *For* $c_3 = 3, c_5 = 0$ *and* $c_4 = 1$ *in (16), if we set* $w(t) = \cos(t/3)\sin(t/3)$ *and* $l(t) = t$ *or* $w(t) = \cosh(t/3)/3$ *and* $l(t) = \sinh(t/5)$ *then the flat normal surface pencils are illustrated in Figure 4.*

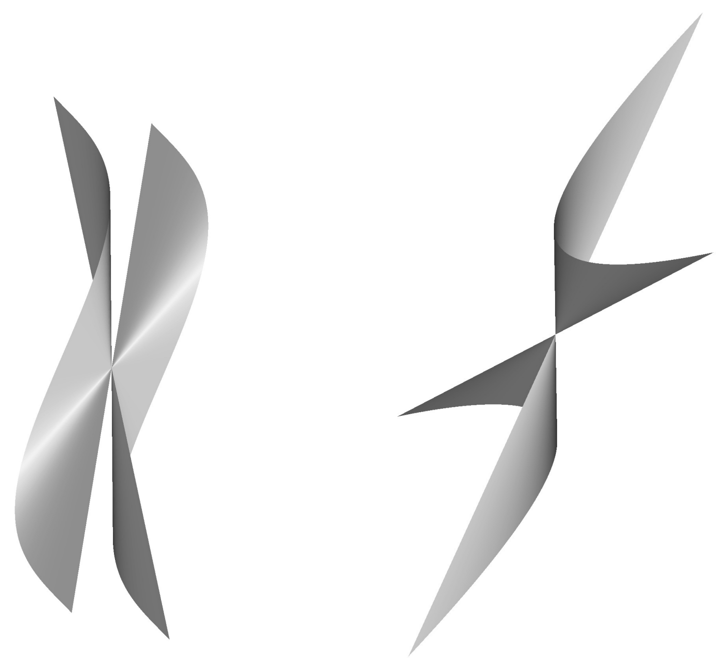

(a) A member of flat normal surface pencil, with $w = \sin(t)\cos(t)$ and $l = t$.

(b) A member of flat normal surface pencil, with $w = t - 5$ and $l = t^3$.

FIGURE 4. Flat normal surface pencil.

Subsubcase 3.4.2) If $l_t(t) = 0(l(t) = c_6, c_6 \in \mathbb{R})$ then the normal surface pencil is a flat surface parameterized by

$$\varphi(s,t) = \alpha(s) + y(s)w(t)\mathbf{e}_1 + z(s)c_6\mathbf{e}_2.$$

Subcase 3.5) If $z_s(s) = 0(z(s) = c_7)$ in equation (15) then the coefficient $C_2(s,t)$ of $l_t^2(t)w_t^2(t)$ is obtained as

$$C_2 = -y_s^2 z^2.$$

Since the case $w_t(t) = 0$ is investigated in subcase 3.1, there are three cases:

Subsubcase 3.5.1) If $z(s) = 0$ or $l_t(t) = 0(l(t) = c_8)$ then the normal surface pencil is a flat surface parameterized by

$$\varphi(s,t) = \alpha(s) + y(s)w(t)\mathbf{n}.$$

and

$$\varphi(s,t) = \alpha(s) + y(s)w(t)\mathbf{n} + c_7c_8\mathbf{b},$$

respectively.

Subsubcase 3.5.2) If $y_s(s) = 0(y(s) = c_9)$, then the equation (9) becomes

$$-l_t y\kappa z^2(yw\kappa - 1)^3(l_{tt}w_t - l_t w_{tt}) = 0.$$

Since we investigated all the cases, we omit all of these cases.

Case 4) If $z(s) = 0$ in equation (10) then we have the coefficient $B_4(s,t)$ of $w_t^4(t)$ as follows

$$B_4 = -y^4\tau^2.$$

For $y(s) \neq 0$ and $w_t(t) \neq 0$ (in these cases it is not a surface) when $\tau = 0$ this case is investigated in subsubcase 3.5.1.

- If l and w are linearly dependent. Then we have $w = c_{10}l$ and the equation (9) becomes

  $$-(c_{10}(-y_s z + yz_s) + \tau c_{10}^2 y^2 + \tau z^2)^2 l_t^4 = 0$$

  where $c_{10} \in \mathbb{R}$. The solution of the above differential equation can be obtained as

  $$y = z\frac{\tan\int\tau + c_{11}}{c_{10}}$$

  where c_{11} is a integration constant. The equation (3) is written as

  $$\varphi(s,t) = \alpha(s) + z(s)(\tan\int\tau + c_{11})l(t)\mathbf{n} + z(s)l(t)\mathbf{b}.$$

Note that if the curve $\alpha(s)$ is an arbitrary speed curve, then one calculates the function $y(s)$ as follows

$$y = z\frac{\tan\int\tau\,\|\alpha'\| + c_{11}}{c_{10}}. \tag{17}$$

Example 5. *Let us consider a space curve parameterized by*

$$\alpha(s) = (2s, s^2, \frac{s^3}{3}).$$

It is easy to see that the curvature and torsion are

$$\kappa = \frac{2}{(s^2+2)^2} = \tau$$

For $z(s) = \cosh(s)$, $w(t) = 6t$ *and* $l(t) = t$, *by using (17) we have*

$$y = \frac{\cosh(s)\tan(\sqrt{2}\arctan(\frac{s\sqrt{2}}{2}))}{6}$$

Moreover if we set $z(s) = (s)$, $w(t) = 6t$ *and* $l(t) = t$, *then we obtain another member of flat normal surface pencil shown in Figure 5.*

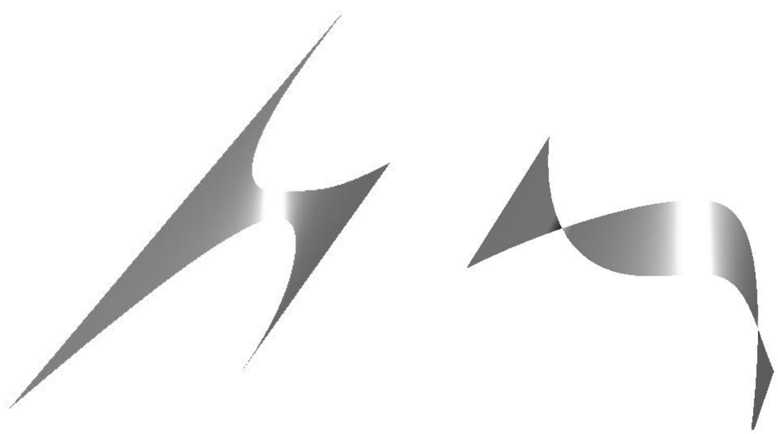

(a) A member of flat normal surface pencil, with $zl = tcosh(s)$ and $w = 6t$.

(b) A member of flat normal surface pencil, with $zl = tcos(s)$ and $w = 6t$.

FIGURE 5. Flat normal surface pencil.

□

3. Conclusion

The surface pencil and flat surfaces are both important subjects in computer aided design (CAD), and in this paper we describe somewhat novel analysis on special cases of flat normal surface pencils. We recommend this new approach for the following reasons:

- We can construct lots of flat normal surface pencil by using this method.
- The designer can select different sets of functions $y(s), w(t), z(s)$ and $l(t)$ to adjust the shape of the surface.
- We have studied this problem without any constraints such as curves that have isoparametric properties.

Declaration of Competing Interests The author declare that he has no competing interest.

References

[1] Kreyszig, E., Differential Geometry, Dover Publications Inc. Courier Corporation, New York, 2013.

[2] Maekawa, T., Patrikalakis, N. M., Sakkalis, T., Yu, G., Analysis and applications of pipe surfaces. *Computer Aided Geometric Design*, 15 (1988) 437-458.

[3] Xu, Z., Feng, R., Sun, J., Analytic and algebraic properties of canal surfaces, *Journal of Computational and Applied Mathematics*, 195 (2006), 220–228. https://doi.org/10.1016/j.cam.2005.08.002

[4] Wang, G. J., Tang, K., Tai, C. L., Parametric representation of a surface pencil with a common spatial geodesic, *Computer Aided Geometric Design*, 36 (5) (2004), 447–459.

[5] Kasap, E., Akyıldız, F. T., Orbay, K., A generalization of surfaces family with common spatial geodesic, *Appl. Math. Comput.*, 201 (2008), 781-789. https://doi.org/10.1016/j.amc.2008.01.016

[6] Li, C. Y., Wang, R. H., Zhu, C. G., Parametric representation of a surface pencil with a common line of curvature, *Computer Aided Design*, 43 (9) (2011), 1110–1117.

[7] Küçükarslan, Z. Y., On a family of surfaces with common asymptotic curve in the Galilean space G_3, *J. Nonlinear Sci. Appl.*, 9 (2016) 518–523.

[8] Lopez, R., Cyclic surfaces of constant Gauss curvature, *Houston J. Math.*, 27 (2001), 799–805.

[9] Lopez, R., Surfaces of constant Gauss Curvature in Lorentz-Minkowski Three-Space, *Rocky Mountain J. Math.*, 33 (2003) 971-993.

[10] Do Carmo, M. P., Differential Geometry of Curves and Surfaces, Prentice Hall, NJ, 1976.

[11] Gray, A., Modern Differential Geometry of Curves and Surfaces with Mathematica, CRC Press. Boca Raton, 1998.

[12] Goemans, W., Van de Woestyne, I., Twisted surfaces in Euclidean and Minkowski 3-space, *In: Pure and Applied Differential Geometry Padge, Shaker Verlag Aachen, Germany*, (2012), 143-151.

[13] Goemans, W., Van de Woestyne, I., Twisted surfaces with null rotation axis in Minkowski 3-space, *Results Math.*, 70(1) (2016), 81-93. https://doi.org/10.1007/s00025-015-0462-2

[14] Lopez, R., Moruz, M., Translation and homothetical surfaces in Euclidean space with constant curvature, *J. Korean Math. Soc.*, 52(3) (2015), 523-535.

[15] Izumiya, S., Takeuchi, N., New special curves and developable surfaces, *Turkish J. Math.*, 28(2) (2004), 153-163.

[16] Zhao, H. Y., Wang, G. J., A new method for designing a developable surface utilizing the surface pencil through a given curve, *Progress in Nature Science*, 18 (2008), 105–110.

[17] Ergün, E., Bayram, E., Kasap, E., Surface pencil with a common line of curvature in Minkowski 3-space, *Acta Mathematica Sinica-English Series*, 30(12) (2014), 2103-2118.

[18] Alegre, P., Arslan, K., Carriazo, A., Murathan C., Öztürk, G., Some special types of developable ruled surface, *Hacettepe Journal of Mathematics and Statistics*, 39(3) (2010), 319–325.

[19] Hanson, A. J., Ma, H., Parallel transport approach to curve framing, *Tech. Report*, 425 (1995).
[20] Dede, M., Helical extension curve of a space curve, *Mediterranean Journal of Mathematics*, 18 (2021), 1-10.
[21] Ates, F., Gok, I., Ekmekci, F., N., Yaylı, Y., Characterizations of inclined curves according to parallel transport frame in $\mathbb{E}^4$ and Bishop frame in $\mathbb{E}^3$, *Konuralp Journal of Mathematics*, 7(1) (2019), 16-24.
[22] Bishop, R. L., There is more than one way to frame a curve, *Amer. Math. Monthly* 82, (1975) 246–251.
[23] Bloomenthal, J., Calculation of Reference Frames Along a Space Curve, Graphics Gems, Academic Press Professional, Inc., San Diego, CA, 1990.

http://communications.science.ankara.edu.tr

Commun.Fac.Sci.Univ.Ank.Ser. A1 Math. Stat.
Volume 72, Number 3, Pages 663–685 (2023)
DOI:10.31801/cfsuasmas.1126025
ISSN 1303-5991 E-ISSN 2618-6470

Research Article; Received: June 4, 2022; Accepted: January 19, 2023

TWO FRACTIONAL ORDER LANGEVIN EQUATION WITH NEW CHAOTIC DYNAMICS

Meriem Mansouria BELHAMITI[1], Zoubir DAHMANI[2] and Mehmet Zeki SARIKAYA[3]

[1]Laboratory of LMPA, Faculty of Exact Sciences and Informatics, UMAB University, Mostaganem, ALGERIA
[2]LMPA, Faculty SEI, UMAB Mostaganem, ALGERIA
[3]Department of Mathematics, Faculty of Science and Arts, Düzce University, Düzce, TÜRKİYE

Abstract. In the present paper, we introduce a two-order nonlinear fractional sequential Langevin equation using the derivatives of Atangana-Baleanu and Caputo-Fabrizio. The existence of solutions is proven using a fixed point theorem under a weak topology, and an illustrative example is then given. Furthermore, we present new fractional versions of the Adams-Bashforth three-step approach for the Atangana-Baleanu and Caputo derivatives. New nonlinear chaotic dynamics are performed by numerical simulations.

1. Introduction

Fractional calculus has several applications in biology, mechanics, physics, viscoelasticity, electromagnetic waves, fractional Brownian motions, image processing, and engineering. Numerous books and essays in the literature cover a wide spectrum of fractional calculus problems, see [2,22,33].
Unfortunately, the fundamental prestigious Caputo and Riemann-Liouville features have such a critical flaw, even though their kernel is non-local, it remains singular. This issue has an impact on the modeling of real-world problems. To address the aforementioned obstacles, Caputo and Fabrizio proposed a new differential operator with non-singular kernel, see for instance the papers [12, 13, 21]. On the other, some researchers have used these derivatives to handle specific challenges, see [3,5,21]. Regrettably, various concerns have been raised in opposition to this novel approach, leading them to conclude that this operator cannot be a derivative

2020 *Mathematics Subject Classification.* 30C45, 39B72, 39B82.
Keywords. Caputo, Caputo-Fabrizio derivative, Atangana–Baleanu derivative, fixed-point theory, three-step Adams-Bashforth scheme.
[1] meriembelhamiti@gmail.com; 0000-0002-3108-7378
[2] zzdahmani@yahoo.fr; 0000-0003-4659-0723
[3] sarikayamz@gmail.com-Corresponding author; 0000-0002-6165-9242.

of fractional order but can be viewed as a regulatory parameter, see [35]. For these reasons, based on the Mittag Leffler function, Atangana and Baleanu devised a new fractional operator, see [4,26].

Nowadays, the most common differential equations observed in engineering and applied research are of second order. They take the form of $\ddot{x} = f(t, x, \dot{x})$.
Among the important examples of second-order equations is the Newton equation: $m\ddot{x} = f(x)$, the RLC circuit equation in electrical engineering: $LC\ddot{x} + RC\dot{x} + x = v(t)$, as well as the forced harmonic oscillator: $m\ddot{x} + b\dot{x} + kx = f(t)$.
The ultimate focus of this paper is to thoroughly explore certain sophisticated fractional differential equations, which can typically produce chaotic behavior such as the Langevin equation. The relevance of the nonlinear Langevin problem arises from its implementation as a model of anomalous systems. Indeed, it is well known that in many cases, the Langevin equation is the most convenient way to measure time changes in Brownian motion velocity, see [11,18,19,23,32,34].
In this contribution, we study the existence of solutions for the nonlinear Langevin equation using a fixed point theorem under a weak topology, see [9,20,21]. The considered problem involves, in particular, two fractional orders with non-local multi-point boundary conditions. For more information, see [1,8,15,17,31].
So let us consider the following problem:

$$D^{\alpha}\left(D^{\beta}-\lambda(t)\right)y(t)=f\left(t,y(t),D^{\beta}y(t)\right),\quad t\in[0,T],\quad 0<\alpha,\beta\leq 1, \tag{1}$$

with its conditions:

$$\begin{aligned} &y(0)=0,\quad D^{\beta}y(0)=\sum_{i=0}^{r}\delta_i J^{\gamma}y(\xi_i),\\ &0<\beta\leq 1,\quad \gamma>0,\quad r\in\mathbb{N}^*,\quad \xi_i\in[0,T], \end{aligned} \tag{2}$$

where D^{α} and D^{β} are fractional differential operators of order $0<\alpha,\beta\leq 1$, J^{γ} is the Rieman Liouville fractional integral operator of order $\gamma>0$ and $\lambda:[0,T]\to\mathbb{R}$ is a given continuous function. Two different approaches are used: the first one is of Caputo-Fabrizio and the second one is of Atangana Baleanu.
Then, inspired by [7,25,27,28], we propose new three-step Adams-Bashforth fractional methods for Caputo and Atangana Baleanu fractional derivatives. Finally, we apply the three-step Adams-Bashforth fractional methods to obtain new nonlinear chaotic dynamics.

The remaining part of the paper is organized into sections. Section 2 provides an overview of some of the fundamental concepts of fractional differentiation and fixed-point theory. In Section 3, we assert the existence of at least one solution to the problem as an outcome of the study. Section 4 discusses the numerical approximation method for fractional derivatives. Section 5 investigates numerical experiments with chaotic fractional differential equations to illustrate the utility of the proposed technique. Finally, we conclude with Section 6.

2. Preliminaries

The following section introduces some fractional calculus notions and concepts, see [4, 9, 13, 20, 23] .

Definition 1. *The Riemann-Liouville fractional integral operator of order* $\alpha \geq 0$*, for a continuous function* f *on* $[a, b]$ *is defined as*

$$J_a^\alpha f(t) = \frac{1}{\Gamma(\alpha)} \int_a^t (t-s)^{\alpha-1} f(s) ds, \quad \alpha > 0, \quad a < t \leq b,$$

where $\Gamma(\alpha) := \int_0^\infty e^{-s} s^{\alpha-1} ds.$

Definition 2. *The Liouville-Caputo fractional derivative of order* $\alpha \in (0, 1)$*, for a differentiable function* f*, is defined by*

$${}^C D^\alpha f(t) = \frac{1}{\Gamma(1-\alpha)} \int_0^t f'(s) \frac{1}{(t-s)^\alpha} ds.$$

Definition 3. *The Laplace transform for the Liouville-Caputo fractional derivative of order* α *is:*

$$\mathcal{L}\left[D^\alpha f(t)\right](s) = s^\alpha \mathcal{L}\{f(t)\}(s) - s^{\alpha-1}\{f(0)\}.$$

Definition 4 ([13]). *The Caputo-Fabrizio derivative of order* $\alpha \in]0, 1[$*, for* $T > 0, f \in H^1(0, T)$*, is given by*

$${}^{CF} D^\alpha f(t) = \frac{1}{2} \frac{M(\alpha)(2-\alpha)}{1-\alpha} \int_0^t f'(s) \exp\left[\frac{-\alpha(t-s)}{1-\alpha}\right] ds,$$

where $M(\alpha)$ *is a normalizing function depending on* α *such that* $M(0) = M(1) = 1$*.*

Definition 5 ([13]). *The Laplace transform for Caputo-Fabrizio derivative is defined as*

$$\mathcal{L}\left\{{}^{CF} D^\alpha f(t)\right\}(s) = \frac{1}{2} \frac{M(\alpha)(2-\alpha)}{1-\alpha} \frac{s\ \mathcal{L}\{f(t)\}(s) - f(0)}{s + \frac{\alpha}{1-\alpha}}.$$

Definition 6 ([23]). *The Caputo Fabrizio integral operator of order* α *is given in the following way:*

$${}^{CF} J^\alpha f(t) = \frac{2(1-\alpha)}{M(\alpha)(2-\alpha)} f(t) + \frac{2\alpha}{M(\alpha)(2-\alpha)} \int_0^t f(s) ds.$$

Definition 7 ([4]). *The Atangana Baleanu fractional derivative in Caputo sense, for* $T > 0, f \in H^1[0, T]$*,* $\alpha \in]0, 1[$*, is given as:*

$${}^{ABC} D^\alpha f(t) = \frac{B(\alpha)}{1-\alpha} \int_0^t f'(s) E_\alpha\left[-\alpha \frac{(t-s)^\alpha}{1-\alpha}\right] ds.$$

The Atangana Baleanu fractional derivative in Riemann-Liouville sense is given as:

$$^{ABR}D_t^{\alpha} f(t) = \frac{B(\alpha)}{1-\alpha} \frac{d}{dt} \int_a^t f(s) E_\alpha \left[-\alpha \frac{(t-s)^\alpha}{1-\alpha} \right] ds,$$

where E_α is Mittag-Leffler function, given by

$$E_\alpha(u) = \sum_{k=0}^{\infty} \frac{u^k}{\Gamma(\alpha k+1)}, \quad \alpha > 0, \quad \alpha \in \mathbb{R}, \quad u \in \mathbb{R},$$

where $B(\alpha)$ has the same properties as $M(\alpha)$ in Caputo-Fabrizio case.

Definition 8 ([4]). *The fractional integral associated to the Atangana-Baleanu fractional derivative is defined as:*

$$^{AB}J^{\alpha} f(t) = \frac{1-\alpha}{B(\alpha)} f(t) + \frac{\alpha}{B(\alpha)\Gamma(\alpha)} \int_a^t f(y)(t-s)^{\alpha-1} ds.$$

Definition 9. *The Laplace transform of Atangana-Baleanu fractional derivative in Caputo sense, is defined by:*

$$\mathcal{L}\left\{ ^{ABC}D^{\alpha} f(t) \right\}(s) = \frac{B(\alpha)}{1-\alpha} \frac{s^\alpha \mathcal{L}\{f(t)\}(s) - s^{\alpha-1} f(0)}{s^\alpha + \frac{\alpha}{1-\alpha}}.$$

Definition 10 ([4]). *The Laplace transform of Atangana-Baleanu fractional derivative in Riemann-Liouville sense is given as:*

$$\mathcal{L}\left\{ ^{ABR}D^{\alpha} f(t) \right\}(s) = \frac{B(\alpha)}{1-\alpha} \frac{s^\alpha \mathcal{L}\{f(t)\}(s)}{s^\alpha + \frac{\alpha}{1-\alpha}}.$$

Definition 11. *Let E and F be two Banach spaces. The operator $f : E \to F$ is weakly sequentially continuous if, for each sequence $(y_n)_n$ with $y_n \to y$, we have $fy_n \to fy$.*

Definition 12. *Let E be a Banach space with a norm $\| \cdot \|_E$. A mapping $\Psi : E \longrightarrow E$ is called D-Lipschitz, if there exists a continuous nondecreasing function $\mathfrak{W} : R^+ \longrightarrow R^+$ satisfying*

$$\|\Psi x - \Psi y\|_E \leq \mathfrak{W}(\|x-y\|_\infty),$$

for all $x, y \in E$ with $\mathfrak{W}(0) = 0$. The function $\mathfrak{W}$ is called a D-function of Ψ on E. Particularly, once $\mathfrak{W}(r) = kr$ for a given $k > 0$ is a Lipschitz mapping with a Lipschitzian constant k. In addition, if $k < 1$ is a contraction on E with a contraction constant k.

Remark 1. *Any Lipitzian correspondence is automatically D-Lipschitz, but the reverse may not be true. If $\mathfrak{W}$ is not necessarily increasing and satisfies $\mathfrak{W}(r) < r$ for $r > 0$, then Ψ is called a nonlinear contraction on E.*

Remark 2. *Note that any weakly sequentially continuous nonlinear contraction is ω-condensing.*

Corollary 1. *Let Ω be a nonempty, convex, and closed set in a Banach space E. Assume that $\Psi : \Omega \longrightarrow \Omega$ is a weakly sequentially continuous and condensing map in Ω. If $\Psi(\Omega)$ is bounded, then, Ψ has at least a fixed point.*

Corollary 2. *Let Ω be a nonempty, bounded, closed, and convex subset of a Banach space E. Assume that $\Phi : \Omega \longrightarrow \Omega$ is weakly sequentially continuous. If $\Phi(\Omega)$ is relatively weakly compact, then Φ has at least a fixed point in Ω.*

Theorem 1 ([9]). *Let Ω be a nonempty, bounded, closed, and convex subset of a Banach space E. Suppose that $\Phi : \Omega \longrightarrow E$ and $\Psi : E \longrightarrow E$ are two weakly sequentially continuous mappings such that:*

(i) *Φ is weakly compact,*
(ii) *Ψ is a nonlinear contraction,*
(iii) *$(y = \Psi x + \Phi y, x \in \Omega) \Longrightarrow y \in \Omega$.*

Then, there exists $y \in \Omega$ such that $y = \Psi y + \Phi y$.

Theorem 2 (Eberlein-Smulian). *Let $\mathcal{B}$ be a weakly closed subset of the Banach space E. Then the following assertions are equivalent:*

* *$\mathcal{B}$ is weakly compact.*
* *$\mathcal{B}$ is weakly sequentially compact.*

Lemma 1. *Let $T > 0, f \in H^1(0,T), \alpha \in]0,1[$. Then the solution of the problem (1)-(2), for Atangana Baleanu fractional derivative in Caputo sense, is*

$$\begin{aligned} y(t) =& \mathcal{A}_1 \left[\begin{array}{l} \displaystyle\int_0^t \left(\frac{(t-u)^{\beta+\alpha-1}}{\Gamma(\beta+\alpha)} + \frac{(1-\alpha)(t-u)^{\beta-1}}{\alpha\Gamma(\beta)} + \frac{(1-\beta)(t-u)^{\alpha-1}}{\beta\Gamma(\alpha)} \right) f(u)du \\ + \dfrac{(1-\beta)(1-\alpha)f(t)}{\beta\alpha} \end{array} \right] \\ &+ \mathcal{B}_1 \left[\int_0^t \frac{(t-u)}{\Gamma(B)}^{\beta-1} \lambda(u)y(u)du + \lambda(0) \left(\frac{1-\beta}{\beta} + \frac{t^\beta}{\Gamma(\beta+1)} \right) \sum_{i=0}^{r} \delta_i J^\gamma y(\xi_i) \right]. \end{aligned} \tag{3}$$

Lemma 2. *Let $T > 0, f \in H^1(0,T), \alpha \in]0,1[$. Then the solution of (1)-(2), for the case of Caputo Fabrizio derivative, is*

$$\begin{aligned} y(t) =& \mathcal{A}_2 \left[\begin{array}{l} \displaystyle\int_0^t \left((t-u) + \frac{(1-\alpha)}{\alpha} + \frac{(1-\beta)}{\beta} \right) F_y(u)du \\ + \dfrac{(1-\beta)(1-\alpha)F_y(t)}{\beta\alpha} \end{array} \right] \\ &+ \mathcal{B}_2 \left[\int_0^t \lambda(u)y(u)du + \lambda(0) \left(\frac{1-\beta}{\beta} + t \right) \sum_{i=0}^{r} \delta_i J^\gamma y(\xi_i) \right]. \end{aligned} \tag{4}$$

Proof of Lemmas 1 and 2 : For computational purposes, we include the following quantity:

$$g(t) \quad := \quad D^\beta y(t) - \lambda(t)y(t),$$

$$\mathcal{A}_1 := \frac{\beta\alpha}{B(\alpha)\ \Big(B(\beta) - \lambda(t)(1-\beta)\Big)},$$

$$\mathcal{B}_1 := \frac{\beta}{B(\beta) - \lambda(t) + \beta},$$

$$\mathcal{A}_2 := \frac{\beta\alpha}{4M(\alpha)\ \Big(\alpha - 2\Big)\Big(M(\beta)(\beta-2) - 2\lambda(t)(1-\beta)\Big)},$$

$$\mathcal{B}_2 := \frac{\beta}{-2\ M(\beta)(\beta-2) - 2\lambda(t)(1-\beta)}.$$

(Proof of Lemma 1) From the property of Laplace transform, we have

$$\mathcal{L}\left\{D^{\alpha}g(t)\right\}(s) = \frac{\frac{B(\alpha)}{1-\alpha}s^{\alpha}}{s^{\alpha} + \frac{\alpha}{1-\alpha}}\mathcal{L}(g(t))(s) + \frac{\frac{B(\alpha)}{1-\alpha}s^{\alpha-1}}{s^{\alpha} + \frac{\alpha}{1-\alpha}}g(0) = \mathcal{L}\left\{f(t)\right\},$$

thus,

$$\mathcal{L}\left\{g(t)\right\}(s) = \frac{s^{\alpha} + \frac{\alpha}{1-\alpha}}{\frac{B(\alpha)}{1-\alpha}s^{\alpha}}\mathcal{L}\left\{f(t)\right\}(s) + \frac{g(0)}{s}.$$

Then, we have

$$\mathcal{L}\left\{D^{\beta}y(t)\right\}(s) = \frac{s^{\alpha} + \frac{\alpha}{1-\alpha}}{\frac{B(\alpha)}{1-\alpha}s^{\alpha}}\mathcal{L}(f(t))(s) + \frac{g(0)}{s} + \mathcal{L}(\lambda(t)y(t))(s) + \frac{y(0)}{s}.$$

Hence, it yields that

$$\begin{aligned}\mathcal{L}\left\{y(t)\right\}(s) =& \frac{\left(s^{\alpha} + \frac{\alpha}{1-\alpha}\right)\left(s^{\beta} + \frac{\beta}{1-\beta}\right)}{\frac{B(\alpha)}{1-\alpha}\frac{B(\beta)}{1-\beta}s^{\alpha+\beta}}\ \mathcal{L}(f(t))(s) + \frac{\left(s^{\beta} + \frac{\beta}{1-\beta}\right)\ g(0)}{\frac{B(\beta)}{1-\beta}s^{\beta+1}} \\ &+ \frac{\left(s^{\beta} + \frac{\beta}{1-\beta}\right)\ \mathcal{L}(\lambda(t)y(t))(s)}{\frac{B(\beta)}{1-\beta}s^{\beta}}.\end{aligned} \tag{5}$$

Substituting the conditions (2) in (5) and thanks to the properties of inverse Laplace transform, we deduce (3), which ends the proof.
(Proof of Lemma 2) Using the same arguments as before, we can write

$$\mathcal{L}\left\{D^{\alpha}g(t)\right\}(s) = \frac{\frac{M(\alpha)(2-\alpha)}{2(1-\alpha)}s}{s + \frac{\alpha}{1-\alpha}}\mathcal{L}(g(t))(s) + \frac{\frac{M(\alpha)(2-\alpha)}{2(1-\alpha)}}{s + \frac{\alpha}{1-\alpha}}g(0) = \mathcal{L}\left\{f(t)\right\}.$$

Then, we have

$$\mathcal{L}\left\{y(t)\right\}(s) = \frac{\left(s+\frac{\alpha}{1-\alpha}\right)\left(s+\frac{\beta}{1-\beta}\right)}{\frac{M(\alpha)(2-\alpha)}{2(1-\alpha)}\frac{M(\beta)(2-\alpha)}{2(1-\alpha)}s}\ \mathcal{L}(f(t))(s) + \frac{\left(s+\frac{\beta}{1-\beta}\right)\ g(0)}{\frac{M(\beta)(2-\beta)}{2(1-\beta)}s^2}$$
$$+\frac{\left(s+\frac{\beta}{1-\beta}\right)\ \mathcal{L}(\lambda(t)y(t))(s)}{\frac{M(\alpha)(2-\alpha)}{2(1-\alpha)}s}.$$

Replacing the conditions (2) in (2), we obtain (4), which completes the proof. □

3. Main Results

The next section addresses the existence of at least one solution to our problem by utilizing two different approaches. We apply a fixed point theorem of Krasnoselskii type. It is based on the sum of two sequentially weakly continuous mappings.
We consider the Banach space:

$$\mathfrak{E} = \left\{y \in \mathcal{C}([0,T],\mathbb{R}),\ D^{\beta}y \in \mathcal{C}([0,T],\mathbb{R})\right\},$$

equipped with norm

$$\|y\|_{\mathfrak{E}} = \sup_{t\in[0,T]} |y(t)| + \sup_{t\in[0,T]} \left|D^{\beta}y(t)\right|.$$

Certainly, $(\mathfrak{E}, \|.\|_{\mathfrak{E}})$ is a Banach space.
Let $\Omega_j := \{y \in \mathfrak{E}, \|y\|_{\mathfrak{E}} \leq \eta_j\}, \quad j = 1, 2.$
The assumptions below are required:

(H1): The function $f : [0,T] \times \mathbb{R}^2 \to \mathbb{R}$ is a jointly continuous function.

(H2): There exist non negative function $h \in \mathcal{C}([0,T],\mathbb{R}^+)$ and a non negative non decreasing function $\mathfrak{W} : \mathbb{R}^+ \to \mathbb{R}^+$, for each $t \in [0,T]$, and for all $x_i,\ y_i \in \mathbb{R}, i = 1, 2$, such that

$$|f(t,x_1,x_2) - f(t,y_1,y_2)| \leq h(t)\ \mathfrak{W}(\|x-y\|_{\mathfrak{E}}).$$

For $x \in \Omega_j, j = 1, 2$, we have

$$|f(t,x_1,x_2)| \leq h(t)\ \mathfrak{W}(\eta_j).$$

To simplify, we consider the following formulas

$$
\begin{aligned}
&F_y(t) := f\left(t, y(t), D^{\beta}y(t)\right),\\
&\quad k_1 := \|h\|_\infty \mathcal{A}_1 \left| \frac{(1-\beta)(1-\alpha)}{\beta\alpha} + \frac{T^{\beta+\alpha}}{\Gamma(\beta+\alpha+1)} + \frac{(1-\alpha)T^{\beta}}{\alpha\Gamma(\beta+1)} + \frac{(1-\beta)T^{\alpha}}{\beta\Gamma(\alpha+1)} \right|,\\
&\quad k_2 := \|h\|_\infty \mathcal{A}_2 \left| \frac{(1-\beta)(1-\alpha)}{\beta\alpha} + \frac{T^2}{2} + \frac{(1-\alpha)T}{\alpha} + \frac{(1-\beta)T}{\beta} \right|,\\
&\quad k_3 := \|h\|_\infty \left| \frac{1-\alpha}{B(\alpha)} + \frac{\alpha T^{\alpha}}{B(\alpha)\Gamma(\alpha+1)} \right|,\\
&\quad k_4 := \|h\|_\infty \left| \frac{-\alpha T^2}{M(\alpha)(\alpha-2)} + \frac{2(\alpha-1)}{M(\alpha)(\alpha-2)} \right|,\\
&\quad p_1 := \mathcal{B}_1|\ \|\lambda\|_\infty \left(\frac{T^{\beta}}{\Gamma(\beta+1)} + \left| \frac{1-\beta}{\beta} + \frac{T^{\beta}}{\Gamma(\beta+1)} \right| \frac{r\delta\xi^{\gamma}}{\Gamma(\gamma+1)} \right),\\
&\quad p_2 = \mathcal{B}_2|\ \|\lambda\|_\infty \left(\frac{T^2}{2} + \left| \frac{1-\beta}{\beta} + T \right| \frac{r\delta\xi^{\gamma}}{\Gamma(\gamma+1)} \right),\\
&\quad p_3 = p_4 = \|\lambda\|_\infty \left(1 + \frac{r\delta\xi^{\gamma}}{\Gamma(\gamma+1)}\right),
\end{aligned}
$$

and

$$1-\rho_1 \neq 0,\ 1-\rho_2 \neq 0, \quad \kappa_1 := k_1+k_3,\ \kappa_2 := k_2+k_4, \quad \rho_1 := p_1+p_3,\ \rho_2 := p_2+p_4.$$

$$\delta := \max\{\delta_i, i = \overline{1,r}\},\ \xi := \max_{\xi_i \in [0,T]}\{\xi_i, i = \overline{1,r}\}$$

Our main results are given by the following theorem:

Theorem 3. *Assume that (H1) and (H2) are satisfied and suppose that* $\frac{\kappa_j}{(1-\rho_j)} \leq \frac{\eta_j}{\mathfrak{W}(\eta_j)},\ j = 1, 2.$
Then problem (1)-(2) *has at least a solution* y, $\|y\|_{\mathfrak{E}} \leq \eta_j,\ j = 1, 2.$

Proof. Let's introduce the applications $\mathcal{H}_j : \mathfrak{E} \to \mathfrak{E}, j = 1, 2,$ by

$$
\begin{aligned}
&\mathcal{H}_1 y(t)\\
&= \mathcal{A}_1 \left[\begin{aligned} &\int_0^t \left(\frac{(t-u)^{\beta+\alpha-1}}{\Gamma(\beta+\alpha)} + \frac{(1-\alpha)(t-u)^{\beta-1}}{\alpha\Gamma(\beta)} + \frac{(1-\beta)(t-u)^{\alpha-1}}{\beta\Gamma(\alpha)} \right) F_y(u)du \\ &+ \frac{(1-\beta)(1-\alpha)F_y(t)}{\beta\alpha} \end{aligned} \right] \qquad (6)\\
&+ \mathcal{B}_1 \left[\int_0^t \frac{(t-u)}{\Gamma(B)}^{\beta-1} \lambda(u)y(u)du + \lambda(0)\left(\frac{1-\beta}{\beta} + \frac{t^{\beta}}{\Gamma(\beta+1)}\right) \sum_{i=0}^{r} \delta_i J^{\gamma} y(\xi_i) \right],
\end{aligned}
$$

and

$$\begin{aligned}\mathcal{H}_2 y(t) =& \mathcal{A}_2 \left[\begin{array}{l} \int_0^t \left((t-u) + \frac{(1-\alpha)}{\alpha} + \frac{(1-\beta)}{\beta} \right) F_y(u)du \\ + \frac{(1-\beta)(1-\alpha)F_y(t)}{\beta\alpha} \end{array} \right] \\ &+ \mathcal{B}_2 \left[\int_0^t \lambda(u)y(u)du + \lambda(0)\left(\frac{1-\beta}{\beta} + t\right) \sum_{i=0}^{r} \delta_i J^\gamma y(\xi_i) \right].\end{aligned} \tag{7}$$

Obviously, the establishment of the existence of solutions for (1)-(2) is equivalent to studying the existence of solutions of equation (6) (for Atangana Baleanu derivative), or the existence of solution of equation (7) (for Caputo Fabrizio derivative). For this aim, let us define the operators:

$$\Psi_j := (\Psi_{j,1}, \Psi_{j,2}) \text{ and } \Phi_j := (\Phi_{j,1}, \Phi_{j,2}), \quad j = 1, 2,$$

such that

$$\Psi_{j,\ i} : \mathfrak{E} \to \mathfrak{E} \text{ and } \Phi_{j,\ i} : \Omega_j \to \mathfrak{E}, \quad i, j = 1, 2,$$

by

$$\Psi_{1,1} y(t) = \mathcal{A}_1 \left[\begin{array}{l} \int_0^t \left(\frac{(t-u)^{\beta+\alpha-1}}{\Gamma(\beta+\alpha)} + \frac{(1-\alpha)(t-u)^{\beta-1}}{\alpha\Gamma(\beta)} + \frac{(1-\beta)(t-u)^{\alpha-1}}{\beta\Gamma(\alpha)} \right) F_y(u)du \\ + \frac{(1-\beta)(1-\alpha)F_y(t)}{\beta\alpha} \end{array} \right],$$

$$\Psi_{2,1} y(t) = \mathcal{A}_2 \left[\int_0^t \left((t-u) + \frac{(1-\alpha)}{\alpha} + \frac{(1-\beta)}{\beta} \right) F_y(u)du + \frac{(1-\beta)(1-\alpha)F_y(t)}{\beta\alpha} \right],$$

$$\Phi_{1,1} y(t) = \mathcal{B}_1 \left[\int_0^t \frac{(t-u)}{\Gamma(\beta)}^{\beta-1} \lambda(u)y(u)du + \lambda(0)\left(\frac{1-\beta}{\beta} + \frac{t^\beta}{\Gamma(\beta+1)}\right) \sum_{i=0}^{r} \delta_i J^\gamma y(\xi_i) \right],$$

$$\Phi_{2,1} y(t) = \mathcal{B}_2 \left[\int_0^t \lambda(u)y(u)du + \lambda(0)\left(\frac{1-\beta}{\beta} + t\right) \sum_{i=0}^{r} \delta_i J^\gamma y(\xi_i) \right],$$

$$\Psi_{1,2} y(t) = \frac{\alpha}{B(\alpha)} \int_0^t \frac{(t-u)^{\alpha-1}}{\Gamma(\alpha)} F_y(u)du + \frac{(1-\alpha)\ F_y(t)}{B(\alpha)},$$

$$\Psi_{2,2} y(t) = \frac{-2\alpha}{M(\alpha)(\alpha-2)} \int_0^t F_y(u)du + \frac{2(\alpha-1)F_y(t)}{M(\alpha)(\alpha-2)},$$

$$\Phi_{1,2} y(t) = \Phi_{2,2} y(t) = \lambda(t)y(t) + \lambda(0) \sum_{i=0}^{r} \delta_i J^\gamma y(\xi_i),$$

where

$$\mathcal{H}_j = \Psi_{j,1} + \Phi_{j,1}, \quad D^\beta \mathcal{H}_j = \Psi_{j,2} + \Phi_{j,2}, \quad j = 1, 2.$$

Firstly, we need to prove that Ψ_1, Φ_1 are two weakly sequential continuous mappings. Let $y_n \in \Omega_j$ be a sequence with $y_n \to y$, for some $y \in \mathfrak{E}$.
By (H_1) and (H_2), for $j = 1, 2$, we can write

$$|\Psi_{j,1}y_n(t) - \Psi_{j,1}y(t)| \leq k_j \ \mathfrak{W}(\ \|y_n - y\|_{\mathfrak{E}} \ ),$$

and

$$|\Psi_{j,2}y_n(t) - \Psi_{j,2}y(t)| \leq k_{j+2} \ \mathfrak{W}(\ \|y_n - y\|_{\mathfrak{E}} \ ).$$

Thus, we can write

$$\|\Psi_j y_n - \Psi_j y\|_{\mathfrak{E}} \leq \kappa_j \mathfrak{W}(\ \|y_n - y\|_{\mathfrak{E}}). \tag{8}$$

With the same arguments as before, we have

$$|\Phi_{j,1}y_n(t) - \Phi_{j,1}y(t)| \leq p_j \|y_n - y\|_\infty$$

and

$$|\Phi_{j,2}y_n(t) - \Phi_{j,2}y_n(t)| \leq p_{j+2} \|y_n - y\|_\infty.$$

Therefore,

$$\|\Phi_j y_n - \Phi_j y\|_{\mathfrak{E}} \leq \rho_j \|y_n - y\|_{\mathfrak{E}}. \tag{9}$$

Since $\|y_n - y\|_{\mathfrak{E}} \to 0$, the right hand sides of (8) and (9) tend to zero, then Ψ_j and Φ_j are weakly sequentially continuous mapping.

Secondly, we show that $\Phi_j(\Omega_j)$ is relatively weakly compact.
Step 1: Let $y \in \Omega_j$ $j = 1, 2, t \in [0, T]$. We prove that $\Phi_j(\Omega_j)$ are bounded.
By (H_2), we get

$$|\Phi_{j,1}y(t)| \leq \eta_j \ p_j \quad \text{and} \quad |\Phi_{j,2}y(t)| \leq \eta_j \ p_{j+2},$$

so that

$$\|\Phi_j y\|_{\mathfrak{E}} \leq \eta_j \ \rho_j. \tag{10}$$

It follows that $\Phi_j(\Omega_j)$ are bounded.
Step 2: Let $y \in \Omega_j$ $j = 1, 2$ and $t_1, t_2 \in [0, T]$ with $t_1 < t_2$, we will show that Φ_j are equicontinuous.

By application of (H_1), for $j=1$, we have

$$\begin{aligned}
&|\Phi_{1,1}y(t_2)-\Phi_{1,1}y(t_1)|\\
&\le \frac{|\mathcal{B}_1|}{\Gamma(\beta)}\int_0^{t_1}\left|(t_2-u)^{\beta-1}-(t_1-u)^{\beta-1}\right| \ |\lambda(u)y(u)|\,du\\
&\quad+\frac{|\mathcal{B}_1|}{\Gamma(\beta)}\left[\ \int_{t_1}^{t_2}\left|(t_2-u)^{\beta-1}\right| \ |\lambda(u)y(u)|\,du\ +\frac{|t_2^B-t_1^B|}{\Gamma(B+1)}\sum_{i=0}^{r}\delta_i J^\gamma y(\xi_i)\ \right]\\
&\le \frac{\eta_1\ |\mathcal{B}_1|\ \|\lambda\|_\infty}{\Gamma(\beta)}\left[\int_0^{t_1}\left|(t_2-u)^{\beta-1}-(t_1-u)^{\beta-1}\right|+\ \int_{t_1}^{t_2}\left|(t_2-u)^{\beta-1}\right|\ du\right]\\
&\quad+\frac{|\mathcal{B}_1|\ \delta\ r\ \eta_1\ \xi^\gamma\ |t_2^B-t_1^B|}{\Gamma(B+1)\Gamma(\gamma+1)}.
\end{aligned}$$

Also, we have

$$|\Phi_{1,2}y(t_2)-\Phi_{1,2}y(t_1)|\le\ |\lambda(t_2)-\lambda(t_1)|\ |y(t_2)-y(t_1)|.$$

Consequently,

$$\begin{aligned}
|\Phi_1y(t_2)-\Phi_1y(t_1)|\le\frac{\eta_1\ |\mathcal{B}_1|\ \|\lambda\|_\infty}{\Gamma(\beta)}&\left[\begin{array}{l}\displaystyle\int_0^{t_1}\left|(t_2-u)^{\beta-1}-(t_1-u)^{\beta-1}\right|du\\ \displaystyle+\ \int_{t_1}^{t_2}\left|(t_2-u)^{\beta-1}\right|\ du\end{array}\right]\\
&+\frac{\delta\ r\ \eta_1\ \xi^\gamma\ |t_2^B-t_1^B|}{\Gamma(B+1)\Gamma(\gamma+1)}+|\lambda(t_2)-\lambda(t_1)|\ |y(t_2)-y(t_1)|.
\end{aligned}\tag{11}$$

In the same way as the previous part, for $j=2$, we get

$$\begin{aligned}
|\Phi_{2,1}y(t_2)-\Phi_{2,1}y(t_1)|\le\ &|\mathcal{B}_2|\left[\ \int_{t_1}^{t_2}|\lambda(u)y(u)|\,du\ +|t_2-t_1|\sum_{i=0}^{r}\delta_iJ^\gamma y(\xi_i)\ \right]\\
&\le\eta_2\ |\mathcal{B}_2|\,|t_2-t_1|\left[\ \|\lambda\|_\infty+\ \delta\ r\ \frac{\xi^\gamma}{\Gamma(\gamma+1)}\right]
\end{aligned}$$

and

$$|\Phi_{2,2}y(t_2)-\Phi_{2,2}y(t_1)|\le\ |\lambda(t_2)-\lambda(t_1)|\ |y(t_2)-y(t_1)|.$$

These imply that

$$\begin{aligned}
|\Phi_2y(t_2)-\Phi_2y(t_1)|\le\eta_2\ |\mathcal{B}_2|\,|t_2-t_1|&\left[\ \|\lambda\|_\infty+\ \delta\ r\ \frac{\xi^\gamma}{\Gamma(\gamma+1)}\right]\\
&+|\lambda(t_2)-\lambda(t_1)|\ |y(t_2)-y(t_1)|,
\end{aligned}\tag{12}$$

when $t_1\to t_2$, the right hand sides of (11) and (12) tends to zero independently of y. Therefore, $\Phi_j,\ j=1,2$, are equicontinuous operators.
Thanks to Arzelà–Ascoli and Eberlein-Smulian theorems, $\Phi_j,\ j=1,2$, is relatively

weakly compact.

Next, we show that the operator $\Psi_j, j = 1, 2$, are nonlinear contractions. In view of (H_1) and (H_2), for each $t \in [0, T]$, we obtain

$$\|\Psi_{j,1}y_2 - \Psi_{j,1}y_1\|_{\infty} \leq k_j \ \mathfrak{W}(\ \|y_2 - y_1\|_{\mathfrak{E}} \ ),$$

and

$$\|\Psi_{j,2}y_2 - \Psi_{j,2}y_1\|_{\infty} \leq k_{j+2} \ \mathfrak{W}(\ \|y_2 - y_1\|_{\mathfrak{E}} \ ),$$

from which we get

$$\|\Psi_j y_2 - \Psi_j y_1\|_{\mathfrak{E}} \leq \kappa_j \ \mathfrak{W}(\ \|y_2 - y_1\|_{\mathfrak{E}} \ ).$$

In addition, we have to prove condition (iii) of Theorem 1 in two steps.
Phase 1: We verify that $\Psi_j(\mathfrak{E}), j = 1, 2$ are bounded.
Let $\Psi_j(\mathfrak{E}) := \{\Psi_j(y), y \in \Omega_j\}, j = 1, 2$, for all $t \in [0, T]$. Thanks to (H_2), we obtain

$$|\Psi_{j,1}y(t)| \leq k_j \ \mathfrak{W}(\eta_j) \quad \text{and} \quad |\Psi_{j,2}y(t)| \leq k_{j+2} \ \mathfrak{W}(\eta_j),$$

which simplifies into

$$\|\Psi_j y\|_{\mathfrak{E}} \leq \ \kappa_j \ \mathfrak{W}(\eta_j). \tag{13}$$

Therefore, $\Psi_j(\mathfrak{E}), j = 1, 2$ are bounded.
Phase 2: Let $z \in \Omega_j, j = 1, 2$, such that $y = \Psi_j z + \Phi_j y$, so we can write:

$$|y(t)| \leq |\Psi_{j,1}z(t)| \ + \ |\Phi_{j,1}y(t)| \quad \text{and} \quad |D^\beta y(t)| \leq |\Psi_{j,2}z(t)| \ + \ |\Phi_{j,2}y(t)|,$$

Thanks to (10) and (13), we obtain

$$\|y\|_{\mathfrak{E}} \leq \ \kappa_j \ \mathfrak{W}(\eta_j) + \eta_j \ \rho_j.$$

Consequently, we have

$$\|y\|_{\mathfrak{E}} \leq \eta_j \Rightarrow y \in \Omega_j.$$

So through the implementation of theorem1, we can state that $\mathcal{H}_j$ has at least one fixed point. Hence problem (1)-(2) has one solution in Ω_j, for $j = 1, 2$. □

4. An Example

Consider the following example:

$$\begin{cases} D^\alpha \left(D^\beta - \lambda(t)\right) y(t) = f\left(t, y(t), D^\beta y(t)\right), \quad t \in [0, T], \quad 0 < \alpha, \beta \leq 1, \\ y(0) = 0, \quad D^\beta y(0) = \displaystyle\sum_{i=0}^{r} \delta_i J^\gamma y(\xi_i), \quad 0 < \beta \leq 1, \quad \gamma > 0 \quad r \in \mathbb{N}^*, \quad \xi_i \in [0, T]. \end{cases}$$

We choose $\alpha = 0.995, \ \beta = 0.995, \ \gamma = 1.33, \ \delta = 0.75, \ \xi = 0.75, \ r = 5,$ and $T = 1$. Define the continuous function by

$$f(t, x_1, x_2) = \frac{e^{\cos(\pi t)}}{(2-t)^4}\left(\sqrt{|x_1 + x_2|}\right), \quad h(t) = \frac{e^{\cos(\pi t)}}{(2-t)^4}, \quad \mathfrak{W}(r) = \sqrt{r}, \quad \lambda(t) = 0.1t.$$

From the above data, for $\eta_1 = 4.5$ and $\eta_2 = 1.6$, we have

$$\kappa_1 = 0.5581,\ \kappa_2 = 0.4138,\ \rho_1 = 0.7293,\ \rho_2 = 0.6708.$$

Obviously,

$$\frac{\kappa_1}{(1-\rho_1)} = 2.0622 \leq \frac{\eta_1}{\mathfrak{W}(\eta_1)} = \sqrt{4.5} \sim 2.1213$$
$$\frac{\kappa_2}{(1-\rho_2)} = 1.2575 \leq \frac{\eta_2}{\mathfrak{W}(\eta_2)} = \sqrt{1.6} \sim 1.2649.$$

By Theorem 1, our problem has at least one solution on $[0,1]$.

5. Numerical Method of Approximation

We recall the following result, which is needed in the next section.

Theorem 4 ([25]). *The three-step Adams-Bashforth scheme for the Caputo Fabrizio fractional derivative is given by*

$$\begin{aligned} y(t_{n+1}) =& y(t_n) + \left(\frac{1-\alpha}{M(\alpha)} + \frac{23\alpha h}{12M(\alpha)}\right) f\left(t_n, y(t_n)\right) \\ &- \left(\frac{1-\alpha}{M(\alpha)} + \frac{16\alpha h}{12M(\alpha)}\right) f\left(t_{n-1}, y(t_{n-1})\right) + \frac{5\alpha h}{12M(\alpha)} f\left(t_{n-2}, y_{n-2}\right). \end{aligned} \tag{14}$$

In what follows, we prove an analogue theorem in the case of Atangana-Baleanu and then in the case of Caputo.

Theorem 5. *The three-step fractional Adams-Bashforth scheme for Atangana-Baleanu derivative in Caputo sense, for $n \in \mathbb{N}$, is given by*

$$\begin{aligned} y(t_{n+1}) =& y(t_n) + \mathfrak{A}\left(f\left(t_n, y_n\right) - f\left(t_{n-1}, y(t_{n-1})\right)\right) \\ &+ f\left(t_n, y\left(t_n\right)\right) \begin{pmatrix} \frac{h^\alpha \mathfrak{B}(n+1)^\alpha}{2}\left[\frac{6}{\alpha} - \frac{5(n+1)}{(\alpha+1)} + \frac{(n+1)^2}{\alpha+2}\right] \\ -\frac{h^\alpha \mathfrak{B} n^\alpha}{2}\left[\frac{2}{\alpha} - \frac{3n}{\alpha+1} + \frac{n^2}{\alpha+2}\right] \end{pmatrix} \\ &+ f\left(t_{n-2}, y\left(t_{n-2}\right)\right) \begin{pmatrix} \frac{h^\alpha \mathfrak{B}(n+1)^\alpha}{2}\left[\frac{2}{\alpha} - \frac{3(n+1)}{a+1} + \frac{(n+1)^2}{\alpha+2}\right] \\ +\frac{h^\alpha \mathfrak{B} n^\alpha}{2}\left[\frac{n}{\alpha+1} - \frac{n^2}{\alpha+2}\right] \end{pmatrix} \\ &- 2f\left(t_{n-1}, y\left(t_{n-1}\right)\right) \begin{pmatrix} \frac{h^\alpha \mathfrak{B}(n+1)^\alpha}{2}\left[\frac{3}{\alpha} - \frac{4(n+1)}{a+1} + \frac{(n+1)^2}{\alpha+2}\right] \\ +\frac{h^\alpha \mathfrak{B} n^\alpha}{2}\left[\frac{2n}{\alpha+1} - \frac{n^2}{\alpha+2}\right] \end{pmatrix}, \end{aligned} \tag{15}$$

where

$$\mathfrak{A} := \frac{1-\alpha}{B(\alpha)}, \quad \mathfrak{B} := \frac{\alpha}{B(\alpha)\Gamma(\alpha)}.$$

Proof. To approach the fractional derivative of Atangana-Baleanu we use [27,28]. First, we take the following differential equation

$${}^{ABC}D_t^{\alpha} y(t) = f(t, y(t)).$$

With respect to the integral representation, we find that

$$y(t) - y(0) = \frac{1-\alpha}{B(\alpha)} f(t, y(t)) + \frac{\alpha}{B(\alpha)\Gamma(\alpha)} \int_0^t (t-\tau)^{\alpha-1} f(\tau, y(\tau)) d\tau.$$

At t_{n+1}, we get

$$y\left(t_{n+1}\right) - y(0) = \frac{1-\alpha}{B(\alpha)} f\left(t_n, y(t_n)\right) + \frac{\alpha}{B(\alpha)\Gamma(\alpha)} \int_0^{t_{n+1}} \left(t_{n+1} - t\right)^{\alpha-1} f(t, y(t)) dt,$$

thus

$$y\left(t_{n+1}\right) - y\left(t_n\right) = \mathfrak{A}\left(f\left(t_n, y_n\right) - f\left(t_{n-1}, y(t_{n-1})\right)\right) + C_1 - C_2, \tag{16}$$

where,

$$C_1 := \frac{\alpha}{B(\alpha)\Gamma(\alpha)} \int_0^{t_{n+1}} \left(t_{n+1} - t\right)^{\alpha-1} f(t, y(t)) dt,$$
$$C_2 := \frac{\alpha}{B(\alpha)\Gamma(\alpha)} \int_0^{t_n} \left(t_n - t\right)^{\alpha-1} f(t, y(t)) dt.$$

To approximate the integral parts, we must use the polynomial approximation for $f(t, y(t))$ that passes through $f\left(t_n, y(t_n)\right), f\left(t_{n-1}, y(t_{n-1})\right)$, and $f\left(t_{n-2}, y_{n-2}\right)$, which is given by

$$\Pi_2(t) = \sum_{i=0}^{2} f\left(t_{n-i}, y_{n-i}\right) L_i(t),$$

where $L_i(t)$ is the Lagrange polynomial for the interpolation points on t_n, t_{n-1} and t_{n-2}, as

$$\begin{aligned}\Pi_2(t) =& \frac{f\left(t_{n-2}, y\left(t_{n-2}\right)\right)}{2h^2}\left(t - t_n\right)\left(t - t_{n-1}\right) - \frac{f\left(t_{n-1}, y\left(t_{n-1}\right)\right)}{h^2}\left(t - t_n\right) \\ &\times \left(t - t_{n-2}\right) + \frac{f\left(t_n, y\left(t_n\right)\right)}{2h^2}\left(t - t_{n-1}\right)\left(t - t_{n-2}\right).\end{aligned}$$

Now, using $u = (t_{n+1} - t)/h$ in C_1, we get

$$C_1 = \frac{h^\alpha (n+1)^\alpha}{2} \left(\begin{array}{l} \left[\frac{6}{\alpha} - \frac{5(n+1)}{(\alpha+1)} + \frac{(n+1)^2}{\alpha+2}\right] f(t_n, y(t_n)) \\ -2\left[\frac{3}{\alpha} - \frac{4(n+1)}{\alpha+1} + \frac{(n+1)^2}{\alpha+2}\right] \times f(t_{n-1}, y(t_{n-1})) \\ +\left[\frac{2}{\alpha} - \frac{3(n+1)}{a+1} + \frac{(n+1)^2}{\alpha+2}\right] f(t_{n-2}, y(t_{n-2})) \end{array} \right). \quad (17)$$

Similarly, taking $u = (t_n - t)/h$ in C_2, we obtain

$$C_2 = \frac{h^\alpha (n)^\alpha}{2} \left(\left[\frac{n^2}{\alpha+2} - \frac{3n}{\alpha-1} + \frac{2}{\alpha}\right] f(t_n, y(t_n)) + 2\left[\frac{2n}{\alpha+1} - \frac{n^2}{\alpha+2}\right] \times f(t_{n-1}, y(t_{n-1})) - \left[\frac{n}{\alpha+1} - \frac{n^2}{\alpha+2}\right] f(t_{n-2}, y(t_{n-2})) \right). \quad (18)$$

Substituting (17) and (18) into (16), we find (15). □

Theorem 6. *The three-step fractional Adams-Bashforth scheme for Caputo derivative, for $n \in \mathbb{N}$, is defined by:*

$$\begin{aligned} y(t_{n+1}) = {} & y(t_n) + f(t_n, y(t_n)) \left(\begin{array}{l} \frac{h^\alpha (n+1)^\alpha}{2\Gamma(\alpha)} \left[\frac{6}{\alpha} - \frac{5(n+1)}{(\alpha+1)} + \frac{(n+1)^2}{\alpha+2}\right] \\ -\frac{h^\alpha n^\alpha}{2\Gamma(\alpha)} \left[\frac{2}{\alpha} - \frac{3n}{\alpha+1} + \frac{n^2}{\alpha+2}\right] \end{array} \right) \\ & + f(t_{n-2}, y(t_{n-2})) \left(\begin{array}{l} \frac{h^\alpha (n+1)^\alpha}{2\Gamma(\alpha)} \left[\frac{2}{\alpha} - \frac{3(n+1)}{a+1} + \frac{(n+1)^2}{\alpha+2}\right] \\ +\frac{h^\alpha n^\alpha}{2\Gamma(\alpha)} \left[\frac{n}{\alpha+1} - \frac{n^2}{\alpha+2}\right] \end{array} \right) \\ & - 2f(t_{n-1}, y(t_{n-1})) \left(\begin{array}{l} \frac{h^\alpha (n+1)^\alpha}{2\Gamma(\alpha)} \left[\frac{3}{\alpha} - \frac{4(n+1)}{a+1} + \frac{(n+1)^2}{\alpha+2}\right] \\ +\frac{h^\alpha n^\alpha}{2\Gamma(\alpha)} \left[\frac{2n}{\alpha+1} - \frac{n^2}{\alpha+2}\right] \end{array} \right), \end{aligned} \quad (19)$$

Proof. For Caputo derivative, we examine the following differential equation

$${}^{c}D_t^\alpha y(t) = f(t, y(t)).$$

The integral representation is given by

$$y(t) - y(0) = \frac{1}{\Gamma(\alpha)} \int_0^t (t-\tau)^{\alpha-1} f(\tau, y(\tau)) d\tau.$$

In a similar manner as before, we obtain (19) □

We further extend the feasibility of the suggested new scheme to explore issues modeled in many applications. In order to reproduce some existing chaotic problems, we adequately replace the classical time derivative by the fractional derivative of Caputo, Caputo-Fabrizio, and Atangana-Baleanu, then we faithfully perform the

simulation with the three-step Adams Bashforth fractional method as it was constructed above.
We note that (1) can be reduced to the following system:

$$\begin{array}{lllll} D^{\beta}y(t) & = & z(t)+\lambda(t)\ y(t) & = & f_1(t,y(t)) \\ D^{\alpha}z(t) & = & f(t,y(t),D^{\beta}y(t)) & = & f_2(t,y(t),D^{\beta}y(t)). \end{array}$$

We can therefore stipulate the conditions (2) as follows

$$y(0)=0, \quad z(0)=\sum_{i=0}^{r}\delta_i J^{\gamma}y(\xi_i), \quad \gamma>0. \tag{20}$$

By (14), (15) and (19), the above system is transformed into the following:
Caputo case

$$\begin{aligned} y(t_{n+1}) =& y(t_n)+f_1\left(t_n,y\left(t_n\right)\right)C_{1,\beta}+f_1\left(t_{n-2},y\left(t_{n-2}\right)\right)C_{2,\beta} \\ &-2f_1\left(t_{n-1},y\left(t_{n-1}\right)\right)C_{3,\beta} \\ z(t_{n+1}) =& z(t_n)+f_2\left(t_n,z\left(t_n\right)\right)C_{1,\alpha}+f_2\left(t_{n-2},z\left(t_{n-2}\right)\right)C_{2,\alpha} \\ &-2f_2\left(t_{n-1},z\left(t_{n-1}\right)\right)C_{3,\alpha}. \end{aligned}$$

Caputo Fabrizio case

$$\begin{aligned} y(t_{n+1}) =& y(t_n)+f_1\left(t_n,y\left(t_n\right)\right)F_{1,\beta}+f_1\left(t_{n-2},y\left(t_{n-2}\right)\right)F_{2,\beta} \\ &-2f_1\left(t_{n-1},y\left(t_{n-1}\right)\right)F_{3,\beta} \\ z(t_{n+1}) =& z(t_n)+f_2\left(t_n,z\left(t_n\right)\right)F_{1,\alpha}+f_2\left(t_{n-2},z\left(t_{n-2}\right)\right)F_{2,\alpha} \\ &-2f_2\left(t_{n-1},z\left(t_{n-1}\right)\right)F_{3,\alpha}. \end{aligned}$$

Atangana-Baleanu case

$$\begin{aligned} y(t_{n+1}) =& y(t_n)+f_1\left(t_n,y\left(t_n\right)\right)A_{1,\beta}+f_1\left(t_{n-2},y\left(t_{n-2}\right)\right)A_{2,\beta} \\ &-2f_1\left(t_{n-1},y\left(t_{n-1}\right)\right)A_{3,\beta} \\ z(t_{n+1}) =& z(t_n)+f_2\left(t_n,z\left(t_n\right)\right)A_{1,\alpha}+f_2\left(t_{n-2},z\left(t_{n-2}\right)\right)A_{2,\alpha} \\ &-2f_2\left(t_{n-1},z\left(t_{n-1}\right)\right)A_{3,\alpha}, \end{aligned}$$

where $A_{i,\alpha},\ A_{i,\beta}, F_{i,\alpha},\ F_{i,\beta},\ C_{i,\alpha}, C_{i,\beta}$, constants obtained from (14), (15), (19) respectively.

6. Numerical Experiments

We use a variety of real-world examples to assess the performance of the new method on our problem, see [10,14,16,29,30,36]. The integration is carried out using the three-step fractional Adams-Bashforth methods for Caputo, Caputo Fabrizio, and Atangana-Baleanu. The classic case is plotted using the three-step Adams-Bashforth method for comparison.

For all the examples, we take $n = 8000$, so $T = n \times h$, $\alpha = 0.999999999$, $\beta = 0.99999999$.

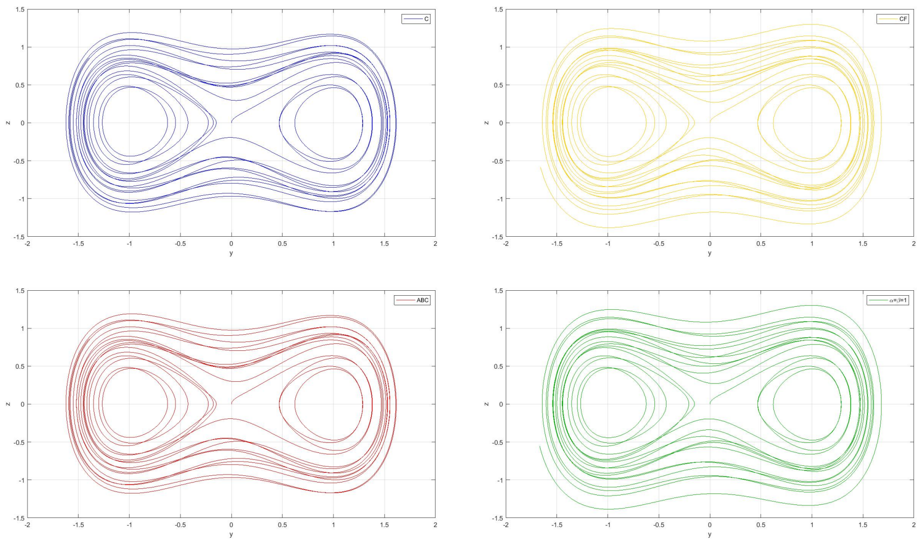

FIGURE 1. 2-D phase portraits for the numerical simulation for (21)

Example 1 (see [14]). *We consider the following general nonlinear Helmholtz–Duffing oscillator:*

$$D^{\alpha}\left(D^{\beta}-\delta\right)y(t)=\gamma\cos(\omega t)+y-(1-\sigma)y^{2}-\sigma y^{3}-0.000001D^{\beta}y(t),\quad t\in[0,T],\ 0<\alpha,\beta\le 1, \tag{21}$$

the equation (21) *can be reduced to the following system:*

$$\begin{aligned}D^{\beta}y(t)&=z(t)+\delta y(t),\\ D^{\alpha}z(t)&=\gamma\cos(\omega t)+y-(1-\sigma)y^{2}-\sigma y^{3}-0.000001D^{\beta}y(t).\end{aligned}$$

With initial conditions $(0, 0.00025)$, $h = 0.01$, $\delta = 0.01$, $\sigma = 1$, $\omega = 0.068$, $\gamma = 1$.

Example 2 (see [16]). *We consider the following problem in light of the Josephson Junction pendulum description and the pendulum system for ultra-subharmonic resonance:*

$$\begin{aligned}D^{\alpha}\left(D^{\beta}-\delta\right)y(t)=&-ay-[1+f_{0}\cos(\Omega t+\Psi)]\sin y+f_{1}\cos(\omega t)\sin(y-\gamma)\\ &-5*10^{(-5)}D^{\beta}y(t),\quad t\in[0,T],\quad 0<\alpha,\beta\le 1.\end{aligned} \tag{22}$$

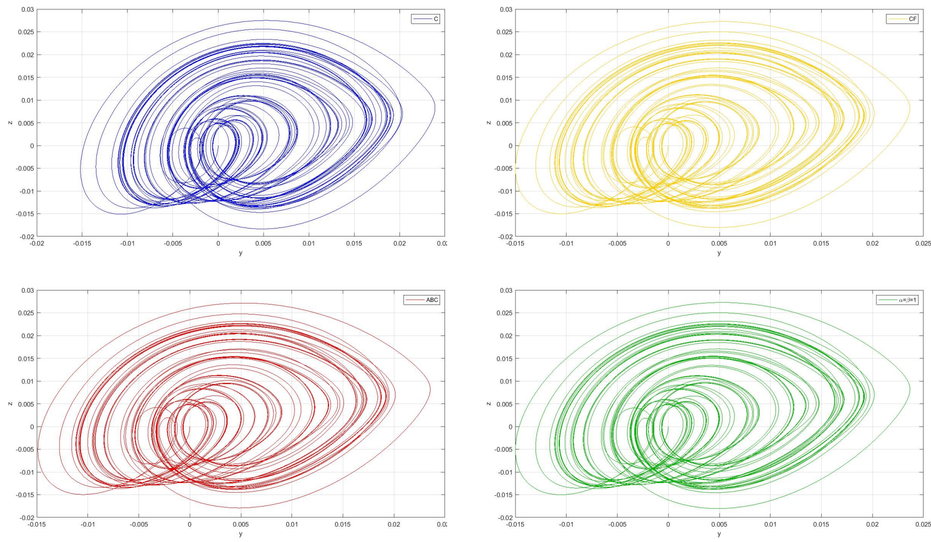

FIGURE 2. 2-D phase portraits for the numerical simulation for (22)

The equation (22) *can be reduced to the following system:*

$$
\begin{aligned}
D^{\beta}y(t) =& z(t) + \delta y(t),\\
D^{\alpha}z(t) =& -ay - [1 + f_0\cos(\Omega t + \Psi)]\sin y + f_1\cos(\omega t)\sin(y-\gamma)\\
& - 5 * 10^{(-5)} D^{\beta}y(t).
\end{aligned}
$$

The initial conditions are: $(0,0)$, $h = 0.01$, $\delta = 0.1$, $a = 0.1$, $\Omega = 0.75$, $\omega = 1.5$, $\Psi = \ 7\pi/4$, $f_0 = 0.2$, $f_1 = 1.381$, $\gamma = 0.01$.

Example 3 (see [30]). *We examine the resulting chaos of a simple nonlinear damped and driven pendulum motion:*

$$
\begin{aligned}
& D^{\alpha}\left(D^{\beta} - q\right)y(t) = a\Omega^2\cos(\Omega_D t) - \Omega^2\sin(y(t)) + 0.001D^{\beta}y(t),\\
& t \in [0,T], \quad 0 < \alpha, \beta \le 1.
\end{aligned} \tag{23}
$$

The equation (23) *can be reduced to the following system:*

$$
\begin{aligned}
D^{\beta}y(t) &= z(t) + qy(t),\\
D^{\alpha}z(t) &= a\Omega^2\cos(\Omega_D t) - \Omega^2\sin(y(t)) + 0.001D^{\beta}y(t).
\end{aligned}
$$

The initial conditions: $(0, 0.8)$, $h = 0.045$. $q = -0.4$, $a = 1.4$, $\Omega = 1$, $\Omega_D = 2/3$.

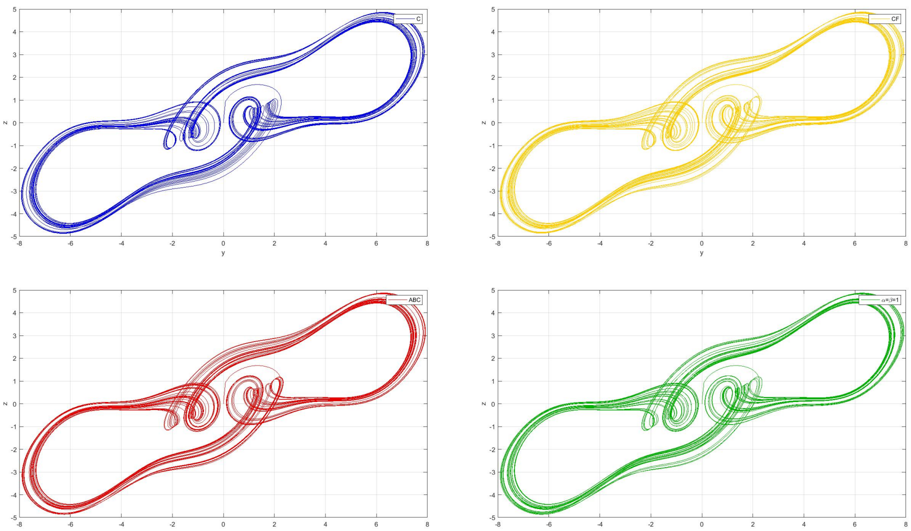

FIGURE 3. 2-D phase portraits for the numerical simulation for (23)

Example 4 (see [10]). *We employ numerical techniques to display chaotic attractors on the dynamics of a vertically driven damped planar pendulum:*

$$D^{\alpha}\left(D^{\beta}-\gamma\right)y(t)=(\chi-\psi\cos\tau)y(t)+0.001D^{\beta}y(t),\quad t\in[0,T],\quad 0<\alpha,\beta\leq 1. \tag{24}$$

The equation (24) *can be reduced to:*

$$\begin{aligned} D^{\beta}y(t)&=z(t)+\gamma y(t),\\ D^{\alpha}z(t)&=(\chi-\psi\cos\tau)y(t)+0.001D^{\beta}y(t). \end{aligned}$$

As initial conditions: $(0, 0.05)$, *and* $h = 0.05$, $\gamma = -0.001$, $\chi = -0.1$, $\psi = 0.545$.

Example 5 (see [24]). *We examine the Mixed Rayleigh Lienard Oscillator Driven by Parametric Periodic Pimping and External Excitation given by:*

$$\begin{aligned} D^{\alpha}\left(D^{\beta}-\left(\alpha_1+\eta\cos vt\right)\right)y(t)=&\,\omega_0^2\left(F_0+F_1\cos\omega t\right)-\beta_0(D^{\beta}y(t))^2\\ &-\beta_1(D^{\beta}y(t))^3+\omega_0^2y(t)-\gamma y(t)^3. \end{aligned} \tag{25}$$

The equation (25) *can be reduced to the following system:*

$$\begin{aligned} D^{\beta}y(t)&=z(t)+\left(\alpha_1+\eta\cos vt\right)y(t),\\ D^{\alpha}z(t)&=\omega_0^2\left(F_0+F_1\cos\omega t\right)-\beta_0(D^{\beta}y(t))^2-\beta_1(D^{\beta}y(t))^3+\omega_0^2y(t)-\gamma y(t)^3. \end{aligned}$$

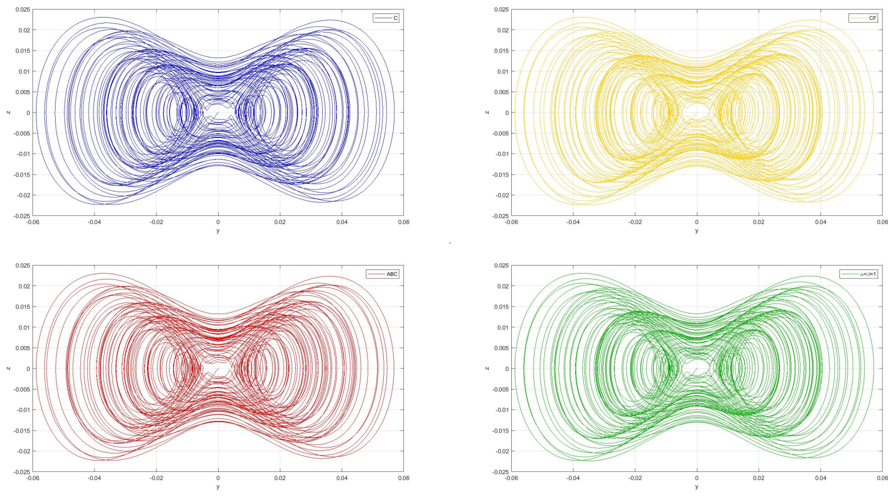

FIGURE 4. 2-D phase portraits for the numerical simulation for (24)

For initial conditions: $(0, -0.5)$, $\omega_0 = F_0 = 0.25$, $\alpha_0 = 0.015$, $\alpha_1 = 0.025$,$\gamma = 1$, $F_1 = 0.5$, $\beta_0 = 0.01$, $\beta_1 = 0.005$, *and* $\omega = v = 0.618$, $v = \frac{\sqrt{5}-1}{2}$, $\eta = 4$.

TABLE 1. Error summary table for each approach

Errors \ Examples	Example 1	Example 2	Example 3	Example 4	Example 5
$\|y_{AB3} - y_{ABc}\|_2$	1.29947854	0.00055533	0.82869035	0.05410987	0.4834849
$\|y_{AB3} - y_{ABcf}\|_2$	0.00062860	0.00000003	0.00009742	0.000023851	0.0011151
$\|y_{AB3} - y_{ABab}\|_2$	0.97326548	0.00047625	0.82859426	0.13071068	0.49796754

- The appearance of chaos under specific parameters demonstrates the convenience and pertinence of the proposed method.
- It is important to underline that some derivatives are more appropriate than others for particular cases but not for others.

7. CONCLUSION

In this study, we have examined the existence of solutions to the above fractional differential Langevin equation with Caputo-Fabrizio and Atangana-Baleanu derivatives. To achieve this, we have used a fixed point theorem based on the sum of two weakly sequentially continuous mappings.

Following that, we have proposed a novel three-step Adam Bashforth approach based on Caputo and Atangan Baleanu fractional derivatives. Numerous nonlinear

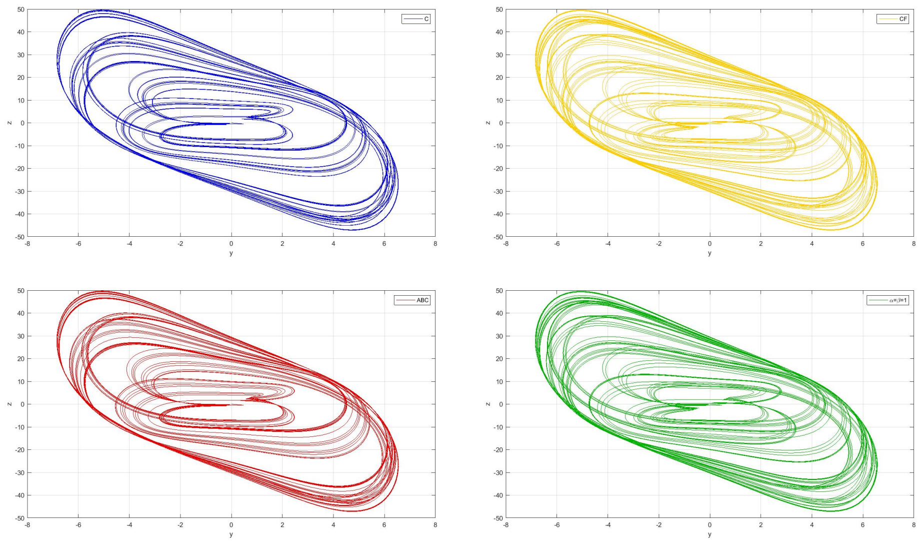

FIGURE 5. 2-D phase portraits for the numerical simulation for (25)

fractional differential equations have been exposed to a range of quantitative experiments. To assess the accuracy of the innovative numerical approach, the classical solution was compared towards the numerical solution for various values. Computational simulation results, for particular instances of α, β, are endowed with chaotic attractors.

Author Contribution Statements Z. DAHMANI proposed the problem and corrected the analytical study of Belhamiti. M.M. BELHAMITI studied the problem in its analytical and numerical studies. M.Z. SARIKAYA organized the paper and corrected some other analytical aspects.

Declaration of Competing Interests The authors declare that they have no competing interests.

Acknowledgements The authors would like to thank the editors and the anonymous reviewers for their helpful comments and suggestions.

REFERENCES

[1] Ahmad, B., Nieto, J.J., Alsaedi, A., El-Shahed, M., A study of nonlinear Langevin equation involving two fractional orders in different intervals, *Nonlinear Anal. Real World Appl.,* 13(2) (2012), 599-606. https://doi.org/10.1016/j.nonrwa.2011.07.052.

[2] Almeida, R., Bastos, R.O., Teresa, M., Monteiro, T., Modeling some real phenomena by fractional differential equations, *Mathematical Methods in the Applied Sciences,* 39(16) (2015). https://doi.org/10.1002/mma.3818.

[3] Atangana, A., Baleanu, D., Caputo - Fabrizio derivative applied to groundwater flow within a confined aquifer, *J. Eng. Mech.,* (2016). https://doi.org/10.1061/(ASCE)EM.1943-7889.0001091.

[4] Atangana, A., Baleanu, D., New fractional derivatives with nonlocal and non-singular kernel, *Thermal Science,* 20 (2016), 763-769. https://doi.org/10.2298/TSCI160111018A.

[5] Atangana, A., On the new fractional derivative and application to nonlinear Fisher's reaction-diffusion equation, *Appl. Math. Comput.,* 273 (2015), 948-56. https://doi.org/10.1016/j.amc.2015.10.021.

[6] Atangana, A., Alqahtani, R.T., Numerical approximation of the space-time Caputo-Fabrizio fractional derivative and application to groundwater pollution equation, *Adv. Diff. Equ.,* 2016(1) (2016), 1-13. https://doi.org/10.1186/s13662-016-0871-x.

[7] Atangana, A., Koca, B.I., Chaos in a simple nonlinear system with Atangana-Baleanu derivatives with fractional order, *Chaos, Solitons and Fractals,* 89 (2016), 447-454. https://doi.org/10.1016/j.chaos.2016.02.012

[8] Belhamiti, M.M., Dahmani, Z., Agarwal, P., Chaotic Jerk Circuit: existence and stability of solutions for a fractional model, *Progr. Fract. Differ. Appl.,* Accepted (2022).

[9] Ben Amar, A., O'Regan, D., Topological Fixed Point Theory for Singlevalued and Multivalued Mappings and Applications, Springer International Publishing Switzerland, 2016. https://doi.org/10.1007/978-3-319-31948-3.

[10] Bartuccelli, M.V., Gentile, G., Georgiou, K.V., On the dynamics of a vertically driven damped planar pendulum, *The Royal Society, Physical and Engineering Sciences,* 457 (2001), 3007-3022. https://doi.org/10.1098/rspa.2001.0841.

[11] Bezziou, M., Dahmani, Z., Jebril, I., Belhamiti, M.M., Solvability for a differential system of Duffing type via Caputo-Hadamard approach, *Appl. Math. Inf. Sci.,* 16(2) (2022), 341-352.

[12] Caputo, M., Fabrizio, M., Applications of new time and spatial fractional derivatives with exponential kernels, *Progress in Fractional Differentiation and Applications,* 2(1) (2016), 1-11. https://doi.org/10.18576/pfda/020101.

[13] Caputo, M., Fabrizio, M., A new definition of fractional derivative without singular kernel, *Progr. Fract. Differ. Appl.,* 1(2) (2015), 73-85.

[14] Cao, H., Seoane, J.M., Sanjuán, M.A.F., Symmetry-breaking analysis for the general Helmholtz Duffing oscillator, *Chaos, Solitons and Fractals,* 34 (2007), 197-212.

[15] Chen, A., Chen, Y., Existence of solutions to nonlinear Langevin equation involving two fractional orders with boundary value conditions, *Boundary Value Problems*, 3 (2011). https://doi.org/10.1155/2011/516481.

[16] Chen, X., Fu, X., Chaos control in a special pendulum system for ultra-subharmonic resonance, *American Institute of Mathematical Sciences, February*, 26(2) (2021), 847-860. https://doi.org/10.3934/dcdsb.2020144.

[17] Dahmani, Z., Belhamiti, M.M., Sarıkaya, M.Z., A three fractional order jerk equation with anti periodic conditions, Submitted paper, (2020).

[18] Gouari, Y., Dahmani, Z. , Belhamiti, M.M., Sarıkaya, M.Z., Uniqueness of solutions, stability and simulations for a differential problem involving convergent series and time variable singularities, *Rocky Mountain Journal of Mathematics,* (2021). https://doi.org/10.22541/au.163673427.78470853/v1.

[19] Hirsch, M.W., Smale, S., Devaney, R.L., Differential Equations, Dynamical Systems, and an Introduction to Chaos, Elsevier, USA, 2004.

[20] Jeribi, A., Krichen, B., Nonlinear Functional Analysis in Banach Spaces and Banach Algebras Fixed Point Theory under Weak Topology for Nonlinear Operators and Block Operator Matrices with Applications, Taylor & Francis Group, LLC., 2016.

[21] Jeribi, A., Hammami, M.A., Masmoudi, A., Applied mathematics in Tunisia, *International Conference on Advances in Applied Mathematics (ICAAM), Hammamet, Tunisia*, (2013).
[22] Kumar, S., Rashidi, M.M., New analytical method for gas dynamics equation arising in shock fronts, *Comput. Phys. Commun.,* 185(7) (2014), 1947-54. https://doi.org/10.1016/j.cpc.2014.03.025.
[23] Losada, J., Nieto, J.J., Properties of a new fractional derivative without singular kernel, *Progress in Fractional Differentiation and Applications*, 2 (2015), 87-92.
[24] Kpomahou, Y.J.F., Hinvi, L.A., Adéchinan, J.A., Miwadinou, C.H., The mixed Rayleigh Lienard oscillator driven by parametric periodic pamping and external excitation, *Hindawi Complexity*, (2021). https://doi.org/10.1155/2021/6631094.
[25] Owolabi, K.M., Analysis and Simulation of Herd Behaviour Dynamics Based on Derivative with Nonlocal and Nonsingular Kernel, Elsevier, 2021. https://doi.org/10.1016/j.rinp.2021.103941.
[26] Mainardi, F., Why the Mittag-Leffler function can be considered the queen function of the fractional calculus?, *Entropy,* 22(12) (2020), 1359. https://doi.org/10.3390/e22121359.
[27] Owolabi, K.M., Atangana, A., Analysis and application of new fractional Adams-Bashforth scheme with Caputo-Fabrizio derivative, *Chaos, Solitons and Fractals,* 105 (2017), 111–119.
[28] Owolabi, K.M., Atangana, A., On the formulation of fractional Adams-Bashforth method with Atangana-Baleanu-Caputo derivative to model chaotic problems, (2021). https://doi.org/10.1063/1.5085490.
[29] Peters, R.D., Chaotic pendulum based on torsion and gravity in opposition, *American Journal of Physics,* 63 (1995), 1128. https://doi.org/10.1119/1.18019.
[30] Rahayu, S.U., Tamba, T., Tarigan, K., Investigation of chaos behaviour on damped and driven nonlinear simple pendulum motion simulated by mathematica, *Journal of Physics Conference Series,* 1811(1) 012014 (2021). https://doi.org/10.1088/1742-6596/1811/1/012014.
[31] Salema, A., Alzahrania, F., Almaghamsia, L., Langevin equation involving one fractional order with three point boundary conditions, *Nonlinear Sci. Appl.,* 12 (2019), 791-798. https://doi.org/10.22436/jnsa.012.12.02.
[32] Singh, H., Kumar, D., Baleanu, D., Methods of Mathematical Modelling, Mathematics and Its Applications: Modelling, Engineering, and Social Sciences, Taylor & Francis Group, 2019. https://doi.org/10.1201/9780429274114.
[33] Atanacković , M.T., Pilipović , S., Stanković , B., Zorica, D., Fractional Calculus with Applications in Mechanics, John Wiley & Sons, 2014. https://doi.org/10.1002/9781118577530.
[34] Tablennehas, K., Dahmani, Z., Belhamiti, M.M., Abdelnebi, A., Sarıkaya, M.Z., On a fractional problem of Lane-Emden type: Ulam type stabilities and numerical behaviors, *Advances in Difference Equations,* (2021).
[35] Tarasov, V., No nonlocality no fractional derivative, *Communications in Nonlinear Science and Numerical Simulation,* 62 (2018). https://doi.org/10.1016/j.cnsns.2018.02.019.
[36] Zaslavsky, G.M., Hamiltonian Chaos and Fractional Dynamics, Oxford University Press, 2005.

http://communications.science.ankara.edu.tr

Commun.Fac.Sci.Univ.Ank.Ser. A1 Math. Stat.
Volume 72, Number 3, Pages 686–700 (2023)
DOI:10.31801/cfsuasmas.1175872
ISSN 1303-5991 E-ISSN 2618-6470

COMMUNICATIONS SERIES A1

Research Article; Received: September 15, 2022; Accepted: March 20, 2023

COMPARISON OF THE SEVERAL TWO-PARAMETER EXPONENTIAL DISTRIBUTED GROUP MEANS IN THE PRESENCE OF OUTLIERS

Mustafa CAVUS[1] and Berna YAZICI[2]

[1,2]Eskisehir Technical University, Department of Statistics, Eskisehir, TÜRKİYE

Abstract. The two-parameter exponential distribution is often used to model the lifetime of a product. The comparison of the mean lifetimes of several products is a main concern in reliability applications. In this study, the performance of the methods to compare the mean lifetimes of several products based on generalized p-value, parametric bootstrap, and fiducial approach are compared in the presence of outliers. The results of Monte-Carlo simulations clearly indicate that there is no uniformly powerful test. The parametric bootstrap test is superior to the others except in the case of the lower number of groups and the presence of outliers. An illustrative example of testing the equality lifetimes of a component is given to perform the proposed tests. The considered tests are implemented in an R package `doex`.

1. Introduction

Testing equality of means of several normal populations under unequal variances is a very common Behrens-Fisher-type problem in social sciences, agriculture, biology, etc. The generalized p-value method is used to solve this problem [1]. The generalized F-test is proposed using the generalized p-value method, and its modifications for non-normality caused by outliers are improved by Cavus et al. [2], caused by skewness by Cavus et al. [3], and performed in a real data application by Cavus et al. [4]. Moreover, there are few parametric methods for testing the equality of means of skewed populations. Tian and Wu [5] proposed a generalized p-value approach for log-normal populations, Tian [6], Ma and Tian [7] improved procedures for inverse Gaussian and Niu et al. [8] proposed a generalized p-value procedure for Birbaum-Saunders distributions.

2020 *Mathematics Subject Classification.* 62J10, 62K99, 62F03.
Keywords. ANOVA, parametric bootstrap penalized power, exponential distribution, lifetime data.
[1] mustafacavus@eskisehir.edu.tr-Corresponding author; 0000-0002-6172-5449
[2] bbabloglu@eskisehir.edu.tr; 0000-0001-9843-7355.

The two-parameter exponential distribution is used in many real-life problems such as modeling extreme rainfalls, the lifetime of a component, the service time of an agent, and so on. Ghosh and Razmpour [9] indicated that two-parameter exponential distribution is used to model the guaranteed time with unknown and possibly unequal failure rates in reliability and life testing. There are some procedures improved for the two-parameter exponential distribution. Chen [10] proposed a range statistic for comparing location parameters of two-parameter exponential distributions. Singh [11] derived a likelihood ratio test for testing the equality of location parameters of two-parameter exponential distributions based on Type II censored samples under unknown scales. Kambo and Awad [12] proposed a test statistic based on doubly censored samples to test the equality of location parameters of k exponential distributions when the scale parameter is unknown. Hsieh [13] proposed an exact test for comparing location parameters simultaneously of several two-parameter exponential distributions under unequal scale parameters with unknown scale parameters. Vaughan and Tiku [14] extended the test developed by Tiku and Vaughan [15] for $k > 2$ populations for testing equality of location parameters of two-parameter exponential populations from censored samples. Ananda and Weerahandi [16] proposed a testing procedure based on generalized p-values for testing the difference between two exponential means. Wu [17] proposed a one-stage multiple comparison procedure for comparing $k - 1$ treatment exponential mean lifetimes with the control based on doubly censored samples under unequal scales. Malekzadeh and Jafari [18] proposed some procedures based on generalized p-values, parametric bootstrap, and fiducial approaches by using Cochran type test statistics for testing the means of several two-parameter exponential distributions under progressively Type II censoring. The two-parameter exponential distribution has scale and location parameters. In the testing equality of means of two-parameter exponential distributions, the scale parameter is a nuisance parameter when it is unknown or unequal. Therefore, the considered problem turns into a Behrens-Fisher-type problem. There is no study on the testing equality of two-parameter exponentially distributed population means for complete data in the presence of outliers.

The article discusses the testing equality means of k two-parameter exponentially distributed populations for complete data in the presence of outliers. In the next section, the procedures proposed by Malekzadeh and Jafari [18] are introduced. A Monte-Carlo simulation study is conducted for comparing the performances of these tests for complete data in the presence of outliers in Sec 3. To show the efficiency of the tests, illustrative examples are given in Sec 4. The results are discussed in the last section.

2. Methodology

In this section, methods proposed by Malekzadeh and Jafari [18] are introduced. The probability density function of the two-parameter exponential distribution is given in (1).

$$f(x;a,b)=\frac{1}{a}\exp\Big\{-\frac{x-b}{a}\Big\}, x>b, a>0 \tag{1}$$

where a is the scale and b is the location parameter. We are interested in the problem of testing the equality of means of k exponentially distributed populations for complete data in (2).

$$\begin{aligned} &H_0 : \mu_1 = \mu_2 = ... = \mu_k \\ &H_A : \mu_i \neq \mu_j \text{ for some } i \text{ and } j \text{ where } i \neq j \end{aligned} \tag{2}$$

Rahman and Pearson [19] revisited the parameter estimations of two-parameter exponential distribution and conducted a simulation study to compare the performance of maximum likelihood, product spacing, and quantile estimation methods. The uniformly minimum variance unbiased estimators of the two-parameter exponential distribution parameters (Malekzadeh and Jafari, [18]):

$$\hat{a}=S/(n-1) \tag{3}$$

$$\hat{b}=X_{(1)} \tag{4}$$

where $X_{(1)}=min(X_1,X_2,...,X_n)$ and $S=\sum_{j=1}^{n}[X_j-X_{(1)}]$. Viveros and Balakrishnan [20] gave the distributions of the following random variables.

$$W=\frac{2(n-1)S}{a}\sim\chi^2_{(2n-2)} \text{ and } Y=\frac{2n(X_{(1)}-b)}{a}\sim\chi^2_{(2)} \tag{5}$$

where W_i and Y_i are independent random variables. Cochran [21] type test statistics are used for Behrens-Fisher problems. Here, it is modified for testing the equality of two-parameter exponential distributed means under unequal scale parameters.

$$T_t=\sum_{i=1}^{k}\frac{n_i\hat{\mu}_i^2}{S_i^2}-\frac{\left(\sum_{i=1}^{k}\frac{n_i\hat{\mu}_i^2}{S_i^2}\right)^2}{\sum_{i=1}^{k}\frac{n_i}{S_i^2}} \tag{6}$$

where $\hat{\mu}$ is the mean estimate and S is the scale estimate of the i^{th} population. The uniformly minimum variance unbiased estimator of $\mu=a+b$ and it can be shown as in (7).

$$\hat{\mu}_i = X_{i(1)} + \frac{n_i - 1}{n_i} S_i = \frac{a_i}{2n_i}(W_i + Y_i) + b_i \sim N(\mu_i, a_i^2/n_i) \tag{7}$$

T_t is used for the rejection rule as a critical value of the Generalized p-value, Parametric Bootstrap, and Fiducial Approach test in the following subsections.

2.1. **Generalized p-value (GP) Based Test.** The generalized p-value method is used to derive the test statistics in the presence of nuisance parameters. Weerahandi [22] proposed the Generalized F-test for testing the equality of several populations' means under unequal variances instead of the Classical F-test. Also, many researchers used this method to derive test statistics for several distributions. In this method, firstly sufficient statistics of parameters of the related distribution are obtained. Using the sufficient statistics of the two-parameter exponential distribution, (i) R_i can be obtained independently from the nuisance parameter, and, (ii) since the observed λ_i values are independent of the nuisance parameter θ_i, generalized pivot value can be estimated.

$$R_i = X_{i(1)} + (n_i - 1)S_i(2n_i - Y_i/n_i W_i) \tag{8}$$

Expected values of $(X_{i(1)}, S_i)$ vector for R_i generalized pivot value and the variance can be obtained as follows:

$$\mu_{Ri} = X_{i(1)} + \frac{(n_i - 1)^2 S_i}{n_i^2 - 2n_i} \tag{9}$$

$$\sigma_{Ri}^2 = \frac{(n_i - 1)^4 S_i^2}{n_i^2 (n_i - 2)^2} \left(\frac{1}{n_i - 3}\right) \tag{10}$$

Cochran test statistic can be obtained as in (11) using expected value of R_i generalized pivot and the variance of it.

$$T_{GP} = \sum_{i=1}^{k} \frac{(R_i - \mu_{Ri})^2}{\sigma_{Ri}^2} - \frac{\left(\sum_{i=1}^{k} \frac{R_i - \mu_{Ri}}{\sigma_{Ri}^2}\right)}{\sum_{i=1}^{k} \frac{1}{\sigma_{Ri}^2}} \tag{11}$$

The rejection rule is H_0 is in (2) rejected when $T_{GP} > T_t$. The p-value of the GP test is computed at least 10.000 Monte-Carlo runs as $p_{GP} = P(T_{GP} \geq T_t)$.

2.2. **Parametric Bootstrap (PB) Based Test.** Krishnamoorthy et al. [23] propose the parametric bootstrap method for testing the equality of normal population means under heteroscedasticity. Let $Y_i \sim \chi^2_{(2)}$ and $W_i \sim \chi^2_{(2n_i-2)}$. The PB test statistic is in (12) obtained for complete data from Malekzadeh and Jafari [18] using the Cochran statistic.

$$T_{PB} = \sum_{i=1}^{k} \frac{n_i \mu_{Bi}^2}{S_{Bi}^2} - \frac{\left(\sum_{i=1}^{k} \frac{n_i \mu_{Bi}^2}{S_{Bi}^2}\right)^2}{\sum_{i=1}^{k} \frac{n_i}{S_{Bi}^2}} \tag{12}$$

where $\mu_{Bi} = (S_i/2n_i)(W_i + Y_i)$ and $S_{Bi} = S_i W_i/(2n_i - 2)$. The rejection rule is H_0 is in (2) rejected when $T_{PB} > T_t$. The p-value of the PB test is computed at least 10.000 Monte-Carlo runs as $p_{PB} = P(T_{PB} \geq T_t)$.

2.3. **Fiducial Approach (FA) Based Test.** Li et al. [24] used the fiducial approach for testing the equality of several populations' means under unequal variances. Let $Y_i \sim \chi^2_{(2)}$ and $W_i \sim \chi^2_{(2n_i-2)}$, and S_i functions can be rewritten as random samples:

$$S_i = \frac{a_i W_i}{2(n_i - 1)}, \quad X_{i(1)} = \frac{a_i Y_i}{2n_i} + b_i \tag{13}$$

Parameter estimations are obtained as follows by using the observed values of $(X_{i(1)}, S_i)$

$$b_i = X_{i(1)} - \frac{(n_i - 1) S_i Y_i}{n_i W_i}, \quad a_i = \frac{2(n_i - 1) S_i}{W_i} \tag{14}$$

Using Cochran test statistic, T_{FA} can be written as in (15).

$$T_{FA} = \sum_{i=1}^{k} \frac{f_i n_i}{S_i n_i^2 W_i^2} - \frac{\left(\sum_{i=1}^{k} \frac{f_i}{S_i^2 n_i W_i}\right)^2}{\sum_{i=1}^{k} \frac{n_i}{S_i^2}} \tag{15}$$

where $f_i = (n_i - 1)(W_i Y_i - 2n_i W_i)$. The rejection rule is H_0 is in (2) rejected when $T_{PB} > T_t$. The p-value of the FA test is computed at least 10.000 Monte-Carlo runs as $p_{FA} = P(T_{FA} \geq T_t)$.

3. Monte-Carlo Simulation Study

In this section, we provide some of our comprehensive simulation study results. The GP, PB, and FA tests, as introduced in the previous subsections, are compared in terms of penalized power and Type I error probability when the nominal level of the test is taken as $\alpha_0 = 0.05$ under different sample sizes and scale parameters. The configuration of the outliers is determined similarly to the illustrative examples in the next section. The first and third groups consist of outlier one each which is five and three times higher than the group median, respectively in $k = 3$ groups design while the second, third, and fourth groups consist of an outlier one each which is one and a half times higher than the group median, respectively in $k = 4$ groups design.

It is known that Monte-Carlo simulation studies are used to compare the performance of the tests in terms of power and Type I error probability. However, any comparison of the powers is invalid when Type I error probabilities are different. Cavus et al. [25] proposed the penalized power approach in (16) to compare the power of the tests when Type I error probabilities are different.

$$\gamma_i = \frac{1-\beta_i}{\sqrt{1+|1-\frac{\alpha_i}{\alpha_0}|}} \tag{16}$$

where β_i is Type II error rate, α_i is Type I error of the test and α_0 is the nominal level. Penalized power adjusts the power function with the square root of the percentile deviation between Type I error probability and the nominal level. Thus, penalized power is used to compare the power of the tests in the simulation studies. The simulations are performed for balanced and unbalanced designs with `doex` package implemented by Cavus and Yazici [26] and Cavus and Yazici [27] in `R`, and the results are based on 10.000 Monte-Carlo runs. The results of the simulations are given in the following subsections.

3.1. **Type I Error Probability Results.** Table 1 shows the Type I error probabilities of the tests under scale parameters 2 and 5 for small, moderate, and large samples with and without outliers. The GP and FA test can not control Type I error probability in small samples for $\alpha_0 = 0.05$ while the PB test controls Type I error probability under unbalanced design $n_i = (5, 10, 15)$. The performance of the PB test to control the Type I error probability is not similar in the presence of outliers. It does not control the Type I error probability and shows a more conservative performance than the design without outliers. The FA and GP test generally has Type I errors close to each other and are more conservative than the PB test. In the presence of outliers, the performance of the GP and FA tests are affected negatively also and show more conservative performance. The PB test performs better than the others in moderate and large samples and controls the error. The performance of the GP and FA test is getting better in large and moderate samples. The performance of the test on controlling the Type I error probability is getting better when the number of groups (k) is increased. Even if the presence of outliers negatively affects the performance of all tests to control the Type I error probability, the increase in sample size eliminates this negative effect for GP and PB tests.

Table 1. Type I error probabilities for $\alpha_0 = 0.05$

				without outliers			with outliers		
k	n_i	a_i	b_i	GP	PB	FA	GP	PB	FA
3	10, 10, 10	2, 2, 2	1, 1, 1	0.0061	0.0087	0.0010	0.0130	0.0100	0.0005
		5, 5, 5		0.0065	0.0101	0.0014	0.0090	0.0095	0.0001
	8, 10, 12	2, 2, 2		0.0068	0.0128	0.0021	0.0140	0.0030	0.0008
		5, 5, 5		0.0083	0.0139	0.0025	0.0130	0.0030	0.0002
	5, 10, 15	2, 2, 2		0.0144	0.0436	0.0072	0.0120	0.0003	0.0009
		5, 5, 5		0.0129	0.0439	0.0079	0.0070	0.0003	0.0008
	30, 30, 30	2, 2, 2		0.0269	0.0407	0.0201	0.0410	0.0580	0.0310
		5, 5, 5		0.0298	0.0462	0.0223	0.0330	0.0540	0.0280
	24, 30, 36	2, 2, 2		0.0309	0.0453	0.0236	0.0440	0.0530	0.0260
		5, 5, 5		0.0298	0.0450	0.0229	0.0350	0.0500	0.0210
	15, 30, 45	2, 2, 2		0.0332	0.0487	0.0242	0.0380	0.0390	0.0220
		5, 5, 5		0.0325	0.0528	0.0248	0.0350	0.0320	0.0150
	50, 50, 50	2, 2, 2		0.0365	0.0473	0.0310	0.0480	0.0650	0.0440
		5, 5, 5		0.0348	0.0455	0.0302	0.0432	0.0604	0.0360
	40, 50, 60	2, 2, 2		0.0359	0.0493	0.0319	0.0490	0.0570	0.0360
		5, 5, 5		0.0368	0.0498	0.0309	0.0470	0.0540	0.0320
	25, 50, 75	2, 2, 2		0.0392	0.0494	0.0308	0.0460	0.0465	0.0320
		5, 5, 5		0.0407	0.0512	0.0339	0.0430	0.0410	0.0283
4	10, 10, 10, 10	2, 2, 2, 2	1, 1, 1, 1	0.0054	0.0094	0.0007	0.0070	0.0100	0.0010
		5, 5, 5, 5		0.0052	0.0090	0.0006	0.0060	0.0100	0.0010
	7, 9, 11, 13	2, 2, 2, 2		0.0086	0.0165	0.0029	0.0070	0.0170	0.0030
		5, 5, 5, 5		0.0083	0.0162	0.0027	0.0070	0.0170	0.0030
	5, 8, 12, 15	2, 2, 2, 2		0.0120	0.0337	0.0059	0.0050	0.0360	0.0080
		5, 5, 5, 5		0.0121	0.0332	0.0056	0.0050	0.0360	0.0080
	30, 30, 30, 30	2, 2, 2, 2		0.0256	0.0404	0.0183	0.0270	0.0450	0.0220
		5, 5, 5, 5		0.0252	0.0399	0.0180	0.0280	0.0460	0.0210
	21, 27, 33, 39	2, 2, 2, 2		0.0320	0.0486	0.0218	0.0250	0.0430	0.0220
		5, 5, 5, 5		0.0310	0.0481	0.0213	0.0280	0.0440	0.0220
	15, 24, 36, 45	2, 2, 2, 2		0.0319	0.0489	0.0245	0.0260	0.0510	0.0300
		5, 5, 5, 5		0.0314	0.0482	0.0241	0.0260	0.0520	0.0300
	50, 50, 50, 50	2, 2, 2, 2		0.0317	0.0444	0.0273	0.0360	0.0490	0.0300
		5, 5, 5, 5		0.0314	0.0442	0.0271	0.0360	0.0500	0.0320
	35, 45, 55, 65	2, 2, 2, 2		0.0312	0.0443	0.0264	0.0330	0.0500	0.0320
		5, 5, 5, 5		0.0310	0.0442	0.0261	0.0340	0.0520	0.0310
	25, 40, 60 ,75	2, 2, 2, 2		0.0360	0.0492	0.0299	0.0290	0.0460	0.0320
		5, 5, 5, 5		0.0350	0.0488	0.0295	0.0290	0.0450	0.0320

3.2. **Penalized Power Results.** Table 2 shows the results of penalized powers of the tests in the case of $k = 3$ for several effect sizes and sample sizes. Recall from Table 1 that the GP and FA tests are very conservative in terms of Type I error probability, while the PB test successfully controls the Type I error probability.

The penalized power results show that the PB test is more powerful than the GP and FA test in most of the scenarios except the case of unbalanced small sample size designs. In higher effect sizes for large samples, penalized power of the tests are higher than 0.85. Also, their performances are better in unbalanced designs than in balanced designs. The performance of the GP and PB tests is affected negatively when the scale parameter is increased while the performance of the FA test is positively affected without outliers. It is seen that the power of the tests decreases in the case of $\theta_i = 5$. For example, the power of the PB test is 0.99 in the case of $\theta_i = 3$ and 0.96 in $\theta_i = 5$, it is the biggest difference between the tests. It is concluded that the effect of the higher scale parameter on the PB test is higher than the others. However, the penalized power of the PB test is the highest in most of the scenarios followed by the GP test and the FA test. When the power of the tests is evaluated according to whether there is an outlier or not, it is seen that the GP and FA tests are higher in the case of outliers than in the case of no outliers, and the contrary, the power of the PB test is lower. The result is that PB is the uniformly most powerful test in the non-presence of an outlier, and GP is the uniformly most powerful test in the case of an outlier.

Table 3 shows the results of penalized powers for $k = 4$. Unlike the results in Table 2, the most powerful test is the PB, the second is GP and the last one is the FA test in the presence and non-presence of outliers. The increase in the number of groups affects the penalized power of the tests negatively in small samples in most of the scenarios. Only the performance of the PB test is better than the case of $k = 3$ in large samples and it is obtained that the least affected test is the PB test.

When the results given in Tables 2 and 3 are examined, the effect of the design configurations such as the presence of outliers and the number of groups on the performance of the tests differs. Therefore, when using tests, the reliability of their results should be carefully examined.

4. Illustrative Examples

In this section, the GP, PB, and FA tests are applied to two real data examples to compare their results in hypothesis testing.

Example 1. Data consists of the lifetimes of a component are different brands in a refrigerator which is collected from a local factory in Turkey and it is available in `doex` package in `R` as component data. It is known that the lifetime data generally follows the exponential distribution. However, to make sure of this, the Cramer-von Mises (CvM) goodness-of-fit test is used to test whether the data follows the two-parameter exponential distribution. As a result of the CvM test, the p-value 0.6786 shows there is not enough evidence to reject the null hypothesis indicating that the data follows a two-parameter exponential distribution at the 0.05 significance level. The sample size of the data is $n_1 = 15, n_2 = 49, n_3 = 54, n_4 = 12$. The estimates of the location parameters are $\hat{b}_1 = 8.38, \hat{b}_2 = 8.40, \hat{b}_3 = 8.41, \hat{b}_4 = 8.62$ and the

Table 2. Penalized power results for $k = 3$

			without outliers			with outliers		
n_i	a_i	b_i	GP	PB	FA	GP	PB	FA
10, 10, 10	2, 2, 3	1, 1, 1	0.0101	0.0143	0.0021	0.0280	0.0193	0.0028
	2, 2, 4		0.0254	0.0334	0.0055	0.0515	0.0432	0.0070
	2, 2, 5		0.0429	0.0581	0.0097	0.0864	0.0648	0.0155
8, 10, 12	2, 2, 3		0.0245	0.0342	0.0039	0.0434	0.0150	0.0281
	2, 2, 4		0.0622	0.0779	0.0096	0.1006	0.0358	0.0091
	2, 2, 5		0.1181	0.1386	0.0177	0.1890	0.0746	0.0141
5, 10, 15	2, 2, 3		0.0559	0.1119	0.0147	0.0889	0.0028	0.0001
	2, 2, 4		0.1590	0.2180	0.0265	0.2231	0.0042	0.0002
	2, 2, 5		0.3010	0.3475	0.0413	0.3572	0.0106	0.0004
30, 30, 30	2, 2, 3		0.1610	0.2420	0.1253	0.2062	0.2748	0.1489
	2, 2, 4		0.4997	0.6363	0.4303	0.5790	0.6685	0.4860
	2, 2, 5		0.7297	0.8488	0.6697	0.8220	0.8718	0.7320
24, 30, 36	2, 2, 3		0.2444	0.3225	0.1755	0.3061	0.3418	0.1824
	2, 2, 4		0.6301	0.7455	0.5232	0.7238	0.7653	0.5392
	2, 2, 5		0.8083	0.9180	0.7411	0.8976	0.9285	0.7587
15, 30, 45	2, 2, 3		0.3307	0.4043	0.2160	0.3681	0.3023	0.1905
	2, 2, 4		0.7178	0.8277	0.5868	0.7696	0.7360	0.5572
	2, 2, 5		0.8447	0.9643	0.7630	0.8791	0.8800	0.7429
50, 50, 50	2, 2, 3		0.3808	0.4686	0.3422	0.4324	0.4323	0.3968
	2, 2, 4		0.8119	0.9107	0.7675	0.8835	0.8068	0.8400
	2, 2, 5		0.8812	0.9700	0.8447	0.9776	0.8761	0.9420
40, 50, 60	2, 2, 3		0.4722	0.5521	0.4015	0.5069	0.4842	0.3836
	2, 2, 4		0.8448	0.9522	0.8029	0.9356	0.8860	0.8158
	2, 2, 5		0.8821	0.9921	0.8549	0.9881	0.9347	0.8812
25, 50, 75	2, 2, 3		0.5582	0.6071	0.4440	0.5831	0.5263	0.3910
	2, 2, 4		0.8840	0.9662	0.8103	0.9343	0.9276	0.8077
	2, 2, 5		0.9063	0.9937	0.8489	0.9593	0.9593	0.8532
10, 10, 10	5, 5, 6	1, 1, 1	0.0215	0.0234	0.0164	0.0133	0.0111	0.0007
	5, 5, 8		0.0298	0.0321	0.0266	0.0266	0.0200	0.0042
	5, 5, 10		0.0419	0.0436	0.0369	0.0385	0.0422	0.0070
8, 10, 12	5, 5, 6		0.0356	0.0367	0.0349	0.0121	0.0071	0.0003
	5, 5, 8		0.0651	0.0642	0.0622	0.0447	0.0172	0.0028
	5, 5, 10		0.1046	0.1051	0.1023	0.0932	0.0394	0.0084
5, 10, 15	5, 5, 6		0.0221	0.0631	0.0094	0.0256	0.0002	0.0001
	5, 5, 8		0.0726	0.1325	0.0171	0.0997	0.0007	0.0003
	5, 5, 10		0.1577	0.2186	0.0266	0.1994	0.0063	0.0005
30, 30, 30	5, 5, 6		0.1509	0.1628	0.1329	0.0587	0.0991	0.0458
	5, 5, 8		0.4060	0.4592	0.3732	0.2531	0.3791	0.1975
	5, 5, 10		0.5755	0.6553	0.5404	0.5425	0.6908	0.4783
24, 30, 36	5, 5, 6		0.0758	0.0868	0.0742	0.0789	0.1090	0.0477
	5, 5, 8		0.2967	0.3371	0.2831	0.3552	0.4340	0.2426
	5, 5, 10		0.5172	0.5825	0.4921	0.6718	0.7910	0.5234
15, 30, 45	5, 5, 6		0.0886	0.1306	0.0588	0.1157	0.0866	0.0467
	5, 5, 8		0.4225	0.4979	0.2934	0.4481	0.3798	0.2316
	5, 5, 10		0.7141	0.8159	0.5891	0.7481	0.7022	0.5307
50, 50, 50	5, 5, 6		0.2984	0.3276	0.2862	0.1058	0.1314	0.0848
	5, 5, 8		0.6130	0.6734	0.5938	0.5366	0.5741	0.4347
	5, 5, 10		0.6634	0.7277	0.6399	0.8419	0.8389	0.7866
40, 50, 60	5, 5, 6		0.1163	0.1323	0.1123	0.1233	0.1299	0.0771
	5, 5, 8		0.4950	0.5549	0.4724	0.6313	0.6350	0.4956
	5, 5, 10		0.6630	0.7370	0.6277	0.9188	0.9160	0.7914
25, 50, 75	5, 5, 6		0.1498	0.1752	0.1097	0.1760	0.1445	0.0958
	5, 5, 8		0.6815	0.7300	0.5755	0.7024	0.6379	0.5091
	5, 5, 10		0.8951	0.9605	0.8291	0.9122	0.8920	0.7883

Table 3. Penalized power results for $k = 4$

			without outliers			with outliers		
n_i	a_i	b_i	GP	PB	FA	GP	PB	FA
10, 10, 10, 10	2, 2, 2, 3	1, 1, 1, 1	0.0086	0.0130	0.0016	0.0102	0.0134	0.0021
	2, 2, 2, 4		0.0149	0.0262	0.0028	0.0146	0.0283	0.0049
	2, 2, 2, 5		0.0227	0.0406	0.0050	0.0175	0.0402	0.0063
7, 9, 11, 13	2, 2, 2, 3		0.0196	0.0319	0.0037	0.0117	0.3182	0.0050
	2, 2, 2, 4		0.0554	0.0687	0.0075	0.0263	0.0651	0.0100
	2, 2, 2, 5		0.1074	0.1142	0.0112	0.0703	0.1086	0.0122
5, 8, 12, 15	2, 2, 2, 3		0.0417	0.0651	0.0090	0.0224	0.0707	0.0103
	2, 2, 2, 4		0.1214	0.1242	0.0133	0.0783	0.1149	0.0154
	2, 2, 2, 5		0.2425	0.1924	0.0177	0.1784	0.1829	0.0243
30, 30, 30, 30	2, 2, 2, 3		0.1254	0.2023	0.0893	0.1191	0.2011	0.0880
	2, 2, 2, 4		0.4084	0.5593	0.3302	0.4063	0.5987	0.3226
	2, 2, 2, 5		0.6623	0.8024	0.5852	0.6728	0.8552	0.6108
21, 27, 33, 39	2, 2, 2, 3		0.2598	0.3147	0.1527	0.2490	0.3175	0.1457
	2, 2, 2, 4		0.6636	0.7661	0.4834	0.6385	0.7258	0.4931
	2, 2, 2, 5		0.8200	0.9441	0.7182	0.7928	0.9075	0.7229
15, 24, 36, 45	2, 2, 2, 3		0.3263	0.3573	0.1700	0.3041	0.3584	0.1656
	2, 2, 2, 4		0.7321	0.8051	0.5376	0.7052	0.8178	0.5628
	2, 2, 2, 5		0.8416	0.9591	0.7532	0.8104	0.9693	0.7885
50, 50, 50, 50	2, 2, 2, 3		0.3099	0.4026	0.2720	0.3394	0.4455	0.2974
	2, 2, 2, 4		0.7457	0.8605	0.7083	0.7919	0.9158	0.7428
	2, 2, 2, 5		0.8467	0.9413	0.8191	0.8785	0.9861	0.8383
35, 45, 55, 65	2, 2, 2, 3		0.4899	0.5281	0.3750	0.4941	0.5520	0.3918
	2, 2, 2, 4		0.8284	0.9155	0.7753	0.8396	0.9650	0.8094
	2, 2, 2, 5		0.8508	0.9459	0.8213	0.8630	0.9990	0.8566
25, 40, 60 75	2, 2, 2, 3		0.5669	0.5865	0.4151	0.5412	0.5725	0.4347
	2, 2, 2, 4		0.8643	0.9664	0.8084	0.8299	0.9439	0.8309
	2, 2, 2, 5		0.8770	0.9878	0.8415	0.8391	0.9622	0.8574
10, 10, 10, 10	5, 5, 5, 6	1, 1, 1, 1	0.0058	0.0077	0.0008	0.0051	0.0111	0.0007
	5, 5, 5, 8		0.0102	0.0154	0.0017	0.0123	0.0149	0.0028
	5, 5, 5, 10		0.0149	0.0262	0.0028	0.0145	0.0290	0.0049
7, 9, 11, 13	5, 5, 5, 6		0.0099	0.0196	0.0026	0.0080	0.0209	0.0028
	5, 5, 5, 8		0.0254	0.0381	0.0045	0.0139	0.0388	0.0057
	5, 5, 5, 10		0.0554	0.0686	0.0075	0.0293	0.0667	0.0100
5, 8, 12, 15	5, 5, 5, 6		0.0160	0.0406	0.0060	0.0094	0.0477	0.0081
	5, 5, 5, 8		0.0539	0.0758	0.0098	0.0340	0.0786	0.0117
	5, 5, 5, 10		0.1207	0.1244	0.0133	0.0834	0.1131	0.0154
30, 30, 30, 30	5, 5, 5, 6		0.0356	0.0649	0.0255	0.0408	0.0692	0.0326
	5, 5, 5, 8		0.1697	0.2679	0.1265	0.1608	0.2780	0.1209
	5, 5, 5, 10		0.4089	0.5607	0.3302	0.4100	0.6100	0.3222
21, 27, 33, 39	5, 5, 5, 6		0.0703	0.1044	0.0413	0.0691	0.0992	0.0440
	5, 5, 5, 8		0.3486	0.4173	0.2074	0.3508	0.4204	0.2113
	5, 5, 5, 10		0.6680	0.7676	0.4840	0.6558	0.7370	0.4963
15, 24, 36, 45	5, 5, 5, 6		0.0828	0.1161	0.0473	0.0723	0.1108	0.0532
	5, 5, 5, 8		0.4269	0.4626	0.2380	0.4035	0.4696	0.2484
	5, 5, 5, 10		0.7331	0.8067	0.5380	0.7069	0.8109	0.5654
50, 50, 50, 50	5, 5, 5, 6		0.0707	0.1042	0.0590	0.0830	0.1240	0.0728
	5, 5, 5, 8		0.4171	0.5298	0.3764	0.4498	0.5810	0.3999
	5, 5, 5, 10		0.7452	0.8605	0.7103	0.7910	0.9260	0.7554

estimates of the scale parameters are $\hat{a}_1 = 1.47, \hat{a}_2 = 1.60, \hat{a}_3 = 1.82, \hat{a}_4 = 1.80$, respectively. It is clearly seen that the scale parameters are different. The lifetimes of the brands are given in Figure 1. The boxplots show that the groups referenced as Brands 2-4 consist of outliers. These outliers are higher than one and a half times higher than the medians. Testing the mean lifetimes of the components under scale parameters, GP, PB, and FA tests are performed by using the `doex`.
The p-value of the GP, PB, and FA tests are $0.6807, 0.7471$, and 0.7545, respectively. Thus, there is no evidence to reject the null hypothesis at $\alpha_0 = 0.05$ and concluded that the mean lifetimes of the components produced by different brands are not different. It is seen that the PB test can control the Type I error probability very close to the nominal level, in the unbalanced moderate, low-scale parameter and outlier design in Table 1. Therefore, it can be said that the results obtained in this example are reliable.

Example 2. In this example, the equality of mean agricultural income of the geographical regions in Turkey is considered. Agricultural incomes of the Central Anatolia (CA), Eastern Anatolia (EA), and Southeastern Anatolia (SA) regions in 2017 are considered and the data is obtained from the Turkish Statistical Institute Database. The Cramer-von Mises (CvM) goodness-of-fit test is used to test whether the data follows the two-parameter exponential distribution. As a result of the CvM test, the p-value 0.4005 shows there is not enough evidence to reject the null hypothesis indicating that the data follows a two-parameter exponential distribution at the 0.05 significance level. The number of city in the geographical regions are $n_{CA} = 13, n_{EA} = 14$, and $n_{SA} = 9$. The estimates of the location parameters are $\hat{b}_{CA} = 0.7503, \hat{b}_{EA} = 0.3649, \hat{b}_{SA} = 0.5811$, and the estimates of the scale parameters are $\hat{a}_{CA} = 2.2122, \hat{a}_{EA} = 1.0558, \hat{a}_{SA} = 1.7988$, respectively. The agricultural income of the geographical regions in Turkey is given in Figure 2. The boxplots show that the groups referenced as CA and SA consist of outliers. The outlier in the geographical region of CA is five times higher than the median while the outlier in the geographical region of SA is three times higher than its median. Testing the mean income of the geographical regions under unequal scale parameters, GP, PB, and FA tests are performed.
The p-value of the GP, PB, and FA tests are $0.0816, 0.0881$, and 0.1489, respectively. Thus, there is enough evidence to reject the null hypothesis at $\alpha_0 = 0.10$ and concluded that the mean incomes of the geographical regions are not different according to the results of the GP and PB test. In Table 2, the GP and PB tests are more powerful than the FA test, that's why it can be said that the results of these two tests are more reliable than the FA test in the presence of outliers.

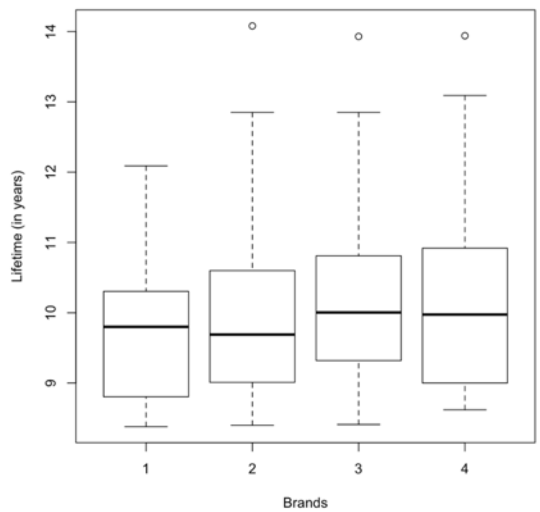

Figure 1. Lifetime of the components in years

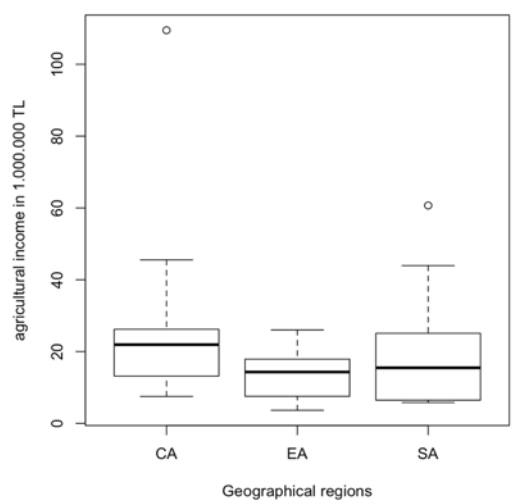

Figure 2. Agricultural income of the geographical regions in Turkey

5. Results and Conclusions

The generalized p-value, parametric bootstrap, and fiducial approach-based test proposed by Malekzadeh and Jafari [18] can be used for complete data. The performance of the tests was compared in terms of Type I error probability and penalized power for complete data and the most powerful test is determined. The results are obtained in balanced and unbalanced designs for small, moderate, and large samples in the presence of outliers. The simulation results clearly show that the PB test is superior to the others to control the Type I error probability and penalized power in most of the cases. Only in the presence of outliers, the GP test is more powerful than the PB test in $k = 3$ group designs. There are also some interesting results obtained such as the negative effect of the balanced designs and higher scale parameters on the performance of the tests. Moreover, illustrative examples are given to perform the tests on a real data example. It is concluded that the lifetimes of the components are not statistically significant. In this study, the PB test is obtained as a powerful test for testing the equality of exponentially distributed populations' means under unequal scale parameters and it can be safely used in reliability analysis, modeling extreme events, sequential analysis, and income inequality.

Author Contribution Statements The authors contributed equally. All authors read and approved the final copy of the paper.

Declaration of Competing Interests The authors declare that they have no known competing financial interests or personal relationships that could have appeared to influence the work reported in this paper.

References

[1] Tsui, K., Weerahandi, S., Generalized p-values in significance testing of hypotheses in the presence of nuisance parameters, *Journal of the American Statistical Association*, 84 (1989), 602–607. https://doi.org/10.2307/2289949

[2] Cavus, M., Yazici, B., Sezer, A., Modified tests for comparison of group means under heteroskedasticity and non-normality caused by outlier(s), *Hacettepe Journal of Mathematics and Statistics*, 46 (2017), 602–607. https://doi.org/10.15672/HJMS.2017.417

[3] Cavus, M., Yazici, B., Sezer, A., A revised generalized F-test for testing the equality of group means under non-normality caused by skewness, *Communications Faculty of Sciences University of Ankara Series A1 Mathematics and Statistics*, 70 (2021), 1036–1054. https://doi.org/10.31801/cfsuasmas.800452

[4] Cavus, M., Yazici, B., Sezer, A., Analyzing regional export data by the modified generalized F-test, *International Journal of Economic and Administrative Studies*, (2018), 541–552. https://doi.org/10.18092/ulikidince.348070

[5] Tian, L., Wu, J., Inferences on the common mean of several log-normal populations: the generalized variable approach, *Biometrical Journal*, 49 (2007), 944–951. https://doi.org/10.1002/bimj.200710391

[6] Tian, L., Testing equality of inverse gaussian means under heterogeneity based on generalized test variable, *Computational Statistics and Data Analysis*, 51 (2006), 1156–1162. https://doi.org/10.1016/j.csda.2005.11.012

[7] Ma, C., Tian, L., A parametric bootstrap approach for testing equality of inverse gaussian means under heterogeneity, *Communications in Statistics-Simulation and Computation*, 38 (2009), 1156–1162. https://doi.org/10.1080/03610910902833470

[8] Niu, C., Guo, X., Xu, W., Zhu, L., Comparison of several Birbaum-Saunders distributions, *Journal of Statistical Computation and Simulation*, 84 (2014), 2721–2733. https://doi.org/10.1080/00949655.2014.881814

[9] Ghosh, M., Razmpour, A., Estimation of the common location parameter of several exponentials, *Sankhya: The Indian Journal of Statistics*, 46 (1984), 383–394. https://www.jstor.org/stable/25050498

[10] Chen, H., A new range statistic for comparisons of several exponential location parameters, *Biometrika*, 69 (1982), 257–260. https://doi.org/10.2307/2335881

[11] Singh, N., The likelihood ratio test for the equality of location parameters of exponential populations based on Type II censored samples, *Technometrics*, 25 (1983), 193–195. https://doi.org/10.1080/00401706.1983.10487852

[12] Kambo, N., Awad, A., Testing equality of location parameters of k exponential distributions, *Communications in Statistics - Theory and Methods*, 14 (1985), 567–583.

[13] Hsieh, H., An exact test for comparing location parameters of k exponential distributions with unequal scaled based on Type II censored data, *Technometrics*, 28 (1986), 157–164. https://doi.org/10.2307/1270452

[14] Vaughan, D., Tiku, M., Testing the equality of location parameters of exponential populations from censored samples, *Communication in Statistics-Theory and Methods*, 22 (1993), 2567–2581. https://doi.org/10.1080/03610928308831169

[15] Tiku, M. Vaughan, D., Testing equality of location parameters of two exponential distributions from censored samples, *Communication in Statistics-Theory and Methods*, 20 (1991), 929–944. https://doi.org/10.1080/03610929108830540

[16] Ananda, M., Weerahandi, S., Testing the difference of two exponential means using generalized p-values, *Communications in Statistics - Simulation and Computation*, 25 (1996), 521–532. https://doi.org/10.1080/03610919608813327

[17] Wu, S., One stage multiple comparisons with the control for exponential mean lifetimes based on doubly censored samples under heteroscedasticity, *Communications in Statistics - Simulation and Computation*, 50 (2021), 1473-1483. https://doi.org/10.1080/03610918.2019.1584302

[18] Malekzadeh, A., Jafari, A., Inference on the equality means of several two-parameter exponential distributions under progressively Type II censoring, *Communications in Statistics - Simulation and Computation*, 49 (2020), 3196-3211. https://doi.org/10.1080/03610918.2018.1538452

[19] Rahman, M., Pearson, L. M., Estimation in two-parameter exponential distributions, *Journal of Statistical Computation and Simulation*, 70 (2001), 371–386. https://doi.org/10.1080/00949650108812128

[20] Viveros, R., Balakrishnan, N., Interval estimation of parameters of life from progressively censored data, *Technometrics*, 36 (1994), 84–91. https://doi.org/10.2307/1269201

[21] Cochran, W. G., Problem arising in the analysis of a series of similar experiments, *Journal of the Royal Statistical Society*, 4 (1937), 102–118. https://www.jstor.org/stable/2984123

[22] Weerahandi, S., ANOVA under unequal error variances, *Biometrics*, 51 (1995), 102–118. https://doi.org/10.2307/2532947

[23] Krishnamoorthy, K., Lu, F., Mathew, T., A parametric bootstrap approach for ANOVA with unequal variances: fixed and random models, *Computational Statistics and Data Analysis*, 51 (2007), 5731–5742. https://doi.org/10.1016/j.csda.2006.09.039

[24] Li, X., Wang, J., Liang, H., Comparison of several means: A fiducial based approach, *Computational Statistics and Data Analysis*, 55 (2011), 1993–2002. https://doi.org/10.1016/j.csda.2010.12.009

[25] Cavus, M., Yazici, B., Sezer, A., Penalized power approach to compare the power of the tests when Type I error probabilities are different, *Communications in Statistics - Simulation and Computation*, 50 (2021), 1912-1926. https://doi.org/10.1080/03610918.2019.1588310

[26] Cavus, M., Yazici, B., Testing the equality of normal distributed and independent groups' means under unequal variances by doex package, *The R Journal*, 12 (2021), 134-154. https://doi.org/10.32614/RJ-2021-008

[27] Cavus, M., Yazici, B., doex: The one-way heteroscedastic ANOVA tests, *R package*, v.1.2.

http://communications.science.ankara.edu.tr

Commun.Fac.Sci.Univ.Ank.Ser. A1 Math. Stat.
Volume 72, Number 3, Pages 701–709 (2023)
DOI:10.31801/cfsuasmas.1199113
ISSN 1303-5991 E-ISSN 2618-6470

Research Article; Received: November 8, 2022; Accepted: February 14, 2023

SUBORDINATION THEOREMS FOR A CLASS RELATED TO Q-FRACTIONAL DIFFERENTIAL OPERATOR

Mohamed Ahmed MOWAFY[1], Adela Othman MOSTAFA[2] and Samer Mohamed MADIAN[3]

[1,2]Mathematics Department, Faculty of Science, Mansoura University, Mansoura 35516, EGYPT
[3]Basic Science Department, Higher Institute for Engineering and Technology, New Damietta, EGYPT

Abstract. By using the definition of q-difference operator, we defined the new q-Al-Oboudi-Al-Amoudi operator, which generalize modified Al-Oboudi-Al-Amoudi operator. Using the new operator, we defined a new class of uniformly functions and obtained subordination result for functions in it. Our results not only generalize previous results but also modified some previous results.

1. Introduction

The class of univalent analytic functions

$$F(z) = z + \sum_{k=2}^{\infty} a_k z^k, (a_k \geq 0),\ z \in \mathcal{D} = \{z \in \mathbb{C} :| z |< 1\}, \tag{1}$$

is denoted by $\mathcal{S}$.

The class of convex functions $\mathcal{K}$ satisfies

$$\text{Re}\left\{1 + \frac{zF^{''}(z)}{F^{'}(z)}\right\} > 0.$$

If F, g are analytic in $\mathcal{D}$, then F is subordinate to g, written F $\prec g$ if there exists a Schwarz function $w(z)$ analytic in $\mathcal{D}$ with $w(0) = 0$ and $|w(z)| < 1$ for all $z \in \mathcal{D}$, such that $F(z) = g(w(z))$. (*see* [14, 16])

2020 *Mathematics Subject Classification.* 30C45.
Keywords. Coefficient estimate, subordination factor sequence, q-difference and fractional operator.

[1] mohamed1976224@gmail.com-Corresponding author; 0000-0002-2308-6826
[2] adelaeg254@yahoo.com; 0000-0002-3911-0990
[3] samar_math@yahoo.com; 0000-0001-7490-9901.

For F given by (1) and g given by

$$g(z)=z+\sum_{k=2}^{\infty}b_kz^k, \tag{2}$$

the Hadamard product (or convolution) is

$$(F*g)(z)=z+\sum_{k=2}^{\infty}a_kb_kz^k=(g*F)(z).$$

For $F\in\mathcal{S},\ 0<q<1$, the $q-$derivative operator ∇_q is given by (Jackson [15]) and many authors studied it for example see ([1], [4 − 6], [9], [16, 17] and [22, 23]).

$$\nabla_qF(z)=\begin{cases}\frac{F(z)-F(qz)}{(1-q)z} & ,z\neq 0\\ F'(0) & ,z=0\end{cases}$$

that is

$$\nabla_qF(z)=1+\sum_{k=2}^{\infty}[k]_qa_kz^{k-1}, \tag{3}$$

where

$$[k]_q=\frac{1-q^k}{1-q},\ [0]_q=0. \tag{4}$$

The fractional $q-$derivative operator of order α for analytic function F defined in a simply connected domain, contains zero is defined by [5],

$$D_{q,z}^{\alpha}F(z)=\frac{1}{\Gamma_q(1-\alpha)}\int_0^z\frac{F(t)}{(z-t)^{\alpha}}d_qt\ ,\ 0\leq\alpha<1,$$

$$\begin{aligned}\Omega_q^{\alpha}F(z) &= \Gamma_q(2-\alpha)\,z^{\alpha}D_{q,z}^{\alpha}F(z), \qquad (5)\\ &= z+\sum_{k=2}^{\infty}\frac{\Gamma_q(k+1)\Gamma_q(2-\alpha)}{\Gamma_q(k+1-\alpha)}a_kz^k\ \ (0<q<1,\ 0\leq\alpha<1),\end{aligned}$$

where multiplicity of $(z-t)^{-\alpha}$ is removed by requiring $\log(z-t)$, to be real when $z-t>0$ (for $q\to 1^-$ see [19], [20]).

Definition 1. *For $\lambda\geq 0,\ 0\leq\alpha<1,\ 0<q<1,\ n\in\mathbb{N}_0=\mathbb{N}\cup\{0\},\ \mathbb{N}=\{1,2,...\}$ and F is given by* (1) *we defined new $q-$fractional derivative operator as follows,*

$$\begin{aligned}D_{\lambda,q}^{0,0}F(z) &= F(z), \qquad (6)\\ D_{\lambda,q}^{1,\alpha}F(z) &= (1-\lambda)\,\Omega_q^{\alpha}F(z)+\lambda zD_q\left(\Omega_q^{\alpha}F(z)\right)=D_{\lambda,q}^{\alpha}F(z),\\ D_{\lambda,q}^{2,\alpha}F(z) &= D_{\lambda,q}^{\alpha}\left(D_{\lambda,q}^{\alpha}F(z)\right),\end{aligned}$$

$$\begin{aligned} D_{\lambda,q}^{n,\alpha}F(z) &= D_{\lambda,q}^{\alpha}\left(D_{\lambda,q}^{n-1,\alpha}F(z)\right), \\ &= z+\sum_{k=2}^{\infty}\Psi_{k,n,q}(\alpha,\lambda)a_k z^k, \end{aligned}$$

where

$$\Psi_{k,n,q}(\alpha,\lambda)=\frac{\Gamma_q(k+1)\Gamma_q(2-\alpha)}{\Gamma_q(k+1-\alpha)}\left[1+\lambda([k]_q-1)\right]^n. \tag{7}$$

We note that:

(i) $D_{1,q}^{n,0}F(z)=D_q^n\ F(z)$ [8, 18].

(ii) $\lim_{q\to 1^-} D_{\lambda,q}^{n,\alpha}F(z)=D_{\lambda}^{n,\alpha}F(z)$, where this operator modified the operator of [3, 7],

(iii) $\lim_{q\to 1^-} D_{\lambda,q}^{0,\alpha}F(z)=D_z^{\alpha}\ F(z)$ (see [19, 20]),

(iv) $\lim_{q\to 1^-} D_{1,q}^{n,0}F(z)=D^nF(z)$ (see [21]),

(v) $\lim_{q\to 1^-} D_{\lambda,q}^{n,0}F(z)=D_{\lambda}^nF(z)$ (see [2]),

Definition 2. *For $\lambda,\mu\geq 0,\ \gamma\geq 1, 0\leq\alpha,\beta<1, 0\leq\delta\leq 1, n\in\mathbb{N}_0$, a function F $\in\mathcal{S}$ is in the class $S_{\lambda,q}^{n,\alpha}(\delta,\gamma,\mu,\beta)$, if*

$$Re\left\{\frac{\gamma z\nabla_q G(z)}{G(z)}-(\gamma-1)\right\}>\mu\left|\frac{\gamma z\nabla_q G(z)}{G(z)}-\gamma\right|+\beta, \tag{8}$$

where

$$G(z)=(1-\delta)D_{\lambda,q}^{n,\alpha}F(z)+\delta z\left(\nabla_q D_{\lambda,q}^{n,\alpha}F(z)\right). \tag{9}$$

We note that as $q\to 1^-$: $S_{\lambda,q}^{n,\alpha}(0,1,\mu,\beta)=SP_{\alpha,\lambda}^n(\mu,\beta)$ and $S_{\lambda,q}^{n,\alpha}(1,1,\mu,\beta)=UCV_{\alpha,\lambda}^n(\mu,\beta)$ [3, 7, with $\Psi_{k,n,q}(\alpha,\lambda)$ of the form (1.7)]. For different values of n,α, $\lambda,\delta,\gamma,\mu$ and β, we get the classes defined by [3], [8], [10 − 13], and [17].

2. Main Results

Unless indicated, let $0\leq\alpha,\beta<1$, $\lambda,\mu\geq 0$, $\gamma\geq 1$, $0\leq\delta\leq 1$, $n\in\mathbb{N}_0$, $0<q<1$ and $\Psi_{k,n,q}(\alpha,\lambda)$ as (7). The following definition and lemma are needed.

Definition 3. [24]. *A sequence $\{b_k\}_{k=1}^{\infty}$ of complex numbers is called a subordinating factor sequence if, whenever $F(z)\in\mathcal{K}$ then,*

$$\sum_{k=1}^{\infty}a_kb_kz^k\prec F(z)\qquad(z\in\mathcal{D};a_1=1).$$

Lemma 1. [24]. *The sequence* $\{b_k\}_{k=1}^{\infty}$ *is a subordinating factor sequence if and only if*

$$\Re\left\{1+2\sum_{k=1}^{\infty} b_k z^k\right\} > 0 \qquad (z \in \mathcal{D}).$$

Theorem 1. *If* $F \in \mathcal{S}$, *satisfies*

$$\sum_{k=2}^{\infty}\left[1-\beta+\gamma\left([k]_q-1\right)(1+\mu)\right]\left[1+\left([k]_q-1\right)\delta\right]\Psi_{k,n,q}(\alpha,\lambda)\left|a_k\right| \leq 1-\beta, \tag{10}$$

then, $F \in S_{\lambda,q}^{n,\alpha}(\delta,\gamma,\mu,\beta)$.

Proof. Assume that (10) holds. Since for real β and complex number w, □

$$\operatorname{Re}(w) \geq \beta \Leftrightarrow |w+(1-\beta)|-|w-(1+\beta)| \geq 0, \tag{11}$$

then by Definition 2 it is sufficient to show that

$$\begin{aligned}&\left|\frac{\gamma z\nabla_q G(z)}{G(z)}-(\gamma-1)-\mu\left|\frac{\gamma z\nabla_q G(z)}{G(z)}-\gamma\right|-(1+\beta)\right| \leq \\ &\left|\frac{\gamma z\nabla_q G(z)}{G(z)}-(\gamma-1)-\mu\left|\frac{\gamma z\nabla_q G(z)}{G(z)}-\gamma\right|+(1-\beta)\right|.\end{aligned} \tag{12}$$

For the right-hand side of (12)

$$\begin{aligned} R \quad : &= \left|\frac{\gamma z\nabla_q G(z)}{G(z)}-(\gamma-1)-\mu\left|\frac{\gamma z\nabla_q G(z)}{G(z)}-\gamma\right|+(1-\beta)\right| \\ &= \frac{1}{|G(z)|}\left|\gamma z\nabla_q G(z)+(2-\beta-\gamma)G(z)-\mu e^{i\theta}\left|\gamma z\nabla_q G(z)-\gamma G(z)\right|\right| \\ &> \frac{|z|}{|G(z)|}\{2-\beta-\sum_{k=2}^{\infty}\left[2-\beta+\gamma\left([k]_q-1\right)(1+\mu)\right] \\ &\times \left[1+\left([k]_q-1\right)\delta\right]\Psi_{k,n,q}(\alpha,\lambda)\left|a_k\right|\}. \end{aligned}$$

Similarly, the left

$$\begin{aligned} L \quad : &= \left|\frac{\gamma z\nabla_q G(z)}{G(z)}-(\gamma-1)-\mu\left|\frac{\gamma z\nabla_q G(z)}{G(z)}-\gamma\right|-(1+\beta)\right| \\ &= \frac{1}{|G(z)|}\left|\gamma z\nabla_q G(z)-(\gamma-1)G(z)-\mu e^{i\theta}\left|\gamma z\nabla_q G(z)-\gamma G(z)\right|-(1+\beta)G(z)\right| \end{aligned}$$

$$< \frac{|z|}{|G(z)|}\{\beta+\sum_{k=2}^{\infty}\left[\gamma\left([k]_q-1\right)(1+\mu)-\beta\right]\left[1+\left([k]_q-1\right)\delta\right]\Psi_{k,n,q}(\alpha,\lambda)\,|a_k|\}.$$

Since

$$\begin{aligned} R-L &> \frac{|z|}{|G(z)|}\{2(1-\beta)-2\sum_{k=2}^{\infty}\left[1-\beta+\gamma\left([k]_q-1\right)(1+\mu)\right] \\ &\times \left[1+\left([k]_q-1\right)\delta\right]\Psi_{k,n,q}(\alpha,\lambda)\,|a_k|\} \\ &\geq 0, \end{aligned}$$

then (12) is satisfied, so $F\in S_{\lambda,q}^{n,\alpha}(\delta,\gamma,\mu,\beta)$.

Let $\acute{S}_{\lambda,q}^{n,\alpha}(\delta,\gamma,\mu,\beta)$ be the class of functions satisfy (10) so $\acute{S}_{\lambda,q}^{n,\alpha}(\delta,\gamma,\mu,\beta)\subset$ $S_{\lambda,q}^{n,\alpha}(\delta,\gamma,\mu,\beta)$.

Theorem 2. *Let* $F\in \acute{S}_{\lambda,q}^{n,\alpha}(\delta,\gamma,\mu,\beta)$ *and* $g\in\mathcal{K}$, *then*

$$\left(\frac{[1-\beta+\gamma q(1+\mu)](1+\delta q)\Psi_{2,n,q}(\alpha,\lambda)}{2\{[1-\beta+\gamma q(1+\mu)](1+\delta q)\Psi_{2,n,q}(\alpha,\lambda)+1-\beta\}}\right)(F*g)(z)\prec g(z) \quad (13)$$

and

$$\Re\{F(z)\}>-\frac{\{[1-\beta+\gamma q(1+\mu)](1+\delta q)\Psi_{2,n,q}(\alpha,\lambda)+1-\beta\}}{[1-\beta+\gamma q(1+\mu)](1+\delta q)\Psi_{2,n,q}(\alpha,\lambda)}. \quad (14)$$

The constant factor $\frac{[1-\beta+\gamma q(1+\mu)](1+\delta q)\Psi_{2,n,q}(\alpha,\lambda)}{2\{[1-\beta+\gamma q(1+\mu)](1+\delta q)\Psi_{2,n,q}(\alpha,\lambda)+1-\beta\}}$ *in* (13) *cannot be replaced by a larger one.*

Proof. Let $F\in \acute{S}_{\lambda,q}^{n,\alpha}(\delta,\gamma,\mu,\beta)$ and $g(z)=z+\sum_{k=2}^{\infty}b_kz^k\in\mathcal{K}$, then □

$$\begin{aligned} &\left(\frac{[1-\beta+\gamma q(1+\mu)](1+\delta q)\Psi_{2,n,q}(\alpha,\lambda)}{2\{[1-\beta+\gamma q(1+\mu)](1+\delta q)\Psi_{2,n,q}(\alpha,\lambda)+1-\beta\}}\right)(F*g)(z) \\ &= \left(\frac{[1-\beta+\gamma q(1+\mu)](1+\delta q)\Psi_{2,n,q}(\alpha,\lambda)}{2\{[1-\beta+\gamma q(1+\mu)](1+\delta q)\Psi_{2,n,q}(\alpha,\lambda)+1-\beta\}}\right)\left(z+\sum_{k=2}^{\infty}a_kb_kz^k\right). \end{aligned} \quad (15)$$

Thus, by Definition 3, (13) will be true if

$$\left\{\frac{\left[1-\beta+\gamma q\left(1+\mu\right)\right]\left(1+\delta q\right)\Psi_{2,n,q}\left(\alpha,\lambda\right)}{2\left\{\left[1-\beta+\gamma q\left(1+\mu\right)\right]\left(1+\delta q\right)\Psi_{2,n,q}\left(\alpha,\lambda\right)+1-\beta\right\}}a_k\right\}_{k=1}^{\infty} \tag{16}$$

is a subordinating factor sequence, with $a_1 = 1$. In view of Lemma 1, this is equivalent to

$$\Re\left\{1+\sum_{k=1}^{\infty}\frac{\left[1-\beta+\gamma q\left(1+\mu\right)\right]\left(1+\delta q\right)\Psi_{2,n,q}\left(\alpha,\lambda\right)}{\left\{\left[1-\beta+\gamma q\left(1+\mu\right)\right]\left(1+\delta q\right)\Psi_{2,n,q}\left(\alpha,\lambda\right)+1-\beta\right\}}a_k z^k\right\}>0, \tag{17}$$

where

$$\Theta\left(k\right)=\left[1-\beta+\gamma\left(\left[k\right]_q-1\right)\left(1+\mu\right)\right]\left[1+\left(\left[k\right]_q-1\right)\delta\right]\Psi_{k,n,q}(\alpha,\lambda)\quad(k\geq 2),$$

is an increasing function of k $(k \geq 2)$, when $|z| = r < 1$, we have,

$$\begin{aligned}
&\Re\left\{1+\sum_{k=1}^{\infty}\frac{\Theta\left(2\right)}{\Theta\left(2\right)+1-\beta}a_k z^k\right\}\\
=\ &\Re\left\{1+\frac{\Theta\left(2\right)}{\Theta\left(2\right)+1-\beta}z+\frac{\sum_{k=2}^{\infty}\Theta\left(2\right)}{\Theta\left(2\right)+1-\beta}a_k z^k\right\}\\
\geq\ &1-\frac{\Theta\left(2\right)}{\Theta\left(2\right)+1-\beta}r-\frac{\sum\limits_{k=2}^{\infty}\Theta(k)|a_k|}{\Theta(2)+1-\beta}r^k\\
>\ &1-\frac{\Theta\left(2\right)}{\Theta\left(2\right)+1-\beta}r-\frac{1-\beta}{\Theta(2)+1-\beta}r\\
=\ &1-r>0\qquad\left(|z|=r<1\right).
\end{aligned}$$

By taking the convex function $g(z) = \frac{z}{1-z} = z + \sum_{k=2}^{\infty} z^k$. To prove the sharpness of $\frac{\Theta(2)}{2[\Theta(2)+1-\beta]}$, the function $F_0(z) \in \acute{S}_{\lambda,q}^{n,\alpha}(\delta,\gamma,\mu,\beta)$ given by

$$F_0(z)=z-\frac{1-\beta}{\left[1-\beta+\gamma q\left(1+\mu\right)\right]\left(1+\delta q\right)\Psi_{2,n,q}\left(\alpha,\lambda\right)}z^2. \tag{18}$$

Thus from (14), we have

$$\frac{\left[1-\beta+\gamma q\left(1+\mu\right)\right]\left(1+\delta q\right)\Psi_{2,n,q}\left(\alpha,\lambda\right)}{2\left\{\left[1-\beta+\gamma q\left(1+\mu\right)\right]\left(1+\delta q\right)\Psi_{2,n,q}\left(\alpha,\lambda\right)+1-\beta\right\}}F_0(z)\prec\frac{z}{1-z}.$$

Moreover, it can easily to verify for $F_0(z)$ given by (18) that

$$\min_{|z|\leq r}\left\{\Re\frac{\left[1-\beta+\gamma q\left(1+\mu\right)\right]\left(1+\delta q\right)\Psi_{2,n,q}\left(\alpha,\lambda\right)}{2\left\{\left[1-\beta+\gamma q\left(1+\mu\right)\right]\left(1+\delta q\right)\Psi_{2,n,q}\left(\alpha,\lambda\right)+1-\beta\right\}}F_0(z)\right\}=-\frac{1}{2} \tag{19}$$

This shows that the $\frac{[1-\beta+\gamma q(1+\mu)](1+\delta q)\Psi_{2,n,q}(\alpha,\lambda)}{2\{[1-\beta+\gamma q(1+\mu)](1+\delta q)\Psi_{2,n,q}(\alpha,\lambda)+1-\beta\}}$ is the best possible .

Taking $\lim_{q\to 1^-}$in Theorem 2, we have

Corollary 1. *Let* $F \in \acute{S}_{\lambda}^{n,\alpha}(\delta,\gamma,\mu,\beta)$ *whose coefficients satisfy* (10) *when* $q \to 1^{-}$ *and* $g(z) = z + \sum_{k=2}^{\infty} b_k z^k \in \mathcal{K}$, *then*

$$\left(\frac{[1-\beta+\gamma(1+\mu)](1+\delta)\Psi_{2,n}(\alpha,\lambda)}{2\{[1-\beta+\gamma(1+\mu)](1+\delta)\Psi_{2,n}(\alpha,\lambda)+1-\beta\}}\right)(F*g)(z) \prec g(z) \tag{20}$$

and

$$\Re\{F(z)\} > -\frac{\{[1-\beta+\gamma(1+\mu)](1+\delta)\Psi_{2,n}(\alpha,\lambda)+1-\beta\}}{[1-\beta+\gamma(1+\mu)](1+\delta)\Psi_{2,n}(\alpha,\lambda)}.$$

The factor $\frac{[1-\beta+\gamma(1+\mu)](1+\delta)\Psi_{2,n}(\alpha,\lambda)}{2\{[1-\beta+\gamma(1+\mu)](1+\delta)\Psi_{2,n}(\alpha,\lambda)+1-\beta\}}$ in (2.11) cannot be replaced by a larger one.

Remark 1. *Note that for* $\gamma = 1$ *and* $\delta = 0, 1$ *respectively in Corollary 1 modified Theorems 2.4 and 2.8 of* [7].

Taking $\gamma = 0$ in Theorem 2, we have

Corollary 2. *Let* $F \in \acute{S}_{\lambda,q}^{n,\alpha}(\delta,0,\mu,\beta)$ *whose coefficients satisfy* (10) *when* $\gamma = 0$ *and* $g \in \mathcal{K}$, *then*

$$\left(\frac{(1-\beta)(1+\delta q)\Psi_{2,n,q}(\alpha,\lambda)}{2[(1-\beta)(1+\delta q)\Psi_{2,n,q}(\alpha,\lambda)+1-\beta]}\right)(F*g)(z) \prec g(z) \tag{21}$$

and

$$\Re\{F(z)\} > -\frac{[(1-\beta)(1+\delta q)\Psi_{2,n,q}(\alpha,\lambda)+1-\beta]}{(1-\beta)(1+\delta q)\Psi_{2,n,q}(\alpha,\lambda)}.$$

The factor $\frac{(1-\beta)(1+\delta)\Psi_{2,n}(\alpha,\lambda)}{2[(1-\beta)(1+\delta)\Psi_{2,n}(\alpha,\lambda)+1-\beta]}$ *in* (2.12) *cannot be replaced by a larger one.*

Taking $\mu = 0$ in Theorem 2, we have

Corollary 3. *Let* $F \in \acute{S}_{\lambda,q}^{n,\alpha}(\delta,\gamma,0,\beta)$ *whose coefficients satisfy* (10) *with* $\mu = 0$ *and* $g \in \mathcal{K}$. *Then*

$$\left(\frac{(1-\beta+\gamma q)(1+\delta q)\Psi_{2,n,q}(\alpha,\lambda)}{2[(1-\beta+\gamma q)(1+\delta q)\Psi_{2,n,q}(\alpha,\lambda)+1-\beta]}\right)(F*g)(z) \prec g(z) \tag{22}$$

and

$$\Re\{F(z)\} > -\frac{[(1-\beta+\gamma q)(1+\delta q)\Psi_{2,n,q}(\alpha,\lambda)+1-\beta]}{(1-\beta+\gamma q)(1+\delta q)\Psi_{2,n,q}(\alpha,\lambda)}.$$

The factor $\frac{(1-\beta+\gamma q)(1+\delta q)\Psi_{2,n,q}(\alpha,\lambda)}{2[(1-\beta+\gamma q)(1+\delta q)\Psi_{2,n,q}(\alpha,\lambda)+1-\beta]}$ *in* (22) *cannot be replaced by a larger one.*

3. Conclusions

Throughout the paper, first by using the definition of $q-$difference operator we defined new q- Al-Oboudi - Al-Amoudi operator and which modified Al-Oboudi - Al-Amoudi operator. After that, we used the new operator to introduce new class $S_{\lambda,q}^{n,\alpha}(\delta,\gamma,\mu,\beta)$ which generalized a class of uniformly univalent functions. Finally, we obtained some subordination factor sequence results for this class and its subclasses. Our results modified previous results.

Author Contribution Statements All authors jointly worked on the results, and they read and approved the final manuscript.

Declaration of Competing Interests The authors declare that they have no competing interests.

Acknowledgements The authors would like to thank Prof. Dr. M. K. Aouf for his helpful in preparing the paper and the referees for their valuable comments and helpful suggest.

References

[1] Risha, M.A., Annaby, M.H., Mansour, Z.S., Ismail, M.E., Linear q-difference equations, *Zeitschrift für Analysis und ihre Anwendungen*, 26(4) (2007), 481-494. doi 10.4171/zaa/1338
[2] Al-Oboudi, F.M., On univalent functions defined by a generalized Sălăgean operator, *International Journal of Mathematics and Mathematical Sciences*, 2004(27) (2004), 1429-1436. https://doi.org/10.1155/S0161171204108090
[3] Al-Oboudi, F.M., Al-Amoudi, K.A., On classes of analytic functions related to conic domains, *Journal of Mathematical Analysis and Applications*, 339(1) (2008), 655-667. https://doi.org/10.1016/j.jmaa.2007.05.087
[4] Annaby, M.H., Mansour, Z.S., Fractional q-difference equations, *q-Fractional Calculus and Equations,* (2012), 223-270.
[5] Aouf, M.K., Mostafa, A.O., Subordination results for analytic functions associated with fractional q-calculus operators with complex order, *Afrika Matematika,* 31(7) (2020), 1387-1396. https://doi.org/10.1007/s13370-020-00803-3
[6] Aouf, M.K., Mostafa, A.O., Some subordinating results for classes of functions defined by Salagean type q derivative operator, *Filomat*, 34(7) (2020), 2283-2292. https://doi.org/10.2298/FIL2007283A
[7] Aouf, M.K., Mostafa, A.O., Some subordination results for classes of analytic functions defined by the Al-Oboudi–Al-Amoudi operator, *Archiv der Mathematik*, 92(3) (2009), 279-286. https://doi.org/10.1007/s00013-009-2984-x
[8] Aouf, M.K., Mostafa, A.O., Al-Quhali, F.Y., A class of $\beta-$ uniformly univalent functions defined by Salagean type q- difference operator, *Acta Univ. Apulensis*, 60 (2019), 19-35.
[9] Aouf, M.K., Mostafa, A.O., Elmorsy, R.E, Certain subclasses of analytic functions with varying arguments associated with q-difference operator, *Afrika Matematika*, 32(3) (2021), 621-630. https://doi.org/10.1007/s13370-020-00849-3
[10] Aouf, M.K., Mostafa, A.O., Hussain, A.A., Properties of certain class of uniformly Starlike and Convex functions defined by convolution, *Int. J. Open Problems Complex Analysis*, 7(2) (2015), 1-15.

[11] Aouf, M.K., Mostafa, A.O., Shahin, A.M., Madian, S.M., Subordination theorem for analytic function defined by convolution, *Indian J. Math.*, 54(1) (2012) , 1-11. https://doi.org/10.2298/FIL2007283A

[12] Aouf, M.K., Shamandy, A., Mostafa, A.O., El-Emam, F., Subordination results associated with $\beta-$uniformly convex and starlike functions, *Proc. Pakistan Acad. Sci*, 46(2) (2009), 97-101.

[13] Aouf, M.K., Shamandy, A., Mostafa, A.O., Madian, S.M., Subordination theorem for analytic function defined by convolution, *Proc. Pakistan Acad. Sci.,* 96(4) (2009) , $227-232$.

[14] Bulboacă, T., Differential subordinations and suberordinations: Recent results, *Casa Cărtii de Stiintă* (2005).

[15] Jackson, F.H., On q-functions and a certain difference operator, *Trans. R. Soc. Edinb.,* 46 (1908), 64–72.

[16] Miller, S.S., Mocanu, P.T., Differential Subordinations: Theory and Applications, CRC Press, 2000.

[17] Mostafa, A.O., Saleh, Z.M., On a class of uniformly analytic functions with q-analogue, *Int. J. Open Problems Complex Analysis*, 13(2) (2021), 1-13.

[18] Murugusundaramoorthy, G., Vijaya, K., Sub classes of bi-univalent functions defined by Salagean type q-difference operator, arXiv preprint arXiv:1710.00143, 1 (2017), 1-10.

[19] Owa, S., On the distortion theorems I, *Kyungpook Mathematical Journal*, 18(1) (1978), 53-59.

[20] Owa, S., Srivastava, H.M., Univalent and starlike generalized hypergeometric functions, *Canadian Journal of Mathematics*, 39(5) (1987), 1057-1077. https://doi.org/10.4153/CJM-1987-054-3

[21] Salagean, G.S., Subclasses of univalent functions, *In complex analysis-fifth Romanian-Finnish seminar*, part-1 (Bucharest, 1981) *of Lecture Notes in Mathematics,* 1013 (1983), 362-372.

[22] Srivastava, H.M., Operators of basic (or q-) calculus and fractional q-calculus and their applications in geometric function theory of complex analysis, *Iranian Journal of Science and Technology, Transactions A: Science*, 44(1) (2020), 327-344. https://doi.org/10.1007/s40995-019-00815-0

[23] Srivastava, H.M., Mostafa, A.O., Aouf, M.K., Zayed, H.M., Basic and fractional q-calculus and associated Fekete-Szegő problem for p-valently q-starlike functions and p-valently q-convex functions of complex order, *Miskolc Mathematical Notes*, 20(1) (2019), 489-509. doi: 10.18514/mmn.2019.2405

[24] Wilf, H.S., Subordinating factor sequences for convex maps of the unit circle, *Proceedings of the American Mathematical Society*, 12(5) (1961), 689-693.

http://communications.science.ankara.edu.tr

Commun.Fac.Sci.Univ.Ank.Ser. A1 Math. Stat.
Volume 72, Number 3, Pages 710–720 (2023)
DOI:10.31801/cfsuasmas.1197154
ISSN 1303-5991 E-ISSN 2618-6470

Research Article; Received: October 31, 2022; Accepted: February 6, 2023

ON SPECIAL SINGULAR CURVE COUPLES OF FRAMED CURVES IN 3D LIE GROUPS

Bahar DOĞAN YAZICI[1], Osman Zeki OKUYUCU[2] and Murat TOSUN[3]

[1,2]Department of Mathematics, Bilecik Şeyh Edebali University, Bilecik, TÜRKİYE
[3]Department of Mathematics, Sakarya University, Sakarya, TÜRKİYE

Abstract. In this paper, we introduce Bertrand and Mannheim curves of framed curves, which are a special singular curve in 3D Lie groups. We explain the conditions for framed curves to be Bertrand curves and Mannheim curves in 3D Lie groups. We give relationships between framed curvatures and Lie curvatures of Bertrand and Mannheim curves of framed curves. In addition, we obtain the characterization of Bertrand and Mannheim curves according to the various frames of framed curves in 3D Lie groups.

1. Introduction

It is known that a moving frame cannot be installed for curves with singular points [1]. However, thanks to the recent studies for smooth singular curves, there are important developments and these studies have important contributions to the singularity theory. Framed curves defined by Honda and Takahashi are one of them [10]. Framed curves that can have singular points are actually smooth curves. Since they are the general form of Legendre curves on unit tangent bundles and of regular curves with linear independent conditions, they have a great contribution to the studies of singular curves. Some of the pioneering work on framed curves is given in [6, 8, 10, 11, 16].

Bertrand and Mannheim curves are special curve types in differential geometry [2, 12, 13]. For curves $\gamma_1, \gamma_2 : I \to \mathbb{R}$ and moving frames $\{\mathcal{T}_1, \mathcal{N}_1, \mathcal{B}_1\}$ and $\{\mathcal{T}_2, \mathcal{N}_2, \mathcal{B}_2\}$ respectively, if $\mathcal{N}_1 = \mathcal{N}_2$ then curves γ_1, γ_2 are called Bertrand couple, if $\mathcal{N}_1 = \mathcal{B}_2$ then curves γ_1, γ_2 are called Mannheim couple [2, 13]. Bertrand and Mannheim curves of singular curves have been given by Honda and Takahashi in

2020 *Mathematics Subject Classification.* 53A04, 22E15.
Keywords. Bertrand curves, Mannheim curves, framed curves, Lie groups.
[1] bahar.dogan@bilecik.edu.tr; 0000-0001-5690-4840
[2] osman.okuyucu@bilecik.edu.tr-Corresponding author; 0000-0003-4379-0252
[3] tosun@sakarya.edu.tr; 0000-0002-4888-1412.

recent years, as well as the studies of regular curves on Bertrand and Mannheim curves [11]. In addition, Honda and Takahashi added nondegenerate condition to Bertrand and Mannheim curves for regular curves in the literature. Also, they gave a theory that is not valid in the regular case. For framed curves, a curve can be both a Bertrand and Mannheim curve.

Lie groups given by bi invariant metric are a structure that has important results in physics as well as its importance in differential geometry. Lie groups have three different forms in mathematics such that S^3, $SO(3)$ and abelian Lie groups [5]. There are some pioneering studies on 3D Lie groups in differential geometry. As a generalization of the characterizations in Euclidean space, helices, slant helices, Bertrand and Mannheim curves have been introduced in 3D Lie groups in various studies [3, 9, 14, 15]. These studies are based on the condition that the curve is regular. Framed curves, a singular curve, were introduced in 3D Lie groups by Yazıcı, Okuyucu and Tosun [7]. They, gave a new perspective to both physical and geometrical forms of Lie groups. Then, they defined various frames of framed curves in 3D Lie groups.

In this study, we investigate Bertrand and Mannheim curves in 3D Lie groups of framed curves, which have an important place in singularity theory. We express the necessary and sufficient conditions for the framed curves to be Bertrand or Mannheim curves in 3D Lie groups.

2. Lie Groups

Let G be a Lie group with a bi-invariant metric $\langle , \rangle$ and ∇ be the Levi-Civita connection of Lie group G. $\mathfrak{g}$ is isomorphic to T_eG where e is neutral element of G and $\mathfrak{g}$ is Lie algebra of G. Since $\langle , \rangle$ is a bi-invariant metric on G, we have

$$\langle P, [Q, R]\rangle = \langle [P, Q], R\rangle$$

and

$$\nabla_P Q = \frac{1}{2}[P, Q].$$

for all $P, Q, R \in \mathfrak{g}$. On the other hand the Lie bracket of two vector fields W_1 and W_2 is given

$$[W_1, W_2] = \sum_{i=1}^{n} w_{1i} w_{2i} [Y_i, Y_j],$$

where $W_1 = \sum_{i=1}^{n} w_{1i} Y_i$ and $W_2 = \sum_{i=1}^{n} w_{2i} Y_i$ with orthonormal basis $\{Y_1, Y_2, ..., Y_n\}$ of $\mathfrak{g}$.

Suppose that $\beta : I \to$ G be an unit speed regular curve. Then the covariant derivative of X along the curve β is given as follows

$$\nabla_{\beta'} X = \nabla_T X = \dot{X} + \frac{1}{2}[T, X],$$

where T is tangent and $\dot{X} = \sum_{i=1}^{n} \dfrac{dx}{dt} Y_i$. Moreover, if W is the left-invariant vector field to the curve, then $\dot{X} = 0$ (see for details [4]).

The representation of the Frenet-Serret formulas in the 3D Lie group G with the covariant derivative is given as follows:

$$\begin{array}{rcl} \nabla_T T & = & \kappa_1 N_1, \\ \nabla_T N_1 & = & -\kappa_1 T + \kappa_2 N_2, \\ \nabla_T N_2 & = & -\kappa_2 N_1, \end{array}$$

where ∇ is connection of G and $\kappa_1 = \|\dot{T}\|$.

2.1. **Framed curves in 3D Lie groups.** In this part, framed curves, general and adapted frames in 3D Lie groups are discussed [7]. Obviously, framed curves in 3D Lie groups [7] are a generalization of framed curves in $\mathbb{R}^3$ [10].

Definition 1. *[7] A curve $(\gamma, \varrho_1, \varrho_2) : I \to \mathrm{G} \times \Delta_{\mathrm{G}}$ in 3D Lie group* G *is a framed curve if $\langle \gamma^{'}(s), \varrho_i(s) \rangle = 0$ for all $s \in I$ and $i = 1, 2$ where*

$$\Delta_{\mathrm{G}} = \{\varrho = (\varrho_1, \varrho_2) \in \mathrm{G} \times \mathrm{G} | \quad \langle \varrho_1, \varrho_1 \rangle = \langle \varrho_2, \varrho_2 \rangle = 1, \langle \varrho_1, \varrho_2 \rangle = 0\}.$$

A unit vector ω is defined by $\omega = \varrho_1 \times \varrho_2$. The covariant derivative of X along the framed curve $(\gamma, \varrho_1, \varrho_2)$ with the help of unit vector ω as follows

$$\nabla_\omega X = \dot{X} + \frac{1}{2}[\omega, X]. \tag{1}$$

A smooth function on I is given as $\gamma^{'}(s) = \alpha(s)\omega(s)$ and it is clear that s_0 is a singular point if and only if $\alpha(s_0) = 0$. Then the representation with Levi-Civita connection of Frenet-Serret type formulas of $(\gamma, \varrho_1, \varrho_2)$ satisfies:

$$\begin{array}{rcl} \nabla_\omega \omega & = & -l_2(s)\varrho_1(s) - l_3(s)\varrho_2(s), \\ \nabla_\omega \varrho_1 & = & l_1(s)\varrho_2(s) + l_2(s)\omega(s), \\ \nabla_\omega \varrho_2 & = & -l_1(s)\varrho_1(s) + l_3(s)\omega(s), \end{array} \tag{2}$$

where ∇ is Levi-Civita connection of G and $\sqrt{l_2^2(s) + l_3^2(s)} = \|\dot{\omega}\|$. If ω is the left-invariant vector field to the framed curve, then $l_2(s) = l_3(s) = 0$ for every $s \in I$.

Proposition 1. *[7] Let $(\gamma, \varrho_1, \varrho_2) : I \to \mathrm{G} \times \Delta_{\mathrm{G}}$ be a framed curve in 3D Lie groups. Then,*

$$[\omega, \varrho_1] = \langle [\omega, \varrho_1], \varrho_2 \rangle \varrho_2 = 2\delta_G \varrho_2,$$

$$[\omega, \varrho_2] = \langle [\omega, \varrho_2], \varrho_1 \rangle \varrho_1 = -2\delta_G \varrho_1.$$

is provided.

Theorem 1. *[7] Let $(\gamma, \varrho_1, \varrho_2) : I \to \mathrm{G} \times \Delta_{\mathrm{G}}$ be a framed curve. The Frenet-Serret type formulas of framed curves in 3D Lie groups are given by*

$$\begin{pmatrix} \dot{\omega} \\ \dot{\varrho_1} \\ \dot{\varrho_2} \end{pmatrix} = \begin{pmatrix} 0 & -l_2(s) & -l_3(s) \\ l_2(s) & 0 & (l_1(s) - \delta_{\mathrm{G}}) \\ l_3(s) & -(l_1(s) - \delta_{\mathrm{G}}) & 0 \end{pmatrix} \begin{pmatrix} \omega \\ \varrho_1 \\ \varrho_2 \end{pmatrix}. \tag{3}$$

where $\delta_{\mathrm{G}} = \frac{1}{2}\langle [\omega, \varrho_1], \varrho_2 \rangle$.

Corollary 1 ([7], **Bishop-type frame in 3D Lie groups**). *The under condition $l_1(s) - \delta_{\mathrm{G}} - \psi^{'}(s) = 0$, we have*

$$\begin{pmatrix} \dot{\omega} \\ \dot{\tilde{\varrho}}_1 \\ \dot{\tilde{\varrho}}_2 \end{pmatrix} = \begin{pmatrix} 0 & -\tilde{l}_2(s) & -\tilde{l}_3(s) \\ \tilde{l}_2(s) & 0 & 0 \\ \tilde{l}_3(s) & 0 & 0 \end{pmatrix} \begin{pmatrix} \omega \\ \tilde{\varrho_1} \\ \tilde{\varrho_2} \end{pmatrix}, \tag{4}$$

where

$$\begin{pmatrix} \tilde{l}_2 \\ \tilde{l}_3 \end{pmatrix} = \begin{pmatrix} \cos\psi(s) & -\sin\psi(s) \\ \sin\psi(s) & \cos\psi(s) \end{pmatrix} \begin{pmatrix} l_2 \\ l_3 \end{pmatrix}.$$

Corollary 2 ([7], **Frenet-type frame in 3D Lie groups**). *The under condition $l_2(s)\sin\psi(s) + l_3(s)\cos\psi(s) = 0$, we get*

$$\begin{pmatrix} \dot{\omega} \\ \dot{\tilde{\varrho}}_1 \\ \dot{\tilde{\varrho}}_2 \end{pmatrix} = \begin{pmatrix} 0 & p(s) & 0 \\ -p(s) & 0 & (q(s) - \delta_{\mathrm{G}}) \\ 0 & -(q(s) - \delta_{\mathrm{G}}) & 0 \end{pmatrix} \begin{pmatrix} \omega \\ \tilde{\varrho_1} \\ \tilde{\varrho_2} \end{pmatrix}. \tag{5}$$

where $q(s) = l_1(s) - \psi^{'}(s)$ and $p(s) \neq 0$.

3. Bertrand Curves of Framed Curves in 3D Lie Groups

Definition 2. *The framed curves $(\gamma, \varrho_1, \varrho_2) : I \to \mathrm{G} \times \Delta_{\mathrm{G}}$ and $(\overline{\gamma}, \overline{\varrho}_1, \overline{\varrho}_2) : I \to \mathrm{G} \times \Delta_{\mathrm{G}}$ are called Bertrand couples if there exists a smooth function $\lambda : I \to \mathbb{R}$ where*

$$\overline{\gamma}(s) = \gamma(s) + \lambda(s)\varrho_1(s) \tag{6}$$

and

$$\varrho_1(s) = \overline{\varrho}_1(s)$$

for all $s \in I$.

Proposition 2. *If $(\gamma, \varrho_1, \varrho_2) : I \to \mathrm{G} \times \Delta_{\mathrm{G}}$ and $(\overline{\gamma}, \overline{\varrho}_1, \overline{\varrho}_2) : I \to \mathrm{G} \times \Delta_{\mathrm{G}}$ are Bertrand couples, $\lambda \neq 0$ is a constant.*

Proof. By differentiating equation (6) in 3D Lie groups and by using equation (3), we have

$$\frac{d\overline{\gamma}(s)}{ds} = \frac{d\gamma(s)}{ds} + \lambda^{'}(s)\varrho_1(s) + \lambda(s)\dot{\varrho}_1(s)$$

$$\overline{\alpha}(s)\overline{\omega}(s) = (\alpha(s) + \lambda(s)l_2(s))\omega(s) + \lambda^{'}(s)\varrho_1(s) + \lambda(s)(l_1(s) - \delta_{\mathrm{G}})\varrho_2(s) \qquad (7)$$

Since $\varrho_1(s) = \overline{\varrho}_1(s)$, we get $\lambda^{'}(s) = 0$. That is, $\lambda(s)$ is a constant function on I. □

Theorem 2. *Let* $(\gamma, \varrho_1, \varrho_2) : I \to \mathrm{G} \times \Delta_{\mathrm{G}}$ *be a framed curve with the curvature* (l_1, l_2, l_3, α) *and Lie curvature* δ_{G}. *Then* $(\gamma, \varrho_1, \varrho_2)$ *is a Bertrand curve if and only if there exist* $\lambda \neq 0$*=constant and a smooth function* $\Phi : I \to \mathbb{R}$ *where*

$$\lambda(l_1(s) - \delta_{\mathrm{G}})\cos\Phi(s) - (\alpha(s) + \lambda l_2(s))\sin\Phi(s) = 0 \qquad (8)$$

Proof. Suppose that $(\gamma, \varrho_1, \varrho_2) : I \to \mathrm{G} \times \Delta_{\mathrm{G}}$ are Bertrand curve. Since $\varrho_1(s) = \overline{\varrho}_1(s)$, there exists a function Φ on I with

$$\overline{\varrho}_2(s) = \cos\Phi(s)\varrho_2(s) - \sin\Phi(s)\omega(s), \qquad (9)$$

$$\overline{\omega}(s) = \sin\Phi(s)\varrho_2(s) + \cos\Phi(s)\omega(s). \qquad (10)$$

If the equations (9) and (10) are substituted in the equation (7), we get

$$\overline{\alpha}(s)\sin\Phi(s) = \lambda(l_1(s) - \delta_{\mathrm{G}}), \qquad (11)$$

$$\overline{\alpha}(s)\cos\Phi(s) = \alpha(s) + \lambda l_2(s). \qquad (12)$$

Therefore, the equation (8) is found. Conversely, suppose that (8) is provided. If we define a mapping $(\overline{\gamma}, \overline{\varrho}_1, \overline{\varrho}_2) : I \to \mathrm{G} \times \Delta_{\mathrm{G}}$ with

$$\overline{\gamma}(s) = \gamma(s) + \lambda\varrho_1(s), \quad \varrho_1(s) = \overline{\varrho}_1(s)$$

and $\overline{\varrho}_2(s) = \cos\Phi(s)\varrho_2(s) - \sin\Phi(s)\omega(s)$, then $(\gamma, \varrho_1, \varrho_2)$ and $(\overline{\gamma}, \overline{\varrho}_1, \overline{\varrho}_2)$ are Bertrand mates in 3D Lie groups. □

Proposition 3. *Let* $(\gamma, \varrho_1, \varrho_2) : I \to \mathrm{G} \times \Delta_{\mathrm{G}}$ *and* $(\overline{\gamma}, \overline{\varrho}_1, \overline{\varrho}_2) : I \to \mathrm{G} \times \Delta_{\mathrm{G}}$ *are Bertrand mates. Then,*

$$\overline{\delta}_{\mathrm{G}} = \delta_{\mathrm{G}}$$

where

$$\delta_{\mathrm{G}} = \frac{1}{2}\langle[\omega, \varrho_1], \varrho_2\rangle,$$

$$\overline{\delta}_{\mathrm{G}} = \frac{1}{2}\langle[\overline{\omega}, \overline{\varrho}_1], \overline{\varrho}_2\rangle.$$

Proof. Suppose that $(\gamma, \varrho_1, \varrho_2) : I \to \mathrm{G} \times \Delta_{\mathrm{G}}$ and $(\overline{\gamma}, \overline{\varrho}_1, \overline{\varrho}_2) : I \to \mathrm{G} \times \Delta_{\mathrm{G}}$ are Bertrand mates. By according to equations (9) and (10), we can write

$$\overline{\delta}_{\mathrm{G}} = \frac{1}{2}\langle[\overline{\omega}, \overline{\varrho}_1], \overline{\varrho}_2\rangle$$

$$= \frac{1}{2}\langle[\sin\Phi(s)\varrho_2(s)+\cos\Phi(s),\varrho_1(s)],\cos\Phi(s)\varrho_2(s)-\sin\Phi(s)\omega(s)\rangle$$
$$= \frac{1}{2}\langle\sin\Phi(s)[\varrho_2(s),\varrho_1(s)]+\cos\Phi(s)[\omega(s),\varrho_1(s)],\cos\Phi(s)\varrho_2(s)-\sin\Phi(s)\omega(s)\rangle$$

Hence, from Lie bracket properties, we get

$$\overline{\delta}_{\mathrm{G}} = \frac{1}{2}\langle[\overline{\omega},\overline{\varrho}_1],\overline{\varrho}_2\rangle = \frac{1}{2}\langle[\omega,\varrho_1],\varrho_2\rangle = \delta_{\mathrm{G}}.$$

□

Proposition 4. *Let $(\gamma,\varrho_1,\varrho_2): I\to \mathrm{G}\times\Delta_{\mathrm{G}}$ and $(\overline{\gamma},\overline{\varrho}_1,\overline{\varrho}_2): I\to \mathrm{G}\times\Delta_{\mathrm{G}}$ are Bertrand mates. Then the curvatures $(\bar{l}_1,\bar{l}_2,\bar{l}_3,\overline{\alpha})$ of $(\overline{\gamma},\overline{\varrho}_1,\overline{\varrho}_2)$ are given by*

$$\begin{aligned}
\bar{l}_1(s) &= l_1(s)\cos\Phi(s)-l_2(s)\sin\Phi(s)+\delta_{\mathrm{G}}(1-\cos\Phi(s)),\\
\bar{l}_2(s) &= l_2(s)\cos\Phi(s)+l_1(s)\sin\Phi(s)-\delta_{\mathrm{G}}\sin\Phi(s),\\
\bar{l}_3(s) &= l_3(s)-\Phi^{'}(s),\\
\overline{\alpha}(s) &= \lambda(l_1(s)-\delta_{\mathrm{G}})\sin\Phi(s)+(\alpha(s)+\lambda l_2(s))\cos\Phi(s).
\end{aligned}$$

Proof. By differentiating equation (9), we have

$$\begin{aligned}
\bar{l}_3(s)\overline{\omega}(s)-(\bar{l}_1(s)-\overline{\delta}_{\mathrm{G}})\overline{\varrho}_1(s) &= (l_3(s)\cos\Phi(s)-\Phi^{'}(s)\cos\Phi(s))\omega(s)\\
&+ (-(l_1(s)-\delta_{\mathrm{G}})\cos\Phi(s)+l_2(s)\sin\Phi(s))\varrho_1(s)\\
&+ (-\sin\Phi(s)\Phi^{'}(s)+l_3(s)\sin\Phi(s))\varrho_2(s).
\end{aligned}$$

Since $\overline{\varrho}_1(s)=\varrho_1(s)$ and $\overline{\delta}_{\mathrm{G}}=\delta_{\mathrm{G}}$, we get

$$\bar{l}_1(s)=l_1(s)\cos\Phi(s)-l_2(s)\sin\Phi(s)+\delta_{\mathrm{G}}(1-\cos\Phi(s)).$$

By using equation (10), we have $\bar{l}_3(s)=l_3(s)-\Phi^{'}(s)$. Also, by differentiating equation (10), we get

$$\begin{aligned}
-\bar{l}_2(s)\overline{\varrho}_1(s)-\bar{l}_3(s)\overline{\varrho}_2(s) &= (l_3(s)\sin\Phi(s)-\Phi^{'}(s)\sin\Phi(s))\omega(s)\\
&+ (-(l_1(s)-\delta_{\mathrm{G}})\sin\Phi(s)-l_2(s)\cos\Phi(s))\varrho_1(s)\\
&+ (\cos\Phi(s)\Phi^{'}(s)-l_3(s)\cos\Phi(s))\varrho_2(s).
\end{aligned}$$

Since $\overline{\varrho}_1(s)=\varrho_1(s)$ and $\overline{\delta}_{\mathrm{G}}=\delta_{\mathrm{G}}$, we have

$$\bar{l}_2(s)=l_2(s)\cos\Phi(s)+l_1(s)\sin\Phi(s)-\delta_{\mathrm{G}}\sin\Phi(s).$$

On the other hand, If the equation (11) is multiplied by $\sin\Phi(s)$ on both sides, and the equation (12) is multiplied by $\cos\Phi(s)$ on both sides, then we get

$$\overline{\alpha}(s)=\lambda(l_1(s)-\delta_{\mathrm{G}})\sin\Phi(s)+(\alpha(s)+\lambda l_2(s))\cos\Phi(s).$$

□

Corollary 3. *Let* $(\gamma, \varrho_1, \varrho_2) : I \to \mathrm{G} \times \Delta_{\mathrm{G}}$ *be a framed curve with the curvatures* (l_1, l_2, l_3, α) *and Lie curvature* δ_{G}.
(i). If $l_1(s) - \delta_{\mathrm{G}} = 0$ *for every* $s \in I$ *, then* $(\gamma, \mu_1, \mu_2) : I \to G \times \Delta_G$ *is a Bertrand curve.*
(ii). If $\alpha(s) + \lambda l_2(s) = 0$ *where* $\lambda \neq 0$*=constant, then* $(\gamma, \varrho_1, \varrho_2) : I \to \mathrm{G} \times \Delta_{\mathrm{G}}$ *is a Bertrand curve.*

Proof. (i). If we assume that $\Phi(s) = 0$, it is clear that equation (7) is realized.
(ii). If we assume that $\Phi(s) = \dfrac{\pi}{2}$, it is clear that equation (7) is realized. □

Corollary 4. *For an adapted frame (Bishop-type frame) in 3D Lie groups, the framed curve is always a Bertrand curve.*

Corollary 5. *For an adapted frame (Frenet-type frame) in 3D Lie groups, the curves are Bertrand couples if and only if there exists* λ*=constant where* $\Phi(s)$ *is a constant. Because, the curvature* $\bar{l}_3(s) = l_3(s) = 0$ *for Frenet-type framed curve and by using equation* $\bar{l}_3(s) = l_3(s) - \Phi^{'}(s)$*, we have* Φ *is a constant.*

Corollary 6. *In the Propositions and Theorems obtained, if* $\delta_{\mathrm{G}} = 0$*, the results correspond to the study [11]. Therefore, these results are a generalization of both study [11] and [15].*

4. Mannheim Curves of Framed Curves in 3D Lie Groups

Definition 3. *The framed curves* $(\gamma, \varrho_1, \varrho_2) : I \to \mathrm{G} \times \Delta_{\mathrm{G}}$ *and* $(\overline{\gamma}, \overline{\varrho}_1, \overline{\varrho}_2) : I \to \mathrm{G} \times \Delta_{\mathrm{G}}$ *are called Mannheim couples if there exists a smooth function* $\lambda : I \to \mathbb{R}$ *where*

$$\overline{\gamma}(s) = \gamma(s) + \lambda(s)\varrho_1(s) \tag{13}$$

and

$$\varrho_1(s) = \overline{\varrho}_2(s)$$

for all $s \in I$.

Proposition 5. *If* $(\gamma, \varrho_1, \varrho_2) : I \to \mathrm{G} \times \Delta_{\mathrm{G}}$ *and* $(\overline{\gamma}, \overline{\varrho}_1, \overline{\varrho}_2) : I \to \mathrm{G} \times \Delta_{\mathrm{G}}$ *are Mannheim couples, then* $\lambda \neq 0$ *is a constant.*

Proof. Firstly, by differentiating equation (13) in 3D Lie groups and by using equation (3), we have

$$\overline{\alpha}(s)\overline{\omega}(s) = (\alpha(s) + \lambda(s)l_2(s))\omega(s) + \lambda^{'}(s)\varrho_1(s) + \lambda(s)(l_1(s) - \delta_{\mathrm{G}})\varrho_2(s) \tag{14}$$

Since $\varrho_1(s) = \overline{\varrho}_2(s)$, we get $\lambda^{'}(s) = 0$. That is, $\lambda(s)$ is a constant function on I. □

Theorem 3. *Let* $(\gamma, \varrho_1, \varrho_2) : I \to \mathrm{G} \times \Delta_{\mathrm{G}}$ *be a framed curve with the curvature* (l_1, l_2, l_3, α) *and Lie curvature* δ_{G}*. Then* $(\gamma, \varrho_1, \varrho_2)$ *is a Mannheim curve if and only if there exist* $\lambda \neq 0$*=constant and a smooth function* $\theta : I \to \mathbb{R}$ *where*

$$\lambda(l_1(s) - \delta_{\mathrm{G}})\sin\theta(s) + (\alpha(s) + \lambda l_2(s))\cos\theta(s) = 0 \tag{15}$$

Proof. Assume that $(\gamma, \varrho_1, \varrho_2) : I \to \mathrm{G} \times \Delta_{\mathrm{G}}$ is a Mannheim curve. Since $\varrho_1(s) = \overline{\varrho}_2(s)$, there exists a function θ on I with

$$\overline{\varrho}_1(s) = \sin\theta(s)\varrho_2(s) + \cos\theta(s)\omega(s), \tag{16}$$

$$\overline{\omega}(s) = \cos\theta(s)\varrho_2(s) - \sin\theta(s)\omega(s). \tag{17}$$

If the equations (16) and (17) are substituted in the equation (14), we get

$$-\overline{\alpha}(s)\sin\theta(s) = \alpha(s) + \lambda l_2(s) \tag{18}$$

$$\overline{\alpha}(s)\cos\theta(s) = \lambda(l_1(s) - \delta_{\mathrm{G}}) \tag{19}$$

Consequently, we have equation (15). Conversely, suppose that (15) is provided. If we define a mapping $(\overline{\gamma}, \overline{\varrho}_1, \overline{\varrho}_2) : I \to \mathrm{G} \times \Delta_{\mathrm{G}}$ with

$$\overline{\gamma}(s) = \gamma(s) + \lambda\varrho_1(s), \quad \varrho_1(s) = \overline{\varrho}_2(s)$$

and $\overline{\varrho}_1(s) = \sin\theta(s)\varrho_2(s) + \cos\theta(s)\omega(s)$, then $(\gamma, \varrho_1, \varrho_2)$ and $(\overline{\gamma}, \overline{\varrho}_1, \overline{\varrho}_2)$ are Mannheim mates. $\square$

Remark 1. *Similar to Proposition 3, by using equations $\varrho_1(s) = \overline{\varrho}_2(s)$, (16) and (17), it can be seen that the Lie curvature of the framed curve and the Lie curvature of the Mannheim curve are the same.*

Proposition 6. *Let $(\gamma, \varrho_1, \varrho_2) : I \to \mathrm{G} \times \Delta_{\mathrm{G}}$ and $(\overline{\gamma}, \overline{\varrho}_1, \overline{\varrho}_2) : I \to \mathrm{G} \times \Delta_{\mathrm{G}}$ are Mannheim mates. Then the curvatures $(\bar{l}_1, \bar{l}_2, \bar{l}_3, \overline{\alpha})$ of $(\overline{\gamma}, \overline{\varrho}_1, \overline{\varrho}_2)$ are given by*

$$\begin{aligned}
\bar{l}_1(s) &= -l_1(s)\sin\theta(s) - l_2(s)\cos\theta(s) + \delta_{\mathrm{G}}(1 + \sin\theta(s)), \\
\bar{l}_2(s) &= -l_3(s) + \theta'(s), \\
\bar{l}_3(s) &= l_1(s)\cos\theta(s) - l_2(s)\sin\theta(s) - \delta_{\mathrm{G}}\cos\theta(s), \\
\overline{\alpha}(s) &= \lambda(l_1(s) - \delta_{\mathrm{G}})\cos\theta(s) - (\alpha(s) + \lambda l_2(s))\sin\theta(s).
\end{aligned}$$

Proof. By differentiating equation (16), we have

$$\begin{aligned}
\bar{l}_2(s)\overline{\omega}(s) + (\bar{l}_1(s) - \overline{\delta}_{\mathrm{G}})\overline{\varrho}_2(s) &= (l_3(s)\sin\theta(s) - \theta'(s)\sin\theta(s))\omega(s) \\
&+ (-(l_1(s) - \delta_{\mathrm{G}})\sin\theta(s) - l_2(s)\cos\theta(s))\varrho_1(s) \\
&+ (\cos\theta(s)\theta'(s) - l_3(s)\cos\theta(s))\varrho_2(s).
\end{aligned}$$

Since $\overline{\varrho}_2(s) = \varrho_1(s)$ and $\overline{\delta}_{\mathrm{G}} = \delta_{\mathrm{G}}$, we get

$$\bar{l}_1(s) = -l_1(s)\sin\theta(s) - l_2(s)\cos\theta(s) + \delta_{\mathrm{G}}(1 + \sin\theta(s)).$$

By using equation (17), we have $\bar{l}_2(s) = -l_3(s) + \theta'(s)$. Moreover, by differentiating equation (17), we get

$$\begin{aligned}
-\bar{l}_2(s)\overline{\varrho}_1(s) - \bar{l}_3(s)\overline{\varrho}_2(s) &= (l_3(s)\cos\theta(s) - \theta'(s)\cos\theta(s))\omega(s) \\
&+ (-(l_1(s) - \delta_{\mathrm{G}})\cos\theta(s) + l_2(s)\sin\theta(s))\varrho_1(s) \\
&+ (-\sin\theta(s)\theta'(s) + l_3(s)\sin\theta(s))\varrho_2(s).
\end{aligned}$$

Since $\overline{\varrho}_2(s) = \varrho_1(s)$ and $\overline{\delta}_{\mathrm{G}} = \delta_{\mathrm{G}}$, we have

$$\bar{l}_3(s) = l_1(s)\cos\theta(s) - l_2(s)\sin\theta(s) - \delta_{\mathrm{G}}\cos\theta(s).$$

On the other hand, If the equation (18) is multiplied by $-\sin\theta(s)$ on both sides, and the equation (19) is multiplied by $\cos\theta(s)$ on both sides, then we get

$$\overline{\alpha}(s) = \lambda(l_1(s) - \delta_{\mathrm{G}})\cos\theta(s) - (\alpha(s) + \lambda l_2(s))\sin\theta(s).$$

□

Corollary 7. *Let $(\gamma, \varrho_1, \varrho_2) : I \to \mathrm{G} \times \Delta_{\mathrm{G}}$ be a framed curve with the curvature (l_1, l_2, l_3, α) and Lie curvature δ_{G}.*
(i). If $l_1(s) - \delta_{\mathrm{G}} = 0$ for all $s \in I$, then $(\gamma, \varrho_1, \varrho_2) : I \to \mathrm{G} \times \Delta_{\mathrm{G}}$ is a Mannheim curve.
(ii). If $\alpha(s) + \lambda l_2(s) = 0$ where $\lambda \neq 0$=constant, then $(\gamma, \varrho_1, \varrho_2) : I \to \mathrm{G} \times \Delta_{\mathrm{G}}$ is a Mannheim curve.

Proof. (i). If we assume that $\theta(s) = \dfrac{\pi}{2}$, it is clear that equation (15) is realized.
(ii). If we assume that $\theta(s) = 0$, it is clear that equation (15) is realized. □

Corollary 8. *For an adapted frame (Bishop-type frame) in 3D Lie groups, the framed curve is always a Mannheim curve.*

Corollary 9. *For an adapted frame (Frenet-type frame) in 3D Lie groups, since $\bar{l}_3(s) = l_3(s) = 0$, by using Proposition (6), the curves are Mannheim couples if and only if there exist $\lambda \neq 0$=constant and a smooth function θ where*

$$\begin{aligned}
&\overline{p}(s) = -\theta'(s),\\
&\overline{q}(s) = -(q - \delta_{\mathrm{G}})\sin\theta(s) + p(s)\cos\theta(s) + \delta_{\mathrm{G}},\\
&\overline{\alpha}(s) = -(\alpha(s) - \lambda p(s))\sin\theta(s) + \lambda(q(s) - \delta_{\mathrm{G}})\cos\theta(s),\\
&p(s)\sin\theta(s) + (q(s) - \delta_{\mathrm{G}})\cos\theta(s) = 0.
\end{aligned}$$

Let us now give a theorem that is not valid for regular Bertrand and Mannheim curves in both Euclidean space and 3D Lie groups:

Theorem 4. *Let $(\gamma, \varrho_1, \varrho_2) : I \to \mathrm{G} \times \Delta_{\mathrm{G}}$ be a framed curve with the curvature (l_1, l_2, l_3, α) and Lie curvature δ_{G}. Then $(\gamma, \varrho_1, \varrho_2) : I \to \mathrm{G} \times \Delta_{\mathrm{G}}$ is a Bertrand curve in 3D Lie groups if and only if $(\gamma, \varrho_1, \varrho_2) : I \to \mathrm{G} \times \Delta_{\mathrm{G}}$ is a Mannheim curve in 3D Lie groups.*

Proof. Assume that $(\gamma, \varrho_1, \varrho_2)$ is a Bertrand curve. Then, there exist $\lambda \neq 0$=constant and a smooth function Φ such that

$$\lambda(l_1(s) - \delta_{\mathrm{G})}\cos\Phi(s) - (\alpha(s) + \lambda l_2(s))\sin\Phi(s) = 0.$$

If $\Phi(s) = \theta(s) - \dfrac{\pi}{2}$, we have

$$\lambda(l_1(s) - \delta_{\mathrm{G})})\sin\theta(s) + (\alpha(s) + \lambda l_2(s))\cos\theta(s) = 0.$$

Then, $(\gamma, \varrho_1, \varrho_2)$ is a Mannheim curve. Conversely, suppose that $(\gamma, \varrho_1, \varrho_2)$ is a Mannheim curve. Then, there exist a constant $\lambda \neq 0$ and a smooth function θ such that

$$\lambda(l_1(s) - \delta_{\mathrm{G})}) \sin\theta(s) + (\alpha(s) + \lambda l_2(s)) \cos\theta(s) = 0.$$

If $\theta(s) = \Phi(s) + \dfrac{\pi}{2}$, then we have,

$$\lambda(l_1(s) - \delta_{\mathrm{G})}) \cos\Phi(s) - (\alpha(s) + \lambda l_2(s)) \sin\Phi(s) = 0.$$

Consequently, $(\gamma, \varrho_1, \varrho_2)$ is a Bertrand curve. □

Corollary 10. *In the Propositions and Theorems obtained, if $\delta_{\mathrm{G}} = 0$, the results correspond to the study [11]. Therefore, these results are a generalization of both study [11] and [9].*

Author Contribution Statements The authors jointly worked on the results and they read and approved the final manuscript.

Declaration of Competing Interests The authors declare no potential conflict of interests.

References

[1] Aminov, Y., Differential Geometry and the Topology of Curves, Translated from the Russian by V. Gorkavy, Amsterdam, the Netherlands: Gordon and Breach Science Publishers, 2000.

[2] Bertrand, J., Mémoire sur la théorie des courbes à double courbure, *J. de Methématiques Pures et Appliquées*, 15 (1850), 332–350 (in French).

[3] Çiftçi, Ü., A generalization of Lancert's theorem, *J. Geom. Phys.*, 59 (2009), 1597–1603. https://doi.org/10.1016/j.geomphys.2009.07.016

[4] Crouch, P., Silva Leite, F., The dynamic interpolation problem: On Riemannian manifolds, Lie groups and symmetric spaces, *J. Dyn. Control Syst.*, 1(2) (1995), 177–202. https://doi.org/10.1007/BF02254638

[5] do Espírito-Santo, N., Fornari, S., Frensel, K., Ripoll, J., Constant mean curvature hypersurfaces in a Lie group with a bi-invariant metric, *Manuscripta Math.*, 111(4) (2003), 459–470. https://doi.org/10.1007/s00229-003-0357-5

[6] Doğan Yazıcı, B., Karakuş, S. Ö., Tosun, M., On the classification of framed rectifying curves in Euclidean space, *Math. Methods Appl. Sci.*, 45(18) (2022), 12089–12098. http://dx.doi.org/10.1002/mma.7561

[7] Doğan Yazıcı, B., Okuyucu, O. Z., Tosun, M., Framed curves in three-dimensional Lie groups and a Berry phase model, *J. Geom. Phys.*, 182 (2022), 104682. https://doi.org/10.1016/j.geomphys.2022.104682

[8] Fukunaga, T., Takahashi, M., Existence conditions of framed curves for smooth curves, *J. Geo.*, 108 (2017), 763–774. https://doi.org/10.1007/s00022-017-0371-5

[9] Gök, İ., Okuyucu, O. Z., Ekmekci, N., Yaylı, Y., On Mannheim partner curves in three dimensional Lie groups, *Miskolc Math. Notes*, 15(2) (2014), 467–479. https://doi.org/10.18514/mmn.2014.682

[10] Honda, S., Takahashi, M., Framed curves in the Euclidean space, *Adv. Geo.*, 16 (2016), 265–276. https://doi.org/10.1515/advgeom-2015-0035

[11] Honda, S., Takahashi, M., Bertrand and Mannheim curves of framed curves in the 3-dimensional Euclidean space, *Turk. J. Math.*, 44 (2020), 883–899. https://doi.org/10.3906/mat-1905-63

[12] Izumiya, S., Takeuchi, N., Generic properties of helices and Bertrand curves, *J. Geo.*, 74 (2002), 97–109. https://doi.org/10.1007/PL00012543

[13] Liu, H., Wang, F., Mannheim partner curves in 3-space, *J. Geo.*, 88 (2008), 120–126. https://doi.org/10.1007/s00022-007-1949-0

[14] Okuyucu, 0. Z., Gök, İ., Yaylı, Y., Ekmekci, N., Slant helices in three dimensional Lie groups, *Appl. Math. Comput.*, 221 (2013), 672–683. https://doi.org/10.1016/j.amc.2013.07.008

[15] Okuyucu, 0. Z., Gök, İ., Yaylı, Y., Ekmekci, N., Bertrand curves in three dimensional Lie groups, *Miskolc Math. Notes*, 17(2) (2017), 999–1010. https://doi.org/10.18514/MMN.2017.

[16] Wang, Y., Pei, D., Gao, R., Generic properties of framed rectifying curves, *Mathematics*, 7(1) (2019), 37. https://doi.org/10.3390/math7010037

http://communications.science.ankara.edu.tr

Commun.Fac.Sci.Univ.Ank.Ser. A1 Math. Stat.
Volume 72, Number 3, Pages 721–736 (2023)
DOI:10.31801/cfsuasmas.1186785
ISSN 1303-5991 E-ISSN 2618-6470

Research Article; Received: October 10, 2022; Accepted: March 21, 2023

EXISTENCE OF SOLUTIONS FOR IMPULSIVE BOUNDARY VALUE PROBLEMS ON INFINITE INTERVALS

Sibel DOĞRU AKGÖL
Department of Mathematics, Atilim University, 06830, İncek, Ankara, TÜRKİYE

Abstract. The paper deals with the existence of solutions for a general class of second-order nonlinear impulsive boundary value problems defined on an infinite interval. The main innovative aspects of the study are that the results are obtained under relatively mild conditions and the use of principal and nonprincipal solutions that were obtained in a very recent study. Additional results about the existence of bounded solutions are also provided, and theoretical results are supported by an illustrative example.

1. Introduction

Differential equations with impulses are very convenient mathematical tools for perfectly modeling real-world phenomena with sudden changes in their states. Since it is more realistic to have abrupt changes or jumps in the state than to show constant behavior, they frequently occur in natural sciences. In addition, the efficiency and richness of the relevant theory have contributed to many researchers paying attention to impulsive differential equations in recent years. We refer the reader to the famous books [6, 16] that involve extensive knowledge about qualitative theory and some applications of impulsive differential equations. On the other hand, boundary value problems (BVPs) on unbounded domains naturally appear in fluid mechanics problems such as the unstable gas flow through a porous medium, in plasma physics, and to model many other phenomena, see [1]. In particular, some applications of impulsive BVPs can be found in the papers [9, 17, 18] that have recently been published. There are many results in the literature regarding the existence of solutions to impulsive BVPs, e.g. [2,3,10–12]. Below, we mention some recent results about impulsive BVPs on unbounded domains.

2020 *Mathematics Subject Classification.* 34B37, 34B40.
Keywords. Second-order, nonlinear, impulsive, boundary value problem, principal/nonprincipal solution.

sibel.dogruakgol@atilim.edu.tr; 0000-0003-3513-1046

In [10], for an impulsive BVP with integral boundary conditions of the form

$$\begin{cases} \frac{1}{a(t)}(a(t)x'(t))' + f(t, x(t), x'(t)) = 0, \quad t \neq \tau_k, \\ \Delta x|_{t=\tau_k} = I_k(x(\tau_k)), \quad k = 1, 2, \dots, \\ \Delta x'|_{t=\tau_k} = J_k(x(\tau_k)), \quad k = 1, 2, \dots, \\ a_1 \lim_{t\to-\infty} x(t) - b_1 \lim_{t\to-\infty} a(t)x'(t) = \int\limits_{-\infty}^{\infty} g(x(s))\varphi(s)\,\mathrm{d}s, \\ a_2 \lim_{t\to\infty} x(t) + b_2 \lim_{t\to\infty} a(t)x'(t) = \int\limits_{-\infty}^{\infty} h(x(s))\varphi(s)\,\mathrm{d}s, \end{cases}$$

the existence of solutions is shown under the following hypotheses:

(i) $a_1b_2 + a_2b_1 + a_1a_2\int_{-\infty}^{\infty}\frac{1}{a(s)}\mathrm{d}s > 0$,

(ii) $f \in C(\mathbb{R}\times[0,\infty)\times\mathbb{R},[0,\infty))$ such that $f(t,y,z) \leq u_1(t)u_2(y,z)$ where $u_1 \in L(\mathbb{R},(0,\infty))$ and $u_2 \in C([0,\infty)\times\mathbb{R},[0,\infty))$,

(iii) $g, h \in C(\mathbb{R},[0,\infty))$ are nondecreasing, and $g(x)$, $h(x)$ are bounded provided that x is defined on a bounded set,

(iv) I_k and J_k are bounded functions, and

$$\left[a_2 + b_2\int_{\tau_k}^{\infty}\frac{1}{a(s)}\mathrm{d}s\right]J_k(x(\tau_k)) - \frac{a_2}{a(\tau_k)}I_k(x(\tau_k)) > 0,$$

(v) $\varphi \in C(\mathbb{R},[0,\infty))$ and $\int\limits_{-\infty}^{\infty}\varphi(s)\,\mathrm{d}s < \infty$,

(vi) $a \in C(\mathbb{R},(0,\infty))$ and $\int\limits_{-\infty}^{\infty}\frac{1}{a(s)}\mathrm{d}s < \infty$.

In [12], the second order impulsive BVP

$$\begin{cases} x''(t) = -f(t, x(t), x'(t)), \quad t \neq \tau_k, \\ x(\tau_k+) = a_kx(\tau_k), \quad k = 1, 2, \dots, \\ a_0x(0) - b_0x'(0) = \alpha, \\ a_1x(1) - b_1x'(1) = \beta \end{cases} \tag{1}$$

is studied, and the existence of solutions is shown via the upper and lower solutions method.

In [2], the existence of solutions was shown for the impulsive BVP

$$\begin{cases} (a(t)y')' + b(t)y = f(t,y), & t \neq \tau_k, \\ \Delta y' + b_ky = g_k(y), & t = \tau_k, \\ y(t_0) = y_0, \\ y(t) = c_1v(t) + c_2u(t) + o(v^{\mu}(t)u(t)), & t \to \infty,\ \mu \in (0,1), \end{cases} \tag{2}$$

where u and v are the principal and nonprincipal solutions of the corresponding homogeneous equation. Observe in (1) that impulse effects occur only on the solutions while (2) has continuous solutions as the impulse effects occur only on the derivatives of the solutions. The method of the paper [2] is different from the other studies in the literature as it relies on principal and nonprincipal solutions. A similar approach was applied in [3] and [7], where a particular case of the impulsive BVP (2) was considered in [3], while [7] dealt with a BVP without impulse effects.

Motivated by the studies above, we consider the second-order nonlinear differential equation under impulse effects

$$\begin{cases} (a(t)y')' + b(t)y = f(t,y), & t \neq \tau_k, \\ \Delta y + a_k y = f_k(y), & t = \tau_k, \\ \Delta(a(t)y') + b_k y + c_k y' = g_k(y), & t = \tau_k, \end{cases} \tag{3}$$

satisfying the boundary conditions

$$y(a) = 0, \quad y(t) = O(v(t)),\ t \to \infty \tag{4}$$

where $a \geq t_0$, $a(t), b(t) \in \mathrm{PLC}([t_0,\infty),\mathbb{R})$ with $a(t) > 0$, $f \in \mathrm{PLC}([t_0,\infty)\times\mathbb{R},\mathbb{R})$, $\{a_k\}$, $\{b_k\}$ and $\{c_k\}$ are sequences of real numbers, $f_k, g_k \in \mathrm{PLC}(\mathbb{R},\mathbb{R})$ for each $k \in \mathbb{N}$, $\{\tau_k\}$ is the sequence of impulses satisfying $\tau_{k+1} > \tau_k$ for all $k \in \mathbb{N}$ and $\lim_{k\to\infty} |\tau_k| = \infty$, and Δ is the impulse operator defined by $\Delta y(\tau_k) = y(\tau_k^+) - y(\tau_k^-)$ with $y(\tau_k^\pm) = \lim_{t\to\tau_k^\pm} y(t)$. Note that $\mathrm{PLC}[t_0,\infty)$ is the set of functions y such that $y(t)$ is continuous on $(\tau_k, \tau_{k+1}]$, $y(\tau_k-) = y(\tau_k)$ and $y(\tau_k+)$ exists for each $k = 1, 2, \ldots$. For brevity, we use the notations $\underline{n}(t) := \inf\{k :\ \tau_k \geq t\}$ and $\overline{n}(t) := \sup\{k :\ \tau_k < t\}$.

We aim to prove the existence of solutions of the second-order nonlinear impulsive BVP (3)-(4) with discontinuous solutions under some mild conditions that depend on the principal and nonprincipal solutions of the homogeneous equation

$$\begin{cases} (a(t)y')' + b(t)y = 0, & t \neq \tau_k, \\ \Delta y + a_k y = 0, & t = \tau_k, \\ \Delta(a(t)y') + b_k y + c_k y' = 0, & t = \tau_k \end{cases} \tag{5}$$

associated with equation (3).

In the present work, the impulses affect both the solutions and their derivatives, and the impulse conditions occurring in the third line of (3) are the so-called mixed type conditions because they include both the solution and its derivative. Hence, the equation under consideration is quite general. On the other hand, the conditions determined on the functions that are on the right-hand side of the nonhomogeneous equation (3) are weaker than the conditions in previous studies. Our conditions do not directly require the functions to be bounded or monotonic. Another novelty is the use of principal and nonprincipal solutions of the corresponding homogeneous equation (5).

2. Preliminaries

In this section, we state some auxiliary lemmas that will be utilized in the rest of the paper.

The existence and some properties of principal and nonprincipal solutions for impulsive differential equations with continuous solutions

$$\begin{cases} (a(t)y')' + b(t)y = 0, & t \neq \tau_k, \\ \Delta a(t)y' + b_k y = 0, & t = \tau_k \end{cases} \tag{6}$$

was proved in [13], where it was shown that equation (6) has two linearly independent solutions u_0 and v_0 satisfying

$$\lim_{t\to\infty} \frac{u_0(t)}{v_0(t)} = 0, \quad \int_a^\infty \frac{\mathrm{d}t}{a(t)u_0^2(t)} = \infty, \quad \int_a^\infty \frac{\mathrm{d}t}{a(t)v_0^2(t)} < \infty, \quad \frac{u_0'(t)}{u_0(t)} < \frac{v_0'(t)}{v_0(t)},\ t \geq a$$

provided that (6) has a positive solution, and a is sufficiently large. Such functions u_0 and v_0 are said to be principal and nonprincipal solutions of (6), respectively.

The counterpart of the above lemma for differential equations having impulse effects not only on the derivative of the solution but also on the solution was given very recently in [4] and improved in [5] for the more general impulsive differential equations of the form (5). The statement of the related lemma is given below for completeness.

Lemma 1. ([5]) Let $(1-a_k)(1-c_k/a(\tau_k)) > 0$, $k \in \mathbb{N}$ and suppose equation (5) has a positive solution. Then, there exist two linearly independent solutions u and v of (5) satisfying the following conditions:

$$\lim_{t\to\infty} \frac{u(t)}{v(t)} = 0, \tag{7}$$

$$\int_a^\infty \frac{\mu(t,a)}{a(t)u^2(t)}\mathrm{d}t = \infty, \quad \int_a^\infty \frac{\mu(t,a)}{a(t)v^2(t)}\mathrm{d}t < \infty,$$

$$\frac{u'(t)}{u(t)} < \frac{v'(t)}{v(t)}, \quad t \geq a,$$

where a is arbitrarily large, and

$$\mu(t,a) = \prod_{k=\underline{n}(a)}^{\overline{n}(t)} (1-a_k)(1-c_k/a(\tau_k)).$$

Namely, u is the principal, and v is a nonprincipal solution.

Remark 1. *If $u > 0$ is a principal solution of* (5)*, then, a nonprincipal solution is of the form*

$$v(t) = u(t) \int_{t_0}^{t} \frac{\mu(s,a)}{a(s)u^2(s)}\mathrm{d}s. \tag{8}$$

Conversely, if $v > 0$ is a nonprincipal solution of (5)*, then, the principal solution is of the form*

$$u(t) = v(t)\int_t^\infty \frac{1}{\mu(\infty,s)a(s)v^2(s)}\mathrm{d}s.$$

In addition, we provide below some definitions and compactness criteria that will be needed in the future.

Definition 1. ([15]) Let $1 \le p < \infty$ and Y be an arbitrary measure space. We define $L^p(Y)$ to be the space of functions f such that

$$||f||_p = \left(\int_Y |f|^p \mathrm{d}\mu\right)^{1/p} < \infty.$$

Definition 2. ([15]) Let $1 \le p < \infty$. We define $\ell^p(Y)$ to be the space of sequences y_k such that

$$\sum_{k=1}^{\infty} |y_k|^p < \infty.$$

Theorem 1. ([14]) Let $Y \in \mathbb{R}^n$. A set $S \subset L^p(Y)$, $1 \le p < \infty$ is compact if

(i) there exists some $a > 0$ such that $\|y\|_{L^p(Y)} \le a$ for all $y \in S$,

(ii) $\|(\varphi_h y) - y\|_{L^p(Y)} \to 0$ as $h \to 0$, where $(\varphi_h y)(x) := y(x_1 + h, x_2 + h \ldots x_n + h)$, $x \in Y$.

Theorem 2. ([8]) Let $Y \in \mathbb{R}^n$. A set $S \subset l^p(Y)$, $1 \le p < \infty$ is totally bounded if, and only if

(i) S is pointwise bounded,

(ii) for every $\epsilon > 0$ and $y \in S$, there is some $n \in \mathbb{N}$ such that $\sum_{k>n} |y_k|^p < \epsilon^p$.

3. Main Results

We define the Banach space

$$X = \left\{ y \in \mathrm{PLC}([a,\infty),\mathbb{R}) : \frac{|y(t)|}{v(t)} \text{ is bounded} \right\}$$

endowed with the norm

$$\|y\| = \sup_{t\in[a,\infty)} \frac{|y(t)|}{v(t)}$$

and, introduce the operator

$$(\mathcal{T}y)(t) = -\,u(t)\Bigg\{\int\limits_a^t \frac{1}{a(s)u^2(s)}\Bigg(\int\limits_s^\infty \frac{u(r)}{\mu(r,s)}f(r,y(r))\mathrm{d}r + \sum_{k=\underline{n}(s)}^{\infty}\frac{h_k}{\mu(k,s)}\Bigg)\mathrm{d}s - \sum_{k=\underline{n}(a)}^{\overline{n}(t)}\frac{f_k(y(\tau_k))}{(1-a_k)u(\tau_k)}\Bigg\}, \tag{9}$$

where $h_k = (1-a_k)u(\tau_k)g_k(y(\tau_k)) - \big[(a(\tau_k)-c_k)u'(\tau_k) - b_k u(\tau_k)\big]f_k(y(\tau_k))$ and $y \in X$.

We aim to show that $\mathcal{T}y$ has at least one fixed point by applying Schauder fixed point theorem.

For this purpose, we define the set $E := \big\{y \in X : |y(t)| \le v(t)\big\}$ which is convex, closed, and bounded, and assume the following hypotheses hold:

(H1) There exist some functions $q_j \in \mathrm{C}(\mathbb{R}_+,\mathbb{R}_+)$, $j=1,2,3$, $p_i \in \mathrm{C}([t_0,\infty),\mathbb{R}_+)$, $i=1,2$ and real sequences $\{\alpha_k\}, \{\beta_k\}$ such that

$$|f(t,y)| \le p_1(t)q_1\left(\frac{|y|}{v(t)}\right) + p_2(t), \quad t \ge a, \tag{10}$$

$$\big|f_k(y)\big| \le \alpha_k q_2\left(\frac{|y|}{v(\tau_k)}\right), \quad \big|g_k(y)\big| \le \beta_k q_3\left(\frac{|y|}{v(\tau_k)}\right), \quad \tau_k \ge a.$$

(H2) $\displaystyle\int_a^\infty \frac{u(s)}{\mu(s,a)}(p_1(s)+p_2(s))\mathrm{d}s + \sum_{k=\underline{n}(a)}^{\infty}\frac{H_k}{\mu(k,a)} = O(1), \quad t\to\infty,$
where $H_k = (1-a_k)u(\tau_k)\beta_k + |(a(\tau_k)-c_k)u'(\tau_k) - b_k u(\tau_k)|\alpha_k$

(H3) $\displaystyle\sum_{k=\underline{n}(a)}^{\overline{n}(t)}\frac{\alpha_k}{(1-a_k)u(\tau_k)} = O(1), \quad t\to\infty.$

Lemma 2. *The operator $\mathcal{T}$ given in (9) maps E onto E.*

Proof. First, we prove that $\mathcal{T}y \in \mathrm{PLC}[a,\infty)$.

Let $y \in X$ and $t_1 \in [a,\infty)$ with $t < t_1$, and $t_1 \ne \tau_l$, $l = 1,2,\ldots$. Then

$$\begin{aligned}|(\mathcal{T}y)(t) - (\mathcal{T}y)(t_1)| \le{}& |u(t)-u(t_1)|\Bigg\{\int\limits_a^t \frac{1}{a(s)u^2(s)}\Bigg(\int\limits_s^\infty \frac{u(r)}{\mu(r,s)}|f(r,y(r))|\mathrm{d}r \\ &+ \sum_{k=\underline{n}(s)}^{\infty}\frac{|h_k|}{\mu(k,s)}\Bigg)\mathrm{d}s + \sum_{k=\underline{n}(a)}^{\overline{n}(t)}\frac{|f_k(y(\tau_k))|}{(1-a_k)u(\tau_k)}\Bigg\} \\ &+ u(t_1)\Bigg\{\int\limits_t^{t_1} \frac{1}{a(s)u^2(s)}\Bigg(\int\limits_s^\infty \frac{u(r)}{\mu(r,s)}|f(r,y(r))|\mathrm{d}r\end{aligned}$$

$$+ \sum_{k=\underline{n}(s)}^{\infty} \frac{|h_k|}{\mu(k,s)}\Big) \mathrm{d}s + \sum_{k=\underline{n}(t)}^{\overline{n}(t_1)} \frac{|f_k(y(\tau_k))|}{(1-a_k)u(\tau_k)}\Big\}.$$

Since $|y(t)|/v(t)$ is bounded, $\exists M > 0$ such that

$$\frac{|y(t)|}{v(t)} \le M.$$

So, from continuity of q_j, there can be found positive constants c_j such that $\max_{0\le t\le M} q_j(t) = c_j$, $j = 1, 2, 3$. Hence, in view of (H1), we have the following estimates:

$$|f(r,y(r))| \le p_1(r)q_1\Big(\frac{|y(r)|}{v(r)}\Big) + p_2(r) \le c_1 p_1(r) + p_2(r) \le c\big[p_1(r) + p_2(r)\big], \quad (11)$$

$$\begin{aligned} |h_k| &\le (1-a_k)u(\tau_k)\beta_k q_3\Big(\frac{|y(\tau_k)|}{v(\tau_k)}\Big) + |(a(\tau_k)-c_k)u'(\tau_k) - b_k u(\tau_k)|\alpha_k q_2\Big(\frac{|y(\tau_k)|}{v(\tau_k)}\Big) \\ &\le c_3(1-a_k)u(\tau_k)\beta_k + c_2|(a(\tau_k)-c_k)u'(\tau_k) - b_k u(\tau_k)|\alpha_k \ \le\ cH_k, \end{aligned} \quad (12)$$

$$|f_k(y(\tau_k))| \le \frac{\alpha_k}{(1-a_k)u(\tau_k)} q_2\Big(\frac{|y(\tau_k)|}{v(\tau_k)}\Big) \le c_2 \frac{\alpha_k}{(1-a_k)u(\tau_k)} \le c\frac{\alpha_k}{(1-a_k)u(\tau_k)}, \quad (13)$$

where $c = \max\{1, c_1, c_2, c_3\}$.

Using the above estimates and the expansion $1/\mu(s,\nu) = \mu(s,a)/\mu(\nu,a)$, we can proceed as follows:

$$\begin{aligned} |(\mathcal{T}y)(t) - (\mathcal{T}y)(t_1)| \le{}& c|u(t) - u(t_1)|\Big\{\int_a^t \Big(\frac{\mu(s,a)}{a(s)u^2(s)} \int_a^\infty \frac{u(r)}{\mu(r,a)}\,(p_1(r)+p_2(r))\,\mathrm{d}r \\ &+ \sum_{k=\underline{n}(a)}^{\infty} \frac{H_k}{\mu(k,a)}\Big)\mathrm{d}s + \sum_{k=\underline{n}(a)}^{\overline{n}(t)} \frac{\alpha_k}{(1-a_k)u(\tau_k)}\Big\} \\ &+ cu(t_1)\Big\{\int_t^{t_1} \frac{\mu(s,a)}{a(s)u^2(s)}\Big(\int_a^\infty \frac{u(r)}{\mu(r,a)}\,(p_1(r)+p_2(r))\,\mathrm{d}r \\ &+ \sum_{k=\underline{n}(a)}^{\infty} \frac{H_k}{\mu(k,a)}\Big)\mathrm{d}s + \sum_{k=\underline{n}(t)}^{\overline{n}(t_1)} \frac{\alpha_k}{(1-a_k)u(\tau_k)}\Big\}. \end{aligned}$$

It follows from (H2) that $(\mathcal{T}y)(t) \to (\mathcal{T}y)(t_1)$ as $t \to t_1-$.

In a similar way, one can show that $\lim_{t\to t_1+}(\mathcal{T}y)(t) = (\mathcal{T}y)(t_1)$ for $t_1 \ne \tau_l$, $l = 1, 2, \ldots$, and $\lim_{t\to\tau_l+}(\mathcal{T}y)(t)$ exist for all $l = 1, 2, \ldots$ Hence, $\mathcal{T}y(t)$ is piecewise left continuous on $[a,\infty)$.

Now, from (11), (12) and (13) one has

$$|(\mathcal{T}y)(t)| \leq cu(t)\bigg\{\int_a^t \frac{\mu(s,a)}{a(s)u^2(s)}\bigg(\int_a^\infty \frac{u(r)}{\mu(r,a)}\big(p_1(r)+p_2(r)\big)\mathrm{d}r + \sum_{k=\underline{n}(a)}^{\infty}\frac{H_k}{\mu(k,a)}\bigg)\mathrm{d}s + \sum_{k=\underline{n}(a)}^{\overline{n}(t)}\frac{\alpha_k}{(1-a_k)u(\tau_k)}\bigg\}.$$

In view of (H2) and (H3) we may write

$$\int_a^\infty \frac{u(r)}{\mu(r,a)}\big(p_1(r)+p_2(r)\big)\mathrm{d}r + \sum_{k=\underline{n}(a)}^{\infty}\frac{H_k}{\mu(k,a)} \leq \frac{1}{2c} \tag{14}$$

and

$$\sum_{k=\underline{n}(a)}^{\overline{n}(t)}\frac{\alpha_k}{(1-a_k)u(\tau_k)} \leq \frac{1}{2c}$$

for some sufficiently large a. Then, from the relation (8) we have

$$|(\mathcal{T}y)(t)| \leq \frac{u(t)}{2}\bigg\{\int_a^t \frac{\mu(s,a)}{a(s)u^2(s)}\mathrm{d}s + \sum_{k=\underline{n}(a)}^{\overline{n}(t)}\frac{\alpha_k}{(1-a_k)u(\tau_k)}\bigg\} = \frac{v(t)}{2} + \frac{u(t)}{2}.$$

Using (7) we conclude that $|(\mathcal{T}y)(t)| \leq v(t)$. Hence, $\mathcal{T}y \in E$. □

Lemma 3. *$\mathcal{T}$ is a continuous operator.*

Proof. Take a sequence $\{y_n\} \in E$ such that $\lim_{n\to\infty} y_n = y \in E$. Using (11), (12) and (13) we can write

$$\begin{aligned}|(\mathcal{T}y_n)(t) - (\mathcal{T}y)(t)| \leq & u(t)\bigg\{\int_a^t \frac{\mu(s,a)}{a(s)u^2(s)}\bigg(\int_s^\infty \frac{u(r)}{\mu(r,a)}|f(r,y_n(r)) - f(r,y(r))|\mathrm{d}r \\ & + \sum_{k=\underline{n}(s)}^{\infty}\frac{1}{\mu(k,a)}\Big[(1-a_k)u(\tau_k)|g_k(y_n(\tau_k)) - g_k(y(\tau_k))| \\ & + |(a(\tau_k)-c_k)u'(\tau_k) - b_k u(\tau_k)|f_k(y_n(\tau_k)) - f_k(y(\tau_k))|\Big]\bigg)\mathrm{d}s \\ & + \sum_{k=\underline{n}(a)}^{\overline{n}(t)}\frac{1}{(1-a_k)u(\tau_k)}|f_k(y_n(\tau_k)) - f_k(y(\tau_k))|\bigg\} \\ \leq & 2cu(t)\bigg\{\int_a^t \frac{\mu(s,a)}{a(s)u^2(s)}\bigg(\int_s^\infty \frac{u(r)}{\mu(r,a)}\left(p_1(r)+p_2(r)\right)\mathrm{d}r\end{aligned}$$

$$+ \sum_{k=\underline{n}(s)}^{\infty} \frac{H_k}{\mu(k,a)}\Big)\mathrm{d}s + \sum_{k=\underline{n}(a)}^{\overline{n}(t)} \frac{\alpha_k}{(1-a_k)u(\tau_k)}\Big\}.$$

From (H2) and (H3), it can be seen that the above expression is finite for all $t \in [a,\infty)$. Thus, applying Lebesgue dominated convergence theorem and Weierstrass-M test, we obtain

$$\lim_{n\to\infty} \|\mathcal{T}y_n - \mathcal{T}y\| \to 0.$$

Hence, $\mathcal{T}$ is a continuous operator.

□

Lemma 4. *$\mathcal{T}$ is a relatively compact operator.*

Proof. Pick an arbitrary sequence $\{y_n\} \in E$. We wish to prove that there exists a subsequence $\{y_{n_i}\} \in E$ such that $\mathcal{T}y_{n_i}$ is convergent in E. If we define

$$f_n(r) := \frac{u(r)}{\mu(r,s)} f(r, y_n(r)), \qquad g_n(\tau_k) := \frac{f_k(y_n(\tau_k))}{(1-a_k)u(\tau_k)},$$

and

$$h_n(\tau_k) := \frac{1}{\mu(k,s)}\big[(1-a_k)u(\tau_k)g_k(y_n(\tau_k)) + [(a(\tau_k)-c_k)u'(\tau_k) - b_k u(\tau_k)]f_k(y_n(\tau_k))\big]$$

then, $\mathcal{T}$ can be decomposed as $\mathcal{T} = \mathcal{T}_1 + \mathcal{T}_2 + \mathcal{T}_3$, where

$$(\mathcal{T}_1 y_n)(t) = u(t) \int_a^t \frac{\mu(s,a)}{a(s)u^2(s)} \int_s^{\infty} f_n(r)\mathrm{d}r\mathrm{d}s,$$

$$(\mathcal{T}_2 y_n)(t) = u(t) \int_a^t \frac{\mu(s,a)}{a(s)u^2(s)} \sum_{k=\underline{n}(s)}^{\infty} h_n(\tau_k)\mathrm{d}s, \qquad (\mathcal{T}_3 y_n)(t) = u(t) \sum_{k=\underline{n}(a)}^{\overline{n}(t)} g_n(\tau_k).$$

As in (14), there is a constant $m_1 > 0$ such that

$$\|f_n\|_{L^1([a,\infty))} \le m_1, \quad n \ge 1.$$

Thus, the first hypothesis of Lemma 1 holds. Now, for $(\varphi_h f)(s) = f(s+h)$ from (10) and (11) we may write

$$\begin{aligned}\int_a^{\infty} |(\varphi_h f_n)(s) - f_n(s)|\mathrm{d}s &\le \int_{a+h}^{\infty} |f_n(s)|\mathrm{d}s + \int_a^{\infty} |f_n(s)|\mathrm{d}s \\ &\le 2\int_a^{\infty} |f_n(s)|\mathrm{d}s \le 2c \int_a^{\infty} \frac{u(s)}{\mu(s,a)}(p_1(s)+p_2(s))\mathrm{d}s.\end{aligned}$$

In view of (H2), we apply the Lebesgue dominated convergence theorem, and we obtain the second hypothesis of Lemma 1. Hence, Lemma 1 asserts that there exists a convergent subsequence $\{f_{n_i}\} \in L^1([a,\infty))$. Since f_{n_i} is continuous, we conclude that

$$\int_a^\infty |\bar{f}(r)|\mathrm{d}r = \lim_{i\to\infty} \int_a^\infty |f_{n_i}(r)|\mathrm{d}r,$$

where

$$\bar{f}(r) = \frac{u(r)}{\mu(r,a)} f(r, y(r)).$$

Then,

$$\frac{|(\mathcal{T}_1 y_{n_i})(t) - (\mathcal{T}_1 y)(t)|}{v(t)} \leq \frac{u(t)}{v(t)} \int_a^t \frac{\mu(s,a)}{a(s)u^2(s)} \int_s^\infty |f_{n_i}(r) - \bar{f}(r)|\mathrm{d}r\mathrm{d}s.$$

In view of (H2), again Lebesgue dominated convergence theorem applies, and so

$$\lim_{i\to\infty} \|\mathcal{T}_1 y_{n_i} - \mathcal{T}_1 y\| = 0.$$

Next, we need to utilize Lemma 2 to show that $\mathcal{T}_2$ is a compact operator. Proceeding as in (12), we see that

$$|h_n(\tau_k)| \leq c\frac{H_k}{\mu(k,a)}.$$

But (H2) and (H3) imply that each element of the sets $\{f_n\}$, $\{h_n\}$ is pointwise bounded. This means that the first hypothesis of Lemma 2 holds.

For an arbitrary $\epsilon > 0$, we may choose a sufficiently large $j \in \mathbb{N}$ so that

$$\sum_{k=j}^\infty \frac{H_k}{\mu(k,a)} < \frac{\epsilon}{c},$$

then we get

$$\sum_{k=j}^\infty |h_n(\tau_k)| < \epsilon.$$

Thus, by virtue of Lemma 2, the set $\{h_n\}$ is compact in $\ell^1([a,\infty))$ which means that there exists a convergent subsequence $\{h_{n_i}\} \in \ell^1([a,\infty))$ such that

$$\lim_{i\to\infty} \sum_{k=\underline{n}(a)}^\infty |h_{n_i}(\tau_k) - \bar{h}_k| = 0,$$

where

$$\bar{h}_k := \frac{h_k}{\mu(k,a)}.$$

Hence,

$$\frac{|(\mathcal{T}_2 y_{n_i})(t) - (\mathcal{T}_2 y)(t)|}{v(t)} \leq \frac{u(t)}{v(t)} \int_a^t \frac{\mu(s,a)}{a(s)u^2(s)} \sum_{k=\underline{n}(s)}^\infty |h_{n_i}(\tau_k) - \bar{h}_k|.$$

Applying Weierstrass-M test it is seen that $\mathcal{T}_2$ has a convergent subsequence in E, i.e.,

$$\lim_{i\to\infty} \|\mathcal{T}_2 y_{n_i} - \mathcal{T}_2 y\| = 0.$$

Finally, since $\mathcal{T}_3$ is a finite sum, it is uniformly convergent. Hence,

$$\lim_{i\to\infty} \frac{|(\mathcal{T}_3 y_{n_i})(t) - (\mathcal{T}_3 y)(t)|}{v(t)} = 0.$$

Since each of $\mathcal{T}_1$, $\mathcal{T}_2$ and $\mathcal{T}_3$ is relatively compact in E, then so is $\mathcal{T}$. This completes the proof. □

Lemma 5. *Let y be a fixed point of the operator* (9). *Then, y is a solution of equation* (3).

Proof. Suppose y is a fixed point of the operator $\mathcal{T}$. Then,

$$y(t) = u(t)\left\{ I(t) + \sum_{k=\underline{n}(a)}^{\overline{n}(t)} \frac{f_k(y(\tau_k))}{(1-a_k)u(\tau_k)} \right\},$$

where

$$I(t) := -\int_a^t \frac{1}{a(s)u^2(s)} \left(\int_s^\infty \frac{u(r)}{\mu(r,s)} f(r, y(r))\mathrm{d}r + \sum_{k=\underline{n}(s)}^{\infty} \frac{h_k}{\mu(k,s)} \right) \mathrm{d}s.$$

For $t \neq \tau_l$, $l = 1, 2, \ldots$, we have

$$y'(t) = u'(t)\left\{ I(t) + \sum_{k=\underline{n}(a)}^{\overline{n}(t)} \frac{f_k(y(\tau_k))}{(1-a_k)u(\tau_k)} \right\} - \frac{J(t)}{a(t)u(t)}$$

where

$$J(t) = \int_t^\infty \frac{u(r)}{\mu(r,t)} f(r, y(r))\mathrm{d}r + \sum_{k=\underline{n}(t)}^{\infty} \frac{h_k}{\mu(k,t)}.$$

Thus,

$$\begin{aligned}(a(t)y'(t))' + b(t)y(t) =& [(a(t)u'(t))' + b(t)u(t)] \left\{ I(t) + \sum_{k=\underline{n}(a)}^{\overline{n}(t)} \frac{f_k(y(\tau_k))}{(1-a_k)u(\tau_k)} \right\} \\ &+ 2a(t)u'(t)I'(t) + u(t)(a(t)I'(t))'.\end{aligned}$$

It is easy to see that

$$2a(t)u'(t)I'(t) = -\frac{2u'(t)}{u^2(t)} J(t)$$

and

$$u(t)(a(t)I'(t))' = \frac{2u'(t)}{u^2(t)} J(t) + \frac{1}{\mu(t,t)} f(t, y(t)).$$

From $\mu(t,t) = 1$, we conclude that

$$(a(t)y'(t))' + b(t)y(t) = f(t, y(t)). \tag{15}$$

Now, we need to show that impulsive conditions hold. Let $t = \tau_l$. Clearly $I(t)$ is a continuous function, namely $I(\tau_l+) = I(\tau_l)$. Thus, we have

$$\begin{aligned}\Delta y|_{t=\tau_l} =& u(\tau_l+)\Big\{I(\tau_l) + \sum_{k=\underline{n}(a)}^{l-1} \frac{f_k(y(\tau_k))}{(1-a_k)u(\tau_k)} + \frac{f_l(y(\tau_l))}{(1-a_l)u(\tau_l)}\Big\} - \\ & u(\tau_l)\Big\{I(\tau_l) + \sum_{k=\underline{n}(a)}^{l-1} \frac{f_k(y(\tau_k))}{(1-a_k)u(\tau_k)}\Big\} \\ =& \Delta u|_{t=\tau_l}\Big\{I(\tau_l) + \sum_{k=\underline{n}(a)}^{l-1} \frac{f_k(y(\tau_k))}{(1-a_k)u(\tau_k)}\Big\} + \frac{u(\tau_l+)f_l(y(\tau_l))}{(1-a_l)u(\tau_l)}.\end{aligned}$$

From $u(\tau_l+) = (1-a_l)u(\tau_l)$ it follows that

$$\Delta y|_{t=\tau_l} + a_l y(\tau_l) = f_l(y(\tau_l)). \tag{16}$$

Finally, using

$$\frac{1}{\mu(k, l+1)} = \prod_{j=l+1}^{k} (1-a_j)^{-1}(1 - c_j/a(\tau_j))^{-1} = (1-a_l)(1-c_l/a(\tau_l))\frac{1}{\mu(k,l)}$$

we can write $J(\tau_l+) = (1-a_l)(1-c_l/a(\tau_l))J(\tau_l) - h_l$, and hence

$$a(\tau_l+)u(\tau_l+)I'(\tau_l+) = -\frac{1}{u(\tau_l+)}J(\tau_l+) = ((a(\tau_l) - c_l))u(\tau_l)I'(\tau_l) + \frac{h_l}{(1-a_l)u(\tau_l)}.$$

Then, we have

$$\begin{aligned}a(\tau_l+)y'(\tau_l+) =& a(\tau_l+)u'(\tau_l+)\Big\{I(\tau_l) + \sum_{k=\underline{n}(a)}^{l} \frac{f_k(y(\tau_k))}{(1-a_k)u(\tau_k)}\Big\} + a(\tau_l+)u(\tau_l+)I'(\tau_l+) \\ =& \big[(a(\tau_l) - c_l)u'(\tau_l) - b_l u(\tau_l)\big]\Big\{I(\tau_l) + \sum_{k=\underline{n}(a)}^{l-1} \frac{f_k(y(\tau_k))}{(1-a_k)u(\tau_k)} + \frac{f_l(y(\tau_l))}{(1-a_l)u(\tau_l)}\Big\} \\ & + a(\tau_l)u(\tau_l)I'(\tau_l) + \frac{h_l}{(1-a_l)u(\tau_l)}\end{aligned}$$

which implies that

$$\Delta(ay') + b_l y(\tau_l) + c_l y'(\tau_l) = g_l(y(\tau_l)). \tag{17}$$

Hence, from (15), (16), and (17) we conclude that $y(t)$ is a solution of (3). □

Theorem 3. *The impulsive differential equation* (3) *with the boundary conditions* (4) *has at least one solution, provided that the hypotheses (H1)-(H3) hold, where u and v are principal and nonprincipal solutions of the homogeneous equation* (5)*.*

Proof. From Lemma 2, Lemma 3 and Lemma 4 it is seen that the Schauder fixed point theorem's all hypotheses hold. Thus, the operator $\mathcal{T}$ given in (9) has a fixed point, say y. In view of Lemma 5, the fixed point y is a solution of the equation (3).

On the other hand, by using the hypotheses (H1)-(H3) it is not hard to see that $I(a) = 0$ which implies

$$y(a) = u(a)\left\{I(a) + \sum_{k=\underline{n}(a)}^{\overline{n}(a)} \frac{f_k(y(\tau_k))}{(1-a_k)u(\tau_k)}\right\} = 0.$$

Proceeding as in Lemma 3, we obtain $|y(t)| \le v(t)$ from which we can write

$$\lim_{t\to\infty} \frac{|y(t)|}{v(t)} \le 1,$$

which means that $y(t) = O(v(t))$ as $t \to \infty$. Thus, the boundary conditions in (4) hold. This completes the proof. □

4. Examples

This section is devoted to illustrative examples that demonstrate the efficiency of the above result.

Example 1. *Consider the impulsive BVP*

$$\begin{cases} (t^2y')' - 2y = \ln\left(1 + \dfrac{y^2}{t^2(y^2+1)}\right), & t \ne \tau_k, \\ \Delta y - \dfrac{y}{k} = \sin\left(\dfrac{y}{k^4(k+1)^2}\right), & t = \tau_k, \\ \Delta(t^2y') - ky' = \arctan(y/k^3), & t = \tau_k, \\ y(1) = 0, \quad y(t) = O(v(t)),\ t \to \infty. \end{cases} \tag{18}$$

Observe that $a(t) = t^2$, $b(t) = -2$, $a_k = -1/k$, $b_k = 0$, $c_k = -k$, *and so* $(1-a_k)(1-c_k/a(\tau_k)) = (1+1/k)^2$. *Furthermore,*

$$f(t,y) = \ln\left(1 + \frac{y^2}{t^2(y^2+1)}\right) \le \frac{1}{t^2}\frac{y^2}{y^2+1} \le \frac{1}{t^2},$$

$$f_k(y) = \sin\left(\frac{y}{k^4(k+1)^2}\right) \le \frac{1}{(k^2+k)^2}\frac{|y|}{k^2}$$

and

$$g_k(y) = \arctan\left(\frac{y}{k^3}\right) \le \frac{1}{k}\frac{|y|}{k^2}.$$

By direct computations, it can be shown that $u(t) = kt^{-2}$ *is the principal, and* $v(t) = kt$, $t \in (k-1, k]$ *is a nonprincipal solution of the associated homogeneous* *impulsive equation*

$$\begin{cases}(t^2y')' - 2y = 0, & t \neq \tau_k,\\ \Delta y - \dfrac{y}{k} = 0, & t = \tau_k,\\ \Delta(t^2y') - ky' = 0, & t = \tau_k.\end{cases}$$

Thus, one may choose $p_1(t) = 1/t^2$, $p_2(t) = 0$, $q_1(y) = 1$, $q_2(y) = q_3(y) = y$, $\alpha_k = 1/(k^2+k)^2$ *and* $\beta_k = 1/k$ *so that (H1) is satisfied.*

Now, we need to check for the validity of the hypotheses (H2) and (H3). Let $a = 2$. *Observe that* $\overline{n}(s) = i$ *if* $s \in (i-1, i]$, *and*

$$\mu(s,a) = \mu(i,2) = \prod_{k=2}^{i} \frac{(k+1)^2}{k^2} = \frac{(i+1)^2}{4}, \quad H_k = \frac{k+1}{k^3} + \frac{2}{k^3(k+1)}.$$

So, we have

$$\begin{aligned}\int_a^\infty \frac{u(s)}{\mu(s,a)}(p_1(s)+p_2(s))\mathrm{d}s + \sum_{k=\underline{n}(a)}^{\infty} \frac{H_k}{\mu(k,a)} &= \sum_{i=3}^{\infty} \int_{i-1}^{i} \frac{4}{(i+1)^2}\frac{i}{s^4}\mathrm{ds}\\ &\quad + \sum_{k=2}^{\infty} \frac{4}{(k+1)^2}\Big(\frac{k+1}{k^3} + \frac{2}{k^3(k+1)}\Big)\\ &= \sum_{i=3}^{\infty} \frac{4i(3i^2-3i+1)}{3(i-1)^3 i^3 (i+1)^2}\\ &\quad + \sum_{k=2}^{\infty}\Big(\frac{4}{k^3(k+1)} + \frac{8}{k^3(k+1)^3}\Big)\end{aligned} \tag{19}$$

and

$$\sum_{k=\underline{n}(a)}^{\overline{n}(t)} \frac{\alpha_k}{(1-a_k)u(\tau_k)} = \sum_{k=2}^{\overline{n}(t)} \frac{1}{(k+1)^3} \tag{20}$$

which are both finite.

Thus, all the hypotheses of Theorem 3 hold, and hence there exists a solution $y(t)$ *of the impulsive BVP* (18).

Remark 2. *If the right-hand sides of the hypotheses (H2) and (H3) are replaced with* $O(1/v(t))$, *where* v *is a nonprincipal solution of the homogeneous impulsive equation* (5), *then the impulsive BVP* (3) *satisfies the boundary condition*

$$y(t) = O(1), \quad t \to \infty,$$

i.e., the solution turns out to be bounded.

Indeed, in Example 1, it can be seen from (19) *and* (20) *that there exist some positive constants C_1 and C_2 such that*

$$\int_a^t \frac{u(s)}{\mu(s,a)}(p_1(s)+p_2(s))\mathrm{d}s + \sum_{k=\underline{n}(a)}^{\overline{n}(t)} \frac{H_k}{\mu(k,a)} \le \frac{C_1}{t^3} + o(t^3) = o(v(t)), \quad t \to \infty$$

and

$$\sum_{k=\underline{n}(a)}^{\overline{n}(t)} \frac{\alpha_k}{(1-a_k)u(\tau_k)} \le \frac{C_2}{k^2} = O\Big(\frac{1}{v(t)}\Big), \quad t \to \infty$$

since $v(t) = kt$, $t \in (k-1,k]$. Hence, the impulsive BVP (18) *has at least one bounded solution.*

5. Conclusion

In this paper, the existence of solutions for impulsive BVPs on an infinite interval was obtained under some weak conditions. As the impulses act on both the solution and its derivative, i.e., the solutions have discontinuities, and both the differential equation and the impulses are nonlinear, it turns out that the impulsive BVP (3) is in a quite general form. The main innovation in the study is to use the principal and nonprincipal solutions of the associated impulsive homogeneous equation. Also, slightly modifying the hypotheses of the main theorem, it was shown that the considered impulsive BVP has a bounded solution.

Declaration of Competing Interests The author declares that there is no competing interest regarding the publication of this paper.

Acknowledgements The author would like to thank anonymous referees for carefully reading the paper and for their helpful suggestions.

References

[1] Agarwal, R. P., O'Regan, D., Infinite Interval Problems for Differential, Difference and Integral Equations, Netherlands: Kluwer Academic Publisher, 2001. https://doi.org/10.1007/978-94-010-0718-4.

[2] Akgöl, S. D., Zafer, A., Boundary value problems on half-line for second-order nonlinear impulsive differential equations, *Math. Meth. Appl. Sci.*, 41 (2018), 5459–5465. https://doi.org/10.1002/mma.5089

[3] Akgöl, S.D., Zafer, A., A fixed point approach to singular impulsive boundary value problems, *AIP Conference Proceedings*, 1863 (2017), 140003. https://doi.org/10.1063/1.4992310

[4] Akgöl, S. D., Zafer, A., Prescribed asymptotic behavior of second-order impulsive differential equations via principal and nonprincipal solutions, *J. Math. Anal. Appl.*, 503(2) (2021), 125311. https://doi.org/10.1016/j.jmaa.2021.125311

[5] Akgöl, S. D., Zafer, A., Leighton and Wong type oscillation theorems for impulsive differential equations, *Appl. Math. Lett.*, 121 (2021), 107513. https://doi.org/10.1016/j.aml.2021.107513

[6] Bainov, D., Simeonov, P., Impulsive Differential Equations: Asymptotic Properties of the Solutions, World Scientific, Singapore, 1995. https://doi.org/10.1142/2413

[7] Ertem, T., Zafer, A., Existence of solutions for a class of nonlinear boundary value problems on half-line, *Bound. Value Probl.*, 43 (2012). https://doi.org/10.1186/1687-2770-2012-43

[8] Hanche-Olsen, H., Holden, H., The Kolmogorov-Riesz compactness theorem, *Expo. Math.*, 28 (2010), 385-394. https://doi.org/10.1016/j.exmath.2010.03.001

[9] Iswarya, M., Raja, R., Rajchakit, G., Cao, J., Alzabut, J., Huang, C., A perspective on graph theory-based stability analysis of impulsive stochastic recurrent neural networks with time-varying delays, *Adv. Differ. Equ.*, 502 (2019). https://doi.org/10.1186/s13662-019-2443-3

[10] Karaca, İ. Y., Aksoy, S., Existence of positive solutions for second-order impulsive differential equations with integral boundary conditions on the real line, *Filomat*, 35(12) (2021), 4197-4208. https://doi.org/10.2298/FIL2112197K

[11] Kayar, Z., An existence and uniqueness result for linear fractional impulsive boundary value problems as an application of Lyapunov type inequality, *Hacet. J. Math. Stat.*, 47(2) (2018), 287-297. Doi: 10.15672/HJMS.2017.463

[12] Li, Z., Shu, X. B., Xu, F., The existence of upper and lower solutions to second-order random impulsive differential equation with boundary value problem, *AIMS Mathematics*, 5(6) (2020), 6189-6210. https://doi.org/10.3934/math.2020398

[13] Özbekler, A., Zafer, A., Principal and nonprincipal solutions of impulsive differential equations with applications, *Appl. Math. Comput.*, 216 (2010), 1158-1168. https://doi.org/10.1016/j.amc.2010.02.008

[14] Riesz, M., Sur les ensembles compacts de fonctions sommables, *Acta Szeged Sect. Math.*, 6 (1933), 136-142.

[15] Royden, H. L., Real Analysis, 2nd. ed. Macmillan, 1968.

[16] Samoilenko, A. M., Perestyuk, N. A., Impulsive Differential Equations, World Scientific, 1995.

[17] Vinodkumar, A., Senthilkumar, T., Hariharan, S., Alzabut, J., Exponential stabilization of fixed and random time impulsive delay differential system with applications, *Math. Biosci. Eng.*, 18(3) (2021), 2384-2400. https://doi.org/10.3934/mbe.2021121

[18] Zada, A., Alam, L., Kumam, P., Kumam, W., Ali, G., Alzabut, J., Controllability of impulsive non–linear delay dynamic systems on time scale, *IEEE Access*, 8 (2020), 93830-93839. https://doi.org/10.1109/ACCESS.2020.2995328.

http://communications.science.ankara.edu.tr

Commun.Fac.Sci.Univ.Ank.Ser. A1 Math. Stat.
Volume 72, Number 3, Pages 737–760 (2023)
DOI:10.31801/cfsuasmas.1133106
ISSN 1303-5991 E-ISSN 2618-6470

COMMUNICATIONS SERIES A1

Research Article; Received: June 20, 2022; Accepted: January 17, 2023

CONSTANT PSEUDO-ANGLE LIGHTLIKE SURFACES

Gül TUĞ

Department of Mathematics, Karadeniz Technical University, Trabzon, TÜRKİYE

Abstract. The oriented angles between lightlike vectors cannot be defined properly compared to the timelike vectors in the Minkowski spacetime. Therefore, we use the pseudo-angles between any non-lightlike or lightlike vectors to develop the theory of lightlike surfaces having constant angle with a fixed non-lightlike direction. We investigate some geometric properties on these surfaces such as being a tangent developable. Besides, we construct the constant angle lightlike ruled surfaces by means of the null helices. We give several examples to illustrate the obtained surfaces.

1. Introduction

In the differential geometry and physics, especially in the theory of general relativity, lightlike hypersurfaces play an important role because they are considered as models for different horizon types of black holes. A black hole is a region of space-time containing a huge mass compacted into an extremely small volume. The gravity inside the black hole is so strong that even light with its remarkable speed cannot escape (see [1]). After the Einstein's theory of gravitation was first published in 1915, numerous research papers were devoted to the mathematical and physical theory of black holes. For subsequent information about black holes and the applications of lightlike hypersurfaces, see [3, 7, 11, 12, 23, 24].
A constant angle surface is a surface which has tangent planes making a constant angle with a fixed constant vector field at every point in the Euclidean meaning (for more detail, see [8, 9, 20]). These surfaces are considered as a generalization of the concept of helix. They represent good models to describe some phenomena in physics of interfaces in liquids crystals and of layered fluids (see [6]). Lopez and Munteanu extend the theory of constant angle surfaces to the three dimensional Minkowski spacetime [18]. However, due to the variety of causal characters

2020 *Mathematics Subject Classification.* 53C50, 51B20, 53Z05.
Keywords. Lightlike surface, pseudo-angle, transversal vector field, ruled surface, Cartan slant helix, null helix, pseudo-null curve.
gguner@ktu.edu.tr; 0000-0001-9453-3809.

of a vector in Minkowski space, there is not a natural concept of angle between two arbitrary vectors so it is only possible to define the angle between timelike vectors. Therefore, they state that a constant angle surface in Minkowski space is actually a spacelike surface whose unit normal vector makes a constant hyperbolic angle with a fixed timelike vector at every point. In that case, it is possible to define the angle since any unit normal vector field of a spacelike immersion is timelike at each point. However, when we come to the concept of lightlike surfaces, following question arises: Is it possible to define the constant angle lightlike surfaces in Minkowski spacetime? To answer this question we use the concept of pseudo-angles between lightlike (null) vectors and the others. Helzer introduced an oriented pseudo-angle between any two null or non-null unit vectors in [13]. Pseudo-angles provide a generalization of the oriented hyperbolic angles between the unit non-null vectors [4]. That is to say, an oriented hyperbolic angle between non-null unit vectors in Minkowski plane is equivalent to the oriented pseudo-angle between those vectors. In [21], the author introduce pseudo-perpendicular vectors in Minkowski plane. In the mentioned work, it is shown that any unit non-null or null vector can be associated exactly eight vectors which are pseudo-perpendicular to it. So it is given geometric interpretations of the oriented pseudo-angles in terms of the hyperbolic arcs by using the pseudo-perpendicular vectors. Pseudo-angles have applications in several fields, such as in computing Polyakov extrinsic energy of Polyakov string solutions [3] or in Backlund transformations [22].

Ruled surfaces are generated by the continuous movement of a straight line in the space and they are one of the most important topics in differential geometry. Also, ruled surfaces play an important role in the study of rational design problems in spatial mechanisms since they represent the trajectories of the oriented lines embedded in a moving rigid body in spatial motion. This kind of a surface can be used in many scientific fields as well as in Computer Aided Geometric Design (CAGD). Different from the Euclidean space, there exist several types of the ruled surfaces according to the Lorentzian casual characters of lines and curves lying on the surface in Minkowski space. In [25], Kim and Yoon give classifications of the ruled surfaces in Minkowski 3-space. Also, Ali [2] introduces two types of non-lightlike ruled surfaces in Minkowski 3-space: Those of constant slope parallel to the tangent of a timelike general helix and those parallel to the normal of a timelike slant helix. However, there is still a gap in the theory of lightlike ruled surfaces in Minkowski 3-space.

In this paper, first we introduce the concept of lightlike constant-pseudo angle surfaces in Section 3. We give Theorem 3 and Theorem 5 to classify these surfaces in two types. Moreover, we show that any constant pseudo-angle lightlike surface is actually a ruled surface along a spacelike base curve with lightlike rulings. We give some related corollaries and examples. In Section 4, we define a constant angle lightlike ruled surface by means of the Cartan frame of a null helix, a pseudo-null curve as a slant helix or a Cartan slant helix. We see that, they are ruled surfaces along a non-null base curve with null rulings similar to the surfaces introduced in the previous section. We investigate such ruled surfaces in three cases depending on the type of chosen helix. We also give some related examples to support the theory.

2. Preliminaries

2.1. **Pseudo-angles in the Minkowski plane.** In this section, we give a brief information on the pseudo-perpendicular vectors in Minkowski plane and introduce the concept of pseudo-angles between lightlike and non-lightlike vectors in terms of the hyperbolic arcs of finite hyperbolic lengths (for detailed information see [13,21]).
The Minkowski plane E_1^2 is an affine plane endowed with the standard indefinite scalar product given by

$$g(x, y) = x_1 y_1 - x_2 y_2$$

for any two vectors $x(x_1, x_2)$ and $y = (y_1, y_2)$. A vector $v \neq 0$ has a casual character spacelike, timelike or lightlike (lightlike) iff $g(v, v) > 0$, $g(v, v) < 0$ or $g(v, v) = 0$, respectively. The vector $v = 0$ is spacelike and the norm of a given vector is defined as $\|v\| = \sqrt{|g(v, v)|}$.
$e_2 = (0, 1)$ is a unit timelike vector and an arbitrary vector v in E_1^2 is called future-pointing or past-pointing if $g(v, e_2) < 0$ or $g(v, e_2) > 0$, respectively. Moreover, any two timelike vectors have the same time-orientation when they are both future pointing or past pointing vectors. On the other hand, if $g(x, y) < 0$ for any two lightlike vectors x and y, we say they have the same time-orientation.
Let $O = e_1, e_2$ be the standard orthonormal basis of E_1^2. Then we define a function $\phi_O(u)$ by

$$\phi_O(u) = \begin{Bmatrix} \ln|a + b| & if & a + b \neq 0 \\ -\ln|a - b| & if & a + b = 0 \end{Bmatrix}$$

where $u = ae_1 + be_2$ is a lightlike or non-lightlike unit vector and $a, b \in \mathbb{R}$ [21].

Definition 1. *If u and v are unit non-lightlike or lightlike vectors, then the oriented pseudo-angle $\phi(u, v)$ from u to v is given by,*

$$\phi(u, v) = \phi_O(u, v) = \phi_O(v) - \phi_O(u)$$

We note that the function $\phi_O(u, v)$ only depends on the orientation of the bases O. Also, one can show that the oriented hyperbolic angles between the unit non-lightlike vectors in the Minkowski plane are actually equal to the oriented pseudo-angles between them [21].

Definition 2. *Let u and v be the unit non-lightlike or lightlike vectors in Minkowski plane. Then we say they are mutually pseudo-perpendicular vectors, if $\phi(u, v) = 0$ [21].*

Moreover, for any unit non-lightlike or lightlike vector in the Minkowski plane, it can be associated eight vectors pseudo-perpendicular to it (for more information see [21]).

Any oriented pseudo-angle $\phi(a,b)$ can be associated a unique hyperbolic arc of finite hyperbolic length. This hyperbolic arc is determined by the central pseudo-angle enclosed by two unit non-lightlike vectors on the non-lightlike unit circle [13] . The central pseudo-angle of the unit spacelike circle is pseudo-angle formed by two unit timelike future-pointing (or past-pointing) vectors. Analogously, central pseudo-angle of the unit timelike circle is pseudo-angle formed by two unit spacelike vectors.

On the other hand, a measure of an unoriented pseudo-angle $|\phi(a,b)|$ is equal to the hyperbolic length of the hyperbolic arc determined by two unit non-lightlike vectors pseudo perpendicular to a and b, where a and b are the unit non-lightlike or lightlike vectors. The oriented and unoriented pseudo-angles between unit non-lightlike or lightlike vectors are distinguished in six cases depending on the causal characters of the vectors a and b in [21].

2.2. **Lightlike surfaces.** In this section, we refer to the fundamental notions about the theory of lightlike surfaces (for a further information on the lightlike surfaces, see [10, 11]).

Let $\bar{M}$ be a 3 dimensional semi-Riemannian manifold endowed with the metric $\bar{g}$. If M is a lightlike surface in $\bar{M}$, there exists a subspace $T_pM^\perp$ at every point such that

$$T_pM^\perp = \left\{ v_p \in T_p\bar{M} : \bar{g}_p\left(v_p, w_p\right) = 0,\ \forall w_p \in T_pM \right\}.$$

where T_pM is the tangent plane on the surface M. Then the radical distribution is defined by,

$$RadT_pM = T_pM \cap T_pM^\perp \neq \{0\},\ \forall p \in M.$$

The rank of $RadTM$ is 1 for the lightlike surface M.

The complement vector bundle to $RadTM$ in TM is $S(TM)$ which is called a *screen distribution.* Clearly, $S(TM)$, is a non-degenerate subspace. Hence, one can write the following decomposition,

$$\begin{aligned} TM &= RadTM \oplus_{ort} S(TM) \\ RadTM &= TM \cap TM^\perp \end{aligned}$$

where $TM^\perp = \bigcap_{p\in M} T_pM^\perp$.

Theorem 1. *Let $(M, g, S(TM))$ be a lightlike surface in $\bar{M}$. If U is a coordinate neighborhood of M and $RadTM = Span\{\xi\}$. There exist a smooth vector field N such that*

$$\bar{g}\left(\xi, N\right) = 1 \quad \text{and} \quad \bar{g}\left(N, W\right) = 0.$$

where W is a non-lightlike vector field in $S(TM)$.

The subspace $ltr(TM) = Span\{N\}$ is called *lightlike transversal vector bundle.* Also, the following decomposition is satisfied;

$$T\bar{M}\mid_M = TM \oplus tr(TM)$$

where $tr(TM) = ltr(TM) \oplus S(TM^{\perp})$. In this case, $\{\xi, W, N\}$ is a quasi-ortonormal basis of $\bar{M}$ along M. The Weingarten equations are

$$\bar{\nabla}_X Y = \nabla_X Y + h(X, Y) \tag{1}$$

$$\bar{\nabla}_X V = -A_V X + \nabla^t_X V \tag{2}$$

where $X, Y \in \Gamma(TM)$ and $V \in \Gamma(tr(TM))$. Also, $\bar{\nabla}$ is the Levi-Civita connection on $\bar{M}$, $\nabla_X Y$ and $\nabla^t_X V$ are the linear connections on M and $tr(TM)$ respectively. Note that ∇ is a torsion free induced linear connection. Also, $A_V X$ and $h(X, Y)$ are the shape operator and second fundamental form on M, respectively. Locally suppose ξ, N is a pair of vector fields on U in Definition 1. Then we define a symmetric bilinear form B and 1-form τ on M by

$$B(X, Y) = \bar{g}(h(X, Y), \xi) \quad \text{and} \quad \tau(X) = \bar{g}(\nabla^t_X N, \xi) \tag{3}$$

The equations (1) and (2) become

$$\bar{\nabla}_X Y = \nabla_X Y + B(X, Y)N \tag{4}$$

$$\bar{\nabla}_X N = -A_N X + \tau(X)N. \tag{5}$$

3. Constant Pseudo-Angle Lightlike Surfaces

Let M be a lightlike surface in E^3_1. The tangent plane of M is spanned by the pseudo orthogonal vector fields $\{e_1, \xi\}$ where ξ belongs to the radical distribution and N be the transversal vector field at every point on M. To describe the constant pseudo-angle lightlike surfaces, we consider a fixed non-lightlike vector field U making a constant pseudo-angle with the vector field N. According to the position of U, we classify such surfaces in two types. In all cases, since U is non-lightlike, there exists a non-lightlike vector ν which is pseudo-perpendicular to N at every point. We consider the pseudo-angle ϕ between the vector fields U and N as defined in the Section 2.

Different from the constant angle surfaces in the Euclidean space, pseudo-angle between the transversal vector field N and the constant direction U can be zero on a lightlike surface. Since U and N are pseudo-perpendicular for $\phi = 0$, U is one of the pre-defined eight vectors given in [21]. We assume that ϕ is a non-zero constant throughout this work.

Type I

Let U lies in the plane of $\{N, \xi\}$. We decompose U as,

$$U = a\xi + bN$$

where a and b are constant functions. By using the logarithmic forms of the inverse hyperbolic functions, we reach to the following form:

$$U = \sinh\phi\xi + \cosh\phi N. \tag{6}$$

We denote $\langle\cdot,\cdot\rangle$ as the Lorentzian metric and $\bar{\nabla}$ as the Levi-Civita connection in E_1^3 when g is the metric and ∇ is the L.C. connection in M. Since U is constant, from (6) we have

$$\sinh\phi\bar{\nabla}_X\xi+\cosh\phi\bar{\nabla}_X N=0$$

where $X\in T_PM$. Also we know that $B(X,\xi)=0$ and N is a lightlike vector field, we have

$$\sinh\phi\langle\nabla_X\xi,N\rangle=0.$$

Then we obtain $\tau(X)=0$ and this implies $\bar{\nabla}_X N=-A_N X$.

Let $\{v_1,v_2\}$ show the local basis in the tangent plane T_PM and we denote

$$b_{ij}=B(v_i,v_j)=-\langle Av_i,v_j\rangle.$$

We can write the following decompositions by using the Gauss and Weingarten formulas given in (2.4) and (2.5):

$$\bar{\nabla}_{v_i}V_j=\nabla_{v_i}V_j+b_{ij}N \tag{7}$$

$$\bar{\nabla}_{v_i}N=b_{i1}v_1+b_{i2}v_2 \tag{8}$$

where V_j is a tangent vector field that extends v_j. Now, take the derivative of (6) with respect to e_1 then we have

$$\sinh\phi\bar{\nabla}_{e_1}\xi+\cosh\phi\bar{\nabla}_{e_1}N=0. \tag{9}$$

By combining (8) and (9), we find

$$\bar{\nabla}_{e_1}\xi=-\coth\phi b_{11}e_1.$$

On the other hand, by taking the derivative of (6) with respect to ξ and combining with (8) we find

$$\sinh\phi\bar{\nabla}_\xi\xi=0$$

and this implies $\bar{\nabla}_\xi\xi=0$.

According to the above calculations, we can give the following theorem without proof:

Theorem 2. *Let M be a constant pseudo-angle lightlike surface of Type I. The linear connection on M is given by*

$$\begin{aligned}\nabla_{e_1}e_1 &= \coth\phi b_{11}\xi\\ \nabla_{e_1}\xi &= -\coth\phi b_{11}e_1\\ \nabla_\xi\xi &= \nabla_\xi e_1=0.\end{aligned}$$

From this point on, we choose coordinates u and v such that

$$\frac{\partial}{\partial u}=\beta e_1 \quad\text{and}\quad \frac{\partial}{\partial v}=\beta\xi$$

where $\beta=\beta(u,v)$ is a certain smooth function on the surface. We will construct the parameterization $x(u,v)$ of a lightlike constant pseudo-angle surface of Type I. We assume $x(u,v)$ twice continuously-differentiable and from Theorem 2 we obtain,

$$\begin{aligned} x_{vv} &= 0 \\ x_{vu} &= \frac{\beta_v}{\beta} x_u \\ x_{uu} &= -\beta\beta_v x_v + \frac{\beta_u}{\beta} x_u + \beta^2 b_{11} N \end{aligned}$$

Since $x_{vu} = x_{uv}$ and $\nabla_{e_1}\xi = -\coth\phi b_{11} e_1$, we find that $\frac{\beta_v}{\beta} = -\coth\phi b_{11}$.

Also we have,

$$\begin{aligned} N_u &= \bar{\nabla}_{x_u} N = b_{11} x_u \\ N_v &= \bar{\nabla}_{x_v} N = 0 \\ N_{uv} &= 0 \end{aligned}$$

Using the fact that $N_{uv} = N_{vu}$ we get

$$(b_{11})_v x_u + b_{11} x_{uv} = 0 \tag{10}$$

Substituting the expression of x_{uv} in the last equation gives $\frac{\partial}{\partial v}(b_{11}\beta) = 0$. Hence there exists a smooth function $\psi(u)$ such that

$$b_{11}\beta = \psi(u). \tag{11}$$

Corollary 1. *Let M be a constant pseudo-angle lightlike surface of Type I. If $b_{11} = 0$, then the surface immersion is affinely equivalent to the graph immersion of a certain function $f : M \to \mathbb{R}$.*

Assume that $b_{11} \neq 0$, then from the equation (10) we have

$$(b_{11})_v - \coth\phi (b_{11})^2 = 0.$$

Hence we obtain

$$b_{11} = \frac{1}{\alpha(u) - v\coth\phi} \tag{12}$$

and from the (11) we get

$$\beta(u,v) = \psi(u)(\alpha(u) - v\coth\phi) \tag{13}$$

We can calculate the second derivatives of $x(u,v)$ by using the last two equations as,

$$\begin{aligned} x_{uu} &= (\psi(u))^2 \coth\phi(\alpha(u) - v\coth\phi) x_v + (\frac{\psi'(u)}{\psi(u)} + \frac{\alpha'(u)}{\alpha(u) - v\coth\phi}) x_u \\ &+ (\psi(u))^2(\alpha(u) - v\coth\phi) N \\ x_{uv} &= \frac{\coth\phi}{v\coth\phi - \alpha(u)} x_u \\ x_{vv} &= 0 \end{aligned} \tag{14}$$

Using the expression of U given in (6), we calculate

$$\langle U, x_u \rangle = 0 \quad \text{and} \quad \langle U, x_v \rangle = -\cosh\phi.$$

It implies $\langle x, U \rangle_v = -\cosh\phi$ and so we have

$$\langle x, U \rangle = -v\cosh\phi + \mu$$

where $\mu \in \mathbb{R}$.

1. Without loss of generality, we can choose the non-lightlike vector U as E_1 with an isometry of E_1^3, then the parameterization $x(u,v)$ of the surface M is (up to translations):

$$x(u,v) = (v\cosh\phi, x_1(u,v), x_2(u,v))$$

Since ξ is a lightlike vector, $\langle x_v, x_v \rangle = 0$. So there exists a function $\Phi(u,v)$ such that

$$x_v = (\cosh\phi, \cosh\phi\cos\Phi(u,v), \cosh\phi\sin\Phi(u,v)) \tag{15}$$

From the equations in (14) and (15), we have $\Phi_v = 0$. Hence the function Φ depends on solely the parameter u. We can rewrite the expression of x_v as,

$$x_v = \cosh\phi((0, f(u)) + (1,0,0)) \tag{16}$$

where $f(u) = (\cos\Phi(u), \sin\Phi(u))$. If we calculate x_{uv} and integrate with respect to v, we obtain

$$x_u = \cosh\phi(0, vf'(u) + h(u))$$

where $h(u)$ is a smooth function. When we substitute the last equation in (14) and equalise it to the derivative of (16), we find that

$$h(u) = -\tanh\phi\alpha(u)f'(u)$$

We can rewrite the expression of x_u by substituting the above function and take the derivative with respect to u, then we obtain

$$x_{uu} = \cosh\phi(v - \alpha(u)\tanh\phi)(0, f''(u)) - \alpha'(u)\sinh\phi(0, f'(u)) \tag{17}$$

Multiplying the expressions of x_{uu} in (14) and (17) by x_v implies that

$$\Phi'(u) = \frac{\psi(u)}{\sqrt{|\cosh\phi\sinh\phi|}}$$

One can make a change in the variable u to obtain $\Phi'(u) = 1$ and this choice does not affect the second derivatives of $x(u,v)$. Then we substitute $\Phi(u)$ in the last expressions of x_u and x_v and obtain

$$x(u,v) = v\cosh\phi(1, \cos u, \sin u) + \eta(u)$$

by integrating x_v. We calculate the function $\eta(u)$ as

$$\eta(u) = \sinh\phi(\int \alpha(u)\sin u du, -\int \alpha(u)\cos u du, 0)$$

2. Now take the non-lightlike vector U as the vector E_3 in E^3_1. Then the parameterization of the surface M is

$$x(u,v) = (x_1(u,v), x_2(u,v), -v\cosh\phi)$$

Following the similar steps in the case i, we obtain

$$x(u,v) = v\cosh\phi(\cosh u, \sinh u, -1) + \eta(u)$$

where the function $\eta(u)$ reads

$$\eta(u) = -\sinh\phi(\int \alpha(u)\sinh u du, \int \alpha(u)\cosh u du, 0).$$

Now we can give the following theorem as a consequence of the above calculations:

Theorem 3. *Let M be a constant pseudo-angle lightlike surface of Type I which is not totally geodesic in E^3_1. Up to the isometries of the ambient space, there exist local coordinates u and v such that M is given by one of the following two parameterizations:*

1.

$$\begin{aligned} x(u,v) &= \eta(u) + v\cosh\phi(1, \cos u, \sin u) \\ \eta(u) &= \sinh\phi(\int \alpha(u)\sin u du, -\int \alpha(u)\cos u du, 0) \end{aligned}$$

2.

$$\begin{aligned} x(u,v) &= \eta(u) + v\cosh\phi(\cosh u, \sinh u, -1) \\ \eta(u) &= -\sinh\phi(\int \alpha(u)\sinh u du, \int \alpha(u)\cosh u du, 0). \end{aligned}$$

where $\alpha(u)$ is a smooth function on a certain interval I and ϕ is the pseudo-angle between the transversal vector field on M and the fixed direction U.

TypeII

Let the fixed direction U lies in the plane of $\{e_1, N\}$. Then we decompose U as,

$$U = U^T + \cosh\phi N$$

where U^T is the projection of U on the tangent plane of M and

$$e_1 = \frac{U^T}{\|U^T\|}.$$

We can write U as in the following form,

$$U = \cosh\phi e_1 + \sinh\phi N. \tag{18}$$

Since U is constant,

$$\cosh\phi\bar{\nabla}_X e_1 + \sinh\phi\bar{\nabla}_X N = 0$$

where $X \in T_P M$. Then we obtain $\tau(e_1) = -b_{11}\coth\phi$ and $\tau(\xi) = 0$. This implies

$$\bar{\nabla}_{v_i} V_j = \nabla_{v_i} V_j + b_{ij} N \tag{19}$$

$$\bar{\nabla}_{v_i} N = b_{i1} v_1 + b_{i2} v_2 - b_{i1} \coth \phi N \tag{20}$$

where V_j is a tangent vector field that extends v_j. We can calculate the Levi Civita connection on M by taking the derivatives of (18) with respect to e_1 and ξ.

Theorem 4. *Let M be a constant pseudo-angle lightlike surface of Type II. The Levi Civita connection on M is given by*

$$\begin{aligned} \nabla_{e_1} e_1 &= -b_{11}(\tanh \phi e_1 + N) \\ \nabla_{e_1} \xi &= b_{11} e_1 \\ \nabla_{\xi} \xi &= \nabla_{\xi} e_1 = 0 \end{aligned}$$

Proof. One can easily reach to the given equations by following straightforward calculations similar to the Theorem 2 in Type I. □

Now we choose coordinates u and v as in Type I. To construct the parameterization $x(u,v)$ of a lightlike constant pseudo-angle surface of Type II, we calculate the second derivatives by using Theorem 3 as follows:

$$\begin{aligned} x_{vv} &= 0 \\ x_{vu} &= \frac{\beta_v}{\beta} x_u \\ x_{uu} &= (-\beta_v \tanh \phi + \frac{\beta_u}{\beta}) x_u \end{aligned} \tag{21}$$

We find that $\frac{\beta_v}{\beta} = b_{11}$ and so $(b_{11})_v + b_{11}^2 = 0$. Choose $b_{11} \neq 0$, then we have

$$b_{11} = \frac{1}{v + \alpha(u)}$$

where $\alpha(u)$ is a smooth function. On the other hand using the derivatives given in (20) we calculate $\frac{\partial}{\partial v}(b_{11}\beta) = 0$. Hence we have $b_{11}\beta = \psi(u)$ where $\psi(u)$ is a smooth function. Then we obtain

$$\beta(u,v) = \psi(u)(v + \alpha(u)).$$

One can easily calculate that

$$\langle x_u, U \rangle = \beta \cosh \phi \quad \text{and} \quad \langle x_v, U \rangle = \sinh \phi$$

Integrating second one of the above equations with respect to v, we get

$$\langle x, U \rangle = v \sinh \phi + \eta(u)$$

and we obtain $\eta(u) = \cosh \phi \int \beta(u,v) du + c$ by taking derivative and integrating with respect to u.

Now we take the spacelike fixed direction U as the vector E_3 in E_1^3. Using (18), we conclude that the parameterization of M is in the form:

$$x(u,v) = (x_1(u,v), x_2(u,v), v \sinh \phi + \cosh \phi \int \beta(u,v) du)$$

up to translations. Since $\langle x_u, x_u\rangle = \beta^2$, there exists a function $\Phi(u,v)$ such that

$$x_u = (\beta \sinh\phi \cosh\Phi, \beta \sinh\phi \sinh\Phi, \beta\cosh\phi) \tag{22}$$

Then we calculate

$$x_{uv} = (\beta_v \sinh\phi\cosh\Phi + \beta\Phi_v \sinh\phi\sinh\Phi, \beta_v \sinh\phi\sinh\Phi + \beta\Phi_v \sinh\phi\cosh\Phi, \beta_v \cosh\phi)$$

We use the equality of the second derivatives of x and integrate the above equation with respect to u to obtain,

$$x_v = (\sinh\phi \int \psi(u)\cosh\Phi du, \sinh\phi \int \psi(u)\sinh\Phi du, \cosh\phi \int \psi(u)du) \tag{23}$$

When we equalise the two expressions of x_{uv} given in (21) and the above equation, we find that $\Phi_v = 0$, hence the fuction Φ only depends on the variable u.

On the other hand we find that

$$\frac{d\Phi}{du} = -\psi(u)\tanh\phi\coth\Phi \tag{24}$$

by following similar steps as in Type I. If we solve the equation (24), we obtain

$$\begin{aligned} \cosh\Phi &= e^{-\tanh\phi\int\psi(u)du} \\ \sinh\Phi &= (e^{-2\tanh\phi\int\psi(u)du} - 1)^{\frac{1}{2}} \end{aligned} \tag{25}$$

Now we integrate the equation (23) with respect to v and we have

$$x(u,v) = (v\sinh\phi \int \psi(u)\cosh\Phi du, v\sinh\phi \int \psi(u)\sinh\Phi du, v\cosh\phi \int \psi(u)du) + \mu(u) \tag{26}$$

Then we take derivative of (26) with respect to u and equalise to the expression of x_u given in (22) to find $\mu(u)$. We have

$$\mu(u) = (\sinh\phi \int \psi(u)\alpha(u)\cosh\Phi du, \sinh\phi \int \psi(u)\alpha(u)\sinh\Phi du, \cosh\phi \int \psi(u)\alpha(u)du)$$

By the help of the above calculations, we give following theorem without proof:

Theorem 5. *Let M be a constant pseudo-angle lightlike surface of Type II which is not totally geodesic in E_1^3. Up to the isometries of the ambient space, there exist local coordinates u and v such that M is given by the following parameterization:*

$$x(u,v) = \mu(u) + v(\sinh\phi \int \psi(u)\cosh\Phi du, \sinh\phi \int \psi(u)\sinh\Phi du, \cosh\phi \int \psi(u)du)$$

$$\mu(u) = (\sinh\phi \int \psi(u)\alpha(u)\cosh\Phi du, \sinh\phi \int \psi(u)\alpha(u)\sinh\Phi du, \cosh\phi \int \psi(u)\alpha(u)du)$$

where $\psi(u)$ and $\alpha(u)$ are smooth functions on a certain interval I, ϕ is the pseudo-angle between the transversal vector field on M and the fixed direction U and

$$\begin{aligned} \cosh\Phi &= e^{-\tanh\phi\int\psi(u)du} \\ \sinh\Phi &= (e^{-2\tanh\phi\int\psi(u)du} - 1)^{\frac{1}{2}}. \end{aligned}$$

Proposition 1. *Let the fixed direction U lies in the plane of $\{e_1, \xi\}$. Then the surface immersion is affinely equivalent to the graph immersion of a certain function $f : M \to \mathbb{R}$.*

Proof. We express U as

$$U = \cosh\phi e_1 + \sinh\phi\xi \tag{27}$$

Since U is constant, we calculate

$$\cosh\phi(\nabla_{e_1}e_1 + b_{11}N) + \sinh\phi\nabla_{e_1}\xi = 0$$

Then we obtain $\nabla_{e_1}e_1 = -b_{11}N$ and this implies $b_{11} = 0$. □

Corollary 2. *Any constant pseudo-angle lightlike surface is a ruled surface along a spacelike base curve with lightlike rulings.*

Theorem 6. *A constant pseudo-angle lightlike surface is totally umbilical.*

Proof. Let $x(u, v)$ be a constant pseudo-angle lightlike surface of Type I or Type II. Since $x_u = \beta e_1$ and $x_v = \xi$ we obtain $B(x_u, x_v) = 0 = g(x_u, x_v)$ and $B(x_v, x_v) = 0 = g(x_v, x_v)$. Also, using the equation

$$B(x_u, x_u) = \langle\bar{\nabla}_{x_u}N, x_u\rangle \tag{28}$$

we have

$$B(x_u, x_u) = \beta^2 b_{11} = b_{11}g(x_u, x_u).$$

□

Corollary 3. *If M is a constant pseudo-angle lightlike surface, then the lightlike sectional curvature is negative.*

Theorem 7. *The constant pseudo-angle lightlike surface of Type I is a lightlike developable.*

Proof. Let M be a lightlike surface of Type I which has one of the two parameterizations given in Theorem 3.3. Then we obtain the following partial differentials of the parameterization given in (1) as:

$$\begin{aligned} X_u &= \eta\prime(u) + v\cosh\phi(0, -\sin u, \cos u) \\ X_v &= \cosh\phi(1, \cos u, \sin u) \\ \eta\prime(u) &= \sinh\phi(0, \alpha(u)\sin u, -\alpha(u)\cos u) \end{aligned}$$

Since $||X_u \times X_v|| = 0$, the surface is a lightlike developable. For the parameterization given by (2), the proof is similar. □

Theorem 8. *The constant pseudo-angle lightlike surface of Type I cannot be a tangent surface.*

Proof. Assume that M is a tangent surface. If M is one of the surfaces given in Corollary 1, then we find that $\cosh\phi = 0$. However, this is a contradiction. □

Theorem 9. *The constant pseudo-angle lightlike surface of Type I is one of the following surfaces:*

i. A part of a lightlike plane
ii. A part of the lightcone

iii. A mix of the above surfaces

Proof. Proof is clear from the Theorem 5.1 in [14]. □

Theorem 10. *The constant pseudo-angle lightlike surface of Type II cannot be a lightlike developable.*

Proof. Let $x(u,v)$ be a lightlike surface of Type II. Assume that it is a lightlike developable. The expressions of x_u and x_v are given in (22) and (23), respectively. By a straightforward calculation we can state that the vector $V = x_u \times x_v$ is lightlike. This property implies that the function Φ is constant. However, we see that it is only possible when $\beta = 0$ by using the equation (24) and this is a contradiction. □

Theorem 11. *Let the constant pseudo-angle lightlike surface of Type II be a tangent surface. Then the function $\psi(u)$ is in the form:*

$$\psi(u) = \frac{e^u}{\tanh\phi \int \alpha(u) e^u du}$$

where $\alpha(u)$ is a smooth function and ϕ is the pseudo-angle between the transversal vector and a fixed direction.

Proof. Let M be a surface given in Theorem 4 If it is a tangent surface, tangent of the base curve must be equal to the rulings. Hence, we have

$$\psi(u)\alpha(u)\cosh\Phi = \int \psi(u)\cosh\Phi du.$$

If we take derivative of the above equation with respect to u, we obtain

$$\alpha(u) = 1 + \frac{\tanh\phi}{\psi(u)} \int (\psi(u))^2 \alpha(u) du$$

On the other hand, we get $\psi(u)\alpha(u) = \int \psi(u)du$ when we equalise the third components of the tangent vector of $\mu(u)$ and the ruling. Hence it must be

$$\psi(u)\alpha(u) = \psi(u) + \tanh\phi \int (\psi(u))^2 \alpha(u) du. \tag{29}$$

Taking derivative of (29) gives a Riccati differential equation and the solution is

$$\psi(u) = \frac{e^u}{\tanh\phi \int \alpha(u) e^u du}.$$

□

We give following examples to illustrate the introduced surfaces by taking different choises of the functions $\psi(u)$ and $\alpha(u)$.

Example 1. *Let $x(u,v)$ be the parameterization of a constant pseudo-angle lightlike surface of Type I as in Theorem 3 (2). Take the pseudo-angle as $\phi = 5$ and the function $\alpha(u) = u$. Then the surface is obtained as*

$$x(u,v) = \begin{bmatrix} 74.21v\cosh(u) - 74.2u\cosh(u) + 74.2\sinh(u) \\ 74.21v\sinh(u) - 74.2u\sinh(u) + 74.2\cosh(u) \\ -74.21v \end{bmatrix}$$

and it can be seen in the Figure 1(a).

Example 2. *Now take $x(u,v)$ as the parameterization of a constant pseudo-angle lightlike surface of Type I as in Theorem 3 (1). We choose the pseudo-angle as $\phi = 5$ and the function $\alpha(u) = e^u$. Then the surface parameterization is*

$$x(u,v) = \begin{bmatrix} 74.21v - 37.1\cos(u)\mathrm{e}^u + 37.1\sin(u)\mathrm{e}^u \\ 74.21v\cos(u) - 37.1\cos(u)\mathrm{e}^u - 37.1\sin(u)\mathrm{e}^u \\ 74.21v\sin(u) \end{bmatrix}$$

It can be seen in the Figure 1(b).

Example 3. *Let $x(u,v)$ be the parameterization of a constant pseudo-angle lightlike surface of Type II as in Theorem 3.4. Take the pseudo-angle as $\phi = 0.5$, $\alpha(u) = 0.001$ and $\psi(u) = -0.5u^3$. We obtained the following parameterization:*

$$x(u,v) = \begin{bmatrix} \left(-0.00008685u^3 - 0.24080v\right)\mathrm{e}^{0.07702}u^3 \\ \left(-0.00008685u^3 - 0.24080v\right)\sqrt{e^{0.1540u^3} - 1} + \arctan\left(\sqrt{\mathrm{e}^{0.1540u^3} - 1}\right) \\ -0.1879u^3(v + 0.001) \end{bmatrix}$$

The surface is illustrated in Figure 1(c).

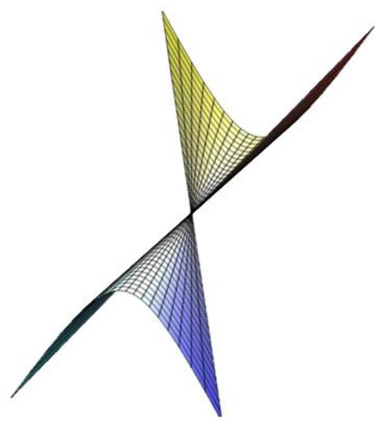

(a) Type I (2) for $\phi = 5$ and $\alpha(u) = u$

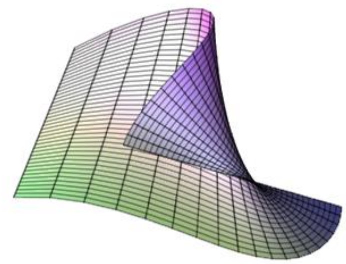

(b) Type I (1) for $\phi = 5$ and $\alpha(u) = e^u$

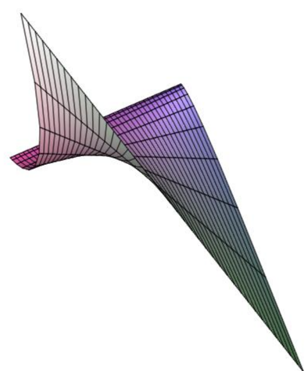

(c) Type II for $\phi = 0.5$, $\alpha(u) = 0.001$ and $\psi(u) = -0.5u^3$

FIGURE 1. Constant pseudo-angle lightlike surfaces of Type I and Type II

4. Constant Angle Lightlike Ruled Surfaces

We investigate the parameterization of a constant angle lightlike ruled surface by means of the Cartan frame on a null helix, a pseudo-null curve as a slant helix or a Cartan slant helix (for further information on these helices see [15], [19], [2], [17], [16], [5]). We classify such ruled surfaces in three cases depending on type of the corresponding helices.

Case 1

Let $\gamma(s)$ be a unit speed null helix equipped with the Cartan frame $\{T, N, B\}$ where the first and second curvatures are $k_1 \neq 0$ and $k_2 = constant$. Here we note that if $k_2 = 0$ then it is a null cubic and the slope axis is a null vector. The slope axis is a non-null vector lies in the rectifying plane if $k_2 \neq 0$.
Now, define a ruled surface as

$$\Psi(s, v) = \alpha(s) + vX(s). \tag{30}$$

Here $\alpha(s)$ and $X(s)$ are expressed by

$$\begin{aligned} \alpha'(s) &= aT + bN + cB \\ X(s) &= x_1T + x_2N + x_3B \end{aligned} \tag{31}$$

where a, b, c, x_1, x_2 and x_3 are smooth functions. If the surface in (30) is lightlike, there exists a lightlike transversal vector field U such that it can be written in the following form by a straightforward calculation:

$$U = U_1T + U_2N + U_3B$$

where

$$U_1 = u_{11} + vu_{12} \quad U_2 = u_{21} + vu_{22} \quad U_3 = u_{31} + vu_{32}. \tag{32}$$

For (30) to be a constant angle surface, we take the lightlike transversal vector U as parallel to the tangent of the curve $\gamma(s)$. Hence $(u_{11}, u_{12}) \neq (0, 0)$. Since there exist spacelike and null vectors in the basis of the tangent plane of $\Psi(s, v)$, we investigate two possibilities:

i. Choose Ψ_v as a null vector, then we have

$$\langle U, \Psi_v\rangle = 1 \quad \text{and} \quad \langle U, \Psi_u\rangle = 0. \tag{33}$$

We can calculate $\langle U, \Psi_v\rangle = x_3U_1 + x_2U_2 + x_1U_3$. Since $U_2 = U_3 = 0$ we have $U_1 = \frac{1}{x_3}$ and this implies $x_3 \neq 0$.
On the other hand, we calculate

$$X'(s) = KT + LN + MB$$

where

$$K = x_1' - x_2k_2 \quad L = x_1 + x_2' + x_3k_2 \quad M = x_3' - x_2. \tag{34}$$

Then we have $c + vM = 0$ which implies $c = 0$ and $x_3' = x_2$. Also, we obtain

$$x_2^2 = -2x_1x_3 \tag{35}$$

$$ax_3 + bx_2 = 0 \tag{36}$$

by using the equations $\langle X, X\rangle = 0$ and $\langle \Psi_s, X\rangle = 0$, respectively. From the equations (35) and (36), we have following ODE;

$$x_3' = \pm\frac{a}{b}x_3. \tag{37}$$

Solving the equation (37) gives

$$\begin{aligned} x_3 &= e^{\pm\int \frac{a}{b}ds} \\ x_2 &= \pm\frac{a}{b}e^{\pm\int \frac{a}{b}ds} \\ x_1 &= -\frac{a^2}{2b^2}e^{\pm\int \frac{a}{b}ds} \end{aligned}$$

where $b \neq 0$.

ii. Now we choose Ψ_s as a null vector. Since

$$\langle U, \Psi_s\rangle = 1 \quad \text{and} \quad \langle U, \Psi_v\rangle = 0$$

we obtain $x_3 = 0$ by using the right hand side of above equation. We also have

$$cu_{11} + v(cu_{12} - x_2u_{11} - vx_2u_{12}) = 1. \tag{38}$$

The equation (38) implies $u_{12} = x_2 = 0$, $u_{11} \neq 0$ and $c \neq 0$. Besides, we can calculate

$$\langle \Psi_v, \Psi_v\rangle = 2x_1x_3 + x_2^2 = 0 \tag{39}$$

and this is a contradiction.

Acording to the above notations, we obtain the expression of a lightlike ruled surface of constant slope as

$$\Psi(s,v) = \int (aT + bN)ds + ve^{\pm\int \frac{a}{b}ds}\left(-\frac{a^2}{2b^2}T + \frac{a}{b}N + B\right) \tag{40}$$

where $b \neq 0$. Note that the surface in (40) is a ruled surface along a spacelike base curve with lightlike rulings. Then we can give the following theorem:

Corollary 4. *Velocity vector of the base curve of a constant angle lightlike ruled surface defined by (40), lies in the osculating plane of a null helix at every point.*

Case 2

Assume that $\gamma(s)$ is a unit speed pseudo-null curve (slant helix) equipped with the Cartan frame $\{T, N, B\}$. If $k_2 = 0$ then any constant vector in E_1^3 can be the slope axis. If $k_2 \neq 0$, the slope axis can be a null or spacelike vector lies in the osculating plane of the curve.

Let the ruled surface defined in (30) with the expressions in (31) be a lightlike surface. We take the transversal vector U expressed in (32) as parallel to the normal vector of $\gamma(s)$. Then we have

$$X' = KT + LN + MB$$

where

$$K = x_1' - x_3 \quad L = x_1 + x_2' \quad M = (x_2 - x_3)k_2 + x_3'.$$

i. We choose Ψ_v as a null vector. Following similar steps as in Case 1, we obtain $x_3 \neq 0$, $u_2 \neq 0$ and $c = 0$. We also have

$$x_2 = x_3 - \frac{x_3'}{k_2} \tag{41}$$

$$-x_2 x_3 = \frac{b^2}{a^2} x_3^2 \tag{42}$$

Substituting (41) in (42), we obtain following ODE:

$$x_3' - k_2(\frac{b^2}{2a^2} + 1)x_3 \tag{43}$$

We find x_1, x_2 and x_3 as;

$$\begin{aligned} x_3 &= e^{\int k_2(\frac{b^2}{2a^2}+1)ds} \\ x_2 &= -\frac{b^2}{2a^2} e^{\int k_2(\frac{b^2}{2a^2}+1)ds} \\ x_1 &= -\frac{b}{a} e^{\int k_2(\frac{b^2}{2a^2}+1)ds} \end{aligned} \tag{44}$$

where $a \neq 0$.

ii. Let Ψ_s be a null vector. Using $\langle U, \Psi_v \rangle = 0$ and $\langle U, \Psi_s \rangle = 1$, we obtain

$$x_2 = 0, u_{22} = 0, c \neq 0 \quad \text{and} \quad u_{21} \neq 0. \tag{45}$$

On the other hand, we find $x_1 = \pm 1$ by calculating $\langle \Psi_v, \Psi_v \rangle = 1$. Hence, one can easily obtain the function c as zero from the equation $\langle \Psi_s, \Psi_s \rangle = 0$. However, this is a contradiction.

Acording to the above notations, we can express a lightlike ruledsurface of constant slope as

$$\Psi(s, v) = \int (aT + bN)ds + ve^{\int k_2(\frac{b^2}{2a^2}+1)ds}(-\frac{b}{a}T - \frac{b^2}{2a^2}N + B) \tag{46}$$

where $a \neq 0$. As in Case 1, the surface in (46) is also a ruled surface along a spacelike base curve with lightlike rulings. So we give the following theorem:

Corollary 5. *Velocity vector of the base curve of a constant angle lightlike ruled surface defined by (46), lies in the osculating plane of a pseudo null curve at every point.*

Case 3

Now, let $\gamma(s)$ be a Cartan slant helix with the attached Cartan frame $\{T, N, B\}$ where $k_2 \neq 0$.

i. Choose Ψ_v as a null vector.

Following similar procedure as in the previous two sections, we find $x_2 \neq 0$, $c \neq 0$, $a \neq 0$ and $b = 0$. Without loss of generality, we also take $ac > 0$. Then the following ODE can be obtained by straightforward calculations:

$$x_3' = \zeta x_3$$

where

$$\zeta = \frac{-(a' + k_2\sqrt{2ac})c + (c' + \sqrt{2ac})a}{2ac}.$$

Using the above equation, we have

$$\begin{aligned} x_3 &= e^{\int \zeta ds} \\ x_2 &= \pm\sqrt{\frac{2a}{c}} e^{\int \zeta ds} \\ x_1 &= -\frac{a}{c} e^{\int \zeta ds} \end{aligned} \tag{47}$$

ii. If we take Ψ_s as a null vector, we find $x_2 = 0$, $u_{22} = 0$, $b \neq 0$, $u_{21} \neq 0$ and $ac = 0$. Using the inner products of the vectors U, Ψ_s and Ψ_v, we obtain $x_1 = -k_2 x_3$. Besides, we also have $\frac{x_1}{x_3} = -\frac{a}{c}$. However, this implies $k_2 = 0$ or indefinite. It is a contradiction.

Acording to the above notations, we can define a constant angle lightlike ruled surface as:

$$\Psi(s,v) = \int (aT + cB)ds + ve^{\int \zeta ds}\left(-\frac{a}{c}T \pm \sqrt{\frac{2a}{c}}N + B\right) \tag{48}$$

where $c \neq 0$ and $a \neq 0$. Similar to the previous cases, the surface in (43) is also a ruled surface along a non-null base curve with lightlike rulings.

Corollary 6. *Velocity vector of the base curve of a constant angle lightlike ruled surface defined by (48), lies in the rectifying plane of a Cartan slant helix at every point.*

Corollary 7. *A constant angle lightlike ruled surface is constructed by null rulings along a non-null base curve.*

According to the above information mentioned in the three cases, we give following theorem without proof.

Theorem 12. *Let $\gamma(s)$ be a space curve in E_1^3. A constant angle lightlike ruled surface can be defined by one of the equations (40), (46) or (48) where γ is a null helix, pseudo-null curve or Cartan slant helix, respectively.*

We give some examples to illustrate the theory.

Example 4. *Let γ_1 be a null helix given by*

$$\gamma_1(s) = (s, \sin s, -\cos s).$$

Then the Cartan frame on γ_1 *is*

$$\begin{aligned} T &= (1, \cos s, \sin s) \\ N &= (0, -\sin s, \cos s) \\ B &= (-\frac{1}{2}, \frac{1}{2}\cos s, \frac{1}{2}\sin s). \end{aligned}$$

Then we obtain the surface given in Figure 2 (a) by choosing the functions $a = 0$ *and* $b = 1$*. Also the base curve* $\alpha(s)$ *can be seen in the Figure 3 (a).*

Example 5. *Let* γ_2 *be a pseudo null curve given by*

$$\gamma_2(s) = (\frac{s^3}{12}, \frac{s^3 + 12s}{12\sqrt{2}}, \frac{s^3 - 12s}{12\sqrt{2}}).$$

Then the Cartan frame on γ_2 *is*

$$\begin{aligned} T &= (\frac{s^2}{4}, \frac{s^2+4}{4\sqrt{2}}, \frac{s^2-4}{4\sqrt{2}}) \\ N &= (\frac{s}{2}, \frac{s}{2\sqrt{2}}, \frac{s}{2\sqrt{2}}) \\ B &= (-\frac{s^3}{16} - \frac{1}{s}, \frac{s}{2\sqrt{2}} + \frac{1}{\sqrt{2}s} - \frac{s^3}{16\sqrt{2}}, -\frac{s}{2\sqrt{2}} + \frac{1}{\sqrt{2}s} - \frac{s^3}{16\sqrt{2}}) \end{aligned}$$

where $k_2 = \frac{1}{s}$*. We obtain the surface given in Figure 2 (b) by choosing the functions* $a = 1$ *and* $b = 1$ *and the base curve* $\alpha(s)$ *can be seen in the Figure 3 (b).*

Example 6. *Let* γ_3 *be a pseudo null curve given by*

$$\gamma_3(s) = (-\frac{s^2}{2}, -\frac{s^2\sqrt{2}(\cos(\ln(s)) + 3\sin(\ln(s)))}{10}, -\frac{s^2\sqrt{2}(\sin(\ln(s)) - 3\cos(\ln(s)))}{10}).$$

Then the Cartan frame on γ_3 *is*

$$\begin{aligned} T &= (-s, -\frac{s\sqrt{2}(\cos(\ln(s)) + \sin(\ln(s)))}{2}, \frac{s\sqrt{2}(-\sin(\ln(s)) + \cos(\ln(s)))}{2}) \\ N &= (-1, -\sqrt{2}\cos(\ln(s)), -\sqrt{2}\sin(\ln(s))) \\ B &= (\frac{1}{s}, \frac{\sqrt{2}\left(2\cos(\ln(s))^3 + 2\cos(\ln(s))^2\sin(\ln(s)) - 3\cos(\ln(s)) + \sin(\ln(s))\right)}{4s\sin(\ln(s))\cos(\ln(s)) - 2s}, \\ &\quad \frac{\sqrt{2}\left(2\cos(\ln(s))^2 - 1\right)}{2s(-\sin(\ln(s)) + \cos(\ln(s)))}) \end{aligned}$$

where $k_2 = \frac{1}{s^2}$*. We obtain the surface given in Figure 2 (c) by choosing the functions* $a = s^2$ *and* $c = s$ *and the base curve* $\alpha(s)$ *can be seen in the Figure 3 (c).*

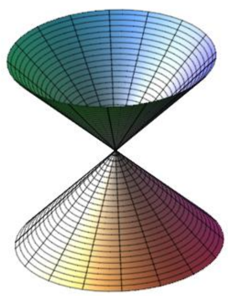

(a) Case 1 for $a = 0$ and $b = 1$

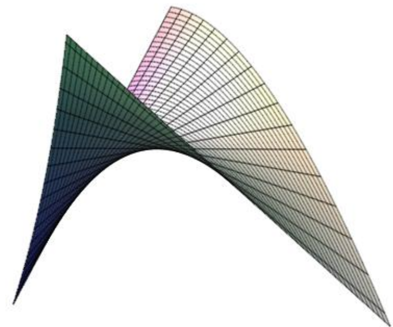

(b) Case 2 for $a = 1$ and $b = 1$

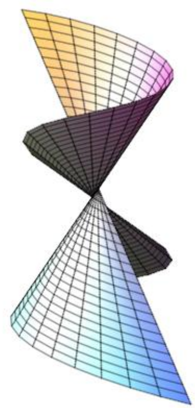

(c) Case 3 for $a = s^2$ and $c = s$

Figure 2. Constant angle lightlike ruled surfaces

5. Conclusion

In this paper, we investigate new methods to obtain the parameterizations of lightlike surfaces making constant pseudo-angles with a fixed direction in the Minkowski space. We classify these surfaces by considering the possible casual characters of the fixed direction and show that such surfaces are actually ruled surfaces based on a spacelike curve. Moreover, we give some corrolaries such as; any constant pseudo-angle lightlike surface is totally umbilical and it has negative lightlike sectional curvature, Type I is a lightlike developable and Type II is not. In the given examples one can see the illustrations related to the obtained surfaces

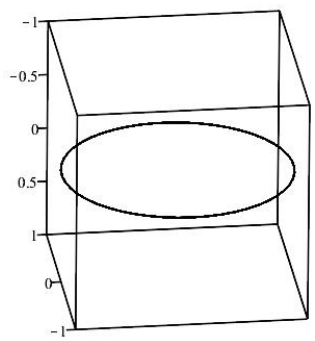

(a) Case 1

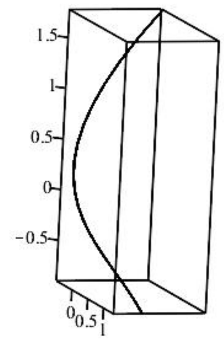

(b) Case 2

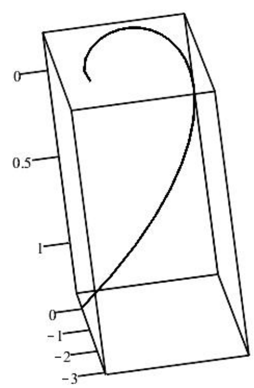

(c) Case 3

FIGURE 3. Base curve $\alpha(s)$ for (a) $-\pi < s < \pi$, (b) and (c) $-\pi/2 < s < \pi/2$

Type I and Type II.
On the other hand, we obtain corresponding constant angle lightlike ruled surfaces by using the Cartan frame on a null helix, a pseudo-null curve or a Cartan slant helix in section 4. We classify such surfaces according to the casual character of the slope axis. When we assume that the surface itself is lightlike, there exists a lightlike transversal vector field U which is parallel to the tangent vector of the initial curve. We state that a constant angle lightlike ruled surface is constructed

by null rulings along a non-null base curve. The theory is supported by several examples and illustrations.

Declaration of Competing Interests Author declares that there is no conflict of interest in the current manuscript.

References

[1] Abdel-Baky A. R., Aldossary M. T., On the null scrolls in Minkowski 3-space, *IOSR J. Math.*, 7 (2013), 11 – 16. https://doi.org/10.9790/5728-0761116

[2] Ali, A. T., Mahmoud, S. R., Position vector of spacelike slant helices in Minkowski 3-space, *Honam Mathematical J.*, 36(2) (2014), 233–251. https://doi.org/10.5831/HMJ.2014.36.2.233

[3] Barros, M., Ferrandez, A., Null scrolls as fluctuating surfaces: A new simple way to construct extrinsic string solutions, *J. High Energ. Phys*, 5 (2012), 1–18. https://doi.org/10.1007/JHEP05(2012)068

[4] Birman, G., Nomizu, K., Trigonometry in Lorentzian geometry, *Amer. Math. Monthly*, 91 (1984), 543–549. https://doi.org/10.2307/2323737

[5] Camcı, Ç., İlarslan, K., Uçum, A., General helices with lightlike slope axis, *Filomat*, 32(2) (2018), 355–367. https://doi.org/10.2298/FIL1802355C

[6] Cermelli, P., Di Scala, A. J., Constant angle surfaces in liquid crystals, *Philos. Magazine*, 87 (2007), 1871–1888. https://doi.org/10.1080/14786430601110364

[7] Chandrasekhar S., The Mathematical Theory of Black Holes, Oxford Univ. Press, 1983.

[8] Dillen, F., Fastenakels, J., Van der Veken, J., Vrancken, L., Constant angle surfaces in S2 × R, *Monaths. Math.*, 152 (2007), 89–96. https://doi.org/10.1007/s00605-007-0461-9

[9] Di Scala, A. C., Ruiz-Hernandez, G., Helix submanifolds of Euclidean spaces, *Monatsh. Math.*, 157(3) (2009), 205–215.

[10] Duggal K. L., Bejancu A., Lightlike Submanifolds of Semi-Riemannian Manifolds and Applications, Dordrecht: Springer Sci. Business Media, 1996.

[11] Duggal K. L., Foliations of lightlike hypersurfaces and their physical interpretation, *Centr. Eur. J. Math.*, 10 (2012), 1789 – 1800.

[12] Hawking S. W., The Event Horizons in Black Holes, Amsterdam, North Holland, 1972.

[13] Helzer, G., A relativistic version of the Gauss–Bonnet formula, *J. Differential Geom.*, 9 (1974), 507–512.

[14] Izumiya, S., Lightlike developables in Minkowski 3-space, *Demonstratio Mathematica*, (2006). https://doi.org/10.1515/dema-2013-0236

[15] Karadağ, H. B., Karadağ, M., Null generalized slant helices in Lorentzian space, *Differential Geometry-Dynamical Systems*, 10 (2008), 178-185.

[16] Kosinka, J., Jüttler, B., Cubic helices in Minkowski space, *Sitzungsber. Abt. II*, 215 (2006), 13–35. https://doi.org/10.1553/SundA2006sSBII-13

[17] Liu, T., Pei, D., Null helices and Cartan slant helices in Lorentz–Minkowski 3-space, *International Journal of Geometric Methods in Modern Physics*, 16(11) (2019), 1950179. https://doi.org/10.1142/S0219887819501792

[18] Lopez, R., Munteanu, M. I., Constant angle surfaces in Minkowski space, *Bull. Belg. Math. Soc. Simon Stevin*, 18 (2011), 271–286. https://doi.org/10.36045/bbms/1307452077

[19] Lucas, P., Ortega-Yagües, J. A., Slant helices: a new approximation, *Turk J Math*, 43 (2019), 473 – 485. https://doi.org/10.3906/mat-1809-16

[20] Munteanu, M. I., Nistor, A. I., A new approach on constant angle surfaces in E3, *Turkish J. Math.*, 33 (2009), 107–116. https://doi.org/10.3906/mat-0802-32

[21] Nesovic, E., On geometric interpretation of pseudo-angle in Minkowski plane, *International Journal of Geometric Methods in Modern Physics*, (2017). https://doi.org/10.1142/S0219887817500682

[22] Palmer, B., Backlund transformations for surfaces in Minkowski space, *J. Math. Phys.*, 31 (1990), 2872–2875. https://doi.org/10.1063/1.528939

[23] Tuğ, G., Ekmekci, N., Construction of the null scrolls along lightlike submanifolds in $\mathbb{R}^m + n_v$, *Int. Elec. Journ. of Geom.*, 10(1) (2017), 31–38.

[24] Tuğ, G., Ekmekci, N., Notes on the lightlike hypersurfaces along spacelike submanifolds, *Ukrainian Mathematical Journal*, 71 (2019), 1105–1114. https://doi.org/10.1007/s11253-019-01701-z

[25] Kim, Y. H., Yoon, D. W., Classification of ruled surface in Minkowski 3-space, *J. Geom. Phys.*, 49(1) (2004), 89–100. https://doi.org/10.1016/S0393-0440(03)00084-6

http://communications.science.ankara.edu.tr

Commun.Fac.Sci.Univ.Ank.Ser. A1 Math. Stat.
Volume 72, Number 3, Pages 761–777 (2023)
DOI:10.31801/cfsuasmas.1150659
ISSN 1303-5991 E-ISSN 2618-6470

Research Article; Received: July 29, 2022; Accepted: April 26, 2023

AN EXACT PENALTY FUNCTION APPROACH FOR INEQUALITY CONSTRAINED OPTIMIZATION PROBLEMS BASED ON A NEW SMOOTHING TECHNIQUE

Nurullah YILMAZ[1] and Hatice OGUT[2]

[1,2]Department of Mathematics, Suleyman Demirel University, Isparta, TÜRKİYE

Abstract. Exact penalty methods are one of the effective tools to solve nonlinear programming problems with inequality constraints. In this study, a new class of exact penalty functions is defined and a new family of smoothing techniques to exact penalty functions is introduced. Error estimations are presented among the original, non-smooth exact penalty and smoothed exact penalty problems. It is proved that an optimal solution of smoothed penalty problem is an optimal solution of original problem. A smoothing penalty algorithm based on the the new smoothing technique is proposed and the convergence of the algorithm is discussed. Finally, the efficiency of the algorithm on some numerical examples is illustrated.

1. Introduction

We consider the following continuous constrained optimization problem

$$(P) \qquad \begin{aligned} &\min_{x\in\mathbb{R}^n} f(x) \\ &s.t.\ \ c_j(x) \le 0, \quad j = 1,2,\ldots,m, \end{aligned}$$

where $f : \mathbb{R}^n \to \mathbb{R}$ and $c_j(x) : \mathbb{R}^n \to \mathbb{R}$, $j \in J = \{1,2,...,m\}$ are continuously differentiable functions. The set of feasible solutions is defined by $C_0 := \{x \in \mathbb{R}^n : c_j(x) \le 0,\ j = 1,2,\ldots,m\}$ and we assume that C_0 is not empty.

One of the most important methods in solving this problem is the penalty function approach. The penalty function approach is based on transforming the constrained optimization problem into an unconstrained problem. When the penalty function approach is applied to problem (P), it turns into the following unconstrained optimization problem:

2020 *Mathematics Subject Classification.* Primary 90C30, 65K05; Secondary 65D15.
Keywords. Constrained optimization, smoothing technique, exact penalty function.
[1] nurullahyilmaz@sdu.edu.tr-Corresponding Author; 0000-0001-6429-7518;
[2] haticeeogutt@gmail.com; 0000-0001-8640-0619.

$$\min_{x\in\mathbb{R}^n} F(x,\rho), \tag{1}$$

where $F(x,\rho) = f(x) + \rho\sum_j G\left(c_j(x)\right)$ and $\rho > 0$ parameter. The most common G functions are $G(t) = \max\{0,t\}^2$, $G(t) = \max\{0,t\}$, $G(t) = \max\{0,t\}^p$ $(0 < p \le 1)$, $G(t) = \log(1 + \max\{0,t\})$ etc [4,24]. Moreover, as the parameter ρ increases, the solution of the problem (1) gets closer to the solution of the problem (P). One of the desirable properties of penalty functions is precision. $F(x,\rho)$ is called as exact penalty function for problem (P) if there is appropriate parameter choice such that the optimal solution to the penalty problem is an optimal solution to the original problem [17,26,27]. We refer the following studies for more details [25,28].

One of the well-known penalty function is called as l_2-penalty function and it is defined as

$$F_2(x,\rho) = f(x) + \rho\sum_j \max\{c_j(x),0\}^2.$$

When f and c_j $(j = 1,2,\ldots,m)$ are continuously differentiable, the l_2 penalty function is smooth, but it is not exact [17]. One of the most popular exact penalty function is called as l_1 penalty function which is defined as

$$F_1(x,\rho) = f(x) + \rho\sum_j \max\{c_j(x),0\},$$

by Eremin [1] and Zangwill [2]. l_1 penalty function is exact but not differentiable. This is the main disadvantage of the l_1 exact penalty function, because it prevents some efficient algorithms (Steepest Descent, Newton, Quasi-Newton, etc.) from being used to solve the penalty problem. On the other hand, in order to increase the effectiveness of the exact penalty function, lower-order exact penalty functions have come to the fore in the literature [3,4]. The lower order l_p-exact penalty function is defined as

$$F_p(x,\rho) = f(x) + \rho\sum_j \max\{c_j(x),0\}^p,$$

where $0 < p < 1$ in [5,6]. Similar to l_1, l_p penalty function is also exact but not differentiable and l_p penalty function is non-Lipschitz when $0 < p < 1$. Moreover, non-smooth penalty function can cause numerical instability in the solution process when the penalty parameter is large. For this reason the smoothing approaches for the penalty function have been emerged [7]. The smoothing approach can be expressed as the representation of the non-differentiable function with a family of smooth functions. A smoothing function is defined as follows:

Definition 1. *[8] A function $\tilde{f} : \mathbb{R}^n \times \mathbb{R}_+ \to \mathbb{R}$ is called a smoothing function of a non-smooth function $f : \mathbb{R}^n \to \mathbb{R}^m$ if, for any $\varepsilon > 0$, $\tilde{f}(x,\varepsilon)$ is continuously differentiable and*

$$\lim_{z\to x,\varepsilon\downarrow 0} \tilde{f}(z,\varepsilon) = f(x)$$

for any $x \in \mathbb{R}^n$.

$\mathbb{R}_+$ represents the non-negative real numbers. Smoothing functions are often used to solve non-smooth optimization problems [9–12]. In addition, there is quite a lot of work in the literature on smoothed penalty functions l_1 and l_p [13–20]. A comprehensive review is presented in [23].

As it is well-known that gradient based methods (e. g. Newtonian methods) which are powerful tools in nonlinear programming usually needs second-order continuously differentiability of an objective function. Therefore, it is essential to develop smoothing techniques which makes l_1 and l_p exact penalty functions the second order continuously differentiable. Although there are different smoothing studies for l_1, l_p and other penalty functions in the literature, there is no smoothing approach that includes all of them.

The aim of this study is to re-define the class of exact penalty functions for problem (P) and propose a new second-order continuously differentiable smoothing technique for a new exact penalty functions in general form. By applying the proposed smoothing technique to exact penalty functions, a smoothed penalty function and a smoothed penalty problem are obtained. The relationships among the solutions which are obtained for original constrained optimization problem, exact penalty problem and the smoothed penalty problem is investigated. Based on the smoothed penalty problem, it is aimed to create an algorithm to solve the problem (P). Numerical experiments are presented by applying this algorithm to test problems.

2. Main Results

2.1. A New Exact Penalty Function.

In this part of the study, we first re-define a class of exact penalty functions as follows:

$$h(t) = \begin{cases} 0, & t < 0, \\ g(t), & t \geq 0, \end{cases}$$

where $g : \mathbb{R}_+ \to \mathbb{R}_+$ second-order continuously differentiable function with (a) $g(0) = 0$ and (b) $g'(t) > 0$ and $g''(t) \leq 0$ for $t > 0$. Based on the above definition, the exact penalty function for problem (P) is defined by

$$F_g(x, \rho) = f(x) + \rho \sum_j h(c_j(x))$$

and the penalty problem is given by

$$(P_g) \qquad \min_{x \in \mathbb{R}^n} F_g(x, \rho).$$

Moreover we have the following properties based on the function $g(t)$:

(i) if $g(t) = t$ then $F_g(x, \rho)$ become l_1-exact penalty function ([2]),

(ii) if $g(t) = t^p$ for $0 < p < 1$ is then $F_g(x, \rho)$ become l_p-lower order exact penalty function ([4,5]),

(iii) if $g(t) = \log(1+t)$ is then $F_g(x,\rho)$ become logarithmic exact penalty function is obtained ([24]).

We need the following assumptions to state the exactness of our penalty function.
Assumption 1. $f(x)$ is a coercive function, i.e., $\lim_{||x||\to\infty} f(x) = \infty$.

Assumption 1 implies that there exist a compact set $Y \subset \mathbb{R}^n$ such that all local minimizer of problem (P) are included in int$Y$.
Assumption 2. The number of local minimizer of the problem (P) is finite.

Theorem 1. *Suppose that Assumptions 1 and 2 hold. Then, there exist a threshold value $\bar{\rho}$ such that $\rho \in [\bar{\rho}, \infty)$, every solution of (P_g) is a solution of (P).*

Proof. The proof is obtained by following the way at the proof of the Corollary 2.3 in [5]. □

2.2. **Smoothing Techniques.** As it is known that, the differentiability of the penalty functions established with the functions given by (i), (ii) and (iii) cannot always be guaranteed. Especially, when $g(t) = 0$, the function h is non differentiable. Therefore, we offer the following smoothing functions for the function h inspiring from the studies [21, 22].

The smoothing function of h is defined as

$$h_{1,\gamma}(t) = \begin{cases} 0, & t < 0, \\ \frac{\gamma g'(\gamma) - 2g(\gamma)}{\gamma^3} t^3 - \frac{\gamma g'(\gamma) - 3g(\gamma)}{\gamma^2} t^2, & 0 \le t \le \gamma, \\ g(t), & t > \gamma, \end{cases} \tag{2}$$

where $\gamma > 0$ is the smoothing parameter.

Lemma 1. *For any $t \in \mathbb{R}$, the smoothing function $h_{1,\gamma}(t)$ satisfies that*

i. *$h_{1,\gamma}(t)$ is continuously differentiable,*
ii. *$\lim_{\gamma\to 0} h_{1,\gamma}(t) = h(t)$.*

Proof. i. For any $\gamma > 0$, we have

$$h'_{1,\gamma}(t) = \begin{cases} 0, & t < 0, \\ 3\frac{\gamma g'(\gamma) - 2g(\gamma)}{\gamma^3} t^2 - 2\frac{\gamma g'(\gamma) - 3g(\gamma)}{\gamma^2} t, & 0 \le t \le \gamma, \\ g'(t), & t > \gamma, \end{cases}$$

and it is easy to see that the function $h'_{1,\gamma}(t)$ is continuous at the transition points $t = 0$ and $t = \gamma$.

ii. The difference between $h(t)$ and $h_{1,\gamma}(t)$ is stated by

$$h(t) - h_{1,\gamma}(t) = \begin{cases} 0, & t < 0, \\ g(t) - \left[\frac{\gamma g'(\gamma) - 2g(\gamma)}{\gamma^3} t^3 - \frac{\gamma g'(\gamma) - 3g(\gamma)}{\gamma^2} t^2\right], & 0 \le t \le \gamma, \\ 0, & t > \gamma, \end{cases}$$

for any $\gamma > 0$. Therefore the maximum difference between $h(t)$ and $h_{1,\gamma}(t)$ arises when $0 \le t \le \gamma$. Let us define the following

$$l_{1,\gamma}(t) = \frac{\gamma g'(\gamma) - 2g(\gamma)}{\gamma^3} t^3 - \frac{\gamma g'(\gamma) - 3g(\gamma)}{\gamma^2} t^2,$$

then for $0 \le t \le \gamma$ we have

$$\begin{aligned} l'_{1,\gamma}(t) &= \frac{1}{\gamma^3}\left[\gamma g'(\gamma)\left(3t^2 - 2\gamma t\right) + g(\gamma)\left(6\gamma t - 6t^2\right)\right] \\ &\ge \frac{g(\gamma)}{\gamma^3}\left[4\gamma t - 3t^2\right] \\ &\ge 0. \end{aligned}$$

Since $l_{1,\gamma}(t) \ge 0$ and it is non-decreasing we obtain

$$h(t) - h_{1,\gamma}(t) = g(t) - l_{1,\gamma}(t) \le g(\gamma). \tag{3}$$

By taking the limit as $\gamma \to 0$, the proof is obtained.

□

For different exact penalty function, the error estimation between $h_{1,\gamma}(t)$ and $h(t)$ can be calculated. For example, if we take $g(t) = t$, then by considering (3) we obtain

$$0 \le h(t) - h_{1,\gamma}(t) \le \gamma.$$

With a similar approach, a second order differentiable smoothing function of $h(t)$ can be generated as:

$$h_{2,\gamma}(t) = \begin{cases} 0, & t < 0, \\ l_{2,\gamma}(t), & 0 \le t \le \gamma, \\ g(t), & t > \gamma, \end{cases} \tag{4}$$

form is obtained. Here

$$\begin{aligned} l_{2,\gamma}(t) &= \frac{\gamma^2 g''(\gamma) - 6\gamma g'(\gamma) + 12g(\gamma)}{2\gamma^5} t^5 - \frac{\gamma^2 g''(\gamma) - 7\gamma g'(\gamma) + 15g(\gamma)}{\gamma^4} t^4 \\ &\quad + \frac{\gamma^2 g''(\gamma) - 8\gamma g'(\gamma) + 20g(\gamma)}{2\gamma^3} t^3, \end{aligned}$$

for $\gamma > 0$.

Lemma 2. *For any $t \in \mathbb{R}$, the smoothing function $h_{2,\gamma}(t)$ satisfies that*

i. *$h_{2,\gamma}(t)$ is second-order continuously differentiable,*
ii. *$\lim_{\gamma \to 0} h_{2,\gamma}(t) = h(t)$.*

Proof. The proof is obtained similarly to the proof of Lemma 1. □

Example 1. *Let us consider the function $y = h(t)$. The graph of $h(t)$, $h_{1,\gamma}$ and $h_{2,\gamma}$ are illustrated in Figs. 1, 2 and 3, when $g(t) = t$, $g(t) = t^p$ with $p = \frac{1}{2}$ and $g(t) = \log(1+t)$, respectively. It is observed that the smoothing functions approach the original function when $\gamma \to 0$.*

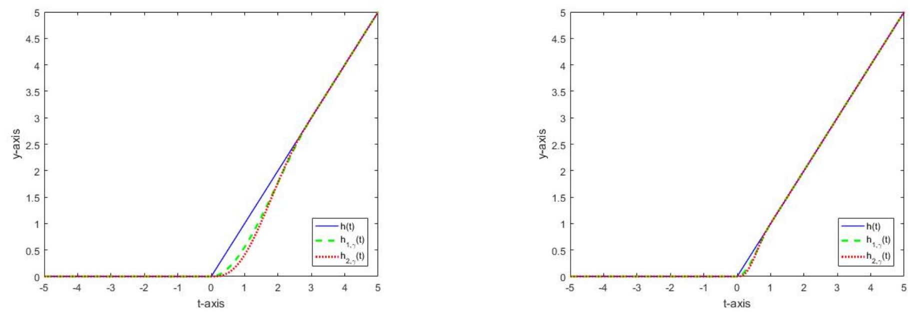

(A) For $\gamma = 3$. (B) For $\gamma = 1$.

FIGURE 1. The blue graph represents $h(t)$ for $g(t) = t$, the green graph is $h_{1,\gamma}(t)$ and the red graph is $h_{2,\gamma}(t)$.

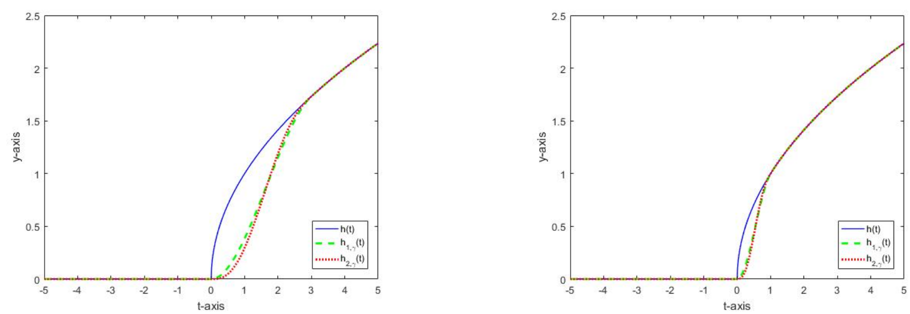

(A) For $\gamma = 3$. (B) For $\gamma = 1$.

FIGURE 2. The blue graph represents $h(t)$ for $g(t) = t^p$, $p = 0.5$, the green graph is $h_{1,\gamma}(t)$ and the red graph is $h_{2,\gamma}(t)$.

Remark 1. *It should be pointed out that the applied smoothing functions are non-convex.*

By using one of the smoothing functions given in (2) and (4), the smoothing exact penalty function is obtained as

$$\tilde{F}_g(x, \rho, \gamma) = f(x) + \rho \sum_{j \in J} h_{i,\gamma}\left(c_j(x)\right),$$

$i = 1, 2$. Therefore the smoothed penalty function problem is stated as

$$(PS_g) \quad \min_{x \in \mathbb{R}^n} \tilde{F}_g(x, \rho, \gamma).$$

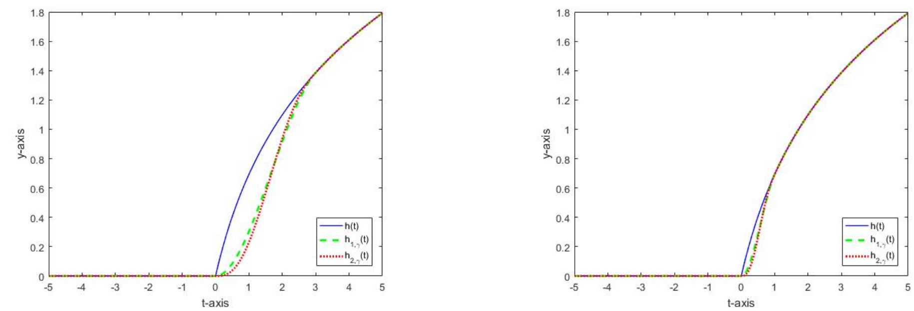

(A) For $\gamma = 3$. (B) For $\gamma = 1$.

FIGURE 3. The blue graph represents $h(t)$ for $\log(1+t)$, the green graph is $h_{1,\gamma}(t)$ and the red graph is $h_{2,\gamma}(t)$.

Now let us investigate the relationship between the exact penalty problem and the smoothed exact penalty problem.

Theorem 2. *For any $x \in \mathbb{R}^n$, we have*

$$0 \leq F_g(x,\rho) - \tilde{F}_g(x,\rho,\gamma) \leq \rho m g(\gamma)$$

and

$$\lim_{\gamma \to 0} \tilde{F}_g(x,\rho,\gamma) = F_g(x,\rho),$$

for $\gamma > 0$.

Proof. For any $\rho, \gamma > 0$, we have

$$\begin{aligned} F_g(x,\rho) - \tilde{F}_g(x,\rho,\gamma) &= f(x) + \rho \sum_{j \in J} h(c_j(x)) - \left[f(x) + \rho \sum_{j \in J} h_{i,\gamma}(c_j(x)) \right] \\ &= \rho \sum_{j \in J} \left[h(c_j(x)) - h_{i,\gamma}(c_j(x)) \right], \end{aligned}$$

for $i = 1, 2$. Therefore, we obtain

$$\begin{aligned} F_g(x,\rho) - \tilde{F}_g(x,\rho,\gamma) &\leq \rho \sum_{j \in J} g(\gamma) \\ &\leq \rho m g(\gamma). \end{aligned}$$

□

It is easy to see that we have the following error estimates:

$$F_1(x,\rho) - \tilde{F}_1(x,\rho,\gamma) \leq \rho m \gamma,$$

for $g(t) = t$,

$$F_p(x,\rho) - \tilde{F}_p(x,\rho,\gamma) \leq \rho m \gamma^p,$$

for $g(t) = t^p$, $0 < p < 1$ and

$$F_{\log}(x,\rho) - \tilde{F}_{\log}(x,\rho,\gamma) \leq \rho m \log(1+\gamma),$$

for $g(t) = \log(1+t)$.

The following corollary indicates that the distance between $F_g(x,\rho)$ and $\tilde{F}_g(x,\rho,\gamma)$ decreases when the smoothing parameter decreases.

Corollary 1. *Let $\{\gamma_k\} \to 0$ and $\{x^k\}$ is an optimal solution of the problem $\min_{x\in\mathbb{R}^n} \tilde{F}_g(x,\rho_k,\gamma_k)$. If $\bar{x}$ is limit point of $\{x^k\}$, then $\bar{x}$ is the optimal solution to the problem (P_g).*

Definition 2. *[17] Let f^* be the optimal objective function value of the problem (P) and x be a feasible solution. If the condition*

$$f(x) - f^* \leq \gamma$$

holds, then x is called $\gamma-$approximate solution.

Definition 3. *[17] If $c_j(x_\gamma) \leq \gamma$ for any $j \in J$ and for $\gamma > 0$, then the x_γ is called as $\gamma-$feasible solution of the problem (P).*

Lemma 3. *[17, 24] Let x^* be the optimal solution to the problem (P_g). If x^* is a feasible solution to the problem (P), then x^* is the optimal solution for (P).*

Thus, we can give the following theorem on the relations of optimal solutions of the problems (P), (P_g) and (PS_g) .

Theorem 3. *Let $\rho > 0$, x^* be an optimal solution to the problem (P_g) and x_γ be and optimal solution to the problem (PS_g). Then the following holds:*

$$\lim_{\gamma\to 0} \tilde{F}_g(x_\gamma,\rho,\gamma) = F_g(x^*,\rho). \tag{5}$$

Moreover, if x^* is the optimal solution to the problem (P) and x_γ is the γ-feasible solution for the problem (P) , then x_γ is the approximate solution to the problem (P).

Proof. Let x^* be an optimal solution of (P_g) and x_γ be an optimal solution of (PS_g). By considering Theorem 2 and following inequalities

$$\begin{aligned} F_g(x^*,\rho) &\leq F_g(x_\gamma,\rho), \\ \tilde{F}_g(x_\gamma,\rho,\gamma) &\leq \tilde{F}_g(x^*,\rho,\gamma), \end{aligned} \tag{6}$$

we obtain

$$\begin{aligned} 0 &\leq F_g(x^*,\rho) - \tilde{F}_g(x^*,\rho,\gamma) \\ &\leq F_g(x^*,\rho) - \tilde{F}_g(x_\gamma,\rho,\gamma) \\ &\leq F_g(x_\gamma,\rho) - \tilde{F}_g(x_\gamma,\rho,\gamma) \end{aligned}$$

$$\leq \quad m\rho g(\gamma).$$

Therefore, (5) is hold. Let x^* be an optimal solution of (P) and x_γ be $\gamma-$feasible solution (P). Since we have

$$0 \leq \left[f(x^*) + \rho \sum_j h(c_j(x^*)) \right] - \left[f(x_\gamma) + \rho \sum_j h_{i,\gamma}(c_j(x_\gamma)) \right] \leq m\rho g(\gamma),$$

$c_j(x^*) \leq 0$ and $c_j(x_\gamma) \leq \gamma$, then we have

$$\rho \sum_j h(c_j(x^*)) = 0, \qquad 0 \leq \rho \sum_j h_{i,\gamma}(c_j(x_\gamma)) \leq m\rho\gamma$$

and we obtain

$$|f(x_\gamma) - f(x^*)| < m\rho\,(\gamma + g(\gamma))\,.$$

□

2.3. **Algorithm.** In this section, the following algorithm is proposed to solve the penalty problem (P) by considering the surrogate problem (PS_g).

Algorithm A

Step 1 Select initial point x^0, and parameters $\gamma_0 > 0$, $\rho_0 > 0$. Determine the auxiliary parameters $\varepsilon > 0$, $N > 1$, $0 < \delta < 1$. Let $k = 0$ and go to Step 2.

Step 2 By using x^k as an initial point, solve the problem $\min_{x \in R^n} \tilde{F}_g(x, \rho_k, \gamma_k)$ with any local search methods. Let x^{k+1} be an optimal solution.

Step 3 If x^{k+1} is the ε-feasible solution to the problem (P), then stop. Otherwise, take $\rho_{k+1} = N\rho_k$, $\gamma_{k+1} = \delta\gamma_k$ and $k = k + 1$, and go back to Step 2 .

Remark 2. *In Step 2 of Algorithm A, any gradient based local search method (e.g. Steepest Descent, Newton, Quasi-Newton and etc.) can be used according to degree of smoothing approximation.*

Remark 3. *From the 3rd step of Algorithm A and Theorem 2, an approximate optimal solution of the problem P can be obtained.*

We denote the following index sets

$$J_\gamma^-(x) = \{j | c_j(x) < \gamma, j \in J\}, \qquad J_\gamma^+(x) = \{j | c_j(x) \geq \gamma, j \in J\}.$$

With these notations; the following theorem is given related to the convergence of Algorithm A.

Theorem 4. *Let the Assumption 1 is hold. Then the sequence $\{x^k\}$ generated by Algorithm A is bounded and the limit point $\bar{x}$ is the optimal solution to the problem (P).*

Proof. Let us first prove that $\{x^k\}$ is bounded. Since the sequence $\{F(x^k, \rho_k, \gamma_k)\}$ is a bounded sequence, then there exist a number L such that

$$\tilde{F}_g(x^k, \rho_k, \gamma_k) \leq L, \quad k = 0, 1, 2, \ldots. \tag{7}$$

Assume to contrary that $\left\{x^k\right\}$ is unbounded. Without loss of generality, let $k \to \infty$, $\|x^k\| \to \infty$. The equation (7) is re-stated as

$$L \geq \tilde{F}_g(x^k, \rho_k, \gamma_k) \geq f(x^k), \quad k = 0, 1, 2, \ldots$$

and it is a contradiction with the Assumption 1. The boundedness of $\{x^k\}$ is obtained.

Let us now show that the limit point $\bar{x}$ of $\{x^k\}$ is the optimal solution to the problem (P). Let us first show that the point $\bar{x}$ is a feasible solution to the problem (P). Let $\lim_{k\to\infty} x^k = \bar{x}$. On the contrary, suppose the point $\bar{x}$ is not a feasible solution to (P). Then there exists $j \in J$ for $c_j(\bar{x}) \geq \alpha > 0$ such that

$$\begin{aligned} \tilde{F}_g(x^k, \rho_k, \gamma_k) &= f(x^k) + \rho_k \sum_{j\in J} h_{i,\gamma_k}(c_j(x^k)) \\ &= f(x^k) + \rho_k \sum_{j\in J^+_{\gamma_k}(x^k)} h_{i,\gamma_k}(c_j(x^k)) \\ &\quad + \rho_k \sum_{j\in J^-_{\gamma_k}(x^k)} h_{i,\gamma_k}(c_j(x^k)). \end{aligned} \tag{8}$$

where $c_j(\bar{x}) \geq \alpha > 0$, the set $\{j : c_j(\bar{x}) \geq \alpha\}$ is non-empty. There is $j_0 \in J$ with $c_{j_0}(\bar{x}) \geq \alpha$. Since $\rho_k \to \infty$ as $k \to \infty$, from the equation (8) we obtain

$$\tilde{F}_g(x^k, \rho_k, \gamma_k) \to \infty.$$

This contradicts the boundedness of the sequence $\{\tilde{F}_g(x^k, \rho_k, \gamma_k)\}$. Thus $\bar{x}$ would be a feasible solution to the (P) problem.

Let us show that the $\bar{x}$ is an optimal solution for (P). Assume x^* is an optimal solution for (PS_g) and x^k is an optimal solution for the problem $\min_{x\in R^n} \tilde{F}_g(x^k, \rho_k, \gamma_k)$ then we have

$$\tilde{F}_g(x^k, \rho_k, \gamma_k) \leq \tilde{F}_g(x^*, \rho_k, \gamma_k), \quad k = 1, 2, \ldots.$$

Similarly, we have

$$f(x^k) + \rho_k \sum_{j\in J} h_{i,\gamma_k}(c_j(x^k)) \leq f(x^*) + \rho_k \sum_{j\in J} h_{i,\gamma_k}(c_j(x^*)), \quad k = 1, 2, \ldots$$

and

$$f(x^k) \leq f(x^*).$$

So while $k \to \infty$,

$$f(\bar{x}) \leq f(x^*). \tag{9}$$

Since x^* is the optimal solution for (P), we have

$$f(\bar{x}) \geq f(x^*). \tag{10}$$

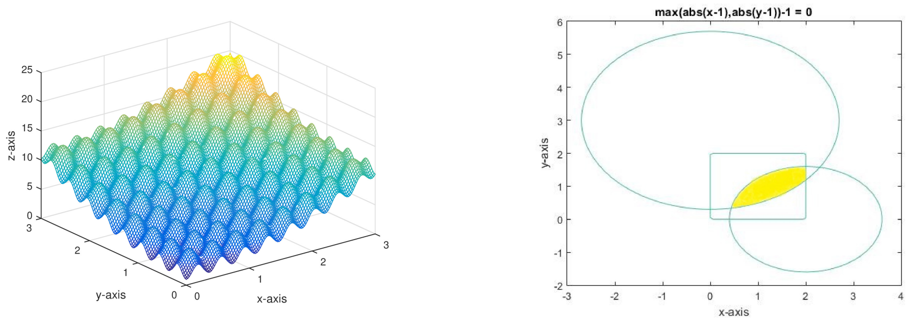

(A) (B)

FIGURE 4. (A) The graph of f (B)The graph of feasible region.

From (9) and (10), we obtain $f(\bar{x}) = f(x^*)$. It means that $\bar{x}$ is the optimal solution for (P). □

3. Numerical Results

In order to analyze the numerical performance of Algorithm A, we apply it on some test problems in the literature. The results are presented in the tables with details and the evaluations on these results are given. Firstly, the abbreviations used in the tables are listed below.

k	:	Number of iterations
x^k	:	the result of $k-$th iteration
ρ_k	:	penalty function parameter in the $k-$th iteration
γ_k	:	smoothing parameter of the $k-$th iteration
$c_j(x^k)$	:	constraint function value at x^k
$\tilde{F}_g(x^k, \rho_k, \gamma_k)$	:	value of function $\tilde{F}_g$ at point x^k.
$f(x^k)$	:	The value of the objective function at x^k

Problem 1. *[14] Consider the following problem*

$$\begin{aligned} \min f(x) \quad &= \quad x_1^2 + x_2^2 - \cos(17x_1) - \cos(17x_2) + 3 \\ s.t. \quad & \quad g_1(x) = (x_1 - 2)^2 + x_2^2 - 1.6^2 \leq 0, \\ & \quad g_2(x) = x_1^2 + (x_2 - 3)^2 - 2.7^2 \leq 0, \\ & \quad 0 \leq x_1 \leq 2, \quad 0 \leq x_2 \leq 2. \end{aligned}$$

We select $x^0 = (1,1)$ as starting point $\rho_0 = 10$, $\gamma_0 = 0.1$, $\eta_0 = 0.1$ and $N = 3$. The obtained numerical results are illustrated in Table 1 and 2.

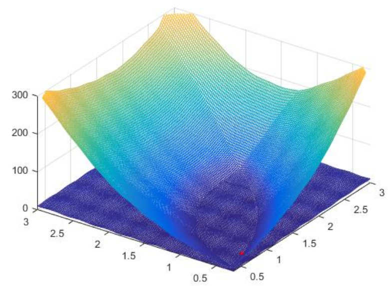

(A) For $g(t) = t$.

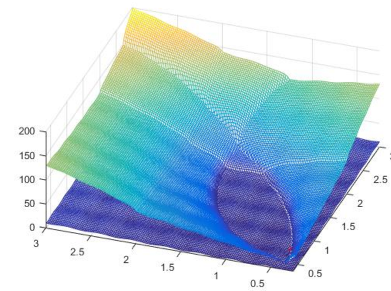

(B) For $g(t) = t^p$, $p = \frac{1}{2}$.

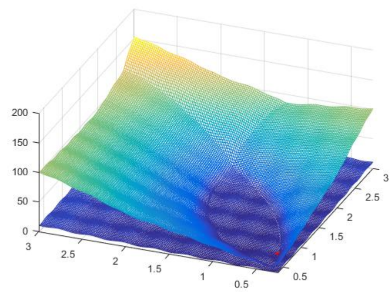

(C) For $g(t) = \log(1 + t)$

FIGURE 5. The graph of $\tilde{F}_g(x, \rho, \gamma)$ with $\rho = 10$, $\gamma = 0.25$.

TABLE 1. Numerical results for the Problem 1

Penalty Function	k	x^{k+1}	ρ_k	γ_k	$(c_1(x^k), c_2(x^k))$	$\tilde{F}_g(x^k, \rho_k, \gamma_k)$	$f(x^k)$
$g(t) = t$	0	$(0.7256, 0.3985)$	10	0.1	$(-0.7770, 0.0044)$	1.8338	1.8301
	1	$(0.7254, 0.3992)$	30	0.01	$(-0.7759, 0.0001)$	1.8374	1.8373
	2	$(0.7254, 0.3993)$	90	0.001	$(-0.7759, 0.0000)$	1.8376	1.8376
$g(t) = t^p$	0	$(0.72540.3991)$	10	0.1	$(-0.7762, 0.0011)$	1.8366	1.8356
	1	$(0.7254, 0.3993)$	30	0.01	$(-0.7759, 0.0000)$	1.8376	1.8376
$g(t) = log(1 + t)$	0	$(0.72560.3985)$	10	0.1	$(-0.77700.0045)$	1.8337	1.8299
	1	$(0.7254, 0.3992)$	30	0.01	$(-0.7759, 0.0001)$	1.8374	1.8373
	2	$(0.7254, 0.3993)$	90	0.001	$(-0.7759, 0.0000)$	1.8376	1.8376

For different penalty types, the global minimizer is found as $x^* = (0.7254, 0.3993)$ with corresponding function value 1.8376. In [14, 17], the resulting global minimizer is found as $x^* = (0.72540669, 0.3992805)$ and the corresponding function value 1.837623, and combining all three approaches our algorithm found the right point as in [14, 17].

TABLE 2. Numerical results for the Problem 1

Penalty Function	iter	feval	Time	$\tilde{F}_g(x^k, \rho_k, \gamma_k)$	$f(x^k)$
$g(t) = t$	3	180	1.1094	1.8376	1.8376
$g(t) = t^p$	2	123	0.8125	1.8376	1.8376
$g(t) = \log(1+t)$	3	177	1.1875	1.8376	1.8376

Problem 2. *[14] Consider the following problem which is called as Rosen-Suzuki problem:*

$$\begin{aligned} \min f(x) &= x_1^2 + x_2^2 + 2x^3 + x_4^2 - 5x_1 - 21x_3 + 7x_4 \\ s.t. \quad & g_1(x) = 2x_1^2 + x_2^2 + x_3^2 + 2x_1 + x_2 + x_4 - 5 \le 0, \\ & g_2(x) = x_1^2 + x_2^2 + x_3^2 + x_4^2 + x_1 - x_2 + x_3 - x_4 - 8 \le 0, \\ & g_3(x) = x_1^2 + 2x_2^2 + x_3^2 + 2x_4^2 - x_1 - x_4 - 10 \le 0. \end{aligned}$$

We select the starting point as $x^0 = (0,0,0,0)$, $\rho_0 = 10$, $\gamma_0 = 0.1$, $\eta_0 = 0.1$ *and* $N = 3$. *The obtained numerical results are illustrated as in Table* 3 *and* 4.

Applying Algorithm A, the minimizer is found as $x^* = (0.1697, 0.8358, 2.0084, -0.9651)$ with the corresponding function value -44.2338. In [14], the resulting global minimizer is found as $x^* = (0.1684621, 0.8539065, 2.000167, -0.9755604)$ with the corresponding function value -44.23040. In [17], the global minimizer is obtained as $x^* = (0.170189, 0.835628, 2.008242, -0.95245)$ with corresponding function value -44.2338. It can be observed that our algorithms provide numerically better results than [14] and find approximate solutions with lower iteration numbers compared to [17].

TABLE 3. Numerical results for Problem 2.

Penalty Function	k	x^{k+1}	ρ_k	γ_k	$(c_1(x^k), c_2(x^k), c_3(x^k))$	$\tilde{F}_g(x^k, \rho_k, \gamma_k)$	$f(x^k)$
$g(t) = t$	0	$(0.1697, 0.8355, 2.0092, -0.9656)$	10	0.1	$(0.0019, 0.0052, -1.8773)$	-44.2396	-44.2455
	1	$(0.1696, 0.8356, 2.0086, -0.9650)$	30	0.01	$(0.0001, 0.0002, -1.8826)$	-44.2340	-44.2342
	2	$(0.1696, 0.8356, 2.0086, -0.9650)$	90	0.001	$(-0.0001, 0.0000, -1.8827)$	-44.2338	-44.2338
$g(t) = t^p$	0	$(0.1696, 0.8356, 2.0088, -0.9651)$	10	0.1	$(0.0005, 0.0013, -1.8815)$	-44.2353	-44.2367
	1	$(0.1695, 0.8355, 2.0086, -0.9650)$	30	0.01	$(-0.0007, 0.0000, -1.8827)$	-44.2338	-44.2338
$g(t) = log(1+t)$	0	$(0.1697, 0.8355, 2.0092, -0.9656)$	10	0.1	$(0.0019, 0.0053, -1.8772)$	-44.2398	-44.2458
	1	$(0.1696, 0.8356, 2.0086, -0.9650)$	30	0.01	$(0.0001, 0.0002, -1.8826)$	-44.2340	-44.2342
	2	$(0.1696, 0.8356, 2.0086, -0.9650)$	90	0.001	$(-0.0001, 0.0000, -1.8827)$	-44.2338	-44.2338

Problem 3. *[17] Consider the following problem*

$$\begin{aligned} \min f(x) &= 1000 - x_1^2 - 2x_2^2 - x_3^2 - x_1x_2 - x_1x_3 \\ s.t. \quad & g_1(x) = x_1^2 + x_2^2 + x_3^2 - 25 = 0, \\ & g_2(x) = (x_1 - 5)^2 + x_2^2 + x_3^2 - 25 = 0 \end{aligned}$$

TABLE 4. Numerical results for Problem 2.

Penalty Function	iter	feval	Time	$\tilde{F}_g(x^k, \rho_k, \gamma_k)$	$f(x^k)$
$g(t) = t$	3	510	1.1406	−44.2338	−44.2338
$g(t) = t^p$	2	475	0.79688	−44.2338	−44.2338
$g(t) = \log(1+t)$	3	460	0.98438	−44.2338	−44.2338

$$g_3(x) = (x_1 - 5)^2 + (x_2 - 5)^2 + (x_3 - 5)^2 - 25 \leq 0.$$

We select $x^0 = (2, 2, 1)$ *as a starting point* $\rho_0 = 100$, $\gamma_0 = 0.1$, $\eta_0 = 0.1$ *and* $N = 3$. *The obtained numerical results are illustrated as in Table* 5 *and* 6.

By considering Algorithm A the global minimizer is found as $x^* = (2.5001, 4.1754, 1.1474)$ with corresponding function value 944.2157 by using $g(t) = t$, and $x^* = (2.5000, 4.2213, 0.9647)$ and corresponding value as 944.2157 by using $g(t) = t^p$ and $g(t) = \log(1+t)$. In [17], the obtained global minimizer is obtained as $x^* = (2.5000, 4.2213, 0.9647)$ with the corresponding function value 944.2157. According to these results, we deduce that by using Algorithm A the correct solutions is obtained with a lower number of iterations than [17].

TABLE 5. Numerical results for Problem 3.

Penalty Function	k	x^{k+1}	ρ_k	γ_k	$(c_1(x^k), c_2(x^k), c_3(x^k))$	$\tilde{F}_g(x^k, \rho_k, \gamma_k)$	$f(x^k)$
$g(t) = t$	0	$(2.5001, 4.1754, 1.1474)$	100	0.1	$(0.0012 - 0.0001 - 3.2283)$	944.3897	944.2571
	1	$(2.5000, 4.1753, 1.1474)$	300	0.01	$(0.0000, 0.0000, -3.2274)$	944.2652	944.2653
$g(t) = t^p$	0	$(2.5012, 4.2220, 0.9649)$	100	0.1	$(0.0123, 0.0007, -1.8682)$	945.4946	944.1889
	1	$(2.5000, 4.2213, 0.9647)$	300	0.01	$(0.0000, -0.0000, -1.8599)$	944.2156	944.2156
$g(t) = log(1+t)$	0	$(2.5000, 4.2213, 0.9648)$	100	0.1	$(0.0004, 0.0000, -1.8607)$	944.3356	944.2148
	1	$(2.5000, 4.2213, 0.9648)$	300	0.01	$(0.0000, 0.0000, -1.8604)$	944.2156	944.2156

TABLE 6. Numerical results for Problem 3.

Penalty Function	iter	feval	Time	$\tilde{F}_g(x^k, \rho_k, \gamma_k)$	$f(x^k)$
$g(t) = t$	2	328	0.8125	944.2652	944.2653
$g(t) = t^p$	2	300	0.70313	944.2156	944.2156
$g(t) = \log(1+t)$	2	300	0.71875	944.2156	944.2156

4. Conclusion

In this study, a new class of exact penalty function is given and smoothing penalty function is proposed for this new exact penalty function. A new minimization algorithm is developed in order to solve the problem (P) by the help of surrogate problem (PS_g). The algorithm is applied to the test problems and satisfactory results are obtained.

The proposed smoothing technique for the non-smooth exact penalty functions has a flexible structure. It is available for both Lipschitz and non-Lipschitz penalty functions. This is the most important feature of our smoothing technique and that distinguishes our smoothing technique from other techniques.

Algorithm A is in all cases highly effective for small and medium scale optimization problems. By applying this algorithm, the optimum value is found quickly and the algorithm offers high accuracy in finding the optimal point.

Author Contribution Statements The authors contributed equally to this work. All authors read and approved the final copy of this paper.

Declaration of Competing Interests The authors declare that they have no known competing financial interest or personal relationships that could have appeared to influence the work reported in this paper.

Acknowledgements This paper was presented in 4th International Conference on Pure and Applied Mathematics (ICPAM - VAN 2022), Van-Turkey, June 22-23, 2022.

References

[1] Eremin, I. I., The penalty method in convex programming, *Cybernetics*, 3(4) (1967), 53-56. https://doi.org/10.1007/BF01071708
[2] Zangwill, W. I., Nonlinear programing via penalty functions, *Management Science*, 13 (1967), 344-358. http://www.jstor.org/stable/2627851.
[3] Rubinov, A. M., Glover, B. M., Yang, X. Q., Decreasing functions with applications to penalization, *SIAM J. Optim.*, 10 (1999), 289-313. https://doi.org/10.1137/S105262349732609
[4] Rubinov, A. M., Yang, X. Q., Bagirov, A. M., Penalty functions with a small penalty parameter, *Optim. Methods Softw.*, 17(5) (2002), 931-964. https://doi.org/10.1080/1055678021000066058
[5] Wu, Z. Y., Bai, F. S., Yang, X. Q., Zhang, L. S., An exact lower-order penalty function and its smoothing in nonlinear programming, *Optimization*, 53(1) (2004), 51-68. https://doi.org/10.1080/02331930410001662199
[6] Bai, F. S., Wu, Z. Y., Zhu, D. L., Lower order calmness and exact penalty function, *Optim. Methods Softw.*, 21(4) (2006), 515-525. https://doi.org/10.1080/10556780600627693
[7] Pinar, M. C., Zenios, S., On smoothing exact penalty functions for convex constrained optimization, *SIAM J. Optim.*, 4(3) (1994), 468-511. https://doi.org/10.1137/0804027
[8] Chen, C., Mangasarian, O. L., A class of smoothing functions for nonlinear and mixed complementarity problem, *Comput. Optim. Appl.*, 5 (1996), 97-138. https://doi.org/10.1007/BF00249052

[9] Bertsekas, D. P., Nondifferentiable optimization via approximation. *In: Balinski, M. L., Wolfe, P. (eds) Nondifferentiable Optimization. Mathematical Programming Studies*, 3 (1975), 1-25. https://doi.org/10.1007/BFb0120696

[10] Zang, I., A smoothing out technique for min-max optimization,*Math. Programm.*, (19) 1980, 61-77. https://doi.org/10.1007/BF01581628

[11] Bagirov, A. M., Al Nuaimat, A., Sultanova, N. Hyperbolic smoothing function method for minimax problems, *Optimization*, 62(6) (2013), 759-782. https://doi.org/10.1080/02331934.2012.675335

[12] Yilmaz, N. and Sahiner, A., On a new smoothing technique for non-smooth, non-convex optimization, *Numer. Algebra Control Optim.*, 10(3) (2020), 317-330. https://doi.org/10.3934/naco.2020004

[13] Wu, Z. Y., Lee, H. W. J., Bai, F. S., Zhang, L. S., Quadratic smoothing approximation to l_1 exact penalty function in global optimization, *J. Ind. Manag. Optim.*, 1(4) 2005, 533-547. https://doi.org/10.3934/jimo.2005.1.533

[14] Lian, S. J., Smoothing approximation to l_1 exact penalty for inequality constrained optimization, *Appl. Math. Comput.*, 219(6) (2012), 3113-3121. https://doi.org/10.1016/j.amc.2012.09.042

[15] Xavier, A. E., Hyperbolic penalty: a new method for nonlinear programming with inequalities, *Int. Trans. Op. Res.*, 8(6) (2001), 659-671. https://doi.org/10.1111/1475-3995.t01-1-00330

[16] Liu, B., On smoothing exact penalty function for nonlinear constrained optimization problem,*J. Appl. Math. Comput.*, 30 (2009), 259-270. https://doi.org/10.1007/s12190-008-0171-z

[17] Xu, X., Meng, Z., Sun, J., Shen, R., A penalty function method based on smoothing lower order penalty function, *J. Comput. Appl. Math.*, 235(14) (2011), 4047-4058. https://doi.org/10.1016/j.cam.2011.02.031

[18] Meng, Z., Dang, C., Jiang, M., Shen, R., A smoothing objective penalty function algorithm for inequality constrained optimization problems, *Numer. Funct. Anal. Optim.*, 32(7) (2011), 806-820. https://doi.org/10.1080/01630563.2011.577262

[19] Sahiner, A., Kapusuz, G., Yilmaz, N., A new smoothing approach to exact penalty functions for inequality constrained optimization problems, *Numer. Algebra Control Optim.*, 6(2) (2016), 161-173. https://doi.org/10.3934/naco.2016006

[20] Xu, X., Dang, C., Chan, F., Wang, Y., On smoothing ℓ_1 exact penalty function for constrained optimization problems, *Numer. Funct. Anal. Optim.*, 40(1) (2019), 1-18. https://doi.org/10.1080/01630563.2018.1483948

[21] Lee, J. and Skipper, D., Virtuous smoothing for global optimization, *J. Glob. Optim.*, 69 (2017), 677-699. https://doi.org/10.1007/s10898-017-0533-x

[22] Xu, L., Lee, J. and Skipper, D., More virtuous smoothing, *SIAM J. Optim.*, 29(2) 2019, 1240-1259. https://doi.org/10.1137/18M11728

[23] Grossmann, C., Smoothing techniques for exact penalty function methods, *In: Panaroma of Mathematics: Pure and Applied Contemporary Mathematics,*, 658 (2016), 249-265.

[24] Hassan M., Baharum, A., Generalized logarithmic penalty function method for solving smooth nonlinear programming involving invex functions, *Arab. J. Basic Appl. Sci.*, 26(1) (2019), 202-214. https://doi.org/10.1080/25765299.2019.1600317

[25] Dolgopolik, M. V., Smooth exact penalty functions: a general approach, *Optim. Lett.*, 10 (2016), 635-648. https://doi.org/10.1007/s11590-015-0886-3

[26] Lucidi S., Rinaldi, F., Exact penalty functions for nonlinear integer programming problems, *J. Optim. Theory Appl.*, 145 (2010), 479-488. https://doi.org/10.1007/s10957-010-9700-7

[27] Di Pillo, G., Lucidi, S., Rinaldi, F., An approach to constrained global optimization based on exact penalty functions, *J. Glob Optim.*, 54 (2012), 251-260. https://doi.org/10.1007/s10898-010-9582-0

[28] Antczak, T., A new exact exponential penalty function method and nonconvex mathematical programming, *Appl. Math. Comput.*, 217(15) (2011), 6652-6662. https://doi.org/10.1016/j.amc.2011.01.051

http://communications.science.ankara.edu.tr

Commun.Fac.Sci.Univ.Ank.Ser. A1 Math. Stat.
Volume 72, Number 3, Pages 778–802 (2023)
DOI:10.31801/cfsuasmas.1159269
ISSN 1303-5991 E-ISSN 2618-6470

COMMUNICATIONS SERIES A1

Research Article; Received: August 8, 2022; Accepted: April 29, 2023

A NEW MEASURE OF PREFERRED DIRECTION FOR CIRCULAR DATA USING ANGULAR WRAPPING

Özge TEZEL,[1] Buğra Kaan TİRYAKİ,[2] Eda ÖZKUL[3] and Orhan KESEMEN[4]

[1,2,3,4]Department of Statistics and Computer Sciences, Karadeniz Technical University, 61080 Trabzon, TÜRKİYE

Abstract. The statistical techniques which are developed for the analysis of data in the linear number system cannot be applied to directional data directly. Circular data may be discontinuous in some principal interval. These discontinuities cause failure results in the circular statistics. Because of that the proposed wrapping operator must be used for data, which are defined in the discontinuous range. However, in both continuity and discontinuity, the wrapping operator works correctly. The most common preferred directions for circular data are circular mean and variance summarizing and comparing them. Although circular data has a very important role in statistics, the literature is weak in terms of statistical analysis of circular data. It creates a gap in this field. This study examines the preferred direction of circular data to fill this gap and presents a new measure of preferred direction for circular data using angular wrapping. Four different artificial and three real datasets are employed to evaluate the performance of the proposed methods. The results demonstrate the superiority of the proposed methods in terms of the absolute error and absolute percentage error. Consequently, it has been seen that the proposed methods give more consistent and more accurate results than the vectorial methods.

1. Introduction

The obtained data from observation can be existed in various measurement spaces. One of the measurement spaces is an angular space in which data are

2020 *Mathematics Subject Classification.* 62H11, 62P10, 62P12, 62-08.
Keywords. Angular wrapping, circular data, angular circular mean, angular circular variance, preferred directions.

[1] ozge_tzl@hotmail.com; 0000-0003-2815-686X;
[2] bugrakaantiryaki@gmail.com; 0000-0003-0995-7389;
[3] eda.ozkul.gs@gmail.com-Corresponding author; 0000-0002-9840-8818;
[4] okesemen@gmail.com; 0000-0002-5160-1178.

expressed as the angular. For instance, a biologist may be measuring the orientation of an animal depending on a factor in the nature or a geologist may be interested in the direction of the earth's magnetic pole. Such directions may be univariate as in the first example or bivariate like the second one ([1]). In general, data identifying in angular space are referred to as directional data. Data showing univariate angular change are called as circular data; data showing bivariate angular change are called as spherical data. If data show more than two angular changes are called as hyper-spherical data.

The statistical techniques which are developed for the analysis of data in the linear number system cannot be applied to directional data directly. The most illustrative example of this situation is to consider a sample of size two on the circle consisting of the angles $350°$ and $10°$, mean direction of these angles is $0°$ when linear mean formula is applied to them, their linear mean is $180°$. Many problems arise when the other statistics such as dispersion measurement and correlation are applied to circular data ([2]). Therefore, circular statistics have been developed for circular data as a branch of statistical science. Circular statistics include statistical techniques to summarize the obtained data in angular space and to interpret that. In the literature several studies were performed for the analysis of directional data and circular statistics were applied to different field of study. Mardia ([3]) is the first reference book for the analysis of circular data. Fisher ([4]), Mardia and Jupp ([5]), and Jammalamadaka and SenGupta ([1]) are good alternative reference books in this field. Statistics of circular data are used in different scientific disciplines such as earth sciences ([6]), meteorology, biology, physics, psychology ([7,8]), mathematics and statistics ([9–18]), image analysis ([19]), medicine ([20–22]), astronomy and agriculture ([23]), geography and marine sciences ([24–27]), computer sciences ([28,29]).

In many research, the usage of appropriate descriptive statistics is useful to summarize the data. Representation of two-dimensional data in the form of angle and vector on the unit circle is not only one. Because the value of circular observation may be changed according to zero direction and the selection of clockwise or anticlockwise. The obtained results are a function of the given observation, and the function does not depend on the arbitrary value. Owing to these properties, circular data analysis is quite different from statistical analysis. The need of arbitrary zero direction and orientation often make many statistical techniques and measures incorrect and meaningless. Therefore, various methods for descriptive statistics of circular data have been developed in the literature. Firstly, these methods were developed by Fisher ([4]). Batschelet ([30]), Fisher ([4]), Zar ([31]), Jammalamadaka and SenGupta ([1]) are the source books for the descriptive statistics of circular data.

The vectorial methods proposed by Mardia ([3]) define circular data as vectors on the unit circle. If the inspected data are vectorial data, vectorial methods are good approximation. If the inspected data are directional or periodic data, the proposed methods by Mardia ([3]) can give the failure or approximate results. Therefore, several statistics such as the angular mean and the angular variance are proposed for circular data by using wrapping operator to eliminate this approximation in this study. In view of this, the motivation of this paper is to merge the burgeoning field of circular statistics with different disciplines as environmental, biological and ecology science to see how the different areas can be of mutual benefit.

The remainder of the paper is organized as follows. Section 2 presents an overview of circular data. The proposed preferred directions for circular data are discussed in Section 3. Experimental results are highlighted in Section 4. Section 5 focusses on the applications of circular statistics in real environmental, biological and ecological problems. Eventually, the conclusions are drawn in Section 6.

2. Overview of Circular Data

Circular variables are defined on a circle curve unlike number line. For this reason, they show periodic changes. In this way, periodic variables are defined as

$$\theta = mod\left(\theta + 2k\pi, 2\pi\right), \left(k = 0, \pm 1, \pm 2, \ldots\right).$$

These variables are periodic with 2π radian period. In the same way, the stability of periodicity in different phase values can alter circle number line's starting point location or definition interval boundaries. The most common mathematical representation of starting point accepts the positive x-axis as starting point and counterclockwise as orientation. Two different approaches are used as the definition interval of radian unit. These are one-sided principal interval $[0, 2\pi)$ and symmetric principal interval $(-\pi, \pi]$ ([32]). The symmetric principal interval is preferred in this study.

Although directional data are continuous at each point on the circle, when directional data addressed linearly, it creates the illusion of discontinuities at the 0 radian point according to the one-sided principal interval and at the π point according to the symmetric principal interval. Therefore, classical statistical techniques are insufficient and occasionally give failure results in the analysis of directional data.

Generally, observed circular data are measured in degrees; however, this study is assumed that circular data are measured in radians. Circular data are converted from degrees (α) to radians (θ) by using following equation

$$\theta = \frac{\alpha}{180}\pi.$$

Circular data can be applied to periodic data as well as data which show the angular change. Periodic data, such as the days of the week and time of the day can be exemplified for this situation. Periodic data (x) are converted into angular space by

$$\theta = \frac{2\pi x}{T},$$

where T gives the period of observed data.

Circular data can be cut across interval boundaries because of some arithmetic operations. In this situation, principal interval can be reduced to symmetric principal interval by using wrapping process. Wrapping process is given in the following equation

$$\theta = mod\,(\phi + \pi, 2\pi) - \pi.$$

In this study, wrapping process is represented by $Wrap_\pi(\cdot)$ operation and it is defined as

$$\theta = Wrap_\pi\,(\phi)\,.$$

2.1. **Addition of Two Circular Values.** The sum of two variables which are in the same unit and show the angular change is the same as in the linear number system. However, in this operation, principal interval boundaries can be cut across. In this situation, the obtained values from the result of addition can be reduced to the symmetric principal interval by

$$\psi = Wrap_\pi\,(\phi + \theta)\,.$$

2.2. **Subtraction of Two Circular Values.** The subtraction involves some complexity. Some equations such as equation (1) may lead to failure results by the reason of the characteristics of the circular data.

$$\psi = \phi - \theta \tag{1}$$

Therefore, if counterclockwise is assumed as positive and clockwise is assumed as negative, the subtraction will be easier. The angle θ is accepted as starting point, so that in the range $(\theta - \pi, \theta)$ is assumed as negative region and in the range $(\theta, \theta + \pi]$ is assumed positive region (Figure 1).

Therefore, we assumed that a value (ϕ) in the range of $(\theta - \pi,\ \theta)$ is smaller than θ and a value (ϕ) in the range of $(\theta,\ \theta + \pi]$ is bigger than θ. Under these circumstances, the smallest difference between two angles is calculated by

$$\psi = Wrap_\pi\,(\phi - \theta)\,.$$

2.3. **Distance of Two Circular Values.** Every pair of distinct points on a circle determines two arcs. If two points are not directly opposite each other, one of these arcs, the minor arc, will subtend an angle at the center of the circle that is less than π radians. The other arc, the major arc, will subtend an angle greater than π radians ([33]).

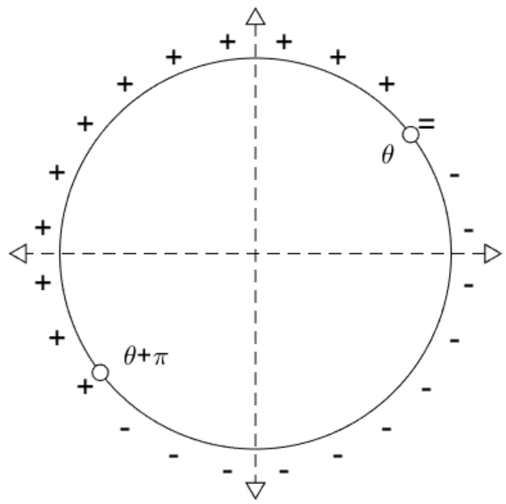

FIGURE 1. Positive and negative region according to θ radian

When the distance between two points on the circle number line is calculated, the minor arc length is preferred. The minor arc length is calculated by using the following equation ([34])

$$\psi_0 = \pi - |\pi - |\phi - \theta|| . \quad (2)$$

This equation gives accurate results in radians. However, ϕ and θ must be in the principal interval. Another alternative equation is given in the following equation ([35])

$$\psi_v = 1 - \cos(\phi - \theta). \quad (3)$$

This equation takes values in $[0, 2]$. It is not equal to the length of the $[0, \pi]$ radian. If this equation multiplies by $\pi/2$, it will be in the desired principal interval. In spite of this improvement, it may not always produce the desired results due to the curvature of the cosine function. Proposed method which is given in the equation (4) gives the best results by taking the absolute value of the subtraction.

$$\psi_a = |Wrap_\pi(\phi - \theta)| \quad (4)$$

2.4. **Circular Mean and Variance.** The mean of the circular data cannot be inherently calculated like mean of linear data. The most illustrative example of

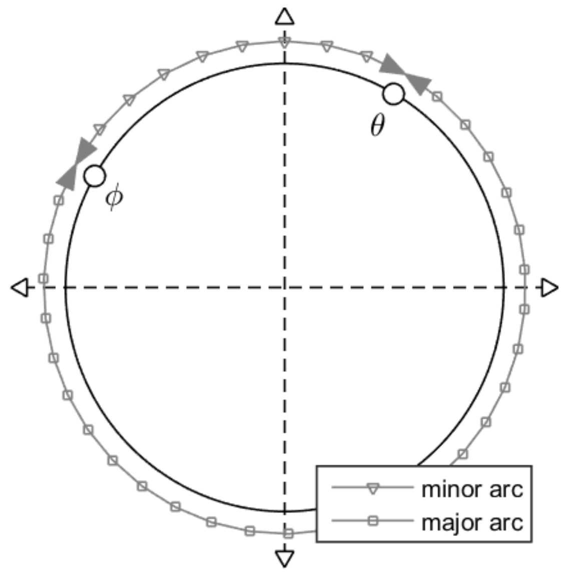

FIGURE 2. The minor arc and the major arc of two points

this situation is to consider a sample of size two on the circle consisting of the angles 355° and 5°, mean direction of these angles is 0° when linear mean formula is applied to these angles, their linear mean is 180°. Angular continuity is exposed to numerical discontinuity; therefore, mean of the circular data cannot be calculated properly. When Mardia and Jupp ([5]) proposed a method to calculate the circular mean; in this method, each observation regarded as unit vectors and the resultant length of these vectors is calculated. The average horizontal component of circular data is calculated by

$$\bar{C} = \frac{1}{n}\sum_{i=1}^{n} \cos(\theta_i),$$

and the average vertical component of circular data is calculated by using equation (5)

$$\bar{S} = \frac{1}{n}\sum_{i=1}^{n} \sin(\theta_i). \tag{5}$$

The resultant length of these components is calculated by the following equation

$$\bar{R} = \sqrt{\bar{C}^2 + \bar{S}^2}.$$

The angle of this resultant length is defined as

$$\bar{\theta} = atan2\left(\bar{S}, \bar{C}\right).$$

In this equation, $\bar{\theta}$ also gives the circular mean where atan2 is an arc tangent function that ranges between $(-\pi, \pi]$. In statistical analysis, variance is the most widely used measure of variability. The sample variance is the sum of the squared differences around the arithmetic mean divided by the sample size minus one. Circular variance is calculated by using vectorial approach as

$$V_v = 1 - \bar{R}.$$

In which the circular variance (V_v) takes value in $[0, 1]$. This method was proposed by Mardia and Jupp ([5]) but this approach is unsuitable for the definition of variance in the linear data.

3. Proposed Preferred Directionsfor Circular Data

The definitions of the mean and the variance are given clearly in the literature. These definitions were altered for circular data because of the special nature of circular data, but these are not suit to the standard definition. Thus, in the literature, several statistics were obtained by using vectorial mean or resultant length. The most common preferred directions for circular data are the circular mean and the variance ([4]). Circular mean and circular variance are the most commonly used parameters to summarize and compare the circular data. Circular variance shows the spread of a dataset. If all circular data are concentrated in one direction, the average resultant vector length will be close to one. If the circular data show a widespread over the unit circle, that is, if they show a uniform distribution, the average resultant vector length will be close to or equal to zero.

3.1. **Circular Mean Based on Angular Difference.** In this study, an iterative method which based on the angular distance of circular data is suggested. Let, $\Theta = \{\theta_1, \theta_2, \ldots, \theta_n\}$ represent the circular data. The first selected value is considered as initial mean and this situation is represented as follows

$$\bar{\theta}_1 = \theta_1.$$

Afterwards, each value is treated with the current mean respectively and equation (6) is obtained.

$$\bar{\theta}_i = \bar{\theta}_{i-1} + \frac{1}{i} Wrap_\pi \left(\theta_i - \bar{\theta}_{i-1}\right), \quad (i = 2, \ldots, n) \tag{6}$$

After all values are treated, general mean is calculated by using equation (7).

$$\bar{\theta} = Wrap_\pi \left(\bar{\theta}_n\right) \tag{7}$$

3.2. **Circular Variance Based on Angular Difference.** The sample variance is the sum of the squared differences around the arithmetic mean divided by the sample size minus one. Vectorial variance proposed by Mardia and Jupp ([5]) is unsuitable for the definition of variance in the linear data. For this reason, vectorial variance method does not perform properly for circular data. Therefore, this study proposes a circular variance by using the angular approach as in equation (8).

$$V_a = \frac{1}{n-1} \sum_{i=1}^{n} Wrap_{\pi}^{2} \left(\theta_i - \bar{\theta} \right) \tag{8}$$

In which $\bar{\theta}$ represents the circular mean which is given in the previous section.

4. Experimental Results

In circular statistics, classical statistical techniques give approximate results because of the special nature of circular data. The angular mean and the angular variance are proposed to eliminate this approximation in this paper. Generally, circular data may be discontinuous in some principal interval. These discontinuities cause failure results in the circular statistics. Because of that the proposed wrapping operator must be used for data, which are defined in the discontinuous range. But discontinuity for variance cannot be mentioned because of the fact that variance is calculated quantitatively. However, in both continuity and discontinuity, the wrapping operator works correctly for circular variance calculation. In this regard, performance criteria are required to show the success of the proposed methods. For this reason, absolute error and dispersion are used as performance criteria for both continuity and discontinuity situations. In addition, a new dispersion measure has been proposed using the wrapping operator as a performance criteria.

4.1. **Performance Criteria for Circular Mean.** The linear sample mean is defined as below

$$\bar{x} = \frac{1}{n} \sum_{i=1}^{n} x_i. \tag{9}$$

Equation (10) can be obtained by subtracting the right side of this equation from both sides of equation (9).

$$n\bar{x} - \sum_{i=1}^{n} x_i = 0 \tag{10}$$

If the equation (10) is regulated, the equation (11) is obtained as

$$\sum_{i=1}^{n} (x_i - \bar{x}) = 0. \tag{11}$$

According to this equation, the sum of deviations from the mean is zero. If this equation is applied to circular data, equation (12) is obtained as

$$Wrap_\pi\left(\sum_{i=1}^{n} Wrap_\pi\left(\theta_i-\bar{\theta}\right)\right)=0. \tag{12}$$

The fact that this is not zero shows that an error is to be occurred. The absolute error for mean is defined as follows

$$E_{mean}=\left|Wrap_\pi\left(\sum_{i=1}^{n} Wrap_\pi\left(\theta_i-\bar{\theta}\right)\right)\right|.$$

Different approaches have been developed in the literature to calculate the distance of two circular values and given in Section 2.3. Therefore, different dispersion measures have been presented for each of the distance approximations. The dispersion of angles $\theta_1,\theta_2,\ldots,\theta_n$ about a given angle α is defined as in the equation (13) and it was developed based on the minor arc length in the equation (2) ([1,4]).

$$d_0(\alpha)=\pi-\frac{1}{n}\sum_{i=1}^{n}\left|\pi-\left|\theta_i-\alpha\right|\right| \tag{13}$$

The other way of the measuring the dispersion of angles about the angle α is given as the following equation which is based on the equation (3) ([5]).

$$d_v(\alpha)=\frac{1}{n}\sum_{i=1}^{n}\left(1-\cos\left(\theta_i-\alpha\right)\right)$$

This paper presents a new measure of preferred direction for circular data using angular wrapping. Therefore, a new measure of dispersion is proposed as a new performance criteria for the preferred directions which is given equation (14)

$$d_a(\alpha)=\frac{1}{n}\sum_{i=1}^{n}\left|Wrap_\pi\left(\theta_i-\alpha\right)\right|. \tag{14}$$

The dispersion of the angles $\theta_1,\theta_2,\ldots,\theta_n$ about the angle α can be calculated by taking as $\alpha=\bar{\theta}_{vectorial}$ and $\alpha=\bar{\theta}_{angular}$, respectively.

4.2. **Performance Criteria for Circular Variance.** The linear sample variance is defined as below

$$V=\frac{1}{n-1}\sum_{i=1}^{n}\left(x_i-\bar{x}\right)^2. \tag{15}$$

Equation (16) can be obtained by subtracting the right side of this equation from both sides of equation (15).

$$\left(n-1\right)V-\sum_{i=1}^{n}\left(x_i-\bar{x}\right)^2=0 \tag{16}$$

If the equation (16) is regulated, the equation (17) is obtained as

$$\sum_{i=1}^{n}\left[(x_i-\bar{x})^2-\frac{(n-1)}{n}V\right]=0. \tag{17}$$

If this equation is applied to circular data, equation (18) is obtained as

$$\sum_{i=1}^{n}\left[Wrap_{\pi}^{2}\left(\theta_i-\bar{\theta}\right)-\frac{n-1}{n}V_a\right]=0. \tag{18}$$

The fact that this is not zero shows that an error is to be occurred. The absolute error for variance is defined as follows

$$E_{var}=\left|\sum_{i=1}^{n}\left[Wrap_{\pi}^{2}\left(\theta_i-\bar{\theta}\right)-\frac{n-1}{n}V_a\right]\right|.$$

4.3. **Simulation of Performances.** In this section, four different examples were selected to compare the proposed method with the conventional method to measure performances of angular mean and angular variance.

Example 1. *It was discussed that discontinuity of circular data may lead to failure results in the previous section. Thus, the first example is selected from the range $[0,\pi]$ where data are continuous. For comparing performance of these methods, we consider the simulation data from the uniform distribution by generating a hundred data points. This process repeated a thousand times and some of the obtained results are shown in Table 1, Table 2 and Table 3.*

The obtained some results are shown in Table 1 and Table 2 which is included the absolute error and dispersion measure to prove the performance of the proposed approach. The linear sample mean, and angular mean give the same results in Table 1, because of the data are continuous in the range of $[0,\pi]$.

According to these results, since the circular data generated in the $[0,\pi]$ interval show continuity, the linear mean $\left(\bar{\theta}_l\right)$ and the proposed angular mean $\left(\bar{\theta}_a\right)$ give the same results, while the vectorial mean $\left(\bar{\theta}_v\right)$ proposed by Mardia gives almost close results. Although the vectorial absolute error $(E_{mean}^{(v)})$ is quite low for continuous circular data, the angular absolute error $(E_{mean}^{(a)})$ of the proposed angular mean $(\bar{\theta}_a)$ using the wrapping operator is equal zero for all iterations. Because the data are continuous in the range $[0,\pi]$, the linear mean and the proposed angular mean are equal. Therefore, it can be concluded that the proposed angular mean performs more consistent and proper than the vectorial mean. Thus, the average errors of vectorial and angular mean are calculated as 1.5225 and 0.000, respectively.

When the results are examined, it is seen that the $d_0(\bar{\theta}_v)$ and $d_0(\bar{\theta}_a)$, which depend on the minor arc length, give almost the same results. In addition, the Table 2 reveals that the values of $d_v(\bar{\theta}_v)$ and $d_v(\bar{\theta}_a)$ depending on the vectorial distance give close results. When the $d_a(\bar{\theta}_v)$ and $d_v(\bar{\theta}_a)$ values depending on the

TABLE 1. Comparison of circular means according to the absolute errors.

i	$\bar{\theta}_l$	$\bar{\theta}_v$	$\bar{\theta}_a$	$E_{mean}^{(v)}$	$E_{mean}^{(a)}$
1	1.528	1.524	1.528	0.377	0.000
100	1.516	1.524	1.516	0.793	0.000
200	1.743	1.770	1.743	2.747	0.000
300	1.606	1.617	1.606	1.051	0.000
400	1.590	1.601	1.590	1.107	0.000
500	1.490	1.489	1.490	0.142	0.000
600	1.568	1.576	1.568	0.805	0.000
700	1.653	1.656	1.653	0.266	0.000
800	1.541	1.533	1.541	0.798	0.000
900	1.491	1.464	1.491	2.729	0.000
1000	1.596	1.616	1.596	2.002	0.000

TABLE 2. Comparison of circular means according to the dispersions.

i	$d_0(\bar{\theta}_v)$	$d_0(\bar{\theta}_a)$	$d_v(\bar{\theta}_v)$	$d_v(\bar{\theta}_a)$	$d_a(\bar{\theta}_v)$	$d_a(\bar{\theta}_a)$
1	0.816	0.817	0.381	0.381	0.004	0.000
100	0.888	0.888	0.431	0.431	0.008	0.000
200	0.734	0.735	0.335	0.335	0.027	0.000
300	0.764	0.764	0.348	0.348	0.011	0.000
400	0.844	0.844	0.408	0.408	0.011	0.000
500	0.761	0.761	0.346	0.346	0.001	0.000
600	0.803	0.804	0.366	0.366	0.008	0.000
700	0.723	0.723	0.320	0.320	0.003	0.000
800	0.710	0.711	0.311	0.311	0.008	0.000
900	0.767	0.767	0.361	0.362	0.027	0.000
1000	0.786	0.786	0.353	0.354	0.020	0.000

proposed wrapping operator are examined, the dispersion of the $\bar{\theta}_a$ *is equal to zero for all repetition. Accordingly, it can be said that the proposed method gives more consistent results than the vectorial method.*

The some of the obtained results are shown in Table 3 which is obtained from the comparison of the angular variance and the linear variance. The linear variance and angular variance give the same results in Table 3, because of the data are continuous in the range of $[0, \pi]$.

According to Table 3, since the circular data generated in the $[0, \pi]$ *interval show continuity, while the linear variance* (V_l) *and the proposed angular variance* (V_a)

TABLE 3. Comparison of the linear and angular variance according to absolute errors.

i	V_l	V_v	V_a	$E_{var}^{(v)}$	$E_{var}^{(v)}$
1	0.872	0.381	0.872	48.585	0.000
100	0.995	0.431	0.995	55.794	0.000
200	0.771	0.335	0.771	43.146	0.000
300	0.790	0.348	0.790	43.792	0.000
400	0.941	0.408	0.941	52.786	0.000
500	0.791	0.346	0.791	44.084	0.000
600	0.829	0.366	0.829	45.862	0.000
700	0.729	0.320	0.729	40.449	0.000
800	0.705	0.311	0.705	39.056	0.000
900	0.835	0.361	0.835	46.838	0.000
1000	0.802	0.353	0.802	44.404	0.000

give the same results, the vectorial variance (V_v) proposed by Mardia gives almost close results with them. The angular absolute error ($E_{var}^{(a)}$) of the proposed angular variance (V_a) using the wrapping operator is equal zero for all iterations. Because the data are contiuous in the range $[0, \pi]$, the linear variance and proposed angular variance are equal. Therefore, it can be concluded that the proposed angular variance performs more consistent and proper than vectorial variance. Thus, the average errors of vectorial and angular variance are calculated as 46.157 and 0.000, respectively.

Example 2. *For comparing performances of these methods, we consider the simulation data from the uniform distribution by generating a hundred data points in the range $[-\pi, \pi]$. This process repeated a thousand times. The linear mean is not used due to discontinuity in Example 2. In this case, angular mean and vectorial mean are compared by using absolute error and measure of dispersion, obtained results are shown in Table 4 and Table 5.*

In this example, the generated circular data shows discontinuity as it is defined in the range $[-\pi, \pi]$. Therefore, the linear mean value cannot be calculated for discontinuous circular data and the vectorial mean $\left(\bar{\theta}_v\right)$ and angular mean $\left(\bar{\theta}_a\right)$ values are used, and absolute error value (E_{mean}) and dispersion of angles ($d(\alpha)$) are used as performance criterias in this example. According to these results, the mean absolute errors of vectorial and angular mean are calculated as 1.5948 and 0.000, respectively. Table 4 shows that the absolute errors for all iterations are equal zero. It can be inferred that the proposed angular mean provides better results than the vectorial mean.

When the results are examined, angular and vectorial dispersion measures give different results due to discontinuity. When the $d_a(\bar{\theta}_v)$ and $d_a(\bar{\theta}_a)$ values depending

Table 4. Comparison of circular means according to the absolute errors.

i	$\bar{\theta}_v$	$\bar{\theta}_a$	$E_{mean}^{(v)}$	$E_{mean}^{(a)}$
1	-3.139	-0.463	2.557	0.000
100	2.837	2.479	1.938	0.000
200	1.009	1.289	2.893	0.000
300	1.040	0.574	2.700	0.000
400	2.971	-2.918	1.759	0.000
500	0.025	-0.783	0.816	0.000
600	2.479	2.312	2.165	0.000
700	0.098	0.355	0.653	0.000
800	-0.238	2.521	0.547	0.000
900	-1.390	2.228	2.688	0.000
1000	1.523	2.438	2.775	0.000

Table 5. Comparison of circular means according to the dispersions.

i	$d_0(\bar{\theta}_v)$	$d_0(\bar{\theta}_a)$	$d_v(\bar{\theta}_v)$	$d_v(\bar{\theta}_a)$	$d_a(\bar{\theta}_v)$	$d_a(\bar{\theta}_a)$
1	1.522	1.598	0.969	1.028	0.026	0.000
100	1.352	1.379	0.842	0.852	0.019	0.000
200	1.430	1.447	0.889	0.893	0.029	0.000
300	1.530	1.507	0.955	0.960	0.027	0.000
400	1.460	1.458	0.905	0.912	0.018	0.000
500	1.523	1.522	0.957	0.971	0.008	0.000
600	1.520	1.514	0.955	0.956	0.022	0.000
700	1.439	1.447	0.900	0.903	0.007	0.000
800	1.419	1.713	0.882	1.110	0.005	0.000
900	1.462	1.669	0.914	1.077	0.027	0.000
1000	1.482	1.511	0.931	0.958	0.028	0.000

on the proposed wrapping operator are examined, the dispersion of the $\bar{\theta}_a$ *is equal to zero for all repetition. It can be said that the proposed method gives more consistent results than the vectorial method. Therefore, it is seen that the proposed method gives more consistent results than the vectorial method.*

The angular variance and vectorial variance are compared by using absolute error and the obtained results are shown in Table 6.

In this example, the generated circular data shows discontinuity as it is defined in the range $[-\pi, \pi]$*. Therefore, the linear variance cannot be calculated for discontinuous circular data, the vectorial variance* (V_v) *and angular variance* (V_a) *are*

TABLE 6. Comparison of the angular and vectorial variance according to absolute errors.

i	$\bar{\theta}_v$	$\bar{\theta}_a$	$E_{var}^{(v)}$	$E_{var}^{(a)}$
1	0.969	3.434	244.038	0.000
100	0.842	2.557	169.831	0.000
200	0.889	2.767	185.994	0.000
300	0.955	3.112	213.511	0.000
400	0.905	2.987	206.140	0.000
500	0.957	3.073	209.457	0.000
600	0.955	3.088	211.124	0.000
700	0.900	2.807	188.807	0.000
800	0.882	3.763	285.193	0.000
900	0.914	3.616	267.541	0.000
1000	0.931	3.122	216.904	0.000

used, and absolute error (E_{var}) is used as performance criteria in this example. According to these results, the mean absolute errors of vectorial and angular variance are calculated as 218.639 and 0.000, respectively. Table 6 shows that the absolute errors for all iterations are equal zero. It can be inferred that the proposed angular variance provides better results than the vectorial variance.

Example 3. *For comparing performance of these methods, we consider the simulation data from the von Mises distribution $\left(vM\left(\mu=\frac{\pi}{2},\kappa=10\right)\right)$ by generating a hundred data points. This process repeated a thousand times. The high values of concentration parameter (κ) reduce to discontinuity of circular data. For this reason, the differences between vectorial mean $\left(\bar{\theta}_v\right)$ and angular mean $\left(\bar{\theta}_a\right)$ decrease. The some of the obtained results are shown in Table 7 which is acquired from the comparison of the circular means and the linear mean. The linear mean $\left(\bar{\theta}_l\right)$ and angular mean $\left(\bar{\theta}_a\right)$ give the same results in Table 7 due to the high values of κ.*

The high values of κ reduce to discontinuity of circular data. For this reason, the differences between vectorial and angular mean decrease. The linear mean $\left(\bar{\theta}_l\right)$ and the proposed angular mean $\left(\bar{\theta}_a\right)$ give the same results, while the vectorial mean $\left(\bar{\theta}_v\right)$ proposed by Mardia ([3]) gives almost close results. Although the vectorial absolute error ($E_{mean}^{(v)}$) is quite low for continuous circular data, the angular absolute error ($E_{mean}^{(a)}$) of the proposed angular mean $\left(\bar{\theta}_a\right)$ using the wrapping operator is equal zero for all iterations. Because of the high values of κ, the data are contiuous and so the linear mean and the proposed angular mean are equal. Therefore, it proves that the proposed angular mean performs more consistent and proper than the vectorial mean. According to these results, the average errors of vectorial and angular mean are calculated as 0.114 and 0.000, respectively.

TABLE 7. Comparison of circular means according to the absolute errors.

i	$\bar{\theta}_l$	$\bar{\theta}_v$	$\bar{\theta}_a$	$E^{(v)}_{mean}$	$E^{(a)}_{mean}$
1	*1.593*	*1.593*	*1.593*	*0.027*	*0.000*
100	*1.591*	*1.588*	*1.591*	*0.285*	*0.000*
200	*1.557*	*1.558*	*1.557*	*0.116*	*0.000*
300	*1.554*	*1.554*	*1.554*	*0.052*	*0.000*
400	*1.609*	*1.609*	*1.609*	*0.053*	*0.000*
500	*1.576*	*1.573*	*1.576*	*0.235*	*0.000*
600	*1.563*	*1.564*	*1.563*	*0.148*	*0.000*
700	*1.527*	*1.528*	*1.527*	*0.056*	*0.000*
800	*1.554*	*1.553*	*1.554*	*0.086*	*0.000*
900	*1.592*	*1.591*	*1.592*	*0.159*	*0.000*
1000	*1.623*	*1.621*	*1.623*	*0.140*	*0.000*

TABLE 8. Comparison of circular means according to the dispersions.

i	$d_0(\bar{\theta}_v)$	$d_0(\bar{\theta}_a)$	$d_v(\bar{\theta}_v)$	$d_v(\bar{\theta}_a)$	$d_a(\bar{\theta}_v)$	$d_a(\bar{\theta}_a)$
1	*0.251*	*0.251*	*0.047*	*0.047*	*0.000*	*0.000*
100	*0.280*	*0.281*	*0.059*	*0.059*	*0.003*	*0.000*
200	*0.249*	*0.249*	*0.048*	*0.048*	*0.001*	*0.000*
300	*0.243*	*0.243*	*0.049*	*0.049*	*0.001*	*0.000*
400	*0.259*	*0.259*	*0.048*	*0.048*	*0.001*	*0.000*
500	*0.254*	*0.254*	*0.052*	*0.052*	*0.002*	*0.000*
600	*0.259*	*0.259*	*0.051*	*0.051*	*0.001*	*0.000*
700	*0.243*	*0.243*	*0.043*	*0.043*	*0.001*	*0.000*
800	*0.265*	*0.265*	*0.053*	*0.053*	*0.001*	*0.000*
900	*0.267*	*0.267*	*0.058*	*0.058*	*0.002*	*0.000*
1000	*0.285*	*0.285*	*0.061*	*0.061*	*0.001*	*0.000*

When the results are examined, it is seen that the $d_0(\bar{\theta}_v)$ *and* $d_0(\bar{\theta}_a)$*, which depend on the minor arc length, give almost the same results. In addition, the values of* $d_v(\bar{\theta}_v)$ *and* $d_v(\bar{\theta}_a)$ *depending on the vectorial distance give close results. When* $d_a(\bar{\theta}_v)$ *and* $d_a(\bar{\theta}_a)$ *values depending on the proposed wrapping operator are examined, the dispersion of the* $\bar{\theta}_a$ *is equal to zero for all repetition. Accordingly, it can be said that the proposed method gives more consistent results than the vectorial method.*

In the same way, the some of the obtained results from the comparison of the angular and vectorial variance are shown in Table 9. The linear variance and angular variance give the same results in Table 9.

TABLE 9. Comparison of the angular and vectorial variance according to absolute errors.

i	V_l	V_v	V_a	$E_{var}^{(v)}$	$E_{var}^{(a)}$
1	0.097	0.047	0.097	4.942	0.000
100	0.123	0.059	0.123	6.339	0.000
200	0.100	0.048	0.100	5.123	0.000
300	0.101	0.049	0.101	5.184	0.000
400	0.098	0.048	0.098	4.996	0.000
500	0.108	0.052	0.108	5.529	0.000
600	0.105	0.051	0.105	5.386	0.000
700	0.089	0.043	0.089	4.529	0.000
800	0.111	0.053	0.111	5.654	0.000
900	0.121	0.058	0.121	6.266	0.000
1000	0.127	0.061	0.127	6.522	0.000

The high values of κ reduce to discontinuity of circular data. For this reason, the differences between vectorial and angular variance decrease. While the linear variance (V_l) and the proposed angular variance (V_a) give the same results, the vectorial variance (V_v) proposed by Mardia ([3]) gives almost close results. Although the vectorial absolute error $E_{var}^{(v)}$ is quite low for continuous circular data, the angular absolute error $E_{var}^{(a)}$ of the proposed angular variance (V_a) using wrapping operator is equal zero for all iterations. Because of the high values of κ, the data are contiuous and so the linear variance and the proposed angular variance are equal. Therefore, it proves that the proposed angular variance performs more consistent and proper than the vectorial variance. According to these results, the average errors of vectorial and angular variance are calculated as 5.416 and 0.000, respectively.

Example 4. *For comparing performance of these methods, we consider the simulation data from the von Mises distribution $\left(vM\left(\mu = \frac{\pi}{2}, \kappa = 2\right)\right)$ by generating a hundred data points. This process repeated a thousand times. The low values of κ increase discontinuity of circular data. For this reason, the difference between vectorial mean and angular mean increase. The linear mean is not used due to the discontinuity in Example 4.*

The angular mean and vectorial mean are compared by using absolute error and measure of dispersion, the obtained results are shown in Table 10 and Table 11.

The low values of κ increase discontinuity of circular data. For this reason, the difference between vectorial mean and angular mean increase. Therefore, the linear

TABLE 10. Comparison of circular means according to the absolute errors.

i	$\bar{\theta}_v$	$\bar{\theta}_a$	$E^{(v)}_{mean}$	$E^{(a)}_{mean}$
1	1.573	1.558	1.507	0.000
100	1.688	1.700	1.277	0.000
200	1.458	1.437	2.052	0.000
300	1.576	1.581	0.525	0.000
400	1.652	1.650	0.208	0.000
500	1.699	1.688	1.079	0.000
600	1.581	1.544	2.620	0.000
700	1.424	1.456	3.042	0.000
800	1.607	1.603	0.389	0.000
900	1.524	1.529	0.584	0.000
1000	1.552	1.535	1.679	0.000

mean $(\bar{\theta}_l)$ cannot be calculated for discontinuous circular data, the vectorial mean $(\bar{\theta}_v)$ and angular mean $(\bar{\theta}_a)$ are used, and absolute error value (E_{mean}) is used as performance criterion in this example. According to these results, the mean absolute errors of vectorial and angular mean are calculated as 1.596 and 0.000, respectively. Table 10 shows that the absolute errors for all iterations are equal zero. It can be inferred that the proposed angular mean provides better results than the vectorial mean.

TABLE 11. Comparison of circular means according to the dispersion.

i	$d_0(\bar{\theta}_v)$	$d_0(\bar{\theta}_a)$	$d_v(\bar{\theta}_v)$	$d_v(\bar{\theta}_a)$	$d_a(\bar{\theta}_v)$	$d_a(\bar{\theta}_a)$
1	0.594	0.595	0.242	0.242	0.015	0.000
100	0.715	0.715	0.331	0.331	0.013	0.000
200	0.676	0.678	0.307	0.308	0.021	0.000
300	0.622	0.623	0.282	0.282	0.005	0.000
400	0.735	0.735	0.344	0.344	0.002	0.000
500	0.634	0.635	0.270	0.270	0.011	0.000
600	0.569	0.568	0.233	0.234	0.026	0.000
700	0.713	0.710	0.330	0.331	0.030	0.000
800	0.643	0.643	0.273	0.273	0.004	0.000
900	0.705	0.705	0.325	0.325	0.006	0.000
1000	0.576	0.576	0.243	0.243	0.017	0.000

When the results are examined, it is seen that the $d_0(\bar{\theta}_v)$ *and* $d_0(\bar{\theta}_a)$*, which depend on the minor arc length, give almost the same results. In addition, the values of* $d_v(\bar{\theta}_v)$ *and* $d_v(\bar{\theta}_a)$ *depending on the vectorial distance give close results. When* $d_a(\bar{\theta}_v)$ *and* $d_a(\bar{\theta}_a)$ *values depending on the proposed wrapping operator are examined, the dispersion of the* $\bar{\theta}_a$ *is equal to zero for all repetition. Accordingly, it can be said that the proposed method gives more consistent results than the vectorial method.*

In the same way, the angular variance and vectorial variance are compared by using absolute error and the obtained results are shown in Table 12.

TABLE 12. Comparison of the angular and vectorial variance according to absolute errors.

i	V_v	V_a	$E_{var}^{(v)}$	$E_{var}^{(a)}$
1	0.242	0.586	34.060	0.000
100	0.331	0.826	49.001	0.000
200	0.307	0.835	52.245	0.000
300	0.282	0.750	46.319	0.000
400	0.344	0.889	53.981	0.000
500	0.270	0.660	38.643	0.000
600	0.233	0.607	37.024	0.000
700	0.330	0.849	51.323	0.000
800	0.273	0.726	44.830	0.000
900	0.325	0.817	48.687	0.000
1000	0.243	0.616	36.930	0.000

The low values of κ *increase discontinuity of circular data. For this reason, the difference between vectorial mean and angular mean increase. Therefore, the linear variance* (V_l) *cannot be calculated for discontinuous circular data, the vectorial variance* (V_v) *and angular variance* (V_a) *are used, and absolute error value* (E_{var}) *is used as performance criteria in this example. According to these results, the mean absolute errors of vectorial and angular variance are calculated as 46.299 and 0.000, respectively. Table 12 shows that the absolute errors for all iterations are equal zero. It can be inferred that the proposed angular variance provides better results than the vectorial variance.*

5. Real Data Applications

In order to compare the performance of the proposed method with the conventional methods and measure performance of angular mean and angular variance, it has been applied on three real dataset that using in environmental and ecological applications. These are movements of ants' dataset ([36]), movements of blue periwinkles' dataset ([37, 38]), and dance directions of bees' dataset ([39]).

5.1. **Movements of ants' dataset.** Route learning is the key to the survival of many ants. Ants show remarkable navigational ability, traveling long distances between profitable foraging areas and their nest. They have low resolution vision. For this reason, ants who travel along a particular route, produce pheromone trails secreted from their abdominal glands. Trail pheromone is used for route learning, and effects on route choice. In this example, we analyze the dataset that presents the orientation of the ants towards a black target when released in a round arena. The ants tended to run towards the target. This experiment was originally conducted by Jander ([36]) and later mentioned in Fisher ([4]). The data consists of 100 observations ([40]). For this data set, the vectorial sample mean and resultant direction are calculated 3.20 radians (183°) and 0.61, respectively ([4]). The directions of the ants are shown in Table 13.

TABLE 13. The directions of the ants.

330	290	60	200	200	180	280	220	190	180	140	40	300	80
180	160	280	180	170	190	180	140	150	150	210	200	170	200
160	200	190	250	180	30	200	180	200	350	210	190	160	170
200	180	120	200	210	130	30	210	200	230	180	140	360	150
180	160	210	190	180	230	50	150	210	180	110	270	180	200
190	210	220	200	60	260	110	180	170	200	220	160	70	190
10	220	180	210	170	90	160	180	170	200	120	150	300	190
160	180												

The circular histogram, the scatter and the vectorial and the proposed angular mean of the movements of the ants' dataset are given in Figure 3.

According to Figure 3, the vectorial and angular mean are calculated as 183.1385° and 184.7°, respectively. The absolute error for vectorial mean and angular mean are computed as 2.7253 and 0.0000, respectively. Since the absolute error for angular mean is equal 0.0000, the proposed angular mean method performs more consistent and proper than the other method. The vectorial variance is 0.3899 and the absolute error of it is 81.1333. The angular variance is calculated as 1.2095 and the absolute error of it is computed as 0.0000. Since the absolute error for angular variance is equal 0.0000, the proposed angular variance method performs more consistent and proper than the other method.

5.2. **Movements of blue periwinkles' dataset.** Blue periwinkles (Nodilittorina unifasciata) are very small blue shells that feed on microscopic algae. They live on the rocky shore in cluster of thousands and are able to survive a long time out of water. They travel up to 12 m in search of food. This dataset contains the directions of small blue periwinkles after they had been relocated down shore from the height at which they normally live. The original dataset not only contains the directions of the movement, but also contains the distances of the periwinkles after

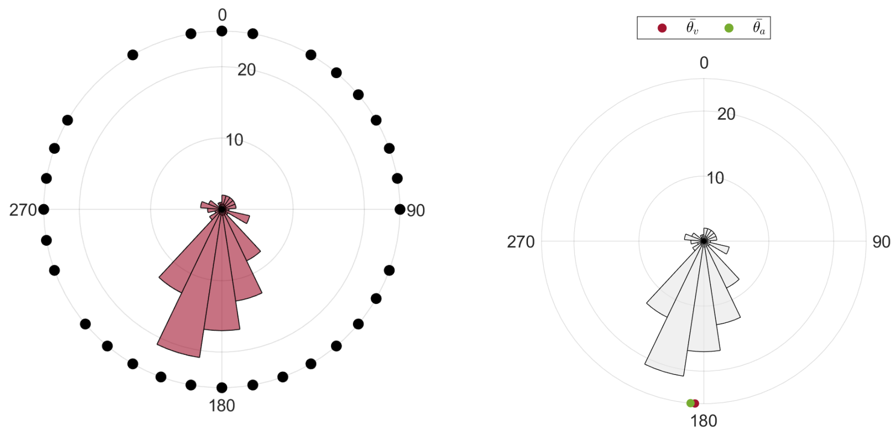

(A) (B)

FIGURE 3. The circular histogram of the movements of the ants' dataset (A) scatter of the data; (B) the vectorial and angular mean of the data

relocation. But in this paper, the distance measurement is omitted. Two different locations are combined for the purposes of this example. A total of 31 animals were involved in the study, 15 of which were measured one day after transplantation and the other 16 of which were measured four days after ([41]). The directions of the blue periwinkles are shown in Table 14.

TABLE 14. The directions of blue periwinkles.

67	66	74	61	58	60	100	89
171	166	98	60	197	98	86	123
165	133	101	105	71	84	75	98
83	71	74	91	38	200	56	

The circular histogram, the scatter and the vectorial and the proposed angular mean of the movements of the blue periwinkles' dataset are given in Figure 4.

According to Figure 4, the vectorial and angular mean are calculated as 92.7931° and 97.3871°, respectively. The absolute error for vectorial mean and angular mean are computed as 2.4856 and 0.0000, respectively. These results show that the proposed angular mean method more consistent and proper than the other method. The vectorial variance is 0.2251 and the absolute error of it is 9.5705. The angular variance is calculated as 0.5441 and the absolute error of it is computed as 0.0000.

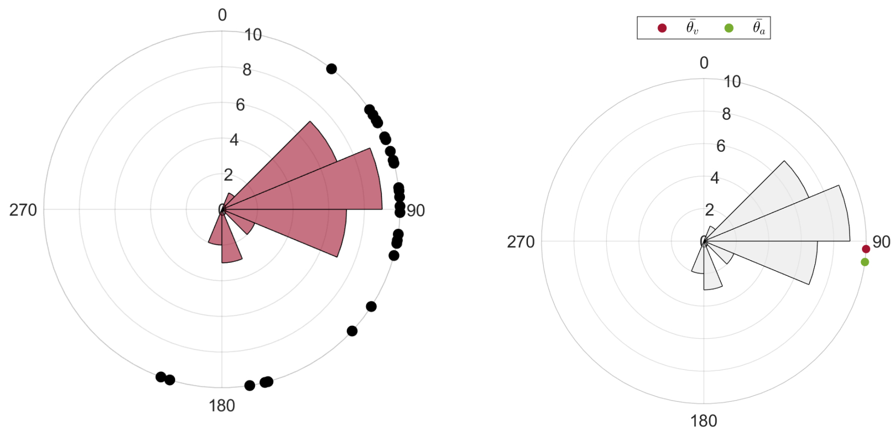

(A) (B)

FIGURE 4. The circular histogram of the movements of the blue periwinkles' dataset (A) scatter of the data; (B) the vectorial and angular mean of the data

These results show that the proposed angular variance method more consistent and proper than the other method.

5.3. **Dance directions of bees' dataset.** How honeybees perceive polarized light from the sky was a longstanding problem in the literature ([42]). It has long been known that bees can use the pattern of polarized light in the sky (e-vector pattern) as a compass cue even if they can see only a small part of the whole pattern ([43]). Honeybees frequently dance with some view of the sky, orienting themselves to the sun or natural polarized skylight ([44]).

This dataset shows the dance directions of 279 honeybees viewing a zenith patch of artificially polarized light. This dataset was measured experimentally to prove that special receptors at the dorsal margin of the eye are required to detect polarized light and derive compass information in sky patterns ([39]). The waggle dances were recorded by a video and were analyzed later by measuring the directions of the individual waggle runs. The dance directions of the honeybees are shown in Table 15.

The circular histogram, the scatter and the vectorial and the proposed angular mean of the dance directions of the bees' dataset are given in Figure 5.

According to Figure 5, the vectorial and angular mean are calculated as 138.2749° and 164.3369°, respectively. The absolute error for vectorial mean and angular mean are computed as 1.2445 and 0.0000, respectively. Since the absolute error for

Table 15. Dance directions of bees.

Direction	0	10	20	30	40	50	60	70	80	90
Frequency	3	8	9	9	6	6	12	9	9	9
Direction	100	110	120	130	140	150	160	170	180	190
Frequency	9	12	5	6	8	12	8	9	12	5
Direction	200	210	220	230	240	250	260	270	280	290
Frequency	5	9	8	5	12	9	8	7	3	8
Direction	300	310	320	330	340	350				
Frequency	12	6	5	5	8	3				

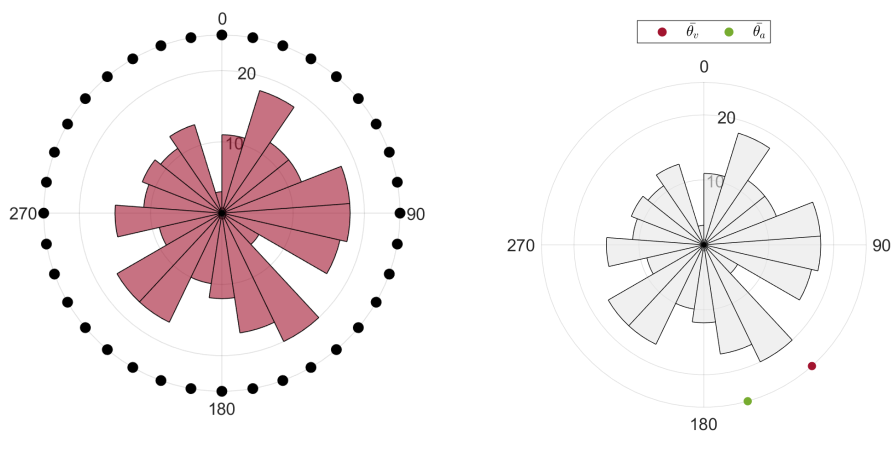

(A) (B)

Figure 5. The circular histogram of the dance directions of the bees' dataset (A) scatter of the data; (B) the vectorial and angular mean of the data

angular mean is equal 0.0000, the proposed angular mean method performs more consistent and proper than the other method. The vectorial variance is 0.9223 and the absolute error of it is 562.7965. The angular variance is calculated as 2.9467 and the absolute error of it is computed as 0.0000. Since the absolute error for angular variance is equal 0.0000, the proposed angular variance method performs more consistent and proper than the other method.

6. Conclusion

In this study, a new approach was proposed for the calculation of the mean and variance of circular data. Circular data can be cut across interval boundaries as a result of some arithmetic operations. In this situation, the principal interval can be reduced to a symmetric principal interval by using the wrapping process. The proposed methods have been developed based on the wrapping process. These methods were compared with Mardia's methods ([3]) in the literature, using both artificial data and real datasets. The absolute error and absolute percentage error which is proposed by using the wrapping process were considered as the performance criteria in the comparisons. In the simulation study, four different artificial data were generated from the uniform and von Mises distribution according to the continuity and discontinuity of the data. The comparisons were performed by changing the interval range for the uniform distribution and altering the κ for the von mises distribution. The attained results showed that the proposed angular mean and variance methods outperform vectorial methods in the literature. In this study, the angular statistics (mean and variance) and the linear statistics (mean and variance) give the same result in the range of $[0, \pi]$. On the other hand, the low values of the κ increase discontinuity of the circular data which generated from von Mises distribution. For this reason, the difference between vectorial statistics and angular statistics increases. These methods give the same results in this situation. In order to compare the performance of the proposed method with the conventional methods and measure the performance of angular mean and angular variance, it has been applied on three real datasets that using in environmental and ecological applications. These are movements of ants' dataset, movements of blue periwinkles' dataset, and dance directions of bees' dataset. The proposed methods achieved more consistent results in the calculation of the mean and variance of the circular data when compared to the vectorial methods. Thus, it has been demonstrated that the proposed method can be easily applied to environmental and ecological data as well as artificial data. Consequently, the simulation study and applications show that the proposed angular methods based on the wrapping process are simple and consistent. It can be easily applied to different datasets in various fields. Also, it is useful for practitioners regarding the applicability.

Author Contribution Statements All authors contributed equally to the writing of this paper. All authors read and approved the final manuscript.

Declaration of Competing Interests The authors declare that they have no competing interests.

References

[1] Jammalamadaka, S. R., SenGupta, A., Topics in Circular Statistics, World Scientific Publishing Co. Pte. Ltd., 2001.
[2] Bowers, J. A., Morto, I. D., Mould, G. I., Directional statistics of the wind and waves, *Appl. Ocean. Res.*, 22(1) (2000), 13-30. https://doi.org/10.1016/S0141-1187(99)00025-5
[3] Mardia, K. V., Statistics of Directional Data, Academic Press, 1972.
[4] Fisher, N., Statistical Analysis of Circular Data, Cambridge University Press, 1993.
[5] Mardia, K. V., Jupp, P. E., Directional Statistics, John Wiley & Sons Inc., 2000.

[6] Lark, L. M., Clifford, D., Waters, C. N., Modelling complex geological circular data with the projected normal distribution and mixtures of von Mises distribution, *Solid Earth*, 5(2) (2014) 631-639. https://doi.org/10.5194/se-5-631-2014

[7] Kempter, R., Leibold, C., Buzsáki, G., Diba, K., Schmidt, R., Quantifying circular–linear associations: Hippocampal phase precession, *J. Neurosci. Methods*, 207(1) (2012), 113-124. https://doi.org/10.1016/j.jneumeth.2012.03.007

[8] La Sorte, F. A., Mannan, R. W., Reynolds, R. T., Grubb, T. G., Habitat associations of sympatric red-tailed hawks and northern goshawks on the Kaibab Plateau, *J. Wildl. Manage.*, 68(2) (2004), 307-317. https://doi.org/10.2193/0022-541X(2004)068[0307:HAOSRH]2.0.CO;2

[9] Jones, M. C., Pewsey, A., Inverse Batschelet distributions for circular data, *Biometrics*, 68(1) (2012), 183-193. https://doi.org/10.1111/j.1541-0420.2011.01651.x

[10] Baayen, C., Klugkist, I., Mechsner, F., Test of order-constrained hypotheses for circular data with applications to human movement science, *J. Mot. Behav.*, 44(5) (2012), 351-363. https://doi.org/10.1080/00222895.2012.709549

[11] Traa, J., Smaragdis, P., Multichannel source separation and tracking with RANSAC and directional statistics, *IEEE/ACM Trans. Audio Speech. Lang. Process.*, 22(12) (2014), 2233-2243. https://doi.org/10.1109/TASLP.2014.2365701

[12] Ehler, M., Galanis, J., Frame theory in directional statistics, *Stat. Probab. Lett.*, 81(2) (2011), 1046-1051. https://doi.org/10.1016/j.spl.2011.02.027

[13] Hawkins, D. M., Lombard, F., Segmentation of circular data, *J. Appl. Stat.*, 42(1) (2015), 88-97. https://doi.org/10.1080/02664763.2014.934665

[14] Klugkist, I., Bullens, J., Postma, A., Evaluating order-constrained hypotheses for circular data using permutation tests, *Br. J. Math. Stat. Psychol.*, 65(2) (2012), 222-236. https://doi.org/10.1111/j.2044-8317.2011.02018.x

[15] Tasdan, F., Cetin, M., A simulation study on the influence of ties on uniform scores test for circular data, *J. Appl. Stat.*, 41(5) (2014), 1137-1146. https://doi.org/10.1080/02664763.2013.862224

[16] Thompson, L. M., van Manen, F. T., King, T. L., Geostatistical analysis of allele presence patterns among American black bears in eastern North Carolina, *Ursus*, 16(1) (2005), 59-69. https://doi.org/10.2192/1537-6176(2005)016[0059:GAOAPP]2.0.CO;2

[17] Kubiak, T., Jonas, C., Applying circular statistics to the analysis of monitoring data, *Eur. J. Psychol. Assess.*, 23(4) (2007), 227-237. https://doi.org/10.1027/1015-5759.23.4.227

[18] Brunsdon, C., Corcoran, J., Using circular statistics to analyse time patterns in crime incidence, *Comput. Environ. Urban Syst.*, 30(3) (2006), 300-319. https://doi.org/10.1016/j.compenvurbsys.2005.11.001

[19] Huang, L., Helmke, B. P., A Semi-automatic method for image analysis of edge dynamics in living cells, *Cell. Mol. Bioeng.*, 4(2) (2011), 205-219. https://doi.org/10.1007/s12195-010-0141-z

[20] Abraham, C., Molinari, N., Servien, R., Unsupervised clustering of multivariate circular data, *Stat. Med.*, 32(8) (2013), 1376-1382. https://doi.org/10.1002/sim.5589

[21] Rocchi, M. B., Perlini, C., Is the time of suicide a random choice? A new statistical perspective, *Crisis*, 23(4) (2002), 161. https://doi.org/10.1027/0227-5910.23.4.161

[22] Le, C. T., Liu, P., Lindgren, B. R., Daly, K. A., Giebink, G. S., Some statistical methods for investigating the date of birth as a disease indicator, *Stat. Med.*, 22(13) (2003), 2127-2135. https://doi.org/10.1002/sim.1343

[23] Chen, L., Singh, V. P., Guo, S., Fang, B., Liu, P., A new method for identification of flood seasons using directional statistics, *Hydrol. Sci. J.*, 58(1) (2013), 28-40. https://doi.org/10.1080/02626667.2012.743661

[24] Wang F., Gelfand, A. E., Modeling space and space-time directional data using projected Gaussian processes, *J. Atmos. Ocean. Technol.*, 8(11) (2014), 1466-1485. https://doi.org/10.1080/01621459.2014.934454

[25] Yurovskaya, M. V., Dulov, V. A., Chapron, B., Kudryavtsev, V. N., Directional short wind wave spectra derived from the sea surface photography, *J. Geophys. Res. Oceans.*, 118(9) (2013), 4380-4394. https://doi.org/10.1002/jgrc.20296

[26] Costa, M., Koivunen, V., Poor, H. V., Estimating directional statistics using wavefield modeling and mixtures of von-mises distributions, *IEEE Signal Process. Lett.*, 21(12) (2014), 1496-1500. https://doi.org/10.1109/LSP.2014.2341651

[27] Mínguez, R., Espejo, A., Tomás, A., Méndez, F. J., Losada, I. J., Directional calibration of wave reanalysis databases using instrumental data, *J. Atmos. Ocean. Technol.*, 28(11) (2011), 1466-1485. https://doi.org/10.1175/JTECH-D-11-00008.1

[28] Schwartz, R. S., Barbosa, R. R. R., Meratnia, N., Heijenk, G., Scholten, H., A directional data dissemination protocol for vehicular environments, *Comput. Commun.*, 34(17), (2011), 2057-2071. https://doi.org/10.1016/j.comcom.2011.03.007

[29] Guo, C., Wu, X., Feng, C., Zeng, Z., Spectrum sensing for cognitive radios based on directional statistics of polarization vectors, *IEEE J. Sel. Areas Commun.*, 31(3) (2013), 379-393. https://doi.org/10.1109/JSAC.2013.130305

[30] Batschelet, E., Circular Statistics in Biology, Academic Press, 1981.

[31] Zar, J. H., Biostatistical Analysis 4th edition, Prentice Hill, 1999.

[32] Easton Jr, R. L., Topics in Circular Statistics, John Wiley & Sons, 2010.

[33] Rhoad, R., Milauskas G., Whipple, R., Geometry for Enjoyment and Challenge, McDougal Littell & Co., 1991.

[34] Ackermann, H., A note on circular nonparametrical classification, *Biom. J.*, 39(5) (1997), 577-587. https://doi.org/10.1002/bimj.4710390506

[35] Lund, U., Cluster analysis for directional data, *Commun. Stat.–Simul. Comput.*, 28(4) (1999), 1001-1009. https://doi.org/10.1080/03610919908813589

[36] Jander, R., Die optische richtungsorientierung der roten waldameise (formica ruea l.), *Z. Vgl. Physiol.*, 40(2) (1957), 162-238. https://doi.org/10.1007/BF00297947

[37] Chapman, M., Assessment of some controls in experimental transplants of intertidal gastropods, *Journal of J. Exp. Mar. Biol. Ecol.*, 103(1-3) (1986), 181-201. https://doi.org/10.1016/0022-0981(86)90140-1

[38] Chapman, M., Underwood, A., Experimental designs for analyses of movements by molluscs, *Proceedings of the third international symposium on littorinid biology*, (1992), 169-180.

[39] Wehner R., Strasser, S., The POL area of the honey bee's eye: behavioural evidence, *Physiol. Entomol.*, 10(3) (1985), 337-349. https://doi.org/10.1111/j.1365-3032.1985.tb00055.x

[40] Ravindran, P., Ghosh, S. K., Bayesian analysis of circular data using wrapped distributions, *J. Stat. Theory Pract.*, 5(4) (2011), 547-561. https://doi.org/10.1080/15598608.2011.10483731

[41] Otieno, B. S., Anderson-Cook, C. M., Measures of preferred direction for environmental and ecological circular data, *Environ. Ecol. Stat.*, 13(3)(2006), 311-324. https://doi.org/10.1007/s10651-004-0014-5

[42] Rossel, S., Wehner, R., Polarization vision in bees, *Nature*, 323(6084) (1986), 128-131. https://doi.org/10.1038/323128a0

[43] Rossel, S., Wehner, R., The bee's map of the e-vector pattern in the sky, *Proc. Natl. Acad. Sci. U.S.A.*, 79(14) (1982), 4451-4455. https://doi.org/10.1073/pnas.79.14.4451

[44] Brines, M. L., Gould, J. L., Bees have rules, *Science*, 206(4418) (1979), 571-573. https://doi.org/10.1126/science.206.4418.571

http://communications.science.ankara.edu.tr

Commun.Fac.Sci.Univ.Ank.Ser. A1 Math. Stat.
Volume 72, Number 3, Pages 803–814 (2023)
DOI:10.31801/cfsuasmas.1194816
ISSN 1303-5991 E-ISSN 2618-6470

Research Article; Received:October 12, 2022; Accepted: July 2, 2023

DISJOINT SETS IN PROJECTIVE PLANES OF SMALL ORDER

Mustafa GEZEK

Department of Mathematics, Tekirdağ Namık Kemal University, Tekirdağ, TÜRKİYE

Abstract. In this paper, results of a computer search for disjoint sets associated with maximal arcs and unitals in projective planes of order 16, and disjoint sets associated with unitals in projective planes of orders 9 and 25 are reported. It is shown that the number of pairs of disjoint unitals in planes of order 9 is exactly *four*, and new pairs and triples of disjoint degree 4 maximal arcs are shown to exist in some of the planes of order 16. New bounds on the number of 104-sets of type $(4, 8)$ and 156-sets of type $(8, 12)$ are achieved. A combinatorial method for finding new maximal arcs, new unitals, and new v-sets of type (m, n) is introduced. All disjoint sets found in this study are explicitly listed.

1. Introduction

We assume familiarity with the basic facts from finite geometries and design theory [3,5,10].

Let q be a prime power and π be a plane of order q^2. A *v-set* of type (m, n) in π is defined to be a set S of v points of π such that any line of π intersects with S in either m or n points.

There are *four* projective planes of order 9 [12]. Through this paper, the following abbreviations will be used for the names of these planes: $PG(2, 9)$, HALL(9), HALL(9)$^\perp$, and HUGHES(9). Up to isomorphism, the number of known projective planes of orders 16 and 25 is 22 and 193, respectively. The following abbreviations will be used for the names of the planes of order 16: PG(2,16), JOHN, MATH, HALL, DEMP, JOWK, SEMI2, SEMI4, DSFP, LMRH, BBH1, BBS4, and BBH2 [15], and we will follow the notations used in [13] for the known planes of order 25.

In this study, we will be interested in disjoint sets associated with $(n(q+1)-q)$-sets of type $(0, n)$ and $(q^3 + 1)$-sets of type $(1, q + 1)$ in projective planes of orders

2020 *Mathematics Subject Classification.* 05B05, 51E10, 51E20.
Keywords. Disjoint set, maximal arc, unital.
mgezek@nku.edu.tr; 0000-0001-5488-9341.

$q^2 \in \{9, 16, 25\}$, where the former set is called a *maximal* $(n(q+1)-q, n)$*-arc* and later is called a *unital*.

The set of lines of π which have no points in common with a maximal $(n(q+1)-q, n)$-arc A determines a maximal $(\frac{q}{n}(q-n+1), \frac{q}{n})$-arc, denoted by $A^{\perp}$, in the dual plane of π. The sets of the intersections of the lines of π with A at n points form a 2-$(n(q+1)-q, n, 1)$ design $D(A)$.

In 1997, for odd prime power q, Ball et al. showed that degree n maximal arcs do not exist in $PG(2,q)$, where $1 < n < q$ [2]. Non-trivial maximal arcs do exist in some of the projective planes of even order with $n = 2^i$, $i \geq 1$ [6–9, 20, 21].

Penttila et al. classified all degree 2 maximal arcs in the known planes of order 16 [15], and it was shown that $PG(2,16)$ contains exactly two inequivalent degree 4 maximal arcs [1]. Maximal $(52,4)$-arcs have not been completely classified in the remaining of the known planes of order 16, yet.

Details of the known degree 4 maximal arcs and unitals in the known planes of order 16 are given in Table 1, where Column 1 gives the name of the planes, Column 2 shows how many degree 4 maximal arcs are known to exist in each plane, Column 3 lists the name of the maximal arcs, and the last column provides the number of known unitals in each plane.

Table 1. The known number of maximal $(52,4)$-arcs and unitals in the known planes of order 16.

Plane	Known number of maximal $(52,4)$-arcs [7–9]	maximal arcs denoted by	Known number of unitals [11, 16, 17, 19]
$PG(2,16)^*$	2	$PG(2,16)$.1 and $PG(2,16)$.2	2
BBH1*	3	bbh1.1, bbh1.2, etc.	16
BBH2	0	-	26
BBS4	0	-	13
DEMP	5	demp.1, demp.2, etc.	4
DSFP	1	dsfp.1	2
HALL	2	hall.1 and hall.2	6
JOHN	4	john.1, john.2, etc.	29
JOWK	2	jowk.1 and jowk.2	7
LMRH	2	lmrh.1 and lmrh.2	2
MATH	7	math.1, math.2, etc.	16
SEMI2*	7	semi2.1, semi2.2, etc.	21
SEMI4*	1	semi4.1	12

The specific point sets of the known degree 4 maximal arcs and unitals in the known planes of order 16 used in this study are from [8] and [17], respectively.

The set of lines of π meeting with a unital U at a single point determines a unital, denoted by $U^{\perp}$, in the dual plane of π. The sets of the intersections of the lines of π with U at $q+1$ points form a 2-$(q^3+1, q+1, 1)$ design $D(U)$.

In 1981, Brouwer constructed 138 non-isomorphic unital 2-$(28, 4, 1)$ designs and showed that *twelve* of them could be embedded as a unital in planes of order 9 [4], and in 1995, Penttila and Royle classified all unitals in planes of order 9 and they showed that there are exactly 18 such sets: *two* in $PG(2, 9)$, *four* in HALL(9) (so *four* in HALL$(9)^{\perp}$), and *eight* in HUGHES(9) [14].

Table 1 shows that the number of known unitals in planes of order 16 is 156, of which 38 of them were found by Stoichev and Tonchev [19], 3 of them were found by Krĉadinac and Smoljak [11] and 115 of them were found by Stoichev and Gezek [17].

The number of known unitals in the known projective planes of order 25 is 477 [18].

In this article, some results of a computer search for disjoint sets in the known planes of orders *nine*, *sixteen* and *twenty-five* are given. It is shown that disjoint sets in a projective plane of order q^2 may be useful to find a complete partitioning of the point set of the plane into disjoint sets associated with degree q maximal arcs and unitals. It is observed that new degree q maximal arcs, new unitals, new v-sets of type (m, n), and new projective planes can be found through disjoint sets as well.

The paper is organized in the following way. In Section 2, types of disjoint sets and some of possible ways of partitioning incidence matrices of projective planes are discussed. In Section 3, new pairs of disjoint degree 4 maximal arcs are shown to exist in BBH1, LMRH, and SEMI2 planes. MATH and SEMI2 planes are shown to contain new triples of disjoint degree 4 maximal arcs. In Section 4, it is shown that pairs of disjoint unitals exist in planes of order 9, and no such sets exists from the known unitals in the known planes of orders 16 and 25. In Section 5, we report the results of computer searches for 156-sets of type $(8, 12)$ associated with maximal arcs and unitals in the known planes of order 16. In Section 6, a combinatorial method for finding a complete partitioning of the point set of a projective plane into disjoint sets associated with maximal arcs and unitals, new maximal arcs, new unitals, new v-sets of type (m, n), and new projective planes is given. Point sets of all newly found disjoint sets discussed in this paper are available online at[1].

2. Types of Disjoint Sets in Projective Planes

It is well-known that some v-sets of type (m, n) might be coming from the unions of pairwise disjoint maximal arcs. In this paper, we will be interested in three different types of disjoint sets as described in Table 2:

Disjoint sets in π can be used to partition an incidence matrix of the plane in one of the following possible forms: if there exists a degree q maximal arc A_1 and

[1]euniversite.nku.edu.tr/testotomasyon/dosyalar/kullanicilar/3705/files/DisjointSets16.pdf

TABLE 2. Types of disjoint sets.

Type I	Disjoint pairs of maximal arcs
Type II	Disjoint pairs of unitals
Type III	A maximal arc disjoint from a unital

a unital U disjoint from A_1, then, WLOG, one may rearrange the columns (rows) of the incidence matrix according to the point sets of A_1 and U ($A_1^{\perp}$ and $U^{\perp}$) as

$$\left[\begin{array}{c||c|c} \overbrace{-\cdots\cdots\cdots-}^{(A_1\cup U)^c} & \overbrace{-\cdots-}^{A_1} & \overbrace{-\cdots-}^{U} \\ \hline q^2-2q & q & q+1 \\ \hline\hline q^2-q & \mathrm{O} & q+1 \\ \hline q^2-q & q & 1 \end{array}\right], \tag{1}$$

where O indicates a $(q^3-q^2+q)\times(q^3-q^2+q)$ zero matrix and numbers in the matrix shows the number of 1's in each row. In addition, if there exists a degree q maximal arc A_2 disjoint from $A_1\cup U$, then we may partition the incidence matrix of π as

$$\left[\begin{array}{c||c|c|c} \overbrace{-\cdots\cdots-}^{(A_1\cup A_2\cup U)^c} & \overbrace{-\cdots-}^{A_2} & \overbrace{-\cdots-}^{A_1} & \overbrace{-\cdots-}^{U} \\ \hline q^2-3q & q & q & q+1 \\ \hline\hline q^2-2q & \mathrm{O} & q & q+1 \\ \hline q^2-2q & q & \mathrm{O} & q+1 \\ \hline q^2-2q & q & q & 1 \end{array}\right]. \tag{2}$$

Sometimes we may not have a Type III disjoint set. Instead, we could have disjoint triples of degree q maximal arcs, that is, if there exists a degree q maximal arc A_3 disjoint from $A_1\cup A_2$, but not disjoint from U, then we may partition the incidence matrix of π as

$$\left[\begin{array}{c||c|c|c} \overbrace{-\cdots\cdots-}^{(A_1\cup A_2\cup A_3)^c} & \overbrace{-\cdots-}^{A_3} & \overbrace{-\cdots-}^{A_2} & \overbrace{-\cdots-}^{A_1} \\ \hline q^2-3q+1 & q & q & q \\ \hline\hline q^2-2q+1 & \mathrm{O} & q & q \\ \hline q^2-2q+1 & q & \mathrm{O} & q \\ \hline q^2-2q+1 & q & q & \mathrm{O} \end{array}\right]. \tag{3}$$

Many more forms as similar above can be derived from an incidence matrix of π, but these three will be enough for our discussion in this study.

3. Type I Disjoint Sets

Type I disjoint sets in a projective plane π are the sets coming from disjoint pairs of maximal arcs. First examples of these sets are seen in $PG(2,4)$:

Theorem 1. *It is possible to partition the points of $PG(2,4)$ into two degree 2 maximal arcs and a unital.*

Proof. $A = \{7,8,10,11,19,20\}$ is a 6-set of type $(0,2)$ in $PG(2,4)$ (the specific line set of the projective plane of order 4 that we use is available online at[2]), a degree 2 maximal arc. It can be shown that $U = \{2,3,4,6,9,15,16,17,18\}$ is a 9-set of type $(1,3)$ in $PG(2,4)$, a unital, disjoint from A. Then, the complement of $A \cup U = \{0,1,5,12,13,14\}$ is a 6-set of type $(0,2)$. □

In the known projective planes of order 16, Hamilton et al. found *thirty-seven* Type I disjoint sets (21 in $PG(2,16)$, 4 in SEMI4, 4 in SEMI2, 3 in MATH, 3 in JOWK, and 2 in BBH1) [9] and Gezek found *thirty-seven* Type I disjoint sets (33 in MATH and 4 in JOHN) [7].

The specific line sets of the known planes of order 16 used in this study are from [8].

Previously, only *four* Type I disjoint sets were known to exist in SEMI2 [9], our computations show that there are more such sets in this plane:

There are *six* isomorphic copies of *semi*2.4 disjoint from *semi*2.1. The collineation stabilizer of the unions of these sets with *semi*2.1 all have order 4, and they are equivalent. This set is denoted by *semi*2.(1, 4).1.

There are *six* isomorphic copies of semi2.5 disjoint from *semi*2.1. The collineation stabilizer of the unions of these sets with *semi*2.1 all have order 4, and they are equivalent. This set is denoted by *semi*2.(1, 5).1.

There are *thirty-six* isomorphic copies of *semi*2.3 disjoint from itself. The collineation stabilizer of the unions of *twenty-four* of these sets with *semi*2.3 have order 16, and

[2] ericmoorhouse.org/pub/planes/pg24.txt

they split into *six* inequivalent classes. These sets are denoted by $semi2.(3,3).1$, $semi2.(3,3).2$, $\cdots$, $semi2.(3,3).6$. The collineation stabilizer of the unions of the remaining *twelve* sets with $semi2.3$ have order 32, and they split into *six* inequivalent classes. These sets are denoted by $semi2.(3,3).7$, $semi2.(3,3).8$, $\cdots$, $semi2.(3,3).12$.

There are *forty-four* isomorphic copies of $semi2.4$ disjoint from itself. The collineation stabilizer of the unions of *twenty-four* of these sets with $semi2.4$ have order 16, and they split into *six* inequivalent classes. These sets are denoted by $semi2.(4,4).1$, $semi2.(4,4).2$, $\cdots$, $semi2.(4,4).6$. The collineation stabilizer of the unions of *twelve* of the remaining sets with $semi2.4$ have order 32, and they split into *six* inequivalent classes. These sets are denoted by $semi2.(4,4).7$, $semi2.(4,4).8$, $\cdots$, $semi2.(4,4).12$. The collineation stabilizer of the unions of the remaining *eight* sets with $semi2.4$ all have order 8, and they are equivalent. This set is denoted by $semi2.(4,4).13$.

There are *sixteen* isomorphic copies of $semi2.5$ disjoint from $semi2.4$. The collineation stabilizer of the unions of these sets with $semi2.4$ all have order 8, and they split into *four* inequivalent classes. These sets are denoted by $semi2.(4,5).1$, $semi2.(4,5).2$, $\cdots$, $semi2.(4,5).4$.

There are *twenty* isomorphic copies of $semi2.5$ disjoint from itself. The collineation stabilizer of the unions of *eight* of these sets with $semi2.5$ have order 8, and they split into *two* inequivalent classes. These sets are denoted by $semi2.(5,5).1$ and $semi2.(5,5).2$. The collineation stabilizer of the unions of the *eight* of the remaining sets with $semi2.5$ have order 4, and they are equivalent. This set is denoted by $semi2.(4,5).3$. The collineation stabilizer of the unions of the remaining *four* sets with $semi2.5$ have order 16, and they split into *two* inequivalent classes. These sets are denoted by $semi2.(5,5).4$ and $semi2.(5,5).5$.

There are *thirty-six* isomorphic copies of $semi2.6$ disjoint from itself. The collineation stabilizer of the unions of these sets with $semi2.6$ all have order 16, and they split into *six* inequivalent classes. These sets are denoted by $semi2.(6,6).1$, $semi2.(6,6).2$, $\cdots$, $semi2.(6,6).6$.

There are *thirty-six* isomorphic copies of $semi2.7$ disjoint from itself. The collineation stabilizer of the unions of these sets with $semi2.7$ all have order 16, and they split into *six* inequivalent classes. These sets are denoted by $semi2.(7,7).1$, $semi2.(7,7).2$, $\cdots$, $semi2.(7,7).6$.

Previously, no Type I disjoint set were known to exist in LMRH. However, our computations show that this plane also contains such sets:

There are *thirty-six* isomorphic copies of $lmrh.2$ disjoint from $lmrh.1$. The collineation stabilizer of the unions of these sets with $lmrh.1$ all have order 8, and they split into *three* inequivalent classes. These sets are denoted by $lmrh.(1,2).1$, $lmrh.(1,2).2$, and $lmrh.(1,2).3$.

There are *twenty-four* isomorphic copies of $lmrh.2$ disjoint from itself. The collineation stabilizer of the unions of *sixteen* of these sets with $lmrh.2$ have order 8, and they split into *two* inequivalent classes. These sets are denoted by $lmrh.(2,2).1$ and $lmrh.(2,2).2$. The collineation stabilizer of the unions of the remaining *eight* sets with $lmrh.2$ have order 16, and they split into *two* inequivalent classes. These sets are denoted by $lmrh.(2,2).3$ and $lmrh.(2,2).4$.

Previously, only *two* Type I disjoint sets were known to exist in BBH1 [9], our computations show that there are more such sets in this plane as well:

There are *four* isomorphic copies of $bbh1.3$ disjoint from itself. The collineation stabilizer of the unions of *two* of these sets with $bbh1.3$ have order 8, and they split into *two* inequivalent classes. These sets are denoted by $bbh1.(3,3).1$, and $bbh1.(3,3).2$. The collineation stabilizer of the unions of the remaining *two* sets with $bbh1.3$ have order 4, and they are equivalent. This set is denoted by $bbh1.(3,3).3$.

All known Type I disjoint sets in the known projective planes of order 16 can be summarized as in Table 3, where Column 1 presents the name of the planes, Column 2 and 3 shows the group orders of the Type I disjoint sets (with their quantities) found in [9], and [7], respectively. Column 4 provides the group orders of the Type I newly discovered disjoint sets (with their quantities). The last column (row) shows the total number of such sets in each plane (study). An entry a^b in Table 3 implies that there are b inequivalent Type I disjoint sets with collineation stabilizer of order a.

TABLE 3. The number of known Type I disjoint sets in the known planes of order 16.

Plane	Hamilton et al. [9]	Gezek [7]	Gezek (2022)	Total
$PG(2,16)^*$	$2^{16}, 4^3, 8^2$			21
BBH1*	$8^1, 16^1$		$4^1, 8^2$	5
JOHN		16^4		4
JOWK	$8^2, 16^1$			3
LMRH			$8^5, 16^2$	7
MATH	$4^1, 8^2$	$4^5, 8^{14}, 16^8, 32^6$		36
SEMI2*	$8^2, 16^2$		$4^3, 8^7, 16^{26}, 32^{12}$	52
SEMI4*	$16^2, 32^2$			4
Total	37	37	58	132

Previously, it was reported that $PG(2,16)$ contains *one* disjoint triples of degree 4 maximal arc having collineation stabilizer of order 2 [9]. A computer program was written to find disjoint triples and disjoint quadruples of degree 4 maximal arcs in the known planes of order 16. In addition to the one found in $PG(2,16)$, our results show that SEMI2 and MATH planes also contain disjoint triples of degree 4 maximal arcs: there is an isomorphic copy of $semi2.4$ disjoint from the union of $semi2.1$ and $semi2.(1,4).1$, having collineation stabilizer of order 8 (this set is denoted by $semi2.(1,4,4).1$). There is an isomorphic copy of $semi2.5$ disjoint from the union of semi2.1 and $semi2.(1,5).1$, having collineation stabilizer of order 8 (this set is denoted by $semi2.(1, 5, 5).1$). There is an isomorphic copy of math.4 disjoint from the union of math.1 and $math.(1, 4).1$, having collineation stabilizer of order 8 (this set is denoted by $math.(1, 4, 4).1$). There is an isomorphic copy of math.5 disjoint from the union of $math.1$ and $math.(1, 5).1$, having collineation stabilizer of order 8 (this set is denoted by $math.(1, 5, 5).1$). Our program found no disjoint quadruples of degree 4 maximal arcs in the known planes of order 16.

4. Type II Disjoint Sets

Type II disjoint sets in a projective plane π are the sets coming from disjoint pairs of unitals.

In HALL(9), there are (up to isomorphism) four unitals. The unital having group order 24 has *six* isomorphic copies disjoint from itself. Up to isomorphism, there are two such pairs of disjoint unitals with collineation stabilizer of order 16. The unions of these sets with the unital having group order 24 in HALL(9) provide 56-sets of type $(5, 8)$ (or, 35-sets of type $(2, 5)$).

$PG(2, 9)$ and HUGHES(9) planes do not contain any Type II disjoint sets, and our computations show that no Type II disjoint sets exists from the known unitals in the known planes of orders 16 and 25.

5. Type III Disjoint Sets

Type III disjoint sets in a projective plane π are the sets coming from a maximal arc A and a unital U in π such that A and U are disjoint. The smallest plane where this type of set exists is $PG(2, 4)$ (see Section 3).

Previously, no Type III disjoint sets were known to exist in the known projective planes of order 16. Our computations show that such sets exist in these planes. We provide details of the Type III disjoint sets found by our algorithm in Table 4, where the first column presents the maximal arcs, and the last column gives for which unital there exists such a set. An entry $\mathbf{j}(k)$ in row i in Table 4 implies that there are k inequivalent Type III disjoint sets coming from maximal arc i and unital $\mathbf{j}$.

Group orders of the Type III disjoint sets found in this study can be summarized as in Table 5, where Column 1 presents the name of the planes, Column 2 shows the group orders of the Type III disjoint sets (with their quantities). The last column (row) shows the total number of such sets in each plane (all planes).

Table 3 shows that the number of disjoint pairs of maximal $(52, 4)$-arcs is at least 132. Union of disjoint pairs of maximal $(52, 4)$-arcs is a 104-set of type $(4, 8)$. Some of the disjoint pairs of the degree 4 maximal arcs given in Table 3 are disjoint from some of the isomorphic copies of unitals: *two* in SEMI2 and *two* in MATH. The complement of the union of these disjoint sets is also a 104-set of type $(4, 8)$: the sets in SEMI2 have collineation stabilizer of orders 4 and 8, and the sets in MATH have collineation stabilizer of orders 4 and 8. None of these sets are equivalent to any Type I disjoint sets given in Table 3. We have

TABLE 4. Type III disjoint sets in the known planes of order 16.

Maximal $(52, 4)$-arc	**Unital No.**(Quantity)
$bbh1.2$	$\mathbf{1}(2), \mathbf{16}(2)$
$john.1$	$\mathbf{26}(1), \mathbf{29}(1)$
$john.2$	$\mathbf{2}(1), \mathbf{26}(1)$
$john.3$	$\mathbf{2}(1), \mathbf{26}(1)$
$john.4$	$\mathbf{26}(1), \mathbf{29}(1)$
$jowk.1$	$\mathbf{7}(1)$
$jowk.2$	$\mathbf{7}(5)$
$lmrh.1$	$\mathbf{1}(1), \mathbf{2}(2)$
$lmrh.2$	$\mathbf{1}(3), \mathbf{2}(8)$
$math.1$	$\mathbf{4}(2), \mathbf{8}(2)$
$math.2$	$\mathbf{2}(1), \mathbf{5}(2), \mathbf{6}(1), \mathbf{10}(1), \mathbf{11}(1)$
$math.3$	$\mathbf{5}(2), \mathbf{7}(1), \mathbf{11}(1), \mathbf{12}(2), \mathbf{15}(1), \mathbf{16}(1)$
$math.4$	$\mathbf{3}(1), \mathbf{5}(2), \mathbf{10}(2), \mathbf{11}(1), \mathbf{13}(2), \mathbf{14}(2)$
$math.5$	$\mathbf{3}(1), \mathbf{10}(1)$
$semi2.1$	$\mathbf{4}(2)$
$semi2.2$	$\mathbf{11}(2)$
$semi2.3$	$\mathbf{1}(1), \mathbf{2}(2), \mathbf{9}(2), \mathbf{10}(2), \mathbf{14}(1) - \mathbf{21}(1)$
$semi2.4$	$\mathbf{2}(2), \mathbf{9}(4), \mathbf{10}(2), \mathbf{11}(2), \mathbf{14}(1), \mathbf{15}(1), \mathbf{16}(2), \mathbf{17}(1) - \mathbf{19}(1)$
$semi2.5$	$\mathbf{11}(1), \mathbf{16}(1)$
$semi2.6$	$\mathbf{5}(1), \mathbf{6}(4), \mathbf{12}(2)$
$semi2.7$	$\mathbf{5}(4), \mathbf{6}(1), \mathbf{13}(2)$
$semi4.1$	$\mathbf{8}(2), \mathbf{10}(2), \mathbf{12}(2)$

TABLE 5. The number of known Type III disjoint sets in the known planes of order 16.

Plane	Gezek (2022)	Total
BBH1*	$8^2, 16^2$	4
JOHN	16^8	8
JOWK	$4^2, 8^2, 16^2$	6
LMRH	$8^{10}, 16^4$	14
MATH	$4^7, 8^{17}, 16^6$	30
SEMI2*	$4^5, 8^{34}, 16^6$	51
SEMI4*	$8^3, 16^2$	5
Total		118

Theorem 2. *The number of* 104*-sets of type* $(4, 8)$ *in planes of order* 16 *is at least* 136*, of which all except four are coming from the unions of pairs of disjoint maximal* $(52, 4)$*-arcs.*

The complement of a Type III disjoint set is a 156-set of type $(8, 12)$. Table 5 shows that the number of 156-sets of type $(8, 12)$ in planes of order 16 is at least 118. As previously it was mentioned, there exist *five* triples of disjoint maximal $(52, 4)$-arcs, their unions provide *five* 156-sets of type $(8, 12)$. None of these sets are equivalent to any of the complement of Type III disjoint sets given in Table 5. We have

Theorem 3. *The number of* 156*-sets of type* $(8, 12)$ *in planes of order* 16 *is at least* 123*, of which five of them are coming from the unions of triples of disjoint maximal* $(52, 4)$*-arcs.*

6. Conclusion

The main purpose of the study presented in this paper is to answer the following question: for any prime power q, is it possible to partition the point set of a projective plane of order q^2 into q pairwise disjoint degree q maximal arcs and a unital? For $q = 2$, the answer is yes (see Section 3).

The first open case where no such partitioning is known to exist is the case for $q = 4$. If a partitioning of the point set of a plane of order 16 (as a union of *four* pairwise disjoint degree 4 maximal arcs and *one* unital) is possible, we get it from either (i) finding appropriate new maximal arcs of degree 4, or (ii) finding appropriate new unitals, or (iii) finding appropriate Type III disjoint sets, or (iv) finding an appropriate partitioning of the complement of the disjoint sets presented in this paper.

An appropriate degree 4 maximal arc in (i) in the matrix form (1) means a maximal arc A disjoint from $A_1 \cup U$ such that we have the matrix form (2), which may lead to a complete partitioning of the incidence matrix of the plane (if there exists an isomorphic copy of A disjoint from $A \cup A_1 \cup U$) and a (possible) new maximal arc (the complement of $A_1 \cup U$ may be a union of triples of disjoint maximal arcs such that maximal arcs in the union are isomorphic to A), or a (possible) new 104-set of type $(4, 8)$. An appropriate degree 4 maximal arc in (i) in the matrix form (2) means a maximal arc A disjoint from $A_1 \cup A_2 \cup U$ such that we have

$$\left[\begin{array}{c||c|c|c|c} \overbrace{-\cdots-}^{A'} & \overbrace{-\cdots-}^{A} & \overbrace{-\cdots-}^{A_2} & \overbrace{-\cdots-}^{A_1} & \overbrace{-\cdots-}^{U} \\ \hline O & 4 & 4 & 4 & 5 \\ \hline\hline 4 & O & 4 & 4 & 5 \\ \hline 4 & 4 & O & 4 & 5 \\ \hline 4 & 4 & 4 & O & 5 \\ \hline 4 & 4 & 4 & 4 & 1 \end{array}\right], \tag{4}$$

which gives a complete partitioning of the incidence matrix of the plane as well as a possible new degree 4 maximal arc A' (A' may be isomorphic to A). An appropriate degree 4 maximal arc in (i) in the matrix form (3) means a maximal arc A disjoint from $A_1 \cup A_2 \cup A_3$ such that

$$\left[\begin{array}{c||c|c|c|c} \overbrace{- \cdots -}^{U'} & \overbrace{- \cdots -}^{A} & \overbrace{- \cdots -}^{A_3} & \overbrace{- \cdots -}^{A_2} & \overbrace{- \cdots -}^{A_1} \\ \hline 1 & 4 & 4 & 4 & 4 \\ \hline\hline 5 & O & 4 & 4 & 4 \\ \hline 5 & 4 & O & 4 & 4 \\ \hline 5 & 4 & 4 & O & 4 \\ \hline 5 & 4 & 4 & 4 & O \end{array}\right], \tag{5}$$

which gives a complete partitioning of the incidence matrix of the plane as well as a new unital U' (this is a new set because U' is disjoint from $A_1 \cup A_2 \cup A_3$ and none of the known unitals have isomorphic copies disjoint from $A_1 \cup A_2 \cup A_3$). Similar arguments can be made for (ii)-(iv) in the matrix forms (1)-(3).

Discussions in this study make us believe that the following is true in general:

Conjecture 1. *The points of $PG(2, q^2)$ can be partitioned into q degree q maximal arcs and a unital.*

We conclude that disjoint sets in a projective plane π may be useful to find a complete partitioning of the point set of the plane into disjoint sets associated with degree q maximal arcs and unitals, new degree q maximal arcs, new unitals, and new v-sets of type (a, b). New projective planes can be found through disjoint sets by studying submatrices in the matrix forms (1)-(3) (a possible future research project). Disjoint sets also dramatically lessen the number of computations for finding new maximal arcs (i.e., from $\binom{273}{52}$ to $\binom{104}{52}$ for the computations in the planes of order 16) and unitals (i.e., from $\binom{273}{65}$ to $\binom{117}{65}$ for the computations in the planes of order 16).

Declaration of Competing Interests The author declares that he has no competing interest.

References

[1] Ball, S., Blokhuis, A., The classification of maximal arcs in small Desarguesian planes, *Bulletin of the Belgian Mathematical Society, Simon Stevin*, 9(3) (2002), 433-445. https://doi.org/10.36045/bbms/1102715068

[2] Ball, S., Blokhuis, A., Mazzocca, F., Maximal arcs in desarguesian planes of odd order do not exist, *Combinatorica*, 17(1) (1997), 31-41. https://doi.org/10.1007/BF01196129

[3] Beth, T., Jungnickel, D., Lenz, H., Design Theory (2nd edition), Cambridge University Press, Cambridge, UK, 1999.

[4] Brouwer, A. E., Some unitals on 28 points and their embeddings in projective planes of order 9, *Geometries and Groups, Springer Lecture Notes in Mathematics*, 893 (1981), 183-188. https://doi.org/10.1007/BFb0091018

[5] Colbourn, C.J., Dinitz J.H., Handbook of Combinatorial Designs (2nd edition), Chapman & Hall/CRC, Boca Raton, FL, USA, 2007.

[6] Denniston, R.H.F., Some maximal arcs in finite projective planes, *Journal of Combinatorial Theory*, 6(3) (1969), 317-319. https://doi.org/10.1016/S0021-9800(69)80095-5

[7] Gezek, M., Combinatorial Problems Related to Codes, Designs and Finite Geometries, PhD Thesis, Michigan Technological University, Houghton, MI, USA, 2017.

[8] Gezek, M., Mathon, R., Tonchev, V.D., Maximal arcs, codes, and new links between projective planes of order 16, *The Electronic Journal of Combinatorics*, 27(1) (2020), P1.62. https://doi.org/10.37236/9008

[9] Hamilton, N., Stoichev, S.D., Tonchev, V.D., Maximal arcs and disjoint maximal arcs in projective planes of order 16, *Journal of Geometry*, 67 (2000), 117-126. https://doi.org/10.1007/BF01220304

[10] Hirschfeld, J.W.P., Projective Geometries over Finite Fields (2nd ed.), Oxford University Press, Oxford, UK, 1998.

[11] Krčadinac, V., Smoljak, K., Pedal sets of unitals in projective planes of order 9 and 16, *Sarajevo Journal of Mathematics*, 7(20) (2011), 255-264.

[12] Lam, C.W.H., Kolesova, G., Thiel, L., A computer search for finite projective planes of order 9, *Discrete Mathematics*, 92 (1991), 187-195. https://doi.org/10.1016/0012-365X(91)90280-F

[13] Moorhouse, G.E., On projective planes of order less than 32, *Finite Geometries, Groups, and Computation*, (2006), 149-162. https://doi.org/10.1515/9783110199741.149

[14] Penttila, T., Royle, G.F., Sets of type (m,n) in the affine and projective planes of order 9, *Designs, Codes and Cryptography*, 6 (1995), 229-245. https://doi.org/10.1007/BF01388477

[15] Penttila, T., Royle, G.F. , Simpson, M.K., Hyperovals in the known projective planes of order 16, *Journal of Combinatorial Designs*, 4 (1996), 59-65. https://doi.org/10.1002/(SICI)1520-6610(1996)4:1<59::AID-JCD6>3.0.CO;2-Z

[16] Stoichev, S.D., Algorithms for finding unitals and maximal arcs in projective planes of order 16, *Serdica Journal of Computing*, 1(3) (2007), 279–292.

[17] Stoichev, S.D., Gezek, M., Unitals in projective planes of order 16, *Turkish Journal of Mathematics*, 45(2) (2021), 1001-1014. https://doi.org/10.3906/mat-2008-46

[18] Stoichev, S.D., Gezek, M., Unitals in projective planes of order 25, *Mathematics in Computer Science*, 17(5) (2023). https://doi.org/10.1007/s11786-023-00556-9

[19] Stoichev, S.D., Tonchev, V.D., Unital designs in planes of order 16, *Discrete Applied Mathematics*, 102(1-2) (2000), 151-158. https://doi.org/10.1016/S0166-218X(99)00236-X

[20] Thas, J.A., Construction of maximal arcs and partial geometries, *Geometriae Dedicata*, 3 (1974), 61-64. https://doi.org/10.1007/BF00181361

[21] Thas, J.A., Construction of maximal arcs and dual ovals in translation planes, *European Journal of Combinatorics*, 1(2) (1980), 189-192. https://doi.org/10.1016/S0195-6698(80)80052-7

http://communications.science.ankara.edu.tr

Commun.Fac.Sci.Univ.Ank.Ser. A1 Math. Stat.
Volume 72, Number 3, Pages 815–825 (2023)
DOI:10.31801/cfsuasmas.1160135
ISSN 1303-5991 E-ISSN 2618-6470

Research Article; Received: August 10, 2022; Accepted: May 23, 2023

STATISTICAL STRUCTURES AND KILLING VECTOR FIELDS ON TANGENT BUNDLES WITH RESPECT TO TWO DIFFERENT METRICS

Murat ALTUNBAŞ

Department of Mathematics, Erzincan Binali Yıldırım University, Erzincan, TÜRKİYE

Abstract. Let (M, g) be a Riemannian manifold and TM be its tangent bundle. The purpose of this paper is to study statistical structures on TM with respect to the metrics $G_1^f = {}^c g + {}^v(fg)$ and $G_2^f = {}^s g_f + {}^h g$, where f is a smooth function on M, ${}^c g$ is the complete lift of g, ${}^v(fg)$ is the vertical lift of fg, ${}^s g_f$ is a metric obtained by rescaling the Sasaki metric by a smooth function f and ${}^h g$ is the horizontal lift of g. Moreover, we give some results about Killing vector fields on TM with respect to these metrics.

1. Introduction

Let (M, g) be a Riemannian manifold and TM be its tangent bundle. In [1], Abbassi and Sarih defined a general "$g-$natural" metric on TM. Some well-known examples of the $g-$natural metric are the Sasaki metric ([6], [14]), the Cheeger-Gromoll metric ([13], [15]), Cheeger-Gromoll type metrics ([4], [7]) and the Kaluza-Klein metric [2]. However, some other metrics can be defined on the tangent bundle which are not subclasses of this $g-$natural metric. As first example, in [9], Gezer and Ozkan defined a metric $G_1^f = {}^c g + {}^v(fg)$, where ${}^c g$ is the complete lift of the metric and ${}^v(fg)$ is the vertical lift of fg and f is a smooth function on M. As second example, in [8], Gezer *et al.* introduced a metric $G_2^f = {}^s g_f + {}^h g$, where ${}^s g_f$ is a metric which is obtained by rescaling the Sasaki metric with a smooth function f on M and ${}^h g$ is the horizontal lift of g. These lifts will be explained later and we will deal with these two metrics in this paper.

2020 *Mathematics Subject Classification.* 53B20, 53C05.
Keywords. Statistical manifold, Riemannian metric, tangent bundle.
maltunbas@erzincan.edu.tr; 0000-0002-0371-9913 .

Statistical manifolds were introduced by Amari [3] in view of information geometry, and they were applied by Lauritzen [10]. These manifolds have a crucial role in statistics as the statistical model often forms a geometrical manifold.

Although curvature related properties of tangent bundles are widely studied, investigating statistical structures on tangent bundles is a relatively new topic. These structures were examined with respect to various Riemannian metrics such as the Sasaki metric [5], the Cheeger-Gromoll metric and a $g-$natural metric which consists of three classic lifts of the metric g [12], the twisted Sasaki metric and the gradient Sasaki metric [11].

In this paper, we study the statistical and Codazzi structures on TM using the horizontal and complete lifts of a linear connection on M when TM is endowed with the metrics G_1^f and G_2^f, respectively. We also investigate the Killing vector fields on TM with respect to such metrics.

2. Preliminaries

Let M be an $n-$dimensional Riemannian manifold and ∇ be a linear connection on M. The tangent bundle TM of the manifold M is a $2n-$dimensional smooth manifold and it is defined by the disjoint union of the tangent spaces at each point of M. If $\{U, x^i\}$ is a local coordinate system in M, then $\{\pi^{-1}(U), x^i, u^i, i = 1, ..., n\}$ is a local coordinate system in TM, where π is the natural projection defined by $\pi : TM \to M$ and (u^i) is the local coordinate system in each tangent space in U with respect to the basis $\{\frac{\partial}{\partial x^i}\}$. We have a direct sum decomposition

$$TTM = VTM \oplus HTM$$

for the tangent bundle of TM, where the vertical subspace VTM is spanned by $\{\frac{\partial}{\partial u^i} := (\frac{\partial}{\partial x^i})^v\}$ and the horizontal subspace HTM is spanned by $\{\frac{\delta}{\delta x^i} := (\frac{\partial}{\partial x^i})^h = \frac{\partial}{\partial x^i} - u^m \Gamma^j_{mi} \frac{\partial}{\partial u^j}\}$. Here Γ^j_{mi} denote the Christoffel symbols of ∇. The vertical, horizontal and the complete lifts of a vector field $X = X^i \frac{\partial}{\partial x^i}$ are defined by, respectively

$$X^v = X^i \frac{\partial}{\partial u^i},\ X^h = X^i \frac{\partial}{\partial x^i} - y^s \Gamma^m_{si} X^i \frac{\partial}{\partial u^m},\ X^c = X^i \frac{\partial}{\partial x^i} + y^s \frac{\partial X^i}{\partial x^s} \frac{\partial}{\partial u^i},$$

where we used Einstein the summation.

The Lie brackets of the vertical lift and the horizontal lift of vector fields satisfy the following relations:

$$[X^h, Y^h] = [X, Y]^h - (R(X, Y)u)^v,\ [X^h, Y^v] = (\nabla_X Y)^v - (T(X, Y))^v,\ [X^v, Y^v] = 0,$$

where R is the curvature tensor field and T is the torsion tensor field of the linear connection ∇, [16].

For a Riemannian metric g on a smooth manifold M, the complete lift ${}^cg$, the vertical lift ${}^vg$ and the horizontal lift ${}^hg$ of g are given by

$${}^cg(X^h, Y^h) = {}^cg(X^v, Y^v) = 0,\ {}^cg(X^h, Y^v) = {}^cg(X^v, Y^h) = g(X, Y),$$
$${}^vg(X^h, Y^h) = g(X, Y),\ {}^vg(X^v, Y^v) = {}^vg(X^h, Y^v) = {}^vg(X^v, Y^h) = 0.$$

$$^{h}g(X^h, Y^h) = 0,\ ^{h}g(X^v, Y^v) = 0,\ ^{h}g(X^h, Y^v) =\ ^{h}g(X^v, Y^h) = g(X, Y).$$

The horizontal lift connection $\overset{h}{\nabla}$ and the complete lift connection $\overset{c}{\nabla}$ are respectively given by, [16]

$$\begin{aligned}
\overset{h}{\nabla}_{X^h} Y^h &= (\nabla_X Y)^h,\ \overset{h}{\nabla}_{X^h} Y^v = (\nabla_X Y)^v,\ \overset{h}{\nabla}_{X^v} Y^h = \overset{h}{\nabla}_{X^v} Y^v = 0, \\
\overset{c}{\nabla}_{X^h} Y^h &= (\nabla_X Y)^h + (R(u, X)Y)^v,\ \overset{c}{\nabla}_{X^v} Y^h = \overset{c}{\nabla}_{X^v} Y^v = 0, \\
\overset{c}{\nabla}_{X^h} Y^v &= (\nabla_X Y)^v,\ \overset{c}{\nabla}_{X^c} Y^c = (\nabla_X Y)^c,\ \overset{c}{\nabla}_{X^c} Y^v = \overset{c}{\nabla}_{X^v} Y^c = (\nabla_X Y)^v.
\end{aligned}$$

Remark 1. *The connection ∇ is a flat and torsionless linear connection if and only if $\overset{h}{\nabla}(\overset{c}{\nabla})$ is a torsionless linear connection, [16].*

In the sequel, we shall denote $\frac{\partial}{\partial x^i}$, $\frac{\delta}{\delta x^i}$ and $\frac{\partial}{\partial u^i}$ as ∂_i, δ_i and $\partial_{\bar{i}}$, for shortness.

The metric G_1^f on TM is defined by

$$G_1^f(X^h, Y^h) = fg(X, Y),\ G_1^f(X^h, Y^v) = G_1^f(X^v, Y^h) = g(X, Y),\ G_1^f(X^v, Y^v) = 0, \tag{1}$$

where f is a strictly positive function on M, [9].

From Theorem 3.1 in [9], we can easily rewrite the Levi-Civita connection of the metric G_1^f in invariant form.

Lemma 1. *Let (M, g) be a Riemannian manifold on (TM, G_1^f) be its tangent bundle with the metric G_1^f defined by (1). The Levi-Civita connection ∇_1^f of the metric G_1^f satisfies the following relations*

$$\begin{aligned}
\nabla^f_{1X^h} Y^h &= (\nabla_X Y)^h + (R(u, X)Y + A_f(X, Y))^v, \\
\nabla^f_{1X^h} Y^v &= (\nabla_X Y)^v,\ \nabla^f_{1X^v} Y^h = \nabla^f_{1X^v} Y^v = 0,
\end{aligned}$$

where X, Y are vector fields on M, ∇ is the Levi-Civita connection of g, R is the Riemannian curvature of ∇ and $A_f(X, Y) = \frac{1}{2}(X(f)Y + Y(f)X - g(X, Y) \circ (df)^*)$.

The metric G_2^f on TM is defined by

$$G_2^f(X^h, Y^h) = fg(X, Y),\ G_2^f(X^h, Y^v) = G_2^f(X^v, Y^h) = g(X, Y), G_2^f(X^v, Y^v) = g(X, Y), \tag{2}$$

where f is a strictly positive function on M, [8].

From [9], we rewrite the Levi-Civita connection of the metric G_2^f in invariant form as follows.

Lemma 2. *Let (M, g) be a Riemannian manifold on (TM, G_2^f) be its tangent bundle with the metric G_2^f defined by (2). The Levi-Civita connection ∇_2^f of the metric G_2^f satisfies the following relations*

$$\nabla^f_{2X^h} Y^h = (\nabla_X Y + \frac{1}{2(f-1)}(R(u, X)Y + R(u, Y)X) + \frac{1}{f-1} A_f(X, Y))^h$$

$$-(\frac{1}{f-1}A_f(X,Y)+\frac{1}{2}R(X,Y)u+\frac{1}{2(f-1)}(R(u,X)Y+R(u,Y)X))^v,$$

$$\nabla^f_{2X^h}Y^v = (\frac{1}{2(f-1)}R(u,Y)X)^h+(\nabla_X Y-\frac{1}{2(f-1)}R(u,X)Y)^v,$$

$$\nabla^f_{2X^v}Y^h = (\frac{1}{2(f-1)}R(u,X)Y)^h-(\frac{1}{2(f-1)}R(u,X)Y)^v,$$

$$\nabla^f_{2X^v}Y^v = 0,$$

where X,Y are vector fields on M, ∇ is the Levi-Civita connection of g, R is the Riemannian curvature of ∇ and $A_f(X,Y)=\frac{1}{2}(X(f)Y+Y(f)X-g(X,Y)\circ(df)^*)$.

Definition 1. *Let (M,g) be a Riemannian manifold and let ∇ be a linear connection on M. The pair (g,∇) is called a Codazzi couple if the Codazzi equation are valid:*

$$(\nabla_X g)(Y,Z)=(\nabla_Z g)(X,Y),$$

for all vector fields X,Y,Z on M. The triplet (M,g,∇) is said to be a Codazzi manifold and ∇ is called a Codazzi connection. Moreover, when ∇ is torsionless, (M,g,∇) is a statistical manifold.

3. Killing Vector Fields and Statistical Structures on (TM,G_1^f)

Definition 2. *Let (M,g) be a Riemannian manifold and ∇ be a linear connection on M. A vector field X is called conformal (respectively, Killing) if $L_X g=2\rho g$ (respectively, $L_X g=0$), where ρ is a smooth function on M.*

Using this definition, we have

$$L_{X^v}G_1^f(Y^v,Z^v) = 0,$$

$$L_{X^v}G_1^f(Y^h,Z^v) = 0,$$

$$L_{X^v}G_1^f(Y^h,Z^h) = g(\nabla_Y X,Z)+g(Y,\nabla_Z X)-g(T(Y,X),Z)-g(T(Z,X),Y)$$

and

$$L_{X^h}G_1^f(Y^v,Z^v) = 0,$$

$$L_{X^h}G_1^f(Y^h,Z^v) = g(\nabla_Y X,Z)+g(T(X,Y),Z)+g(Y,T(X,Z)),$$

$$L_{X^h}G_1^f(Y^h,Z^h) = X(f)g(Y,Z)+f(L_X g)(Y,Z)+g(R(X,Y)u,Z)+g(R(X,Z)u,Y).$$

So, we have the following proposition.

Proposition 1. *Let (TM,G_1^f) be the tangent bundle of a Riemannian manifold (M,g). Then the following statements are true:*

(i) If ∇ is a torsionless linear connection on M, then the vector field X^v is Killing if and only if X is a parallel vector field on (M,g).

(ii) If ∇ is a torsionless linear connection on M, then the vector field X^h is Killing if and only if X is a $\nabla-$parallel vector field, X is a conformal vector field

such that $(L_X g)(Y,Z) = -\frac{X(f)}{f} g(Y,Z)$ *and* $R(X,Y)Z = 0$ *for all the vector fields* Y, Z *on* M.

(iii) If ∇ *is a torsionless linear connection,* f *is a constant function and* X *is a parallel vector field on* M, *then the vector field* X^h *is Killing if and only if the vector field* X *is Killing on* (M,g) *and* $R(X,Y)Z = 0$ *for all the vector fields* Y, Z *on* M.

(iv) If ∇ *is a flat connection,* X *is a* $\nabla-$*parallel vector field and* f *is a constant function on* (M,g)*, then the vector field* X^h *is Killing if and only if the vector field* X *is Killing on* (M,g).

Proof. The truthfulness of the assertions are clear from the definition of the Killing vector fields. □

Now, we obtain the components of $\overset{h}{\nabla} G_1^f$. We have

$$\begin{aligned}
(\overset{h}{\nabla}_{\delta_i} G_1^f)(\delta_j, \delta_k) &= \partial_i(f) g_{jk} + f(\nabla_{\partial_i} g)(\partial_j, \partial_k), \\
(\overset{h}{\nabla}_{\delta_j} G_1^f)(\delta_k, \delta_i) &= \partial_j(f) g_{ki} + f(\nabla_{\partial_j} g)(\partial_k, \partial_i), \\
(\overset{h}{\nabla}_{\delta_k} G_1^f)(\delta_i, \delta_j) &= \partial_k(f) g_{ij} + f(\nabla_{\partial_k} g)(\partial_i, \partial_j),
\end{aligned} \tag{3}$$

$$(\overset{h}{\nabla}_{\partial_{\bar{i}}} G_1^f)(\partial_{\bar{j}}, \partial_{\bar{k}}) = 0, \; (\overset{h}{\nabla}_{\partial_{\bar{i}}} G_1^f)(\partial_{\bar{j}}, \delta_k) = (\overset{h}{\nabla}_{\partial_{\bar{j}}} G_1^f)(\delta_k, \partial_{\bar{i}}) = (\overset{h}{\nabla}_{\delta_k} G_1^f)(\partial_{\bar{i}}, \partial_{\bar{j}}) = 0,$$

$$(\overset{h}{\nabla}_{\delta_i} G_1^f)(\delta_j, \partial_{\bar{k}}) = (\nabla_{\partial_i} g)(\partial_j, \partial_k), \; (\overset{h}{\nabla}_{\delta_j} G_1^f)(\partial_{\bar{k}}, \delta_i) = (\nabla_{\partial_j} g)(\partial_k, \partial_i), \; (\overset{h}{\nabla}_{\partial_{\bar{k}}} G_1^f)(\delta_i, \delta_j) = 0. \tag{4}$$

So, we can express the following theorem.

Theorem 1. *Let* (TM, G_1^f) *be the tangent bundle of a Riemannian manifold* (M,g) *and* ∇ *be a linear connection. Then the following statements are true:*

(i) If $(TM, G_1^f, \overset{h}{\nabla})$ *is a Codazzi manifold, then* f *is a constant function on* M *and* ∇ *is a metric connection.*

(ii) If $(TM, G_1^f, \overset{h}{\nabla})$ *is a statistical manifold, then* ∇ *is flat,* f *is a constant function on* M *and* ∇ *is the Levi-Civita connection of* g. *In this case, the connections* $\overset{h}{\nabla}$ *and* ∇_1^f *coincide.*

(iii) If ∇ *is the Levi-Civita connection of* g *and* f *is a constant function on* M, *then* $\overset{h}{\nabla}$ *is compatible with the metric* G_1^f. *In particular, if* ∇ *is flat, then the connections* $\overset{h}{\nabla}$ *and* ∇_1^f *coincide.*

Proof. (i) From (3) and (4) we see that if $(TM, G_1^f, \overset{h}{\nabla})$ is a Codazzi manifold, then f is a constant function on M and ∇ is a metric connection.

(ii) If $(TM, G_1^f, \overset{h}{\nabla})$ is a statistical manifold, then $\overset{h}{\nabla}$ is torsionless. From Remark 1, we see that ∇ is flat. It follows from (i) and the definition of the connections $\overset{h}{\nabla}$ and ∇_1^f.

(iii) It is clear from the definition of the Levi-Civita connection and the connections $\overset{h}{\nabla}$ and ∇_1^f.

□

Now, we repeat this process for $(TM, G_1^f, \overset{c}{\nabla})$. By direct calculations we have

$$\begin{aligned}
(\overset{c}{\nabla}_{\delta_i} G_1^f)(\delta_j, \delta_k) &= \partial_i(f) g_{jk} + f(\nabla_{\partial_i} g)(\partial_j, \partial_k) - u^s R_{sij}^t g_{kt} - u^s R_{sik}^t g_{jt}, \quad (5)\\
(\overset{c}{\nabla}_{\delta_j} G_1^f)(\delta_k, \delta_i) &= \partial_j(f) g_{ki} + f(\nabla_{\partial_j} g)(\partial_k, \partial_i) - u^s R_{sjk}^t g_{it} - u^s R_{sji}^t g_{tk},\\
(\overset{c}{\nabla}_{\delta_k} G_1^f)(\delta_i, \delta_j) &= \partial_k(f) g_{ij} + f(\nabla_{\partial_k} g)(\partial_i, \partial_j) - u^s R_{ski}^t g_{jt} - u^s R_{skj}^t g_{ti},
\end{aligned}$$

$$(\overset{c}{\nabla}_{\partial_{\bar{i}}} G_1^f)(\partial_{\bar{j}}, \partial_{\bar{k}}) = 0, \ (\overset{c}{\nabla}_{\partial_{\bar{i}}} G_1^f)(\partial_{\bar{j}}, \delta_k) = (\overset{c}{\nabla}_{\partial_{\bar{j}}} G_1^f)(\delta_k, \partial_{\bar{i}}) = (\overset{c}{\nabla}_{\delta_k} G_1^f)(\partial_{\bar{i}}, \partial_{\bar{j}}) = 0,$$

$$(\overset{c}{\nabla}_{\delta_i} G_1^f)(\delta_j, \partial_{\bar{k}}) = (\nabla_{\partial_i} g)(\partial_j, \partial_k), \ (\overset{c}{\nabla}_{\delta_j} G_1^f)(\partial_{\bar{k}}, \delta_i) = (\nabla_{\partial_j} g)(\partial_k, \partial_i), \ (\overset{c}{\nabla}_{\partial_{\bar{k}}} G_1^f)(\delta_i, \delta_j) = 0. \quad (6)$$

Thus, we give the following theorem.

Theorem 2. *Let (TM, G_1^f) be the tangent bundle of a Riemannian manifold (M, g) and let ∇ be a torsionless linear connection. Then the following statements are true:*

i) If $(TM, G_1^f, \overset{c}{\nabla})$ is a Codazzi (respectively statistical) manifold, then ∇ is flat, f is a constant function on M. Furthermore, $\overset{c}{\nabla}$ is a metric connection (respectively, $\overset{c}{\nabla}$ becomes the Levi-Civita connection of G_1^f).

ii) If $(TM, G_1^f, \overset{c}{\nabla})$ is a statistical manifold and f is a constant function on M, then ∇ is the Levi-Civita connection of g and $\overset{c}{\nabla}$ becomes the Levi-Civita connection of G_1^f.

(iii) If ∇ is the Levi-Civita connection of g, f is a constant function on M and ∇ is a flat connection, then the connections $\overset{c}{\nabla}$ and ∇_1^f coincide.

Proof. (i) If $(TM, G_1^f, \overset{c}{\nabla})$ is a Codazzi manifold, then from (6) we obtain that ∇ is a metric connection. Differentiating $(5)_1$ with respect to u^m gives us $R_{mij}^t g_{kt} + R_{mik}^t g_{jt} = 0$. Similarly, by differentiating $(5)_2$ and $(5)_3$ with respect to u^m, we obtain $R_{mjk}^t g_{it} + R_{mji}^t g_{tk} = 0$ and $R_{mki}^t g_{jt} + R_{mkj}^t g_{ti} = 0$, respectively. So, ∇ is a flat connection. We also occur that f is a constant function on M. If $\overset{c}{\nabla}$ is torsionless, it becomes the Levi-Civita connection of G_1^f.

(ii) We get immediately from Remark 1, the definition of the Levi-Civita connection and the complete lift connection $\overset{c}{\nabla}$.

(iii) Definitions of the connections $\overset{c}{\nabla}$ and ∇_1^f give the results. $\square$

Now, we assume that (TM, G_s, ∇_1^f) is a statistical manifold. The metric G_s is called the Sasaki metric and it is defined by

$$G_s(X^h, Y^h) = g(X, Y),\ G_s(X^h, Y^v) = G_s(X^v, Y^h) = 0,\ G_s(X^v, Y^v) = g(X, Y),$$

for all vector fields X, Y, Z on M. Using Lemma 1, we get

$$\begin{aligned}
(\nabla^f_{1\delta_i} G_s)(\delta_j, \delta_k) &= (\nabla^f_{1\delta_j} G_s)(\delta_k, \delta_i) = (\nabla^f_{1\delta_k} G_s)(\delta_i, \delta_j) = 0, \qquad (7)\\
(\nabla^f_{1\partial_{\bar{i}}} G_s)(\partial_{\bar{j}}, \partial_{\bar{k}}) &= 0,\ (\nabla^f_{1\partial_{\bar{i}}} G_s)(\partial_{\bar{j}}, \delta_k) = (\nabla^f_{1\partial_{\bar{j}}} G_s)(\delta_k, \partial_{\bar{i}}) = (\nabla^f_{1\delta_k} G_s)(\partial_{\bar{i}}, \partial_{\bar{j}}) = 0,\\
(\nabla^f_{1\delta_i} G_s)(\delta_j, \partial_{\bar{k}}) &= -u^s R^m_{sij} g_{mk} + \frac{1}{2} g_{mk}(f_i \delta^m_j + f_j \delta^m_i - g_{ij} f^m_{\cdot}),\\
(\nabla^f_{1\delta_j} G_s)(\partial_{\bar{k}}, \delta_i) &= -u^s R^m_{sji} g_{mk} + \frac{1}{2} g_{mk}(f_j \delta^m_i + f_i \delta^m_j - g_{ji} f^m_{\cdot}),\\
(\nabla^f_{1\partial_{\bar{k}}} G_s)(\delta_i, \delta_j) &= 0,
\end{aligned}$$

where, $f_i = \partial_i f$ and $f^m_{\cdot} = g^{mh} f_h$. So, we have the following theorem.

Theorem 3. *Let (TM, G_1^f) be the tangent bundle of a Riemannian manifold (M, g) and let ∇_1^f is the Levi-Civita connection of the metric G_1^f. If (TM, G_s, ∇_1^f) is a statistical manifold, then ∇ is flat and f is a constant function on M.*

Proof. If (TM, G_s, ∇_1^f) is a statistical manifold, by differentiating $(7)_3$ and $(7)_4$ with respect to u^t, we occur $R^m_{tij} g_{mk} = R^m_{tji} g_{mk} = 0$. Moreover, we see that f is a constant function on M. $\square$

4. Killing Vector Fields and Statistical Structures on (TM, G_2^f)

In this final section, we follow the same line in the previous section for the metric G_2^f. The proofs of the results will be similar.
From Definition 2, we have

$$\begin{aligned}
L_{X^v} G_2^f(Y^v, Z^v) &= 0,\\
L_{X^v} G_2^f(Y^h, Z^v) &= g(\nabla_Y X, Z) - g(T(Y, X), Z),\\
L_{X^v} G_2^f(Y^h, Z^h) &= g(\nabla_Y X, Z) - g(T(Y, X), Z) + g(\nabla_Z X, Y) - g(T(Z, X), Y)
\end{aligned}$$

and

$$\begin{aligned}
L_{X^h} G_2^f(Y^v, Z^v) &= (\nabla_X g)(Y, Z) + g(T(X, Y), Z) + g(Y, T(X, Z)),\\
L_{X^h} G_2^f(Y^h, Z^v) &= g(\nabla_Y X, Z) + g(R(X, Y)u, Z) + g(T(X, Y), Z) + g(Y, T(X, Z)),\\
L_{X^h} G_2^f(Y^h, Z^h) &= X(f) g(Y, Z) + f(L_X g)(Y, Z) + g(R(X, Y)u, Z) + g(R(X, Z)u, Y).
\end{aligned}$$

It is clear that if ∇ is a torsionless linear connection, then the vector field X^v is Killing if and only if $\nabla X = 0$. On the other hand, if ∇ is the Levi-Civita connection of g, then X^h is a Killing vector field if and only if X is $\nabla-$parallel, X is Killing, the function f is constant and ∇ is flat. More precisely, we have

Proposition 2. *Let (TM, G_2^f) be the tangent bundle of a Riemannian manifold (M, g). Then the following statements are true:*

(i) If ∇ is a torsionless linear connection on M, then the vector field X^v is Killing if and only if X is a parallel vector field.

(ii) If ∇ is a torsionless linear connection, f is a constant function and X is a $\nabla-$parallel vector field on M, then the vector field X^h is Killing if and only if X is Killing vector field on M, ∇ is the Levi-Civita connection of (M, g) and $R(X, Y)Z = 0$ for all the vector fields Y, Z on M.

(iii) If ∇ is the flat Levi-Civita connection, X is a $\nabla-$parallel vector field and f is a constant function on (M, g), then the vector field X^h is Killing if and only if the vector field X is Killing on (M, g).

Here, we compute the components of $\overset{h}{\nabla} G_2^f$. We obtain

$$\begin{aligned}
(\overset{h}{\nabla}_{\delta_i} G_2^f)(\delta_j, \delta_k) &= \partial_i(f) g_{jk} + f(\nabla_{\partial_i} g)(\partial_j, \partial_k), \\
(\overset{h}{\nabla}_{\delta_j} G_2^f)(\delta_k, \delta_i) &= \partial_j(f) g_{ki} + f(\nabla_{\partial_j} g)(\partial_k, \partial_i), \\
(\overset{h}{\nabla}_{\delta_k} G_2^f)(\delta_i, \delta_j) &= \partial_k(f) g_{ij} + f(\nabla_{\partial_k} g)(\partial_i, \partial_j),
\end{aligned}$$

$$\begin{aligned}
(\overset{h}{\nabla}_{\partial_{\bar{i}}} G_2^f)(\partial_{\bar{j}}, \partial_{\bar{k}}) &= 0, \ (\overset{h}{\nabla}_{\partial_{\bar{i}}} G_2^f)(\partial_{\bar{j}}, \delta_k) = (\overset{h}{\nabla}_{\partial_{\bar{j}}} G_2^f)(\delta_k, \partial_{\bar{i}}) = 0, \\
(\overset{h}{\nabla}_{\delta_k} G_2^f)(\partial_{\bar{i}}, \partial_{\bar{j}}) &= (\nabla_{\partial_k} g)(\partial_i, \partial_j),
\end{aligned}$$

$$\begin{aligned}
(\overset{h}{\nabla}_{\delta_i} G_2^f)(\delta_j, \partial_{\bar{k}}) &= (\nabla_{\partial_i} g)(\partial_j, \partial_k), \ (\overset{h}{\nabla}_{\delta_j} G_2^f)(\partial_{\bar{k}}, \delta_i) = (\nabla_{\partial_j} g)(\partial_k, \partial_i), \\
(\overset{h}{\nabla}_{\partial_{\bar{k}}} G_2^f)(\delta_i, \delta_j) &= 0.
\end{aligned}$$

From the above equations, we deduce that if $(TM, G_2^f, \overset{h}{\nabla})$ is a Codazzi manifold, then f is a constant function on M and ∇ is a metric connection. So, we can write the following theorem.

Theorem 4. *Let (TM, G_2^f) be the tangent bundle of a Riemannian manifold (M, g) and ∇ be a linear connection. Then the following statements are true:*

(i) If $(TM, G_2^f, \overset{h}{\nabla})$ is a Codazzi manifold, then f is a constant function on M and ∇ is a metric connection.

(ii) If $(TM, G_2^f, \overset{h}{\nabla})$ is a statistical manifold, then ∇ is flat, f is a constant function on M and ∇ is the Levi-Civita connection of g. In this case, the connections $\overset{h}{\nabla}$ and ∇_2^f coincide.

(iii) If ∇ is the Levi-Civita connection of g and f is a constant function on M, then $\overset{h}{\nabla}$ is compatible with the metric G_2^f. In particular, if ∇ is flat, then the connections $\overset{h}{\nabla}$ and ∇_2^f coincide.

Now, we follow this process for $(TM, G_2^f, \overset{c}{\nabla})$. By direct calculations we have

$$\begin{aligned} (\overset{c}{\nabla}_{\delta_i} G_2^f)(\delta_j, \delta_k) &= \partial_i(f) g_{jk} + f(\nabla_{\partial_i} g)(\partial_j, \partial_k) - u^s R_{sij}^t g_{kt} - u^s R_{sik}^t g_{jt}, \quad (8) \\ (\overset{c}{\nabla}_{\delta_j} G_2^f)(\delta_k, \delta_i) &= \partial_j(f) g_{ki} + f(\nabla_{\partial_j} g)(\partial_k, \partial_i) - u^s R_{sjk}^t g_{it} - u^s R_{sji}^t g_{tk}, \\ (\overset{c}{\nabla}_{\delta_k} G_2^f)(\delta_i, \delta_j) &= \partial_k(f) g_{ij} + f(\nabla_{\partial_k} g)(\partial_i, \partial_j) - u^s R_{ski}^t g_{jt} - u^s R_{skj}^t g_{ti}, \end{aligned}$$

$$(\overset{c}{\nabla}_{\partial_{\bar{i}}} G_2^f)(\partial_{\bar{j}}, \partial_{\bar{k}}) = 0, \; (\overset{c}{\nabla}_{\partial_{\bar{i}}} G_2^f)(\partial_{\bar{j}}, \delta_k) = (\overset{c}{\nabla}_{\partial_{\bar{j}}} G_2^f)(\delta_k, \partial_{\bar{i}}) = (\overset{c}{\nabla}_{\delta_k} G_2^f)(\partial_{\bar{i}}, \partial_{\bar{j}}) = 0,$$

$$\begin{aligned} (\overset{c}{\nabla}_{\delta_i} G_2^f)(\delta_j, \partial_{\bar{k}}) &= (\nabla_{\partial_i} g)(\partial_j, \partial_k) + u^s R_{sij}^t g_{kt}, \quad (9) \\ (\overset{c}{\nabla}_{\delta_j} G_2^f)(\partial_{\bar{k}}, \delta_i) &= (\nabla_{\partial_j} g)(\partial_k, \partial_i) + u^s R_{sji}^t g_{kt}, \\ (\overset{c}{\nabla}_{\partial_{\bar{k}}} G_2^f)(\delta_i, \delta_j) &= (\nabla_{\partial_k} g)(\partial_i, \partial_j). \end{aligned}$$

If $(TM, G_2^f, \overset{c}{\nabla})$ is a Codazzi manifold, then from (9) we obtain that ∇ is a flat metric connection. We also deduce that from $(8)_1$ f is a constant function on M. Thus, we have the following theorem.

Theorem 5. *Let (TM, G_2^f) be the tangent bundle of a Riemannian manifold (M, g) and let ∇ be a torsionless linear connection. Then the following statements are true:*

i) If $(TM, G_2^f, \overset{c}{\nabla})$ is a Codazzi (respectively statistical) manifold, then ∇ is flat, f is a constant function on M. Furthermore, $\overset{c}{\nabla}$ is a metric connection (respectively, $\overset{c}{\nabla}$ becomes the Levi-Civita connection of G_2^f).

ii) If $(TM, G_2^f, \overset{c}{\nabla})$ is a statistical manifold and f is a constant function on M, then ∇ is the Levi-Civita connection of g and $\overset{c}{\nabla}$ becomes the Levi-Civita connection of G_2^f.

(iii) If ∇ is the Levi-Civita connection of g, f is a constant function on M and ∇ is a flat connection, then the connections $\overset{c}{\nabla}$ and ∇_2^f coincide.

Now, we assume that (TM, G_s, ∇_2^f) is a statistical manifold. Using Lemma 2

$$\begin{aligned} (\nabla^f_{2\delta_i} G_s)(\delta_j, \delta_k) &= -\frac{1}{2(f-1)}(u^s R_{sij}^m + u^s R_{sji}^m + f_i \delta_j^m + f_j \delta_i^m - f_{.}^{m} g_{ij}) g_{mk} \\ &\quad -\frac{1}{2(f-1)}(u^s R_{sik}^m + u^s R_{ski}^m + f_i \delta_k^m + f_k \delta_i^m - f_{.}^{m} g_{ik}) g_{mj} \\ (\nabla^f_{2\partial_{\bar{i}}} G_s)(\partial_{\bar{j}}, \partial_{\bar{k}}) &= 0, \quad (10) \end{aligned}$$

$$
\begin{aligned}
(\nabla^f_{2\partial_{\bar{i}}} G_s)(\partial_{\bar{j}}, \delta_k) &= \frac{1}{2(f-1)} u^s R^m_{sik} g_{mj}, \\
(\nabla^f_{2\delta_k} G_s)(\partial_{\bar{i}}, \partial_{\bar{j}}) &= \frac{1}{2(f-1)} (u^s R^m_{ski} g_{mj} + u^s R^m_{skj} g_{mi}), \\
(\nabla^f_{2\delta_i} G_s)(\delta_j, \partial_{\bar{k}}) &= [\frac{1}{2(f-1)} (u^s R^m_{sij} + u^s R^m_{sji} + f_i \delta^m_j + f_j \delta^m_i - f^m_{.} g_{ij}) \\
&\quad + \frac{1}{2} u^s R^m_{ijs}] g_{km} - \frac{1}{2(f-1)} u^s R^m_{ski} g_{jm}, \\
(\nabla^f_{2\partial_{\bar{k}}} G_s)(\delta_i, \delta_j) &= -\frac{1}{2(f-1)} (u^s R^m_{ski} g_{mj} + u^s R^m_{skj} g_{mi}),
\end{aligned}
$$

where $f_i = \partial_i f$ and $f^m_{.} = g^{mh} f_h$. If (TM, G_s, ∇^f_2) is a statistical manifold, by differentiating $(10)_3$ with respect to u^t we occur $R^m_{tik} g_{mj} = 0$ (other equations which have curvature components of ∇ is similar). Moreover, we see that f is a constant function on M. So, we have the theorem below.

Theorem 6. *Let (TM, G^f_2) be the tangent bundle of a Riemannian manifold (M, g) and let ∇^f_2 is the Levi-Civita connection of the metric G^f_2. If (TM, G_s, ∇^f_2) is a statistical manifold, then ∇ is flat and f is a constant function on M.*

Declaration of Competing Interests The author declares that he has no known competing financial interests or personal relationships that could have appeared to influence the work reported in this paper.

Acknowledgements The author would like to thank the referees for their valuable suggestions and comments.

References

[1] Abbassi, M. T. K., Sarih, M., On natural metrics on tangent bundles of Riemannian manifolds, *Arch. Math. (Brno)*, 41 (2005), 71-92.

[2] Altunbaş, M, Gezer, A., Bilen, L., Remarks about the Kaluza-Klein metric on tangent bundle, *Int. J. Geom. Met. Mod. Phys.*, 16(3) (2019), 1950040. https://doi.org/10.1142/S0219887819500403

[3] Amari, S., Differential geometric methods in statistics- Lect. Notes in Stats., Springer, New York, 1985.

[4] Anastasiei, M., Locally conformal Kaehler structures on tangent bundle of a space form, *Libertas Math.*, 19 (1999), 71-76.

[5] Balan, V., Peyghan, E., Sharahi, E., Statistical structures on the tangent bundle of a statistical manifold with Sasaki metric, *Hacettepe J. Math. Stat.*, 49(1) (2020), 120-135. https://doi.org/10.15672/HJMS.2019.667

[6] Dombrowski, P., On the geometry of the tangent bundle, *J. Reine Angew. Math.*, 210 (1962), 73-88. https://doi.org/10.1515/crll.1962.210.73

[7] Gezer, A., Altunbaş, M., Some notes concerning Riemannian metrics of Cheeger Gromoll type, *J. Math. Anal. App.*, 396(1) (2012), 119-132. https://doi.org/10.1016/j.jmaa.2012.06.011

[8] Gezer, A., Bilen, L., Karaman, Ç., Altunbaş, M., Curvature properties of Riemannian metrics of the forms Sgf +Hg on the tangent bundle over a Riemannian manifold (M,g), *Int. Elec. J. Geo.*, 8(2) (2015), 181-194. https://doi.org/10.36890/iejg.592306

[9] Gezer, A., Ozkan, M., Notes on the tangent bundle with deformed complete lift metric, *Turkish J. Math.*, 38 (2014), 1038-1049. https://doi.org/10.3906/mat-1402-30

[10] Lauritzen, S., Statistical manifolds. In Differential geometry in statistical inference, IMS lecture notes monograph series (10), Institute of Mathematical Statistics, Hyward, CA, USA, 96-163, 1987.

[11] Peyghan, E., Seifipour, D., Blaga, A., On the geometry of lift metrics and lift connections on the tangent bundle, *Turkish J. Math.*, 46(6) (2022), 2335-2352. https://doi.org/10.55730/1300-0098.3272

[12] Peyghan, E., Seifipour, D., Gezer, A., Statistical structures on tangent bundles and Lie groups. *Hacettepe J. Math. Stat.*, 50 (2021), 1140-1154. https://doi.org/10.15672/hujms.645070

[13] Salimov, A., Kazimova, S., Geodesics of the Cheeger-Gromoll metric, *Turkish J. Math.*, 33(1) (2009), 99-105. https://doi.org/10.3906/mat-0804-24

[14] Sasaki, S., On the differential geometry of tangent bundles of Riemannian manifolds, *Tohoku Math. J.*, 10 (1958), 338-358. https://doi.org/10.2748/tmj/1178244668

[15] Sekizawa, M., Curvatures of tangent bundles with Cheeger-Gromoll metric, *Tokyo J. Math.* 14(2) (1991), 407-417. https://doi.org/10.3836/tjm/1270130381

[16] Yano, K., Ishihara, S., Tangent and cotangent bundles, Marcel Dekker Inc., New York, 1973.

http://communications.science.ankara.edu.tr

Commun.Fac.Sci.Univ.Ank.Ser. A1 Math. Stat.
Volume 72, Number 3, Pages 826–838 (2023)
DOI:10.31801/cfsuasmas.1172289
ISSN 1303-5991 E-ISSN 2618-6470

Research Article; Received: September 7, 2022; Accepted: May 14, 2023

CHARACTERIZATION OF A PARASASAKIAN MANIFOLD ADMITTING BACH TENSOR

Uday Chand DE[1], Gopal GHOSH[2] and Krishnendu DE[3]

[1]Department of Pure Mathematics, University of Calcutta, West Bengal, INDIA
[2] Department of Basic Science and Humanities, Cooch Behar Government Engineering College, Harinchawra, Cooch Behar, Kol- 736170, West Bengal, INDIA
[3]Department of Mathematics, Kabi Sukanta Mahavidyalaya,The University of Burdwan, Bhadreswar, P.O.-Angus, Hooghly, Pin 712221, West Bengal, INDIA

Abstract. In the present article, our aim is to characterize Bach flat paraSasakian manifolds. It is established that a Bach flat paraSasakian manifold of dimension greater than three is of constant scalar curvature. Next, we prove that if the metric of a Bach flat paraSasakian manifold is a Yamabe soliton, then the soliton field becomes a Killing vector field. Finally, it is shown that a 3-dimensional Bach flat paraSasakian manifold is locally isometric to the hyperbolic space $H^{2n+1}(1)$.

1. Introduction

Adati and Matsumoto [1] introduced the concept of paraSasakian (briefly, P-Sasakian) manifolds, which are considered as a specific case of an almost paracontact manifold initiated by Sato [15]. Matsumoto and Mihai studied P-Sasakian manifolds that admit W_2 or E-Tensor fields and also some curvature conditions [17]. In ([18], [19]) the authors investigated P-Sasakian manifolds obeying certain curvature conditions. In another way, on a pseudo-Riemannian manifold M^{2n+1} Kaneyuki and Kozai [21] introduced the almost paracontact structure and set up the almost paracomplex structure on $M^{2n+1} \times \mathbb{R}$. The main difference between the almost paracontact metric manifold in the sense of Sato [15] and Kaneyuki et al [20] is the signature of the metric. In [27], Zamkovoy introduced paraSasakian manifolds as a normal paracontact manifold whose metric is pseudo-Riemannian and acquired

2020 *Mathematics Subject Classification.* 53C25; 53C15; 53D10.
Keywords. Bach tensor, cotton tensor, paraSasakian manifold.
1 uc_de@yahoo.com-Corresponding author; 0000-0002-8990-4609;
2 ghoshgopal.pmath@gmail.com; 0000-0001-6178-6340;
3 krishnendu.de@outlook.in; 0000-0001-6520-4520.

a necessary and sufficient condition for which a paracontact metric manifold is a paraSasakian manifold. ParaSasakian manifolds have been investigated by many geometers such as De and De [5], Erken, Dacko and Murathan ([9], [10], [11]), Ghosh et al. [8], Zamkovoy [27] and many others.
On the other hand in [13], Hamilton introduced the idea of Yamabe soliton. In a complete Riemannian manifold (M^{2n+1}, g), the metric g is named a Yamabe soliton if it obeys

$$\pounds_Y g = (\lambda - r)g, \tag{1}$$

where Y is a smooth vector field and λ, $\pounds$ and r indicate a real number, the Lie-derivative operator and the scalar curvature, respectively. For further information about Yamabe solitons see ([4], [6], [16], [26]).

To initiate the investigation of the conformal relativity with regards to conformally Einstein spaces, Bach introduced a new tensor named Bach tensor [2]. We know that the Bach tensor is a trace-free tensor of rank 2 and is also conformally invariant in 4 dimensions [2]. Bach tensor was the single known conformally invariant tensor before 1968 which was algebraically independent of the Weyl tensor [25]. Therefore, as an alternative of the Hilbert-Einstein functional, one chooses the functional

$$\mathcal{W}(g) = \int_M \| W \|_g^2 \, d\mu_g, \tag{2}$$

for 4-dimensional manifolds, where W indicates the Weyl tensor defined by

$$\begin{aligned} W(X,Y)Z &= R(X,Y)Z - \frac{1}{2n-1}[S(Y,Z)X - S(X,Z)Y \\ &\quad + g(Y,Z)QX - g(X,Z)QY] \\ &\quad + \frac{r}{2n(2n-1)}[g(Y,Z)X - g(X,Z)Y], \end{aligned} \tag{3}$$

where R and S indicate the Riemannian curvature tensor and the Ricci tensor, respectively and Q is the Ricci operator defined by $g(QX,Y) = S(X,Y)$.

Critical points of the functional (2) are characterized by the vanishing of certain symmetric 2-tensor B, which is generally named as Bach tensor. Also, if $B = 0$, then the metric is called Bach flat. In a Riemannian manifold (M^{2n+1}, g), the Bach tensor B is defined by

$$\begin{aligned} B(X,Y) &= \frac{1}{2n-2}\sum_{k,j=1}^{2n+1}((\nabla_{e_k}\nabla_{e_j}W)(X,e_k)e_j, Y) \\ &\quad + \frac{1}{2n-1}\sum_{k,j=1}^{2n+1} S(e_k,e_j)W(X,e_k,e_j,Y), \end{aligned} \tag{4}$$

where $\{e_k\}_{k=1}^{2n+1}$ is a local orthonormal basis on M. Using the expression of Cotton tensor

$$C(X,Y)Z = (\nabla_X S)(Y,Z) - (\nabla_Y S)(X,Z) - \frac{1}{4n}[(Xr)g(Y,Z) - (Yr)g(X,Z)], \quad (5)$$

and the Weyl tensor (3), the Bach tensor can be written as

$$B(X,Y) = \frac{1}{2n-1}\sum_{k=1}^{2n+1}[(\nabla_{e_k} C)(e_k, X)Y) + S(e_k, e_k)W(X, e_k, e_k, Y)]. \quad (6)$$

In the event that the manifold M is conformally related locally with an Einstein space, B needs to vanish. However, there exist Riemannian manifolds equipped with $B = 0$, that are not conformally related with Einstein spaces [14]. From the equation (6), it is not difficult to notice that Bach flatness is the inherent generalization of conformal and Einstein flatness. For additional insights concerning Bach tensor, we reffer to see ([3], [12], [23], [24], [25]).

In 2017, Ghosh and Sharma [23] initiated the study of purely transversal Bach tensor in Sasakian manifold. Specifically, they established that assuming a Sasakian manifold M^{2n+1} admitting a purely transversal Bach tensor, g has a constant scalar curvature $\geq 2n(2n-1)$ and S has a constant norm. It is also noticed that the previously stated equality holds if and only if the metric is Einstein. Likewise, they studied (k,μ)-contact manifolds with $B = 0$ and divergence-free Cotton tensor in [24]. The investigations of Ghosh and Sharma ([23], [24]) revolve our concentration to investigate Bach tensor in the context of certain classes of paracontact metric manifolds, in particular paraSasakian manifolds.

In this paper, we consider the Bach flat (2n+1)-dimensional paraSasakian manifolds and we establish the subsequent results.

Theorem 1. Let $M^{2n+1}(n > 1)$ be a paraSasakian manifold. If the manifold admits a purely transversal Bach tensor, then the scalar curvature is constant.

Corollary 1. If the metric of a Bach flat paraSasakian manifold is a Yamabe soliton, then the soliton field becomes a Killing vector field.

Theorem 2. If a 3-dimensional paraSasakian manifold M admits a purely transversal Bach tensor, then M is locally isometric to the hyperbolic space $H^{2n+1}(1)$.

2. ParaSasakian Manifolds

Let M^{2n+1} be a differentiable manifold. If there exits a triplet (φ, ξ, η) , where $\boldsymbol{\varphi}, \xi, \eta$ indicate a tensor field, a vector field and a 1-form, respectively on M^{2n+1} which obey the relation [15]

$$\varphi^2 = I - \eta \otimes \xi, \ \ \eta(\xi) = 1, \ \varphi\xi = 0, \ \eta \circ \varphi = 0, \quad (7)$$

then we name the structure (φ, ξ, η) is an almost paracontact structure. Hence, M is an almost paracontact manifold.

Additionally, if M with the structure (φ, ξ, η) admits a pseudo-Riemannian or semi-Riemannian metric g which obeys the equation [21]

$$g(X, Y) = -g(\varphi X, \varphi Y) + \eta(X)\eta(Y), \tag{8}$$

then M has an almost paracontact metric structure (φ, ξ, η, g). Here, g is named a compatible metric having signature $(n + 1, n)$.

In M, the fundamental 2-form is written by

$$\Phi(X, Y) = g(X, \varphi Y).$$

An almost paracontact metric structure reduces to a paracontact metric structure if

$$d\eta(X, Y) = g(X, \varphi Y)$$

for any vector fields X, Y, where

$$d\eta(X, Y) = \frac{1}{2}[X\eta(Y) - Y\eta(X) - \eta([X, Y])].$$

An almost paracontact structure is named normal if and only if $N_\varphi - 2d\eta \otimes \xi = 0$, where Nijenhuis tensor of φ is defined by: $N_\varphi(X, Y) = [\varphi, \varphi](X, Y) = \varphi^2[X, Y] + [\varphi X, \varphi Y] - \varphi[\varphi X, Y] - \varphi[X, \varphi Y]$ [27]. A normal paracontact metric manifold is named as paraSasakian manifold. Let ∇ be the Levi-Civita connection with respect to the pseudo-Riemannian metric. Then from [27], it is noticed that an almost paracontact manifold is paraSasakian manifold if and only if

$$(\nabla_X \varphi)Y = -g(X, Y)\xi + \eta(Y)X, \tag{9}$$

for any X, Y. From (9), we acquire

$$\nabla_X \xi = -\varphi X. \tag{10}$$

Besides, for M^{2n+1} ParaSasakian manifolds R and S satisfy [27]

$$R(X, Y)\xi = -(\eta(Y)X - \eta(X)Y), \tag{11}$$

$$R(\xi, X)Y = -g(X, Y) + \eta(Y)X, \tag{12}$$

$$S(X, \xi) = -2n\eta(X), \tag{13}$$

$$Q\xi = -2n\xi. \tag{14}$$

Zamkovoy [27] proved the subsequent proposition :

Proposition 2.1. In a paraSasakian manifold M^{2n+1}, we have

$$S(X, \varphi Y) = -S(\varphi X, Y) - g(X, \varphi Y). \tag{15}$$

3. Bach Flat ParaSasakian Manifolds

Before proving the main theorem we first present the subsequent lemma.

Lemma 1. *Let M^{2n+1} be a paraSasakian manifold. Then*
(i)
$$\sum_{k=1}^{2n+1} g((\nabla_X Q)\varphi e_k, e_k) = 0$$
and
(ii)
$$\sum_{k=1}^{2n+1} g((\nabla_{e_k} Q)Y, \varphi e_k) = (-4n^2 - r)\eta(Y) - \frac{1}{2}(\varphi Y)r$$
.

Proof. From Proposition 2.1. it follows
$$\varphi QX = Q\varphi X - \varphi X. \tag{16}$$
Now
$$g((\nabla_X Q)\varphi Y, Z) + g((\nabla_X Q)Y, \varphi Z) = g((\nabla_X Q\varphi Y - Q\nabla_X \varphi Y), Z) \tag{17}$$
$$+g((\nabla_X QY - Q\nabla_X Y), \varphi Z).$$
Using the equation (9) and (16) in (17), we acquire
$g((\nabla_X Q)\varphi Y, Z)+g((\nabla_X Q)Y, \varphi Z) = g((\nabla_X \varphi)QY, Z)-g(Q(\nabla_X \varphi)Y, Z)+g(Q(\nabla_X \varphi)Y, Z)$.
Again using (9) and (13) in the above equation, we get
$$g((\nabla_X Q)\varphi Y, Z) + g((\nabla_X Q)Y, \varphi Z) = -g(X, QY)\eta(Z) + \eta(QY)g(X, Z) \tag{18}$$
$$-(2n + 1)g(X, Z)\eta(Y) - g(QX, Z)\eta(Y) + g(X, Z)\eta(Y).$$
Putting $Y = Z = e_k$ in the foregoing equation and summing over k $(1 \le k \le 2n+1)$, we obtain
$$\sum_{k=1}^{2n+1} g((\nabla_X Q)\varphi e_k, e_k) + \sum_{k=1}^{2n+1} g((\nabla_X Q)e_k, \varphi e_k) = 0.$$
That is,
$$\sum_{k=1}^{2n+1} g((\nabla_X Q)\varphi e_k, e_k) = 0.$$
This completes the proof of (i).
Again, substituting $X = Z = e_k$ in the equation (18) yields

$$\sum_{k=1}^{2n+1} g((\nabla_{e_k} Q)Y, \varphi e_k) = (-4n^2 - r)\eta(Y) - \frac{1}{2}(\varphi Y)r$$
.

This completes the proof of (ii). □

Proof of Theorem 1. Replacing ξ for Z in (5), we get

$$C(X,Y)\xi = g((\nabla_X Q)Y,\xi) - g((\nabla_Y Q)X,\xi) - \frac{1}{4n}[(Xr)g(Y,\xi) - (Yr)g(X,\xi)]. \tag{19}$$

Now using (10) and (14), we have

$$(\nabla_X Q)\xi = 2n\varphi X + Q\varphi X. \tag{20}$$

From the above equation it follows that

$$g((\nabla_X Q)Y,\xi) = 2ng(\varphi X,Y) + g(Q\varphi X,Y). \tag{21}$$

Using (21) in (19) implies

$$C(X,Y)\xi = 2ng(\varphi X,Y) + g(Q\varphi X,\varphi Y) - 2ng(\varphi Y,X) - g(Q\varphi Y,X) + g(QY,\varphi X) + g(Y,\varphi X) - \frac{1}{4n}[(Xr)\eta(Y) - (Yr)\eta(X)]. \tag{22}$$

Differentiating (22) along Z, provides

$$(\nabla_Z C)(X,Y)\xi = \nabla_Z C(X,Y)\xi - C(\nabla_Z X,Y)\xi - C(X,\nabla_Z Y)\xi - C(X,Y)\nabla_Z\xi. \tag{23}$$

Using (10) and (22) in (23) and after some calculations, we obtain

$$\begin{aligned}(\nabla_Z C)(X,Y)\xi &= 2ng((\nabla_Z\varphi)X,Y) - g((\nabla_Z Q)X,\varphi Y)\\ &-g(QX,(\nabla_Z\varphi)Y) - g(X,(\nabla_Z\varphi)Y) - 2ng((\nabla_Z\varphi)Y,X)\\ &+g((\nabla_Z Q)Y,\varphi X) + g(QY,(\nabla_Z\varphi)X) + g(Y,(\nabla_Z\varphi)X)\\ &-\frac{1}{4n}[g(\nabla_Z Dr,X)\eta(Y) - g(\nabla_Z Dr,Y)\eta(X)\\ &-g(\varphi Z,Y)(Xr) + g(\varphi Z,X)(Yr)].\end{aligned} \tag{24}$$

Now we calculate the 2nd term of right hand side of (23), which follows from (22) as

$$\begin{aligned}C(\nabla_Z X,Y)\xi &= 2ng(\varphi\nabla_Z X,Y) - g(Q\nabla_Z X,\varphi Y)\\ &-g(\nabla_Z X,\varphi Y) - 2ng(\varphi Y,\nabla_Z X) + g(QY,\varphi\nabla_Z X)\\ &+g(Y,\varphi\nabla_Z X) - \frac{1}{4n}[((\nabla_Z X)r)\eta(Y) - (Yr)\eta(\nabla_Z X)].\end{aligned} \tag{25}$$

Similarly from (22), it follows that

$$\begin{aligned}C(X,\nabla_Z Y)\xi &= 2ng(\varphi X,\nabla_Z Y) - g(QX,\varphi\nabla_Z Y)\\ &-g(X,\varphi\nabla_Z Y) - 2ng(\varphi\nabla_Z Y,X) + g(Q\nabla_Z Y,\varphi X)\\ &+g(\nabla_Z Y,\varphi X) - \frac{1}{4n}[(Xr)\eta(\nabla_Z Y) - ((\nabla_Z Y)r)\eta(X)].\end{aligned} \tag{26}$$

Again from (5), we have

$$C(X,Y)\nabla_Z\xi = (\nabla_X S)(Y,\varphi Z) - (\nabla_Y S)(X,\varphi Z) \qquad (27)$$
$$-\frac{1}{4n}[(Xr)g(Y,\varphi Z) - (Yr)g(X,\varphi Z)].$$

Using (24), (25), (26) and (27) in (23) we have,

$$(\nabla_Z C)(X,Y)\xi = 2ng((\nabla_Z\varphi)X,Y) - g((\nabla_Z Q)X,\varphi Y) \qquad (28)$$
$$-g(QX,(\nabla_Z\varphi)Y) - g(X,(\nabla_Z\varphi)Y) - 2ng((\nabla_Z\varphi)Y,X)$$
$$+g((\nabla_Z Q)Y,\varphi X) + g(QY,(\nabla_Z\varphi)X) + g(Y,(\nabla_Z\varphi)X)$$
$$-\frac{1}{4n}[g(\nabla_Z Dr,X)\nabla(Y) - g(\nabla_Z Dr,Y)\eta(X) - g(\varphi Z,Y)(Xr)$$
$$+g(\varphi Z,X)(Yr)] - 2ng(\varphi\nabla_Z X,Y) + g(Q\nabla_Z X,\varphi Y)$$
$$+g(\nabla_Z X,\varphi Y) + 2ng(\varphi Y,\nabla_Z X) - g(QY,\varphi\nabla_Z X) - g(Y,\varphi\nabla_Z X)$$
$$+\frac{1}{4n}[((\nabla_Z X)r)\eta(Y) - (Yr)\eta(\nabla_Z X)] - 2ng(\varphi X,\nabla_Z Y)$$
$$+g(QX,\varphi\nabla_Z Y) + g(X,\varphi\nabla_Z Y) + 2ng(\varphi\nabla_Z Y,X)$$
$$-g(Q\nabla_Z Y,\varphi X) - g(\nabla_Z Y,\varphi X) + \frac{1}{4n}[(Xr)\eta(\nabla_Z Y)$$
$$-((\nabla_Z Y)r)\eta(X)] - (\nabla_X S)(Y,\varphi Z) + (\nabla_Y S)(X,\varphi Z)$$
$$+\frac{1}{4n}[(Xr)g(Y,\varphi Z) - (Yr)g(X,\varphi Z)].$$

Putting $X = Z = e_k$ in (28) and summing over k $(1 \le k \le (2n+1))$, we have,

$$\sum_{k=1}^{2n+1}(\nabla_{e_k}C)(e_k,Y)\xi = \sum_{k=1}^{2n+1}[2ng(e_k,Y)\eta(e_k) \qquad (29)$$
$$+g((\nabla_{e_k}Q)\varphi e_k,Y) + g(Qe_k,Y)\eta(e_k)$$
$$-\frac{1}{4n}\{g(\nabla_{e_k}Dr,e_k)\eta(Y) - g(\nabla_{e_k}Dr,Y)\eta(e_k)\}.$$

Applying Lemma 3.1 into the foregoing equation yields

$$\sum_{k=1}^{2n+1}(\nabla_{e_k}C)(e_k,Y)\xi = (-4n^2 - r)\eta(Y) - \frac{1}{2}(\varphi Yr) \qquad (30)$$
$$-\frac{1}{4n}[(divDr)\eta(Y) - g(\nabla_\xi Dr,Y)].$$

Replacing Z by ξ in (3) we infer

$$W(X,Y)\xi = R(X,Y)\xi - \frac{1}{2n-1}[S(Y,\xi)X - S(X,\xi)Y \qquad (31)$$
$$+\eta(Y)QX - \eta(X)QY] + \frac{r}{2n(2n-1)}[\eta(Y)X - \eta(X)Y].$$

Using the equation (11) and (13) in (31), we acquire

$$QW(X,Y)\xi = [1 - \frac{2n}{2n-1} + \frac{r}{2n(2n-1)}](\eta(Y)QX - \eta(X)QY) \quad (32)$$
$$-\frac{1}{2n-1}(\eta(Y)Q^2X - \eta(X)Q^2Y).$$

Now taking inner product with U in (32) and then putting $Y = U = e_k$ and summing over $k(1 \le k \le 2n+1)$, we obtain

$$\sum_{k=1}^{2n+1} g(QW(X,e_k)\xi, e_k) = -\frac{r^2-4n^2}{2n(2n-1)}\eta(X) \quad (33)$$
$$+\frac{1}{2n-1}[\frac{|Q|^2 - 4n^2}{2n-1}].$$

Now

$$g(Qe_k, e_j)g(W(X,e_k)e_j), Y) \quad (34)$$
$$= -g(W(X,e_k)Y, Qe_k) = -g(QW(X,e_k)Y, e_k).$$

Using (4) and (34) we have

$$B(X,Y) = \frac{1}{2n-1}[\sum_{i=1}^{2n+1}(\nabla_{e_k}C)(e_k,X,Y) - \sum_{i=1}^{2n+1} g(QW(X,e_k)Y,e_k)]. \quad (35)$$

By hypothesis, $B(Y,\xi) = 0$.

Then equation (30) and (33) together reveal

$$(4n - 4n^2 + r)\eta(Y) - \frac{1}{2}(\varphi Y r) - \frac{1}{4n}[(divDr)\eta(Y) - g(\nabla_\xi Dr, Y)] \quad (36)$$
$$+\frac{r^2-4n^2}{2n(2n-1)}\eta(Y) - \frac{1}{2n-1}[\frac{|Q|^2 - 4n^2}{2n-1}]\eta(Y).$$

Replacing Y by φY in the above equation provides

$$\nabla_\xi Dr = 2n\varphi Dr. \quad (37)$$

As ξ is a Killing vector field, we get

$$\pounds_\xi r = 0 \quad (38)$$

Taking exterior derivative d on it we can obtain

$$\pounds_\xi dr = 0,$$

which implies

$$\pounds_\xi Dr = 0. \quad (39)$$

Using (10) in (39), we have

$$\pounds_\xi Dr = -\varphi Dr. \tag{40}$$

Finally, using the equation (37) and (40) yields $\varphi Dr = 0$, that is, $Dr = 0$. Hence, r, the scalar curvature is constant.

This finishes the proof. □

Proof of Corollary 1. Since r =constant, the equation (1) becomes

$$\pounds_Y g = 2cg,$$

where $c = \frac{\lambda - r}{2} = constant.$

Therefore, Y, the soliton vector field becomes a homothetic vector field [7]. For a homothetic vector field Y, we get

$$\pounds_Y r = -2cr. \tag{41}$$

Since r =constant, it follows from the above equation $c = 0$. Thus the soliton fields turn into a Killing vector field. □

Remarks: Recently Erken [11] proved that if the metric of a 3-dimensional paraSasakian manifold is a Yamabe soliton then the soliton field is Killing and the scalar curvature is constant.

Therefore, Corollary 1 is an improvement of the result of Erken.

4. 3-Dimensional Bach Flat ParaSasakian manifolds

In a 3-dimensional paraSasakian manifold the Riemannian curvature tensor is given by

$$\begin{aligned} R(X,Y)Z &= g(Y,Z)QX - g(X,Z)QY + S(Y,Z)X - S(X,Z)Y \\ &\quad -\frac{r}{2}[g(Y,Z)X - g(X,Z)Y]. \end{aligned} \tag{42}$$

Substituting $X = Z = \xi$ in (42) and making use of (12), (13) and (14) implies

$$QY = (-3 - \frac{r}{2})\eta(Y)\xi + (1 + \frac{r}{2})Y. \tag{43}$$

From the forgoing equation it is quite clear that

$$Q\varphi = \varphi Q. \tag{44}$$

Now we establish the subsequent lemma:

Lemma 2. *Let M be a 3-dimensional paraSasakian manifold. Then*
(i)

$$\sum_{k=1}^{3} g((\nabla_X Q)\varphi e_k, e_k) = 0$$

and
(ii)

$$\sum_{k=1}^{3} g((\nabla_{e_k} Q)Y, \varphi e_k) = (r-2)\eta(Y) - \frac{1}{2}(\varphi Y)r$$

.

Proof. Using (44), we get
$g((\nabla_X Q)\varphi Y, Z) + g((\nabla_X Q)Y, \varphi Z) = g((\nabla_X \varphi)QY, Z) + g(Q(\nabla_X \varphi)Y, Z).$
Again using (9) and (44) in the above equation yields

$$g((\nabla_X Q)\varphi Y, Z) + g((\nabla_X Q)Y, \varphi Z) = -g(X, QY)\eta(Z) \\ -2g(X,Z)\eta(Y) + 2g(X,Y)\eta(Z) + g(QX,Z)\eta(Y). \tag{45}$$

Putting $Y = Z = e_k$ in the previous equation and taking summation over $k(1 \leq k \leq 3)$, we have

$$\sum_{k=1}^{3} g((\nabla_X Q)\varphi e_k, e_k) + \sum_{k=1}^{3} g((\nabla_X Q)e_k, \varphi e_k) = 0.$$

That is,

$$\sum_{k=1}^{3} g((\nabla_X Q)\varphi e_k, e_k) = 0.$$

This completes the proof of (i).
On the other hand substituting $X = Z = e_k$ in (45) yields

$$\sum_{k=1}^{3} g((\nabla_{e_k} Q)Y, \varphi e_k) = (r-2)\eta(Y) - \frac{1}{2}(\varphi Y)r.$$

This completes the proof of (ii).

□

Proof of Theorem 2. Using (10) and (43), we infer that

$$(\nabla_X Q)\xi = Q\varphi X. \tag{46}$$

From (19) and (46) we have

$$C(X,Y)\xi = -2g(Q\varphi X, Y) - \frac{1}{4}[(Xr)\eta(Y) - (Yr)\eta(X)]. \tag{47}$$

Using (5), (9), (43) and (47) in (23) yields

$$(\nabla_X C)(Y,Z)\xi = g((\nabla_Y Q)Z, \varphi X) - g((\nabla_Z Q)Y, \varphi X) \\ +2g((\nabla_X Q)\varphi Y, Z) + 4g(X,Y)\eta(Z) + 2S(QX,Z)\eta(Y)$$

$$+\frac{1}{4}[g(Z,\varphi X)(Yr)-g(\nabla_X Dr,Y)\eta(Z)$$
$$-g(\varphi X,Z)(Y)-g(\nabla_X Dr,Z)\eta(Y)]. \quad (48)$$

Putting $X=Y=e_k$ in the equation (48) and summing over $k(1\leq k\leq 3)$, we get

$$\begin{aligned}(\nabla_{e_k}C)(e_k,Z)\xi &= g((\nabla_{e_k}Q)Z,\varphi e_k)-g((\nabla_Z Q)e_k,\varphi e_k)\\ &+2g((\nabla_{e_k}Q)\varphi e_k,Z)+12\eta(Z)+2S(Qe_k,Z)\eta(e_k)\\ &+\frac{1}{4}[g(Z,\varphi e_k)(e_k r)-g(\nabla_{e_k}Dr,e_k)\eta(Z)\\ &-g(\varphi e_k,Z)(e_k)-g(\nabla_{e_k}Dr,Z)\eta(e_k)]. \quad (49)\end{aligned}$$

Applying Lemma 4.1 and using (43) in (49) implies

$$\begin{aligned}(\nabla_{e_k}C)(e_k,Z)\xi &= 3(r+6)\eta(Z)-\frac{3}{2}g(\varphi Z,Dr)\\ &+\frac{1}{4}[(divDr)\eta(Z)-g(\nabla_\xi Dr,Z)]. \quad (50)\end{aligned}$$

Since in a 3-dimensional paraSasakian manifold Weyl curvature tensor vanishes, so equation (6) reduces to

$$B(X,Y)=\sum_{k=1}^{3}[(\nabla_{e_k}C)(e_k,X)Y)]. \quad (51)$$

Replacing Y by ξ in (51) and use the the hypothesis, along with equation (50) provides

$$\begin{aligned}&3(r+6)\eta(X)-\frac{3}{2}g(\varphi X,Dr) \quad (52)\\ &+\frac{1}{4}[(divDr)\eta(X)-g(\nabla_\xi Dr,X)]=0.\end{aligned}$$

Replacing X by φX in (52) implies

$$\nabla_\xi Dr=-6(\varphi Dr). \quad (53)$$

From (40) and (53), we have $Dr=0$, that is r is constant. Then from (52), it follows that $r=-6$. Putting $r=-6$ in (43) yields

$$QY=-2Y. \quad (54)$$

Hence, the manifold is an Einstein manifold. Therefore, using $r=-6$ and the equation (54) in (42), we acquire

$$R(X,Y)Z=-[g(Y,Z)X-g(X,Z)Y].$$

Hence, the manifold is locally isometric to the hyperbolic space $H^{2n+1}(1)$ (p. 228, [22]). □

Acknowledgments We would like to thank the anonymous referees and the Editor for reviewing the paper carefully and their valuable comments to improve the quality of the paper.

Author Contribution Statements The authors jointly worked on the results and they read and approved the final manuscripts.

Declaration of Competing Interests The authors declare that they have no competing interest.

References

[1] Adati, T., Matsumuto. K., On conformally recurrent and conformally symmetric P-Sasakian manifolds, *TRU Math.*, 13 (1977), 25-32.

[2] Bach, R., Zur weylschen relativitatstheorie und der Weylschen erweiterung des krummungstensorbegriffs, *Math. Z.*, 9 (1921), 110-135.

[3] Bergman, J., Conformal Einstein spaces and Bach tensor generalization in n-dimensions, Thesis, Linkoping (2004).

[4] Deshmukh, S., Chen, B. Y., A note on Yamabe solitons, *Balk. J. Geom. Appl.*, 23 (2018), 37-43.

[5] De, K., De, U. C., A note on almost Ricci soliton and gradient almost Ricci soliton on para-Sasakian manifolds, *Korean J. Math.*, 28 (2020), 739-751. https://doi.org/10.11568/kjm.2020.28.4.739

[6] De, K., De, U. C., δ-almost Yamabe solitons in paracontact metric manifolds, *Mediterr. J. Math.*, 18, 218 (2021). DOI:10.1007/s00009-021-01856-9

[7] Duggal, K. L., Sharma, R., Symmetries of spacetimes and Riemannian manifolds, Kluwer Academic Publishers, 1999.

[8] De, U. C., Ghosh, G., Jun, J. B., Majhi, P., Some results on paraSasakian manifolds, *Bull. Translivania Univ. Brasov, Series III:Mathematics, Informatics, Physics.*, 60 (2018), 49-64.

[9] Erken, I. K., Dacko, P. and Murathan, C., Almost paracosymplectic manifolds, *J. Geom. Phys.*, 88 (2015), 30-51. DOI: 10.21099/tkbjm/1496164721

[10] Erken, I. K. and Murathan, C., A complete study of three-dimensional paracontact $(\tilde{\kappa}, \tilde{\mu}, \tilde{\nu})$-spaces, *Int. J. Geom. Methods Mod. Phys.*, 14 (2017), 1750106. https://doi.org/10.1142/S0219887817501067

[11] Erken, I. K., Yamabe solitons on three-dimensional normal almost paracontact metric manifolds, *Periodica Mathematica Hungarica*, 80 (2020), 172-184. https://doi.org/10.1007/s10998-019-00303-3

[12] Fu, H. P. and Peng, J. K., Rigidity theorems for compact Bach-flat manifolds with positive constant scalar curvature, *Hokkaido Math. J.*, 47 (2018), 581-605. https://doi.org/10.14492/HOKMJ/2F1537948832

[13] Hamilton, R., The Ricci flow on surface, *Contemp. Math.*, 71 (1988), 237-267.

[14] Pedersen, H., Swann, A., Einstein-Weyl geometry, the Bach tensor and conformal scalar curvature, *J. Reine Angew. Math.*, 441 (1993), 99-113.

[15] Sato, I., On a structure similar to the almost contact structure, *Tensor, N. S.*, 30 (1976), 219-224.

[16] Suh, Y. J., De, U. C., Yamabe soliton and Ricci solitons on almost co-Kahler manifolds, *Can. Math. Bull.*, 62 (2019), 653-661. http://dx.doi.org/10.4153/S0008439518000693

[17] Matsumuto. K., Ianus, S. and Mihai, I., On P-Sasakian manifolds which admit certain tensor fields, *Publ. Math. Debrecen.*, 33 (1986), 61-65.

[18] Mihai, I., Rosca, R., On Lorentzian P-Sasakian Manifolds, Classical Analysis, World Scientific Publ., 156-169 (1992).

[19] Mihai, I., Some structures defined on the tangent bundle of a P-Sasakian manifold, *Bull. Math. Soc. Sci. Math. R. S. Roumanie (N. S)*, 77 (1985), 61-67.

[20] Kaneyuki, S., Willams, F. L., Almost paracontact and parahodge structures on manifolds, *Nagoya Math. J.*, 99 (1985), 173-187.

[21] Kaneyuki, S., Kozai, M., Paracomplex structures and affine symmetric spaces, *Tokyo J. of Math.*, 08 (1985), 81-98.

[22] O'Neill, B., Semi-Riemannian Geometry with Applications to the Relativity, Academic Press, New York-London, 1983.

[23] Sharma, R., Ghosh, A., Sasakian manifolds with purely transversal Bach tensor, *J. Math. Phys.*, 58 103502 (2017). doi: 10.1063/1.4986492

[24] Sharma, R., Ghosh, A., Classification of (k, μ)-contact manifolds with divergence free Cotton tensor and Vanishing Bach tensor, *Ann. Polon. Math.*, (2019). DOI: 10.4064/ap 180228-13-11

[25] Szekeres, P., Conformal tensors, *Proceedings of the Royal Society of London. Series A, Mathematical and Physical Sciences*, 304, No. 1476 (Apr. 2, 1968), 113-122.

[26] Wang, Y., Yamabe solitons on three dimensional Kenmotsu manifolds, *Bull. Belg. Math. Soc.*, 23 (2016), 345-355. http://dx.doi.org/10.36045/bbms/1473186509

[27] Zamkovoy, S., Canonical connection on paracontact manifolds, *Ann. Glob. Anal. Geom.*, 36 (2009), 37-60. http://dx.doi.org/10.1007/s10455-008-9147-3

http://communications.science.ankara.edu.tr

Commun.Fac.Sci.Univ.Ank.Ser. A1 Math. Stat.
Volume 72, Number 3, Pages 839–856 (2023)
DOI:10.31801/cfsuasmas.1202192
ISSN 1303-5991 E-ISSN 2618-6470

Research Article; Received:November 10, 2022; Accepted: March 6, 2023

STABILIZED FEM SOLUTION OF MHD FLOW OVER ARRAY OF CUBIC DOMAINS

Selçuk Han AYDIN

Department of Mathematics, Faculty of Science, Karadeniz Technical University, Trabzon, TÜRKİYE

Abstract. In this study, 3D magnetohydrodynamic (MHD) equations are considered in array of cubic domains having insulated external boundaries separated by conducting thin walls. In order to obtain stable solutions, stabilized version of the Galerkin finite element method is used as a numerical scheme. Different problem parameters and configurations are tested in order to visualize the accuracy and efficiency of the proposed algorithm. Obtained solutions are visualized as contour lines of 2D slices taken from the obtained 3D domain solutions.

1. Introduction

Magnetohydrodynamic (MHD) flow is the popular working area both for the engineers and scientists because of its popular and up-to-date modern applications among different areas such as in astronomy, geophysics, industry, biology and in engineering. The general theory of the MHD is based on the Navier-Stokes equations, Maxwell equations through Ohm's law with the Lorentz force which brings a system of coupled partial differential equations as a mathematical model. One can find the general theory and corresponding equations in references [1–3]. The analytical solutions of the MHD flow problem have been already given by Dragos [3], Shercliff [2] and Davidson [4] for the single duct case having for the circular or square cross sectional channels. Behind this exact solutions, there are considerable amount of numerical studies in the literature using different numerical schemes for several problem domain configurations (see [5–17] and references there in). Due to the original form of the equations, there are also many important studies about the 3D cases of the MHD equations. As far as our knowledge, Salah et al. [18] provided the first basic study using FEM for the solution of 3D incompressible

2020 *Mathematics Subject Classification.* 65N30, 76E25, 76W05.
Keywords. 3D MHD flow, stabilized FEM, array of cubic domains.
shaydin@ktu.edu.tr 0000-0002-1419-9458.

MHD flows. Additionally, solutions of the non-linear MHD systems using two-level iterative finite element algorithms with Newton iteration for the 2D and 3D cases in [19–21]. One can find some theoretical results about the convergence and optimal convergence analysis of iterative solution procedures in references [22, 23]. Li and Zheng [24] studied about 3D MHD equations with mixed finite element method using Newton-Krylov and Picard-Krylov solvers and compared the methods over some test problems. Finally, even there are dozens of MHD papers in recent years, let's consider just a few of them. Incompressible MHD equations are analyzed in the sense of second-order temporal accuracy and unconditional energy stability aspects in [25]. The numerical simulation of the 3D MHD equations has been given for the large Reynolds number by Skala et al. [26]. Also 3D MHD duct flow was studied for the case of insulating flow channel on poloidal ducts in [27]. As a finite volume application of 3D MHD equations are solved in conservative form by Huba and Lyon [28] and on unstructured Lagrangian meshes by Barnes and Rousculp [29]. As an other 3D study of the MHD equations, Wu [30] worked on about the priori bounds, real analyticity and global regularity conditions. Due to the it's importance, many other authors also analyzed the regularity criteria of the 3D MHD equations [31–35]. Finally, there are many other applications of the 3D MHD equations in different areas such as heat transfer [36], massive-star wind [37], intermittent initial data [38] and large initial data [39].

In this study we consider the stabilized FEM solution of the magnetohydrodynamic flow equations in an array of cubic domains connected with the electrically conducting thin walls. No-slip boundary conditions are imposed over all the walls for the velocity component. The continuity of the magnetic field between the cubic domains and walls are satisfied with the coupling of the MHD equations and Laplace, respectively. The influence of the walls for the both co-flow and counter-flow cases are considered for different problem configurations. As an application, these types of problem configuration may be encountered in the heat and mass transfer process of fusion blanket. Analytical solution of this problem has been already given by Bluck [40] for one, two and three ducts cases in 2D using Fourier series approach. Previously, we have also obtained the stabilized FEM solution of MHD flow in an array of electromagnetically coupled rectangular ducts for the arbitrary wall thickness and different problem configurations again defined on 2D case [42]. Therefore, this work can be assumed as the 3D extension of that study with different directions of the externally applied magnetic field of the previous paper and some part of this study has been already presented in the conference [43]. We tried to obtain stable solutions also for the high values of the Hartmann number which appears as a constant parameter in the equations some how similar to the convection coefficient. In such a case problem takes convection dominated behavior in which cases some boundary and/or interior layers may exists depending on the value of the problem parameter. Noticed that, the finite element method (FEM) is the most popular, powerful and convenient numerical method for the solutions of the such a system of partial differential equations. In recent years, many researchers performed different extended versions of the FEM in order to obtain the approximate solutions of the wide variety of engineering problems. But, the Galerkin finite element version is still the basic one among them. However, using the standard Galerkin finite element method brings some numerical instabilities in the solutions of such a convection-dominated problems. In order to eliminate these difficulties, as a first possibility, one can choose the small mesh size depending on the value of the problem parameter. Unfortunately, this approach increases the size of the resulting linear system so the computational cost. Alternatively, it is possible to use some stabilization technique in the numerical formulation. The most popular stabilization technique is referred as the Streamline Upwind Petrov-Galerkin (SUPG) method [44] which achieves stability by adding mesh-dependent terms to the standard Galerkin FEM formulation. After considering the stabilization in the FEM, many authors are used this idea in their research. Salah et al. [45] and Shadid et al. [46] are considered the stabilized finite element formulation for the solution of the 3D MHD equations and for the 2D case in [47–51] (see also references therein). Also, stabilized FEM formulation is applied to the many other flow problems [52–55]. In this study, we have also used SUPG in the numerical scheme.

The rest of the paper is organized as follows: In the next section, we describe the mathematical modeling and the FEM formulation with SUPG type stabilization. Numerical results and discussions are given in Section 3 to show the efficiency of the proposed approach. Finally, some concluding remarks are proposed in Section 4.

2. Mathematical Modelling

The non-dimensional MHD equations which are obtained from Navier-Stokes equations of continuum mechanics and Maxwell's equations of electromagnetic field through Ohm's law in an array of cubic ducts Ω_i with length a separated by conducting walls W_i with thickness b at the outher and $2b$ at the interior ([3, 40]) as

$$\left.\begin{aligned} \nabla^2 V_i + M_{i_x}\frac{\partial B_i}{\partial x} + M_{i_y}\frac{\partial B_i}{\partial y} + M_{i_z}\frac{\partial B_i}{\partial z} &= -P_i \\ \nabla^2 B_i + M_{i_x}\frac{\partial V_i}{\partial x} + M_{i_y}\frac{\partial V_i}{\partial y} + M_{i_z}\frac{\partial V_i}{\partial z} &= 0 \end{aligned}\right\} \quad \text{in } \Omega_i \tag{1}$$

$$\nabla^2 B_i^w = 0 \qquad \text{in } W_i \tag{2}$$

where V_i is the velocity of the fluid and B_i is induced magnetic field on the duct Ω_i with no-slip conditions $V_i = 0$ on all the duct boundaries $\partial\Omega_i$ and on all the walls W_i (See Figure 1). Conditions for the induced magnetic are $B_i^w = B_i$ on the interior sides of the ducts, and $B_i^w = 0$ and $B_i = 0$ on the external boundaries. P_i is the pressure gradient in Ω_i, The Hartmann number Ha is defined as $Ha = B_0 a\sqrt{\frac{\sigma}{\eta}}$ with characteristic length a, electric conductivity σ and viscosity coefficient η. B_0

is the intensity of the applied magnetic field. α_i and β_i are the angles between z-axis and x-axis on $Duct_i$. Then the vector $\mathbf{M}_i$ is defined as

$$\mathbf{M}_i = (M_{i_x}, M_{i_y}, M_{i_z}) \tag{3}$$

with the components $M_{i_x} = \cos\beta_i \sin\alpha_i Ha$, $M_{i_y} = \sin\beta_i \sin_i \alpha Ha$, $M_{i_z} = \cos\alpha_i Ha$.

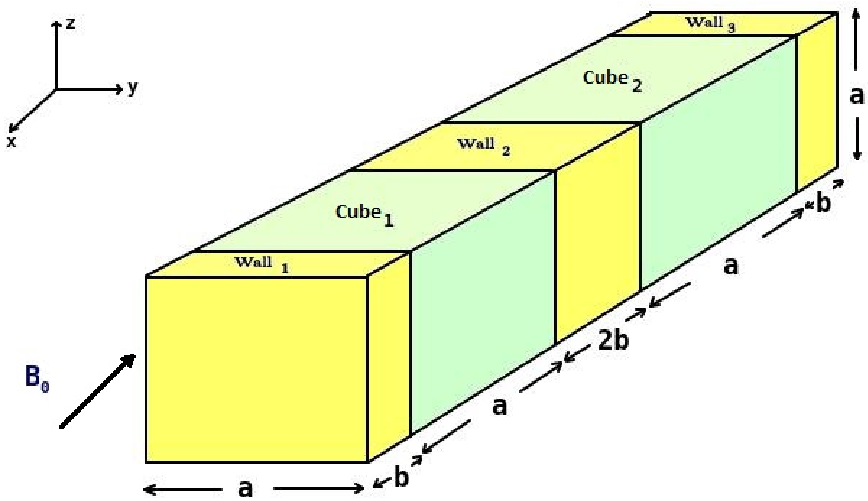

FIGURE 1. Problem configuration for two cubes

Standard Galerkin FEM type weak formulation by employing the linear function space $L = (H_0^1(\Omega))^2$ which is the Sobolev subspace of the space of square integrable functions over the domain Ω as [56]: Find $\{V_i, B_i, B_i^w\} \in \{L \times L \times L\}$ such that

$$\mathfrak{a}(\nabla V_i, \nabla w_{i_1}) - \mathfrak{b}(\mathbf{M}\cdot\nabla B_i, w_{i_1}) + \mathfrak{a}(\nabla B_i, \nabla w_{i_2}) + \mathfrak{b}(\mathbf{M}\cdot\nabla V_i, w_{i_2}) + \mathfrak{a}(\nabla B_i^w, \nabla w_{i_3}) = \mathfrak{b}(P_i, w_{i_1}) \tag{4}$$

$\forall\{w_{i_1}, w_{i_2}, w_{i_3}\} \in \{L \times L \times L\}$ where

$$\mathfrak{a}(\nabla u, \nabla v) = \iiint_\Omega \left(\frac{\partial u}{\partial x}\frac{\partial v}{\partial x} + \frac{\partial u}{\partial y}\frac{\partial v}{\partial y} + \frac{\partial u}{\partial z}\frac{\partial v}{\partial z}\right) d\Omega \quad \text{and} \quad \mathfrak{b}(u,v) = \iint_\Omega (uv)\, d\Omega.$$

It is seen that the equations are in a coupled form. It is well known that using the standard Galerkin finite element for these coupled equations, bring some numerical instabilities for the high values of the Hartmann number. Therefore we should consider the SUPG typed stabilization technique.

Let's decouple the Eqns. (1) to the convection-diffusion type form in order to apply SUPG type stabilization by using the new variables $U_1(x,y,z)$ and $U_2(x,y,z)$ which are defined as

$$\begin{aligned} U_{i_1} &= V_i + B_i \\ U_{i_2} &= V_i - B_i \end{aligned} \tag{5}$$

then equations become

$$\begin{aligned} \nabla^2 U_{i_1} + \mathbf{M}\cdot\nabla U_{i_1} &= -P_i \\ \nabla^2 U_{i_2} - \mathbf{M}\cdot\nabla U_{i_2} &= -P_i. \end{aligned} \tag{6}$$

Galerkin FEM type weak formulation of the equations (2) and (5) is obtained by employing the linear function space $L = (H_0^1(\Omega))^2$ as: Find $\{U_{i_1}, U_{i_2}, B_i^w\} \in \{L \times L \times L\}$ such that

$$\mathcal{B}(U_{i_1}; U_{i_2}; B_i^w, v_{i_1}; v_{i_2}; w_{i_3}) = \mathfrak{b}(P_i, v_{i_1}) + \mathfrak{b}(P_i, v_{i_2}) \tag{7}$$

$\forall\{v_{i_1}, v_{i_2}, v_{i_3}\} \in \{L \times L \times L\}$ where

$$\begin{aligned} \mathcal{B}(U_{i_1}; U_{i_2}; B_i^w, v_{i_1}; v_{i_2}; w_{i_3}) &= \mathfrak{a}(\nabla U_{i_1}, \nabla v_{i_1}) - \mathfrak{b}(\mathbf{M}\cdot\nabla U_{i_1}, v_{i_1}) \\ &+ \mathfrak{a}(\nabla U_{i_2}, \nabla v_{i_2}) + \mathfrak{b}(\mathbf{M}\cdot\nabla U_{i_2}, v_{i_2}) + \mathfrak{a}(\nabla B_i^w, \nabla w_{i_3}). \end{aligned} \tag{8}$$

The variational formulation is written by the choice of finite dimensional subspaces $L_h \subset L$, defined by regular tetrahedralization of the domain. Find $\{U_{i_1}^h, U_{i_2}^h, B_i^{w_h}\}$ $\in \{L^h \times L^h \times L^h\}$ such that

$$\mathcal{B}(U_{i_1}^h; U_{i_2}^h; B_i^{w_h}, v_{i_1}^h; v_{i_2}^h; w_{i_3}^h) = \mathfrak{b}(P_i^h, v_{i_1}^h) + \mathfrak{b}(P_i^h, v_{i_2}^h) \tag{9}$$

$\forall\{v_{i_1}^h, v_{i_2}^h, w_{i_3}^h\} \in \{L^h \times L^h \times L^h\}$ where

$$\begin{aligned} \mathcal{B}(U_{i_1}^h; U_{i_2}^h; B_i^{w_h}, v_{i_1}^h; v_{i_2}^h; w_{i_3}^h) &= \mathfrak{a}(\nabla U_{i_1}^h, \nabla v_{i_1}^h) - \mathfrak{b}(\mathbf{M}\cdot\nabla U_{i_1}^h, v_{i_1}^h) \\ &+ \mathfrak{a}(\nabla U_{i_2}^h, \nabla v_{i_2}^h) + \mathfrak{b}(\mathbf{M}\cdot\nabla U_{i_2}^h, v_{2_1}^h) + \mathfrak{a}(\nabla B_i^{w_h}, w_{i_3}^h) \end{aligned} \tag{10}$$

Now, we can write the SUPG typed variational formulation of these equations using linear tetrahedron elements as [44]:

Using linear tetrahedron elements; Find $\{U_{i_1}^h, U_{i_2}^h, B_i^{w_h}\} \in \{L^h \times L^h \times L^h\}$ such that

$$\begin{aligned} &\mathcal{B}(U_{i_1}^h; U_{i_2}^h; B_i^{w_h}, v_{i_1}^h; v_{i_2}^h; v_{i_3}^h) \\ &+\tau_K \left\{\mathfrak{b}(\mathbf{M}_i\cdot\nabla U_{i_1}^h - P_i^h, \mathbf{M}_i\cdot\nabla v_{i_1}^h)\right. \\ &\quad \left.+\mathfrak{b}(\mathbf{M}_i\cdot\nabla U_{i_2}^h - P_i^h, \mathbf{M}_i\cdot\nabla v_{i_2}^h)\right\} = \mathfrak{b}(\Delta P_i^h, v_{i_1}^h) + \mathfrak{b}(\Delta P_i^h, v_{i_2}^h) \end{aligned} \tag{11}$$

$\forall\{v_{i_1}^h, v_{i_2}^h, w_{i_3}^h\} \in \{L^h \times L^h \times L^h\}$ with the stabilization parameter

$$\tau_K = \begin{cases} \dfrac{h_K}{2Ha} \text{ if } Pe_k \geq 1 \\ \\ \dfrac{h_K^2}{12} \text{ if } Pe_k < 1 \end{cases} \tag{12}$$

where h_K is the diameter of the element K which is calculated as the longest side of the corresponding tetrahedron element and $Pe_K = \dfrac{h_K Ha}{6}$ is the Peclet number.

Back transformations $V_i^h = (U_{i_1}^h + U_{i_2}^h)/2$ and $B_i^h = (U_{i_1}^h - U_{i_2}^h)/2$;
Find $\{V_i^h, B_i^h, B_i^{w_h}\} \in \{L^h \times L^h \times L^h\}$ such that

$$\begin{aligned} &\mathfrak{a}(\nabla V_i^h, \nabla w_{i_1}^h) - \mathfrak{b}(\mathbf{M}_i \cdot \nabla B_{i_1}^h, w_{i_1}^h) + \tau_K \mathfrak{b}(\mathbf{M}_i \cdot \nabla V_i^h, \mathbf{M}_i \cdot \nabla w_{i_1}^h) \\ &+\mathfrak{a}(\nabla B_{i_h}, \nabla w_{i_2}^h) - \mathfrak{b}(\mathbf{M}_i \cdot \nabla V_{i_1}^h, w_{i_2}^h) + \tau_K \mathfrak{b}(\mathbf{M}_i \cdot \nabla B_i^h, \mathbf{M}_i \cdot \nabla w_{i_2}^h) \\ &+\mathfrak{a}(\nabla B_i^{w_h}, \nabla w_{3_i}^h) = (\Delta P_i^h, w_{i_1}^h) - \tau_K(\Delta P_{i_h}, \mathbf{M}_i \cdot \nabla w_{i_2}^h) \end{aligned} \tag{13}$$

$\{w_{i_1}^h, w_{i_2}^h, w_{i_3}^h\} \in \{L^h \times L^h \times L^h\}$.

The solution of this system of linear equations give the velocity of the fluid on the cubic domains, and the induced magnetic field everywhere of the problem domain. Noticed that, It it is clear that, the FEM formulation brings a sparse form linear system of equations. Therefore the resulting system should be solved using an efficient sparse solver.

3. Numerical Results and Discussion

In this section, we will perform some tests for the considered numerical scheme using different cases and different problem parameters. Obtained solutions will be presented in terms of contour plots.

MHD flow equations (1) and (2) are solved using stabilized FEM formulation (13) in single, double and triple cubic domains separately by taking the Hartmann number values $Ha = 1, 10, 100$ and 500. Additional to the velocity and induced magnetic field, we also calculated the current density J which is defined as

$$J = \sqrt{\left(\frac{\partial B}{\partial x}\right)^2 + \left(\frac{\partial B}{\partial y}\right)^2 + \left(\frac{\partial B}{\partial z}\right)^2}$$

in order to compare the obtained results with the literature ones [40, 42]. In all test cases, the wall and duct lengths are taken as $a = 1.0$ and $b = 0.1$ except in Figures 8 and 9. It is easily seen that, the size of the linear system obtained from the discretized equations is very huge especially for the two and three ducts cases. Therefore, the resulting linear system of equations are stored as a sparse matrix form and they are solved using open source UMFPACK sparse solver with the author modified version in order to gain a good accuracy and efficiency.

The volume integrals over linear tetrahedron elements are calculated numerically using 5 point Gauss quadrature method over the unit tetrahedron via transformation which gives the analytical result for the linear shape functions as

$$\iiint_{\Omega} f(x,y,z)d\Omega = \sum_{i=1}^{5} w_i F(\xi_i, \eta_i, \nu_i)$$

where the corresponding values are given in Table 1.

TABLE 1. Gauss Quadrature Values

i	w_i	ξ_i	η_i	ν_i
1	-4/30	1/4	1/4	1/4
2	9/120	1/2	1/6	1/6
3	9/120	1/6	1/2	1/6
4	9/120	1/6	1/6	1/2
5	9/120	1/6	1/6	1/6

Finally, the mesh information and corresponding data sizes are displayed in Table 2.

TABLE 2. Mesh and data information.

	# of ducts		
	1 Duct	2 Ducts	3 Ducts
# of nodes	471836	770047	1015748
# of elements	2733606	4495468	5939642
# of unknowns	943672	1540095	2031496
# of boundary nodes	192360	294712	373544
Size of the system	890516843584	2371892609025	4126975998016
# of non-zero entries	20755732	34313073	45814784

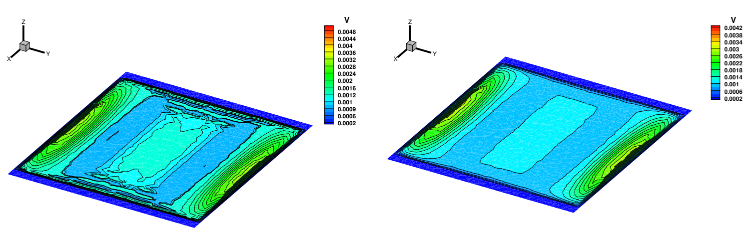

FIGURE 2. $2D$ slices of the velocity without stabilization (left) and with SUPG (right) for $Ha = 100$ at $z = 0$ for $\alpha = \pi/2, \beta = 0$.

Before start to present the obtained results, let's visualize the effect of the stabilization on the numerical solution. Noticed that, the stabilization is more effective especially velocity component. Therefore, in Figure 2, we have displayed the solution contours for both non-stabilized and stabilized formulations over rough mesh for $Ha = 100$. It is clearly seen that, there are numerical instabilities and oscillations on the solution obtained from the without stabilized formulation ($\tau_K = 0$) which are almost eliminated using stabilization.

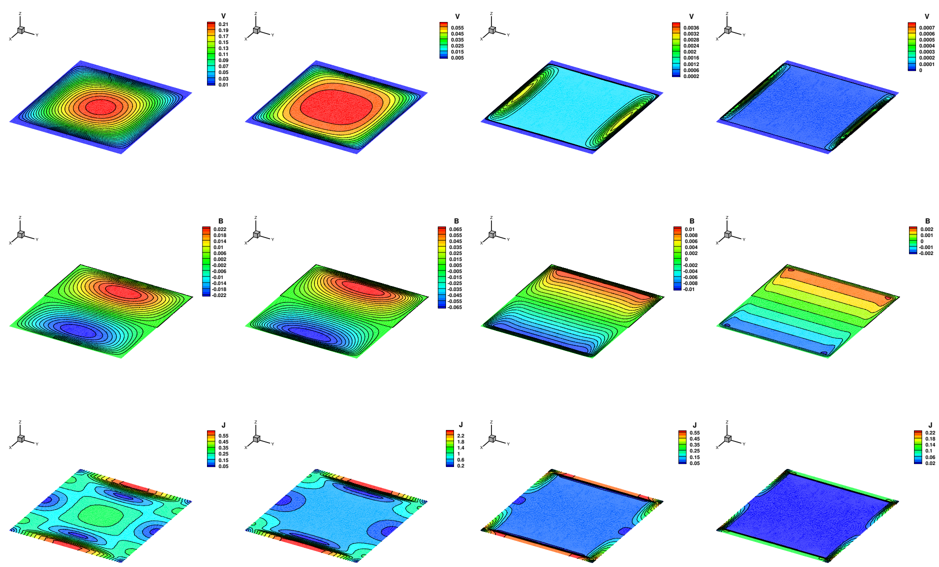

FIGURE 3. $2D$ slices of the velocity (above), induced magnetic field(middle) and current density(below) for $Ha = 1$ (1^{st} column),$Ha = 10$ (2^{nd} column), $Ha = 100$ (3^{rd} column) and $Ha = 500$ (4^{th} column) for the one duct case at $z = 0$ for $\alpha = \pi/2, \beta = 0$.

3.1. **Single Cube.** In the first case, we considered the MHD flow equation on a single cubic duct having conducting walls placed horizontally on the $y - z$ planes. We presented the velocity, induced magnetic field and current density solutions in terms of $2D$ slices at $z = 0$ in Figure 3 and at $y = -0.75$ and $y = 0.25$ in Figure 4 for $Ha = 1, 10, 100$ and 500 for the applied magnetic field angle $\alpha = \pi/2$ and $\beta = 0$ which means that externally applied magnetic field is parallel to x-axis. Existence of the boundary layer formation on the side walls (the walls perpendicular to the applied magnetic field) which is the well known behavior of the MHD flow as the Hartmann number is getting large can be observed explicitly from the solution

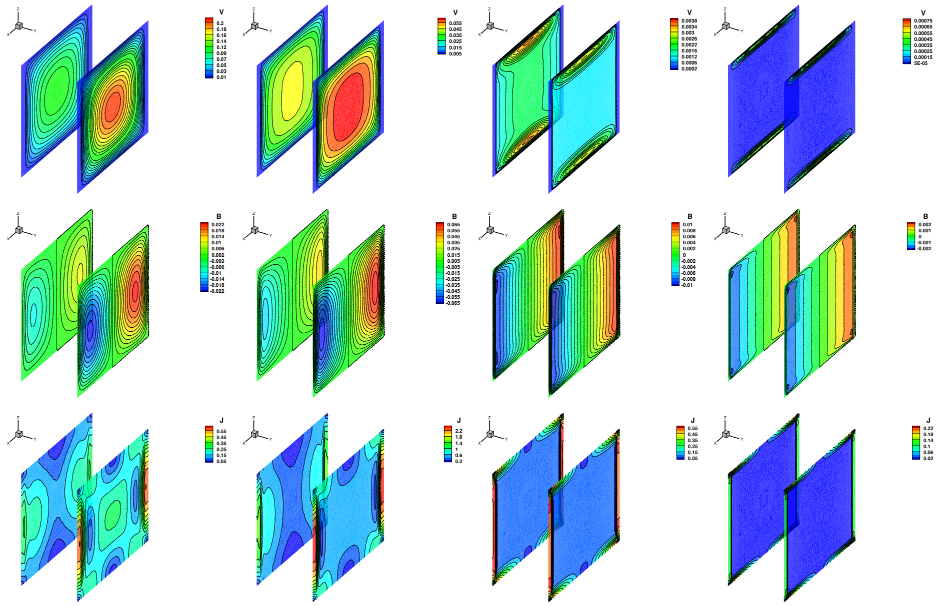

FIGURE 4. $2D$ slices of the velocity (above), induced magnetic field(middle) and current density(below) for $Ha = 1$ (1^{st} column),$Ha = 10$ (2^{nd} column), $Ha = 100$ (3^{rd} column) and $Ha = 500$ (4^{th} column) for the one duct case at $y = -0.75$ and $y = 0.25$ for $\alpha = \pi/2, \beta = 0$.

contours. Also the velocity takes its maximum value at the center of the cube and the flow is flattened as Ha getting large. Induced magnetic field contours create two loops (peaks) which are symmetric with respect to $x = 0$ plane and becomes stagnant through the domain. We also provided the current density solutions in order to compare the previously obtained $2D$ case solutions [40]. In Figure 4 we displayed different y-slices on the same figure in order to display the changes in the solutions contours as the flow approaches the sides of the duct. Finally, if one compare these solutions with the literature results for the $2D$ case of the similar problems, the good agreement is seen with the ones in ([3, 40–42, 57]).

3.2. **Double Cubes.** As a second configuration, we consider the pressure driven MHD flow in two cubic ducts in two different cases named as co-flow ($P_1 = P_2 = 1$) and counter flow ($P_1 = 1, P_2 = -1$). Noticed that due to the no-slip boundary conditions, at all the exterior sides of the ducts and walls both velocity and induced magnetic field components are vanish. Therefore, the velocity values are all 0 which is indicated as blue color on the color-legend. Also due to the continuity condition for the induced magnetic field on the interior walls, the continuation of the contour lines at the interface of the ducts can be observed from the figures.

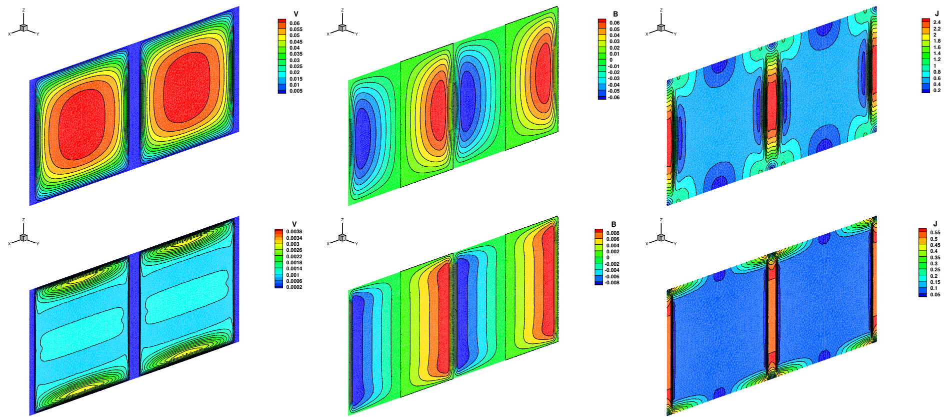

FIGURE 5. $2D$ slices of the velocity (left), induced magnetic field(center) and current density(right) for $Ha = 10$ (above) and $Ha = 100$ (below) for the co-flow case ($P_1 = P_2 = 1$) for the two ducts at $y = 0$ for $\alpha_i = \pi/2, \beta_i = 0$.

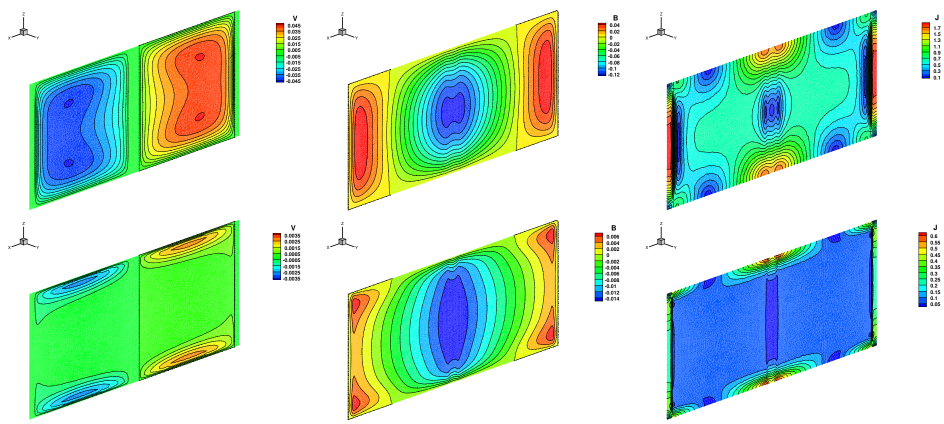

FIGURE 6. $2D$ slices of the velocity (left), induced magnetic field(center) and current density(right) for $Ha = 10$ (above) and $Ha = 100$ (below) for the counter-flow case ($P_1 = 1, P_2 = -1$) for the two ducts at $y = 0$ for $\alpha_i = \pi/2, \beta_i = 0$.

We compared the flow behaviors the co-flow and counter-flow cases in in Figure 5 and in Figure 6, respectively for both $Ha = 10$ and $Ha = 100$. Noticed that the flow behavior is exactly same in all components in both domains for the co-flow case. However, there are strong interactions and symmetric behavior with respect to interior wall in the counter-flow case. If the maximum/minimum values are

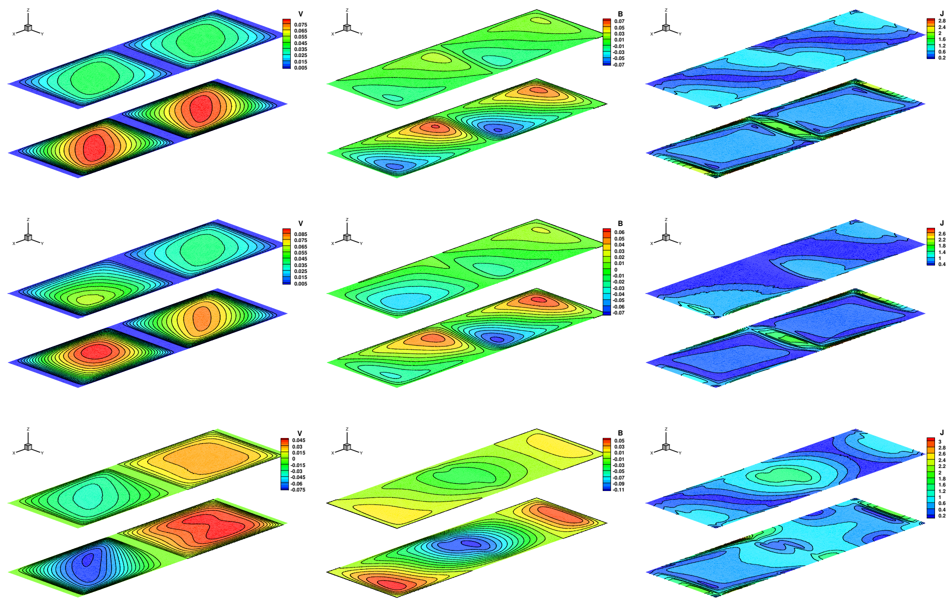

FIGURE 7. $2D$ slices of the velocity (left), induced magnetic field(center) and current density(right) for $\alpha_i = \pi/2, \beta_i = \pi/4$ (above) and $\alpha_1 = \pi/2, \alpha_2 = \pi/4, \beta_i = \pi/4$ (middle) for the co-flow cases and $\alpha_i = \pi/2, \beta_1 = 0, \beta_2 = \pi/4$ (below) for the counter-flow case for $Ha = 10$ the two ducts at $z = -0.25$ and $z = 0.85$

compared for the two different flow regime, it is seen that the magnitude in all components (velocity, induced magnetic field and current density) are absolutely a bit larger in co-flow case compared to contour-flow case. Also, as Hartmann number is getting large again the flow becomes almost stagnant away from the walls. These solutions are also agree with the previous studies [40, 42]. The effect of the direction of the externally applied magnetic field on the flow behavior is demonstrated in Figure 7 by taking (α_i, β_i) combinations for the different flow regime. The solutions contours are displayed at different z-values. It is seen that the positions of the boundary layers and the locations of the maximum/minimum values are changing depending on both the selected slice and angles. One can easily see that both mirroring and symmetries are broken in different domains. Finally, we have tested the affect of the wall length b on the flow behavior for the co-flow case in Figure 8 and for the counter-flow case in Figure 9 for $Ha = 10$. It is seen that as the wall length (b) is getting large, the separation between the domains is more pronounced in both cases.

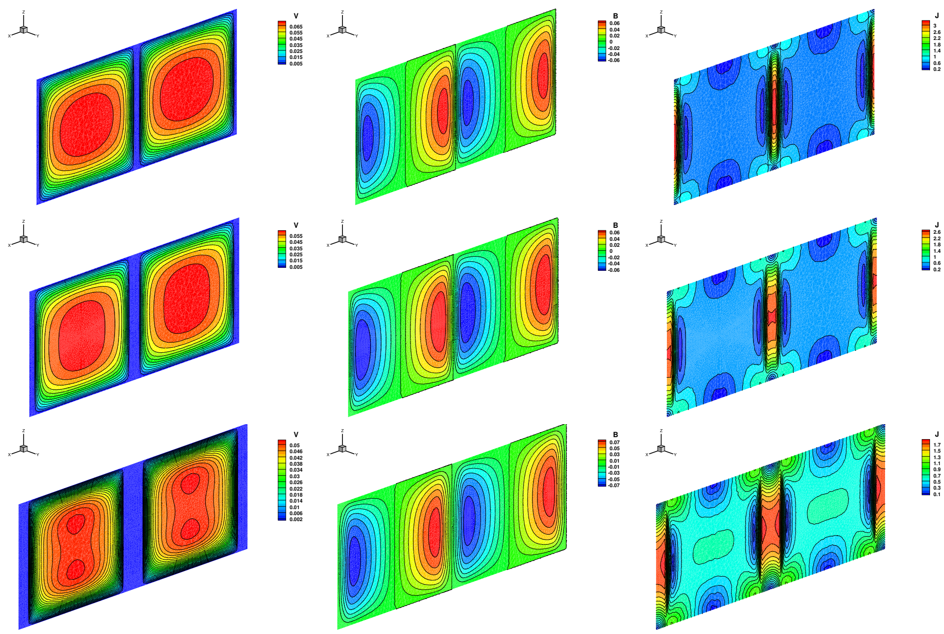

FIGURE 8. $2D$ slices of the velocity (left), induced magnetic field(center) and current density(right) for the wall length $b = 0.05$ (top), $b = 0.1$ (center) and $b = 0.2$ (bottom) for the co-flow case ($P_1 = P_2 = 1$) for the two ducts at $y = 0$ for $Ha = 10$, $\alpha_i = \pi/2, \beta_i = 0$.

3.3. **Triple Cubes.** As a final test, we considered the three cubes case. It is clear that, the size of the obtained resulting system 13 is very huge. Therefore, one of the originality of this work is to obtain accurate and stable solutions from such a big system. For this purpose, we have modified the open source sparse solver UMFPACK for the Fortran version on PC. Similar to two cubes cases, we considered both co-flow ($P_1 = P_2 = P_3 = 1$) and counter-flow ($P_1 = P_3 = 1, P_2 = -1$) cases in Figure 10 for $Ha = 10$ by considering the $2D$ contours of the solutions by taking the slice at $y = 0$. One can see that the core flow is reversed in the central cube and there is a strong connection between the cubes for the counter-flow case and the flow behaviors are all same on each cube for the co-flow case having same α and β values.

Noticed that the effect of the direction of the externally applied magnetic field on the flow behavior can be displayed more clearly by selecting different values α_i and β_i on each cube which is possible to visualize for the several cubes case. We consider different (α_i, β_i) combinations both for the co-flow and counter-flow cases in Figure 11 and Figure 12. Not only the angle values but also depending on the selected slice, the flow displays different behaviors on each cube still obeying the continuity

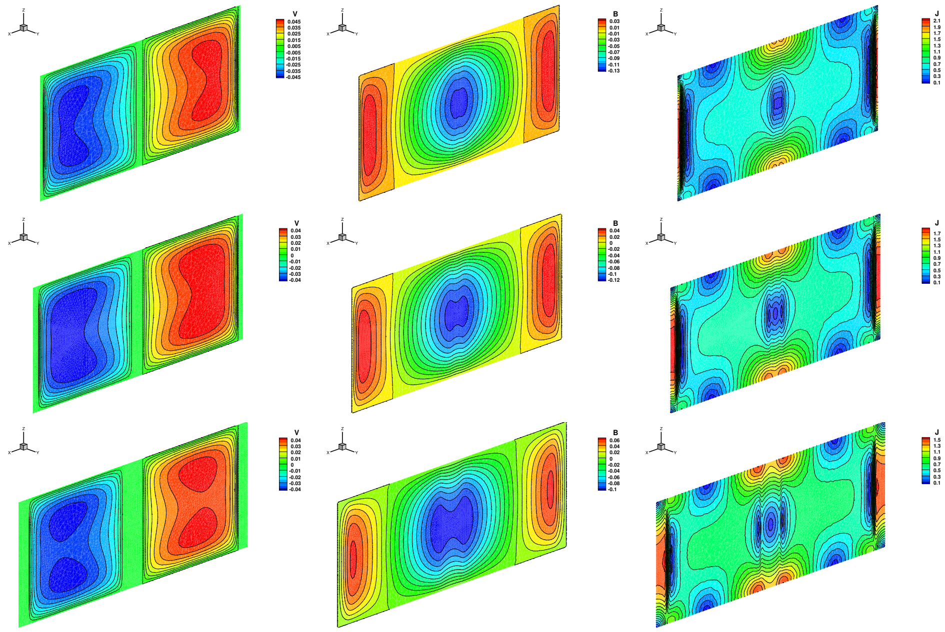

FIGURE 9. $2D$ slices of the velocity (left), induced magnetic field(center) and current density(right) for the wall length $b = 0.05$ (top), $b = 0.1$ (center) and $b = 0.2$ (bottom) for the counter-flow case ($P_1 = 1, P_2 = -1$) for the two ducts at $y = 0$ for $Ha = 10$, $\alpha_i = \pi/2, \beta_i = 0$.

conditions between the cubes. Noticed that, in general, all the components of flow (velocity, magnetic field, current density) are still consistent with the double cubes case.

4. Conclusion

We considered the stabilized FEM solution to MHD flow in an array of cubic domains having electrically insulated internal walls and conducting external walls with the no-slip boundary conditions for the velocity. The problem is tested for the different Hartmann number values. The comparison of flow behaviors for the different number of ducts, co-flow and counter-flow cases and different values of the externally applied magnetic field angle are provided. Obtained stable solutions are displayed in terms of the $2D$-slices taken from different axis. One can observe that the provided formulation is accurate and efficient even for the several cubes cases.

Declaration of Competing Interests The author declares that I have no known competing financial interests or personal relationships that could have appeared to

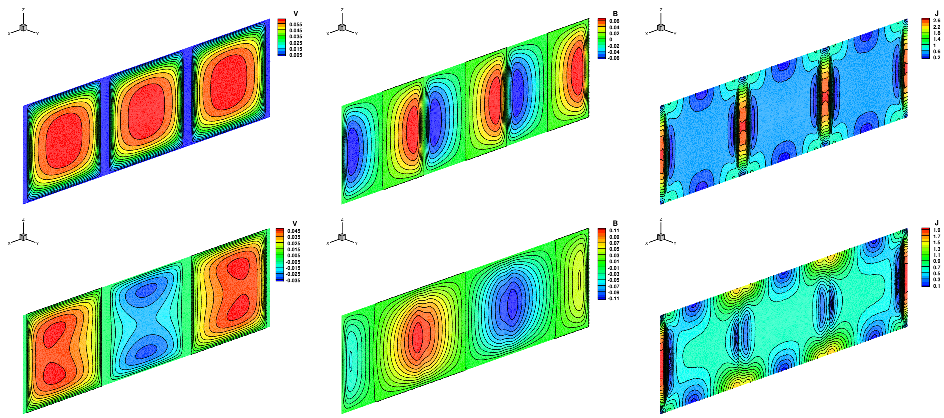

FIGURE 10. $2D$ slices of the velocity (left), induced magnetic field(center) and current density(right) for $Ha = 10, \alpha_i = \pi/2, \beta_i = 0$ for the three ducts in co-flow $(P_1 = P_2 = P_3 = 1)$(above) and counter-flow $(P_1 = P_3 = 1, P_2 = -1)$(below) cases at $y = 0$.

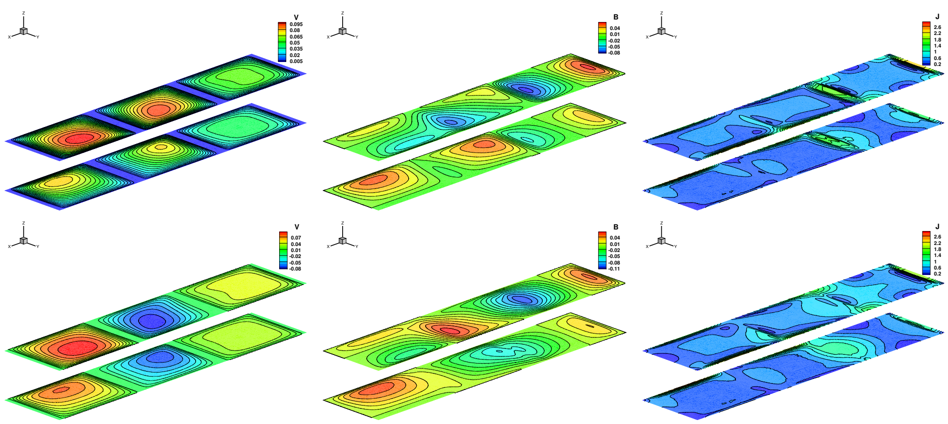

FIGURE 11. $2D$ slices of the velocity (left), induced magnetic field(center) and current density(right) for $Ha = 10, \alpha_1 = \pi/2, \beta_1 = 0, \alpha_2 = \pi/4, \beta_2 = \pi/4, \alpha_3 = \pi/4, \beta_3 = \pi/2$ for the three ducts in co-flow (above) and counter-flow (below) cases at $z = -0.75$ and $z = 0.25$.

influence the work reported in this paper.

Acknowledgements The author wish to thank Prof. Dr. M. Tezer-Sezgin for her valuable support, comments and suggestions.

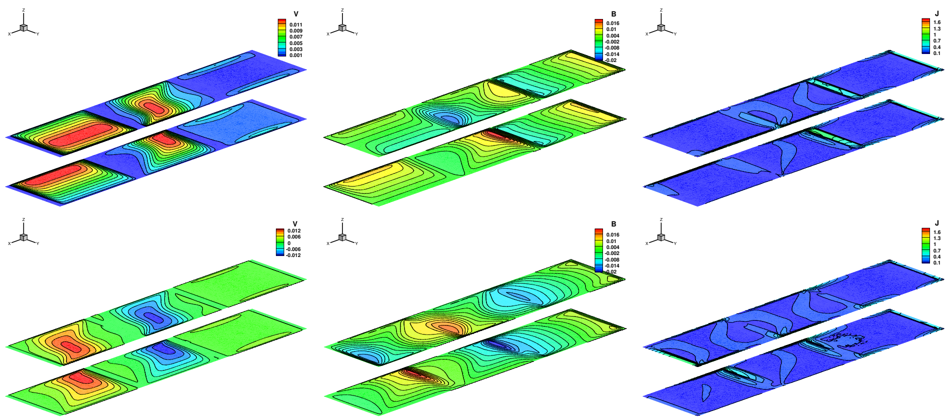

FIGURE 12. $2D$ slices of the velocity (left), induced magnetic field(center) and current density(right) for $Ha = 100, \alpha_1 = \pi/2, \beta_1 = 0, \alpha_2 = \pi/4, \beta_2 = \pi/4, \alpha_3 = \pi/4$ for the three ducts in co-flow for $\beta_3 = \pi/2$(above) and counter-flow for $\beta_3 = \pi/4$)(below) cases at $z = -0.75$ and $z = 0.25$.

REFERENCES

[1] Hartmann, J., Theory of the laminar flow of an electrically conductive liquid in a homogeneous magnetic field, *K. Dan. Vidensk. Selsk. Mat. Fys. Medd.*, 15(6) (1937), 1–28.

[2] Shercliff, J.A., Steady motion of conducting fluid in a pipes under transverse magnetic fields, *J. Fluid Mech.*, 1(6) (1956), 644–666. https://doi.org/10.1017/S0022112056000421

[3] Dragoş, L., Magnetofluid Dynamics, Abacus Pres, 1975.

[4] Davidson, P.A., An Introduction to Magnetohydrodynamic, Cambridge Texts in Applied Mathematics, Vol. 1, Cambridge University Press, 2001. https://doi.org/10.1017/CBO9780511626333

[5] Carabineanu, A., Dinu, A., Oprea, I., The application of the boundary element method to the magnetohydrodynamic duct flow, *The Journal of Applied Mathematics and Physics (ZAMP)*, 46 (1995), 971–981. https://doi.org/10.1007/BF00917881

[6] Meir, A.J., Finite element analysis of magnetohydrodynamic pipe flow, *Applied Mathematics and Computation*, 57 (1993), 177–196. https://doi.org/10.1016/0096-3003(93)90145-5

[7] Sheu, T.W.H., Lin, R.K., Development of a ranvection-diflusion-reaction magnetohydrodynamic solver on nonstaggared grids, *International Journal for Numerical Methods in Fluids*, 45 (2004), 1209–1233. https://doi.org/10.1002/fld.738

[8] Singh, B., Lal, J., Finite element method of MHD channel flow with arbitrary wall conductivity, *Journal of Mathematical and Physical Sciences*, 18 (1984), 501–516.

[9] Tezer-Sezgin, M., Han Aydin, S., Dual reciprocity boundary element method for magnetohydrodynamic flow using radial basis functions, *International Journal of Computational Fluid Dynamics*, 16(1) (2002), 49–63. https://doi.org/10.1080/10618560290004026

[10] Tezer-Sezgin, M., Bozkaya, C., Boundary-element method solution of magnetohydrodynamic flow in a rectangular duct with conducting walls parallel to applied magnetic field, *Computational Mechanics*, 41 (2008), 769–775. https://doi.org/10.1007/s00466-006-0139-5

[11] Tezer-Sezgin, M., Han Aydin, S., BEM solution of MHD flow in a pipe coupled with magnetic induction of exterior region, *Computing*, 95(1) (2013), 751–770. https://doi.org/10.1007/s00607-012-0270-4

[12] Carabineanu, A., Lungu, E., Pseudospectral method for MHD pipe flow, *Int. J. Numer. Methods Eng.*, 68(2) (2006), 173–191. https://doi.org/10.1002/nme.1706

[13] Han Aydın, S., Tezer-Sezgin, M., DRBEM solution of MHD pipe flow in a conducting medium, *J. Comput. Appl. Math.*, 259(B) (2014), 720–729. https://doi.org/10.1016/j.cam.2013.05.010

[14] Tezer-Sezgin, M., Han Aydın, S., FEM Solution of MHD Flow Equations Coupled on a Pipe Wall in a Conducting Medium, PAMIR, 2014.

[15] Cai, X., Qiang, H., Dong, S., Lu, J., Wang, D., Numerical simulations on the fully developed liquid-metal MHD flow at high Hartmann numbers in the rectangular duct, *Advances in Intelligent Systems Research*, 143 (2018), 68–71. https://doi.org/10.2991/ammsa-18.2018.14

[16] Dehghan, M., Mirzai, D., Meshless local boundary integral equation (LBIE) method for the unsteady magnetohydrodynamic(MHD) flow in rectangular and circular pipes, *Computer Physics Communications*, 180 (2009), 1458–66. https://doi.org/10.1016/j.cpc.2009.03.007

[17] Loukopoulos, V.C., Bourantas, G.C., Skouras, E.D., Nikiforidis, G.C., Localized meshless point collocation method for time-dependent magnetohydrodynamic flow through pipes under a variety of wall conductivity conditions, *Computational Mechanics*, 47(2) (2011), 137–159. https://doi.org/10.1007/s00466-010-0535-8

[18] Salah, N.B., Soulaimani, A., Habashi, W.G., A finite element method for magnetohydrodynamics, *Comput. Methods Appl. Mech. Engrg.*, 190 (2001) 5867–5892. https://doi.org/10.1016/S0045-7825(01)00196-7

[19] Dong, X., He, Y., Two-level Newton iterative method for the 2D/3D stationary incompressible magnetohydrodynamics, *J. Sci. Comput.*, 63 (2015), 426–451. https://doi.org/10.1007/s10915-014-9900-7

[20] Wang, L., Li, J. Huang, P., An efficient two-level algorithm for the 2D/3D stationary incompressible magnetohydrodynamics based on the finite element method, *International Communications in Heat and Mass Transfer*, 98 (2018), 183–190. https://doi.org/10.1016/j.icheatmasstransfer.2018.02.019

[21] Xu, J., Feng, X., Su, H., Two-level Newton iterative method based on nonconforming finite element discretization for 2D/3D stationary MHD equations, *Computers and Fluids*, 238 (2022), 105372. https://doi.org/10.1016/j.compfluid.2022.105372

[22] Dong, X., He, Y., Zhang, Y., Convergence analysis of three finite element iterative methods for the 2D/3D stationary incompressible magnetohydrodynamics, *Comput. Methods Appl. Mech. Engrg.*, 276 (2014), 287–311. https://doi.org/10.1016/j.cma.2014.03.022

[23] Xu, J., Su, H., Li, Z., Optimal convergence of three iterative methods based on nonconforming finite element discretization for 2D/3D MHD equations, *Numerical Algorithms.* https://doi.org/10.1007/s11075-021-01224-4 (2021)

[24] Li, L., Zheng, W., A robust solver for the finite element approximation of stationary incompressible MHD equations in 3D, *Journal of Computational Physics*, 351 (2017), 254–270. https://doi.org/10.1016/j.jcp.2017.09.025

[25] Zhang, G.D., He, X., Yang, X., A fully decoupled linearized finite element method with second-order temporal accuracy and unconditional energy stability for incompressible MHD equations, *Journal of Computational Physics*, 448 (2022), 110752. https://doi.org/10.1016/j.jcp.2021.110752

[26] Skala, J., Baruffa, F., Buechner, J., Rampp, M., The 3D MHD Code GOEMHD3 for large-Reynolds-number astrophysical plasmas, *Astron. Astrophys.*, 580 (2015), A48. https://doi.org/10.1051/0004-6361/201425274

[27] Sutevski, D., Smolentsev, S., Morley, N., Abdou, M., 3D numerical study of MHD flow in a rectangular duct with a flow channel insert, *Fusion Science and Technology*, 60(2) (2011), 513-517. https://doi.org/10.13182/FST11-A12433

[28] Huba, J.D., Lyon, J.G., A new 3D MHD algorithm: the distribution function method, *J. Plasma Physics.*, 61(3) (1999), 391–405. https://doi.org/10.1017/S0022377899007503

[29] Barnes, D.C., Rousculp, C.L., Accurate, finite-volume methods for 3D MHD on unstructured Lagrangian meshes, Nuclear explosives code developers conference (NECDC), Las Vegas, NV (United States), October, 1998.

[30] Wu, J., Bounds and new approaches for the 3D MHD equations, *J. Nonlinear Sci.*, 12 (2002), 395–413. https://doi.org/10.1007/s00332-002-0486-0

[31] Ni, L., Guo, Z., Zhou, Y., Some new regularity criteria for the 3D MHD equations, *J. Math. Anal. Appl.*, 396 (2012), 108–118. https://doi.org/10.1016/j.jmaa.2012.05.076

[32] Zhang, Z., Ouyang, X., Zhong, D., Qiu, S., Remarks on the regularity criteria for the MHD equations in the multiplier spaces, *Boundary Value Problems*, (2013), 270. https://doi.org/10.1186/1687-2770-2013-270

[33] Jia, X., Zhou, Y., Regularity criteria for the 3D MHD equations involving partial components, Nonlinear Analysis, *Real World Applications*, 13 (2012), 410–418. https://doi.org/10.1016/j.nonrwa.2011.07.055

[34] Yea, Z., Zhang, Z., A remark on regularity criterion for the 3D Hall-MHD equations based on the vorticity, *Applied Mathematics and Computation.*, 301 (2017), 70–77. https://doi.org/10.1016/j.amc.2016.12.011

[35] Caoa, C., Wu, J., Two regularity criteria for the 3D MHD equations, *J. Differential Equations*, 248 (2010), 2263–2274. https://doi.org/10.1016/j.jde.2009.09.020

[36] Tassone, A., Gramiccia, L., Caruso, G., Three-dimensional MHD flow and heat transfer in a channel with internal obstacle, *International Journal of Heat and Technology*, 36(4) (2018), 1367-1377. https://doi.org/10.18280/ijht.360428

[37] Ud-Doula, A., Sundqvist, J., Owocki, S.P., Petit, V., Townsend, RHD First 3D MHD simulation of a massive-star magnetosphere with application to H alpha emission from theta(1) Ori C, *Monthly Notices of the Royal Astronomical Society*, 428(3) (2013), 2723-2730. https://doi.org/10.1093/mnras/sts246

[38] Fernández-Dalgo, P.G., Jarrin, O., Weak suitable solutions for 3D MHD equations for intermittent initial data, hal-02490130 (2020).

[39] Liu, F., Wang, Y.Z., Global solutions to three-dimensional generalized MHD equations with large initial data, *Z. Angew. Math. Phys.*, 70(69) (2019). https://doi.org/10.1007/s00033-019-1113-3

[40] Bluck, M.J., Wolfandale, M.J., An analytical solution to electromagnetically coupled duct flow in MHD, *Journal of Fluid Mechanics*, 771 (2015), 595–623. https://doi.org/10.1017/jfm.2015.202

[41] Hunt, J.C.R., Stewartson, K., Magnetohydrodynamics flow in rectangular ducts. II., *Journal of Fluid Mechanics*, 23(3) (1965), 563–581. https://doi.org/10.1017/S0022112065001544

[42] Tezer-Sezgin, M., Aydin, S.H., FEM solution of MHD flow in an array of electromagnetically coupled rectangular ducts, *Progress in Computational Fluid Dynamics, An International Journal.*, 20 (2020), 40–50. https://doi.org/10.1504/PCFD.2020.104706

[43] Aydin, S.H., 3-D MHD flow over array of cubic ducts, *International Conference on Applied Mathematics in Engineering (ICAME 21),* September 1-3, (2021), Balikesir, Turkey.

[44] Brooks, A.N., Hughes, T.J.R., Streamline upwind/Petrov-Galerkin formulations for convection dominated flows with particular emphasis on the incompressible Navier-Stokes equations, *Comput. Methods Appl. Mech. Engrg.*, 32 (1982), 199–2592. https://doi.org/10.1016/0045-7825(82)90071-8

[45] Salah, N.B., Soulaimani, A., Habashi, W.G., Fortin, M., A conservative stabilized finite element method for the magnet-hydrodynamic equations, *Internation Journal for Numerical Methods in Fluids*, 29 (1999), 535–554. https://doi.org/10.1002/(SICI)1097-0363(19990315)29:5<535::AID-FLD799>3.0.CO;2-D

[46] Shadid, J.N., Powlowski, R.P., Cyr, E.C., Tuminaro, R.S., Chacón, L., Weber, P.D., Scalable implicit incompressible resistive MHD with stabilized FE and fully-coupled Newton-Krylov-AMG, *Comput. Methods Appl. Mech. Engrg.*, 304 (2016), 1–25. https://doi.org/10.1016/j.cma.2016.01.019

[47] Gerbeau, J.F., A stabilized finite element method for the incompressible magnetohydrodynamic equations, *Numerische Mathematik*, 87 (2000), 83–111. https://doi.org/10.1007/s002110000193

[48] Nesliturk, A.I., Tezer-Sezgin, M., The finite element method for MHD flow at high Hartmann numbers, *Comput. Methods Appl. Mech. Engrg.*, 194 (2005), 1201–1224. https://doi.org/10.1016/j.cma.2004.06.035

[49] Nesliturk, A.I., Tezer-Sezgin, M., Finite element method solution of electrically driven magnetohydrodynamic flow, *Journal of Computational and Applied Mathematics*, 192 (2006), 339–352. https://doi.org/10.1016/j.cam.2005.05.015

[50] Codina, R., Silva, N.H., Stabilized finite element approximation of the stationary magneto-hydrodynamics equations, *Computational Mechanics*, 38 (2006), 344–355. https://doi.org/10.1007/s00466-006-0037-x

[51] Aydin, S.H., Nesliturk, A.I., Tezer-Sezgin, M., Two-level finite element method with a stabilizing subgrid for the incompressible MHD equations, *International Journal for Numerical Methods in Fluids*, 62(2) (2010), 188–210. https://doi.org/10.1002/fld.2019

[52] Marchandise, E., Remacle, J.F., A stabilized finite element method using a discontinuous level set approach for solving two phase incompressible flows, *Journal of Computational Physics*, 219 (2006), 780–800. https://doi.org/10.1016/j.jcp.2006.04.015

[53] Nesliturk, A.I., Aydin, S.H., Tezer-Sezgin, M., Two-level finite element method with a stabilizing subgrid for the incompressible Navier-Stokes equations, *International Journal for Numerical Methods in Fluids*, 58 (2007), 551–572. https://doi.org/10.1002/fld.1753

[54] Hachem, E., Rivaux, B., Kloczko, T., Digonnet, H., Coupez, T., Stabilized finite element method for incompressible flows with high Reynolds number, *Journal of Computational Physics*, 229 (2010), 8643–8665. https://doi.org/10.1016/j.jcp.2010.07.030

[55] Wang, A., Zhao, X., Qin, P., Xie, D., An oseen two-level stabilized mixed finite-element method for the 2D/3D stationary Navier-Stokes equations, *Abstract and Applied Analysis*, 2012 (2012), 1–12. https://doi.org/10.1155/2012/520818

[56] Reddy, J.N., An Introduction to the Finite Element Method, 2nd ed., McGraw-Hill, New York, 1993.

[57] Muller, U., Buhler, L., Magnetofluiddynamics in Channels and Containers, Springer, 2001.

http://communications.science.ankara.edu.tr

Commun.Fac.Sci.Univ.Ank.Ser. A1 Math. Stat.
Volume 72, Number 3, Pages 857–866 (2023)
DOI:10.31801/cfsuasmas.1232916
ISSN 1303-5991 E-ISSN 2618-6470

Research Article; Received: January 11, 2023; Accepted: February 15, 2023

THE BISPECTRAL REPRESENTATION OF MARKOV SWITCHING BILINEAR MODELS

AHMED GHEZAL[1] and IMANE ZEMMOURI[2]

[1]Department of Mathematics and Computer Sciences, University Center of Mila, ALGERIA
[2]Department of Mathematics, University of Annaba, Elhadjar 23, Annaba, ALGERIA

Abstract. This article formulae for the third-order theoretical moments for superdiagonal and subdiagonal of the Markov-switching bilinear

$$X_t = c\left(s_t\right) X_{t-k} e_{t-l} + e_t,\ k,\ l\ \in \mathbb{N},$$

and an expression for the bispectral density function are obtained.

1. Introduction

The series is nonlinear the spectral will not adequately characterize the series. For instance, for some types of nonlinear time series (e.g. Markov switching bilinear models). As well, spectral analysis will not necessarily show up any features of nonlinearity (or nongaussianity) present in the series. It may be necessary, therefore, to perform higher order spectral analysis on the series in order to detect departures from linearity and Gaussianity. The simplest type of bispectral analysis notably by Rosenblatt and Van Ness (1965), Rosenblatt (1966), Van Ness (1966) and Brillinger and Rosenblatt (1967a, b).

Markov switching time series models (MSM) have recently received a growing interest because of their ability to adequately describe various observed time series subjected to change in regime. An (MSM) is a discrete-time random process $((X_t, s_t), t \in \mathbb{Z})$ such that (i): $(s_t, t \in \mathbb{Z})$ is not observable, finite state, discrete-time and homogeneous Markov chain and (ii): the conditional distribution of X_k relative to its entire past, depends on (s_t) only through s_k. Flexibility is one of the main advantages of (MSM). The changes in regime can be smooth or abrupt, and they occur frequently or occasionally depending on the transition probability

2020 *Mathematics Subject Classification.* 62F12, 62M05.

Keywords. Markov-switching superdiagonal and subdiagonal bilinear processes, third-order moments, bispectral density function.

[1] a.ghezal@centre-univ-mila.dz-Corresponding author; 0000-0001-6939-0199
[2] imanezemmouri25@gmail.com; 0000-0001-8397-4924.

of the chain. Markov-switching models were introduced to the econometric mainstream by Hamilton [c,f., [7]] , [c,f., [8]] and continue to gain popularity especially in financial time series analysis in order to integrate the mentioned characteristics in the conditional mean through local linearity representation. In this paper we alternatively propose a Markov switching bilinear $(MS - BL)$ representation, in which the process follows locally from a bilinear characterization. This is in order to give a general, flexible and economic framework for Markov switching modelling and $(MS - BL)$ has been extensively studied by Bibi and Aknouche (2010). In this paper we shall consider a Markov-switching bilinear model defined by

$$X_t = c\left(s_t\right) X_{t-k} e_{t-l} + e_t,\ t \in \mathbb{Z}, \tag{1}$$

where $(e_t, t \in \mathbb{Z})$ is a strictly stationary and ergodic sequence of random variables with mean $E\left(e_t\right) = 0$ and variance $E\left(e_t^2\right) = 1$, for all t. The functions $a_i\left(s_t\right), b_j\left(s_t\right)$ and $c_{ij}\left(s_t\right)$ depends upon a time homogeneous Markov chain $(s_t, t \in \mathbb{Z})$ with finite state space $S = \{1; \ldots; d\}$, irresuctible, aperiodic and ergodic, initial distribution $\pi(i) = P(s_1 = i), i = 1; \ldots; d$, $n-$step transition probabilities matrix $\mathbb{P}^n = \left(p_{ij}^{(n)}\right)_{(i,j)\in\mathbb{S}\times\mathbb{S}}$ where $p_{ij}^{(n)} = P(s_t = j\,|s_{t-n} = i)$ with $\mathbb{P} := (p_{ij})_{(i,j)\in\mathbb{S}\times\mathbb{S}}$ where $p_{ij} := p_{ij}^{(1)} = P(s_t = j\,|s_{t-1} = i)$ for $i; j \in \mathbb{S}$. In addition, we assume that e_t and $\{(X_{s-1}, s_t), s \leq t\}$ are independent, we shall note

$$\mathbb{P}\left(M\right) = \begin{pmatrix} p_{11}M\left(1\right) & \ldots & p_{1d}M\left(1\right) \\ \vdots & \ldots & \vdots \\ p_{d1}M\left(d\right) & \ldots & p_{dd}M\left(d\right) \end{pmatrix},\quad \Pi\left(M\right) = \begin{pmatrix} \pi\left(1\right)M\left(1\right) \\ \vdots \\ \pi\left(d\right)M\left(d\right) \end{pmatrix},$$

and $I_{(n)}$ is the $n \times n$ identity matrix. The model (1) is known as a superdiagonal model if $k > l$, and subdiagonal model for $k < l$. Let $(X_t, t \in \mathbb{Z})$ be a stationary time series satisfying the $MS - BL$ model (1), and the necessary condition for $(X_t, t \in \mathbb{Z})$ to be strictly stationary (see Bibi and Aknouche (2010)). A sufficient condition for stationarity is $\gamma_L(A) < 0$, where $\gamma_L(A)$ is the Lyapunov exponent.
The third-order moments of (X_t) are defined by (c,f., [6])

$$\begin{aligned} R\left(r_1, r_2\right) &= E\left\{\left(X_t - \mu\right)\left(X_{t-r_1} - \mu\right)\left(X_{t-r_2} - \mu\right)\right\} \\ &= E\left(X_t\ X_{t-r_1} X_{t-r_2}\right) - \mu\left(\gamma\left(r_1\right) + \gamma\left(r_2\right) + \gamma\left(r_1 - r_2\right)\right) + 2\mu^3, \end{aligned} \tag{2}$$

where $\mu = E\left(X_t\right),\ \gamma\left(r\right) = E\left(X_t\ X_{t-r}\right)$. It is sufficient to calculate $R\left(r_1, r_2\right)$ in the sector $0 \leq r_1 \leq r_2$ and the other values of $R\left(r_1, r_2\right)$ are determined from its symmetric relations (see Subba Rao and Gabr, (1984)).
Lii and Rosenblatt (1982) have shown how bispectral density function, can be used for estimating the phase relationships, and this in turn can be applied to the problem of deconvolution of e.g. seismic traces, quite a number of seismic records are observed to be nongaussian, and in many geophysical problems it is often required to estimate the coefficients. Also, the bispectral density function

could, in principle be used for testing linearity. The bispectrum has been used in a number of investigations as a data analytic tool; we mention in particular the work of Hasselman, Munk and MacDonald (1963) on ocean waves, the papers of Lii and Rosenblatt (1979) on the energy transfer in grid generated turbulence. In this paper, we shall use the third-order moments to derive the bispectral density function of $MS-BL$ models.

2. Spectral and Bispectral

We now consider the evaluation of the spectral and bispectral of the process (X_t) when the process satisfies some linear time series models. Firstly, we consider the following model

$$X_t = \sum_{j=0}^{q} b_j\left(s_t\right) e_{t-j}, \tag{3}$$

we have

$$E\left(X_t\right) = 0, \text{ for all } t,$$

$$\gamma\left(r\right) = E\left(X_t\ X_{t-r}\right) = \begin{cases} \sum\limits_{j=r}^{q} \underline{1}'_{(d)} \mathbb{P}\left(\underline{b}_j\right) \pi\left(\underline{b}_{j-r}\right) & \text{if } 0 \le r \le q \\ 0 & \text{if } \ r > q \end{cases}.$$

The spectral density function $f\left(.\right)$ of the process (X_t) define by

$$f\left(\omega\right) = \frac{1}{2\pi} \sum_{r=-\infty}^{+\infty} \gamma\left(r\right) \exp\left(-ir\omega\right), \quad -\pi \le \omega \le \pi,$$

of (2) the spectral density function of the process (X_t) is given by $f\left(\omega\right) = \gamma\left(0\right) + 2\sum\limits_{r=1}^{q} \gamma\left(r\right) \cos\left(\omega r\right)$, all ω, the bispectral density function $f\left(\omega_1, \omega_2\right)$ is given by $f\left(\omega_1, \omega_2\right) = 0$, all $\omega_1, \omega_2 \in [-\pi, \pi]$. Secondly, we consider the following model

$$X_t = \sum_{i=1}^{p} a_i\left(s_t\right) X_{t-i} + \sum_{j=1}^{q} b_j\left(s_t\right) e_{t-j} + e_t, \tag{4}$$

Franq and Zakoïan (2001), propose the following representation of (4)

$$\begin{aligned} \underline{X}_t &= \left(X_t, X_{t-1}, ..., X_{t-p+1}, e_t, e_{t-1}, ..., e_{t-q+1}\right)' \in \mathbb{R}^{p+q} \\ &= A\left(s_t\right) \underline{X}_{t-1} + \underline{e}_t, \end{aligned}$$

where $\underline{e}_t = (e_t, 0, ..., 0)' \in \mathbb{R}^{p+q}$ and

$$A(s_t) = \begin{bmatrix} a_1(s_t) & ... & a_p(s_t) & b_1(s_t) & ... & b_q(s_t) \\ 1 & 0 & ... & ... & ... & 0 \\ 0 & 1 & 0 & ... & ... & 0 \\ \vdots & \ddots & \ddots & \ddots & \ddots & \vdots \\ 0 & ... & ... & 0 & 1 & 0 \\ 0 & ... & ... & ... & ... & 0 \\ 0 & 1 & 0 & ... & ... & 0 \\ \vdots & \ddots & \ddots & \ddots & \ddots & \vdots \\ 0 & ... & ... & 0 & 1 & 0 \end{bmatrix}.$$

$\underline{\gamma}(r) = E\left(\underline{X}_t\ \underline{X}'_{t-r}\right)$ is the autocovariance of $\underline{X}_t$, then for all $r > 0$,

$$\pi(i) E\left(\underline{X}_t\ \underline{X}'_{t-r} \middle| s_t = i\right) = \sum_{j=1}^{d} A(i) E\left(\underline{X}_{t-1}\ \underline{X}'_{t-r} \middle| s_{t-1} = j\right) p_{ji}\pi(j),$$

we note $\underline{W}(r) = \left(\pi(1) E\left(\underline{X}_t\ \underline{X}'_{t-r} \middle| s_t = 1\right), ..., \pi(d) E\left(\underline{X}_t\ \underline{X}'_{t-r} \middle| s_t = d\right)\right)'$ (see Pataracchia (2011)) from which we have

$$\underline{W}(r) = \mathbb{P}(\underline{A})\underline{W}(r-1) = \mathbb{P}^r(\underline{A})\underline{W}(0), \forall r > 0,$$

where $\underline{A} = (A(1), ..., A(d))'$. Hence, we can compute the autocovariance of the process X_t:

$$\gamma(r) = \left(\underline{H}' \otimes \underline{1}'_{(d)}\right)\underline{W}(r)\underline{H}.$$

For $r < 0$, let us define

$$\underline{\tilde{W}}(r) = \left(\pi(1) E\left(\underline{X}_t\ \underline{X}'_{t-r} \middle| s_{t-r} = 1\right), ..., \pi(d) E\left(\underline{X}_t\ \underline{X}'_{t-r} \middle| s_{t-r} = d\right)\right)'.$$

Then for $r < 0$,

$$\underline{\tilde{W}}^{(i)}(r) = \pi(i) E\left(\underline{X}_t\ \underline{X}'_{t-r} \middle| s_{t-r} = i\right) = \left(\underline{W}^{(i)}(-r)\right)',$$

from which we have $\underline{\tilde{W}}(r) = \underline{W}(-r) = \mathbb{P}^{-r}(\underline{A})\underline{W}(0), \forall r < 0$. Hence, for negative r, we can compute the autocovariance of the process X_t: $\gamma(r) = \left(\underline{H}' \otimes \underline{1}'_{(d)}\right)\underline{\tilde{W}}(r)\underline{H}$, from which it can be verified that $\gamma(r) = \gamma(-r), \forall r < 0$.

Spectral representation which defines the spectral as Fourier transform of the autocovariance function

$$\begin{aligned} f(\omega) &= \frac{1}{2\pi}\sum_{r=-\infty}^{+\infty}\gamma(r)\exp(-ir\omega), \quad -\pi \le \omega \le \pi \\ &= \frac{1}{2\pi}\left(\underline{H}' \otimes \underline{1}'_{(d)}\right)\sum_{r=-\infty}^{+\infty}\mathbb{P}^{|r|}(\underline{A})\exp(-ir\omega)\underline{W}(0)\underline{H} \end{aligned}$$

$$= \frac{1}{2\pi}\left(\underline{H}'\otimes\underline{1}'_{(d)}\right)\left(\mathbb{P}\left(\underline{A}\right)-\mathbb{P}^{-1}\left(\underline{A}\right)\right)\left(2\cos\omega\ I_{(d)}-\left(\mathbb{P}\left(\underline{A}\right)+\mathbb{P}^{-1}\left(\underline{A}\right)\right)\right)\underline{W}\left(0\right)\underline{H},$$

on conditional $\rho\left(\mathbb{P}\left(\underline{A}\right)\right) < 1$ (see Costa and all (2005)), the bispectral density function $f\left(\omega_1,\omega_2\right)$ is given by $f\left(\omega_1,\omega_2\right)=0$, for all $\omega_1,\omega_2\in[-\pi,\pi]$.
Finally, we consider the $MS-$bilinear model

$$X_t=\sum_{i=1}^{p}a_i\left(s_t\right)X_{t-i}+\sum_{j=1}^{q}b_j\left(s_t\right)e_{t-j}+\sum_{i,j=1}^{P,Q}c_{ij}\left(s_t\right)X_{t-i}e_{t-j}+e_t, \qquad (5)$$

Bibi, A., Aknouche, A. (2010), propose the following representation of (5)

$$\underline{X}_t=B\left(s_t\right)\underline{X}_{t-1}+\underline{e}_t,$$

same result is obtained

$$f\left(\omega\right)=\frac{1}{2\pi}\left(\underline{H}'\otimes\underline{1}'_{(d)}\right)\left(\mathbb{P}\left(\underline{B}\right)-\mathbb{P}^{-1}\left(\underline{B}\right)\right)$$
$$\times\left(2\cos\omega\ I_{(d)}-\left(\mathbb{P}\left(\underline{B}\right)+\mathbb{P}^{-1}\left(\underline{B}\right)\right)\right)\underline{W}\left(0\right)\underline{H},$$

where $\underline{B}=\left(B\left(1\right),...,B\left(d\right)\right)'$. We note that sepectral representation does not allow us to distinguish linear models for nonlinear models and therefore should be talking about higher order spectral (bispectral).

2.1. **Superdiagonal models.** The superdiagonal model may be written as

$$X_t=c\left(s_t\right)X_{t-k}e_{t-k+m}+e_t,\ k\geq 2,\ 1\leq m\leq k-1, \qquad (6)$$

we have

$$\mu=E\left(X_t\right)=0,\text{ for all }t,$$
$$\gamma\left(r\right)=E\left(X_t\ X_{t-r}\right)=\begin{cases}\underline{1}'_{(d)}\left(I_{(d)}-\mathbb{P}^k\left(\underline{c}^2\right)\right)^{-1}\underline{\pi} & \text{if } r=0\\ 0 \quad \text{if } r\neq 0\end{cases}.$$

Lemma 1. *For the* superdiagonal *model* (6) *all the third-order moments* $R\left(r_1,r_2\right)$ *are equal to zero except at* $r_1=k-m$, $r_2=k$, *viz.,* $R(k-m,k)=\underline{1}'_{(d)}\mathbb{P}^k\left(\underline{c}\right)\pi\left(\underline{V}\right)$ *where* $\pi\left(\underline{V}\right)=\left(\pi\left(1\right)E\left(X_t^2\left|s_t=1\right.\right),...,\pi\left(d\right)E\left(X_t^2\left|s_t=d\right.\right)\right)'$.

Proof. Consider the case $r_1=r_2=0$. Using (6) it can be shown that

$$E\left(X_t^3\left|s_t=i\right.\right)=c^3\left(i\right)E\left(X_{t-k}^3e_{t-k+m}^3\left|s_t=i\right.\right)+3c\left(i\right)E\left(X_{t-k}e_{t-k+m}\left|s_t=i\right.\right)=0,$$

using (2) we obtain, $R(0,0)=0$. For $r_1=r_2=r$, say, where $r>0$, we expand X_t using (3) to give

$$E\left(X_tX_{t-r}^2\left|s_t=i\right.\right)=c\left(i\right)E\left(X_{t-k}X_{t-r}^2e_{t-k+m}\left|s_t=i\right.\right)=0,$$

using (2) we obtain, $R(r,r)=0$. Now, we consider the case $r_1=0$ and $r_2=r$. Squaring both sides of (3), multiplying by X_{t-r} and taking expectations, we get

$$E\left(X_t^2X_{t-r}\left|s_t=i\right.\right)=c^2\left(i\right)E\left(X_{t-k}^2X_{t-r}e_{t-k+m}^2\left|s_t=i\right.\right)=0,$$

then $R(0,r)=0$. Lastly, consider the case $r_1=r$ and $r_2=r+s$. When $r\geq 1$ and $s\geq 1$, it can be shown that

$$E\left(X_t X_{t-r} X_{t-r-s}\left|s_t=i\right.\right)=c\left(i\right)E\left(X_{t-k} X_{t-r} X_{t-r-s} e_{t-k+m}\left|s_t=i\right.\right),$$

□

$$E\left(X_t X_{t-r} X_{t-r-s}\left|s_t=i\right.\right)=\begin{cases} c\left(i\right)E\left(X_{t-k}^2\left|s_t=i\right.\right) & \text{if } r_1=k-m, r_2=k \\ 0 & \text{otherwise}\end{cases},$$

using (2) we obtain, $R(k-m,k)=\underline{1}'_{(d)}\mathbb{P}^k\left(\underline{c}\right)\pi\left(\underline{V}\right).$

2.2. **Subdiagonal models.** The subdiagonal model may be written as

$$X_t=c\left(s_t\right)X_{t-1}e_{t-2}+e_t, \tag{7}$$

in which X_{t-1} and e_{t-2} are dependent, and therefore the derivation of the moments is more complicated and rather long. For this reason, we will present the final results. We have

$$\mu=E\left(X_t\right)=0, \text{ for all } t,$$

$$var\left(X_t\right)=E\left(X_t^2\right)=\underline{1}'_{(d)}\left\{\underline{\pi}+\left(I_{(d)}-\mathbb{P}\left(\underline{c}^2\right)\right)^{-1}\left(I_{(d)}+2\mathbb{P}\left(\underline{c}^2\right)\right)\pi\left(\underline{c}^2\right)\right\},$$

and

$$\gamma\left(r\right)=E\left(X_t\ X_{t-r}\right)=\begin{cases}\underline{1}'_{(d)}\mathbb{P}\left(\underline{c}\right)\pi\left(\underline{c}\right) & \text{if } r=3\\ 0 & \text{otherwise}\end{cases}.$$

Moreover, the third-order moments are given by

$$R\left(r_1,r_2\right)=E\left(X_t\ X_{t-r_1}X_{t-r_2}\right)=\underline{1}'_{(d)}\times$$
$$\begin{cases}\pi\left(\underline{c}\right)+3\left(I_{(d)}+3\left(I_{(d)}-\mathbb{P}\left(\underline{c}^2\right)\right)^{-1}\mathbb{P}\left(\underline{c}^2\right)\right)\mathbb{P}\left(\underline{c}\right)\pi\left(\underline{c}^2\right) & \text{if } r_1=1,\ r_2=2\\ 2\mathbb{P}^2\left(\underline{c}\right)\pi\left(\underline{c}\right) & \text{if } r_1=2,\ r_2=4\\ \underline{O}_{(d)} & \text{otherwise}\end{cases}$$

3. Bispectral Structure

The bispectral density function is defined as

$$f\left(\omega_1,\omega_2\right)=\frac{1}{4\pi^2}\sum_{r_1=-\infty}^{+\infty}\sum_{r_2=-\infty}^{+\infty}R\left(r_1,r_2\right)\exp\left(-ir_1\omega_1-ir_2\omega_2\right),$$

where $R\left(r_1,r_2\right)$ is the third-order central moment defined by (2). Using the well known symmetric relations for both $R\left(r_1,r_2\right)$ and $f\left(\omega_1,\omega_2\right)$ (see, e.g., Subba Rao and Gabr, 1984) the bispectral density function $f(\omega_1,\omega_2)$ of the $MS-BL$ model (1) is given as follows. For the superdiagonal model (6)

$$f(\omega_1,\omega_2)=\frac{R(k-m,k)}{4\pi^2}\left\{\begin{array}{c} H(k-m,k)+H(k,k-m)+H(-m,-k) \\ +H(-k,-m)+H(m,-k+m)+H(-k+m,m) \end{array}\right\}, \tag{8}$$

where $H(r_1,r_2)=\exp(-ir_1\omega_1-ir_2\omega_2)$. For the subdiagonal model (7), $f(\omega_1,\omega_2)$ given by

$$f(\omega_1,\omega_2)=\frac{1}{4\pi^2}\left\{\begin{array}{c} R(1;2)\left\{\begin{array}{c} H(1;2)+H(2;1)+H(1;-1)+ \\ H(-1;1)+H(-1,-2)+H(-2,-1) \end{array}\right\} \\ R(2;4)\left\{\begin{array}{c} H(2;4)+H(4;2)+H(2;-2)+ \\ H(-2;2)+H(-4,-2)+H(-2,-4) \end{array}\right\} \end{array}\right\}. \tag{9}$$

Example 1. *The modulus of* $f(\omega_1,\omega_2)$, *given by* (3.1), *is plotted for* $d=2$, $c(1)=0.7$, $c(2)=0.8$ *and* $k=2$, $m=1$; $k=3$, $m=1$; $k=5$, $m=1$; $k=7$, $m=5$ *in Figures* 1, 2, 3 *and* 4. *Finally, Figures* 5 *and* 6 *represent the bispectral modulus of subdiagonal model with* $d=2$, $c(1)=0.7$, $c(2)=0.8$ *and* $d=5$, $c(1)=c(2)=c(4)=0.7$, $c(3)=0.8$, $c(5)=0.6$ *respectively.*

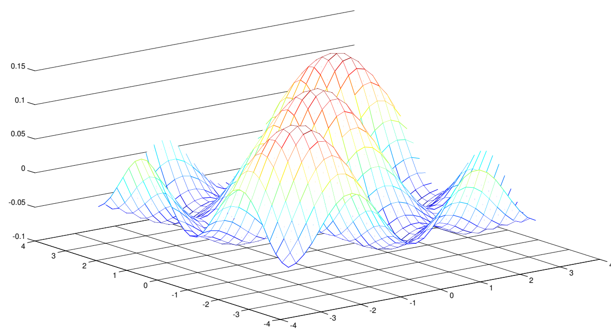

Figure 1. Bispectral modulus of the superdiagonal model $X_t=c(s_t)X_{t-2}e_{t-1}+e_t$.

4. Conclusion

For the superdiagonal and subdiagonal bilinear models we have obtained all the theoretical third-order central moments and also explicit expressions for the bispectral density function. In practice, given real data $\{X_1,X_2,,...,X_N\}$, both third-order moments and bispectral density function could be estimated (see, e.g., Subba Rao and Gabr, 1984).

Author Contribution Statements All authors contributed equally to the writing of this paper. All authors read and approved the final manuscript.

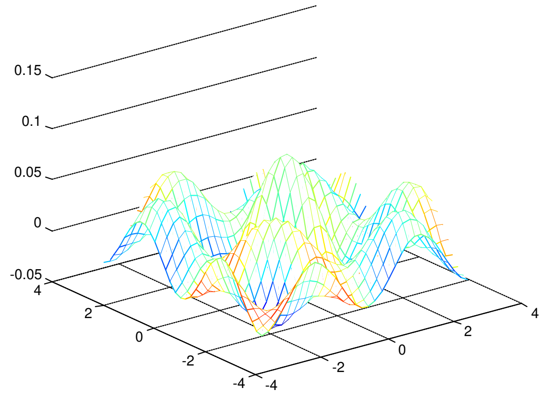

FIGURE 2. Bispectral modulus of the superdiagonal model $X_t = c(s_t) X_{t-3} e_{t-2} + e_t$.

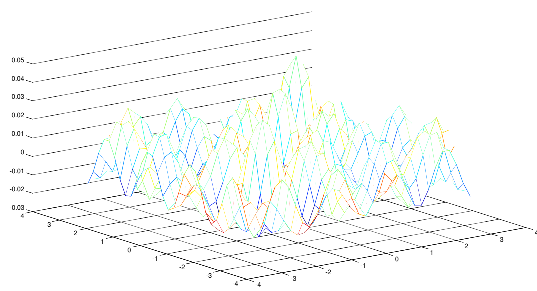

FIGURE 3. Bispectral modulus of the superdiagonal model $X_t = c(s_t) X_{t-5} e_{t-4} + e_t$.

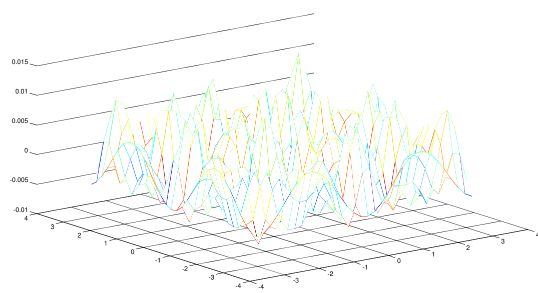

FIGURE 4. Bispectral modulus of the superdiagonal model $X_t = c(s_t) X_{t-7} e_{t-2} + e_t$.

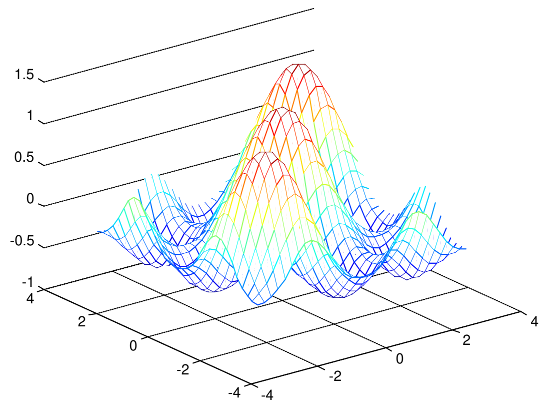

FIGURE 5. Bispectral modulus of the subdiagonal model $X_t = c\,(s_t)\,X_{t-1}e_{t-2} + e_t$.

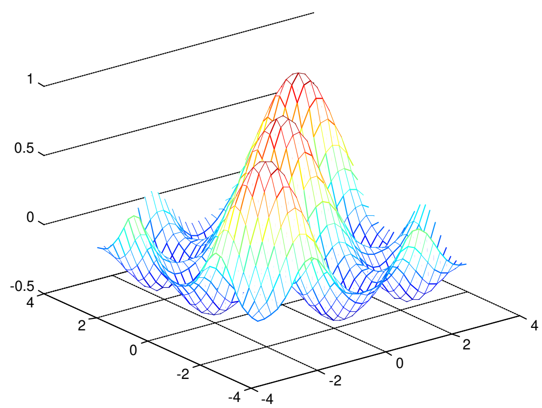

FIGURE 6. Bispectral modulus of the subdiagonal model $X_t = c\,(s_t)\,X_{t-1}e_{t-2} + e_t$.

Declaration of Competing Interests The authors declare that they have no competing interests.

Acknowledgements We thank the editor-in-chief of the journal, the associate editor, and the two anonymous referees for their constructive comments and very useful suggestions and remarks which were most valuable for improvement of the final version of the paper.

References

[1] Bibi, A., Aknouche, A., Stationnarité et β-mélange des processus bilinéaires généraux à changement de régime markovien, *C.R. Acad. Sci. Paris, Ser. I.,* 348(3-4) (2010), $185-188$. https://doi.org/10.1016/j.crma.2009.12.015

[2] Brillinger, D.R., Rosenblatt, M., Asymptotic theory of estimates of k^{th} order spectra, *In Spectral Analysis of Time Series, (ed. by B. Harris),* Proc. Nat.l. Acad. Sci. USA., 57(2) (1967*a*) , 206-210. https://doi.org/10.1073/pnas.57.2.206

[3] Brillinger, D.R., Rosenblatt, M., Computation and Interpretation of k^{th} Order Spectra, *In Spectral Analysis of Time Series, (ed. by B. Harris),* Wiley, New York, 1967, 189-232.

[4] Costa, O.L.V., Fragoso, M.D., Marques, R.P., Discrete Time Markov Jump Linear Systems, Springer, London, 2005. https://doi.org/10.1007/b138575

[5] Gabr, M.M., Subba Rao, T., The estimation and prediction of subset bilinear time series models with applications, *J. Time Series Anal.,* 2(3) (1981), 155-171. https://doi.org/10.1111/j.1467-9892.1981.tb00319.x

[6] Gabr, M.M., On the third-order moment structure and bispectral analysis of some bilinear time series, *J. Time Series Anal.,* 9(1) (1988), $11-20$. https://doi.org/10.1111/j.1467-9892.1988.tb00449.x

[7] Hamilton, J.D., A new approach to the economic analysis of nonstationary time series and the business cycle, *Econometrica,* 57(2) (1989), 357-384. https://doi.org/10.2307/1912559

[8] Hamilton, J.D., Analysis of time series subject to changes in regime, *Journal of Econometrics,* 45(1-2) (1990), $39-70$. https://doi.org/10.1016/0304-4076(90)90093-9

[9] Hasselmann, K., Munk, W., MacDonald, G., Bispectra of Ocean Waves, *Proc. Symp. Time Series Analysis, (ed. M. Rosenblatt.)*, John Wiley, 1963, $135-139$.

[10] Francq, C., Zakoïan, J.M., Stationaruty of multivariate Markov switching $ARMA$ models, *Journal of Econometrics,* 102(2) (2001) , $339-364$. https://doi.org/10.1016/S0304-4076(01)00057-4

[11] Helland, K.N., Lii, K.S., Rosenblatt, M., Bispectra and energy transfer in grid-generated turbulence, *Developments in Statistics, (Ed. P. R. Krishnaiah),* Academic Press, New York, 2 (1979) , $123-155$. https://doi.org/10.1016/B978-0-12-426602-5.50009-8

[12] Lii, K.S., Rosenblatt, M., Deconvolution and estimation of transfer function phase and coefficients for non-Gaussian linear processes, *Ann. Statist.,* 10(4) (1982) , $1195-1208$. https://doi.org/10.1214/aos/1176345984

[13] Pataracchia, B., The spectral representation of Markov switching $ARMA$ models, *Economics Letters,* 112(1) (2011) , $11-15$. https://doi.org/10.1016/j.econlet.2011.03.003

[14] Rosenblatt, M. Remarks on Higher Order Spectra, *Multivariate Analysis,* Academic Press, New York, 1966, $383-389$.

[15] Rosenblatt, M., Van Ness, J.W., Estimation of the bispectrum, *Ann. Math. Statist.,* 36(4) (1965) , $1120-1136$. https://doi.org/10.1214/aoms/1177699987

[16] Subba Rao, T., On the theory of bilinear time series models, *J. Roy. Statist. Soc. B,* 43(2) (1981), $244-255$. https://doi.org/10.1111/j.2517-6161.1981.tb01177.x

[17] Subba Rao, T., Gabr, M.M., An Introduction to Bispectral Analysis and Bilinear Time Series Models, *Lecture Notes in Statistics,* Berlin: Springer-Verlag, 1984. https://doi.org/10.1007/978-1-4684-6318-7

[18] Van Ness, J.W., Asymptotic normality of bispectral estimates, *Ann. Math. Statist.,* 37(5) (1966) , $1257-1275$. https://doi.org/10.1214/aoms/1177699269

INSTRUCTIONS TO CONTRIBUTORS

Communications Faculty of Sciences University of Ankara Series A1 Mathematics and Statistics (Commun. Fac. Sci. Univ. Ank. Ser. A1 Math. Stat.) is a single-blind peer reviewed open access journal which has been published biannually since 1948 by Ankara University, accepts original research articles written in English in the fields of Mathematics and Statistics. It will be published four times a year from 2022. Review articles written by eminent scientists can also be invited by the Editor.

The publication costs for Communications Faculty of Sciences University of Ankara Series A1 Mathematics and Statistics are covered by the journal, so authors do not need to pay an article-processing and submission charges. The PDF copies of accepted papers are free of charges and can be downloaded from the website. Hard copies of the paper, if required, are due to be charged for the amount of which is determined by the administration each year.

All manuscripts should be submitted via our online submission system https://dergipark.org.tr/en/journal/2457/submission/step/manuscript/new. Note that only two submissions per author per year will be considered. Once a paper is submitted to our journal, all co-authors need to wait 6 months from the submission date before submitting another paper to Commun. Fac. Sci. Univ. Ank. Ser. A1 Math. Stat. Manuscripts should be submitted in the PDF form used in the peer-review process together with the COVER LETTER and the TEX file (Source File). In the cover letter the authors should suggest the most appropriate Area Editor for the manuscript and potential four reviewers with full names, universities and institutional email addresses. Proposed reviewers must be experienced researchers in your area of research and at least two of them should be from different countries. In addition, proposed reviewers must not be co-authors, advisors, students, etc. of the authors. In the cover letter, the author may enter the name of anyone who he/she would prefer not to review the manuscript, with detailed explanation of the reason. Note that the editorial office may not use these nominations, but this may help to speed up the selection of appropriate reviewers.

Manuscripts should be typeset using the LATEX typesetting system. Authors should prepare the article using the Journal's templates (commun.cls and commun.cst). Manuscripts written in AMS LaTeX format are also acceptable. A template of manuscript can be downloaded in tex form from the link https://dergipark.org.tr/en/download/journal-file/22173(or can be reviewed in pdf form). The title page should contain the title of the paper, full names of the authors, affiliations addresses and e-mail addresses of all authors. Authors are also required to submit their Open Researcher and Contributor ID (ORCID)'s which can be obtained from http://orcid.org as their URL address in the format http://orcid.org/xxxx-xxxx-xxxx-xxxx. Please indicate the corresponding author. Each manuscript should be accompanied by classification numbers from the Mathematics Subject Classification 2020 scheme. The abstract should state briefly the purpose of the research. The length of the Abstract should be between 50 to 5000 characters. At least 3 keywords are required. Formulas should be numbered consecutively in the parentheses. All tables must have numbers (TABLE 1) consecutively in accordance with their appearance in the text and a legend above the table. Please submit tables as editable text not as images. All figures must have numbers (FIGURE 1) consecutively in accordance with their appearance in the text and a caption (not on the figure itself) below the figure. Please submit figures as EPS, TIFF or JPEG format. Authors Contribution Statement, Declaration of Competing Interests and Acknowledgements should be given at the end of the article before the references. Authors are urged to use the communication.bst style in BibTeX automated bibliography. If manual entry is preferred for bibliography, then all citations must be listed in the references part and vice versa. Number of the references (numbers in squared brackets) in the list can be in alphabetical order or in the order in which they appear in the text. Use of the DOI is highly encouraged. Formal abbreviations of the journals can be used. The Editor may seek the advice of two, or three referees, depending on the response of the referees, chosen in consultation with appropriate members of the Editorial Board, from among experts in the field of specialization of the paper. The reviewing process is conducted in strict confidence and the identity of a referee is not disclosed to the authors at any point since we use a single-blind peer review process.

Declarations/Ethics:
With the submission of the manuscript authors declare that:

- All authors of the submitted research paper have directly participated in the planning, execution, or analysis of study;
- All authors of the paper have read and approved the final version submitted;
- The contents of the manuscript have not been submitted, copyrighted or published elsewhere and the visual-graphical materials such as photograph, drawing, picture, and document within the article do not have any copyright issue;
- The contents of the manuscript will not be copyrighted, submitted, or published elsewhere, while acceptance by the Journal is under consideration.
- The article is clean in terms of plagiarism, and the legal and ethical responsibility of the article belongs to the author(s). Author(s) also accept that the manuscript may go through plagiarism check using iThenticate software;
- The objectivity and transparency in research, and the principles of ethical and professional conduct have been followed. Authors have also declared that they have no potential conflict of interest (financial or non-financial), and their research does not involve any human participants and/or animals.

Research papers published in **Communications Faculty of Sciences University of Ankara** are archived in the Library of Ankara University and in Dergipark immediately following publication with no embargo.

Editor in Chief
http://communications.science.ankara.edu.tr
Ankara University, Faculty of Sciences
06100, Besevler - ANKARA TURKEY

C O M M U N I C A T I O N S

FACULTY OF SCIENCES
UNIVERSITY OF ANKARA

DE LA FACULTE DES SCIENCES
DE L'UNIVERSITE D'ANKARA

Series A1: Mathematics and Statistics

Volume: 72 **Number: 3** **Year:2023**

Research Articles